Table of Contents

Section VIII. MMIRS Electrical Design

1. IR Array Electronics
2. Instrument Electronics
3. Instrument Electronics Rack Packaging
4. Electronics Rack Thermal Analysis

Section IX. MMIRS Software Design

1. Overview
2. Derived Requirements
3. Design Principles
4. Computer and Software Architecture

Software Components

5. Libraries
6. Servers
7. Graphical User Interfaces, GUI's
8. System Management
9. Testing and Verification
10. Data Products
11. Schedules and Milestones

Section X. Miscellaneous

1. Observatory Interface
    a. MMIRS Observatory Interface
    b. MMT Telescope Bearing Moment
    c. Magellan Telescope Bearing Moment
2. Vacuum System
3. Temperature Sensing
4. Gate Valve Interlock

Section XI. Operations and Maintenance

1. Observing Overview
2. Slit Mask Exchange Procedure
3. Warm Up and Cool Down Procedure
4. Maintenance and Serviceability
5. Shipping and Installation Plans
6. Assembly and Test Plan

Section XII. Management

1. MMIRS Project Schedule
2. MMIRS Integration & Test Flow Chart
3. Status of PDR Action Items
4. Known/Open Issues

Section I.

MMIRS Instrument Overview

1. MMIRS Overview
2. MMIRS Functional and Performance Specification

MMIRS OVERVIEW

Brian McLeod
May 3, 2005

1 INTRODUCTION

This document describes the design of MMIRS, the MMT and Magellan InfraRed Spectrograph, a JHK imager and multiobject spectrograph that will be used at the f/5 focus of the 6.5 meter MMT and Magellan Clay telescopes. MMIRS will allow imaging of a 7′ by 7′ field with 0.2″ sampling on a 2048 by 2048 pixel Hawaii 2 array, as well as multiobject spectroscopy with slitlets over a 4′ by 7′ field. A spectral resolution of ~3000 is achieved with coverage of the complete J, H or K bands. Currently, neither MMT nor Magellan users have regular access to either a wide-field, near-infrared imager or spectrograph. We plan to ship MMIRS to Magellan for one observing run per year, nominally three months long. At Magellan[1], MMIRS will be operated in campaign mode with Megacam, SAO's large CCD array. At the MMT, MMIRS would be scheduled as requested by observers.

The FLAMINGOS instrument, a near-infrared multiobject spectrograph developed by Richard Elston's group at the University of Florida, has been brought to the MMT as a visitor instrument. The design of MMIRS builds upon FLAMINGOS and FLAMINGOS-2, currently under development for Gemini. We are developing MMIRS at the Smithsonian Astrophysical Observatory (SAO), but are collaborating with the University of Florida team to use existing FLAMINGOS mechanical and dewar designs. This collaboration will allow us to build MMIRS on an accelerated schedule for less money than would otherwise be possible. The University of Florida will receive telescope time at the MMT and Magellan (separate from the TSIP allocation) in return for this assistance.

The SAO instrument team has delivered six major instruments to the MMT: the f/5 wide-field refractive corrector, the Hectospec and Hectochelle fiber-fed bench spectrographs, the Hectospec/Hectochelle robotic fiber positioner, Megacam (a 36 CCD optical imager), and a dedicated f/5 wavefront sensor. MMIRS builds upon this program, and makes use of software, detector electronics, and stepper motor drive systems.

2 SCIENTIFIC CAPABILITIES

2.1 INTRODUCTION

MMIRS will enable forefront research in stellar and extragalactic astrophysics. We illustrate the scientific capabilities of MMIRS by describing a mix of programs that might be carried out by members of the Magellan and MMT Partner institutions or by investigators from the US community at large who will have access to this instrument as part of the TSIP program. We consider topical problems in star formation, the physics of supernovae, the growth of black holes, and the formation and evolution of galaxies.

[1] The Magellan project has procured an f/5 secondary blank for Magellan 2, and this mirror will be polished at the Steward Observatory Mirror Lab. The mirror is currently being generated at Kodak.

MMIRS is a versatile instrument. Its wide field of view and its changeable multislit aperture plates allow for simultaneous spectroscopic observations of 30 to 70 objects. Its low-resolution modes allow maximum spectral coverage and high sensitivity to broad spectral features (e.g., molecular bands), while the highest resolution modes allow one to work effectively between the telluric OH emission lines to achieve maximum sensitivity. This versatility makes MMIRS a powerful tool in many other areas of astrophysics (e.g., planetary science, stellar populations, photospheric abundances) that we do not have space to discuss.

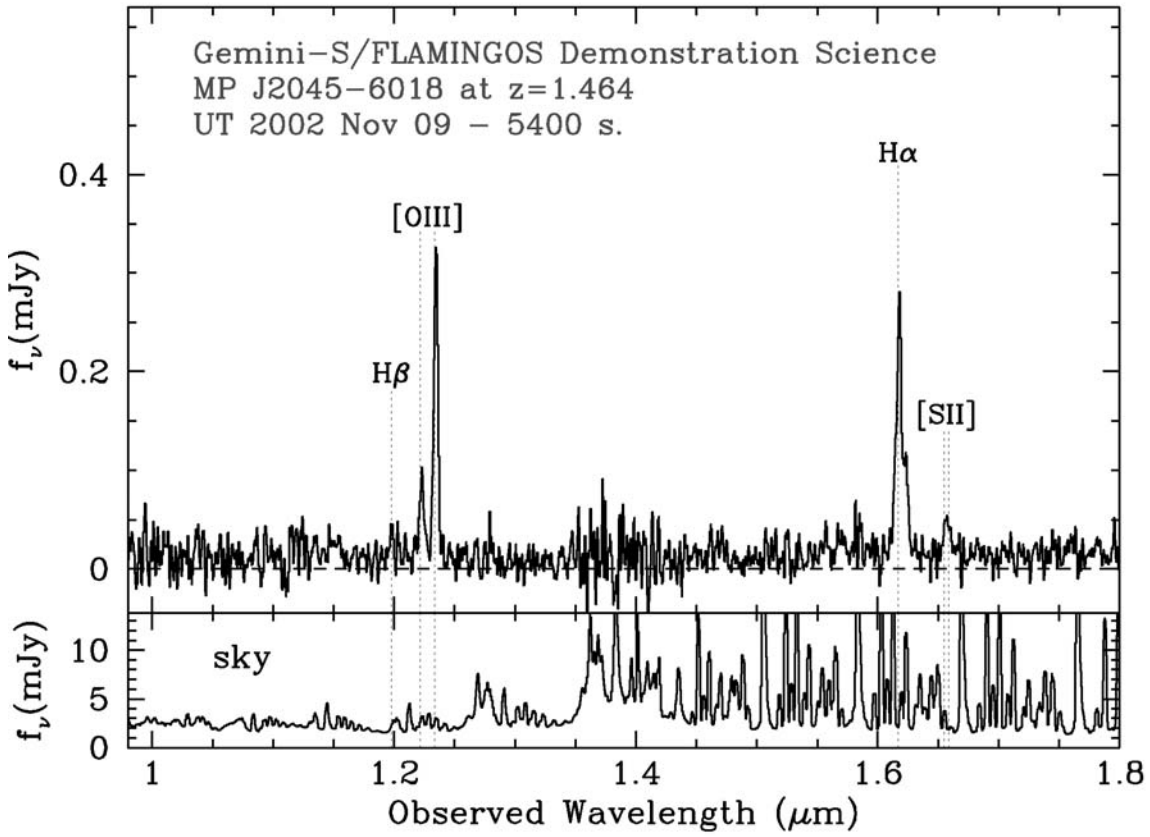

Figure 1. FLAMINGOS J and H spectrum of MP J2045-6018 at R=600 obtained at Gemini South. MP J2045-6018 is an extremely luminous radio source identified with a very red AGN (K=18).

2.2 FORMATION OF STARS AND SUBSTELLAR OBJECTS

Star formation is central to galaxy formation, interstellar medium physics, and planet formation. Despite substantial progress over the last two decades, fundamental puzzles remain. (1) What determines the stellar initial mass function (IMF)? (2) Does the IMF depend upon environment? (3) Are accretion disks as important in the formation of high and low mass stars as in the formation of solar-type stars? The importance of wide-field near-infrared multiple object spectroscopy at R = 300-3000 for studies of star and planet formation was stressed in "The First Workshop on the Ground-Based O/IR System" sponsored by NOAO in Oct. 2000.

Many specific theories can be tested with MMIRS. (1) Do high-mass stars preferentially form at the centers of clusters (e.g., Hillenbrand & Hartmann 1998; Testi et al. 1999), or do they simply sink to cluster centers as dynamical mass segregation proceeds (Kroupa 2002)? (2) Do brown dwarfs form in isolation, or are they formed in circumstellar disks around other stars and then dynamically ejected (Reipurth & Clarke 2001; Bate et al. 2002)? (3) Are planetary-mass objects also ejected from multiple stellar systems (Luhman et al. 2000; Zapatero-Osorio et al. 2000; Hillenbrand & Carpenter 2000; Lucas & Roche 2000)? (4) Do proto-stars accrete most of their mass in short bursts from circumstellar disks (Hartmann & Kenyon 1996)? Testing these and other theories of star formation and of the origin of the IMF require the study of stellar populations at very early ages, when proto-stellar accretion may still be occurring, dynamical evolution is least advanced, and brown dwarfs and possible free-floating planets are brightest. Near-infrared, wide-field spectroscopy on large telescopes is required to address these questions. Observations must be made at infrared wavelengths to penetrate the dusty environments of young star-forming regions; spectroscopic capability is essential to identify spectral types and thus stellar masses, and to determine mass accretion rates through key spectral features. Multi-object capability is vital to obtaining large enough samples to make statistically significant tests of the IMF, and large telescopes are required to observe the lowest-mass systems. Near-infrared spectroscopy will be essential in interpreting the results of sensitive photometric studies from both ground- and space-based (e.g., SIRTF) telescopes.

In the most embedded clusters of OB stars, the He I and H I lines in the near-IR are the only way to classify the spectra of the higher-mass stars. The MMIRS resolution of 3000 is needed to identify these diagnostic absorption features. Emission line observations also can be used to estimate extinction corrections. Accurate spectral typing of > 0.1 solar mass young stars also requires the MMIRS resolving power, in the spectral region of 2.1-2.4 μm. Observations of the Brγ emission line at 2.17 μm, at similar resolutions, can be used to determine accretion rates in low-mass protostars down to low levels (Muzerolle et al. 1998). In addition, the (Paschen β (1.28 μm))/(Brγ) ratio can be used to estimate extinctions in these systems (Muzerolle et al. 2001). Fields at least 20′ in diameter need to be imaged to fully characterize populations of relatively nearby embedded clusters, a project of reasonable scale with the MMIRS imaging field of view.

Likewise, fields 30′ in diameter must be imaged to K=21 to advance surveys for Jupiter-mass free-floating brown dwarfs within nearby clusters. Such a survey would offer an order of magnitude improvement over current work (Burrows et al. 1997; Baraffe et al. 1998). With MMIRS at the MMT or Magellan, this task can be done in about 1.5 hr per field. Because of the broad molecular bands expected in spectra of young brown dwarfs at 1-10 Jupiter masses (1000-2000 °K), low-resolution spectroscopy is ideal for confirming the cool temperatures and sub-stellar nature of candidates identified in the imaging. About 20-100 brown dwarf candidates are available for spectroscopy in single MMIRS fields in the Trapezium and IC348 fields (Luhman et al. 2000, Luhman 1999).

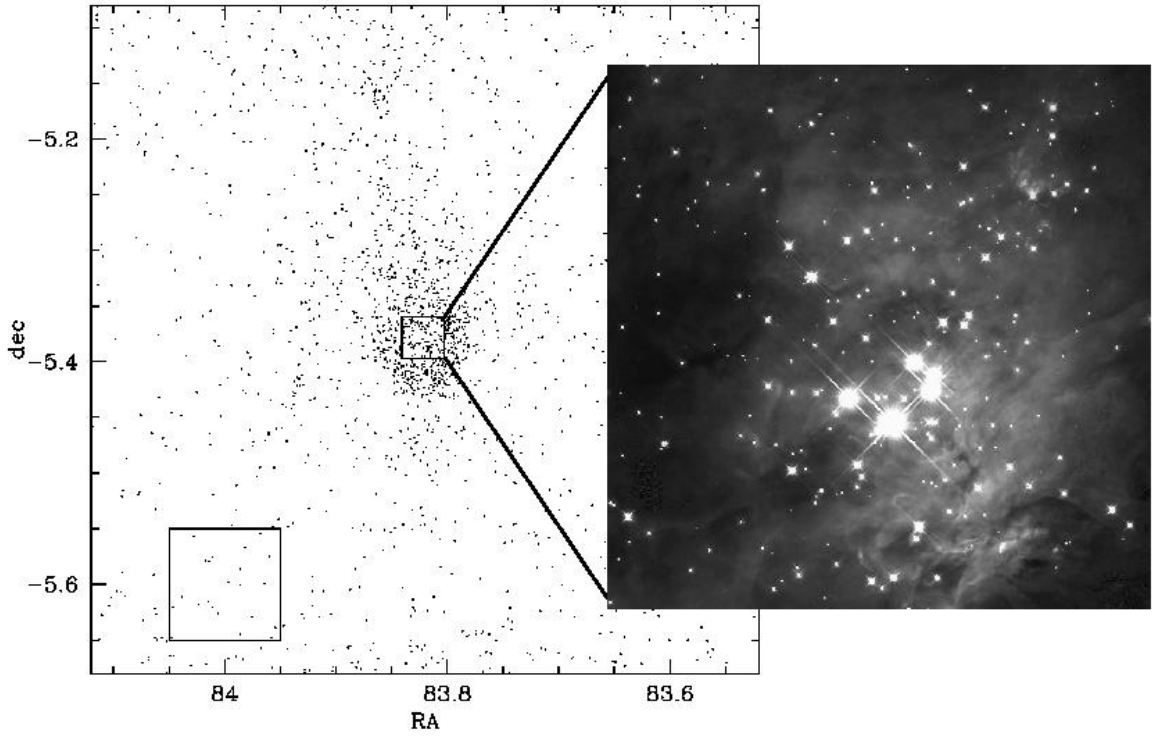

Figure 2. Young stars and brown dwarfs in the Orion Nebula Cluster. The main panel shows 2000 IR stars detected by Ali & Depoy (1995) and McCaughrean and Stauffer (1994). Many of these stars are invisible at optical wavelengths. The box to the lower left is 6′ square, comparable in size to the MMIRS imaging field. The panel to the right is an HST NICMOS image (Luhman et al. 2000); approximately 50 candidate brown dwarfs (with masses 10 to 80 Jupiter masses) lie in this region. Multiobject spectroscopy with MMIRS could be used to derive initial mass functions and to determine the cluster structure in this and other regions.

2.3 THE PHYSICS OF SNe

The last years have witnessed enormous progress in our knowledge of the optical properties of supernovae (SNe) of all types. Comparatively little is known, however, about SNe spectra at near-infrared (NIR) wavelengths. MMIRS will access a virtually unexplored window on the physics of SNe. Below we list three areas in which NIR spectroscopy is critical to resolving outstanding problems in SNe structure and evolution.

Type Ic SNe: Significant effort has gone into determining the presence of He features in optical spectra of these supernovae to determine their progenitors. While the He optical lines are blended with other species, making them difficult to identify, the He I 1.083 μm and 2.058 μm lines are much more isolated and offer a substantial advantage for the detection of He in type Ic supernovae. He I 1.083 μm absorption from a type Ibc SNe is shown in Figure 3.

Type Ib SNe: IR spectra would provide an important constraint on the He abundances in the atmospheres of Type Ib supernovae and help to determine whether the progenitors of Type Ib supernovae are single or binary stars.

Type Ia SNe: The identification of the progenitors of Type Ia supernovae is a longstanding and important problem. Identification of contaminating hydrogen and helium stripped from the companion star (Marietta et al. 2000) would help discriminate between the many Type Ia progenitor scenarios. Unfortunately the spectral region near Hα is contaminated with numerous Fe and Co lines. Telluric water vapor absorption makes searches for Paα (1.87 μm) from the ground problematic. Paβ (1.28 μm), on the other hand, can be detected from the ground, as can the He lines at 1.083 μm and 2.05 μm. Late-time (~1 yr) optical/IR spectra can be used in combination with atmosphere models to determine the mass of Fe produced in the explosion, which provides a

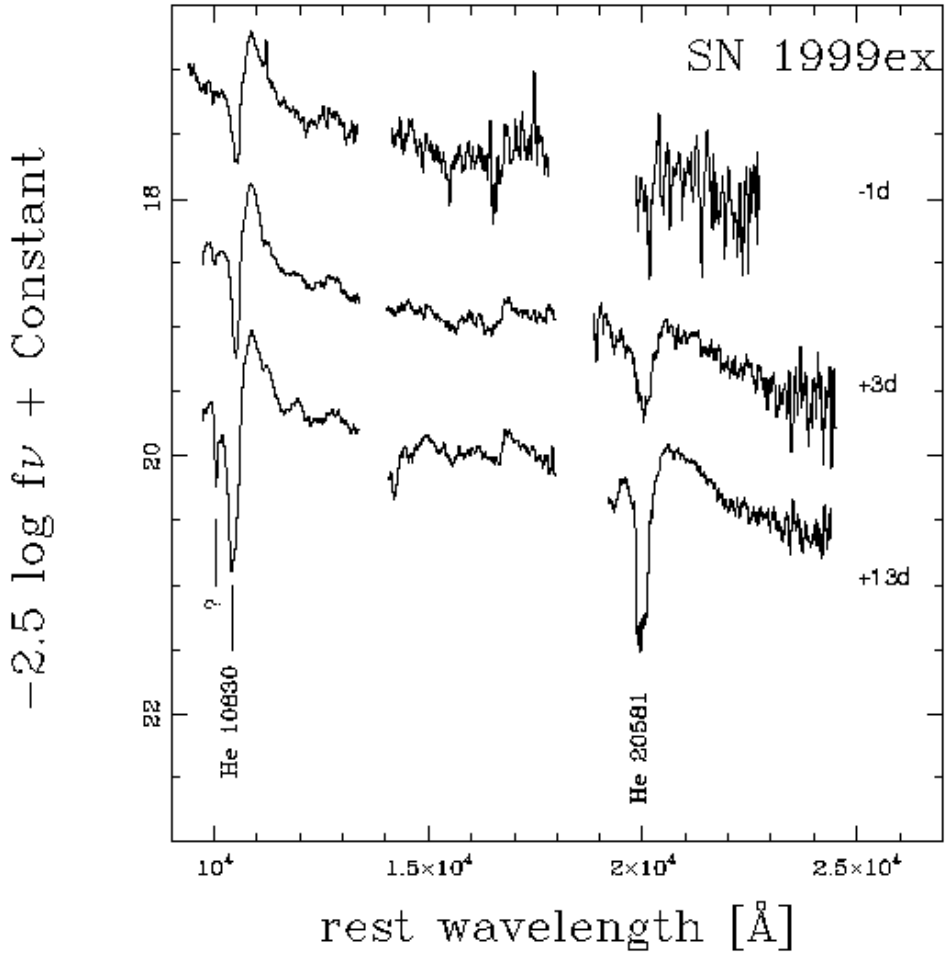

Figure 3. NIR evolution of the spectrum of SN 1999ex (days relative to maximum light are indicated next to each spectrum). The two most prominent features are due to He I. These absorption features allow us to estimate the He abundance in Type Ib/c events. Observations like this will help us to discriminate between binary or single progenitors for these core collapse supernovae. (Data from ISAAC on the VLT.)

fundamental test of the explosion models for Type Ia supernovae, and allows a direct determination of the mass of Ni produced (Spyromilio et al. 1992). Combined optical and

IR spectroscopic observations during the first weeks after explosion can also be used to test various explosion models, as shown by Hoeflich et al. (2002). MMIRS thus offers a clear avenue from which to address the critical question of the type Ia progenitors. In a 1 hr exposure, MMIRS will reach a signal-to-noise ratio of 5 for R=700 at K=19.5, sufficient to observe the broad spectral features characteristic of Sne. High quality spectra of type Ia SNe at or before maximum light can be obtained to z=0.10 in a three hr exposure. Good quality spectra 30 days past maximum can be obtained in hour-long exposures to z~0.07 for Ia SNe and to z~0.03 for type II SNe. Approximately 12 such objects are discovered each year. In longer exposures, spectra up to one year past maximum can be obtained for Ia's to the distance of Virgo. Such objects are rare (~2 per year) but they provide an important laboratory for studying the interactions between SNe ejecta and the surrounding ISM.

2.4 BLACK HOLE DEMOGRAPHICS

Recent work has shown that the masses (M) of black holes at the centers of galaxies are strongly correlated with the velocity dispersions (σ) in their host galaxy spheroids (Ferrarese & Merritt 2000; Gebhardt et al. 2000). This M - σ relationship implies some co-evolution between galaxies and black holes, yet its origin remains a mystery. Substantial progress can be made with a determination of the redshift evolution of supermassive black holes in large numbers of QSOs, where M is increasing rapidly, via measurement of σ for QSOs. While the bright, blue QSO continuum completely swamps the host galaxy stellar absorption features in the visible, the QSO continuum is at a minimum in the rest-frame H-band (e.g., Elvis et al. 1994). Recent observations in that wavelength regime have indicated that the galaxy spectrum can be well enough detected to allow an accurate σ to be measured (Martini et al., in prep). NIR measurements of σ for large numbers of QSOs using the long slit mode of MMIRS can therefore track the evolution of accretion history and supermassive black hole growth and help to unravel the origin of the co-evolution between black holes and galaxies.

2.5 CHEMICAL EVOLUTION IN DISTANT GALAXIES

Several lines of evidence point to the z = 1 to 3 era as the major epoch of galaxy formation (e.g., Lilly et al. 1995, Madau et al. 1996, Fall et al. 1996). The evolution of galaxies through star formation should be accompanied by a rapid evolution in the abundance of both stellar and interstellar matter. Optical surveys are very effective at identifying populations of star forming galaxies at intermediate and high redshift. These studies are keyed to strong, and usually saturated, resonance lines and so they do not provide strong constraints on chemical composition. The emission lines used in the traditional nebular abundance determinations are redshifted to the NIR at high redshifts (Pettini et al. 2002, see Figure 4). Fortunately, most of the strong nebular emission lines (e.g., Hα, [NII], [OIII], Hβ, [OII]) fall within transparent atmospheric windows in a number of interesting redshift ranges (see Figure 4). At z = 2.5, Hα, [OIII]λ5007 and Hβ, and [OII]λ3727 fall in the K, H, and J bands, respectively. The line strengths for galaxies with modest star formation rates can be readily detected with the MMT and Magellan telescopes. While the temperature sensitive lines (e.g., [OIII]λ4363) that are typically used in nebular abundance work are not likely to be detected at z = 2.5, there are well

documented techniques (e.g., Kewley & Dopita 2002) for determining gas-phase abundances using just the [OIII], [OII], and Balmer emission-lines.
In addition to providing sensitive diagnostics of elemental abundances, the Balmer lines provide a good measure of the instantaneous star formation rate (e.g., Kennicutt 1998). MMIRS will reach line-flux limits of ~10^{-17} erg cm^{-2} (or 10^{-20} W m^{-2}) in exposure times of a few hr. At z=2.5 (where Hα is in the K-window) this translates to a star formation rate of ~3 solar masses yr^{-1}, barely one order of magnitude larger than the current Milky Way star formation rate.

Photometric techniques (e.g., photometric redshifts, Lyman-break, Balmer-break) allow for efficient selection of galaxy samples in redshift bins of width ~ 0.15 in z. The favorable redshift ranges for emission-line spectroscopy in the NIR, $0.7 < z < 0.9$ (Hα in J-band), $1.1 < z < 1.4$ (Hα in H-band, [OIII] in J-band), and $2.0 < z < 2.7$ (Hα in K-band, [OIII] in H-band, [OII] in J-band), allow abundance determinations over a critical range of redshifts. At K = 20 the surface density of galaxies in the $0.8 < z < 1.7$ range is roughly 2 per square arcminute. Using the JH grism one could sample 50 to 80 objects per slit mask in a redshift range that samples Hα. MMIRS will allow a determination of the Hα luminosity function (LF), and hence star formation rate, with far greater confidence. Previous determinations of the Hα LF (e.g., Yan et al.) were based on samples of 35 objects. A modest MMIRS program could sample several hundred Hα emitters in the critical $1 < z < 2$ range. MMIRS will allow us to sample the LF down to levelscorresponding to star formation rates below 1 solar mass yr^{-1}.
The K band offers a window on star forming galaxies in the range between IR selected z~1 samples and the traditional Ly-break samples. For galaxies in this redshift range both Hα and Lyα can be detected from the ground. While the sky density of objects bright enough for continuum detections at K is low at these redshifts, emission-line spectroscopy will go much deeper. We expect to be able to observe ~10-20 objects per slit mask, making MMIRS considerably more powerful than single-object IR spectrographs on larger telescopes. Object selection will be based on multi-band imaging, particularly J and K photometry obtained with MMIRS in the imaging mode.

In Figure 5 we show the Hα LF in the $0.8 < z < 1.8$ range as derived from NICMOS spectroscopy (Yan et al. 1999). Using MMIRS we will be able to extend this LF to lower luminosities (by a factor of 3-5) and to z = 2.5. MMIRS observations will allow a determination of the evolution in the global star formation rate based on a single diagnostic, avoiding the differential extinction problems that plague other studies.

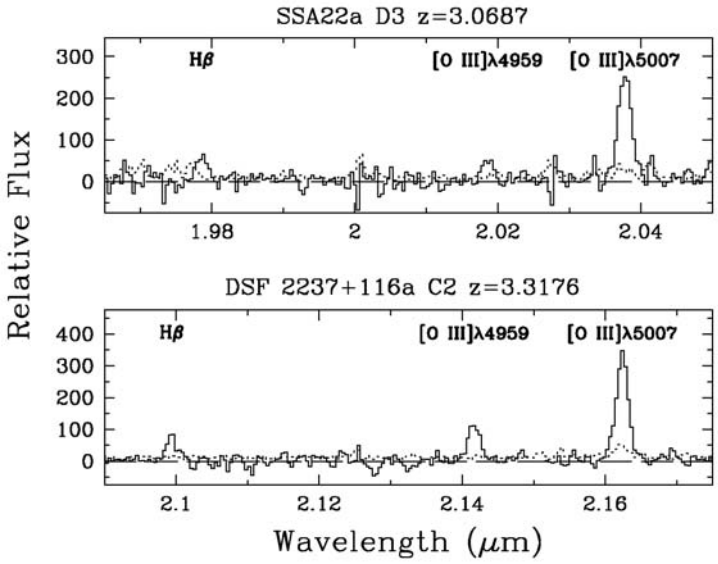

Figure 4. K-band spectra of two Ly-break galaxies from Pettini et al. (2001). Strong [OIII] and Hβ lines are clearly seen in both objects. Photometric techniques now allow one to select star-forming galaxies at redshifts that place Hα in the K-band and [OIII], Hβ in the H-band and [OII] in the J-band, thus allowing nebular abundance determinations over a range of redshifts.

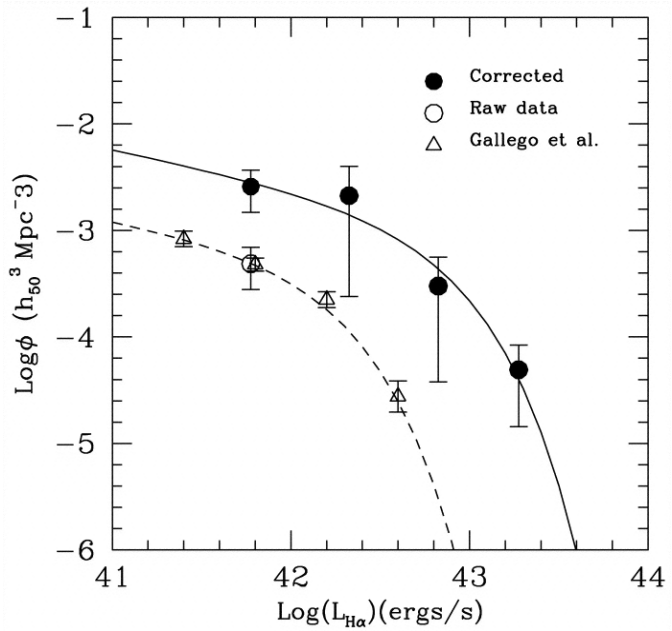

Figure 5. Hα luminosity function in the 0.8 < z < 1.8 range as derived from NICMOS spectroscopy (Yan et al. 1999). This luminosity function is based on a sample of 35 objects; MMIRS would easily allow expansion of this work to samples an order of magnitude larger, including galaxies with star formation rates below 1 solar mass yr^{-1} .

2.6 SCIENTIFIC REFERENCES

Ali, B. & Depoy, D.L. 1995, AJ, 109, 709
Baraffe, I., Chabrier, G., Allard, F. & Hauschildt, P. H. 1998, A&A, 337, 403
Bate, M. R., Bonnell, I. A. & Bromm, V. 2002, MNRAS, 332, L65
Burrows, A. et al. 1997, ApJ, 491, 856
Kewley, L.J., & Dopita, M. A. 2002, ApJS, 142, 35
Elvis, M. et al. 1994, ApJS, 95, 1
Fall, S. M., Carlot, S. & Pei, Y. C. 1996, ApJ, 464, L43
Fassia, A. et al. 2001, MNRAS, 325, 907
Ferrarese, L. & Merritt, D. 2000, ApJ, 539, L9
Gebhardt, K. et al. 2000, ApJ, 539, L13
Hartmann, L. & Kenyon, S. J. 1996, ARAA, 34, 207
Hillenbrand, L. A. & Carpenter, J. M. 2000, ApJ, 540, 236
Hillenbrand, L. A. & Hartmann, L. W. 1998, ApJ, 492, 540
Hoeflich, P., Gerardy, C. L., Fesen, R. A. & Sakai, S. 2002, ApJ, 568, 791
Kennicutt, R. 1998, ARAA, 36, 189
Kroupa, P. 2002, Science, 295, 82
Lilly, S. J., Tresse, L., Hammer, F., Crampton, D. & Le Fevre, O. 1995, ApJ, 455, 108
Lucas, P. W. & Roche, P. F. 2000, MNRAS, 314, 858
Luhman, K.L. 1999, ApJ, 545, 466
Luhman, K. L. et al. 2000, ApJ, 540, 1016
Madau, P., Ferguson, H., Dickinson, M., Giavalisco, M., Steidel C., & Fruchter, A. 1996, MNRAS, 283, 1388
Marietta, E., Burrows, A. & Fryxell, B. 2000, ApJS, 128, 615
McCaughrean, M.J. & Stauffer, J.R. 1994, AJ, 108, 1382
Muzerolle, J., Calvet, N. & Hartmann, L. 2001, ApJ, 550, 944
Muzerolle, J., Hartmann, L. & Calvet, N. 1998, AJ, 116, 2965
Pettini, M., et al. 2001, ApJ, 554, 981
Pettini, M., Ellison, S.L., Bergeron, J. & Petitjean, P. 2002, A&A, 391, 21
Reipurth, B. & Clarke, C. 2001, AJ, 122, 432
Spyromilio, J., Meikle, W., Allen, D. A. & Graham, J. R. 1992, MNRAS, 258, 53
Testi, L., Palla, F. & Natta, A. 1999, A&A, 342, 515
Yan, L., McCarthy P., Freudling, W., Teplitz, H., Malumuth, E., Weymann, R., and Malkan, M. 1999, Ap J, 519, L47
Zapatero Osorio, M. R. et al. 2000, Science, 290, 103

3 TECHNICAL DESCRIPTION

3.1 INSTRUMENT OVERVIEW

MMIRS is a JHK imager and multislit spectrograph based on a 2048 by 2048 pixel Hawaii-2 detector that will be used at the f/5 Cassegrain foci of the MMT and Magellan-2 telescopes. MMIRS incorporates a two element CaF_2 coma corrector that replaces the large fused silica coma corrector used at optical wavelengths. If a coma corrector is not used, the images are unacceptably soft at the MMIRS slit plane. The fused silica used in the optical coma corrector has an OH content of ~1000 ppm, and would offer low throughput in the K-band.

MMIRS will be constructed in two sections. The first section will contain the coma corrector lenses, the slit mask and aperture selection wheels, the guider assembly, and a gate valve which can be closed to separate the first section from the second. The lead coma corrector lens will serve as the dewar window. The slit mask, aperture selection wheels, guider pickoff mirror, and baffles will be cooled to LN_2 temperature by an independent dewar, but the rest of the first section will be operated at ambient temperature. To exchange slit masks, the gate valve between the two sections will be closed and the slit mask and aperture selection wheels will be warmed up. The exchange cycle can be accomplished during the daytime to prepare for nighttime observing. The second section of MMIRS contains the collimator optics, the grism and filter wheels, the camera optics, and the Hawaii-2 array. These will all be operated at LN_2 temperature to minimize the thermal background.

The Hawaii-2 detector will be operated with a modified version of the array controller we have developed for Megacam's 36 CCD arrays. An engineering grade Hawaii-2 has already been deployed at the MMT in SWIRC, a J- and H-band direct imager.

3.2 SCIENTIFIC GOALS AND MMIRS DESIGN

Perhaps the strongest scientific imperative for MMIRS is timeliness: apart from J-and H-band imaging with SWIRC, there is currently no wide-field near-infrared (NIR) imager or spectrograph at the MMT or Magellan. This lack of NIR capability results in a serious lack of scientific opportunity at two large observatories. This situation drives a good deal of our thinking about the MMIRS design: in order to complete MMIRS as quickly as possible we wish to minimize risk and unnecessary development wherever possible.

The broader requirements, that we amplify below, are minimizing scattered light and thermal background to allow sensitive spectroscopy, achieving as high throughput as possible, and offering the option of high spectral resolution to resolve out sky lines. There is a range of opinion in the IR community as to the minimum resolution required to work between the sky lines, but almost all agree that R~3000 is sufficient. There is a fortunate convergence here that R~3000 is the maximum resolution possible while still covering an entire J, H or K-band with a multislit spectrograph and a 2048 pixel array. A 2048 pixel array offers 1024 two-pixel resolution elements; at R=3000 at 2.2 μm, each resolution element corresponds to ~7 Å. The total spectral coverage is therefore ~0.7 μm, allowing slits to be displaced 1′ in the spectral direction and still cover the full 0.5 μm wide K-band. Yet another fortunate convergence is that R~3000 is near the maximum resolution that can be attained with high efficiency from conventional grisms.

The pixel sampling that we have chosen, 0.2″ per pixel, is a tradeoff between field of view and sampling. At both the MMT and Magellan, 0.4″ FWHM images have been routinely obtained in the H and K bands, suggesting that choosing sampling cruder than 0.2″ per pixel would be a mistake. Many of the imaging and spectroscopic observations anticipated with MMIRS could use as large a field of view as possible, suggesting that we operate near critical sampling.

MMIRS offers a large gain in spectroscopic performance as compared with FLAMINGOS 1. With its short focal length camera, FLAMINGOS 1 can achieve a maximum (two pixel) resolution of R~1500 with efficient conventional grisms, compromising its ability to work between the sky lines. MMIRS's large collimated beam also eases the optical design of the camera by reducing the required acceptance angles, resulting in better overall image quality.

Table 1: Comparison of MMIRS to FLAMINGOS 1 and 2

	MMIRS	FLAMINGOS 1	FLAMINGOS-2
Telescope focal ratio	f/5.3	for f/9 at MMT	f/16 (Gemini)
Collimated beam diameter	100 mm	40 mm	100 mm
Collimator focal length	530 mm	350 mm	1600 mm
Camera focal length	285 mm	135 mm	260 mm
Pixel scale	0.20″	0.17″	0.18″

3.3 ESTIMATED MMIRS SENSITIVITY

We have used the observed count rates with FLAMINGOS 1 at the MMT to estimate the sensitivity of MMIRS for unresolved sources with either the MMT or Magellan telescopes.

Table 2: S/N per resolution element at R=3000

Exposure Time (hrs)	Magnitude	J	H	K	J_{dark}	H_{dark}
1	15	118	142	109	125	165
2	15	166	201	155	177	233
4	15	236	285	219	251	329
1	17	35	36	22	46	61
2	17	50	51	31	66	86
4	17	71	72	44	93	122
1	19	7	7	4	13	18
2	19	10	9	5	19	25
4	19	15	13	7	27	35

The J, H, and K columns use the background levels averaged across the band. The J_{dark} and H_{dark} columns assume a background 20 times lower than the average level, appropriate for the regions between the OH airglow lines. At R=3000 approximately

40% of the spectrum will meet the low background condition (Martini & Depoy, 2000, SPIE, 4008, 695).

3.4 OPTICAL DESIGN

The MMIRS optics consist of 14 singlets: a two element coma corrector, a six element collimator with one aspheric surface, and a six element camera (Figure 6). The optics were designed by H. Epps with contributions by D. Fabricant. The design includes eight lenses, one BaF_2 lens, two S-FTM16 lenses (an IR-transmitting Ohara glass), one ZnSe lens, and one IR-grade fused quartz lens. All of the optical materials are readily available in the necessary diameters and thicknesses and we have verified material availability with suppliers. The largest elements in the MMIRS coma corrector, collimator, and camera have clear apertures of 202mm, 134mm and 149mm respectively.

The impossibility of coupling lenses to form multiplets at cryogenic temperatures is a severe optical design constraint. However, ambitious wide-field optical spectrographs have a comparable optical complexity. For example, the IMACS instrument has 12 lens groups counting the ADC/coma corrector, the collimator and the wide-field camera. For either optical or IR spectrographs effective antireflection coatings are essential for high performance. All of the optical materials used in MMIRS transmit well in the J, H, K bands, and as a result, the MMIRS optical throughput is dominated largely by surface reflection losses.

The coma corrector provides excellent images (0.1″ RMS diameter) on a flat focal surface, allowing high transmission through narrow slits when the seeing is at its best. At the detector, the image quality is also superb with RMS image diameters of ~ one pixel (0.2″) and 90% encircled energy image diameters of ~ two pixels (0.4″).

We have designed a suite of 5 grisms: 2 low resolution grisms covering the JH and HK bands, and 3 higher resolution grisms covering the individual J, H and K bands each at a resolution of approximately 3000 with a 2 pixel (0.4″) slit. The spectrum covers 1400 of the 2048 pixels which allows a 2′ wide field for multiobject spectroscopy with full wavelength overage. A 4’ field will be covered with slightly reduced wavelength coverage. Approximate grism parameters are shown in the table below. Theoretical grating efficiencies were determined using PCGrate software.

Table 3: Grism Design Summary

Grism	Wavelength Range	Grooves/mm	Prism Angle	Facet Angle	Resolution (2 pixel slit)	Theoretical Efficiency across band
J	1.11-1.39	230	41°	32°	3000	64-70%
H	1.45-1.82	175	41°	32°	3000	64-70%
K	1.95-2.45	130	41°	32°	3000	64-70%
JH	0.95-1.82	94	18°	14°	1300	55-80%
HK	1.45-2.45	80	21°	17°	1300	55-80%

3.5 MECHANICAL DESIGN

The MMIRS mechanical design makes heavy use of the successful heritage of the FLAMINGOS design. MMIRS will incorporate proven assemblies, such as the detector mount and wheel mechanisms, from the FLAMINGOS design. Modifications have been made to the dewar design, cryogenic system, and telescope interface to accommodate our telescopes and goals. The mechanical layout of MMIRS is shown in Section III.

3.5.1 Dewar Design

The two dewar sections will be constructed from 7075-T6 aluminum. The LN_2 tanks will be welded to the work surfaces; all welds will be rough machined, heat treated to relieve stress, and finally fine machined. The work surface and LN_2 tank assembly in each dewar will be suspended from very stiff G10 rings. Kapton heater pads epoxied on the LN_2 tanks will allow rapid thermal cycling of the dewars.

3.5.1.1 Cryogenics

The bulk of the MMIRS thermal mass, the optics, filters, grisms, and detector, is housed in the collimator/camera dewar. LN_2 cooling will provide excellent temperature stability and will minimize thermal gradients on the optical bench.

3.5.1.2 Wheels

We use a common wheel design for all the MMIRS mechanisms. This is the same wheel design used in FLAMINGOS and TRECS. Wheel positions are defined by mechanical detents, while the home position is defined by a mechanical micro-switch. We expect wheel positions to be repeatable to within 10 μm. The wheels are driven by Phytron cryogenic rated stepper motors. The wheel drive gear/worm placement is designed for proper engagement at cryogenic temperatures. The collimator/camera dewar will have two filter wheels and one grism wheel, located in the collimated beam adjacent to the Lyot stop. Each filter wheel will carry 5 filters with one open slot. Filters with thicknesses of up to 10 mm will be accommodated. The initial complement of filters will include the standard Y, J, H, and K filters, the spectroscopic JH and HK blocking filters, and a dark blocker. The grisms will be carried in a wheel nearly identical to the filter wheels. We use grisms as the primary disperser for MMIRS because of their high efficiency, simple mounting, and the compact instrument design they allow. The Lyot pupil stop will be fixed.

3.5.1.3 Optic Mounts

The optics mounts are athermalized using springs. Axially, the lenses are constrained against three fixed aluminum pads with a thin Kapton spacer. They are spring loaded from the opposite side with a Belleville washer. Radially, the lens rests against 2 fixed Nylon pads and is spring loaded with a third Nylon pad. The thicknesses of the Nylon pads are chosen so that the lenses will be centered both at room temperature and at the operating temperature.

3.5.1.4 Detector Mount.

The mount for the Hawaii-2 array in MMIRS will follow the design used in SWIRC. Electrical connections are made with a multilayer fan-out board. The biases, clock, and signals from the amplifiers are brought out using separate wiring harnesses to help reduce system noise and cross talk. The Hawaii-2 array is cooled by way of the central pins in the chip carrier. The pins are coupled to two copper layers in the fan-out board, which in turn are thermally clamped to the dewar. Because the Hawaii-2 zero insertion force socket does not allow location against a defining surface, alignment will be accomplished using spring loaded screw assemblies and predefined mechanical surfaces. The array must be held flat and located relative to the final element of the camera to roughly 10 μm.

3.5.2 MOS Dewar

The MOS dewar accommodates the interchange of slit masks for MultiObject Spectroscopic observations. The entrance window of the slit mask dewar is the first of the two elements in the coma corrector. The second element of the coma corrector is housed inside the slit mask dewar but will be operated near ambient temperture. An advantage of operating this lens near the ambient temperature is that it will prevent the dewar window from cooling radiatively and condensing water from the air. The slit mask dewar can be thermally cycled during the daytime independently of the camera/collimator dewar that carries the optics.

3.5.2.1 Gate Valve

The slit mask dewar is isolated from the collimator/camera dewar with a gate valve. The gate valve allows us to keep the collimator and camera optics at cryogenic temperatures when thermally cycling the slit mask dewar, and eliminates the need for a warm window below the slit mask. In interlock system prevents the gate valve from opening when it could endanger the cold optics and detector.

3.5.2.2 Rapid Thermal Cycling

MMIRS slit masks must be replaced during the daytime between consecutive nights at the telescope. One of the greatest challenges in achieving rapid thermal cycling is providing efficient heat transfer to the slit mask wheel. We have followed the FLAMINGOS design and used sapphire bearings in a bearing race to maximize thermal conductivity to the wheels. The multislit masks must be cooled to less than 140 K to keep the mask thermal background below the detector dark current (0.1 e^- sec^{-1}).

3.5.2.3 Slit Masks

The mask wheel will hold 9 multislit plates, 7 fixed long slits, and a full-field imaging aperture. To make efficient use of the area on the slit mask wheel the slit masks must be tightly spaced. An aperture selection wheel will precede the slit mask wheel to define the appropriate field of view and ensure that light passes through only a single slit mask or long slit. The coma corrector provides a flat focal plane well suited to multislit masks. Thin sheet metal masks offer high thermal conductivity and low front face emissivity to allow the masks to reach an equilibrium temperature of 140 K. A two pixel wide slit at the detector scale is 60 μm wide at the telescope focal plane scale. The slit edges should be uniform to 0.6 μm RMS so that slit transmission variations are kept below 1%. This

uniformity will facilitate flat-fielding and sky subtraction. The laser slit mask cutting systems have advertised repeatabilities of 0.1 μm and accuracies of 0.25 μm, meeting this requirement. At the MMT, at least initially, we anticipate using an outside vendor to cut the slit masks. At Magellan, a laser machining system already exists.

3.6 Electronics

We have developed a CCD controller capable of driving the 36 CCDs (72 channels) in the Megacam mosaic camera and this controller has since been modified to drive the Hawaii-2 array. A Hawaii-2 engineering array has been in operation with SWIRC at the MMT since last summer. We have ordered an ND-14 Dewar to test the MMIRS detector electronics with the science array. This testing should begin in two months and will enable verification of all the detector electonics and cabling, independent of the main MMIRS cryostat.

3.7 Guiding and Wavefront Sensing

The MOS dewar will contain two fixed pickoff mirrors which will divert the outer parts of the 14 arcmin diameter corrected field to two Guider/Wavefront sensor modules. These units are very similar to the current guider units in use at Magellan. They contain optics for direct viewing of the guide star and also for Shack-Hartmann wavefront sensing. Continuous wavefront sensing will be done with one guide star and autoguiding on the other has proven very effective at Magellan. At the MMT, MMIRS will be the first wide-field instrument capable of offering *continuous* wavefront sensing.

3.8 Software

We have already developed many of the software pieces required to operate MMIRS. These modules are in operation at the MMT with Hectospec, Megacam, and SWIRC. Details are given below, but key existing components are: data acquisition routines, a GUI based exposure sequencing system that allows for efficient observing, and autoguiding software. A new, highly-configurable motor control system has been implemented for the Megacam at Magellan effort and this system will also be used with MMIRS. Additional required software will include modules to monitor the various temperature and vacuum systems, guide camera control, and a Magellan telescope communications module.

FUNCTIONAL AND PERFORMANCE REQUIREMENTS FOR THE MMIRS

SPECIFICATION NUMBER
S-MMIRS-200

Brian McLeod & Paul Martini
Center for Astrophysics
Smithsonian Astrophysical Observatory
Cambridge, MA

Revision History

Version 0.0— Draft, January 2004 G. Nystrom
Version 1.0— Draft, July 2004 B. McLeod
Version 1.1— Released Version, August 2004 P. Martini
Version 1.2— Added Section 315, 13 Sept 2004 B. McLeod
Version 1.2a – Added annotations for CDR 31 March 2005 B. McLeod
Version 1.3 – Reconciled conflicts for CDR 29 April 2005 B. McLeod

Table of Contents

Purpose of this Document

The purpose of the Functional and Performance Requirements document for the MMIRS (MMT & MAGELLAN INFRARED SPECTROMETER) is to provide the CFA Scientific community with an understanding of what MMIRS will do. This document answers the question *What?* but not the question *How?* The *How?* is the design which is derived from and traceable to this document. This document takes precedence over the design and fabrication documents.

The design must serve the requirements in this document completely. This means every feature of MMIRS is traceable to a requirement in this document. This document was written using the FLAMINGOS-2 Functional and Performance Requirements document as a general guide.

Referenced Documents

Magellan 03SE004	*Interfaces between the Magellan Clay telescope and the SAO F/5 Cassegrain Instruments and wide field corrector*
MMTO Conversion Technical Memo #00-1	*6.5m Instrument Rotator Performance Goals and Specifications, Rev 3**
MMT Drawing D-MMT0245	*As Built Principal Datums*
MMT Drawing B-MMT0217	*MMT 6.5m Conversion Instrument Rotator Inner-Race/Turntable Addendum(Sheet #25)*
SAO M-CE100-S1	*SAO Drawing Standards*

Acronym List

FLAMINGOS	***FL***orid***A*** ***M***ulti-object ***I***maging ***N***ear-IR ***G***rism ***O***bservational ***S***pectrometer, built by the University of Florida, funded by the NSF
ICD	***I***nterface ***C***ontrol ***D***ocumentation
ICS	***I***nstrument ***C***ontrol ***S***ystem
CFA	***C***enter ***F***or ***A***strophysics
SAO	***S***mithsonian ***A***strophysical ***O***bservatory
CIR	***C***assegrain ***I***nstrument **R**otator (MMT & Magellan Rotator)
TCS	***T***elescope ***C***ontrol ***S***ystem
GWFS	***G***uider-***W***ave***F***ront ***S***ensor
SNR	***S***ignal-to-***N***oise ***R***atio
FWHM	***F***ull ***W***idth at ***H***alf ***M***aximum
MOS	***M***ulti-***O***bject ***S***pectrometer (MMIRS component)

100 Optical Requirements

110 Science Requirements

MMIRS shall meet all scientific requirements listed below.

111 Wavelength Range

MMIRS shall operate as a spectrograph and imager in the wavelength range 0.9 to 2.4 μm.

See Fabricant, "MMIRS Preconstruction Design" in Section II.

112 Detector Format

MMIRS shall use a HgCdTe Hawaii-2 array 2048 x 2048, with 18 μm square pixels.

By design

113 Spectral Resolution

MMIRS shall provide a low dispersion mode with $R \equiv \lambda/\delta\lambda \sim 1300$ (2-pixel resolution) that permits the full octave ranges of 0.9–1.8 μm or 1.25–2.5 μm to be covered by the detector array. MMIRS shall also provide an intermediate dispersion mode with $R \sim 3000$ (2-pixel resolution) which will allow observations of each of the *J, H,* and *K* atmospheric windows on the array, one at a time.

See McLeod, "MMIRS Grism Design" in Section II.

114 Field of View

MMIRS shall provide a 7 arcminute square field of view with 0.2 arcsecond pixels.

See Fabricant "MMIRS Preconstruction Design" in Section II.

115 Multi-Slit Capability

MMIRS shall provide a multi-slit capability with 8 rectangular multi-slit plates. These multi-slit plates shall provide coverage of a 4 by 7 arcminute field of view. See Nystrom, "MOS Dewar Specifications" and "MOS Design", in Section III. The full spectral range shall be achieved for a 2 by 7 arcminute field of view. See McLeod, "MMIRS Grism Design" in Section II. The slit plates shall be exchangeable during the course of daylight operations

of one day (less than 9 hours). See Park, "MOS Transient Analysis" in Section VII.

116 Long Slits

MMIRS shall provide a mimimum of 7 long slits. All long slits shall be 7 arcminutes in the spatial direction with spectral widths of 1, 2, 3, 4, 6, 8, and 12 pixels. See Nystrom, "MOS Dewar Specifications" and "MOS Design", in Section III.

117 Imaging Aperture

MMIRS will have one imaging aperture 7 arcminutes square. See Nystrom, "MOS Dewar Specifications" and "MOS Design", in Section III.

120 Optical Specifications

Instrumental image quality specifications for MMIRS do not include the telescope system or atmospheric turbulence.
These specifications are all addressed in Martini "MMIRS Optical Specifications", in Section II.

121 Pre-Slit Image Quality at Telescope Focus

The preslit image quality shall not degrade the throughput of a 2-pixel slit (0.4 arcseconds) by more than 10% of the idealized MMT and Magellan telescopes. For a beta=2.5 Moffat profile, this requires an instrumental image profile with FWHM < 20 μm at the slit mask plane.

122 Post-Slit Image Quality

The instrumental image profile at the detector shall not degrade the expected median seeing (0.6 arcseconds FWHM) by more than 25%. For a beta=2.5 Moffat profile, this requires an instrumental profile with FWHM < 28 μm (0.31 arcseconds).

123 Spectral Direction

The instrumental image quality in the spectral direction shall produce less than a 25% change in the spectral resolution of a 2-pixel slit (0.4 arcseconds) over the full spectral bandpass. For a beta=2.5 Moffat, this requires an instrumental image profile with FWHM < 28 μm (0.31 arcseconds).

130 Target Acquisition

MMIRS shall provide a means for target acquisition through imaging on the science detector.
See Martini "Observing Overview", in Section XI.

140 Baffling

MMIRS shall be properly baffled to minimize stray radiation. The stray light falling on the detector, but not passing through the entire optical system, shall be less than the detector dark current.

141 Thermal shielding

The MMIRS shall contain sufficient thermal shielding to minimize heat loading on the cryogenic systems.

See Park, "MOS Steady State Analysis" and Park "Camera Steady State and Transient Analysis", in Section VII.

142 Optical Baffling

MMIRS shall contain proper optical baffling to reduce stray radiation to levels below that of the telescope plus sky background as seen by the science detector.

See Martini, "Stray Light Analysis" in Section II.

143 Lyot Stop

MMIRS shall provide a cold Lyot stop at an image of the telescope pupil (the primary mirror). The position and size of the Lyot stop shall be designed to optimize the SNR.

Awaiting dimensional input from MMTO and Magellan.

144 Ghost Images

The MMIRS optical design shall have no ghost image with a diameter less than 230 μm and fractional illumination per pixel greater 10^{-6} the original intensity.

See Martini "Ghost Image Analysis", in Section II.

145 Ghost Pupils

The sum of all ghost pupils shall result in a <1% peak-to-valley intensity variation across the field.

This particular calculation has not been done. An analysis of the worst ghosts is in Martini "Ghost Image Analysis", in Section II.

150 Internal Instrument Background

MMIRS shall have an internal instrument background less than either the natural background from the observed science field or the dark current of the detector, whichever is greater.

151 MOS Section

All components visible by the detector in spectroscopic mode must be cooler than 140 K in order to have a negligible contribution to the instrument background.
See Park "MOS Steady State Analysis", in Section VII.

152 Camera Section

All components visible by the detector must be cooler than 100 K in order to have a negligible contribution to the instrument background.

See Park, "Camera Steady State and Transient Analysis," in Section VII.

160 Throughput

MMIRS shall be designed to maximize throughput to take maximum advantage of the MMT and Magellan telescopes' performance. Optical throughput for the entire optical train should be >30% for spectroscopy (goal 40%) and >50% for direct imaging (goal 70%). These throughputs are measured on the optical axis and include filters and gratings but do not include the telescope, atmosphere, or detector.

See McLeod "MMIRS Grism Design" and Martini "MMIRS Throughput Calculation", in Section II.

170 General Optics Hardware Requirements

171 Optical Coatings

The following characteristics of all optical coatings shall be specified in the design documentation:

- Transmission <2% loss (goal 1%) within each atmospheric window.
- Environmental testing.
- Hardness or equivalent ISO standard.
- Adherence or equivalent ISO standard.
- Abrasion or equivalent ISO standard.
- Humidity.
- Cleanability.

- Water solubility.
- Radioactivity.

- Surface appearance (flaking, peeling, finger prints, pinholes, *etc.*).
- All coatings shall be unaffected by repeated thermal cycling over the operating, storage, and transportation temperature ranges.

See MMIRS-S-207 "Coating Specification", in Section II.

172 Vacuum Environment

All optical components and coatings shall meet all performance requirements when operated in a vacuum of less than 10^{-7} Torr at operational temperatures.

173 Thermal Cycling and Stress in Optics

Thermal cycling of the instrument over the ranges specified in Section 720 and during normal operation shall not degrade or destroy the optics and coatings. To avoid damage to the optics, stress levels shall be limited to +/- 400 PSI for CaF2, BaF2, and ZnSe elements, and +/-500 PSI for Fused Silica and S-FTM16,

A somewhat pessimistic model indicates a maximum stress of 600PSI in Lens3. See McLeod, Temperature and Stress in Optics, in Section VII.

200 Array and Array Controller Interfaces

210 Science Detector Array Interface

MMIRS design shall provide an integrated array controller for its primary science array.

Geary, "MMIRS IR Array Controller". Need to review to make sure we address these points.

211 Characteristics

MMIRS shall be designed to take the fullest possible advantage of a HgCdTe Hawaii-2 detector with the following characteristics:

Pixels (Number and Format)	2048 × 2048
Architecture	4 independent quadrants of 1024 × 1024 pixels (8 readouts each)
Pixel size	18 µm, square
Number of outputs	32 (8 per quadrant)
Maximum frame rate	0.5 second single-read^{-1} frame^{-1}
IR material	HgCdTe
Full Well (linear range)	100,000 electrons
Wavelength range	0.9-2.5 μm
Nominal operating temperature	77 K
Dark current	<0.1 electron second^{-1}
Read noise	<20 electrons (*RMS*), goal is <5 electrons
Quantum efficiency	40-60% (0.9-2.5 μm)

220 Science Array Controller Interface

MMIRS shall include all electronic, thermal and mechanical interfaces needed for its science array controller to function on both the MMT and Magellan.

221 Science Array Controller Mechanical Interface

The array controller and all associated analog electronics shall be mounted on the MMIRS instrument and be included in the total mass, moment and space envelope specifications, as per MMT and Magellan observatory requirements and/or specifications.

Holwell, Electronics Packaging, in Section VIII, and Nystrom, Observatory Requirements, Section X.

222 Science Array Controller Thermal Interface

The array controller, power supplies and associated analog electronics shall be enclosed in a thermal rack enclosure.

Holwell, Electronics Packaging, in Section VIII.

230 Science Array Data Handling System Interface

Deleted.

240 Guider Wave Front Sensor

The MMIRS design shall contain two combination Shack-Hartmann wavefront sensors/guide cameras to calculate telescope tracking errors, miscollimation, and primary mirror figure errors.

Except as noted see McLeod "MMIRS Guider/Wavefront Sensor Design", Section V for all items below.

241 GWFS Array Characteristics

The MMIRS GWFS CCD array shall be large enough to accommodate up to a 20x20 spot Shack Hartmann array. The CCD shall be back-illuminated and must be read out in at least 0.1 seconds.

242 GWFS Array Mechanical Interface

The GWFS shall patrol the area of the MMIRS 14.0 arcminute diameter corrected field outside the 7 arcminute square science field to provide a high probability of finding a guide star.

243 GWFS Array Thermal Interface

The CCD array shall be contained within a separate dewar and cooled to reduce the dark current below the level of the night sky, (nominally -30C).

244 GWFS Array Optical Interface

The optical feed of the GWFS shall provide a working pixel scale in the range 0.1 to 0.25 arcsec pixel^{-1} and a field stop matched to the lenslet array. The field of view for the guide camera shall be at least 30x30 arcseconds.

245 GWFS Array Contoller Mechanical Interface

The array controller and all associated analog electronics shall be mounted on the MMIRS instrument within a 1m cable run of the CCD array.

246 GWFS Array Controller Thermal Interface

The array controller shall be cooled by the MMT and Magellan facility coolant supplies.

See Holwell, “Electronics Rack Packaging”, in Section VIII.

247 GWFS Array Software Interface

The guide camera software shall deliver images to the existing facility MMT and Magellan guiding and wavefront sensing software.
See Software, Servers, Guiding, in Section IX.

300 Mechanical Requirements

310 Rigidity and Repeatability

MMIRS shall be designed to be rigid, and to meet all the requirements listed below.

311 Alignment of the Instrument to the Telescope

The alignment of the MMIRS Lyot stop with the primary mirror shall be set and maintained such that the SNR is degraded by < 2%.

Martini, Optical Specifications, in Section II.

312 Tracking with Guider-Wavefront Sensor

The GWFS image shall not flex relative to the slit masks by more than an amount that shall lead to a 10% loss in throughput due to centering errors in a 2-pixel wide slit during a 2 hour observation. This corresponds to a relative flexure of 0.25 times the width of the slit, or <16 microns. The focus at the guide camera, relative to the slit, shall not change by more than 45microns over a 30 degree elevation change, with a goal of less than 45 microns over a 60 degree elevation change.

Awaiting publishing of Bergner, Guider-WFS Analysis, in Section VII.

313 Motion of Slit Image on Detector

The image of the slit mask on the detector shall not move by more than an amount which will lead to a 10% degradation in SNR for a 2-pixel FWHM spectral line in 20 minutes. This correspods to 16 microns of image motion over 30 degrees, with a goal of less than 8 microns. The focus at the IR array shall not change by more than 15 microns over a 30 degree change in elevation, with a goal of <15 microns over a 60 degree elevation change.

See Martini, Fringing Memo, Bergner, Flexure Analysis

314 Mechanism Repeatability

All mechanisms with the exception of the Guider/WFS shall return to a normal position with a repeatability that limits motion of the slit image on the detector to 0.2 pixel and of the object image on the slit to 10 microns.

See Holwell, Camera Mechanical Design, in Section IV.

315 Guider/WFS Mechanism Repeatability

The X, Y, and Select mechanisms in the Guider/WFS shall repeat to 200 microns absolute positioning. The encoder shall be capable of reading the actual position to a accuracy of 10 microns. The focus stage shall repeat to 40 microns with 25microns of encoder accuracy.

See GWFS Mechanical Design, in Section V.

320 Thermal Performance

Thermal gradients in the MMIRS optical bench shall be minimized to prevent degradation of image quality.

See Martini "Optical Specifications", in Section II. and Park "Camera Steady State and Transient Analysis", in Section VII.

330 Space Requirements

MMIRS shall fit within the normal MMT or Magellan Clay telescopes envelopes for instruments mounted on the CIR, as specified in MMTO Conversion Technical Memo #00-1 and Magellan 03SE004.

Nystrom, Observatory Requirements in Section X

331 Electronic Enclosures

All MMIRS electronic enclosures mounted to the CIR shall be included when evaluating the MMIRS instrument against the allowable MMT or Magellan envelope, as well as the mass and center of gravity requirements listed in section 340.

Nystrom, Observatory Requirements in Section X

332 Access to Liquid Nitrogen Ports

Liquid nitrogen ports and valves on MMIRS shall be accessible without removing the instrument from the CIR, removing any parts or disconnecting any cables.

McCracken, MOS Design, in Section III & Holwell, Camera Design. Section IV.

333 Electrical Connections

All external electrical connections on MMIRS shall be accessible without removing the instrument from the CIR.

McCracken, MOS Design, Section III & Holwell, Camera Design, Section IV.

334 Access to MOS Plate Exchange Port

Multi-slit plates shall be exchangeable without any instrument disassembly outside removal of the access port when the MOS section is at atmospheric temperature and pressure.

McCracken, MOS Design, in Section III.

340 Mass and Center of Gravity Requirements

MMIRS shall meet all mass and center of gravity requirements listed below. The requirements are derived from MMTO #00-1 and Magellan #03SE004. Items below discussed in Nystrom, "Observatory Requirements", in Section X.

341 Total Mass

MMIRS shall have a mass of <4400 pounds including any adapter to the CIR.

342 Center of Gravity

MMIRS shall have a center of gravity such that its cantilever moment is <150,000 in-lbs relative to the CIR and its rotational unbalance is <12,000 in-lbs..

343 Ballast Weight

A ballast weight and its supporting structure shall be supplied if required to meet the above requirements.

344 Electronic Enclosures

All MMIRS electronic enclosures mounted on the CIR shall count in the mass and center of gravity requirements listed above.

350 Cryogenic Requirements

MMIRS shall meet all cooling system requirements listed below.

351 Cryostat

The total time to pump and thermally cycle MMIRS shall not exceed one week, including one day for cold tests and one day for engineering when the instrument is warm.

See Martini, Warm Up and Cool Down Procedure, in Section XI,

and Park, Camera Steady State and Transient Analysis, in Section VII.

352 MOS Section

The total time to thermally cycle the MOS section (with the gate valve closed) and exchange all slit masks shall not exceed nine hours. The MOS slits shall be cooled to < 120K and shall reach within 10K of their equilibrium temperature before observing starts.

See Park, MOS Transient Analysis, in Section VII.

353 Hold Time

The steady-state hold time of the MOS and Camera Dewars shall each be at least 30 hours.

See Park "MOS Steady State Analysis" and "Camera Steady State and Transient Analysis in Section VII.

354 Thermal Stability

The science detector assembly shall be thermally coupled to the LN2-cooled worksurface to provide maximum stability without requiring active control of the detector temperature during science operations.

See Park, "Camera Detector Steady State and Transient Analysis", in Section VII.

355 Science Array Thermal Interface

The array's fanout board shall be thermally strapped to the cryo-worksurface, and it shall additionally be controlled with a heater and temperature sensor mounted on the fanout board. The maximum rate of temperature change for the detector during warm up and cool down shall not exceed 0.2 K/min. The detector must be the warmest part of the instrument during warmup to protect it from contamination.

See Park, "Camera Detector Steady State and Transient Analysis", in Section VII and Martini "Operational Procedures", in Section XI.

356 Autofill

MMIRS shall be equipped with an autofill system for the camera section when not mounted on the telescope and not in transport..

Not yet designed.

360 Vacuum System

MMIRS shall be provided with a built-in turbo pump system. It will be used for evacuation of the MMIRS MOS and the entire instrument. It will provide evacuation of the MOS section when the camera section is valved off.

The camera section will have a blanked off port for evacuation by a laboratory pumping system when the MOS assembly is not present, otherwise the MOS pumping system will be used for evacuation of the entire instrument. The turbo pump's roughing pump must be a contamination-free pump (no oil) and contained in the electronics rack frame.

Nystrom, Vacuum system design, in Section XI.

361 Pumpout times

The pumpout times for the entire instrument and for the MOS section alone shall be consistent with the requirements in section 350. Pumpout time means to a pressure such that LN_2 can be introduced to that section for cooling the instrument to its operational temperature. A pressure of less than 10^{-4} Torr will achieve this goal.

Nystrom, Vacuum system design, in Section XI

362 Vacuum duration

The MMIRS Camera section shall be capable of being kept cold continuously and operated without measurable degradation of LN_2 hold time for 6 months.

Nystrom, Vacuum system design, in Section XI.

363 Gauges

The Camera and MOS sections will each be outfitted with pressure measurement devices that operate over the range 760 to $5 \cdot 10^{-9}$ Torr. The gauges shall be chosen and positioned so that they do not emit light that can be detected by the science or guider arrays. If this is not possible, then the gauge power must be controllable by software. It must be possible to monitor the output from these gauges with a computer.
Burke, "MMIRS Electrical Design", Section VIII, and Software Servers, in Section IX.

364 Isolation Gate Valve

The MOS and Camera sections shall be separated by an isolation gate valve. The valve shall have an interlock system that prevents it from being opened when the Camera section is at vacuum and the MOS section is at ambient pressure, or when the Camera section is cold and the MOS section is warm.

See McLeod, “MMIRS Valve Interlock”, in Section X.

365 Backfill System

MMIRS shall have a backfill system that allows pure dry nitrogen to be added to the MOS section to bring it from vacuum to ambient pressure. This operation shall be performed before the MOS access panel is removed. An interlock system shall prevent the backfill from operating when the isolation gate valve is open and the Camera section is cold.
See McLeod, “MMIRS Valve Interlock”, in Section X.

370 Operational Requirements for Mechanisms

MMIRS mechanisms shall meet the requirements listed below.

371 Safety

No mechanism shall be back-driveable in the event of loss of power.

McCracken, “MOS Design”, in Section III and Holwell, Camera Design, Section IV.

372 Time to Function

The goal for all individual mechanisms is to take no more than 10 seconds to operate from any position to any other position. The maximum allowable time is 30 seconds. The time to re-zero or datum any mechanism from an unknown position shall not exceed 60 seconds.

See Compliance Matrix in McCracken, “MOS Design”, in Section III and Holwell, Camera Design, Section IV

373 MOS Slitmask Exchange

There shall be a switch to disconnect external control of the MOS mechanisms during slit mask exchange as well as a buttom to move the slit mask wheel in increments of one position.

See Burke, MMIRS Electrical Design, Section VIII.

374 Slitmask Barcode Reader

Each slit mask shall have an identifying barcode cut in it. The instrument shall provide a barcode reader which can view that barcode on an installed mask.

See Burke, MMIRS Electrical Design, Section VIII.

380 Instrument Handling

MMIRS shall be designed so that it can be mounted to the CIR using either MMIRS handling equipemt or MMT-Magellan Facility equipment.

Nystrom, Shipping and Installation Plans, Section XI.

390 Dimensioning

Inch dimensions shall be used in MMIRS with the exception of the optics drawings and specifications, which shall have metric primary dimensions and inch reference dimensions.

In compliance.

391 American Standard Dimensions on Drawings

Drawings will be carried out in compliance with SAO drafting standard M-CE100-S1.

392 Inch Fasteners

All screws, bolts, nuts, tapped holes, and fasteners shall be of standard inch sizes. Metric screws can be used if required to mount equipment having such hardware requirements.

393 Simplification

Every attempt shall be made to minimize the number of hardware sizes and drives required for instrument assembly and maintenance. The goal is to identify only two, distinct fastener sizes to use throughout MMIRS.

400 Electrical and Electronic Requirements

410 Electronic Design Requirements

411 Grounding and Shielding

Separate ground returns shall be provided for low level signals, noisy components such as heaters and motors, and hardware components such as mechanical enclosures, chassis, and racks.

Burke, MMIRS Electrical Design, Section VIII.

412 Electronics Discharge

The MMIRS design shall protect sensitive components from electrostatic discharge.

See Burke, MMIRS Electrical Design, Section VIII.

420 Temperature Monitoring

Sensors are required to monitor the cryo environment within the instrument, including the detector. Critical locations for temperature sensors include the detector mount, the optical bench, and the radiation shields.
See Martini, “Temperature Sensing”, in Section X, and Burke, “Electrical Design”, in Section VIII.

421 Sensor Interfaces

The temperature sensor read-out interface shall be part of the Engineering Interface.
See Software, GUIS, Section IX.

500 Software Requirements

See Software Section IX.

510 Software Design Requirements

511 Required Capabilities

- Provide high level observing software that coordinates data acquisition, telescope motion, and interaction with the GWFS.
- Provide automated means to center targets onto longslit or multislit masks.
- Take and record images with the IR array including with multiple endpoint sampling.
- Control and read positions of all mechanisms in the cryostat.
- Take images with the GWFS cameras and deliver them to the facility guider and WFS software.
- Control GWFS mechanisms.
- Provide automatic selection of guide stars.
- Provide and maintain status and health information for the cryostat and electronics racks.
- Raise alarm conditions of appropriate severity.
- Log and display meaningful messages when in debug mode or in the event of an error.
- Provide a Motion Control Engineering Interface for all mechanisms.
- Insure the camera section is sealed before and while the MOS section is warmed up and brought to ambient pressure.

512 Required Performance

- Acquire sequences of data with an overhead of less than 5 seconds between exposures (in addition to readout time) when moving the telescope less than 30 arcsec.
- Allow for complete configuration changes in 30 seconds or less with a goal of 10 seconds or less.
- Allow simultaneous motion of mechanisms. Goal is to have sufficient power available to drive all mechanisms at once.

600 Observatory Physical Interfaces

610 Instrument Support Structure

MMIRS shall interface mechanically to the MMT instrument rotator bearing per Multiple Mirror Telescope Observatory drawing B-MMT 0217 of the latest revision. The Magellan interface will be the CFA mounting adapter. It will be identical to the MMT interface for mounting and optical interfacing.

See Telescope Truss Design, in Section X for this and following 2 items.

611 Instrument Mounting Plate Material

The MMIRS mounting interface shall take into account the material of which the CIR is made and shall hold differential temperature effects to a level that permits MMIRS to meet all the optical alignment requirements over the entire operating temperature range.

612 Fasteners

All fasteners shall be of the Unified National Standard (UNS) series. Metric fasteners maybe used when interfacing with equipment made to ISO standards. All fasteners must be sized appropriately to effectively carry applied loads and shall be preloaded to approximately 80% of their ultimate strength.

620 Optical Feed

MMIRS shall accept and use both the MMT and Magellan telescopes optical feed, which is approximately *f/5* and combined with a MMIRS corrector the focal length is 33.7159 *meters*. The beam comes to focus nominally 1430.149 *mm* (56.31 in.) behind the primary mirror's vertex. or 11.3 *mm* (0.44 in) inside the CIR mounting surface.
Fabricant, MMIRS Preconstruction Design, Section II.

630 Electrical Power Interface

MMIRS shall derive its electrical power through a standard 60-Hz 120V 3-prong AC power connection.
Will likely use Hubbell type locking connector. See Burke, MMIRS Electrical Design, in Section VIII for following items.

631 Number of Electrical Connections

MMIRS shall have one electrical power connection. The entire instrument will be run off of clean, UPS supported power. MMIRS shall have appropriate local power runs to serve all instrument power needs.

632 Length of Electrical Line Runs

A single set of electical lines will be provided which will allow MMIRS to be mounted on the CIR. A means of dressing the cables to a length appropriate shall be provided.

633 Electric Power Line Flexibility

The electrical power line from MMIRS to facility power shall be flexible enough to permit easy routing, connection, disconnection, and dressing for operation.

634 Type of Electrical Connectors

The Instrument Interface shall have a single, standard connector for power, an emergency stop buttom, and wiring for a remote emergency stop. Two channels of switched 120VAC, 60Hz, shall be provided for the MMIRS instrument rack. All lines shall be protected against line surges and lightning induced transients at both ends of the cable run. A separate, identical, cable and power/control channels shall be provided for test purposes and routed to the allocated test area. This will be implemented such that no cable demating and mating shall be required at the rack interface panel location.

640 Optical Fibers

MMIRS shall contain optical fiber interfaces for the detectors and ethernet. These fibers shall be duplex SC-SC fibers in black cladding to avoid light leakage.
Burke, MMIRS Electrical Design, Section VIII.

641 Camera Interfaces

The infrared array and the two guide cameras shall each have a fiber interface.

642 Ethernet

Ethernet shall run through a single 1000BaseT fiber.

650 Coolant Interface

MMIRS shall contain an internal rack cooling system that limits its heat dissipation into the ambient environment to 50 Watts or less. The cooling system shall connect to the MMT and Magellan facility coolant supplies.

See Holwell, Electronics Packaging, Section VIII.

651 Number of Plumbing Connections

MMIRS shall have one coolant supply connection and one return line connection for the entire instrument. MMIRS shall have appropriate tees from these lines to serve all instrument cooling water needs.

652 Length of Cooling Fluid Runs

Coolant lines will be provided that permit MMIRS to be used at the CIR or in an instrument preparation lab. A means of dressing the cooling water lines to an appropriate length shall be provided.

653 Cooling Fluid Line Flexibility

The supply and return lines from MMIRS mounted on the telescope to the facility supply shall be flexible enough to permit easy routing, connection, disconnection, and dressing for operation.

654 Resistance to Glycol or Methanol

The cooling fluid lines and connectors shall not be damaged in any way when used with a cooling solution containing glycol or methanol; stainless steel hardware connectors shall be used.

655 Cold plate interface to electronics assemblies

Heat exchangers shall be mounted and thermally coupled to the rack-mounted electronics in such a manner that the rack-mounted electronics can be removed without disconnecting the cooling lines.

656 Electronics Racks

The temperature of the rack-mounted electronics will be monitored. The enclosed electronics shall be protected from overheating with an alarm system and a thermostat cutoff.

Burke, Electronics Design, Section VIII.

660 Liquid Nitrogen

MMIRS shall be provided with fittings for adding liquid nitrogen when the instrument is on the telescopes' CIR.

Plumbing design is not yet complete, but compliance is expected.

661 Number of Liquid Nitrogen Connectors

A single supply line will be used to supply the Camera dewar and the MOS dewar. A T-fitting with two valves will be part of MMIRS and will direct the LN2 flow to either dewar, or both simultaneously.

662 Length of Liquid Nitrogen Runs

A single line will be provided to reach from a large liquid nitrogen tank on the observatory floor to the liquid nitrogen connector on the MMIRS.

663 Types of Liquid Nitrogen Connectors

A standard ½ inch flare connector shall be used.

670 Dry Air Purge

To avoid condensation on the cryostat window, MMIRS shall be equipped with plumbing to blow clean, dry air across the window. It requires a single supply line, with no return. The fitting type shall be compatible with the MMT and Magellan facilities.

McCracken, MOS Section Design, Section III.

700 Environment Requirements

710 Altitude Environment

MMIRS shall be capable of being transported, stored, and operated at either the MMT or Magellan Clay telescopes.

See Nystrom, Shipping and Installation Plan, Section X.

711 Transportation Altitudes

MMIRS shall be capable of transport at any altitude between -200 feet and 10,000 feet by any transportation mode. MMIRS shall be capable of transport by commercial jet with pressurized cargo compartments at altitudes up to 50,000 feet. MMIRS shall not be at cryogenic temperature when under transport. If shipping under vacuum is not permitted by shipper regulations, then MMIRS shall be back filled with dry nitrogen or dry air.

712 Storage Altitudes

MMIRS shall be capable of storage in or out of its shipping container at any altitude between -200 feet and 10,000 feet.

713 Operation Altitudes

MMIRS shall be capable of operation at any altitude between -200 and 10,000 feet.

720 Temperature Environment

721 Operational Environment

MMIRS operational environment shall be limited to -15 to +40 °C.
See Holwell, Electronics Packaging, in Section VIII

722 Survival Environment

MMIRS shall be capable of surviving a temperature of -51 to +71 °C without damage per MIL-STD-810E.

723 Transportation Environment

MMIRS shall be capable of withstanding a temperature of -51 to +71 °C during transport without damage.

730 Humidity Environment

731 Transportation Environment

MMIRS shall be capable of transport and storage at a wide range of altitude environments in the range of 0 to 100% relative humidity and with condensing moisture.

See Nystrom, Shipping and Installation, in Section X.

732 Operational Environment

MMIRS shall be capable of operation in relative humidities ranging from 0% to 90%. To prevent condensation on the dewar window, this may require an ambient temperature clean air purge and/or heating of the perimeter of the dewar window.

McCracken, MOS Section Design, Section III.

732 Battery backup

Any required window heating system must include battery backup power for up to 24 hours during lightning power-down times.

Thermal analysis indicates Lens1 temp won't drop significantly so no heater is required. See Park, MOS Steady State Analysis, Section VII.

740 Mechanical Environment

MMIRS shall be capable of operation in the mechanical environments of the MMT and Magellan Clay telescopes and their base facilities, and shall be capable of withstanding shipment among Cambridge, Tucson, and Las Campanas.

800 Other Requirements

810 Documents

MMIRS shall be delivered with adequate documentation to facilitate the operation, maintenance, and repair of the instrument.

811 Software Maintenance Manual

This document shall describe the software at a level of detail sufficient for a competent programmer, not initially familiar with the software, to maintain it properly. This includes detailed verbal descriptions of all software systems and sub-systems written by SAO at a high level, including purpose, organization, and interaction with any other software systems and sub-systems. Included are any systems analyses, data flow diagrams, data dictionaries, structure charts, and mini-specs developed during the software design process, updated to reflect as-built conditions. Also included are listings of all software delivered as part of MMIRS, including firmware in ROM's, PROM's, and Xilinx processors. All software source code modules shall include a standard header documenting the module contents, and each module shall contain a sufficient number of comments explaining the purpose and function of each section of code such that a programmer unfamiliar with the software can understand it. Any systems engineering analyses that led to the allocation of functions between hardware and software or the software design shall also be included.

The CDR Software document largely fills this role. Source code will be maintained in a CVS repository.

812 Users Manual

The users manual shall contain sufficient detail of both instrument operation and instrument performance that MMIRS observations can be carried out by both general users and observatory staff.

The Users Manual will be written during the MMIRS commissioning phase.

813 Service and Calibration Manual

The service and calibration manual shall detail all routine calibration and testing needed to ensure that MMIRS is operating with its design parameters. The service manual shall list and explain all routine service procedures needed to maintain MMIRS in an operational state.

An outline is provided in the Assembly and Test Plan, in Section XI. Detailed procedures will be developed during the Assembly and Test phase.

814 As-Built Drawings

The as-built drawings shall show all dimensions in inches, down to 0.01 inches, or higher precision if needed for proper tolerance. All fasteners specified in these drawings shall be standard inch sizes. All drawings shall otherwise be to SAO-CE standards used in instruments of similar size, function, and complexity.

In compliance.

815 Drawing Standards

The drawings shall comply to SAO standard M-CE100-S1.

In compliance.

816 Drawing Numbering

A separate numbering system shall be instituted for the MMIRS program with number assignments conforming with SAO standard M-CE100-S1. All drawings and documenation shall also be accessable on a MMIRS web site.

The numbering system shall conform to SAO standard M-CE100-S1, where;

- MMIRS is the alpha component identifying the program, it is followed by the numeric section identifying disciplines and other documentation. The numeric attributes are as follows:

- 001-099 Conceptual designs and layouts
- 200-399 Procedures, Specifications, Test procedures
  This series requires a prefix to denote type, ie P-MMIRS-200, S-MMIRS-200 or TP-MMIRS-200
- 400-499 Mechanical interface control drawings
- 500-3999 Mechanical assemblies, source control drawing, altered item drawings and detail drawings.
- 4000-4999 Mechanical ground support drawings (all types).
- 5000-5099 Electrical interface control drawings
- 5100-7999 All Electrical drawings for instrument
- 8000-9999 All Electrical ground support equipment

In compliance.

820 Training

The MMIRS development team shall provide training documentation and a training course to MMT and Magellan operations personnel on the operation, maintenance, and repair of MMIRS.

To be done during commissioning. See Maintenance and Serviceability, in Section XI.

830 Reliability

See Maintenance and Serviceability, in Section XI.

831 Downtime

MMIRS shall have a total downtime of 2%, with 1% as a goal. Where possible, component failure shall result in gradual performance degradation. Single point failures that may result in significant downtime shall be determined and, where necessary, critical spares shall be identified.

832 Continuous Duty

MMIRS shall be designed and built for continuous operation. Modules containing moving parts shall be designed or selected to meet observational requirements without excessive downtime.

840 Maintainability and Serviceability

MMIRS shall meet the following requirements for maintainability, as outlined in our Proposal.

See Maintenance and Serviceability, in Section XI.

841 Standard Components

Whenever possible, MMIRS shall use unmodified, commercially available, standard components, and components taken from FLAMINGOS, FLAMINGOS-2 and other SAO instruments for the MMT and Magellan.

842 Modularity

To the extent possible, the MMIRS shall be designed to be modular.

843 Access

Access to components and subassemblies shall be considered in the MMIRS design, particularly for those elements that are accessed frequently. Tool and hand clearances shall be considered, as well as space required to remove modules, visual access to components (or a means to feel their correct position and alignment, e.g., for electronic connectors).

844 Alignment

Alignment of optical components shall be achieved to the extent possible by accurate machining of component features.

Nystron, Optic Mounting Description, in Section IV

845 Relative Equipment Arrangements

Equipment shall be located with due consideration of the sequence of operations involved in maintenance procedures. To the extent possible, the most accessible locations shall be reserved for the items requiring most frequent access.

Holwell, Electrical Packaging, in Section VIII

846 Subassemblies

Subassemblies of the equipment that require more frequent service (inspection, adjustments, repair, or replacement) shall be configured as plug-in modules or, if in racks, as drawers that can be withdrawn easily.

Holwell, Electrical Packaging, in Section VIII

847 Handling

Modules greater than 20 kg in mass shall have suitable handles for use in removing, replacing, and carrying them. Handles shall be located such that the vector sum of resultant handling forces shall pass close to the center of gravity of the unit.
McCracken, MOS Design, in Section III and Holwell, Camera Design, Section IV.

850 Lifetime

The MMIRS shall be designed for an operational lifetime of 10 years without a major overhaul. Components likely to affect the lifetime requirement shall be identified.

See Maintenance and Serviceability, in Section XI.

860 Safety

MMIRS shall be designed in such a way that it will not present a safety hazard to personel while in transport, attached to the CIR, or during operation.

861 Emergency Stop

A power cutoff switch for the instrument mechanisms shall be attached to the instrument in an easily accessible location. A second switch attached to a long cable shall be added during assembly and testing..

Burke, MMIRS Electrical Design, in Section VIII.

862 Cautions

Placards shall be attached to indicate areas were caution must be exercised.

See MOS Section Design, in Section III.

870 Slit Masks

The goal turnaround time for fabricating masks shall be less than 5 days from the time imaging data is taken until masks are ready for installation in MMIRS. This allows preparatory imaging and spectroscopy of a given field during the same observing run.

Abandoned this goal. Masks must be designed 4 weeks in advance, in conformance with other Magellan instruments.

871 Mask Material

The mask material must be opaque at near-IR wavelengths (over 0.9–2.6 μm). By opaque we require attenuation of at least 1 part in 10^5 (12.5 magnitudes) so that the background will be reduced to below the detector dark current.

The mask material must have sufficiently high heat conductivity and appropriate thermal finishes so that the center of the mask will be cold enough to meet the requirements of section 150 when exposed to room temperature thermal radiation on the upper side.

Expect 3 K center-to-edge gradient even with a black surface looking up.

The recommended mask material is anodized alumimum sheeting, 0.003 inches thick, as used in FLAMINGOS.

Adopted.

872 Mask Cutting

MMIRS shall use a mask material which can be machined using the existing Magellan IMACS laser cutter. The performance goal for this mask maker for MMIRS is that it should machine slits as narrow as 0.2 arcseconds with a regularity on pixel-to-pixel scales less than 1% along the spatial direction.

The mask maker should be capable of making irregular or curved slits if desired.

See above.

873 Mask Design Software

MMIRS shall have mask design software. The goal is that MMIRS shall use the same mask design sofware as IMACS, Binospec, or Flamingos.

See Software, Section IX.

900 Shipping and Handling

See Nystrom, Shipping and Handling in Section XI.

910 Shipping equipment

The MMIRS instrument shall be broken down into components for shopment. All components shall be placed in sealed containers. The containers shall provide vibration and shock attenuation, dessicant, pressure control, and lifting provisions. The containers shall also have labels to identify any special handling or safety requirements.

920 Container sizes

All containers shall be sized to allow air transport and shall be provided with handles, lift devices, and forklift ports, as required. All containers must be sized to allow passage into the observatoriy buildings.

930 Instrument cart

A MMIRS intrument cart shall be designed to allow holding the assembled cryostat for transport within a laboratory space and to provide for instrument rotation of 90 degrees. Rotation with the telescope mounting truss and electronics racks are installed is not required.

The instrument cart shall also serve to install the MMIRS on the MMT telescope with the telescope mount and the electronics racks attached. At the Magellan telescope the cart will be used for instrument assembly, test, and storage, but a separate lift cart will be used for installation on the telescope.

Section II.

Optic Design and Analysis

1. Optical Design Description
2. Optical Specification
3. Ghost Analysis
4. Throughput Calculations
5. Coatings
6. Grism Design
7. Fringing
8. Stray Light Analysis

MMIRS Preconstruction Design

Daniel Fabricant
October 20, 2004, rev a

1 What is a Preconstruction Design?

A preconstruction design has sufficient design maturity to serve as a basis for mechanical design and to obtain quotes for the optics. **A preconstruction design should not be built. Further optimization and design refinement is required. Every element drawing from the preconstruction design should have a clear stamp: "for quotation only, do not build".** Furthermore, the camera and collimator optics in the design are at cryogenic temperatures, and all spacings, thicknesses and radii need to be translated to room temperature for fabrication.

What work remains on the MMIRS optics? We need to carefully check over all of the cryogenic refractive index data, check the effect of working in vacuum (absolute indices as opposed to the current indices relative to air), obtain meltsheet data for the S-FTM16, determine the final working temperature for each optic, and reoptimize the optics using these data. In order to translate the cryogenic design to construction at room temperature we need to have accurate coefficients of thermal expansion. If possible, we would like to sharpen up the collimator's pupil image without giving up a significant amount of image quality. In addition, a careful ghost image analysis should be performed and documented.

2 Where Did This Design Come From?

The MMIRS preconstruction design uses a new collimator by Harland Epps (RUN101804BF) and a camera by Daniel Fabricant (CAM022204L_REOPT). The camera is based on an original design by Harland Epps, but further developed by Dan. The REOPT refers to the fact that it was reoptimized against Dan's COL_022704D after its original optimization in perfectly parallel light. The lens radii and final focus were allowed to readjust, but element spacings and lens thicknesses were fixed for this reoptimization. In the preconstruction design, Dan switched to the new NEW_EPPSIR refractive indices and refocussed, but did not further reoptimize. Attempts to further reoptimize the CAM022204L_REOPT against the RUN101804BF collimator did not result in improvement.

3 Prescription

The preconstruction design uses a single aspheric on the leading edge of the first collimator element. The diameters shown are the minimum clear apertures. The collimator apertures have been taken from Harland Epp's calculation, which gave slightly larger numbers than ZEMAX. The camera numbers are the maximums from the multi-configuration ZEMAX file. The coma corrector elements have been sized for a 14′

diameter field. I would allow ~5 mm margin on all clear apertures to avoid scattered light and reflections, plus whatever is required for mounting.

C:\docs\Zemax_Files\MMIRS\Precons\MMIRS_col_101804bf_cam_022204l._new_reopt.ZMX
Date : WED OCT 20 2004

Surf	Type	Comment	Radius	Thickness	Glass	Diameter	Conic
OBJ	STANDARD		Infinity	Infinity		0	0
STO	STANDARD		-16255.300	-6179.233	MIRROR	6502.400	-1
2	STANDARD		-5150.890	6179.233	MIRROR	1593.118	-2.6947
3	STANDARD		Infinity	1430.149		436.154	0
4	STANDARD		2126.526	50.000	CAF2	208.4	0
5	STANDARD		-1502.700	20.000		201.6	0
6	STANDARD		229.680	20.000	CAF2	189.2	0
7	STANDARD		162.313	310.000		177.2	0
8	STANDARD	FOCUS	Infinity	100.000		98.795	0
9	EVENASPH		242.930	51.000	NEW_CAF2/IN	124.3	0
10	STANDARD		-169.512	154.063		124.9	0
11	STANDARD		-84.406	6.000	NEW_CAF2/IN	74.4	0
12	STANDARD		107.521	83.746		76.0	0
13	STANDARD		Infinity	23.000	NEW_BAF2/IN	111.0	0
14	STANDARD		-104.197	7.234		113.1	0
15	STANDARD		-132.397	8.000	NEW_ZNSE/IN	111.6	0
16	STANDARD		-148.777	10.000		115.7	0
17	STANDARD		Infinity	11.000	NEW_FQTZ/IN	115.3	0
18	STANDARD		413.230	26.554		115.1	0
19	STANDARD		1132.434	21.000	NEW_CAF2/IN	117.5	0
20	STANDARD		-214.539	65.000		118.3	0
21	STANDARD	STOP	Infinity	165.000		107.6	0
22	STANDARD		281.500	38.000	NEW_CAF2/IN	139.1	0
23	STANDARD		-305.335	17.359		138.5	0
24	STANDARD		-243.673	6.993	NEW_S-FTM16/IN	134.6	0
25	STANDARD		6459.728	10.739		135.6	0
26	STANDARD		273.225	33.806	NEW_CAF2/IN	137.7	0
27	STANDARD		Infinity	181.385		135.6	0
28	STANDARD		192.218	22.000	NEW_BAF2/IN	113.0	0
29	STANDARD		-969.285	28.270		109.7	0
30	STANDARD		160.890	38.000	NEW_CAF2/IN	92.5	0
31	STANDARD		1906.067	26.090		76.5	0
32	STANDARD		-138.260	8.000	NEW_S-FTM16/IN	60.3	0
33	STANDARD		139.853	23.853		56.4	0
IMA	STANDARD		Infinity				0

SURFACE DATA DETAIL:

Surface 9 : EVENASPH
Coeff on r 2 : 0
Coeff on r 4 : -4.813075e-008
Coeff on r 6 : 1.9562193e-012
Coeff on r 8 : -4.4717975e-017

GLOBAL VERTEX COORDINATES, ORIENTATIONS, AND ROTATION/OFFSET MATRICES:

Surf	R11	R12	R13	X
	R21	R22	R23	Y
	R31	R32	R33	Z
1	1.0000000000	0.0000000000	0.0000000000	0.000000000E+000
	0.0000000000	1.0000000000	0.0000000000	0.000000000E+000
	0.0000000000	0.0000000000	1.0000000000	0.000000000E+000
2	1.0000000000	0.0000000000	0.0000000000	0.000000000E+000
	0.0000000000	1.0000000000	0.0000000000	0.000000000E+000
	0.0000000000	0.0000000000	1.0000000000	-6.179232967E+003
3	1.0000000000	0.0000000000	0.0000000000	0.000000000E+000
	0.0000000000	1.0000000000	0.0000000000	0.000000000E+000
	0.0000000000	0.0000000000	1.0000000000	0.000000000E+000
4	1.0000000000	0.0000000000	0.0000000000	0.000000000E+000
	0.0000000000	1.0000000000	0.0000000000	0.000000000E+000
	0.0000000000	0.0000000000	1.0000000000	1.430149000E+003
5	1.0000000000	0.0000000000	0.0000000000	0.000000000E+000
	0.0000000000	1.0000000000	0.0000000000	0.000000000E+000
	0.0000000000	0.0000000000	1.0000000000	1.480149000E+003
6	1.0000000000	0.0000000000	0.0000000000	0.000000000E+000
	0.0000000000	1.0000000000	0.0000000000	0.000000000E+000
	0.0000000000	0.0000000000	1.0000000000	1.500148950E+003
7	1.0000000000	0.0000000000	0.0000000000	0.000000000E+000
	0.0000000000	1.0000000000	0.0000000000	0.000000000E+000
	0.0000000000	0.0000000000	1.0000000000	1.520148950E+003
8	1.0000000000	0.0000000000	0.0000000000	0.000000000E+000
FOCUS				
	0.0000000000	1.0000000000	0.0000000000	0.000000000E+000
	0.0000000000	0.0000000000	1.0000000000	1.830148950E+003
9	1.0000000000	0.0000000000	0.0000000000	0.000000000E+000
	0.0000000000	1.0000000000	0.0000000000	0.000000000E+000
	0.0000000000	0.0000000000	1.0000000000	1.930148905E+003
10	1.0000000000	0.0000000000	0.0000000000	0.000000000E+000
	0.0000000000	1.0000000000	0.0000000000	0.000000000E+000
	0.0000000000	0.0000000000	1.0000000000	1.981148868E+003
11	1.0000000000	0.0000000000	0.0000000000	0.000000000E+000
	0.0000000000	1.0000000000	0.0000000000	0.000000000E+000
	0.0000000000	0.0000000000	1.0000000000	2.135211528E+003
12	1.0000000000	0.0000000000	0.0000000000	0.000000000E+000
	0.0000000000	1.0000000000	0.0000000000	0.000000000E+000
	0.0000000000	0.0000000000	1.0000000000	2.141211525E+003
13	1.0000000000	0.0000000000	0.0000000000	0.000000000E+000

```
      0.0000000000   1.0000000000   0.0000000000  0.000000000E+000
      0.0000000000   0.0000000000   1.0000000000  2.224957664E+003

14    1.0000000000   0.0000000000   0.0000000000  0.000000000E+000
      0.0000000000   1.0000000000   0.0000000000  0.000000000E+000
      0.0000000000   0.0000000000   1.0000000000  2.247957613E+003

15    1.0000000000   0.0000000000   0.0000000000  0.000000000E+000
      0.0000000000   1.0000000000   0.0000000000  0.000000000E+000
      0.0000000000   0.0000000000   1.0000000000  2.255191798E+003

16    1.0000000000   0.0000000000   0.0000000000  0.000000000E+000
      0.0000000000   1.0000000000   0.0000000000  0.000000000E+000
      0.0000000000   0.0000000000   1.0000000000  2.263191794E+003

17    1.0000000000   0.0000000000   0.0000000000  0.000000000E+000
      0.0000000000   1.0000000000   0.0000000000  0.000000000E+000
      0.0000000000   0.0000000000   1.0000000000  2.273191790E+003

18    1.0000000000   0.0000000000   0.0000000000  0.000000000E+000
      0.0000000000   1.0000000000   0.0000000000  0.000000000E+000
      0.0000000000   0.0000000000   1.0000000000  2.284191785E+003

19    1.0000000000   0.0000000000   0.0000000000  0.000000000E+000
      0.0000000000   1.0000000000   0.0000000000  0.000000000E+000
      0.0000000000   0.0000000000   1.0000000000  2.310746097E+003

20    1.0000000000   0.0000000000   0.0000000000  0.000000000E+000
      0.0000000000   1.0000000000   0.0000000000  0.000000000E+000
      0.0000000000   0.0000000000   1.0000000000  2.331746074E+003

21    1.0000000000   0.0000000000   0.0000000000  0.000000000E+000 STOP
      0.0000000000   1.0000000000   0.0000000000  0.000000000E+000
      0.0000000000   0.0000000000   1.0000000000  2.396746074E+003

22    1.0000000000   0.0000000000   0.0000000000  0.000000000E+000
      0.0000000000   1.0000000000   0.0000000000  0.000000000E+000
      0.0000000000   0.0000000000   1.0000000000  2.561746074E+003

23    1.0000000000   0.0000000000   0.0000000000  0.000000000E+000
      0.0000000000   1.0000000000   0.0000000000  0.000000000E+000
      0.0000000000   0.0000000000   1.0000000000  2.599746220E+003

24    1.0000000000   0.0000000000   0.0000000000  0.000000000E+000
      0.0000000000   1.0000000000   0.0000000000  0.000000000E+000
      0.0000000000   0.0000000000   1.0000000000  2.617105465E+003

25    1.0000000000   0.0000000000   0.0000000000  0.000000000E+000
      0.0000000000   1.0000000000   0.0000000000  0.000000000E+000
      0.0000000000   0.0000000000   1.0000000000  2.624098186E+003

26    1.0000000000   0.0000000000   0.0000000000  0.000000000E+000
      0.0000000000   1.0000000000   0.0000000000  0.000000000E+000
      0.0000000000   0.0000000000   1.0000000000  2.634837276E+003

27    1.0000000000   0.0000000000   0.0000000000  0.000000000E+000
      0.0000000000   1.0000000000   0.0000000000  0.000000000E+000
```

```
      0.0000000000   0.0000000000   1.0000000000  2.668642905E+003

28    1.0000000000   0.0000000000   0.0000000000  0.000000000E+000
      0.0000000000   1.0000000000   0.0000000000  0.000000000E+000
      0.0000000000   0.0000000000   1.0000000000  2.850028214E+003

29    1.0000000000   0.0000000000   0.0000000000  0.000000000E+000
      0.0000000000   1.0000000000   0.0000000000  0.000000000E+000
      0.0000000000   0.0000000000   1.0000000000  2.872028269E+003

30    1.0000000000   0.0000000000   0.0000000000  0.000000000E+000
      0.0000000000   1.0000000000   0.0000000000  0.000000000E+000
      0.0000000000   0.0000000000   1.0000000000  2.900298746E+003


31    1.0000000000   0.0000000000   0.0000000000  0.000000000E+000
      0.0000000000   1.0000000000   0.0000000000  0.000000000E+000
      0.0000000000   0.0000000000   1.0000000000  2.938298748E+003

32    1.0000000000   0.0000000000   0.0000000000  0.000000000E+000
      0.0000000000   1.0000000000   0.0000000000  0.000000000E+000
      0.0000000000   0.0000000000   1.0000000000  2.964389120E+003

33    1.0000000000   0.0000000000   0.0000000000  0.000000000E+000
      0.0000000000   1.0000000000   0.0000000000  0.000000000E+000
      0.0000000000   0.0000000000   1.0000000000  2.972389161E+003

34    1.0000000000   0.0000000000   0.0000000000  0.000000000E+000
      0.0000000000   1.0000000000   0.0000000000  0.000000000E+000
      0.0000000000   0.0000000000   1.0000000000  2.996242173E+003
```

4 Performance

```
Executing C:\DOCS\ZEMAX_FILES\MACROS\QSPOTALL.ZPL.

Zemax file is: MMIRS_col_101804bf_cam_022204l_multi_new_reopt.ZMX
Date: WED OCT 20 2004  Zemax Ver: 40722
```

Configuration: 1, Y-Band Imaging

```
Averaged over all wavelengths and field angles with refocus 0.00300000

            rms    80%    90%    95%  diameters (microns)
           16.2   20.7   23.8   25.2

         X Field angles (arcmin):
                       0.0000    2.4990    4.0002    5.0000
         Y Field angles (arcmin):
                       0.0000    0.0000    0.0000    0.0000

         RMS Image Diameters:
            0.90000      29.1      19.1      15.6      22.1
            0.95000      15.2       6.9       7.8      10.7
            1.00000       2.9      10.7      15.8      10.4
            1.05000       8.7      19.4      24.3      17.6
            1.10000      13.6      24.2      28.8      21.6


         80% Encircled Energy Diameters:
            0.90000      34.5      22.7      19.5      26.1
            0.95000      16.7       8.7       9.0      12.7
            1.00000       4.4      15.0      22.9      11.8
            1.05000      12.1      26.6      31.9      22.7
            1.10000      18.8      31.7      37.7      28.3


         90% Encircled Energy Diameters:
            0.90000      38.6      24.9      21.4      31.1
            0.95000      19.5       9.4      11.1      15.0
            1.00000       5.2      17.2      25.7      18.6
            1.05000      12.7      28.3      36.7      30.0
            1.10000      19.3      34.3      42.4      35.1


         95% Encircled Energy Diameters:
            0.90000      38.6      26.8      24.1      33.8
            0.95000      19.5       9.6      11.7      15.8
            1.00000       5.3      18.2      26.4      21.4
            1.05000      12.7      31.1      38.5      32.4
            1.10000      19.3      37.2      45.0      37.2


         X Centroids:
            0.90000    0.0000  -13.1527  -21.0397  -26.3196
            0.95000    0.0000  -13.1534  -21.0405  -26.3198
            1.00000    0.0000  -13.1538  -21.0407  -26.3194
```

```
   1.05000    0.0000  -13.1543  -21.0411  -26.3193
   1.10000    0.0000  -13.1549  -21.0419  -26.3199


Y Centroids:
   0.90000    0.0000    0.0000    0.0000    0.0000
   0.95000    0.0000    0.0000    0.0000    0.0000
   1.00000    0.0000    0.0000    0.0000    0.0000
   1.05000    0.0000    0.0000    0.0000    0.0000
   1.10000    0.0000    0.0000    0.0000    0.0000


Traced Rays/Rays in Entrance Pupil:
   0.90000  113/ 113  113/ 113  113/ 113  113/ 113
   0.95000  113/ 113  113/ 113  113/ 113  113/ 113
   1.00000  113/ 113  113/ 113  113/ 113  113/ 113
   1.05000  113/ 113  113/ 113  113/ 113  113/ 113
   1.10000  113/ 113  113/ 113  113/ 113  113/ 113
```

Configuration: 2, J-Band Imaging

Averaged over all wavelengths and field angles with refocus -0.05000000

```
    rms    80%    90%    95%  diameters (microns)
    9.6   12.0   14.1   14.9

X Field angles (arcmin):
              0.0000    2.4990    4.0002    5.0000
Y Field angles (arcmin):
              0.0000    0.0000    0.0000    0.0000

RMS Image Diameters:
   1.00000      15.1       6.9       7.4      10.5
   1.10000       2.7      11.1      15.8       9.7
   1.20000       2.7      10.8      14.9       8.7
   1.30000       7.9       5.3       8.2       7.0
   1.40000      16.7       8.4       7.0      14.5


80% Encircled Energy Diameters:
   1.00000      16.7       8.6       8.7      12.7
   1.10000       4.1      15.5      22.5      11.4
   1.20000       4.1      14.5      20.6      10.8
   1.30000       9.1       6.4      10.6       8.1
   1.40000      18.4      10.3       8.7      17.6


90% Encircled Energy Diameters:
   1.00000      19.4       9.4      10.4      14.7
   1.10000       4.9      17.9      25.3      16.9
   1.20000       4.9      17.4      24.1      14.5
```

```
   1.30000       9.2       8.8      14.8      10.0
   1.40000      21.4      10.7       9.2      18.5


95% Encircled Energy Diameters:
   1.00000      19.4       9.5      11.7      15.7
   1.10000       4.9      19.5      26.7      19.0
   1.20000       5.0      18.8      25.7      17.1
   1.30000       9.2       9.2      15.2      10.5
   1.40000      21.4      11.2       9.5      19.8


X Centroids:
   1.00000    0.0000  -13.1511  -21.0365  -26.3144
   1.10000    0.0000  -13.1523  -21.0378  -26.3150
   1.20000    0.0000  -13.1540  -21.0401  -26.3174
   1.30000    0.0000  -13.1557  -21.0428  -26.3204
   1.40000    0.0000  -13.1573  -21.0451  -26.3230



Y Centroids:
   1.00000    0.0000    0.0000    0.0000    0.0000
   1.10000    0.0000    0.0000    0.0000    0.0000
   1.20000    0.0000    0.0000    0.0000    0.0000
   1.30000    0.0000    0.0000    0.0000    0.0000
   1.40000    0.0000    0.0000    0.0000    0.0000


Traced Rays/Rays in Entrance Pupil:
   1.00000  113/ 113  113/ 113  113/ 113  113/ 113
   1.10000  113/ 113  113/ 113  113/ 113  113/ 113
   1.20000  113/ 113  113/ 113  113/ 113  113/ 113
   1.30000  113/ 113  113/ 113  113/ 113  113/ 113
   1.40000  113/ 113  113/ 113  113/ 113  113/ 113
```

Configuration: 3, H-Band Imaging

Averaged over all wavelengths and field angles with refocus 0.03200000

```
    rms    80%    90%    95%  diameters (microns)
   10.1   12.6   14.3   14.8

X Field angles (arcmin):
              0.0000    2.4990    4.0002    5.0000
Y Field angles (arcmin):
              0.0000    0.0000    0.0000    0.0000

RMS Image Diameters:
   1.40000       5.5      15.0      18.1      10.6
   1.50000       4.6       7.4       9.8       6.8
   1.60000      10.3       4.7       5.4      10.9
```

1.70000	14.3	6.9	6.2	15.4
1.80000	16.1	8.6	7.9	18.1

80% Encircled Energy Diameters:

1.40000	7.7	19.8	24.2	14.4
1.50000	6.5	10.2	13.4	8.1
1.60000	11.3	6.0	6.6	13.6
1.70000	14.8	8.9	8.2	19.1
1.80000	16.9	10.5	9.9	21.6

90% Encircled Energy Diameters:

1.40000	8.1	22.5	27.8	17.5
1.50000	6.9	12.5	16.9	9.8
1.60000	12.0	6.7	8.4	15.1
1.70000	17.2	9.6	9.0	20.3
1.80000	19.4	11.4	10.9	23.0

95% Encircled Energy Diameters:

1.40000	8.3	23.9	29.2	19.2
1.50000	7.0	12.9	17.3	10.0
1.60000	12.0	6.9	9.1	15.7
1.70000	17.2	10.1	9.3	20.5
1.80000	19.4	11.9	11.9	23.8

X Centroids:

1.40000	0.0000	-13.1614	-21.0515	-26.3307
1.50000	0.0000	-13.1626	-21.0532	-26.3326
1.60000	0.0000	-13.1634	-21.0543	-26.3336
1.70000	0.0000	-13.1638	-21.0547	-26.3337
1.80000	0.0000	-13.1638	-21.0545	-26.3331

Y Centroids:

1.40000	0.0000	0.0000	0.0000	0.0000
1.50000	0.0000	0.0000	0.0000	0.0000
1.60000	0.0000	0.0000	0.0000	0.0000
1.70000	0.0000	0.0000	0.0000	0.0000
1.80000	0.0000	0.0000	0.0000	-0.0000

Traced Rays/Rays in Entrance Pupil:

1.40000	113/ 113	113/ 113	113/ 113	113/ 113
1.50000	113/ 113	113/ 113	113/ 113	113/ 113
1.60000	113/ 113	113/ 113	113/ 113	113/ 113
1.70000	113/ 113	113/ 113	113/ 113	113/ 113
1.80000	113/ 113	113/ 113	113/ 113	113/ 113

Configuration: 4, K-Band Imaging

Averaged over all wavelengths and field angles with refocus 0.01300000

rms	80%	90%	95%	diameters (microns)
13.6	16.8	18.9	20.7	

X Field angles (arcmin):

0.0000	2.4990	4.0002	5.0000

Y Field angles (arcmin):

0.0000	0.0000	0.0000	0.0000

RMS Image Diameters:

2.00000	18.7	11.3	11.2	22.6
2.12500	14.0	7.5	8.1	19.7
2.25000	7.7	5.8	6.8	15.6
2.37500	6.6	12.4	12.5	13.0
2.50000	16.1	22.9	22.3	16.3

80% Encircled Energy Diameters:

2.00000	19.7	13.5	12.9	26.9
2.12500	15.5	10.0	9.9	23.0
2.25000	11.1	6.8	8.1	18.6
2.37500	9.1	16.2	16.3	14.6
2.50000	23.9	29.9	29.2	21.3

90% Encircled Energy Diameters:

2.00000	21.9	14.4	14.7	28.7
2.12500	15.8	11.0	11.6	26.1
2.25000	11.1	7.6	9.4	22.0
2.37500	10.5	18.0	19.2	16.5
2.50000	27.1	32.6	34.2	25.2

95% Encircled Energy Diameters:

2.00000	21.9	15.9	15.7	29.4
2.12500	15.8	11.4	12.9	27.6
2.25000	11.3	9.9	10.5	24.4
2.37500	10.5	22.7	23.4	18.1
2.50000	27.1	39.3	39.3	26.7

X Centroids:

2.00000	0.0000	-13.1622	-21.0512	-26.3281
2.12500	0.0000	-13.1613	-21.0494	-26.3249
2.25000	0.0000	-13.1601	-21.0470	-26.3211
2.37500	0.0000	-13.1588	-21.0443	-26.3167
2.50000	0.0000	-13.1572	-21.0412	-26.3119

Y Centroids:

2.00000	0.0000	0.0000	0.0000	-0.0000

```
   2.12500    0.0000    0.0000    0.0000   -0.0000
   2.25000    0.0000    0.0000    0.0000   -0.0000
   2.37500    0.0000    0.0000    0.0000   -0.0000
   2.50000    0.0000    0.0000    0.0000   -0.0000


Traced Rays/Rays in Entrance Pupil:
   2.00000  113/ 113  113/ 113  113/ 113  113/ 113
   2.12500  113/ 113  113/ 113  113/ 113  113/ 113
   2.25000  113/ 113  113/ 113  113/ 113  113/ 113
   2.37500  113/ 113  113/ 113  113/ 113  113/ 113
   2.50000  113/ 113  113/ 113  113/ 113  113/ 113
```

Configuration: 5, 230 gpm, J-Band Spectroscopy

Averaged over all wavelengths and field angles with refocus -0.04000000

```
    rms    80%    90%    95%  diameters (microns)
   11.4   13.8   17.6   20.1

X Field angles (arcmin):
              0.0000    1.7400    2.7840    3.4800
Y Field angles (arcmin):
              0.0000    0.0000    0.0000    0.0000

RMS Image Diameters:
   1.02200       8.7       9.3      10.0      10.9
   1.12350       8.5      12.8      17.3      18.6
   1.22500       2.8       7.3      13.2      15.7
   1.33250       7.9       6.7       8.0       8.4
   1.44000      14.6      13.9      15.1      19.1


80% Encircled Energy Diameters:
   1.02200       9.3      10.8      11.7      13.0
   1.12350       8.3      16.5      23.0      24.6
   1.22500       3.4       9.7      17.4      21.0
   1.33250       9.5       7.9       9.8       9.9
   1.44000      16.8      14.9      16.1      22.6


90% Encircled Energy Diameters:
   1.02200      13.7      14.0      15.7      15.7
   1.12350      14.8      20.3      28.4      30.1
   1.22500       4.4      11.7      20.3      24.3
   1.33250      10.7       9.8      13.0      13.9
   1.44000      20.5      20.9      21.9      27.1


95% Encircled Energy Diameters:
   1.02200      14.9      16.1      18.4      18.4
```

```
   1.12350      18.2      21.8      29.5      33.4
   1.22500       4.4      12.6      22.2      26.6
   1.33250      13.2      11.7      14.1      16.2
   1.44000      25.6      25.4      27.9      30.8


X Centroids:
   1.02200    0.0000   -9.1832  -14.6836  -18.3488
   1.12350    0.0000   -9.1682  -14.6585  -18.3161
   1.22500    0.0000   -9.1645  -14.6522  -18.3076
   1.33250    0.0000   -9.1709  -14.6626  -18.3208
   1.44000    0.0000   -9.1876  -14.6898  -18.3556


Y Centroids:
   1.02200  -18.4564  -18.5081  -18.5888  -18.6637
   1.12350   -9.0485   -9.0930   -9.1623   -9.2265
   1.22500    0.0563    0.0180   -0.0417   -0.0968
   1.33250    9.4298    9.3974    9.3471    9.3010
   1.44000   18.5776   18.5512   18.5105   18.4734


Traced Rays/Rays in Entrance Pupil:
   1.02200  113/ 113  113/ 113  113/ 113  113/ 113
   1.12350  113/ 113  113/ 113  113/ 113  113/ 113
   1.22500  113/ 113  113/ 113  113/ 113  113/ 113
   1.33250  113/ 113  113/ 113  113/ 113  113/ 113
   1.44000  113/ 113  113/ 113  113/ 113  113/ 113
```

Configuration: 6, 175 gpm, H-Band Spectroscopy

```
Averaged over all wavelengths and field angles with refocus 0.03000000

    rms    80%    90%    95%  diameters (microns)
   12.0   14.8   17.7   20.2

X Field angles (arcmin):
              0.0000    1.7400    2.7840    3.4800
Y Field angles (arcmin):
              0.0000    0.0000    0.0000    0.0000

RMS Image Diameters:
   1.34000      17.0      18.9      18.9      16.4
   1.47250       5.4       7.9      11.3      11.9
   1.60500      11.1       6.8       5.0       5.6
   1.74250      14.2      11.1       9.1       9.2
   1.88000      13.4      12.9      14.5      19.2


80% Encircled Energy Diameters:
```

1.34000	21.2	25.2	25.6	21.4
1.47250	6.4	9.4	15.2	15.5
1.60500	11.9	8.7	6.5	6.5
1.74250	15.7	13.1	11.0	11.2
1.88000	15.5	15.0	16.8	23.3

90% Encircled Energy Diameters:

1.34000	27.0	30.9	31.0	25.8
1.47250	7.7	12.7	18.8	20.1
1.60500	12.8	9.2	7.0	8.3
1.74250	18.4	15.4	13.8	13.0
1.88000	18.0	18.8	20.3	25.7

95% Encircled Energy Diameters:

1.34000	32.0	33.6	34.1	31.2
1.47250	10.5	13.9	20.5	22.3
1.60500	13.2	9.5	7.1	9.2
1.74250	21.7	18.0	15.3	15.8
1.88000	21.0	21.9	24.7	28.7

X Centroids:

1.34000	0.0000	-9.1887	-14.6920	-18.3588
1.47250	0.0000	-9.1743	-14.6681	-18.3278
1.60500	0.0000	-9.1704	-14.6614	-18.3188
1.74250	0.0000	-9.1758	-14.6701	-18.3298
1.88000	0.0000	-9.1906	-14.6943	-18.3606

Y Centroids:

1.34000	-18.2207	-18.2720	-18.3522	-18.4266
1.47250	-8.8507	-8.8949	-8.9638	-9.0276
1.60500	0.2197	0.1815	0.1221	0.0674
1.74250	9.3740	9.3416	9.2914	9.2453
1.88000	18.3160	18.2895	18.2485	18.2112

Traced Rays/Rays in Entrance Pupil:

1.34000	113/ 113	113/ 113	113/ 113	113/ 113
1.47250	113/ 113	113/ 113	113/ 113	113/ 113
1.60500	113/ 113	113/ 113	113/ 113	113/ 113
1.74250	113/ 113	113/ 113	113/ 113	113/ 113
1.88000	113/ 113	113/ 113	113/ 113	113/ 113

Configuration: 7, 130 gpm, K-Band Spectroscopy

Averaged over all wavelengths and field angles with refocus 0.01500000

rms	80%	90%	95%	diameters (microns)
13.9	17.1	20.6	22.8	

X Field angles (arcmin):

0.0000	1.7400	2.7840	3.4800

Y Field angles (arcmin):

0.0000	0.0000	0.0000	0.0000

RMS Image Diameters:

1.78800	16.3	15.5	17.0	21.7
1.96900	17.0	13.7	11.4	11.7
2.15000	12.3	8.6	6.3	6.4
2.33500	7.6	9.7	11.3	10.6
2.50000	21.8	22.4	20.5	16.6

80% Encircled Energy Diameters:

1.78800	18.6	17.1	19.8	26.9
1.96900	18.8	15.9	14.0	14.7
2.15000	14.1	10.9	8.6	8.7
2.33500	8.9	11.2	13.9	13.3
2.50000	27.7	30.2	27.3	22.2

90% Encircled Energy Diameters:

1.78800	21.3	22.1	24.4	30.7
1.96900	20.6	18.6	15.9	16.3
2.15000	14.6	12.0	9.6	9.6
2.33500	13.4	16.1	17.8	17.4
2.50000	36.1	35.3	33.6	27.0

95% Encircled Energy Diameters:

1.78800	24.0	25.3	27.4	33.4
1.96900	23.6	20.3	18.1	17.9
2.15000	14.6	12.4	10.5	10.3
2.33500	15.6	18.3	21.2	18.4
2.50000	40.5	38.9	36.0	29.6

X Centroids:

1.78800	0.0000	-9.1906	-14.6948	-18.3619
1.96900	0.0000	-9.1745	-14.6680	-18.3271
2.15000	0.0000	-9.1690	-14.6588	-18.3150
2.33500	0.0000	-9.1732	-14.6653	-18.3231
2.50000	0.0000	-9.1848	-14.6842	-18.3470

Y Centroids:

1.78800	-18.4484	-18.4996	-18.5797	-18.6540
1.96900	-8.8779	-8.9219	-8.9905	-9.0540
2.15000	0.3924	0.3545	0.2956	0.2413
2.33500	9.6164	9.5843	9.5345	9.4888

```
   2.50000   17.6696   17.6426   17.6011   17.5631


Traced Rays/Rays in Entrance Pupil:
   1.78800  113/ 113  113/ 113  113/ 113  113/ 113
   1.96900  113/ 113  113/ 113  113/ 113  113/ 113
   2.15000  113/ 113  113/ 113  113/ 113  113/ 113
   2.33500  113/ 113  113/ 113  113/ 113  113/ 113
   2.50000  113/ 113  113/ 113  113/ 113  113/ 113
```

Configuration: 8, 94 gpm, JH-Band Spectroscopy

Averaged over all wavelengths and field angles with refocus 0.00000000

```
    rms    80%    90%    95%  diameters (microns)
   17.4   20.7   25.1   27.8

X Field angles (arcmin):
              0.0000    1.7400    2.7840    3.4800
Y Field angles (arcmin):
              0.0000    0.0000    0.0000    0.0000

RMS Image Diameters:
   0.90000      24.8      22.0      20.3      21.2
   1.10000      16.4      21.3      26.1      27.4
   1.41000       5.3       3.8       8.0      10.0
   1.73500      21.1      17.6      14.9      15.0
   2.06000      16.1      15.7      17.8      23.3


80% Encircled Energy Diameters:
   0.90000      30.2      24.3      21.7      23.9
   1.10000      18.0      27.8      34.1      35.4
   1.41000       7.0       5.0      10.8      13.7
   1.73500      23.8      19.9      16.8      16.9
   2.06000      18.4      17.8      21.1      28.2


90% Encircled Energy Diameters:
   0.90000      34.4      31.9      29.9      30.1
   1.10000      26.1      31.1      40.5      41.4
   1.41000       7.3       5.5      13.9      17.2
   1.73500      27.5      23.3      21.3      21.6
   2.06000      21.3      22.1      23.7      31.5


95% Encircled Energy Diameters:
   0.90000      37.7      36.8      36.4      36.5
   1.10000      29.2      33.3      41.8      45.9
   1.41000       7.4       5.7      14.3      17.5
   1.73500      31.1      26.4      24.4      24.2
```

```
   2.06000      23.3      24.5      27.5      32.1


X Centroids:
   0.90000    0.0000   -9.1758  -14.6715  -18.3334
   1.10000    0.0000   -9.1691  -14.6600  -18.3179
   1.41000    0.0000   -9.1680  -14.6577  -18.3144
   1.73500    0.0000   -9.1747  -14.6684  -18.3277
   2.06000    0.0000   -9.1893  -14.6923  -18.3582


Y Centroids:
   0.90000  -14.7622  -14.7851  -14.8211  -14.8546
   1.10000   -8.8969   -8.9162   -8.9464   -8.9744
   1.41000    0.0624    0.0481    0.0259    0.0054
   1.73500    9.3496    9.3404    9.3261    9.3132
   2.06000   18.5702   18.5663   18.5606   18.5558


Traced Rays/Rays in Entrance Pupil:
   0.90000  113/ 113  113/ 113  113/ 113  113/ 113
   1.10000  113/ 113  113/ 113  113/ 113  113/ 113
   1.41000  113/ 113  113/ 113  113/ 113  113/ 113
   1.73500  113/ 113  113/ 113  113/ 113  113/ 113
   2.06000  113/ 113  113/ 113  113/ 113  113/ 113
```

Configuration: 9, 80 gpm, HK-Band Spectroscopy

```
Averaged over all wavelengths and field angles with refocus 0.00000000

    rms    80%    90%    95%  diameters (microns)
   15.2   18.7   22.3   25.1

X Field angles (arcmin):
              0.0000    1.7400    2.7840    3.4800
Y Field angles (arcmin):
              0.0000    0.0000    0.0000    0.0000

RMS Image Diameters:
   1.17500      21.8      23.5      23.2      20.1
   1.54250      12.9       9.7       7.8       7.7
   1.91000      23.9      19.4      15.3      14.4
   2.27000       8.4       7.1       7.0       7.1
   2.50000      18.5      20.0      19.5      16.5


80% Encircled Energy Diameters:
   1.17500      27.3      30.9      30.6      26.9
   1.54250      14.4      11.6       9.4       9.6
   1.91000      26.6      21.2      17.6      16.4
```

2.27000	10.6	9.4	8.5	8.7
2.50000	22.1	26.3	25.3	21.0

90% Encircled Energy Diameters:

1.17500	34.0	38.2	36.6	30.6
1.54250	16.3	14.0	12.0	11.6
1.91000	29.6	22.4	18.1	17.5
2.27000	11.7	10.5	9.6	10.6
2.50000	32.3	31.6	31.5	28.3

95% Encircled Energy Diameters:

1.17500	40.2	39.8	39.6	36.6
1.54250	20.0	16.4	13.2	13.8
1.91000	29.7	26.4	22.6	21.4
2.27000	12.6	11.4	11.9	11.4
2.50000	35.7	34.9	33.7	30.3

X Centroids:

1.17500	0.0000	-9.1864	-14.6884	-18.3545
1.54250	0.0000	-9.1740	-14.6674	-18.3269
1.91000	0.0000	-9.1695	-14.6597	-18.3165
2.27000	0.0000	-9.1725	-14.6643	-18.3220
2.50000	0.0000	-9.1785	-14.6741	-18.3343

Y Centroids:

1.17500	-18.6093	-18.6375	-18.6817	-18.7229
1.54250	-9.1893	-9.2113	-9.2458	-9.2777
1.91000	0.0736	0.0567	0.0306	0.0064
2.27000	9.0464	9.0344	9.0159	8.9991
2.50000	14.7444	14.7356	14.7223	14.7103

Traced Rays/Rays in Entrance Pupil:

1.17500	113/ 113	113/ 113	113/ 113	113/ 113
1.54250	113/ 113	113/ 113	113/ 113	113/ 113
1.91000	113/ 113	113/ 113	113/ 113	113/ 113
2.27000	113/ 113	113/ 113	113/ 113	113/ 113
2.50000	113/ 113	113/ 113	113/ 113	113/ 113

5 Layout

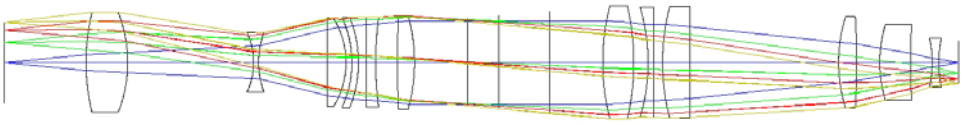

Figure 1. Layout of Preconstruction Design

6 Polychromatic Imaging Mode Spots

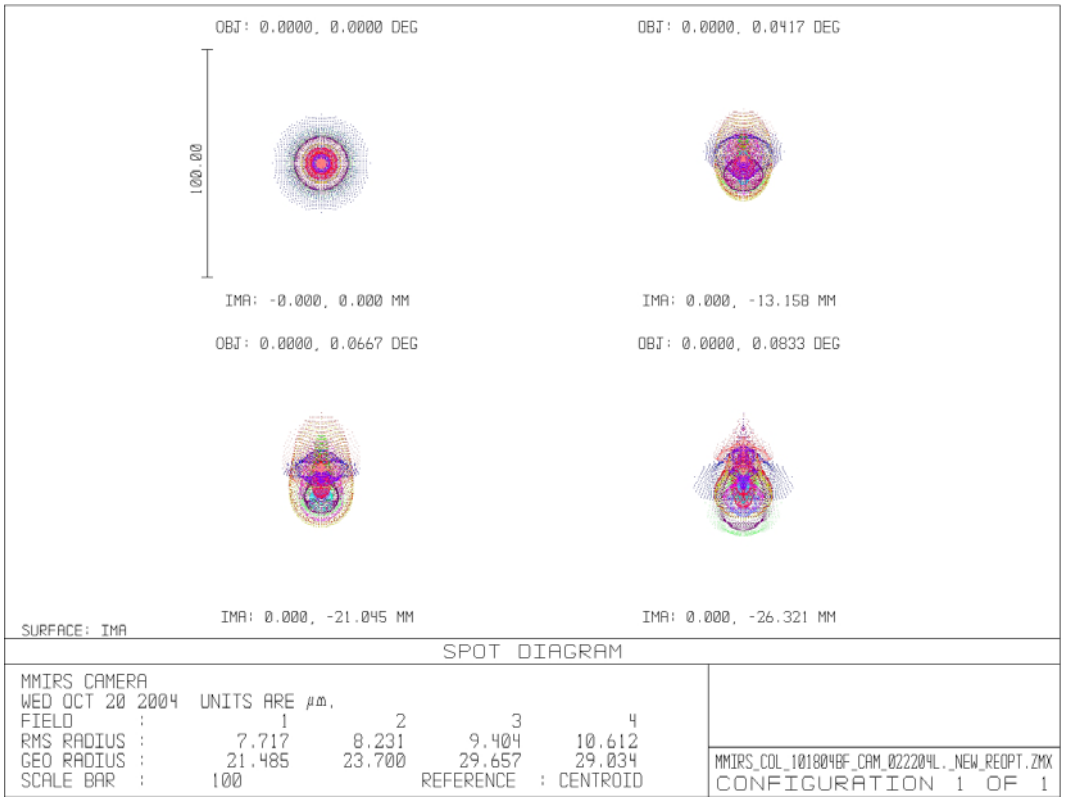

Figure 2. Polychromatic Spots (0.9-2.5 µm)

7 Matrix Imaging Spots

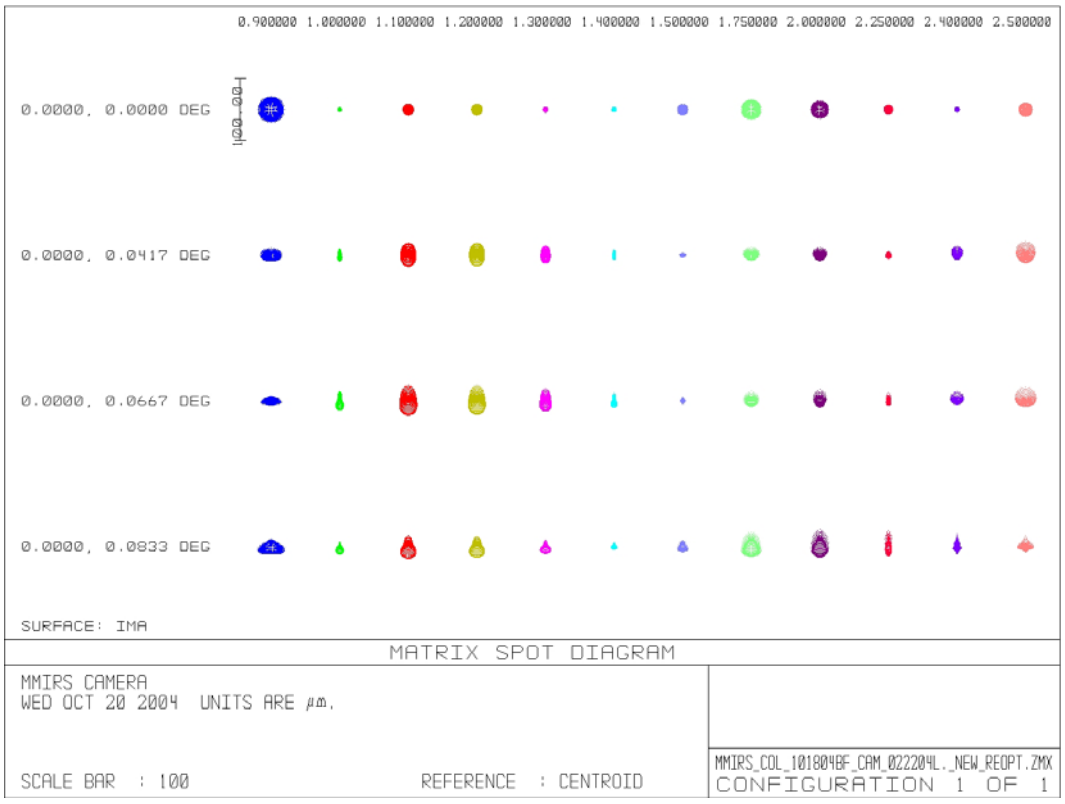

Figure 3. Matrix Imaging Spots.

MMIRS Optical Specifications

Paul Martini
April 28, 2005

100 Overview

This document describes the optical specifications for the MMIRS instrument, and in particular the image quality requirements outlined in section 120 of the MMIRS Functional and Performance Requirements (F&P; S-MMIRS-200). The F&P is the instrument's controlling document, so if there are any discrepancies between this document and the F&P, the F&P shall prevail.

The image quality requirements stated in the F&P are <20 microns FWHM in the slit plane (F&P section 121) and <28 microns FWHM at the detector, whether in imaging mode (section 122) or spectroscopic mode (section 123). These image quality requirements set the total allowable error budget for the MMIRS optics. This error budget includes lens fabrication errors, mechanical errors due to misalignments in the lens mounts, image motion due to systematic lens misalignments, and the impact of temperature gradients. This document calculates the fabrication and mechanical tolerances in detail, as well as several particular flexure and thermal scenarios, and the requirements for mounting the instrument on the telescope. The main result of this analysis is that the specifications outlined here will meet the image quality requirements of the F&P with ample contingency.

Below is a diagram of the optical layout with labels of the surfaces (4-34), lenses (L1-L14) and several groups of lenses (G1-G6). These labels are used throughout this document.

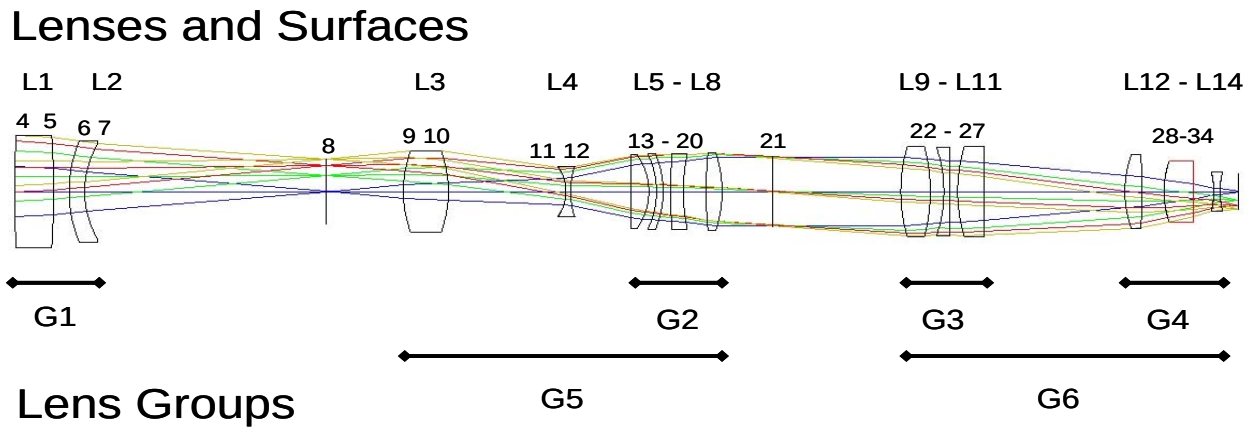

Note that this document does not include the GWFS or the grisms, which are described separately.

200 Tolerance Analysis

The two relevant quantities for the tolerance analysis are the image quality at the slit plane and at the detector. The image quality at the slit plane is important for the spectroscopic mode as this determines the fraction of the light from an unresolved source that passes through the slit. This image quality is determined by the first two optical elements, which will also be referred to as the Corrector. The image quality at the detector is important for both the imaging and spectroscopic modes. This analysis is based on the design presented in the document "MMIRS Preconstruction Design rev a" by D. Fabricant. While this is not the final design, the differences in the error budget between this and the final design are expected to be negligible.

210 Figure of Merit

The optical design produces images with an rms spot radius of 10.5 microns or better over the full science field of view at the detector, an rms spot radius of 4.5 microns or better over the full science field at the slit plane, and an rms spot radius of 10.5 microns or better for the guider/wavefront sensor field.

220 Tolerance Parameters

As noted above, the image quality produced by the 'as built' design will be degraded by both lens fabrication and mechanical errors. The 4-letter ZEMAX codes for each potential error source are:

Lens fabrication tolerances:

TRAD	Surface radius (in lens units)
TFRN	Radius in fringes for flat or nearly flat surfaces
TTHI	Lens thickness
TSD(X,Y)	Surface decenter
TST(X,Y)	Surface tilt
TIRR	Surface irregularity

Mechanical tolerances:

TTHI	Element airspace
TED(X,Y)	Element decenter
TET(X,Y)	Element tilt

The mechanical tolerance parameters were used to both tolerance individual elements and groups of elements.

230 Description of Tolerance Calculations

The error budget was calculated with the tolerancing tools in ZEMAX. This implementation requires initial estimates of the uncertainties for each parameter, which were obtained from the typical performance quoted by optics manufacturers, input from the project engineers, the Flamingos-2 CDR package, and the requirements for the PANIC near-infrared camera. The impact of these initial tolerance estimates were then iteratively rebalanced after measurement of the impact of each parameter on the image quality (using the Inverse Limit option in the Tolerance Tool) with the requirement that no one parameter degrade the image quality more than approximately 5%. A series of Monte Carlo simulations were then run and the error budget was further rebalanced until the required image quality was obtained in

at least 90% of the simulations. The following three sections present the tolerance parameters from this analysis and are followed by the error budget.

240 Lens Fabrication Tolerances

The table below specifies the manufacturing requirements for the radii, thicknesses, surface tilts, and surface irregularities for the optical elements. These values are used to generate the lens fabrication specifications for the optics package, which are summarized below in section 600.

Table 1: Fabrication Tolerances

Surface	TRAD/TFRN [% or fringes]	TTHI [mm]	TSTY/Y [mrad]	TIRR [fringes]	Note
4	0.1	0.1	0.01	0.5	L1
5	0.1	0.1	0.01	0.5	
6	0.1	0.1	0.01	0.5	L2
7	0.1	0.1	0.01	0.5	
9	0.1	0.1	0.01	0.5	L3
10	0.1	0.1	0.01	0.5	
11	0.1	0.1	0.01	0.5	L4
12	0.1	0.1	0.01	0.5	
13	1	0.1	0.01	0.5	L5, Flat
14	0.1	0.1	0.01	0.5	
15	0.1	0.1	0.01	0.5	L6
16	0.1	0.1	0.01	0.5	
17	1	0.1	0.01	0.5	L7, Flat
18	0.1	0.1	0.01	0.5	
19	0.1	0.1	0.01	0.5	L8
20	0.1	0.1	0.01	0.5	
22	0.1	0.1	0.01	0.5	L9
23	0.1	0.1	0.01	0.5	
24	0.1	0.1	0.01	0.5	L10
25	0.1	0.1	0.01	0.5	
26	0.1	0.1	0.01	0.5	L11
27	1	0.1	0.01	0.5	Flat
28	0.1	0.1	0.01	0.5	L12
29	0.1	0.1	0.01	0.5	
30	0.1	0.1	0.01	0.5	L13
31	0.1	0.1	0.01	0.5	
32	0.1	0.1	0.01	0.5	L14
33	0.1	0.1	0.01	0.5	

250 Mechanical Tolerances for Lens Mounts

The following table lists the maximum allowed decenters, tilts, and lens spaces for lenses L1-L14. For the lens spaces, the requirement is on the space between the lens in a given row of the table and the next lens in the optical path.

Table 2: Mechanical Tolerances

Element	Decenter (mm)	Tilt (mrad)	Tilt (degrees)	Space (mm)
L1*	0.05	0.2	0.01146	0.05
L2*	0.05	0.2	0.01146	0.05
L3	0.05	0.1	0.00573	0.05
L4	0.05	0.11**	0.00573	0.05
L5	0.05	0.12**	0.00573	0.05
L6	0.05	0.1	0.00573	0.05
L7	0.05	0.11**	0.00573	0.05
L8	0.05	0.11**	0.00573	0.05
L9	0.05	0.1	0.00573	0.05
L10	0.05	0.1	0.00573	0.05
L11	0.05	0.1	0.00573	0.05
L12	0.05	0.1	0.00573	0.05
L13	0.05	0.1	0.00573	0.05
L14	0.05	0.1	0.00573	(focus)

*Note that the tolerance on L1 and L2 are actually set by the image quality at the slit plane, rather than the detector.
**These tolerances were loosened slightly to accommodate the lens mount design. This loosening had a negligible (<2%) impact on the total error budget.

260 Mechanical Tolerances for Lens Groups

Several groups of elements were also defined to mimic the effect of systematic misalignments in the instrument. G1 describes an offset of the MOS section relative to the rest of the Camera Section, G5 is the first VEE block, G6 is the second VEE block, G5+G6 is the entire Camera Section, and G2-G4 describe individual lens groups within the VEE blocks.

Table 3: Lens Group Tolerances

Group	Decenter (mm)	Tilt (mrad)	Tilt (degrees)
G1 (MOS Section)	0.1	0.1	0.00573
G2	0.05	0.1	0.00573
G3	0.05	0.1	0.00573
G4	0.05	0.1	0.00573
G5 (VEE Block 1)	0.1	0.1	0.00573
G6 (VEE Block 2)	0.1	0.1	0.00573
G5+G6 (Camera Section)	0.1	0.1	0.00573

Note that the image quality is substantially less sensitive to pure decenters between the MOS and Camera sections, as well as between the camera and collimator lens groups.

270 Redistribution of Lens Fabrication and Mechanical Errors

The physical parameters of lenses can be measured much more precisely than they can be specified prior to fabrication. For example, the radius of curvature is typically specified to approximately 0.1%, yet

interferometric techniques can measure the radius to a fringe or better. This substantially higher measurement precision can be exploited to reduce the contribution of fabrication tolerances to the error budget through use of a pickup surface and/or a fine-tuning of the element airspaces and a focus adjustment. In particular, radii can be measured to better than 0.05% and lens thicknesses can be measured to better than 0.01mm.

The potential gain from this approach was estimated by running 20 Monte-Carlo simulations with the fabrications errors tabulated above, choosing the worst case, and reoptimizing the airspaces in the design. This yielded an rms spot radius less than 5% greater than the original value. Subsequent tolerance simulations to investigate mechanical errors adopted errors on the radii and element thicknesses of 0.01% and 0.01mm, respectively.

280 Error Budget Summary

The following table summarizes the contribution of the main sources of error described above. All of these error estimates are based on Monte Carlo simulations with ZEMAX and reflect the image quality performance of better than 90% of all realizations.

When interpreting the individual error sources in the table below, it is important to note that the errors are NOT independent, and therefore a summation of all individual sources of error will underestimate the final uncertainty.

Table 4: Error Budget Summary

	RMS Image Quality [microns radius]
Nominal	9.3
Lenses [As Specified]	11.1
Lenses [As Fabricated, after Optimization]	9.3
Lens Mounts	10.8
Airspaces	9.3
Element Group Misalignments	9.6
All	12.4
Requirement	14.0

Some additional potential sources of error are discussed in the next section.

300 Mechanical Case Studies

The following sections describe calculations for particular scenarios that may not have been completely addressed with the Monte Carlo simulations described above. In several cases this is because the proper compensator is a telescope refocus, rather than an instrument refocus.

310 Tolerance on L1-L2 spacing

The L1-L2 spacing uncertainty shall be less than +/-0.5mm. This tolerance specifically addresses uncertainty in the final seating of L1 on its O-ring seal. Note that the quoted uncertainty can be corrected with a telescope refocus.

320 Misalignment of Camera and MOS Sections

The alignment of the camera section (the entire optical bench) relative to the MOS section was modeled by insertion of a coordinate break before L3. To keep image degradation less than 5%, the alignment of the Camera Section (including the detector) relative to the MOS must have a decenter less than 1mm and a tilt of less than 0.1mrad. A shift of the optical bench parallel to the optical axis can be removed by adjusting focus. The refocus scales linearly with the amount of shift along the z-axis, where 1mm of shift results in a focus change of 0.28mm. The optical bench should be placed in the correct position along the optical bench to within 1mm

330 Systematic Errors in Lens Thickness

The lens manufacturers are likely to produce lenses that are systematically larger than the requested value, even if they fall within the requested range, and this scenario is not properly accounted for by the Monte Carlo simulations. This case was therefore explicitly addressed by increasing the thickness of each lens to the maximum value of the allowed range. Provided the lens thicknesses are known, this systematic error can be completely accounted for by simply reducing the airspaces between the lenses by the corresponding amount.

340 Pupil Misalignment and Shimming the Instrument

The pupil radius is 53mm in radius and the collimator focal length is 500mm. A shift of 0.5mm in the pupil position can thus be achieved with a tilt of 0.06 degrees. Instrument tilt does not significantly begin to degrade image quality until 0.06 degrees, corresponding to 5% degradation at the edge of the field. A tilt of 0.12 degrees corresponds to 10% degradation (and 1mm pupil shift). To insure that shimming the instrument does not significantly degrade image quality, the tilt should be kept to less than 0.06 degrees, which requires pupil placement with to better than 1mm. Note that image degradation quoted here was calculated after a refocus. We do not expect to need to shim the instrument since this tolerance should be easy to achieve.

350 Note on Flexure

Flexure in the optical system was considered separately with the Binosens software package, which combines information about the optical design with a finite element analysis. This analysis is described elsewhere in a series of memos by H. Bergner.

400 Telescope Mounting Specifications

This section specifically addresses the precision with which the instrument shall be mounted on the telescope and therefore is relevant to the design of the telescope mounting truss. The three particular specifications considered here are the degree to which the instrument must be aligned with respect to the optical axis of the telescope, the maximum allowed instrument tilt relative to the telescope axis, and the allowable offset of the instrument along the optical axis relative to the nominal focus position. These quantities were estimated by treating the instrument as a solid body and the tilts and decenters were applied to a point 600mm behind the front surface of L1, which is approximately where the truss is attached.

410 Tilt relative to the Telescope's Optical Axis

The tilt of the entire instrument relative to the optical axis of the telescope shall be less than 0.05 degrees.

420 Centration relative to the Telescope's Optical Axis
The instrument shall be centered on the optical axis of the telescope to less than +/-0.5mm.

430 Offset along Telescope's Optical Axis
The instrument shall be positioned at the nominal focus position along the optical axis with an uncertainty of less than +/-1mm. Note that a placement error of less than 1mm along the optical axis can be corrected with a telescope refocus. Spherical aberration begins to be significant for larger offsets.

The instrument shall maintain this fixed position in the z-direction to +/- 0.05mm for an elevation change of 30 degrees or less at any fixed rotator angle.

500 Temperature Case Studies
The thermal models indicate that several degree temperature gradients may be present. The primary effect of these temperature gradients is on the airspaces between lenses, although thermal gradients will also have an impact on surface curvature and refractive index. Here the temperature gradients are assumed to adjust the element spaces relative to those expected for a uniform optical bench. The CTE of Al-6061 has been assumed to be 18e-6/K, although at cryogenic temperatures the value is closer to 6e-6/K. The estimates below are thus likely to be strong upper limits and neither of the cases considered below affect the image quality.

510 Temperature Gradient between L3 and L4
L3 and its mount is likely to be warmer than the other elements because it is the first element in the camera dewar and it has the longest conductive path to the LN2 reservoir. The distance between L3 and L4 is 151mm. A 5K gradient corresponds to a change of 9e-5 or an increase in the separation of approximately 0.01mm. This does not affect image quality.

520 10K temperature gradient between L3 and L8
This case considers a temperature gradient from L3 through the end of the collimator VEE block and is intended to mimic instrument behavior as the cryogen is depleted. This temperature gradient was input into ZEMAX by distributing the increased distances among all of the airspaces from L3 to L8 according to the size of the separation. This larger temperature gradient similarly did not affect image quality.

530 Impact of Temperature Gradients on Index Data and Surface Curvature
A preliminary analysis indicates that a 3K temperature change degrades the image quality by 10%. A more detailed analysis of how temperature gradients affect image quality will be done before the final optimization of the optical design.

600 Requirements for Optics Bid Package
This section describes the fabrication requirements for the optical elements that are to be included in the Optics Bid Package.

610 Parameters for all surfaces
The following sections provide an overview of the terms used in the fabrication specifications.

611 Material

The glass for the lens shall be clearly specified. In cases where there are multiple grades of a given material, the grade must also be noted. A recommended vendor for the raw material may also be specified. SAO will supply the raw material for the S-FTM16 lenses.

612 Reference Wavelength

The reference wavelength for interferometric tests shall be specified on each drawing. The reference wavelength is 6328 Angstroms.

613 Center Thickness Tolerance

This is the thickness of the lens at the center of curvature of each surface and shall be met to within 0.05mm. The manufacturer shall measure and report the thickness of the lens to 0.01mm.

614 Surface Quality

Surface quality shall be in compliance with MIL-O-13830A. Spherical surfaces and the aspheric surface shall have a scratch/dig of 40-20. All other surfaces shall have a scratch-dig of 80-50.

615 Surface Figure

Surface finish is a tolerance on small-scale irregularities. This shall be specified in terms of Angstroms rms measured within a fixed aperture. The spherical surfaces shall not depart from a purely spherical shape by more than 0.5 fringes over the entire clear aperture.

616 Radius of Curvature Tolerance

The tolerance on the radius of curvature is a measure of the deviation from the specified sagittal power. The radius of curvature must be measured in a temperature-controlled environment at a temperature of 20+/-1 C. The radius of curvature tolerance will be specified in units of radius (mm). The formula to convert a dimensional radius tolerance to a tolerance in fringes is:

$$N = \frac{2\Delta R}{\lambda}\left[1 - \sqrt{1 - \left(\frac{\phi}{2R}\right)}\right]$$

where N is the number of fringes, ΔR is the dimensional radius tolerance, λ is the reference wavelength, φ is the diameter of the clear aperture, and R is the radius of curvature. This equation can be approximated by

$$N = \frac{\Delta R}{4\lambda}\frac{\phi^2}{R^2}$$

for the case where φ/R is small.

The radius of curvature must be within 0.1% of the specified radius value and reported to within 1 fringe or better. This measurement shall be performed in a temperature-controlled environment between 20-25 C and the temperature at the time of measurement shall be reported to 0.5 C.

617 Centration or Lens Thickness Runout or Edge Thickness Difference

The centration of the surfaces on the lens shall be expressed in terms of either the lens thickness runout or the edge thickness differences. The edge thickness difference is the difference between the maximum and minimum thickness of the lens measured at the radius of the clear aperture. The edge thickness difference

(ETD) is related to surface tilt (TSTX/Y) by the equation: TSTX(Y)=ETD/φ. The edge thickness difference is a measure of either surface tilt or decenter for spherical surfaces.

618 Diameter of lens

The diameter of the lens shall be within 0.1mm of the specified value and the manufactured diameter shall be measured with a precision of 0.01mm.

620 Additional Specifications for Aspheric Surface

Slope errors on the aspheric surface shall be less than 0.00001 radians on all scales up to the clear aperture diameter. The aspheric surface error shall be less than 0.5 fringes over the entire clear aperture diameter. The aspheric surface shall be measured with a CGH.

630 Specifications for Coatings

The coatings specifications are summarized in the document MMIRS-S-207.

MMIRS Ghost Analysis

Paul Martini
October 22, 2004

100 Overview

This document describes a ghost analysis of the MMIRS preconstruction design, which is described in "MMIRS_Preconstruction_Design_rev_a.pdf" by D. Fabricant. This document is in reference to the Ghost Image and Pupil requirements of the MMIRS Functional and Performance Requirements, in particular sections 144 and 145.

For every potential double-bounce reflection in the instrument, the ZEMAX Ghost Focus Generator was used to determine the distance of the ghost focus and ghost pupil from the image plane. The separation of each ghost focus and ghost pupil from the image plane was calculated with both the output distance from ZEMAX and the effective f/# of the double bounce system. Below I summarize the worst ghost foci and ghost pupils and attach accompanying figures of the ZEMAX files for several cases. **The result of this analysis is that none of these ghosts are significant**.

200 Ghost Focii

Several of the worst case ghost foci are:

S1	S2	F/#	RMS [mm]	Distance [mm]	D/(F/#)
17	4	2.48	6.78	-5.76	-2.32
25	11	7.45	1.23	17.73	2.38
27	13	5.19	4.18	-18.44	-3.55
28	6	2.29	1.89	-15.49	-6.75

All of these double-bounce reflections produce ghosts greater than 2mm in diameter and most only produce these images on axis. Spot diagrams for reflections 17-4 and 25-11 are presented in Figures 1 and 2. The intensities of both of these ghost images are below 10^{-6} of the original image.

300 Ghost Pupils

Several of the worst case ghost pupils are:

S1	S2	F/#	RMS [mm]	Distance [mm]	D/(F/#)
33	32	1240.5	2.65	-49.23	-0.04
30	13	770.64	5.21	-311.05	-0.40
33	25	106.51	9.03	73.89	0.69
29	17	1.23	26.7	-1.61	-1.31

None of these reflections produce significant ghost pupils. Ray diagrams and the relative illumination plots are shown for reflections 33-32 and 30-13 in Figures 3 and 4

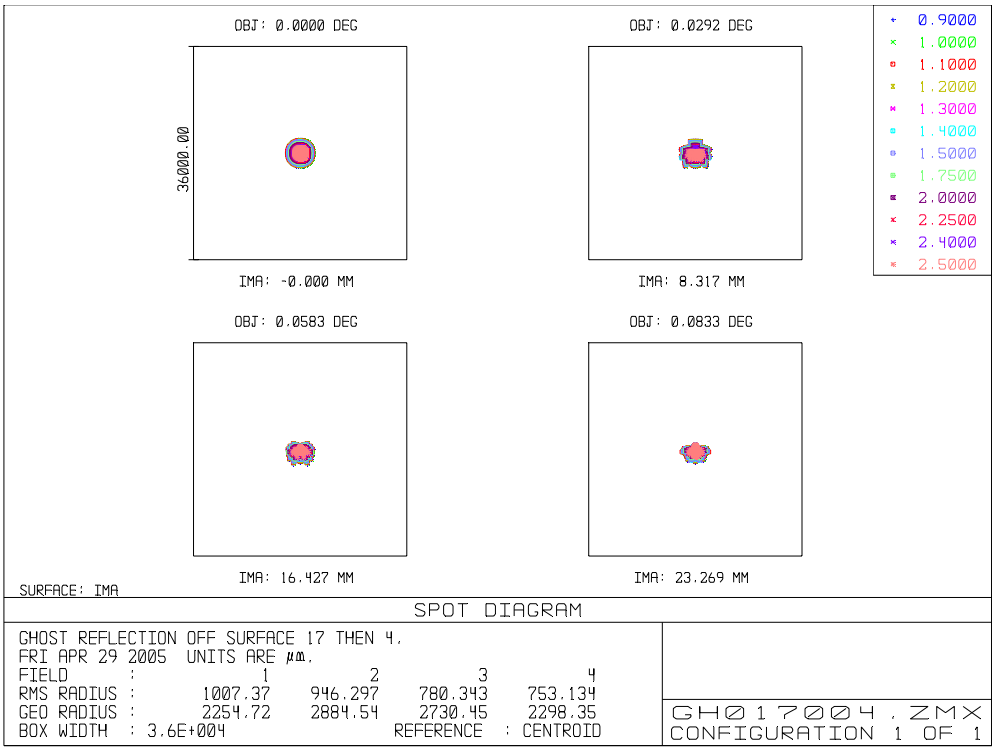

Figure 1: Ghost Image produced by double-bounce reflection off surface 17 and then off surface 4.

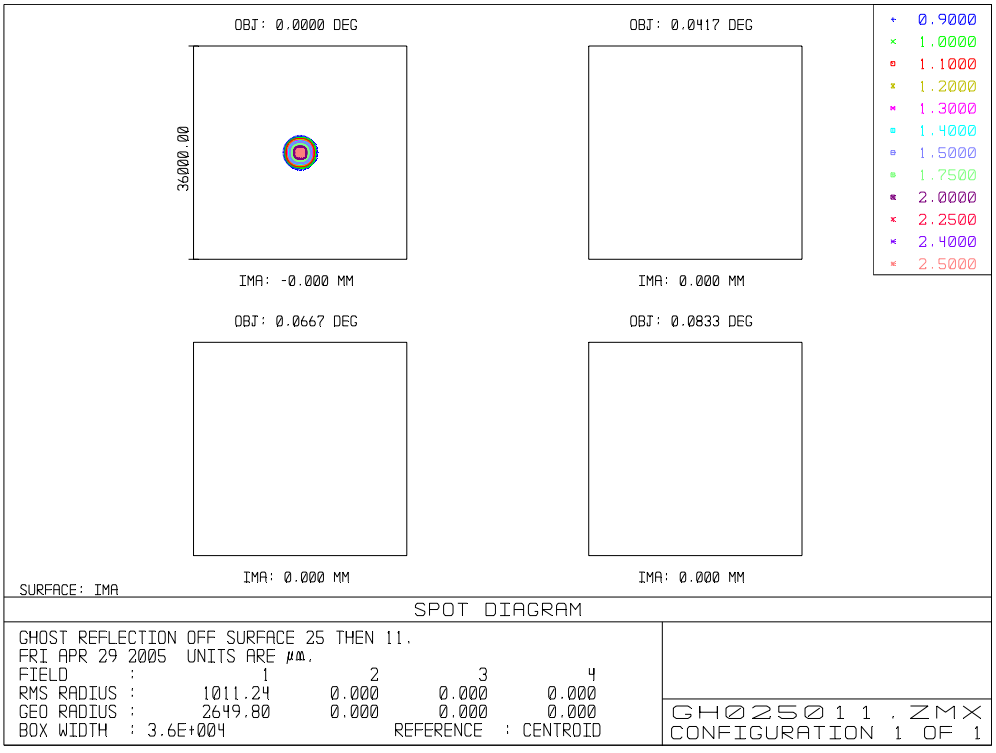

Figure 2: Ghost Image produced by double-bounce reflection off surface 25 and then off surface 11. This ghost is only important on-axis. Rays more than 2 arcminutes off axis are vignetted.

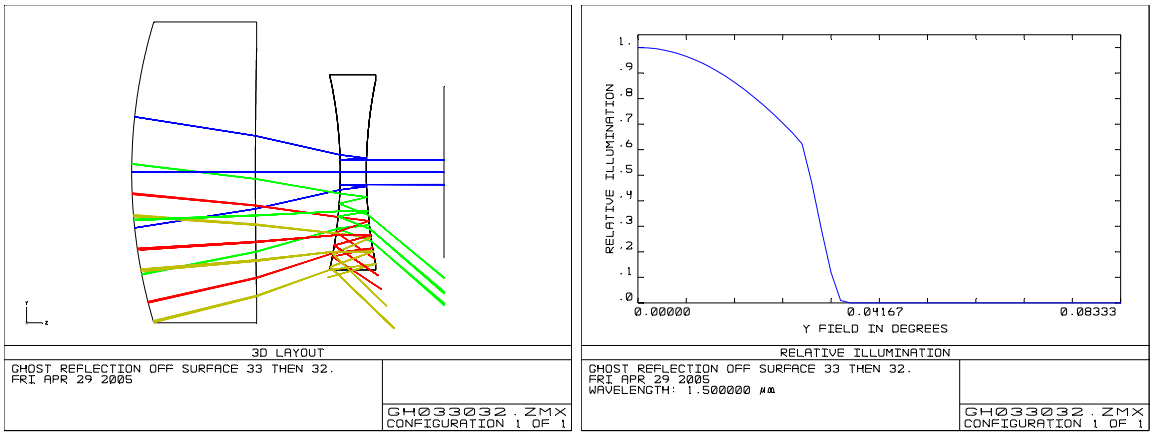

Figure 3: Ray diagram (left) and relative illumination (right) for a ghost reflection off surfaces 33 and then 32. The ray diagram includes lenses 13 and 14.

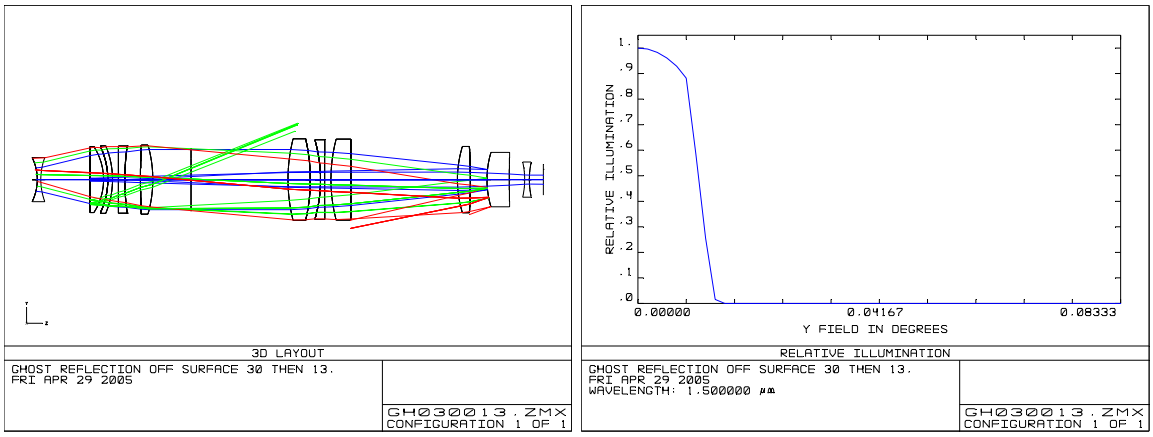

Figure 4: Ray diagram (left) and relative illumination (right) for a ghost reflection off surfaces 30 and then 13. The ray diagram includes lenses 5 and 14.

MMIRS Throughput Calculation

Paul Martini
April 26, 2005

Overview

This document describes the throughput of the MMIRS instrument in relation to section 160 of the MMIRS Functional and Performance Requirements (F&PR; S-MMIRS-200). The F&PR is the instrument's controlling document, so if there are any discrepancies between this document and the F&PR, the F&PR shall prevail. The throughput requirements are >50% throughput in imaging mode (goal 70%) and >30% in spectroscopic mode (goal 40%). These requirements are for the instrument's optical elements alone and do not include the atmosphere, telescope, or detector.

Imaging Mode

In imaging mode there are 14 single lenses (28 surfaces) and a filter. For 1% coatings on these 28 surfaces and 90% throughput for a filter the total throughput is 68%. The throughput is 51.1% for 2% coatings. An average coating of 2% or better will therefore meet the requirement and an average of 1% or better will meet the goal.

Spectroscopic Mode

In spectroscopic mode there is an additional surface on the grism (31 surfaces) and additional losses in the grating. For an assumed grating loss of 25% and 1% coatings the throughput is 50.4% and 37.6% for 2% coatings.

MMIRS-S-207
Coating Specifications

Version 2005.03.03

Overview: The MMIRS instrument contains 19 optical elements comprised of 14 lenses and 5 prisms in two, interconnected vacuum dewars. Lens 1 is the window of one dewar and its first surface faces ambient atmospheric conditions. Lens 2 operates inside the same dewar and will operate at a temperature approximately 10° C below ambient. Lenses 3 through 14 and the 5 prisms are in the second vacuum dewar and operate at a temperature of approximately -196° C. Each of these 19 optical elements is listed below, along with the reference drawing number, material, wavelength ranges of operation, and the maximum incidence angle of rays relative to the surface normal.

Element	Drawing	Material	Wavelength Ranges				Max Incidence (°)
			1	2	3	4	
1	MMIRS-1001	CaF2	Y	Y	Y	Y	10
2	MMIRS-1002	CaF2	Y	Y	Y	Y	12
3	MMIRS-1003	CaF2		Y	Y	Y	15
4	MMIRS-1004	CaF2		Y	Y	Y	18
5	MMIRS-1005	BaF2		Y	Y	Y	12
6	MMIRS-1006	ZnSe		Y	Y	Y	13
7	MMIRS-1007	FQTZ		Y	Y	Y	13
8	MMIRS-1008	CaF2		Y	Y	Y	8
9	MMIRS-1009	CaF2		Y	Y	Y	10
10	MMIRS-1010	S-FTM16		Y	Y	Y	4
11	MMIRS-1011	CaF2		Y	Y	Y	7
12	MMIRS-1012	BaF2		Y	Y	Y	14
13	MMIRS-1013	CaF2		Y	Y	Y	21
14	MMIRS-1014	S-FTM16		Y	Y	Y	11
P41-1	MMIRS-1015	CaF2		Y			0
P41-2	MMIRS-1015	CaF2			Y		0
P41-3	MMIRS-1015	CaF2				Y	0
P21	MMIRS-1016	CaF2		Y	Y		0
P18	MMIRS-1017	CaF2			Y	Y	0

1. **Lens Reflectivity Requirement:** The mean reflectivity requirements are specified separately for four wavelength ranges:
    - **Range 1:** 500-900nm, 5%
    - **Range 2:** 900-1250nm, 0.5%
    - **Range 3:** 1400-1800nm, 0.5%
    - **Range 4:** 1950-2350nm, 0.5%

The peak reflectivity shall be less than 1.0 % in wavelength ranges 2-4 and the spatial uniformity of the coatings shall be better than 0.2% rms. These specifications are for the average of the S and P polarizations.

2. **Angle of Incidence Requirement:** All coatings shall meet the reflectivity requirement for incidence angles up to the value provided in the Table. These incidence angles are relative to the surface normal.

3. **Operational Pressure:** All coatings shall meet the performance requirements at both atmospheric pressure and in vacuum.

4. **Operational Temperature:** The coatings on lenses 1 and 2 shall meet the performance requirements over the temperature range -20° to +40° C. The coatings on lenses 3 through 14 and the prisms shall meet the performance requirements over the temperature range from -200° to +40° C.

5. **Radioactivity:** The coatings shall not employ radioactive materials

6. **Durability:**

    - **Cleaning:** The coatings shall survive without damage 20 brief (ten minute or less), gentle cleanings with a cotton swab wetted with ethyl alcohol, isopropyl alcohol, acetone, or a mild detergent solution.
    - **Condensation:** The coatings shall survive without damage 10 brief (twenty minute or less) incidents of water condensation, such as produced by material temperatures below the ambient dew point.
    - **Thermal and pressure cycling of lenses 1 and 2:** The coatings shall survive without damage daily cycling between temperatures of -20° and +40° C and pressures between vacuum and atmospheric for a period of ten years.
    - **Thermal and pressure cycling of lenses 3 through 14 and prisms:** The coatings shall survive without damage for 100 cycles between temperatures of -200° and +40° C and pressures between vacuum and atmospheric over a period of ten years.

7. **Testing:**

    - **Reflectivity:** The reflectivity of each surface over its operational wavelength range shall be measured and reported to SAO. Witness samples of each material at normal and the maximum angles reported in the Table for the respective material shall be coated and measured. Witness sample material (including S-FTM16) shall be provided by the vendor.
    - **Durability:** The witness samples shall be exposed to ten chemical cleanings with a cotton swab and thermally cycled between approximately -196° and 20° C. The reflectivity of the coatings over the operational wavelength range shall then be measured and reported to SAO.

MMIRS Grism Design

Brian McLeod 28 April 2006

Wavelength Coverage

MMIRS will have five grisms. Three will provide R=3000 coverage of each of the J, H, and K windows. The fourth will cover J+H simultaneously and the fifth, H+K simultaneously, each at a resolution of 1300. The spectrum will map onto 1400 pixels of the 2048 pixel detector. This allows for a 2 arcminute wide strip of the sky to receive full spatial coverage: (2048-1400)*0.2"/pix = 130". The slit mask plates will be 4 arcminutes wide, allowing for additional spatial coverage with incomplete spectral coverage.
The exit angle from the grism that corresponds to +/-700 pixels is +/-2.60 degrees

The wavelength ranges to be covered were specified in the initial MMIRS proposal as

Table 1 (from MMIRS proposal)

Grism	Wavelength Range	Grooves/mm	Prism Angle	Facet Angle	Resolution (2 pixel slit)	Theoretical Efficiency across band
J	1.11-1.39	230	41°	32°	3000	64-70%
H	1.45-1.82	175	41°	32°	3000	64-70%
K	1.95-2.45	130	41°	32°	3000	64-70%
JH	0.95-1.82	94	18°	14°	1300	55-80%
HK	1.45-2.45	80	21°	17°	1300	55-80%

In Table 2, I have substituted the values for the Flamingos2 JH and HK gratings and recomputed the wavelength ranges using the current optical prescription, assuming a CaF2 prism (n=1.43). The wavelength ranges are shown graphically in Figure 1.

Table 2

Grism	Grooves/mm	Prism Angle	Resolution (2 pixel slit)	Wavelength at -2.6 deg	Straight through wavelength	Wavelength at +2.6 deg
J	230	41°	3000	1.08	1.23	1.38
H	175	41°	3000	1.42	1.61	1.81
K	130	41°	3000	1.91	2.17	2.44
JH	98.264	18°	1300	0.92	1.35	1.79
HK	81.571	21°	1300	1.38	1.89	2.41

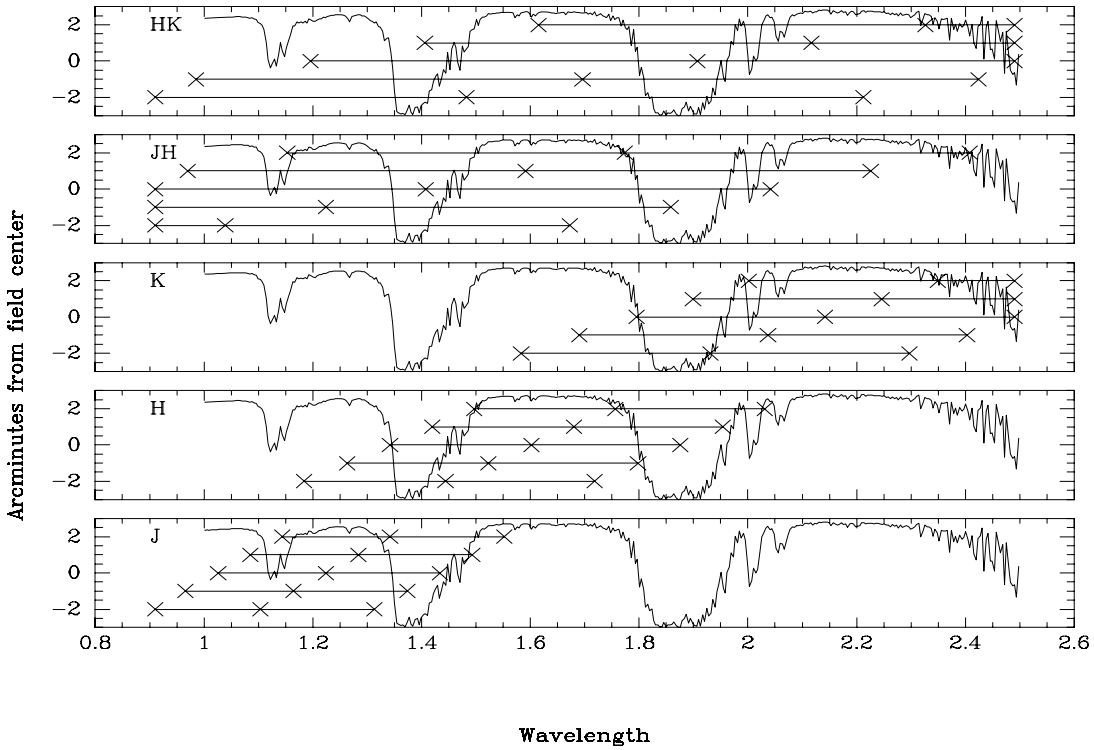

Figure 1. The range of wavelengths falling on the 2048 pixel wide detector is shown for each of 5 field angles (-2',-1',on-axis,+1',+2'). The vertical axis is in arcmin, the horizontal is wavelength in microns. The atmospheric transmission is shown for reference.

Grating Efficiency

In this section I show plots of theoretical grating efficiency computed with PCGrate2000MLT. I have assumed that the resin index is 1.53. The grating parameters are summarized in the Table 3. Note that the incident angle differs from the prism angle due to refraction when passing from the prism into the resin.

Table 3. (Note: as of this writing I am unsure of the Facet Angle actually being used in the Flamingos2 JH and HK grisms. The numbers in the table are my optimization.)

Grism	Grooves/mm	Prism Angle	Incident Angle	Facet Angle
J	230	41°	38°	32°
H	175	41°	38°	32°
K	130	41°	38°	32°
JH	98.264	18°	17°	?? 14°
HK	81.571	21°	19°	?? 17°

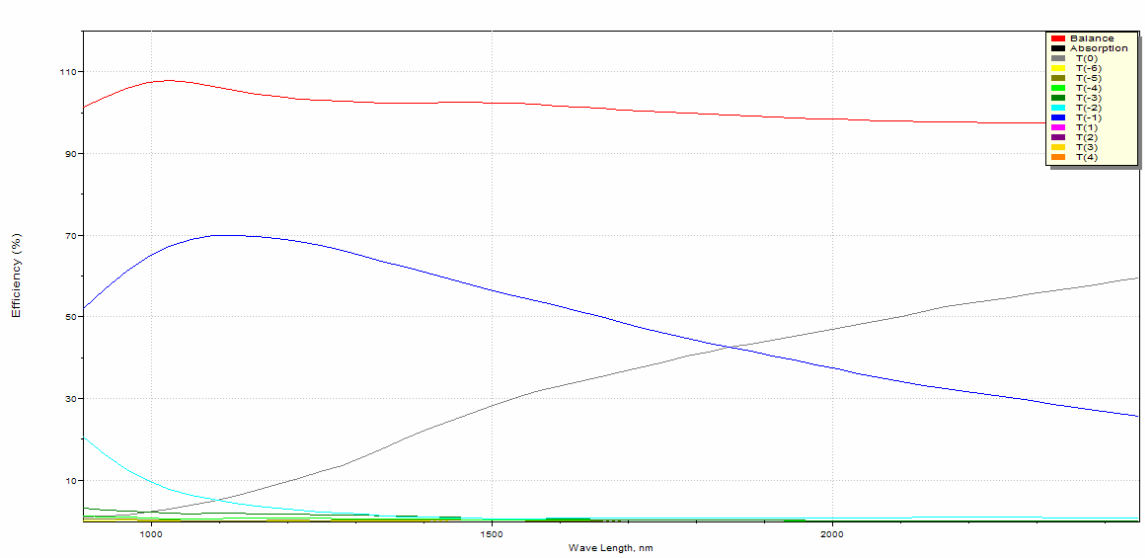

Figure 2. J grating efficiency. The top curve (red) is the total power in all orders (nominally 100%). The curve of interest is the second from the top (blue), representing 1st order.

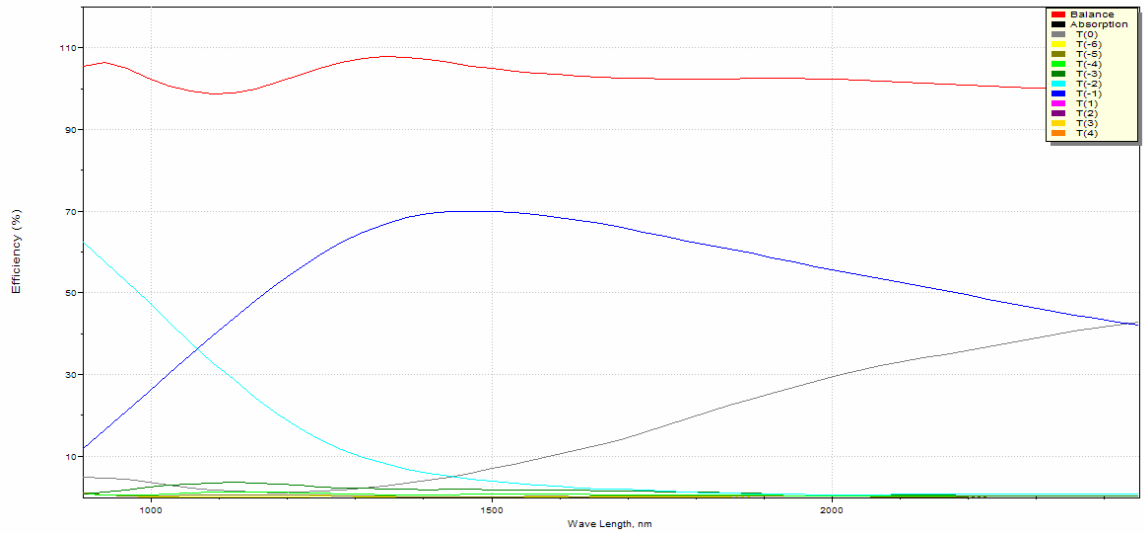

Figure 3. H grating efficiency. The top curve (red) is the total power in all orders (nominally 100%). The curve of interest is the second from the top (blue), representing 1st order.

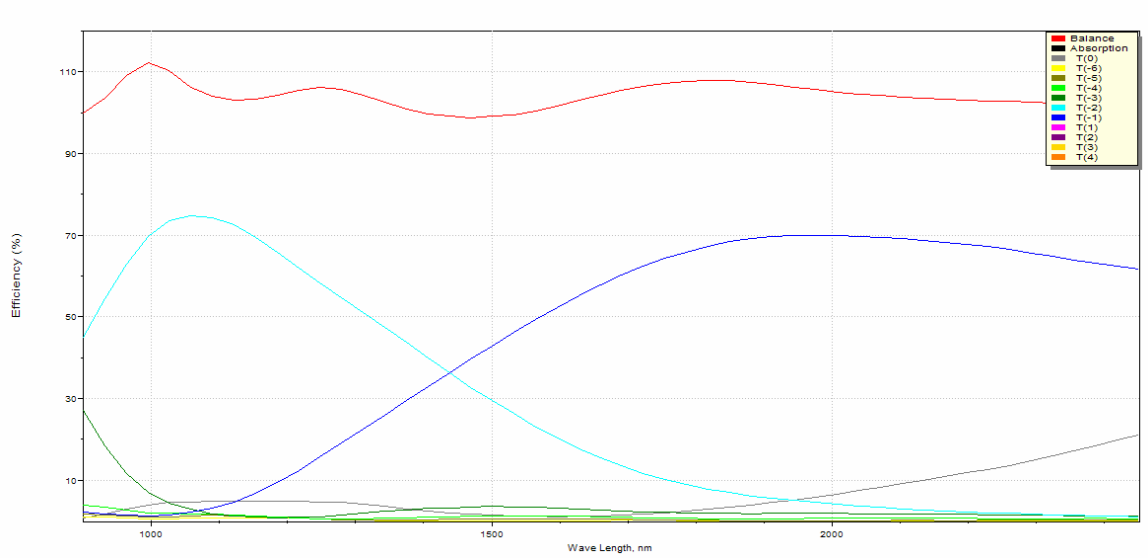

Figure 4. K grating efficiency. The top curve (red) is the total power in all orders (nominally 100%). The curve of interest is the second from the top (blue), representing 1st order.

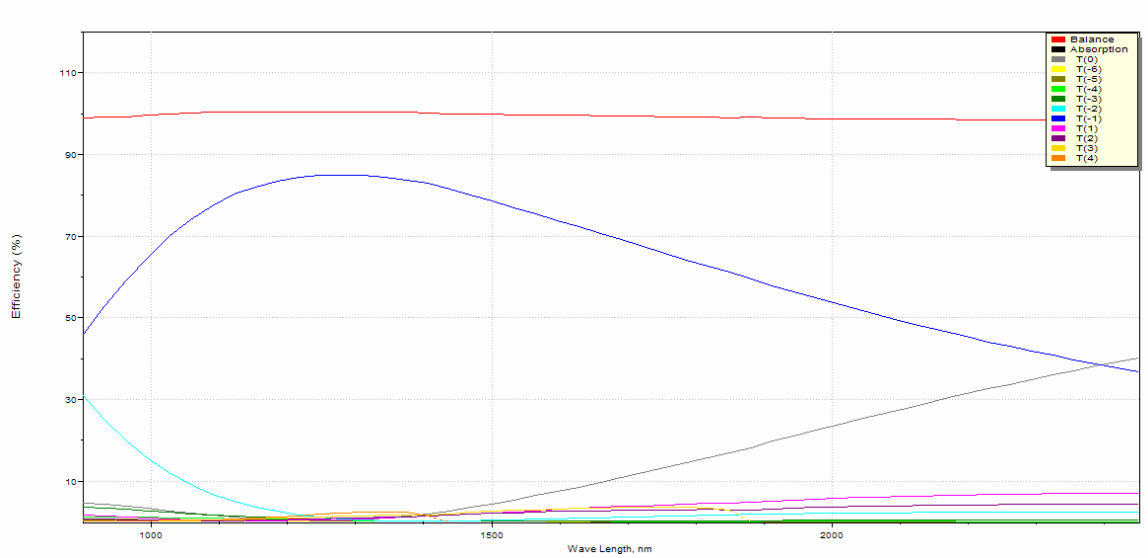

Figure 5. JH grating efficiency. The top curve (red) is the total power in all orders (nominally 100%). The curve of interest is the second from the top (blue), representing 1st order.

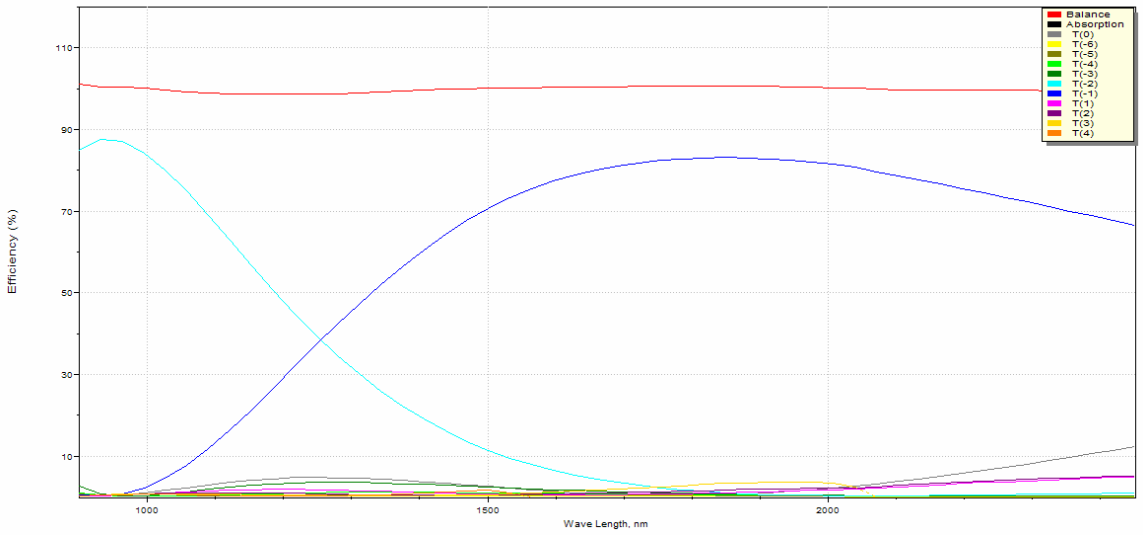

Figure 6 HK Grating efficiency. The top curve (red) is the total power in all orders (nominally 100%). The curve of interest is the second from the top (blue), representing 1st order.

A single grating for J, H, and K at R=3000?

For comparison we plot the efficiency of using a single grating at R=3000 in orders 4, 3 and 2 to get spectra at J, H, and K. While the peak transmission is slightly higher than using the gratings in first order as shown above, the transmission falls off fairly rapidly with wavelength and so we prefer the separate grating approach. This grating has 67gpm with 38 degree incident angle, and 32 degree facet angle.

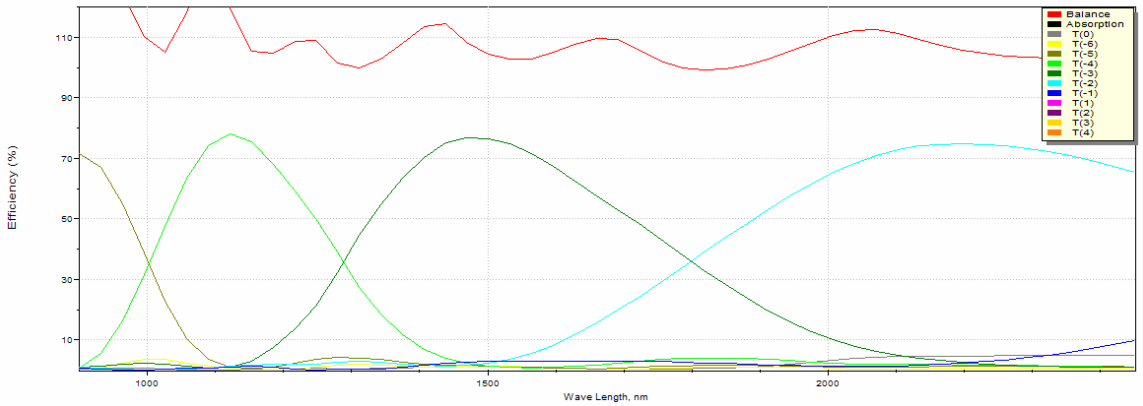

MMIRS Fringing Report

Paul Martini
February 11, 2005

Updated April 29, 2005 [PM]

100 Overview

The MMIRS Hawaii-2 detector array will experience fringing due to optical interference in the detector's sapphire substrate. Fringing causes a modulation of the detector's sensitivity when illuminated by dispersed light and therefore can adversely affect spectroscopic observations. In principle, fringing can be removed by dividing by a flat field. However, any shift in the way light is dispersed onto the detector between the flat field and the science observations, most notably due to instrument flexure, will result in an imperfect fringing correction. This document describes the origin of the fringing, calculates its periodicity for the MMIRS spectroscopic modes, and estimates the magnitude of the error as a function of flexure. The final result of this analysis is that flexure should be less than 0.1 pixels between the science and flatfield observations and therefore a flatfield mechanism should be developed so that flatfields can be obtained at the same instrument orientation as the science observations.

200 Nature of Fringing

The Hawaii detectors manufactured by Rockwell have a sapphire layer above the HgCdTe detector material. Fringing is caused by multiple reflections and optical interference within the sapphire layer. In spectroscopic mode, the wavelength of light striking the detector will vary with position. This linear dispersion in microns per pixel due to a grism can be described by the following formula:

$$d = \frac{dl}{dx} = \frac{\cos t}{mgf} p$$

where cos *t* is the prism angle, *m* (=1) is the grating order, *g* is the groove spacing, *f* is the MMIRS camera focal length (=285mm), and *p* is the pixel size (18 microns).

The multiple reflections of light inside the sapphire layer are very analogous to a Fabry-Perot and the order of the interference as a function of wavelength can be calculated with the Fabry-Perot equation:

$$m(l) = \frac{2nd \cos y}{l}$$

where *m* is now the interference order (not the order of the dispersed light, which is always 1 for the MMIRS grisms), *l* is the wavelength of the dispersed light in microns, *n* is the refractive index of sapphire layer (=1.74), *d* is the thickness of this layer (=381 microns; McGregor 2000), and *y* is the incident angle of the light on the sapphire layer. This is shown in Figure 1 below. Note that for small values of *y* the order is essentially independent of *y*.

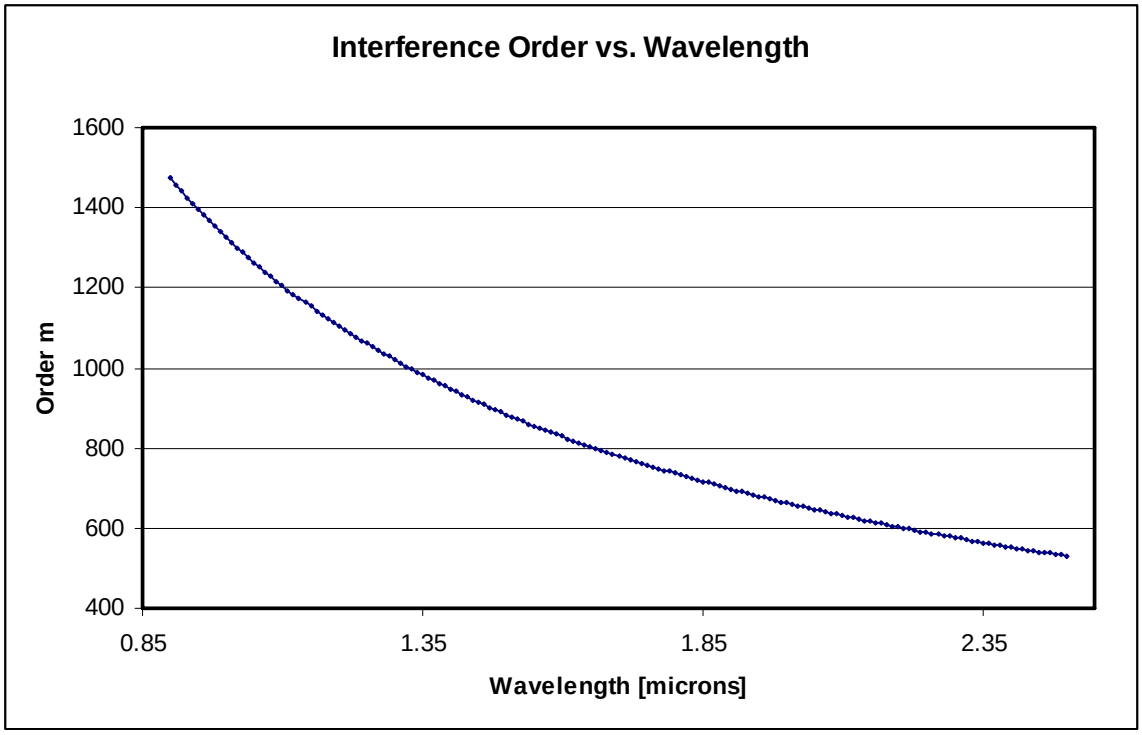

Figure 1: Expected Interference Order vs. Wavelength for the MMIRS detector.

Here *y* is assumed to be zero and the actual interference order for some *y* can be calculated by multiplying the value of *m* by cos *y*.

230 Fringe Periodicity

The interference order *m* is a function of wavelength and the fringe spacing in pixels at a given wavelength is set by both the wavelength difference between *m(l)* and *m(l)+1* and the linear dispersion of the grism. The fringe spacing *F* as therefore a function of wavelength:

$$F(l) = \frac{l}{d\left[\frac{2nt\cos y}{l} + 1\right]}$$

for a linear dispersion *d* (in microns per pixel). For a given flexure error in pixels and fixed fringe amplitude, the wavelengths and resolution modes with the closest fringe spacings will produce the largest errors in the fringe correction. The above equation therefore indicates that shorter wavelengths and lower linear dispersions are likely most sensitive to errors in the fringing correction. The next five figures (Figure 2 collectively) show the fringe spacing *F* in pixels as a function of wavelength for the five MMIRS spectroscopic modes.

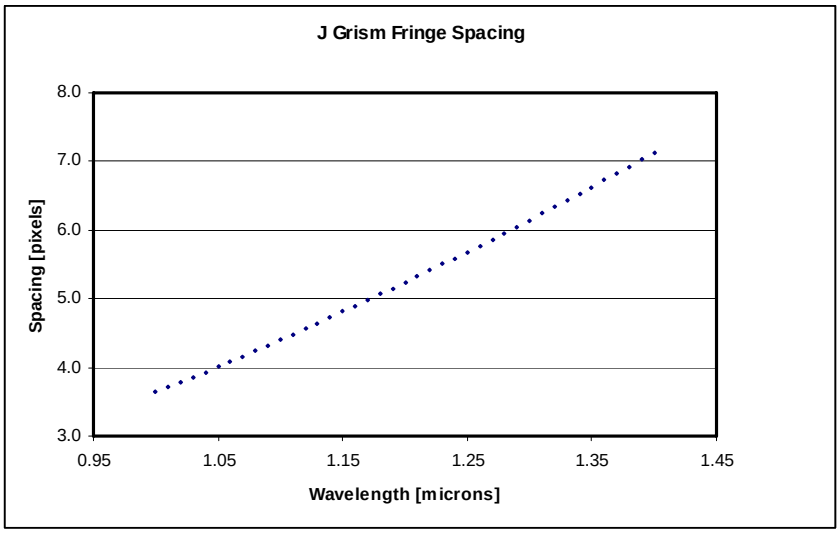
J Grism Fringe Spacing
Spacing [pixels]
8.0
7.0
6.0
5.0
4.0
3.0
0.95
1.05
1.15
1.25
1.35
1.45
Wavelength [microns]

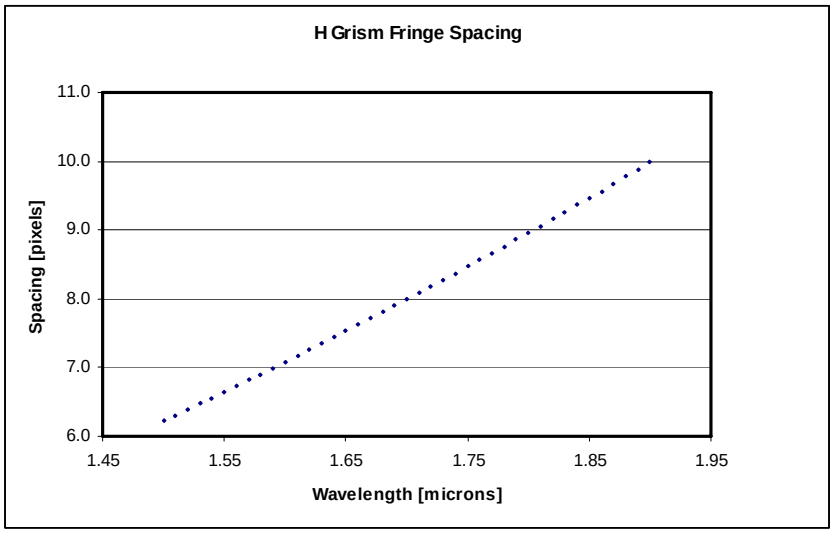
H Grism Fringe Spacing
Spacing [pixels]
11.0
10.0
9.0
8.0
7.0
6.0
1.45
1.55
1.65
1.75
1.85
1.95
Wavelength [microns]

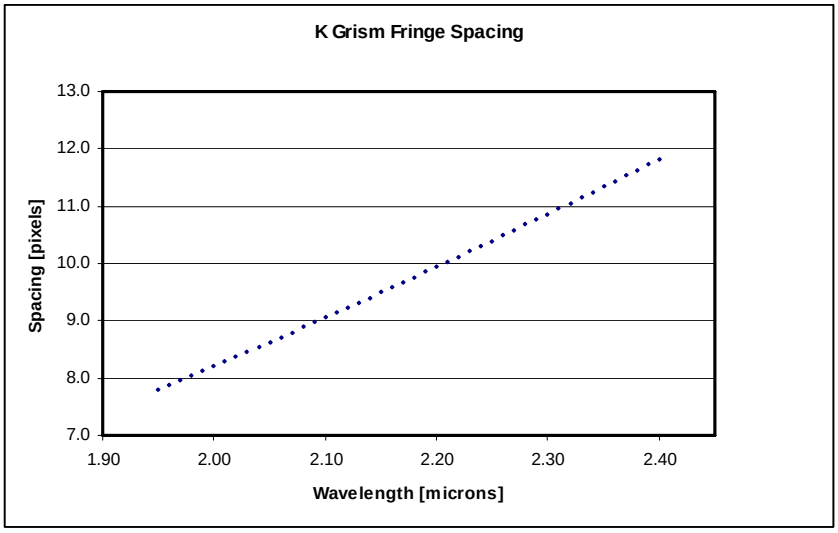
K Grism Fringe Spacing
Spacing [pixels]
13.0
12.0
11.0
10.0
9.0
8.0
7.0
1.90
2.00
2.10
2.20
2.30
2.40
Wavelength [microns]

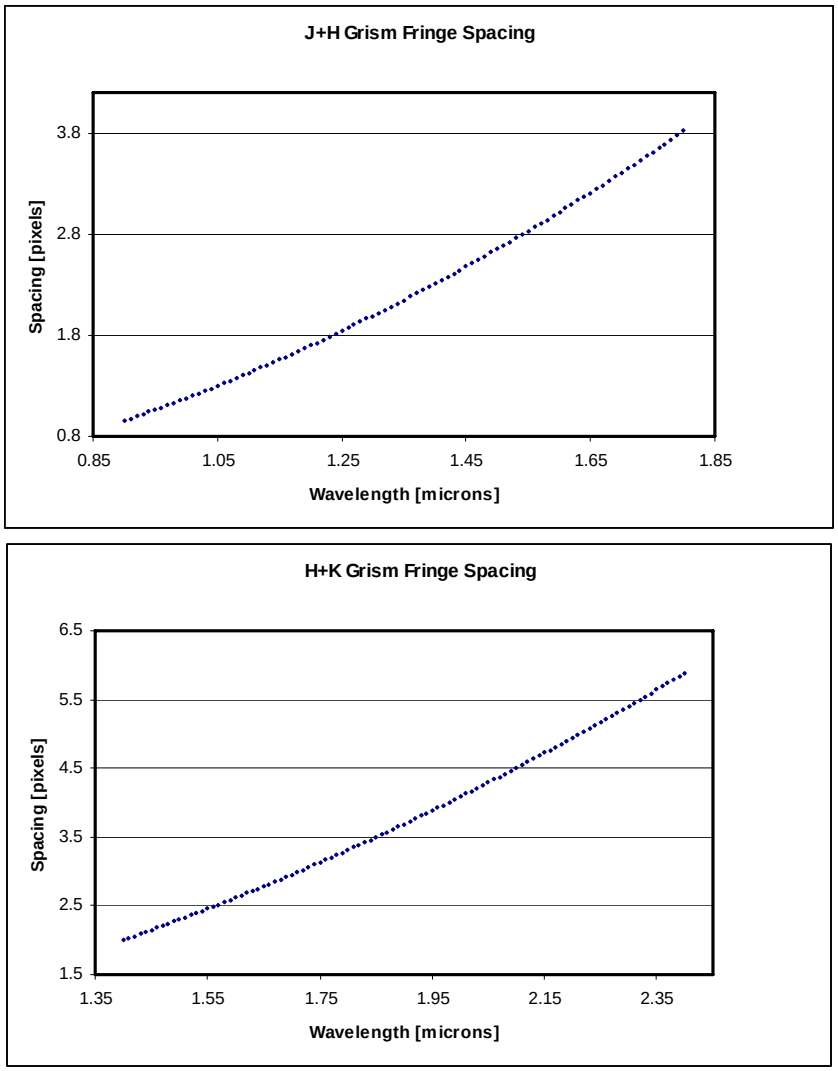

Figure 2: Fringe Spacing vs. Wavelength for the five MMIRS spectroscopic modes.

300 Impact of Flexure on Calibration

The total pixel-to-pixel sensitivity variation can be expressed as some background level *B* and an additional fringing modulation with amplitude *A* whose functional form can be described by a cosine:

$$f(p) = B + A\cos\left(\frac{2\pi p}{F}\right)$$

where *F* is the wavelength-dependent fringe spacing in pixels and *p* is the pixel coordinate. The fringing modulation is actually integrated over each pixel, so the contribution per pixel is:

$$\Gamma = B + \frac{AF}{2\pi}\left[\sin\left(\frac{2\pi(p+1)}{F}\right) - \sin\left(\frac{2\pi p}{F}\right)\right]$$

If there is some flexure *df* in pixels, the fringing modulation is:

$$\Gamma' = B + \frac{AF}{2\pi}\left[\sin\left(\frac{2\pi(p+df+1)}{F}\right) - \sin\left(\frac{2\pi(p+df)}{F}\right)\right]$$

If there has been some amount of flexure *df* between the observation and the flatfield, the error as a function of fringe spacing can be expressed as:

$$E(df,F) = \frac{\Gamma}{\Gamma'} = \frac{1 + \frac{AF}{2\pi B}\left[\sin\left(\frac{2\pi(p+1)}{F}\right) - \sin\left(\frac{2\pi p}{F}\right)\right]}{1 + \frac{AF}{2\pi B}\left[\sin\left(\frac{2\pi(p+df+1)}{F}\right) - \sin\left(\frac{2\pi(p+1)}{F}\right)\right]}$$

For a given grism, the magnitude of the error induced by flexure at any given pixel depends on the fractional amplitude of the fringing *A/B* and the size of the flexure relative to the fringe spacing at that pixel. According the NIFS documentation (MacGregor 2000), which quotes a report from Hodapp et al. (1996) on the Hawaii-1 detector, this amplitude is approximately 10%. For factor of two or less changes in the amplitude, the fringing error scales linearly with amplitude.

The size of the error at any given pixel depends on wavelength because the fringe spacing depends on wavelength and therefore the flexure *df* and the fringe spacing *F* beat against one another like waves of different frequency. While the errors at the locations of the brightest OH sky lines may be the most critical quantities for accurate sky subtraction, the maximum fractional deviation from a perfect correction (*E=1*) is a reasonable, and more general, measure of the error induced by flexure. This quantity, termed the 'Fringe Correction Error' is shown in Figure 3 below for all five spectroscopic modes of MMIRS as a function of flexure in pixels.

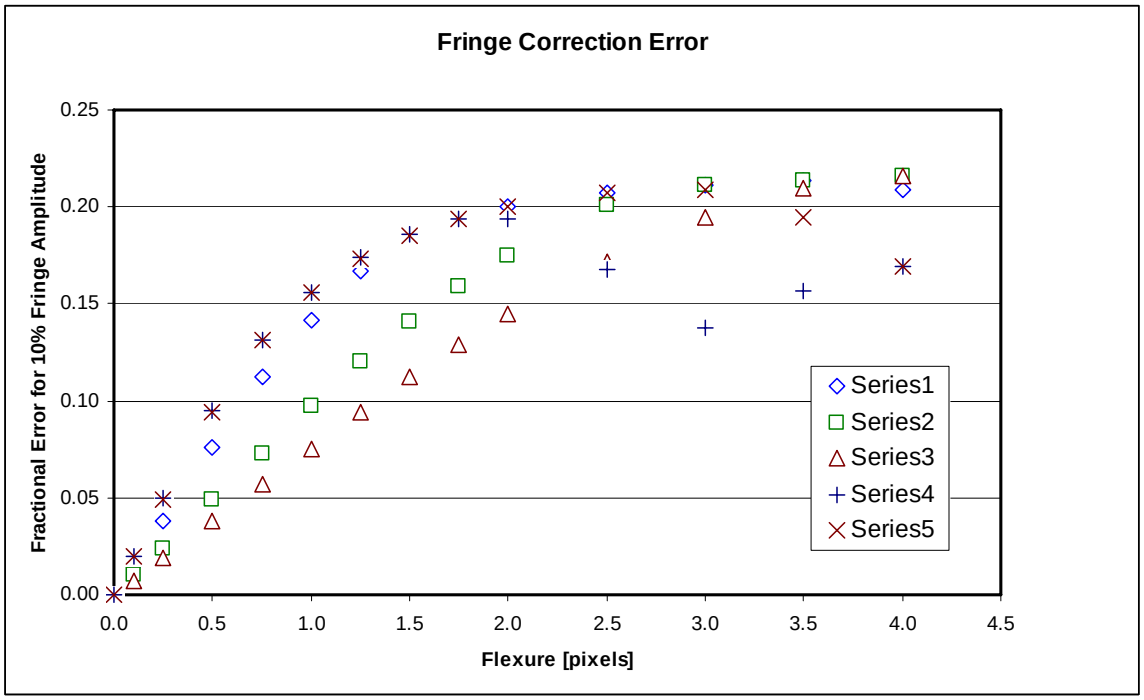

Figure 3: Series 1, 2, and 3 correspond to the medium resolution J, H, and K grisms, respectively. Series 4 and 5 correspond to the lower resolution J+H and H+K grisms, respectively.

For the moderate resolution grisms, the fractional error is largest with the shortest-wavelength *J* grism. This is because the fringe spacing is smallest at the shortest wavelengths and thus a given amount of flexure corresponds to a larger fraction of the fringe spacing *F*. The error 'saturates' at approximately half the typical fringe spacing for a given setting at a value approximately twice the fringe amplitude. For the *J+H* and *H+K* grisms the fractional errors are nearly identical for all but the smallest flexures. This appears to be because the fringe spacing is within a factor of a few for these grisms.

400 Conclusion

Based on this analysis, flexure of less than 0.1 pixels is necessary to achieve calibrations good to 1%. As MMIRS does not have an active flexure compensation mechanism, it is unlikely that the mechanical design will achieve this goal. The best solution for critical applications is therefore to obtain flatfield observations with the same instrument orientation as the science observations. One possible solution is to include a diffuser in the Dekkar wheel. Note that better than 1% calibrations are likely to be limited by variations in the time- and wavelength-dependent telluric absorption. The best solution in this case may be to include a relatively flat-spectrum object in one of the spectroscopic slits.

References

- McGregor, P. (2000), "Fringing Effects in the NIFS Science Detector," SDN0008.10, http://www.mso.anu.edu.au/nifs/sdns/sdn0008.10.htm.
- Hodapp, K. et al. (1996), New Astronomy, 1, 177.

Section II.8

Stray Light Analysis

This document will be available at the CDR.

Section III.

MOS Section Design

1. MOS Specifications
2. MOS Section Mechanical Design
3. MOS Design Supporting Calculations
   a. MOS and Dekker Wheel Drivetrain Calculations
   b. MOS and Dekker Wheel Repeatability Calculations
   c. Guider and WFS Mechanism Calculations
   d. MOS Long Slit Sizing Calculations

MMIRS MOS SPECIFICATIONS

S-MMIRS-201

George Nystrom
February 23, 2004

Updated May 27, 2004 by GN [PDR version]
Updated April 20, 2005 by GN [edits]
Updated April 29, 2005 by PM [reformatted, minor edits]

100 Introduction

This document details the specifications for the Multi-Object Slit Section (MOS Section) of the MMIRS instrument. The MMIRS Functional and Performance Requirements document (F&P; document number S-MMIRS-200) is the instrument's controlling document. If there are any discrepancies between the F&P and this document, the F&P shall prevail.

The MOS Section mounts directly to the Camera Section's front vacuum bulkhead and provides the structural attachment points and a vacuum enclosure for all of the assemblies listed below. The MOS Section includes thermal shields, an LN2 reservoir and feedthroughs, electrical interface connectors, a G10 support ring, and the structural interface to the Camera Section. The specifications for the Camera Section are presented in the document S-MMIRS-203.

The following F&P requirements and specifications are particularly relevant to the MOS Section:

1. Section 100—Optical Requirements
2. Section 300—Mechanical Requirements
3. Section 400—Electrical and Electronic Requirements
4. Section 600—Observatory Physical Interface
5. Section 700 – Environmental Requirements
6. Section 800—Other requirements

Note also that the MOS Section must meet the rigidity specifications for the MMIRS instrument when combined with the Camera Section.

200 Vacuum integrity

The MOS assembly shall be leak tight to less the 5×10^{-6} STD cc of helium/sec. Proper material selection and cleanliness during assembly must be exercised to minimize contamination due to out gassing. All enclosed volumes, such as tapped holes, must be vented. The vacuum system requirements are provided in section 900 below.

300 Axis definitions

The optical axes are defined as follows: the Z axis is along the optical axis with +Z towards the detector, Y is the elevation axis, and X is perpendicular to the Y-Z plane. These axis definitions apply only when the telescope rotator is at the "0" position.

400 Optics

The MOS Section supports the two corrector lenses. The first corrector element (lens 1) is also a vacuum window for the MOS section. The following specifications must be satisfied for the optical elements:

1. Positioning is provided in the MMIRS Optical Specification document.
2. Temperature range:
    a. First element follows ambient temperature: 313 to 258 degrees Kelvin (40 to -15 Celsius).
    b. Second element is 313 to 248 degrees Kelvin (40 to -25 Celsius).
3. Pressure:
    a. The first lens must support one (1) atmosphere across its entire surface at sea level. The lens shall be bonded to an aluminum cell to provide a radial restraint. In turn, the cell shall provide a vacuum seal to its mounting surface with an O-ring. The O-ring must be fully seated at 0.75 atmospheres.
    b. The second element is in equilibrium with its pressure environment and the design must provide adequate venting paths. Its pressure range is from one atmosphere to 1×10^{-7} Torr.
4. Moisture:
    The first corrector lens cell shall have a dry air line or dry nitrogen fitting to allow connection to a purge line. The gas flow must be sufficient to prevent condensation on the lens.
5. Mounting:
    The lens cells must not distort the lenses with either thermal or mechanical stresses. The lens stress level must not exceed ±200 psi due to thermal, vibrational, and mechanical sources. The first lens is to use the bonding system developed for other MMT lens systems. This lens will not be subjected to Cryogenic temperatures. The second lens shall be mounted using standard flexure techniques. The cell designs shall allow for their removal. A spacer is required between the second lens and its mounting surface to allow for small adjustments in the distance between the two corrector lenses.
6. Stray light baffles:
    Baffles to reduce stray light are required. Refer to MMIRS Stray Light Analysis for their size and positioning.

500 Guider and Wave Front Sensor

Two optical guide cameras and wavefront sensors (GWFS) are required and shall be fed by identical optical systems. The optical diagram and design requirements for the GWFS are presented in the document S-MMIRS-204. The GWFS units shall be located outside of the MOS vacuum vessel on fixed supports. The pickoff mirrors for the GWFS shall be mounted on a structural support attached to the cold plate, which will provide a conductive thermal path for the mirrors. The mirrors shall be sized to cover the full 14 arc-minute field of view of the corrector lens system. They shall be placed as close as possible to the MOS focal plane and must not occult the science beam or scatter light into the entrance slit.

The folded optical beam to each GWFS must pass through a window, which shall serve as a vacuum seal. Each re-imaging lens system is carried on a stepper motor driven Y - Z stage that shall have sufficient range of travel to cover the full field provided by the pick-off mirror. A focus stage will also be provided for the detector. The optics required to select the wavefront sensor mode shall reside on a translation stage that can be inserted into the optical path.

600 Dekker wheel

The Dekker wheel is used to prevent light from entering the science beam through neighboring, unused slit wheel apertures. The Dekker wheel shall have apertures:

Long slit aperture
MOS aperture
Imaging aperture
Blank aperture
Long slit diffuser
MOS aperture diffuser

The aperture designs shall allow adequate optical clearance for the science beam and not vignette or scatter light into the science beam. The individual apertures shall follow the Flamingos2 design concept, except for size. The imaging aperture must be oversized to allow a full 7.0 arc-minute image on the detector.

610 Dekker wheel design parameters

The Dekker wheel shall have a stepper-motor driven worm gear system capable of satisfying the following requirements:

1. A minimum factor of safety of 2.5 times the worst-case expected drive torque.
2. Unlimited angular rotation in the clockwise and counterclockwise directions.
3. The wheel's detent system shall have positional accuracies as specified in F&P section 310. Those requirements are repeated here; however they must be verified against the F&P
   a. Repeatability: within ± 250 microns on all axes.
   b. Stability: within ± 150 microns in all axes for one full instrument rotation about the -Z axis over the telescope's elevation range.
   c. Detent offset: less than 100 microns slit to detent (non-cumulative).
   d. Alignment of Dekker apertures to the MOS wheel slits: ± 150 microns.
4. Micro-switch sensing systems:
   a. One switch shall sense the detent position.
   b. A Home micro-switch shall allow the stepper counter to be re-set. The identification of mask positions will be done in software using both step counting and the micro-switch information.
   c. The home switch shall be located at the Dekker wheel's open position.
5. Maximum time to move 180 degrees shall not exceed 30 seconds with 10 seconds as a goal. The software shall determine the direction to use to minimize travel time.
6. All designs must operate in a vacuum ($\approx 1 \times 10^{-7}$ Torr) and at both ambient temperature conditions and at an operating temperature of ≈ 80 to 140 degrees Kelvin.
7. All designs shall use vacuum compatible materials and consider temperature effects.

8. An intermediate electrical interface connector is required between the Dekker assembly and the Vacuum chamber interface connector. This allows ease of motor and/or switch replacement.
9. The desired wheel/mask operating temperature is less than 120 K. The wheel must meet its target temperature in the time specified in F&P section 350.
10. The Dekker wheel and all other precision manufactured parts must be cycled to cryogenic temperatures during the manufacturing process to relieve stress and to increase cryogenic temperature stability. This process is specified in the document S-MMIRS-202.

700 Multi-Object Slit (MOS) wheel

The MOS wheel is used to position slit masks in the telescope's focal plane. The slit's spectral direction is perpendicular to its radius and the spatial direction is parallel to its radius. The MOS wheel shall have the following three types of apertures and number of each type:

MOS	9 apertures
Long Slits	7 apertures
Imaging	1 aperture

The MOS area is 7.0 arc-minutes (69.14mm) in the spatial direction and ±2.0 arc-minutes (39.51mm) in the spectral direction at the MOS slit. The MOS slits shall be oversized to 69.34 x 39.71 mm to allow for detent error. The slits will have various patterns depending on the observed celestial field. The long slits shall all be 7.0 arc-minutes in the spatial direction and have widths of 1, 2, 3, 4, 6, 8 and 12 detector pixels. These widths correspond to 0.033mm (0.0013in), 0.069 (0.0027), 0.102 (0.004), 0.137 (0.0054), 0.206 (0.0081), 0.274 (0.0108) and 0.409mm (.0161in), respectively. The imaging aperture will be oversized to ensure filling the detector surface. It shall be 70 mm square.

The slit wheel apertures shall allow sufficient optical clearance for the science beam so as not to introduce any vignetting and/or scattered light. The individual MOS slit masks shall follow the Flamingos2 design concept, except for size. The plate scale at the slit plane is 9.8799mm/arc-minute. The slit masks must be thermally coupled to the slit wheel with their cold operating temperature < 120 degrees Kelvin with a maximum change during the night observing time of 10 degrees Kelvin.

710 MOS wheel design parameters

The MOS wheel shall have a stepper-motor driven worm gear system capable of satisfying the following requirements:

1. A minimum factor of safety of 2.5 times the worst case expected drive torque.
2. Unlimited angular rotation in either the clockwise or counterclockwise directions.
3. The wheel detent system shall have positional accuracies as specified in F&P section 310. Those requirements are repeated here; however, they must be verified against the F&P.
    a. Repeatability: within ± 25 microns in X & Y axis
    d. Stability: within ± 6 microns in X & Y axis for one full instrument rotation about optical axis.
    b. Detent offset: less than 100 microns slit to detent (non-cumulative).
4. Micro-switch sensing systems:
    a. One switch shall sense the detent position.

   b. A home micro-switch shall allow the stepper counter to be reset. The identification of the mask position will be done in software using both step counting and micro-switch information.
   c. The home switch shall not be located at a detent position.
5. The maximum time to move 180 degrees shall not exceed 30 seconds with a goal of 10 seconds. The software shall determine the direction to use for the minimum rotational travel.
6. All designs must operate in a vacuum ($\approx 1 \times 10^{-7}$ Torr) at both ambient temperature and at a temperature of less than 120 Kelvin.
7. All designs shall use vacuum-compatible materials and consider temperature effects.
8. An electrical interface connector is required between the MOS wheel drive assembly and the vacuum chamber interface connector. This is for ease of motor and/or switch replacement.
9. The desired wheel operating temperature is less than 12 Kelvin. The wheel must meet the temperature requirements and times presented in F&P section 300.
10. The wheel shall have a common mounting plane for all slits to within ±12.5 microns in the plane perpendicular to the Z-axis.
11. The long slits and imaging aperture shall be permanently fixed to the wheel by screws and have adequate thermal coupling to attain a temperature of less than 120 Kelvin in the required time.
12. The MOS slit plates shall be removable. They shall have repeatable positioning within 200 microns of their nominal position in the X and Y planes. The reflectivity of the plates on the side facing the detector shall be minimized to avoid ghost reflections.
13. The MOS wheel and all other precision manufactured parts must be cycled to cryogenic temperatures during the manufacturing process to relieve stress and to increase their cryogenic temperature stability.
14. The MOS slit plates shall have a bar code for identification.

800 Dekker and MOS Mounting Plate

Dekker and MOS mounting plate shall provide a rigid mounting surface for the following:

1. Dekker wheel assembly
2. MOS wheel assembly
3. LN2 reservoir
4. GWFS pickoff mirrors
5. Thermal sensors
6. MOS Heater
7. Detent mechanisms
8. Radiation shields

The MOS Dewar shall be designed to provide a structural interface to the G10 isolation ring and provide the required LN2 capacity to satisfy F&P requirements specified in section 300. The MOS Dewar shall also be instrumented with heaters, thermal sensors and insulation based on MMIRS thermal design. The MOS Dewar shall meet the required positioning tolerances specified in this document and F&P sections 200 & 300. The mounting plate shall be thermally isolated from the MOS vacuum vessel, yet have sufficient rigidity to satisfy the required positioning tolerances. The mounting plate and MOS wheels shall provide a light-tight barrier about the entrance slit, yet have sufficient conductance so that they do not limit the pump-down time of the Camera Section.

900 Vacuum system

The MOS structural shell shall provide the necessary interfaces to mount the vacuum components as specified on drawing number: C-MMIRS-102.

The MOS vacuum system requires that a safety interlock system be developed to prevent accidental venting of the MOS structural shell while the Camera section's isolation valve is open. This requires that both the Camera Isolation Valve and MOS Vent Valve be safety inter-locked. The design of this system requires a safety review prior to implementation.

The vacuum system shall be capable of evacuating the MOS volume to below 10^{-4} Torr within 20 minutes. Cyrogens can be introduced once this pressure is achieved.

The vacuum system shall be manually operated, with the exception of the camera's isolation valve.

The total cryostat pump down time (after initial bakeout and several pump-down cycles) shall be less than 4 hours to achieve a pressure of 1 times 10^{-4} Torr.

1000 Cryogenic systems

The MOS Cryogenic system is used to cool all entrance slits and Dekker masks to temperature specified above and to maintain their temperatures for 30 hours. Also, the design shall allow for rapid warm-up to allow changing of MOS slits during the daytime. A heating system must be properly sized for this requirement. Refer to F&P sections 100 and 440 for these requirements.

1. The LN_2 Reservoir shall have a minimum LN2 capacity to maintain all MOS cryogenic components to R&PR specified temperatures for a minimum hold time of 30 hours when at operating vacuum pressure.
2. The LN_2 Fill and Vent lines shall be designed to minimize thermal conduction to the MOS shell. The Flamingos2 LN2 designs are to be used as a reference.
3. The MOS structural shell shall be isolated by a system of thermal shields thereby limiting thermal losses.
4. A Heating circuit needs to be designed using Kapton heaters to warm the MOS Dewar to allow daytime changing of the MOS slits.

1100 Radiation Shields

A system of radiation shields shall be used to minimize heat transfer to the cold components from the surrounding vacuum vessel. Their effectiveness must satisfy the hold time requirements stated in F&P section 353. The use of thermal blankets is allowable; however, they must use low out-gassing materials and be properly prepared for vacuum use.

MOS SECTION MECHANICAL DESIGN

Ken McCracken
Center for Astrophysics
Smithsonian Astrophysical Observatory
Cambridge, MA

Table of Contents

100 MOS Section

The Multi-Object Slit (MOS) section houses the following components in an aluminum vacuum vessel:

- Corrector Lens System
- Guider/Wave Front Sensor Pick-off Mirror and Optical baffles
- Dekker Wheel
- Multi-Object Slit Wheel
- Liquid Nitrogen Dewar
- Thermal Shields, Heaters and Temperature Monitoring Devices.

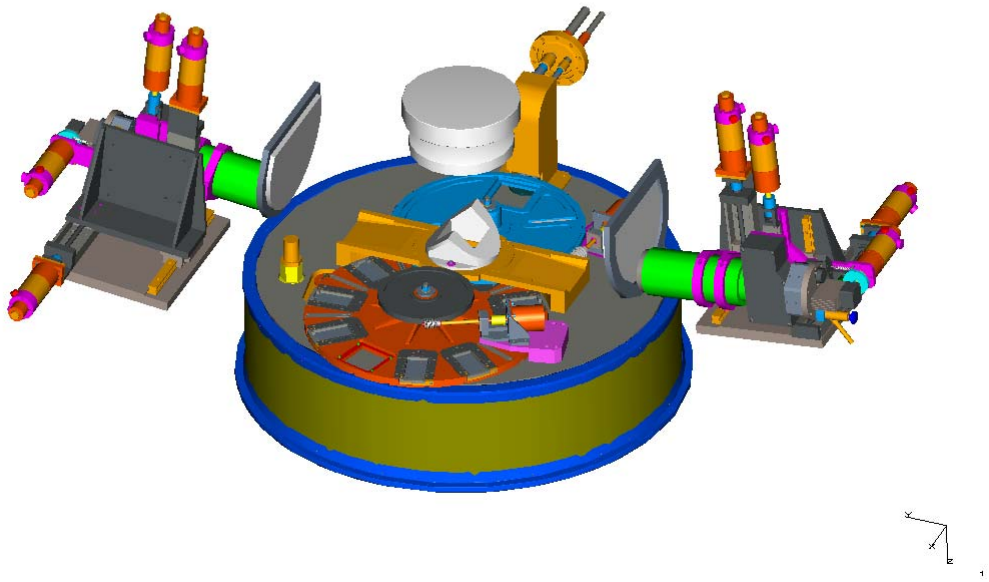

Figure 1 – MOS Section Interior 3D View

The following components are part of the MOS section; however external to the vacuum vessel:

- Guider/Wavefront Sensor Assembly (For additional Details see MMIRS Guider and Wave Front Sensor Section)
- Turbo Pumping System
- Pfeiffer Vacuum Gauge

The performance and operating characteristics for the MOS Section are defined in SAO specification S-MMIRS-201.

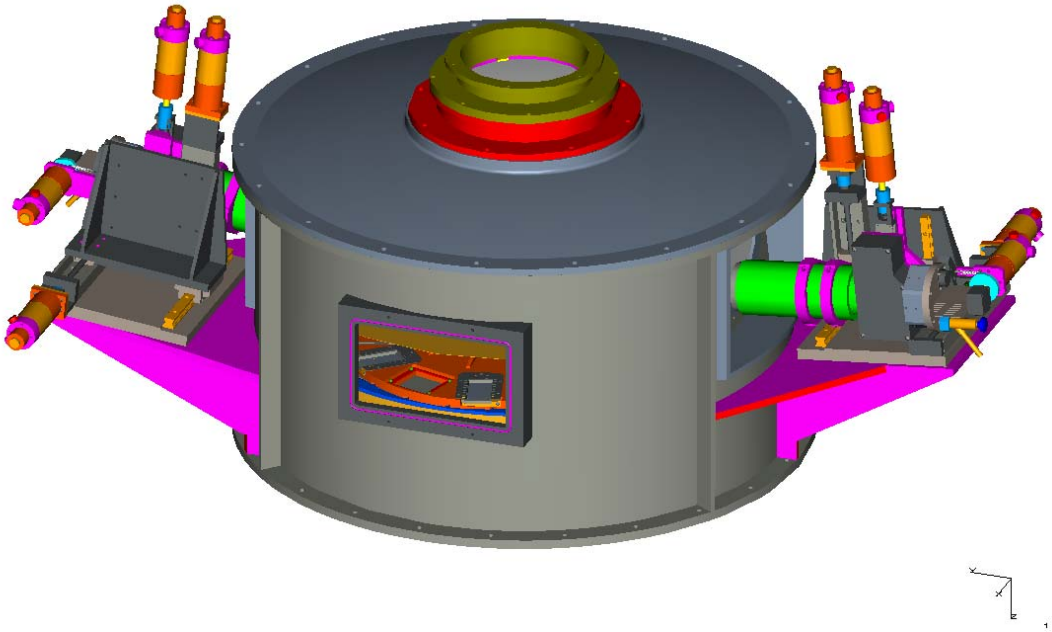

Figure 2 – MOS Section Exterior 3D View – MOS access side

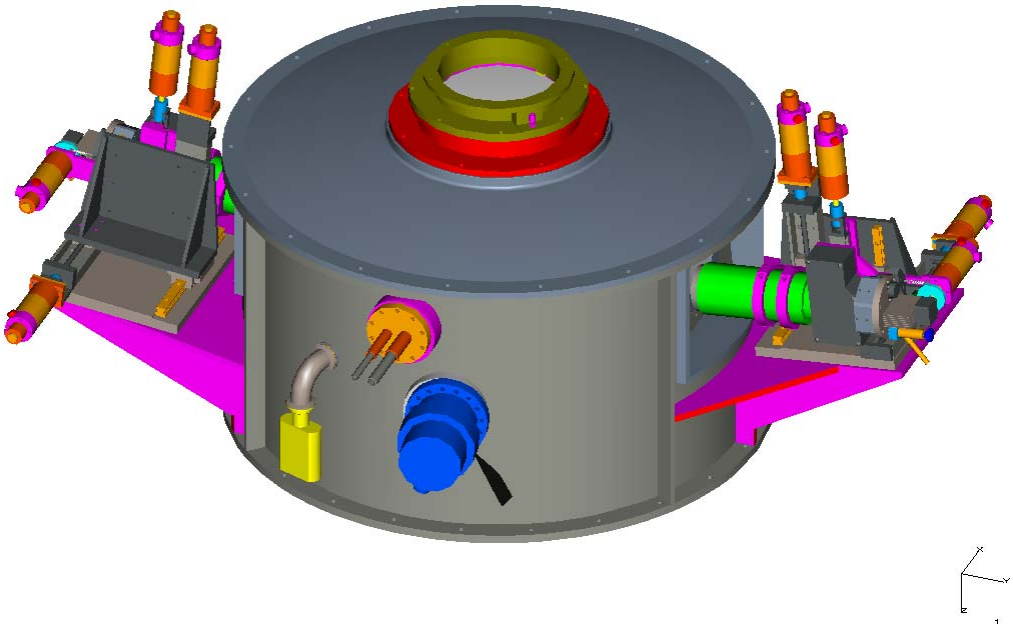

Figure 3 – MOS Section Exterior 3D View – Vacuum / LN_2 Fill/Vent Side

101 Vacuum Vessel and Top Plate

The MOS Section vacuum vessel consists of two components made of 6061 aluminum. The slightly domed Top Plate is nominally .125 inch thick. The top plate supports the Corrector assembly. The cylindrical portion is nominally .187 inch thick and has supports for the Guider/WFS assemblies and allows access to the removeable MOS plates. The lower flange bolts to the Instrument Bulkhead (see the Camera section). Tapped holes are available for lifting and handling each piece. An O-ring seals the vacuum at the Top Plate to MOS Chamber interface and the MOS Chamber to Instrument Bulkhead interface.

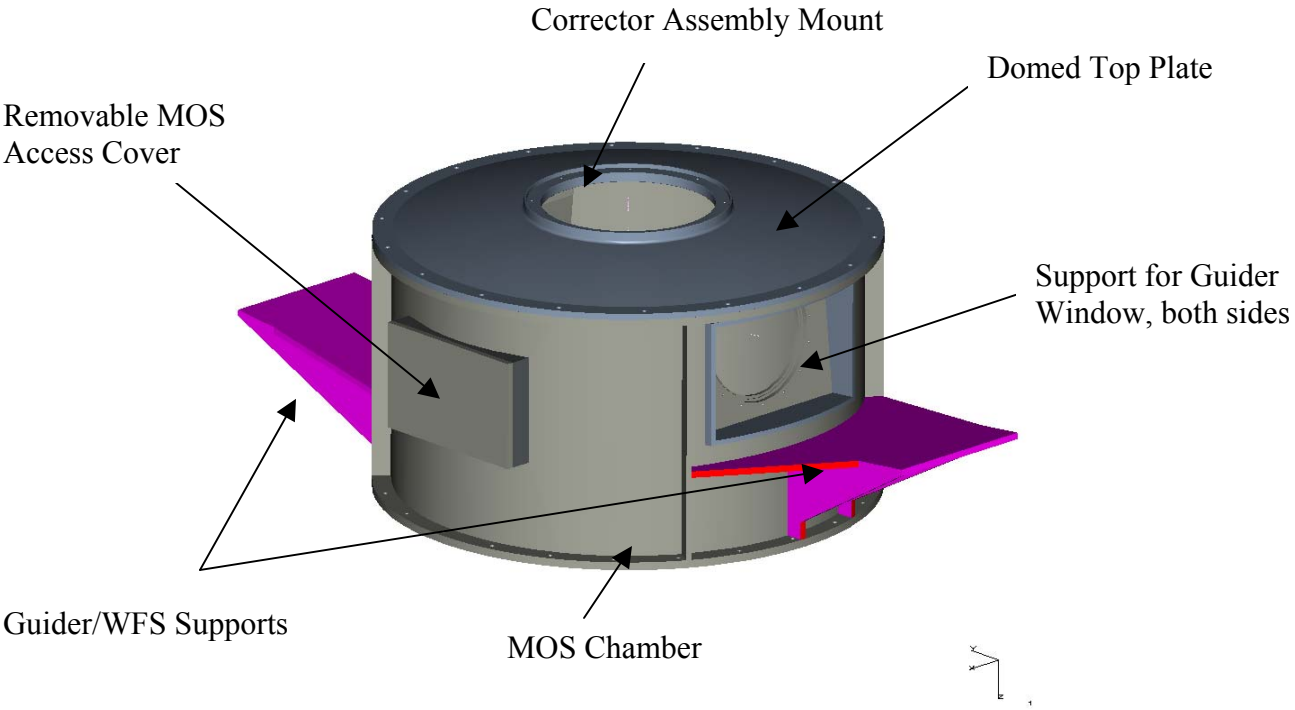

Figure 4 – MOS Vacuum Vessel

110 Internal Components

111 Corrector Lens System

The two-element corrector lens system brings the 14 arc-min diameter telescope field to focus at the MOS slit. The central 7 arc-minute square field is the science field.

The first element (Lens 1) of the corrector is RTV-bonded to its cell using techniques developed for other MMT instruments. Lens 1 serves as an optical element and as the entrance window providing the necessary vacuum seal. The second element (Lens 2) is mounted in a standard three-point restraint where one restraint has compliance (spring loaded). Lens 1 is predicted to operate approximately 4°C below ambient. Provisions for blowing dry air over the outside surface of the lens have been made to prevent condensation. Lens 2 is predicted to operate approximately 7° below ambient.

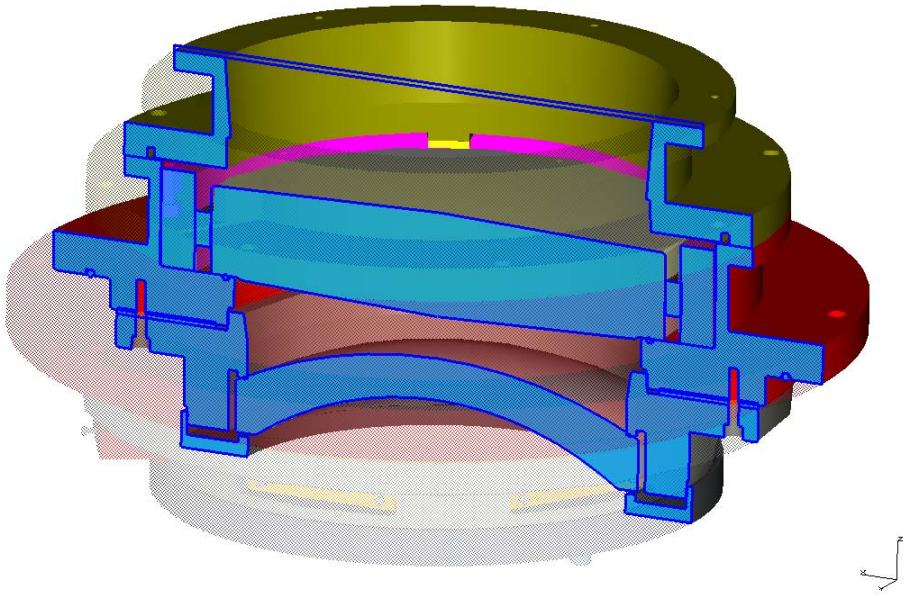

Figure 5 – Corrector Assembly

112 Guider/Wave Front Sensor Pick-off Mirror and Optical Baffles

The field outside the science field is used for guiding and wave front sensing. A pickoff mirror is used to fold this field through windows to the externally mounted Guider/Wavefront Sensor Assembly. The pickoff mirror is a diamond-turned 6061 aluminum mirror thermally coupled to the dewar. A cold shield surrounds the 14' field from the corrector to the pickoff mirror to limit the thermal background to the IR detector. Baffles mounted to the vacuum vessel shield the guide field as it exits the chamber to the guider/WFS assemblies. These warm guider baffles will be insulated with MLI to reduce thermal coupling to the dewar.

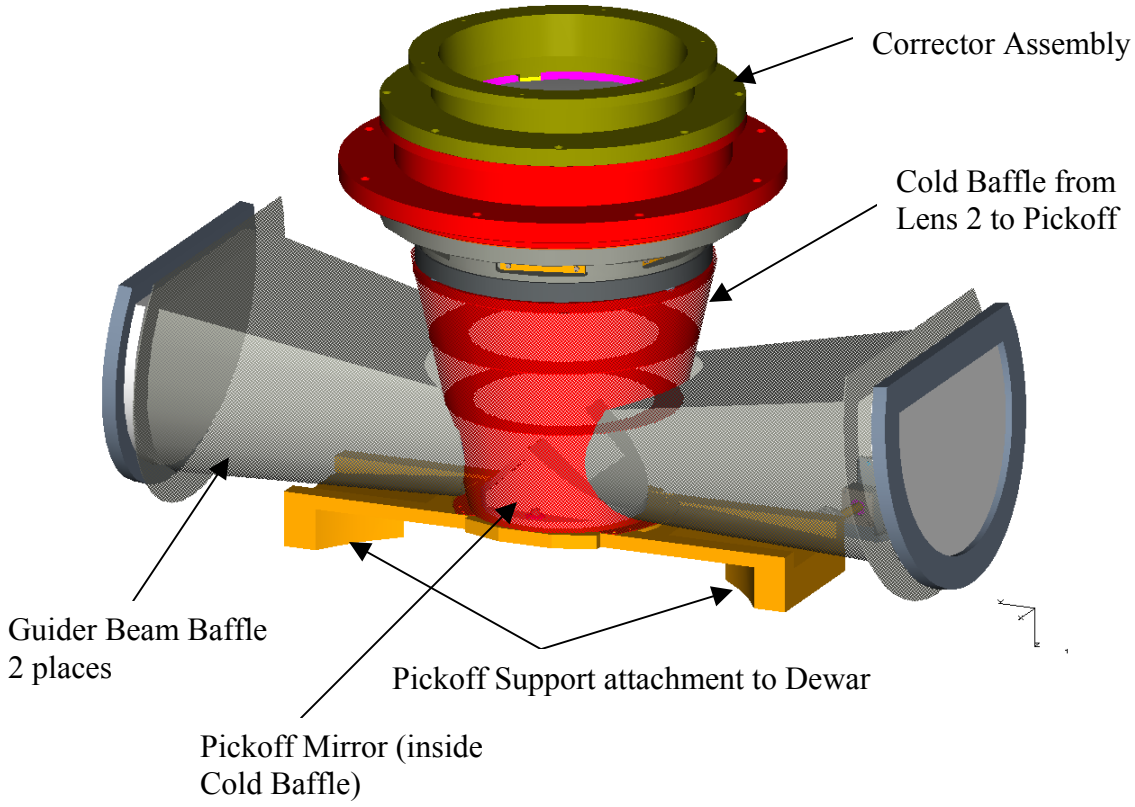

Figure 6 – Guider Pickoff Mirror and Optical Baffles

113 Dekker Wheel

The Dekker wheel is used to limit the MOS slit's field of view. It has six positions, one mask for each slit type, a diffuser for each slit type, blanking and open apertures. The wheel is a motor driven worm gear arrangement with home and detent indicating microswitches. A mechanical detent will control the wheel's position. The home detent microswitches are explained in the Multi-Object Slit Wheel Section. The wheel is to be balanced to within the bearing friction minimizing the required detent force. The small lead angle of the single thread worm and the balanced wheel will eliminated any backdriving potential. The wheel is spaced off the top of the dewar by sapphire balls creating a thermally conductive bearing.

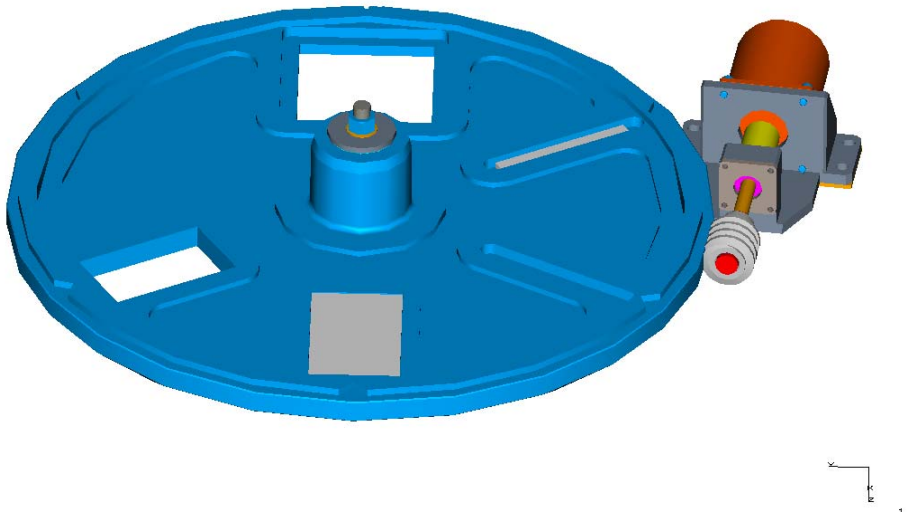

Figure 7 – Dekker Wheel and Drive

114 Multi-Object Slit Wheel

The MOS wheel positions the slit masks at the telescope's focus for spectroscopy and imaging. The MOS wheel has 9 MOS slits, 7 long slits, and one imaging aperture. The MOS slits provide a usable aperture of 7' spatially by 4' spectrally. The MOS slits are populated with interchangeable assemblies containing plates machined specifically for the planned observation. The long slits are not interchangeable and will be available in seven spectral widths by 7' in the spatial direction.

The MOS wheel is driven in a similar manner to the Dekker wheel (see Figure 10). The worm drive backlash will be adjusted to allow a clearance of 2-3 steps. This will allow the detent mechanism to control the wheel's position. The detent microswitch (not shown in Figure 7) will sense when the roller enters and exits the detent feature. The wheel will be commanded to the desired location and then commanded one stop in the reverse direction. The purpose of the reverse step is to disengage the worm drive from the wheel so that the detent can position the wheel. The motion control system will record the exact motor step at which the detent switch is activated. This will be used to verify arrival at the correct location.

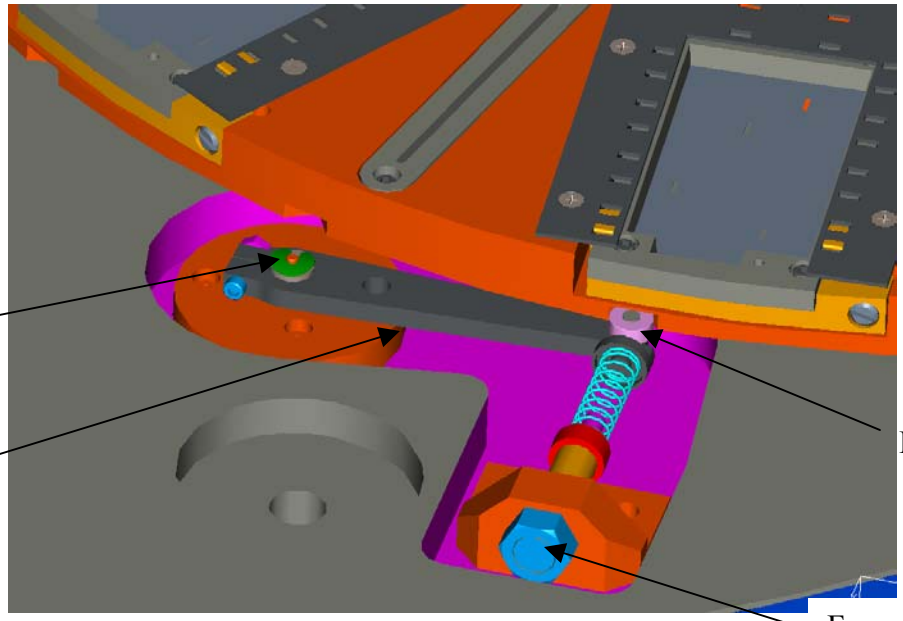

Figure 8 - MOS Wheel Detent

The home position is not at a detent. A cam having identical slopes allowing activation from either direction will be used for the home switch. To serve as a precision reference it must be approached only in one direction.

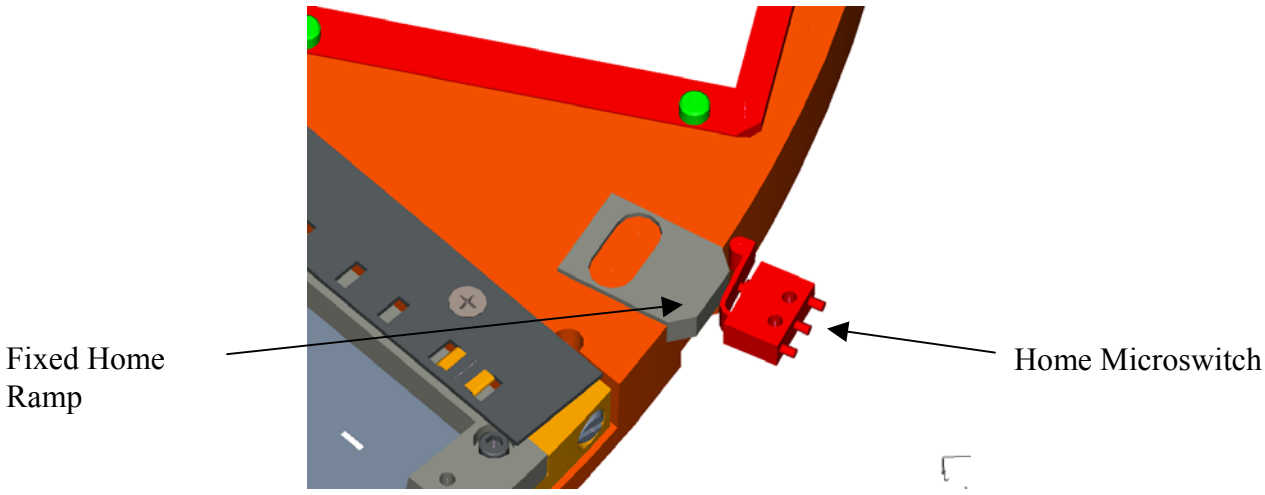

Figure 9 - Home Switch

The MOS wheel is to be balanced to within the bearing friction. This is required so that the worm is always pushing the wheel no matter what the gravity orientation is. The wheel is spaced off the top of the dewar by sapphire balls creating a thermally conductive bearing. The MOS wheel is predicted to operate at 82°K during observation, well below the requirement of 120°K. The wheel is predicted to be within 10°K of the steady state temperature in 2 hours.

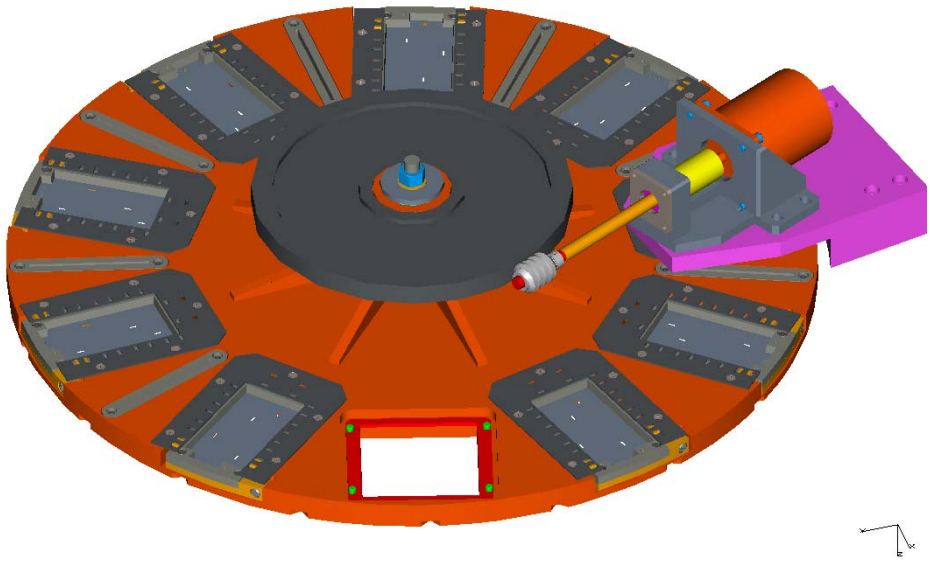

Figure 10 - MOS Wheel and Drive

115 Liquid Nitrogen Dewar

The Liquid Nitrogen dewar has fill and vent lines arranged to limit spillage caused by extreme telescope orientations. These limits are taken to be 1) horizon pointing with the instrument rotator at 0, and 30 degrees elevation with the rotator at +/-115 degrees. The MOS and Camera fill lines will connect to a common manfold allowing both dewars to fill from one connection. The maximum MOS dewar LN2 volume is 55-liters. A hold time greater than 30 hours has been calculated assuming a 50% fill.

The dewar's front reinforced surface is the mounting surface for the Dekker, MOS and Pickoff mirror assemblies. The 6061 aluminum dewar will be stress relieved by cooling from room temperature to 77K at various steps during the machining process.

A G10 tube bonded into 6061 aluminum rings structurally connects the dewar to the vacuum vessel. G10 minimizes the conductive heat loss from the dewar and provides a compliant support. Compliance is required of the support due to the thermal contraction and expansion undergone when filling and heating the dewar. The G10 support is bolted and pinned to the Dewar and MOS Chamber.

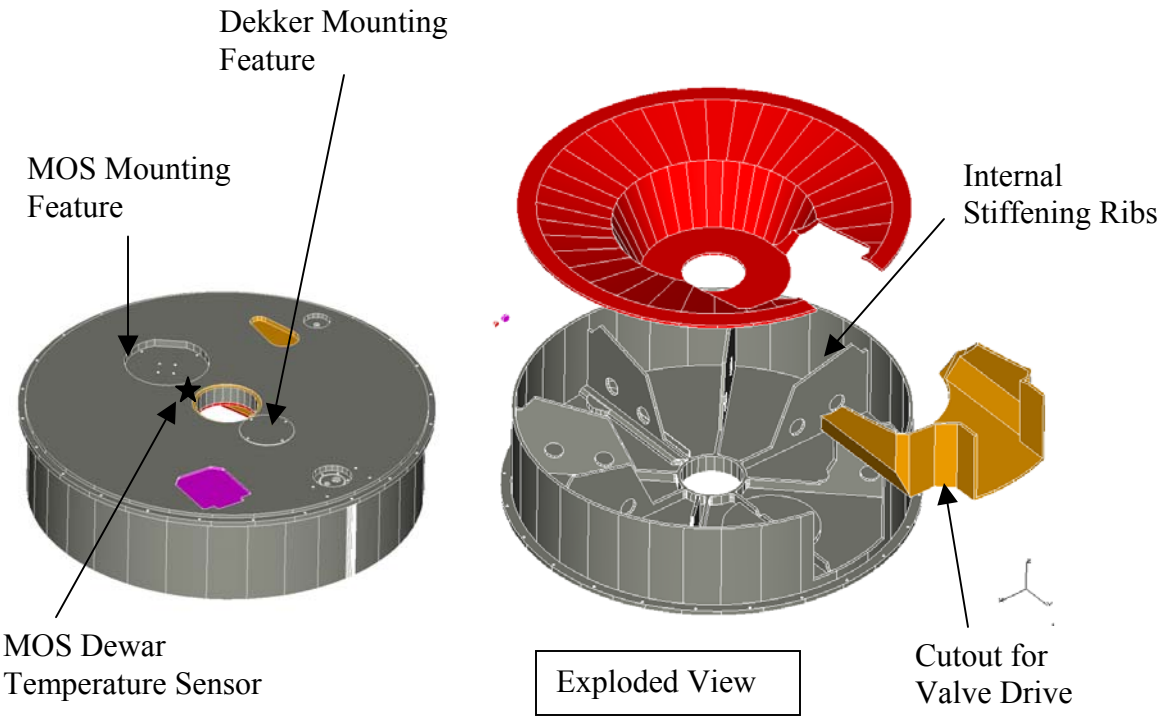

Figure 11 – MOS LN_2 Dewar

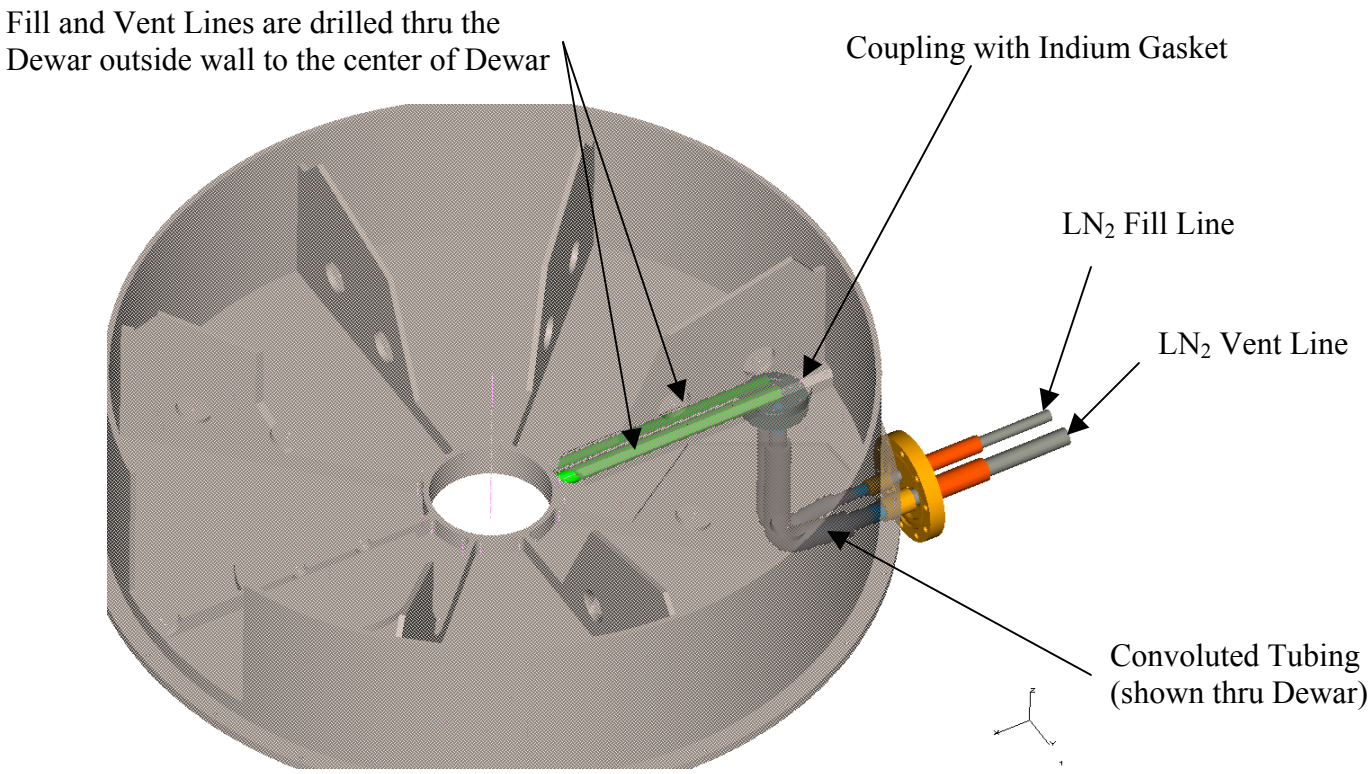

Figure 12 – Interior View of Dewar with LN2 Fill and Vent Lines shown thru the top of the Dewar

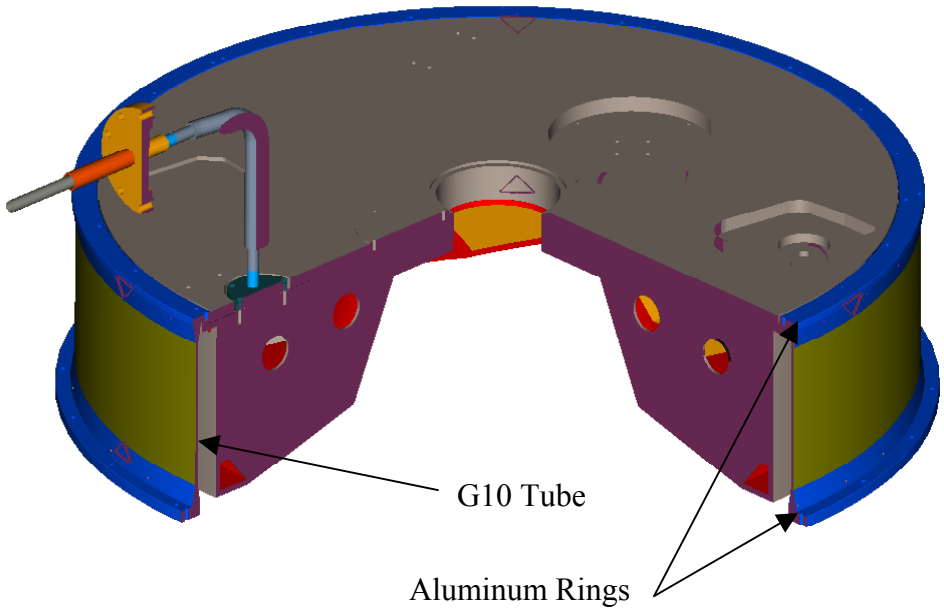

Figure 13 – Section Cutaway from Dewar and G10 Support Structure

116 Thermal Shields, Heaters and Temperature Monitoring Devices

An arrangement of thermal shields are shown in Figures 14 and 15. These limit thermal exchanges between the warm and cold surfaces with temperature sensors placed in areas of concern. The required MOS section temperature sensors are located as follows:

- MOS Dewar (Figure 11)
- MOS Cold Shield (Figure 15)

The MOS Dewar temperature sensor will be used to control the MOS section heaters. The MOS Cold Shield temperature sensor will be used for the Isolation valve safety interlock logic.

The following locations will be provided with temperature sensors for initial instrument assembly and checkout (locations not shown):

- Lens 2 attached to the lens mount material
- Pickoff Mirror attached to the mirror base
- L2 Baffle attached to the outside surface facing the access port
- GWFS Baffle attached to the outside top facing the top dome
- MOS Wheel attached to wheel rim (static test only!)

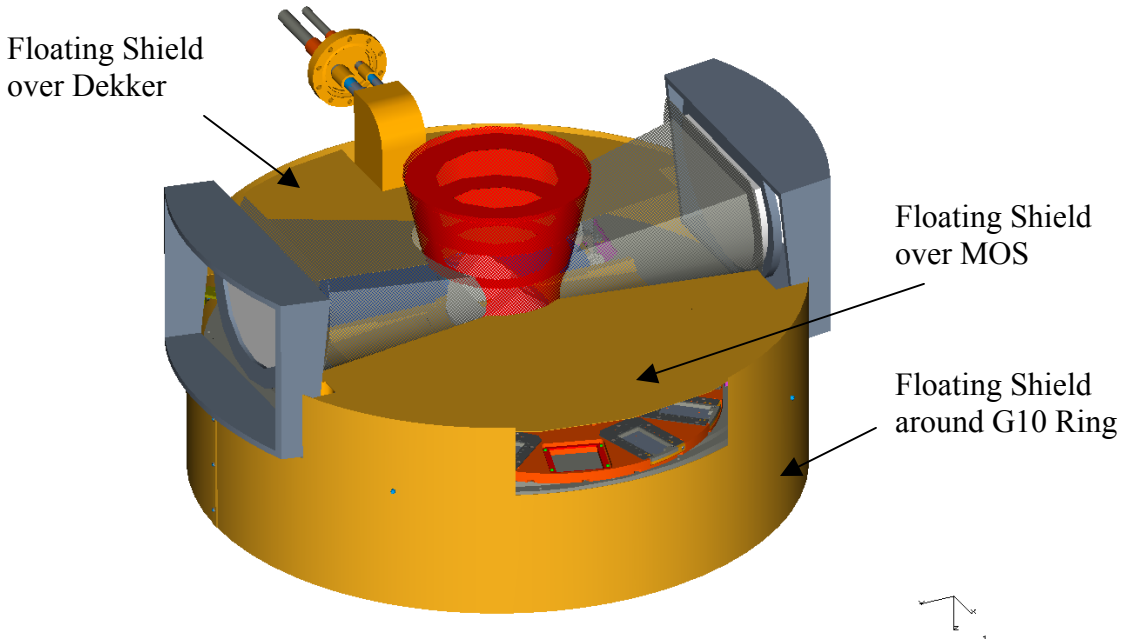

Figure 14 – Floating Thermal shields

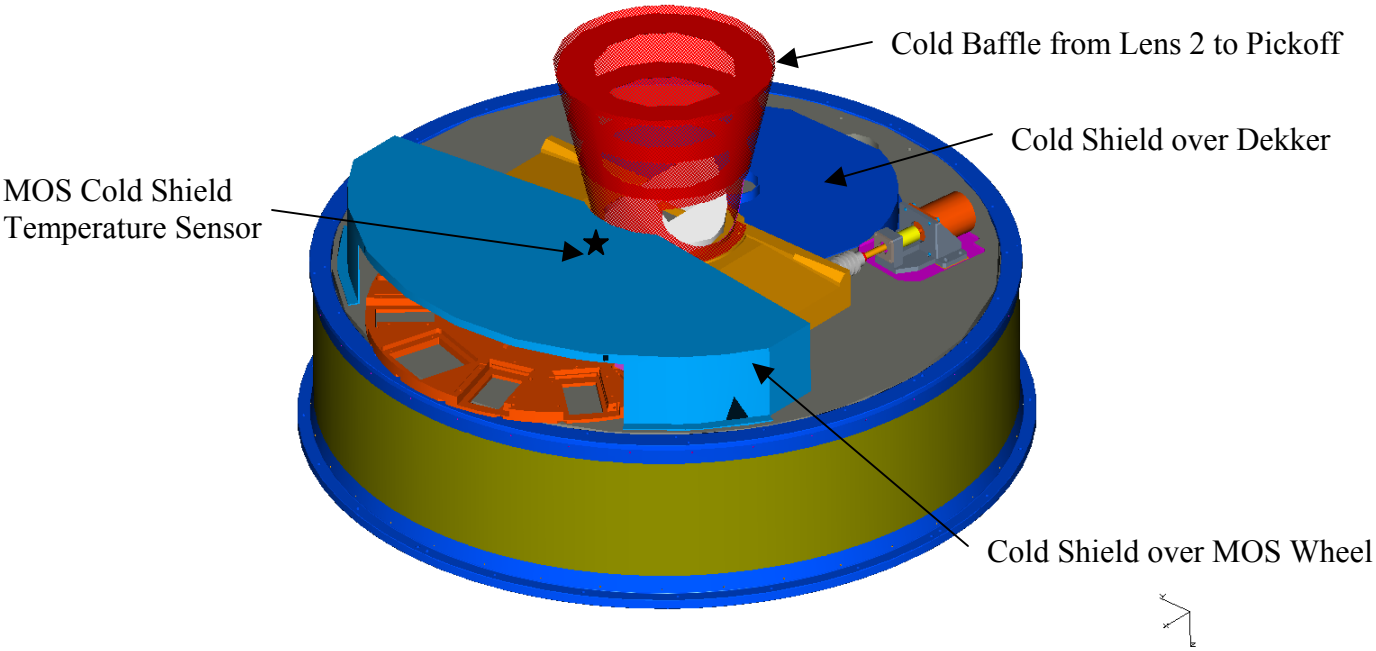

Figure 15 – Cold Shields

120 External Components

The components connected to the outside of the MOS chamber are shown in Figure 16 and described elsewhere. They are:

- LN_2 plumbing
- Turbo pump
- Vacuum gauge
- Guider/WFS assemblies
- Calibration lamps (not shown)

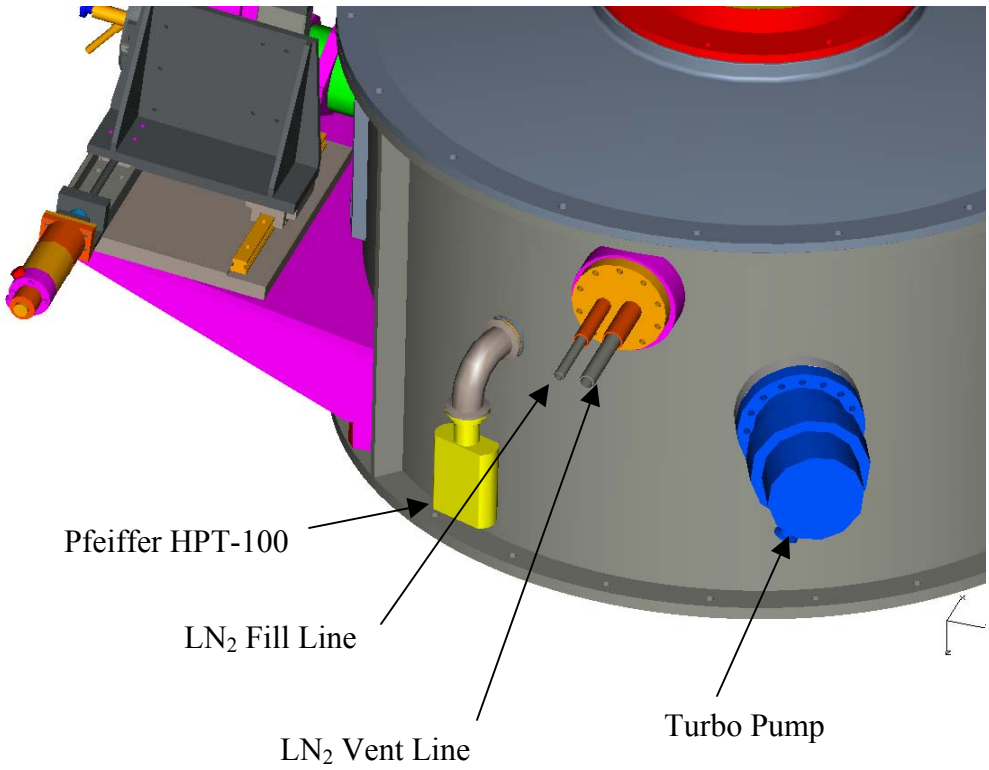

Figure 16 – External items

200 MOS Section Compliance Matrix

Issue	Requirement	Document	MMIRS Value
Mulit-Slit Capability	Provide (8) 4' x 7' exchangable multi-slit plates	S-MMIRS-200 / Section 115 / p. 10	Design provides for (9) 4' x 7' exchangable mulit-slit plates
Long Slit Capability	Provide (7) long slits 7' x 1,2,3,4,6,8, and 12 pixels wide spectrally	S-MMIRS-200 / Section 116 / p.11	By Design
Imaging Aperture	Provide (1) 7' square imaging aperture	S-MMIRS-200 / Section 117 / p. 11	By Design
MOS Wheel Mechanism Repeatability	±25 microns in X and Y axis	S-MMIRS-201 / Section 710 / p. 4	±8.8 microns X ±9.7 microns Y
Dekker Wheel Mechanism Repeatability	±250 microns in all axis	S-MMIRS-201 / Section 610 / p. 3	±8.8 microns X ±9.5 microns Y
Access to Liquid Nitrogen Ports	LN2 ports and valves shall be accessible without instrument removal from CIR	S-MMIRS-200 / Section 332 / p. 19	By Design
Access to Electrical Connections	Connections shall be accessible without instrument removal from CIR	S-MMIRS-200 / Section 333 / p. 19	By Design
Access to MOS Plate Exchange Port	Access shall be made without instrument disassembly	S-MMIRS-200 / Section 334 / p.20	By Design
Safety - Mechanism back driving	No mechanism shall be backdriveable in the event of loss of power	S-MMIRS-200 / Section 371 / p.23	By design
MOS Wheel Time to Function	Maximum of 30 seconds to any wheel position	S-MMIRS-200 / Section 372 / p.23	12.4 sec

Dekker Wheel Time to Function	Maximum of 30 seconds to any wheel position	S-MMIRS-200 / Section 372 / p.23	18.3 sec
MOS Motor Drive Torque	Minimum Factor of Safety = 2.5	S-MMIRS-201 / Section 710 / p.4	FS = 45.0
Dekker Motor Drive Torque	Minimum Factor of Safety = 2.5	S-MMIRS-201 / Section 610 / p.3	FS = 59.3
Lens 1 Window Condensation	Provide plumbing for dry air purge over external window surfaces	S-MMIRS-200 / Section 670 / p.30	By Design

MMIRS

MOS and Dekker Drivetrain Calculations

Constants:

$\text{arcmin} := \left(\frac{1}{60}\right)\text{deg}$ $\text{arcsec} := \left(\frac{1}{3600}\right)\text{deg}$ $\text{ozf} := g \cdot \text{oz}$

$\text{hz} := \frac{1}{\text{sec}}$ $\text{rev} := 360 \cdot \text{deg}$ $\text{rev} = 6.283\,\text{rad}$

$\text{rpm} := \frac{\text{rev}}{1 \cdot \text{min}}$ $\text{rpm} = 360\,\frac{\text{deg}}{\text{min}}$ $\text{rps} := \text{rpm} \cdot 60\,\frac{\text{sec}}{\text{min}}$

$g = 9.807\,\frac{\text{m}}{\text{s}^2}$ $\mu\text{m} := 10^{-6}\text{m}$ *

MOS Wheel Section:

The allowable factor of safety on motor torque is 2.5.

$FS_{torque} := 2.5$

Motor Characteristics - Phytron VSS 52 - From Phytron datasheets:

MotorSteps := 200 (motor steps per rev)

$Nmotor\_max := 300 \cdot \frac{rev}{min}$

$T_{MotorMax} := 33N \cdot cm$ From Phytron: tested motor at 77K - for design calcs use 33Ncm (46.7 in oz) at 300 rpm, 60V)

$Jmotor := .15kg \cdot cm^2$ $Jmotor = 1.5 \times 10^{-5} kg\,m^2$

MOS Wheel Parameters

MOSWheelDiameter := 480mm $Dens := 2710 \frac{kg}{m^3}$

MOSWheelThickness := .625in

Gearing component selection (Steel Worm (single thread), Alum w/ hard anodizing on Worm Gear):

Nwg := 120 Worm Gear Teeth

$Dia_{wg\_pitch} := 7.5 \cdot in$ Diametral Pitch of 16

Nw := 1 Worm Threads

$\phi_n := 14.5 \cdot deg$ Pressure Angle

$\lambda_w := 5.7167 \cdot deg$ Worm Lead Angle

f := .025

$E_w := \frac{\tan(\lambda_w) \cdot ((1 - f \cdot \tan(\lambda_w)))}{(f + \tan(\lambda_w))}$ $E_w = 0.798$ efficiency-from BostonGear

$Nf := \frac{Nwg}{Nw}$ $\boxed{Nf = 120}$

Calculate the component inertias for MOS Wheel Drive:

$$Jwheel := \left(\frac{\pi}{4}\right)\cdot MOSWheelThickness\cdot Dens\cdot\left(\frac{MOSWheelDiameter}{2}\right)^4 \qquad Jwheel = 0.112\,kg\,m^2$$

$$Jshaft := \left(\frac{\pi}{32}\right)\cdot 3Dens\cdot\left[(2.66in)\cdot(.5in)^4 + .94in\cdot(.315in)^4\right] \qquad Jshaft = 1.481\times 10^{-6}\,kg\,m^2$$

$$Jworm := \left(\frac{\pi}{32}\right)\cdot 3Dens\cdot(1.497in)\cdot\left[(1.0in)^4 - (0.5in)^4\right] \qquad Jworm = 1.184\times 10^{-5}\,kg\,m^2$$

$$Jwormgear := \left(\frac{\pi}{32}\right)\cdot Dens\cdot(.75in)\cdot(7.5in)^4 \qquad Jwormgear = 6.675\times 10^{-3}\,kg\,m^2$$

Calculate the torque due to bearing friction (using μ=.0025 for ball and .006 for angular contact bearings, p. 482, Machine Design, sapphire estimated using angular Contact value):

$$Dia_{ball\_bearing} := 25mm$$

$$Dia_{sapphire\_bearing} := 5.125in$$

$$Load_{bearing} := 103lbf$$

$$T_{ball\_bearings} := \frac{\left[\left(.0025\cdot\frac{Load_{bearing}}{10} + .006\cdot Load_{bearing}\right)\cdot Dia_{ball\_bearing}\right]}{2} \qquad T_{ball\_bearings} = 0.036\,N\cdot m$$

*

$$T_{sapphire\_bearing} := \frac{\left[(.006)\cdot Load_{bearing}\cdot Dia_{sapphire\_bearing}\right]}{2} \qquad T_{sapphire\_bearing} = 0.179\,N\cdot m$$

*

$$T_{bearing\_total} := T_{sapphire\_bearing} + T_{ball\_bearings} \qquad T_{bearing\_total} = 0.215\,N\cdot m$$

Calculate the detent force to overcome friction (assume an additional margin of 4X on the spring force):

$Margin_{spring} := 4$

$R_{wheel} := 237.879mm$

$$F_{spring} := \frac{\left(T_{bearing\_total} \cdot Margin_{spring}\right)}{\sin\left(\frac{\pi}{4}\right) \cdot \sin\left(\frac{\pi}{4}\right) \cdot R_{wheel}} \qquad F_{spring} = 7.221\,N$$

From the wheel geometry, the additional spring deflection to get the roller out of the detent feature is:

$Deflection_{additional} := 3.591mm$

Find a spring that gives the required holding force (Fspring) and only increases by 20% at the peak of the detent feature:

$F_{spring\_2} := 1.2 \cdot F_{spring}$

$$deflection := \frac{Deflection_{additional}}{.2} \qquad deflection = 17.955\,mm$$

$$k_{spring} := \frac{F_{spring}}{deflection} \qquad k_{spring} = 0.402\,\frac{N}{mm}$$

$$k_{spring} = 2.297\,\frac{lbf}{in}$$

From Century Spring, use PN 71061S (k=2.4 lb/in, max load = 2.6 lb).

Calculate actual torque at top of detent based on additional force at top of detent:

$$T_{detent} := \sin\left(\frac{\pi}{4}\right) \cdot F_{spring\_2} \cdot \left(R_{wheel} + Deflection_{additional}\right) \qquad T_{detent} = 1.48\,N \cdot m$$

Calculate MOS wheel acceleration based on the maximum motor torque available.

$Jload := Jwheel + Jwormgear$

$$Jeq := \left(\frac{Jload}{Nf^{2}\cdot E_{w}}\right) + (Jshaft + Jworm) \qquad Jeq = 2.366\times 10^{-5}\,kg\,m^{2}$$

$Jtotal := Jmotor + Jeq$ $\qquad Jtotal = 3.866\times 10^{-5}\,kg\,m^{2}$

Calculate MOS Motor maximum available acceleration (still assuming a FS_torque of 2.5):

$$\alpha_{motor\_max\_avail} := \frac{\left[\left(\frac{T_{MotorMax}}{FS_{torque}}\right) - \left[\frac{T_{detent} + T_{bearing\_total}}{(Nf\cdot E_{w})}\right]\right]}{Jtotal}$$

$$\alpha_{motor\_max\_avail} = 2.957\times 10^{3}\,\frac{rad}{sec^{2}}$$

For consistancy across drives(and for a more reasonable acceleration), use the same acceleration as Grism (5718 steps/sq sec):

$$\alpha_{Grism} := 179.64\,\frac{rad}{sec^{2}}$$

$\alpha_{motor} := \alpha_{Grism}$ $\qquad \alpha_{motor} = 179.64\,\frac{1}{s^{2}}$

$$\alpha_{wheel} := \frac{\alpha_{motor}}{Nf} \qquad \alpha_{wheel} = 1.497\,\frac{1}{s^{2}}$$

Calculate the factor of safety on motor torque:

$T_{reqd} := Jtotal\cdot\alpha_{motor}$ $\qquad T_{reqd} = 6.945\times 10^{-3}\,N\cdot m$

$$FS_{torque\_MOS} := \frac{T_{MotorMax} - \frac{(T_{detent} + T_{bearing\_total})}{Nf\cdot E_{w}}}{T_{reqd}} \qquad FS_{torque\_MOS} = 44.972$$

Calculate positioning time period:

$\omega_{initial} := 0 \cdot \frac{rev}{min}$

$\omega_{wheel\_final} := \frac{Nmotor\_max}{Nf}$ $\omega_{wheel\_final} = 2.5\,rpm$

$\omega_{motor\_final} := Nmotor\_max$ $\omega_{motor\_final} = 300\,rpm$

$time_{accel} := \frac{(\omega_{motor\_final} - \omega_{initial})}{\alpha_{motor}}$ $time_{accel} = 0.175\,s$

$Position\_Angle := \pi rad$

$time_{position} := \frac{(Position\_Angle \cdot Nf)}{Nmotor\_max} + 2time_{accel}$ $\boxed{time_{position} = 12.35\,s}$

Calculate Inertia ratio:

$J_{ratio} := \frac{(Jeq)}{Jmotor}$ $\boxed{J_{ratio} = 1.577}$

Dekker Wheel Section:

The Dekker Wheel uses the same Motor as the MOS Wheel.

Dekkar Wheel Parameters

DekkerWheelDiameter := 388.3mm

DekkerWheelThickness := .5in

Gearing component selection (Steel Worm (single thread), Alum w/ hard anodizing on Worm Gear):

$DiaPitch_{Dekker} := 12$ Diametral Pitch of gearing

$Nwg\_d := 181$ Number of teeth on worm gear

$Dia_{wg\_D\_pitch} := \frac{Nwg\_d}{DiaPitch_{Dekker}}$ * $Dia_{wg\_D\_pitch} = 15.083$

$Nw\_d := 1$ Number of starts on worm

$\lambda_{w\_d} := 4.76667 \cdot deg$ Lead Angle

$E_{w\_d} := \frac{\left[\tan\left(\lambda_{w\_d}\right)\cdot\left(\left(1 - f\cdot\tan\left(\lambda_{w\_d}\right)\right)\right)\right]}{\left(f + \tan\left(\lambda_{w\_d}\right)\right)}$ Efficiency

$E_{w\_d} = 0.768$

$Nf\_D := \frac{Nwg\_d}{Nw\_d}$ * $Nf\_D = 181$ Final Gear Ratio

Calculate the component inertias for Dekker Wheel Drive

$$Jwheel\_D := \left(\frac{\pi}{4}\right)\cdot DekkerWheelThickness\cdot Dens\cdot\left(\frac{DekkerWheelDiameter}{2}\right)^4$$

$Jwheel\_D = 0.038\,kg\,m^2$

The torque due to bearing friction uses all the same assumptions as in MOS section.

Calculate the detent force to overcome friction (assume an additional margin of 4X on the spring force):

$R_{wheel\_d} := 183.036mm$

$$F_{spring\_d} := \frac{\left(T_{bearing\_total} \cdot Margin_{spring}\right)}{\sin\left(\frac{\pi}{4}\right) \cdot \sin\left(\frac{\pi}{4}\right) \cdot R_{wheel\_d}} \qquad F_{spring\_d} = 9.385\,N$$

From the wheel geometry, the additional spring deflection to get the roller out of the detent feature is:

$Deflection_{additional\_d} := 3.591mm$

Find a spring that gives the required holding force (Fspring) and only increases by 20% at the peak of the detent feature:

$F_{spring\_d\_2} := 1.2 \cdot F_{spring\_d}$

$$deflection\_d := \frac{Deflection_{additional\_d}}{.2} \qquad deflection\_d = 17.955\,mm$$

$$k_{spring\_d} := \frac{F_{spring\_d}}{deflection\_d} \qquad k_{spring\_d} = 0.523\,\frac{N}{mm}$$

$$k_{spring\_d} = 2.985\,\frac{lbf}{in}$$

From Century Spring, use PN 71473S (k=3.0lb/in, max load = 3.3 lb).

Calculate actual torque at top of detent based on additional force at top of detent:

$$T_{detent\_d} := \left[\sin\left(\frac{\pi}{4}\right) \cdot F_{spring\_d\_2} \cdot \left(R_{wheel\_d} + Deflection_{additional\_d}\right)\right]$$

$$T_{detent\_d} = 1.486\,N \cdot m$$

Calculate Dekker wheel acceleration based on the maximum motor torque available.

$Jload\_d := Jwheel\_D$

$$Jeq\_d := \left(\frac{Jload\_d}{Nf\_D^2 \cdot E_{w\_d}}\right) + (Jshaft + Jworm)$$

$$Jeq\_d = 1.485 \times 10^{-5}\,kg\,m^2$$

$Jtotal\_d := Jmotor + Jeq\_d$

$$Jtotal\_d = 2.985 \times 10^{-5}\,kg\,m^2$$

Calculate Dekker Motor maximum acceleration (still assuming a FS_torqueof 2.5):

$$\alpha_{motor\_max\_avail\_d} := \frac{\left(\frac{T_{MotorMax}}{FS_{torque}}\right) - \frac{\left(T_{detent\_d} + T_{bearing\_total}\right)}{\left(Nf\_D \cdot E_{w\_d}\right)}}{Jtotal\_d}$$

$$\alpha_{motor\_max\_avail\_d} = 4.012 \times 10^{3}\,\frac{rad}{sec^2}$$

For consistancy across drives (and for a more reasonable acceleration) use the same acceleration as Grism (5718 steps/sq sec)

$\alpha_{motor\_d} := \alpha_{Grism}$

$$\alpha_{motor\_d} = 179.64\,\frac{rad}{sec^2}$$

$$\alpha_{wheel\_d} := \frac{\alpha_{motor\_d}}{Nf\_D}$$

$$\alpha_{wheel\_d} = 0.992\,\frac{1}{s^2}$$

Calculate the factor of safety on motor torque:

$T_{Dekker\_reqd} := Jtotal\_d \cdot \alpha_{motor\_d}$

$$T_{Dekker\_reqd} = 5.362 \times 10^{-3}\,N \cdot m$$

$$FS_{torque\_Dekker} := \frac{T_{MotorMax} - \frac{\left(T_{detent\_d} + T_{bearing\_total}\right)}{Nf\_D \cdot E_{w\_d}}}{T_{Dekker\_reqd}}$$

$$FS_{torque\_Dekker} = 59.257$$

Calculate positioning time period:

$\omega_{in\_d} := 0 \cdot \frac{rev}{min}$

$\omega_{w\_d\_final} := \frac{Nmotor\_max}{Nf\_D}$ $\omega_{w\_d\_final} = 0.174 \frac{1}{s}$

$\omega_{m\_d\_final} := Nmotor\_max$ $\omega_{m\_d\_final} = 31.416 \frac{1}{s}$

$time_{accel\_d} := \frac{(\omega_{m\_d\_final} - \omega_{in\_d})}{\alpha_{motor\_d}}$ $time_{accel\_d} = 0.175\,s$

$time_{position\_d} := \frac{(Position\_Angle \cdot Nf\_D)}{Nmotor\_max} + time_{accel\_d}$ $\boxed{time_{position\_d} = 18.275\,s}$

Calculate Inertia ratio:

$J_{ratio\_d} := \frac{Jeq\_d}{Jmotor}$ $\boxed{J_{ratio\_d} = 0.99}$

MOS WHEEL REPEATABILITY

MOS WHEEL

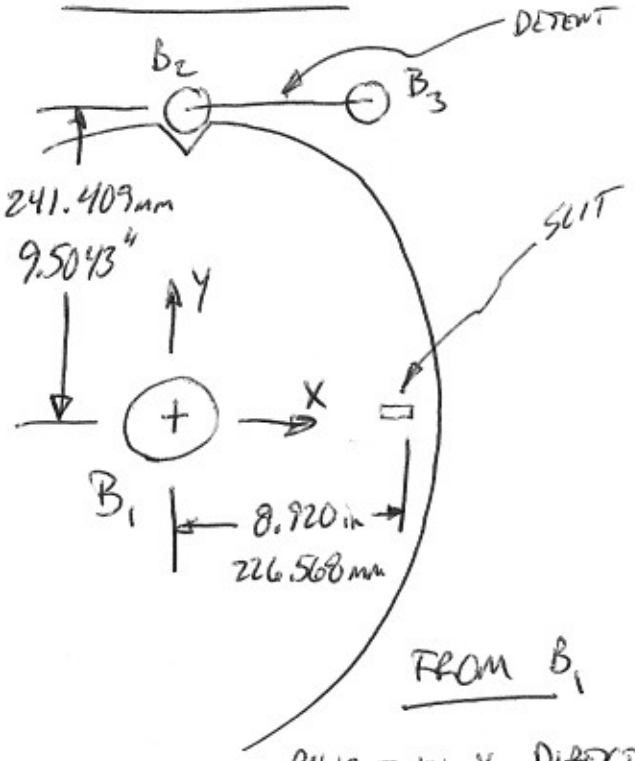

RUNOUT ASSUMPTIONS

$B_1 = \pm .0002"$

$B_2 = \pm .0002"$

$B_3 = \pm .0002"$

FROM B_1

RUNOUT IN X DIRECTION RESULTS IN TILT OF SLIT

$\theta = \text{invtan} \frac{.0002 in}{9.5043 in}$ $\quad \theta = .001206^\circ$

$\delta_y = (\sin .001206)(8.920 in)$ $\quad \delta_y = .000188 in$

δ_x = ASSUME SIMPLE TRANSLATION $\quad \delta_x = .0002 in$

FROM B1

RUNOUT IN Y DIRECTION RESULTS IN TRANSLATION OF SLIT

$\delta_y = .0002 in$

$\delta_x = 0 in$

FROM B_2

RUNOUT IN Y DIRECTION – NO CHANGE – SPRING ON DETENT

RUNOUT IN X DIRECTION – SAME TILT AS B_1 X DIRECTION RESULTS

FROM B_3

RUNOUT IN Y DIRECTION – NO CHANGE

RUNOUT IN X DIRECTION – SAME TILT AS B_1 X DIRECTIONS RESULTS

MOS SUMMARY

BEARING RUNOUT	δ_x	δ_y
B_1 X DIRECTION	.0002	.000188
B_1 Y DIRECTION	0	.0002
B_2 X DIRECTION	.0002	.000188
B_2 Y DIRECTION	0	0
B_3 X DIRECTION	.0002	.000188
B_3 Y DIRECTION	0	0
RSS	±.000346 in 8.8 μm	±.000382 in 9.7 μm

DEKKER WHEEL

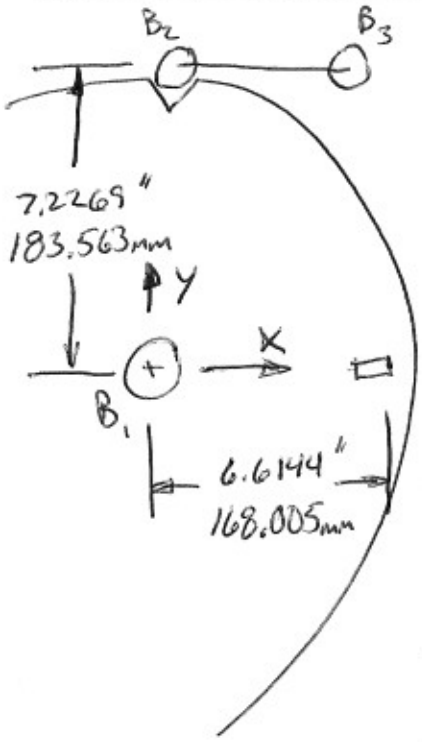

WITH SAME BEARING RUNOUT ASSUMPTIONS AS THE MOS WHEEL

FROM B_1

RUNOUT IN X DIRECTION RESULTS IN TILT OF MASK

$$\theta = \text{INV tan}\frac{.0002\,in}{7.2269\,in} = .001586^\circ$$

$$\delta_y = \left(\sin(.001586^\circ)\right)(6.6144_{in}) = .000183\,in$$

$$\delta_x = .0002\,in$$

DEKKER SUMMARY

BEARING RUNOUT	δ_x	δ_y
B_1 x DIRECTION	.0002	.000183
B_1 y DIRECTION	0	.0002
B_2 x DIRECTION	.0002	.000183
B_2 y DIRECTION	0	0
B_3 x DIRECTION	.0002	.000183
B_3 y DIRECTION	0	0
RSS	± .000346 in 8.8 μm	± .000382 in 9.7 μm

MMIRS

Guider/WFS Mechanism Calculations

Constants:

$arcmin := \left(\frac{1}{60}\right)deg$ $arcsec := \left(\frac{1}{3600}\right)deg$ $ozf := g \cdot oz$

$hz := \frac{1}{sec}$ $rev := 2 \cdot \pi \cdot rad$ $deg = 0.017$

$rpm := \frac{rev}{min}$ $g = 9.807 \frac{m}{s^2}$

Specifications: MMIRS F&P:

The Guider X and Z axis stages must meet the following specs:

$Mechanism\_Repeatability := 200\left(10^{-6}\right)m$

$Encoder\_Resolution := 10\left(10^{-6}\right)m$ *

Mechanism required move time is (WFS move times per Brian 9/9/04 email):

$Time_{move\_Reqd} := 30sec$

$Time_{move\_Desired} := 10sec$

$Time_{move\_WFS\_Reqd} := 10sec$

$Time_{move\_WFS\_Desired} := 5sec$

Minimum Factor of Safety on motor torque is to be:

$FS_{torque} := 2.5$

Guider Horizontal "X" Stage Calculations:

From I-deas modelling as of 4-21-05 the moveable mass on this stage and travel requirements are:

$Mass_{GuiderX} := 17.39kg$

$Travel_X := 140mm$

Since this mass will be moved by a ball screw, calculate the force to turn the screw with the mass loaded in the gravity direction.

For the "YX" Stage ballscrew:

$lead := 6.0\frac{mm}{rev}$ Distance the load moves per revolution of the screw

$E_{bs} := .9$ Ball Screw Efficiency

$\mu_{bs} := .3$ Ball Screw Friction coefficient

Torque to overcome gravity:

$Force := Mass_{GuiderX} \cdot g$ $Force = 170.538\,N$

$T_{Xgravity} := \frac{(Force \cdot lead)}{(E_{bs})}$ $T_{Xgravity} = 0.181\,N \cdot m$

Screw Friction Torque (from preload). Assume the preload force is 30% of the load force:

$Force_{preload} := 0.3 \cdot Force$

$T_{Xpreload} := (Force_{preload} \cdot lead \cdot \mu_{bs})$ $T_{Xpreload} = 0.015\,N \cdot m$

Calculate the torque required to accelerate the load assuming a reasonable linear acceleration:

$a_{linear} := .025 \cdot g$ $a_{linear} = 0.245\frac{m}{s^2}$

$T_{X\_Acc\_load} := \frac{T_{Xgravity} \cdot a_{linear}}{g}$ $T_{X\_Acc\_load} = 4.524 \times 10^{-3}\,N \cdot m$

Calculate inertia of leadscrew:

$\rho_{ss} := 7920 \frac{kg}{m^3}$

$Dia_{ls} := .01m$

$L_{ls} := .325m$

$J_{ls} := \frac{\pi}{32} \cdot \rho_{ss} \cdot L_{ls} \cdot Dia_{ls}^4$ $J_{ls} = 2.527 \times 10^{-6} kg m^2$

Stepper Motor Specifications: Phytron ZSS 52 w/ gearhead and brake:

$MotorSteps := \frac{200}{rev}$

$J_{motor} := .15kg \cdot cm^2$

$T_{rated\_peak} := .45N \cdot m$

Phytron ZSS 52.200. at 70V and:
1400rpm, T = .22 Nm
1094rpm T = .245 Nm
910rpm T = .266 Nm
700rpm T = .283 Nm:

$T_{rated\_continuous} := .245N \cdot m$

From Phytron single stage planetary gearhead data:

$\eta_{gh} := .96$ $J_{gh} := .06kg \cdot cm^2$

$N_{gh} := 6.25$

$T_{gh\_Max\_Rated} := 1.5N \cdot m$

From Phytron telecon (Wahid) 4-25-05:

$J_{brake} := .021kg \cdot cm^2$

$T_{Brake\_Rated} := 0.7N \cdot m$

Calculate "X" Stage step size:

$$StepSize_X := \frac{lead}{MotorSteps \cdot N_{gh}} \quad *$$

$$StepSize_X = 4.8 \times 10^{-6}\,m$$

From THKGeneral Catalog, for KR33, precision grade LM Guide (p. E-17):

$$Repeatability_{Stage\_X} := .003mm$$

Calculate total stage positioning repeatability:

$$Repeatability_{Total\_X} := StepSize_X + Repeatability_{Stage\_X}$$

$$Repeatability_{Total\_X} = 7.8 \times 10^{-6}\,m$$

Calculate the ballscrew rotational acceleration:

$$\alpha := \frac{a_{linear}}{lead}$$

$$\alpha = 256.737\,\frac{rad}{s^2}$$

Calculate the required stage speed assuming the desired positioning time of the "Y" stage (from the F&P):

- Assume that the acceleration time is 20% of the positioning period and the decceleration time equals the acceleration time.

$$time_{accelerating} := 0.2 \cdot Time_{move\_Desired}$$

$$time_{accelerating} = 2\,s$$

$$time_{constant} := Time_{move\_Desired} - 2 \cdot time_{accelerating} \quad *$$

$$time_{constant} = 6\,s$$

$$accel := \frac{Travel_X}{\left[time_{accelerating}^{\,2} + \left(time_{accelerating} \cdot time_{constant}\right)\right]} \quad *$$

$$accel = 8.75 \times 10^{-3}\,\frac{m}{s^2}$$

$$V_{cont} := accel \cdot time_{accelerating}$$

$$V_{cont} = 0.018\,\frac{m}{s}$$

$$\omega_{Screw\_Required} := \frac{V_{cont}}{lead}$$

$$\omega_{Screw\_Required} = 175\,rpm$$

Calculate the required motor speed, torque and torque factor of safety:

$$\omega_{motor} := \omega_{Screw\_Required} \cdot N_{gh} \qquad \omega_{motor} = 1.094 \times 10^{3}\,\text{rpm}$$

$$\alpha_{motor} := \alpha \cdot N_{gh} \qquad \alpha_{motor} = 1.605 \times 10^{3}\,\frac{\text{rad}}{\text{sec}^2}$$

Calculate Peak motor torque required:

$$T_{X\_Motor\_Peak} := \alpha_{motor} \cdot \left(J_{motor} + J_{brake} + J_{gh} + \frac{J_{ls}}{N_{gh}^{2} \cdot \eta_{gh}} \right) + \left(\frac{T_{Xgravity} + T_{Xpreload} + T_{X\_Acc\_load}}{N_{gh} \cdot \eta_{gh}} \right)$$

$$T_{X\_Motor\_Peak} = 0.071\,\text{N}\cdot\text{m}$$

$$FS_{X\_Motor\_Peak} := \frac{T_{rated\_peak}}{T_{X\_Motor\_Peak}} \qquad FS_{X\_Motor\_Peak} = 6.38$$

Calculate Continuous motor torque required:

$$T_{X\_Motor\_Reqd\_Cont} := \frac{T_{Xgravity} + T_{Xpreload}}{\left(N_{gh} \cdot \eta_{gh}\right)} \qquad T_{X\_Motor\_Reqd\_Cont} = 0.033\,\text{N}\cdot\text{m}$$

$$FS_{Motor\_Torque\_Cont} := \frac{T_{rated\_continuous}}{T_{X\_Motor\_Reqd\_Cont}} \qquad FS_{Motor\_Torque\_Cont} = 7.515$$

Calculate the gearhead factor of safety:

$$FS_{Gearhead} := \frac{T_{gh\_Max\_Rated}}{T_{X\_Motor\_Reqd\_Cont}} \qquad FS_{Gearhead} = 46.012$$

Calculate backdriving torque due to load:

$$T_{Backdriving} := \frac{(Force \cdot lead \cdot E_{bs})}{(N_{gh} \cdot \eta_{gh})} \qquad T_{Backdriving} = 0.024\,N \cdot m$$

Calculate Brake Factor of Safety:

$$FS_{Brake} := \frac{T_{Brake\_Rated}}{T_{Backdriving}} \qquad FS_{Brake} = 28.656$$

Guider Vertical "Z" Stage:

From I-deas modelling as of 4-21-05 the moveable mass on this stage and travel requirements are:

$Mass_{GuiderZ} := 11.06kg$

$Travel_Z := 70mm$

Since this mass will be moved by a ball screw, calculate the force to turn the screw with the mass loaded in the gravity direction.

For the "Z" Stage leadscrew:

$lead_Z := 6.0\frac{mm}{rev}$ Distance the load moves per revolution of the screw

Torque to overcome gravity:

$Force_Z := Mass_{GuiderZ} \cdot g$ $Force_Z = 108.462\,N$

$T_{Zgravity} := \frac{(Force_Z \cdot lead_Z)}{(E_{bs})}$ $T_{Zgravity} = 0.115\,N \cdot m$

Screw Friction Torque (from preload). Assume the preload force is 30% of the load force:

$Force_{preloadZ} := 0.3 \cdot Force_Z$

$T_{Zpreload} := (Force_{preloadZ} \cdot lead_Z \cdot \mu_{bs})$ $T_{Zpreload} = 9.322 \times 10^{-3}\,N \cdot m$

Calculate the torque required to accelerate the load assuming a reasonable linear acceleration:

$a_{linear\_z} := .025 \cdot g$ $a_{linear\_z} = 0.245\frac{m}{s^2}$

$T_{Z\_Acc\_load} := \frac{T_{Zgravity} \cdot a_{linear\_z}}{g}$ $T_{Z\_Acc\_load} = 2.877 \times 10^{-3}\,N \cdot m$

Calculate inertia of leadscrew:

$Dia_{ls\_Z} := .01m$

$L_{ls\_Z} := .235m$

$J_{ls\_Z} := \frac{\pi}{32} \cdot \rho_{ss} \cdot L_{ls\_Z} \cdot Dia_{ls\_Z}^{4}$ $J_{ls\_Z} = 1.827 \times 10^{-6} kg\,m^2$

The motor / gearhead / brake is a Phytron 52 (the same as the "X" stage):

Calculate "Z" Stage step size:

$StepSize_Z := \frac{lead_Z}{MotorSteps \cdot N_{gh}}$ * $StepSize_Z = 4.8 \times 10^{-6} m$

From THKGeneral Catalog, for KR33, precision grade LM Guide (p. E-17):

$Repeatability_{Stage\_Z} := .003mm$

Calculate total stage positioning repeatability:

$Repeatability_{Total\_Z} := StepSize_Z + Repeatability_{Stage\_Z}$

$Repeatability_{Total\_Z} = 7.8 \times 10^{-6} m$

Calculate the ballscrew rotational acceleration:

$$\alpha_z := \frac{a_{linear\_z}}{lead_Z} \qquad \alpha_z = 256.737 \frac{rad}{s^2}$$

Calculate the required stage speed assuming the desired positioning time of the "Z" stage (from the F&P):

- Assume that the acceleration time is 20% of the positioning period and the decceleration time equals the acceleration time.

$$accel_z := \frac{Travel_Z}{\left[time_{accelerating}^{2} + \left(time_{accelerating} \cdot time_{constant}\right)\right]} \quad * \quad accel_z = 4.375 \times 10^{-3} \frac{m}{s^2}$$

$$V_{cont\_z} := accel_z \cdot time_{accelerating} \qquad V_{cont\_z} = 8.75 \times 10^{-3} \frac{m}{s}$$

$$\omega_{Screw\_Required\_Z} := \frac{V_{cont\_z}}{lead_Z} \qquad \omega_{Screw\_Required\_Z} = 87.5\,rpm$$

Calculate the required motor speed, torque and torque factor of safety:

$$\omega_{motor\_z} := \omega_{Screw\_Required\_Z} \cdot N_{gh} \qquad \omega_{motor\_z} = 546.875\,rpm$$

$$\alpha_{motor\_z} := \alpha_z \cdot N_{gh} \qquad \alpha_{motor\_z} = 1.605 \times 10^{3} \frac{rad}{sec^2}$$

Calculate Peak motor torque required:

$$T_{Z\_Motor\_Peak} := \alpha_{motor\_z} \cdot \left(J_{motor} + J_{brake} + J_{gh} + \frac{J_{ls\_Z}}{N_{gh}^{2} \cdot \eta_{gh}} \right) + \frac{\left(T_{Zgravity} + T_{Zpreload} + T_{Z\_Acc\_load}\right)}{\left(N_{gh} \cdot \eta_{gh}\right)}$$

$$T_{Z\_Motor\_Peak} = 0.058\,N \cdot m$$

$$FS_{Z\_Motor\_Peak} := \frac{T_{rated\_peak}}{T_{Z\_Motor\_Peak}} \qquad FS_{Z\_Motor\_Peak} = 7.711$$

Calculate Continuous motor torque required:

$$T_{Z\_Motor\_Reqd\_Cont} := \frac{\left(T_{Zgravity} + T_{Zpreload}\right)}{\left(N_{gh} \cdot \eta_{gh}\right)} \qquad T_{Z\_Motor\_Reqd\_Cont} = 0.021\,N \cdot m$$

$$FS_{Z\_Motor\_Cont} := \frac{T_{rated\_continuous}}{T_{Z\_Motor\_Reqd\_Cont}} \qquad FS_{Z\_Motor\_Cont} = 11.816$$

Calculate the gearhead factor of safety:

$$FS_{Gearhead\_Z} := \frac{T_{gh\_Max\_Rated}}{T_{Z\_Motor\_Reqd\_Cont}} \qquad FS_{Gearhead\_Z} = 72.346$$

Calculate backdriving torque due to load:

$$T_{Backdriving\_Z} := \frac{\left(Force_Z \cdot lead_Z \cdot E_{bs}\right)}{\left(N_{gh} \cdot \eta_{gh}\right)} \qquad T_{Backdriving\_Z} = 0.016\,N \cdot m$$

Calculate Brake Factor of Safety:

$$FS_{Brake\_Z} := \frac{T_{Brake\_Rated}}{T_{Backdriving\_Z}} \qquad FS_{Brake\_Z} = 45.057$$

Guider Wave Front Sensor Stage:

From I-deas modelling as of 4-21-05 the moveable mass on this stage and travel requirements are:

$Mass_{WFS} := 1.5kg$ Model shows 0.9 kg - 50% factor applied.

$Travel_{WFS} := 40mm$

Since this mass will be moved by a ball screw, calculate the force to turn the screw with the mass loaded in the gravity direction.

For the WFS Stage leadscrew:

$lead_{WFS} := 6.0\frac{mm}{rev}$ Distance the load moves per revolution of the screw

Torque to overcome gravity:

$Force_{WFS} := Mass_{WFS} \cdot g$ $Force_{WFS} = 14.71\,N$

$T_{WFSgrav} := \frac{(Force_{WFS} \cdot lead_{WFS})}{(E_{bs})}$ $T_{WFSgrav} = 0.016\,N \cdot m$

Screw Friction Torque (from preload). Assume the preload force is 30% of the load force:

$Force_{preloadWFS} := 0.3 \cdot Force_{WFS}$

$T_{WFSpreload} := (Force_{preloadWFS} \cdot lead_{WFS} \cdot \mu_{bs})$ $T_{WFSpreload} = 1.264 \times 10^{-3}\,N \cdot m$

Calculate the torque required to accelerate the load assuming a reasonable linear acceleration:

$a_{linear\_WFS} := .025 \cdot g$ $a_{linear\_WFS} = 0.245\frac{m}{s^2}$

$T_{WFS\_Acc\_load} := \frac{T_{WFSgrav} \cdot a_{linear\_WFS}}{g}$ $T_{WFS\_Acc\_load} = 3.902 \times 10^{-4}\,N \cdot m$

Calculate inertia of leadscrew:

$Dia_{ls\_WFS} := .01m$

$L_{ls\_WFS} := .150m$

$J_{ls\_WFS} := \frac{\pi}{32} \cdot \rho_{ss} \cdot L_{ls\_WFS} \cdot Dia_{ls\_WFS}^{4}$ $J_{ls\_WFS} = 1.166 \times 10^{-6} kg m^2$

The motor / gearhead / brake is a Phytron 52 (the same as the "X" stage):

Calculate "WFS" Stage step size:

$StepSize_{WFS} := \frac{lead_{WFS}}{MotorSteps \cdot N_{gh}}$ * $StepSize_{WFS} = 4.8 \times 10^{-6} m$

From THKGeneral Catalog, for KR30H, precision grade LM Guide (p. E-17):

$Repeatability_{Stage\_WFS} := .003mm$

Calculate total stage positioning repeatability:

$Repeatability_{Total\_WFS} := StepSize_{WFS} + Repeatability_{Stage\_WFS}$

$Repeatability_{Total\_WFS} = 7.8 \times 10^{-6} m$

Torque required to accelerate the leadscrew, motor and brake is:

$\alpha_{WFS} := \frac{a_{linear\_WFS}}{lead_{WFS}}$ $\alpha_{WFS} = 256.737 \frac{rad}{sec^2}$

Calculate the required stage speed assuming the desired positioning time of the "WFS" stage (from the F&P):

- Assume that the acceleration time is 20% of the positioning period and the decceleration time equals the acceleration time.

$$accel_{WFS} := \frac{Travel_{WFS}}{\left[time_{accelerating}^{2} + \left(time_{accelerating} \cdot time_{constant}\right)\right]} \quad cel_{WFS} = 2.5 \times 10^{-3} \frac{m}{s^2}$$

$$V_{cont\_WFS} := accel_{WFS} \cdot time_{accelerating} \qquad V_{cont\_WFS} = 5 \times 10^{-3} \frac{m}{s}$$

$$\omega_{Screw\_Required\_WFS} := \frac{V_{cont\_WFS}}{lead_{WFS}} \qquad \omega_{Screw\_Required\_WFS} = 50\,rpm$$

Calculate the required motor speed, torque and torque factor of safety:

$$\omega_{motor\_WFS} := \omega_{Screw\_Required\_WFS} \cdot N_{gh} \qquad \omega_{motor\_WFS} = 312.5\,rpm$$

$$\alpha_{m\_WFS} := \alpha_{WFS} \cdot N_{gh} \qquad \alpha_{m\_WFS} = 1.605 \times 10^{3} \frac{rad}{sec^2}$$

Calculate Peak motor torque required and torque factor of safety:

$$T_{WFS\_Peak} := \alpha_{m\_WFS} \cdot \left(J_{motor} + J_{brake} + J_{gh} + \frac{J_{ls\_WFS}}{N_{gh}^{2} \cdot \eta_{gh}} \right) + \frac{\left(T_{WFSgrav} + T_{WFSpreload} + T_{WFS\_Acc\_load}\right)}{\left(N_{gh} \cdot \eta_{gh}\right)}$$

$$T_{WFS\_Peak} = 0.04\,N \cdot m$$

$$FS_{WFS\_Motor\_Peak} := \frac{T_{rated\_peak}}{T_{WFS\_Peak}} \qquad FS_{WFS\_Motor\_Peak} = 11.252$$

Calculate the Continuous motor torque required and torque factor of safety:

$$T_{WFS\_Motor\_Reqd\_Cont} := \frac{T_{WFSgrav} + T_{WFSpreload}}{\left(N_{gh} \cdot \eta_{gh}\right)}$$

$$T_{WFS\_Motor\_Reqd\_Cont} = 2.812 \times 10^{-3}\ N \cdot m$$

$$FS_{WFS\_Motor\_Cont} := \frac{T_{rated\_continuous}}{T_{WFS\_Motor\_Reqd\_Cont}} \qquad FS_{WFS\_Motor\_Cont} = 87.127$$

Calculate the gearhead factor of safety:

$$FS_{Gearhead\_WFS} := \frac{T_{gh\_Max\_Rated}}{T_{WFS\_Motor\_Reqd\_Cont}} \qquad FS_{Gearhead\_WFS} = 533.428$$

Calculate backdriving torque due to load:

$$T_{Backdriving\_WFS} := \frac{\left(Force_{WFS} \cdot lead_{WFS} \cdot E_{bs}\right)}{\left(N_{gh} \cdot \eta_{gh}\right)}$$

$$T_{Backdriving\_WFS} = 2.107 \times 10^{-3}\ N \cdot m$$

Calculate Brake Factor of Safety:

$$FS_{Brake\_WFS} := \frac{T_{Brake\_Rated}}{T_{Backdriving\_WFS}} \qquad FS_{Brake\_WFS} = 332.218$$

Camera Focus Stage:

Calculate the camera focus stage resolution required knowing the camera pixel size and guide camera f#. From the geometry on part mmirs9, the Fnumber is calculated (between 3 and 3.28):

$Fnumber := 3.28deg$

$Pixel\_Size_{CCD} := 13\left(10^{-6}\right)m$ *

$$DepthofFocus := \frac{\left(\frac{Pixel\_Size_{CCD}}{2}\right)}{\tan(Fnumber)} \qquad DepthofFocus = 4.465 \times 10^{-3}\,in$$

Required resolution of camera focus stage is:

$$Res_{Camera\_Reqd} := \frac{DepthofFocus}{2}$$

$$Res_{Camera\_Reqd} = 2.233 \times 10^{-3}\,in$$

$$Res_{Camera\_Reqd} = 5.671 \times 10^{-5}\,m$$

Specifications: MMIRS F&P:

The Camera Focus axis stage must meet the following specs:

$Mechanism\_Repeatability_{Camera} := 40\left(10^{-6}\right)m$

$Encoder\_Resolution_{Camera} := 25\left(10^{-6}\right)m$ *

From I-deas modelling as of 4-21-05 the moveable mass on this stage and travel requirements are:

$Mass_{Camera} := 1.7kg$

$Travel_{Camera} := 2mm$

Phytron ZSS 52 motor ratings:

$F_{Bearing\_Radial\_gh} := 250N$

Using a cam determine the travel size of one motor step.

$$CamTravelperStep := \frac{Travel_{Camera} \cdot 360 \frac{deg}{rev}}{N_{gh} \cdot MotorSteps \cdot (330deg)} \quad * \qquad CamTravelperStep = 1.745 \times 10^{-6} m$$

The step size results in a step travel of "Factor" greater than the camera focus repeatability requirement.

$$Factor := \frac{Mechanism\_Repeatability_{Camera}}{CamTravelperStep} \qquad Factor = 22.917$$

Calculate the focus stage minimum motor speed:

$$\omega_{focus\_motor} := \frac{\left[(330deg) \cdot N_{gh}\right]}{Time_{move\_Desired}} \quad * \qquad \omega_{focus\_motor} = 34.375\,rpm$$

The ramp angle of the cam is:

$$theta := atan\left[\frac{(2mm)}{\pi \cdot (2 \cdot 25.4)\,mm \cdot \left(\frac{330}{360}\right)}\right] \quad * \qquad theta = 0.783\,deg$$

Assuming the springs pull the camera against the cam with 5g's of force, determine the factor of safety on the motor bearing radial rating and the factor of safety on backdriving torque vs.the brake rating:

$$Force_{Camera} := 5 \cdot g \cdot Mass_{Camera} \qquad Force_{Camera} = 83.357\,N$$

$$FS_{Bearing\_Radial} := \frac{F_{Bearing\_Radial\_gh}}{Force_{Camera}} \qquad FS_{Bearing\_Radial} = 2.999$$

$$Radius_{CameraCamMax} := 27.4mm$$

$$Backdriving\_Torque_{Camera} := \frac{\left(Force_{Camera} \cdot \sin(theta) \cdot Radius_{CameraCamMax}\right)}{\left(N_{gh} \cdot \eta_{gh}\right)} \ *$$

$$Backdriving\_Torque_{Camera} = 5.204 \times 10^{-3}\,N \cdot m$$

$$FS_{CameraTorque} := \frac{T_{Brake\_Rated}}{Backdriving\_Torque_{Camera}} \qquad FS_{CameraTorque} = 134.522$$

CHAPTER HEADING

MOS Slit sizing calculations:

Calculate MOS Long Slit widths based on specifications in F&PR and MOS Section Spec.:

$$\text{arcminute} := \frac{1\text{deg}}{60}$$

$\text{MOS\_Slit\_Width} := 69.14\text{mm}$

$\text{MOS\_Slit\_Angle} := 7\text{arcminute}$ $\quad \text{MOS\_Slit\_Angle} = 0.117\,\text{deg}$

$$\text{Plate\_Scale} := \frac{\text{MOS\_Slit\_Width}}{\text{MOS\_Slit\_Angle}} \qquad \text{Plate\_Scale} = 9.877\,\frac{\text{mm}}{\text{arcminute}}$$

$\text{Detector\_Pixel\_Size} := 18\left(10^{-6}\right)\text{m}$

$\text{Detector\_Pixels} := 2048$

$\text{Detector\_Width} := \text{Detector\_Pixels}\cdot\text{Detector\_Pixel\_Size}$ $\quad \text{Detector\_Width} = 36.864\,\text{mm}$

$$\text{Optical\_Magnification} := \frac{\text{Detector\_Width}}{\text{MOS\_Slit\_Width}} \qquad \text{Optical\_Magnification} = 0.533$$

$\text{Pixels} := 1, 2 .. 12$

$$\text{Slit\_Width}(\text{Pixels}) := \frac{(\text{Pixels}\cdot\text{Detector\_Pixel\_Size})}{\text{Optical\_Magnification}}$$

$\text{Slit\_Width}(\text{Pixels}) =$ in

$1.3291\cdot10^{-3}$
$2.6582\cdot10^{-3}$
$3.9874\cdot10^{-3}$
$5.3165\cdot10^{-3}$
$6.6456\cdot10^{-3}$
$7.9747\cdot10^{-3}$
$9.3039\cdot10^{-3}$
0.0106
0.012
0.0133
0.0146
0.0159

Section IV.

Camera Section Design

1. Camera Specifications
2. Camera Section Mechanical Design
3. Camera Design Supporting Calculations
4. Cryostat Optics Mounting System
5. Collimator and Camera Lens Mount Calculations

MMIRS CAMERA SECTION SPECIFICATIONS

S-MMIRS-203

George Nystrom
February 23, 2004

Updated May 27, 2004 by GN [PDR version]
Updated June 6, 2004 by GN
Updated May 2, 2005 by PM [reformatted, minor edits]

100 Introduction

The Camera Section is composed of the sub-assemblies specified below. The MMIRS Functional and Performance Requirements (F&P) document (S-MMIRS-200) is the Camera Section's controlling document. If there are any discrepancies between the F&P and this document, the F&P shall prevail.

The Camera Section structural assembly (or optical bench) provides the structural attachment points for two lens assemblies, a grism wheel, two filter wheels, an IR array detector mount, and an LN2 reservoir and feedthroughs. The Camera Section also includes a vacuum enclosure, thermal shields, and electrical interface connectors. The warm bulkhead is the structural interface to the MOS Section and the MMIRS telescope mounting truss.

The following F&P requirements and specifications are particularly relevant to the Camera Section:

1. Section 100—Optical Requirements
2. Section 300—Mechanical Requirements
3. Section 400—Electrical and Electronic Requirements
4. Section 600—Observatory Physical Interface
5. Section 700 – Environmental Requirements
6. Section 800—Other requirements

Note also that the Camera Section must meet the rigidity specifications for the MMIRS instrument when combined with the MOS Section.

200 Vacuum integrity

The Camera Section shall be leak tight to less than 5×10^{-6} STD cc of helium/sec. Proper material selection and cleanliness during assembly must be exercised to minimize contamination due to out gassing. All enclosed volumes, such as tapped holes, must be vented.

300 Axes definitions

The optical axes are defined as follows: Z axis is along the optical axis with –Z towards the detector, Y is the elevation axis, and X is the azimuth axis. These axis definitions apply only when the telescope rotator is at the "0" position.

400 Optics

The Camera Section positions and holds lens 3 –14. The lens positions are shown on MMIRS optical diagram MMIRS -100. The following specifications must be satisfied for the optical elements:

1. Positioning is per the MMIRS Optical Specifications.
2. Temperature range: 300 to 80 ± 3 degrees Kelvin.
3. Pressure: One atmosphere to 1 times 10^{-7} Torr.
4. Mounting:
   Lens cells must not distort the optic by either thermal or mechanical stressing. The allowable lens stress level must not exceed ± 200 psi. All lenses or lens combinations shall be mounted in a cell that allows for their removal. A spacer is required between all lens cells for setting their inter-optic spacing.
5. Maximum lens cooling rate: See Table 1 below.
6. Stray light baffles:
   Baffles to reduce stray light are required. Refer to the optic diagram MMIRS-100, sheet 3 of for their size and positioning.
7. Venting:
   The lens cell shall provide an evacuation path for all internal cavities, which shall not allow external illumination to enter directly.

500 Filter and Grism wheels

The two Filter Wheels are used to introduce various spectral filters into the optical beam. The Grism Wheel is used to place a series of grisms into the beam to disperse objects onto the IR array.

510 Filter Wheels

There shall be two identical Filter Wheels having six positions: Five of these positions shall have filters and the sixth shall be an open aperture. The filters are 125 mm in diameter and 5-10 mm thick.

520 Grism Wheel

The Grism Wheel shall have 6 positions and will carry 5 grisms and one open aperture. The entrance beam diameter at the base of each grism is 120 mm and the mounting size is138 mm times 5 mm in height. The grism maximum height is 120 mm above its mounting surface. Each grism must have a flat on its mounting diameter to define its rotational angle about the -Z axis

The Lyot stop positions a precision aperture that is matched to the telescope's entrance pupil. The Lyot stop will be mounted on the main support structure for the Filter and Grism wheels. The Lyot stop shall be fixed and designed to block the telescope's secondary obscuration. The Lyot stop is defined on drawing MMIRS-100, sheet 3 of 3. The filter wheel closest to the Lyot stop will carry aperture stops to limit the field of view for the K and H+K bands to minimize background.

The design of the filter and grism mounts shall follow the design shown in the Flamingos-2 CDR package. These elements will reside within a recess in the wheels having sufficient clearance to eliminate thermal stressing and be clamped in place using a spring-loaded retainer. The wheels shall allow adequate optical clearance for the science beam and will neither vignette nor scatter light into the science beam. All

optics must be thermally coupled to their respective wheels and shall operate at a temperature of 80 ± 3 Kelvin.

600 Wheel Design Parameters

The Grism and Filter Wheels shall have stepper motor driven worm gear systems capable of satisfying the following requirements:

1. A minimum factor of safety of 2.5 times the worst case expected drive torque.
2. Unlimited angular rotation in either the clockwise or counterclockwise directions.
3. The detent system shall have positional accuracies as specified in F&P section 300. Those requirements are repeated here; however, they must be verified against the F&P.
   a. Repeatability: within ± 50 microns (1 arc-min) measured at the optical axis.
   b. Stability: ± 25 microns for the filters and grisms measured at the optical axis. This is for one full cryostat rotation about the Z axis over the telescope's elevation range.
   c. All grisms must be oriented so that their spectra are aligned with the detector's pixel coordinate system within 1 mrad.
   d. Detent offset: less than 100 microns optic centerline to detent centerline.
4. Micro-switch sensing systems:
   a. One switch shall sense the detent position.
   b. A home micro-switch shall allow the step counter to be reset. The identification of the mask position shall be done in software using both step counting and micro-switch information.
   c. The home switch shall be located at the open position of all wheels.
5. The maximum time to move 180 degrees shall not exceed 30 seconds with 10 seconds as a goal. The software shall determine the direction that will minimize travel time.
6. All designs must operate in a vacuum (≈$1x10^{-7}$ Torr) and at a temperature of 80± 3 degrees K.
7. All designs shall use vacuum-compatible materials and consider temperature effects.
8. An interface connector is required for each wheel drive system and the vacuum interface cable. This allows ease of replacement.
9. The desired wheel operating temperature is 80 ± 3 Kelvin. The wheels must meet the required target temperatures and times per F&P section 350.
10. The wheels shall have a common mounting plane for all optics to within ±250 microns as measured along the optical axis and perpendicular to the optical beam within 25 microns in the X – Y plane.
11. All wheels and all other precision manufactured parts must be cycled to Cryogenic temperatures during the manufacturing process to relieve stress and to increase their cryogenic temperature stability.
12. The Grism Wheel shall allow adjustment for positioning of the Lyot stop in all three axes.

700 Detector Mount

The Detector Mount shall follow the Flamingos 2 design for the mounting and thermal attachment of the IR array detector. The detector shall be mounted on a translation stage similar to the Flamingos 2 design; however it will be driven by a Phytron motor using a Cam and employ an LVDT sensor for position readout. The slide travel direction is in the focus direction with a range of travel of 12-15 mm. The focus drive (Cam) shall provide ± 2.5 mm of travel with a position resolution of ≅5 microns. The focus drive

shall be adjustable over the slide's range of travel to allow setting its cam's range about the optimal focus position.

The detector shall not have a temperature rate of change (cooling and heating) greater than 0.2 degrees per minute. The IR detector shall be centered on the optical axis within 0.1mm and perpendicular to the entrance slit within 5 microns over the width of the detector. A thermal sensor shall be located near the detector to provide temperature data. The detector electronics shall be based on those developed for the SWIRC program, although the detailed electronic board sizes and packaging design may differ.

The vacuum enclosure shall allow access to the detector at its domed end. The access port shall also allow the array's cables to exit the vacuum system. The detector's pre-amplifiers shall be mounted outside of the vacuum enclosure at the access port. This design is intended to minimize the length of the signal cables.

800 Cryogenic System

The optical bench is design to provide an integral LN_2 reservoir with a capacity up to 100 liters. The Camera Section shall be designed to provide a minimum hold time of 30 hours once it has been cooled to its operating temperature and filled with LN2. This requirement is specified in section 353 of the F&P. A G10 thermal isolation ring shall be used to support the optical bench from the Camera Section's warm front bulkhead and provide the necessary thermal isolation and structural strength.

The LN_2 reservoir shall have two isolated lines, which shall pass through the vacuum wall. One line shall be a fill line and the other a vent line. These lines must be vacuum-tight and use a standard bellows for thermal isolation. The fill line shall extend down to the reservoir's detector end. This will allow the reservoir to be purged prior to warm up by pressurizing the LN2 reservoir through the vent line.

810 Design Parameters

The LN_2 fill and vent lines shall be designed to minimize thermal conduction to the camera vacuum enclosure. The Flamingos 2, LN2 design shall be used as a reference.

1. The rate of temperature change of the optical bench during warm up and cool down shall be set by the detector's heating and cooling rate of 0.2 degrees Kelvin per minute. This rate is set in Section 350 of the F&P. The maximum temperature gradients in the lenses listed in Table 1 shall also not be exceeded.
2. A heating system shall be designed to allow warm-up of the camera section. It shall be designed using Kapton flexible heaters bonded to the LN2 reservoir.
3. A system of radiation shields shall be designed to minimize heat loss between the cold components and the surrounding vacuum enclosure. Their effectiveness must satisfy the requirements for hold time stated above.
4. A system of temperature sensors shall be used to characterize the Camera Section's thermal behavior. The number and placement of these sensors shall be determined through a preliminary thermal analysis.

900 Vacuum system

The Camera Section vacuum enclosure shall provide the necessary interfaces to mount the vacuum components as specified on drawing number C-MMIRS-102.

The Camera Section has no active pumping equipment and will be evacuated with the MOS Section turbo pump. The total cryostat (MOS and Camera Sections combined) pump down time (after initial bake-out and several initial pump-down cycles) shall be less than 4 hours to a pressure of 10^{-4} Torr. The Camera Section shall have two passive absorption cartridges. One will be conductively coupled to the LN2 dewar and the other thermally isolated from it. These cold charcoal absorption cartridges are for pumping nitrogen and other noble gases during the heating and cooling times. A Zeolite absorption cartridge shall also be placed on the outside of the vacuum vessel. It shall be mounted to a valve to allow its removal for recharging.

The vacuum enclosure shall have an evacuation port for use during testing when the MOS Section is not present. This port shall be capped off once the MOS Section is attached. The Camera Section shall then be evacuated through the gate valve described below.

A vacuum gauge shall be mounted on a right angle elbow on the vacuum enclosure's external wall with appropriate baffling to eliminate illumination within the Camera section. It shall provide pressure readout from one atmosphere to 10^{-9} Torr.

A gate valve shall be employed to provide vacuum isolation of the Camera Section while the MOS Section is either vented to atmosphere or its temperature is above 85 degrees Kelvin. This valve must be leak tight to less the 10^{-8} std. cc of helium per sec. The gate valve shall provide adequate conductance to allow efficient evacuation of the Camera Section. The vacuum valve requires that a safety interlock system be developed with the MOS vent valve to prevent accidental venting. The design of this interlock system requires a safety review prior to implementation.

The vacuum vessel shall be constructed of aluminum with its internal surface polished to 4-6 micro inch roughness. All welds must be vacuum-tight such that the vessel is leak tight to less than 10^{-9} std. cc of helium per sec. Also, a thermal coating maybe specified for the vessels internal/external walls.

Table 1: Allowable Lens Temperature Gradients [in degrees C]

lens number	radial gradient	axial gradient	dimetral gradient
3	2.18	46.30	222.22
4	1.39	48.31	555.56
5	3.97	42.74	370.37
6	4.83	222.22	1111.11
7	92.59	2777.78	22222.22
8	2.78	42.74	555.56
9	2.58	44.44	370.37
10	3.58	113.38	1234.57
11	2.47	44.44	358.42
12	3.83	48.31	483.09
13	2.22	46.30	252.53
14	5.05	156.49	1221.00

MMIRS CAMERA SECTION DESIGN

Table of Contents

100 Camera Section Design

The Camera section houses the following components in an aluminum vacuum vessel with an internal liquid nitrogen dewar:

- Optical bench / dewar assembly
- Collimator lens assembly
- Grism assembly
    - Filter wheel assemblies (2)
    - Lyot stop
    - Grism wheel assembly
- Camera lens assembly
- Detector assembly
- Detector pre-amplifier assembly
- Thermal shields and temperature monitoring devices

The following components are part of the camera section, however are external to the vacuum vessel:

- Zeolite sorption pump
- Pfeiffer vacuum gauge
- Vacuum isolation valve
- Electrical connectors and LN_2 feedthrus

The performance and operating characteristics for the Camera Section are defined in SAO specification S-MMIRS-202.

Figures 1 and 2 below show 3-D views of the camera section with the vacuum housing and thermal shields removed for clarity. Figure 3 shows a cross-sectional view of the camera section through the optical axis.

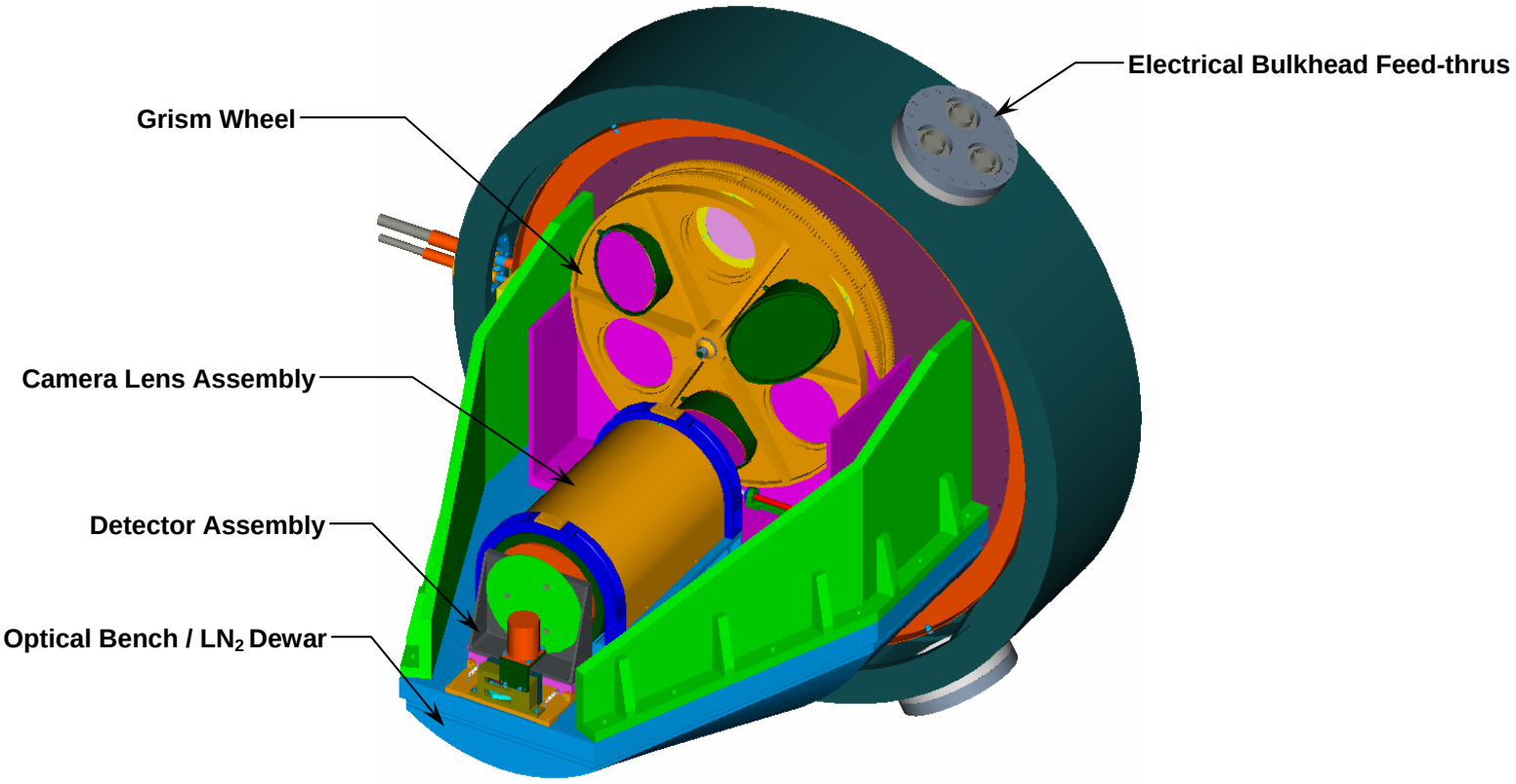

Figure 1 - Camera Section Rear 3-D View

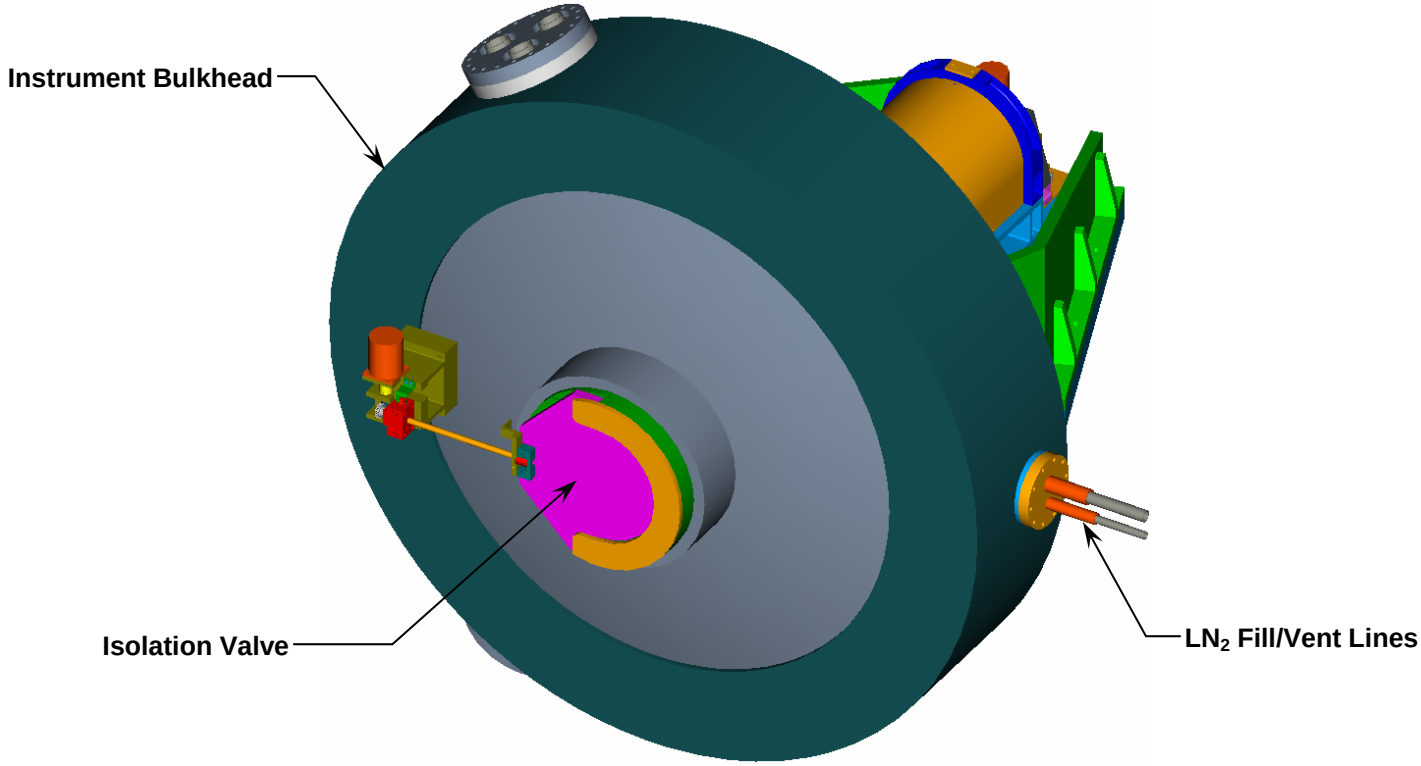

Figure 2 - Camera Section Front 3-D View

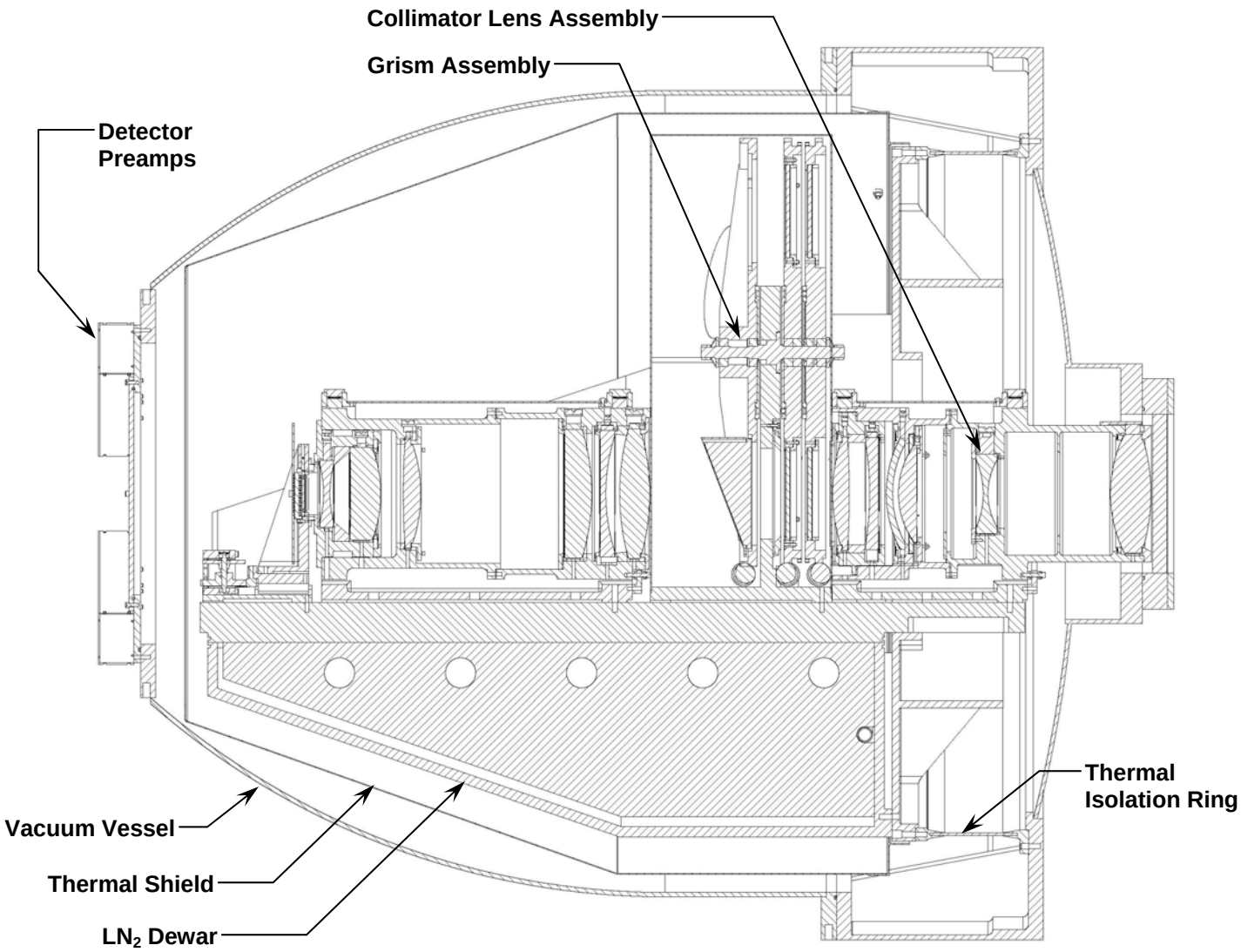

Figure 3 - Camera Section Cross-Section View

110 Internal Camera Components

111 Optical Bench/Dewar Assembly

The optical bench/dewar assembly is used to mount all the internal components listed in the previous section. The assembly is composed of four main structural elements:

- The front bulkhead is a deep section forging which provides the mounting interface to the telescope truss. It also provides the MOS/Camera vacuum separation via a specially designed vacuum isolation valve. The vacuum LN_2 and electrical feed-thrus penetrate the bulkhead.

- A G10 bonded ring assembly with aluminum end fittings is designed to provide the required thermal isolation and structural stiffness. It is similar to MOS section G10 ring previously described.

- A support ring provides the coupling between the G10 ring and bench structure. It is a deep section aluminum machined ring that is secured to the optical bench's top plate, at the dewar outer radius, and to the side plates. This provides a wide structural footprint that transfers structural loads directly into the G10 ring.

- The Optical bench/dewar is complex structure composed of a top plate, side rails and a LN_2 storage container. A two inch, light-weighted top plate is welded to the LN_2 reservoir. The welds are recessed to avoid damage during assembly/handling and are a continuous around bench's perimeter. Three stiffening ribs internal to the reservoir provide both structural stiffness and thermal wetting to the LN_2. The LN_2 fill and vent lines are fastened internally before welding the dewar closed.

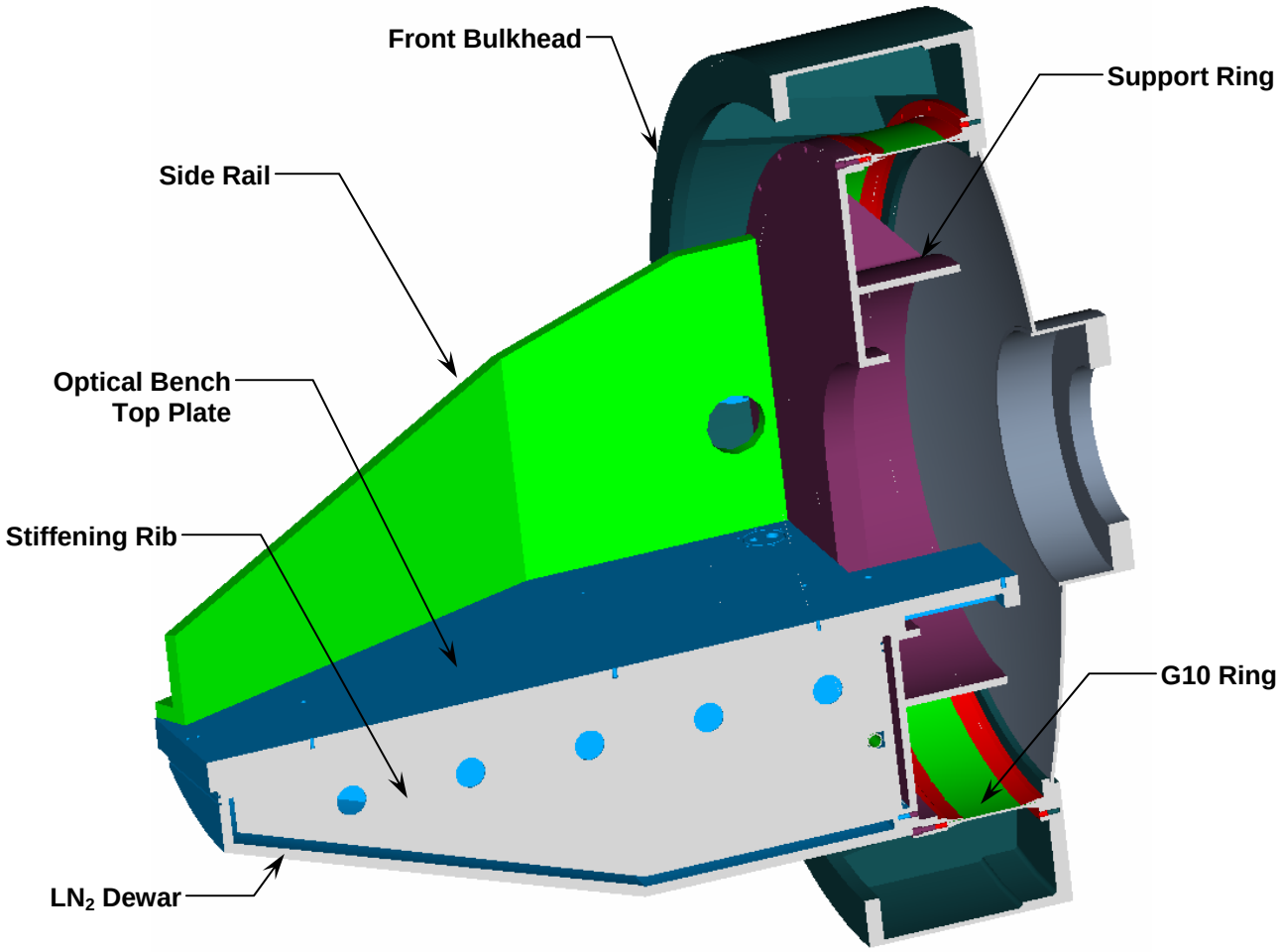

Figure 4 - Optical Bench Structural Assembly

112 Collimator Lens Assembly

The collimator assembly is discussed in the Optics Mounts document in this section.

113 Grism Assembly

The Grism assembly is composed of the following components:

- Six-position filter wheel
- Six-position filter wheel with aperture stops
- Lyot stop
- Six-position grism wheel
- Cover

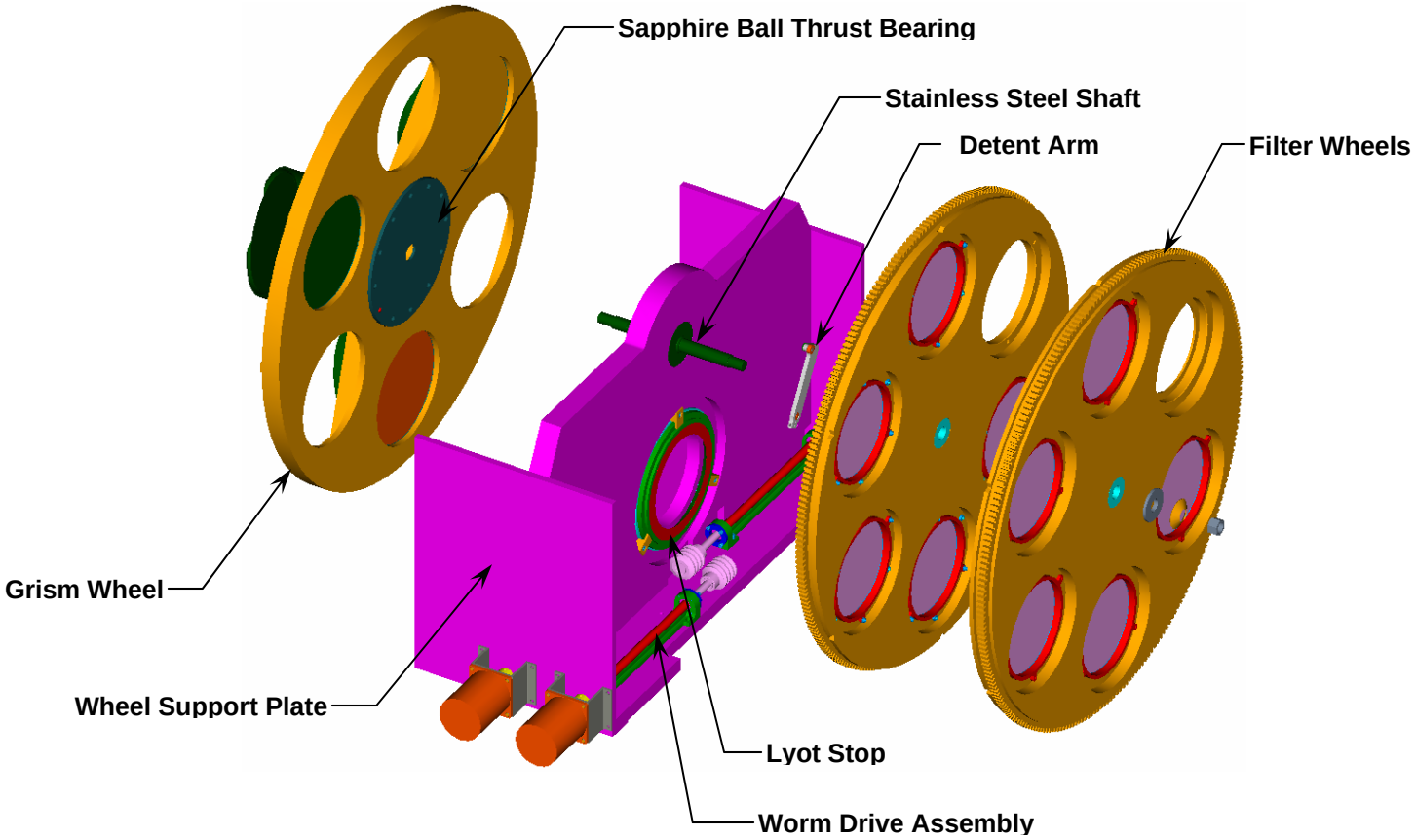

Figure 5 - Grism Assembly

The two filter wheels are identical in design. Each wheel carries up to five filters leaving one open aperture. A single filter or a combination of two filters can be introduced into the beam using both wheels. The wheels have a central hub containing a set of bearings for radial definition and a thrust bearing made from sapphire balls for axial definition. The wheel is a motor driven worm

gear arrangement with a micro switch for homing. A spring loaded detent provides positional stability. The detent also contains a micro switch. The stepper motor is 200 steps/rev and is common with the all of the cold motors in the MOS section. It is specified to maintain the filter temperatures between 77 K - 83 K. The filter wheels' performance and operating characteristics are defined in Camera Specification S-MMIRS-202.

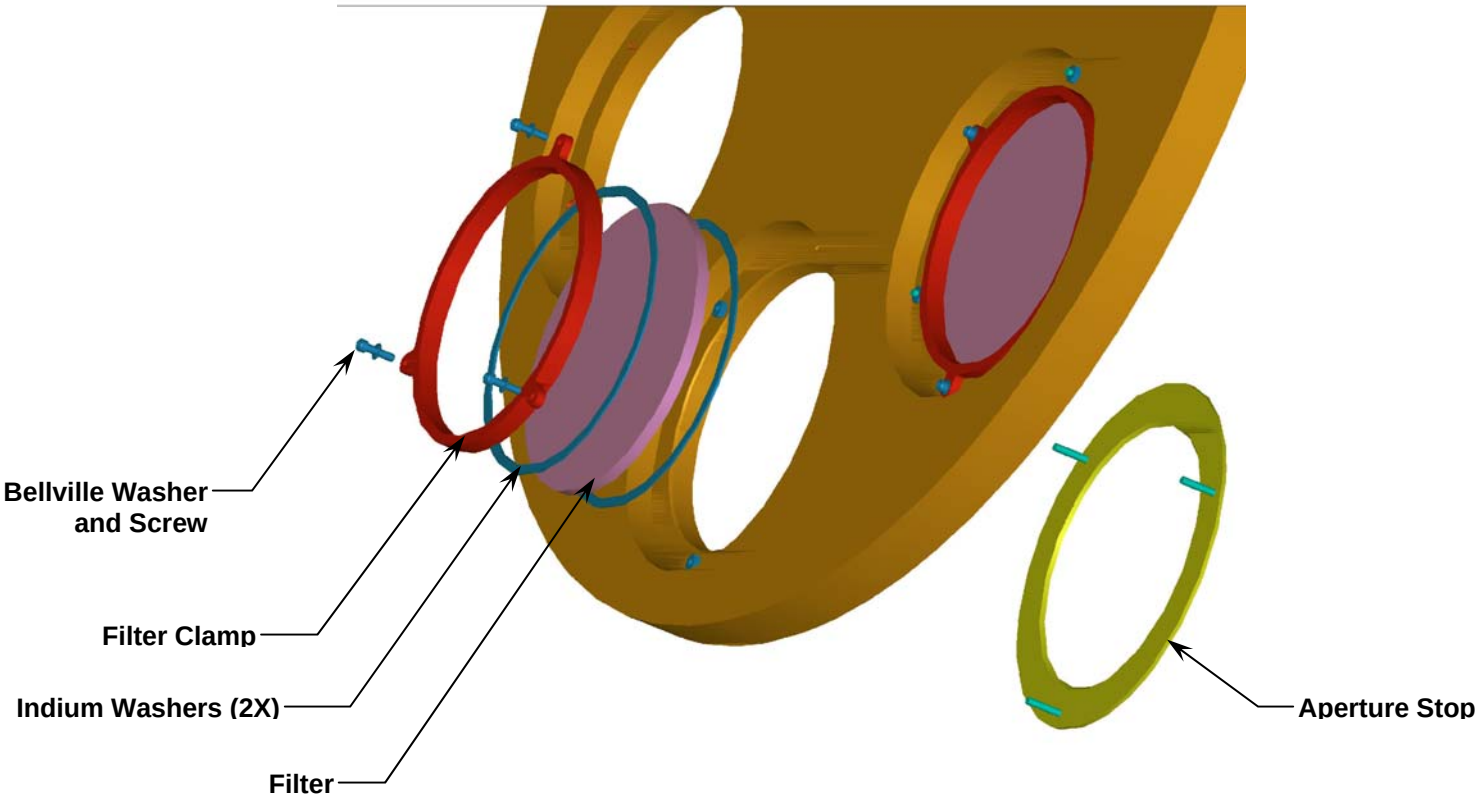

Figure 6 - Filter Wheel with Aperture Stop

The Lyot stop is a fixed stop held within the grism wheel support structure. Its pattern masks the telescopes obscuration pattern and has an adjustable mount allowing radial positioning. Shims are planned for axial placement if required.

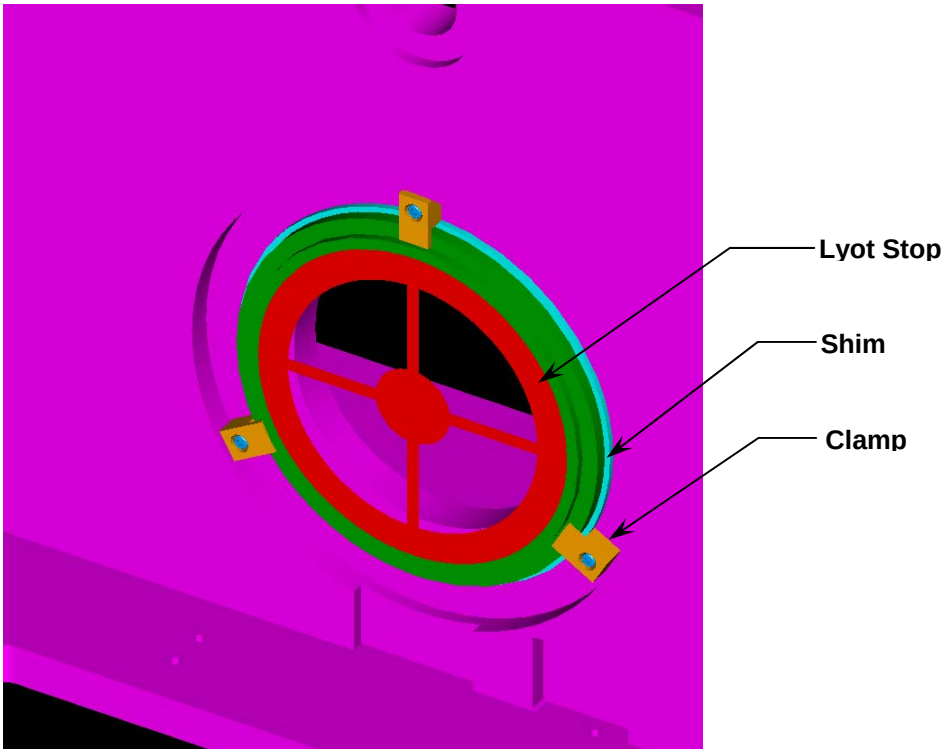

Figure 7 - Lyot Stop

The Grism wheel is a six-position wheel intended to carry five grisms with one permanent open aperture. The grism mounting design follows the Univ. of Florida scheme, which provides rigid positioning and thermal coupling. The grisms fit into a wheel recess with a compression clamp against its mounting foot. The compression clamp has copper fingers that wipe the grisms outer diameter to provide an additional thermal conductive path. The wheel has a central hub containing a set of bearings for radial definition and a thrust bearing made from sapphire balls for axial definition. The grism wheel drive is identical to the filter wheels'. The grism wheel performance and operating characteristics are defined in Camera Specification S-MMIRS-202.

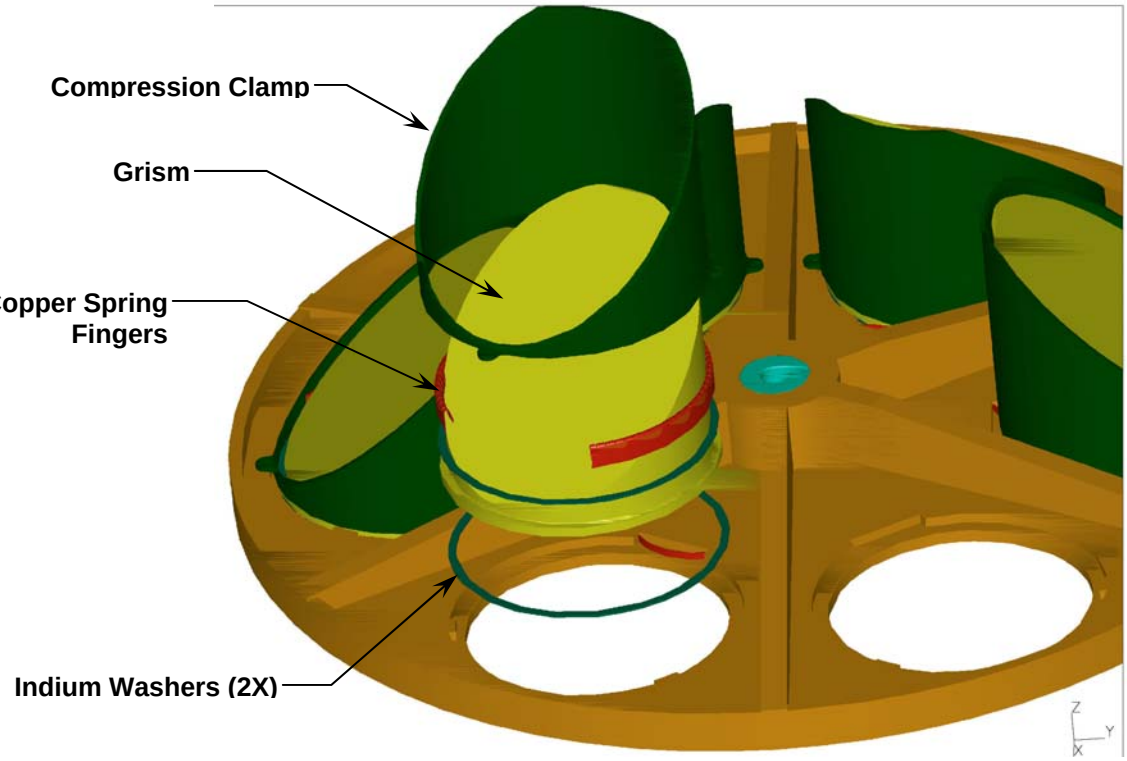

Figure 8 - Grism Wheel

The grism assembly has a thin aluminum cover to provide radiative coupling to the wheel assembly and to limit scattered light from entering the optical path.

114 Camera Lens Assembly

The camera lens assembly is also discussed in the Optics Mounts document.

115 Detector Assembly

The Detector mount is based on the SAO design developed in the SWIRC program. A PCB called the header board serves as mechanical support for the imager, conduit for all signals to and from the imager, and thermal path for primary heat extraction. It mounts a soldered ZIF socket into which the Rockwell Hawaii 2 IR imager plugs. The header board is spring loaded against the detector support bracket, which interfaces with the focus slide.

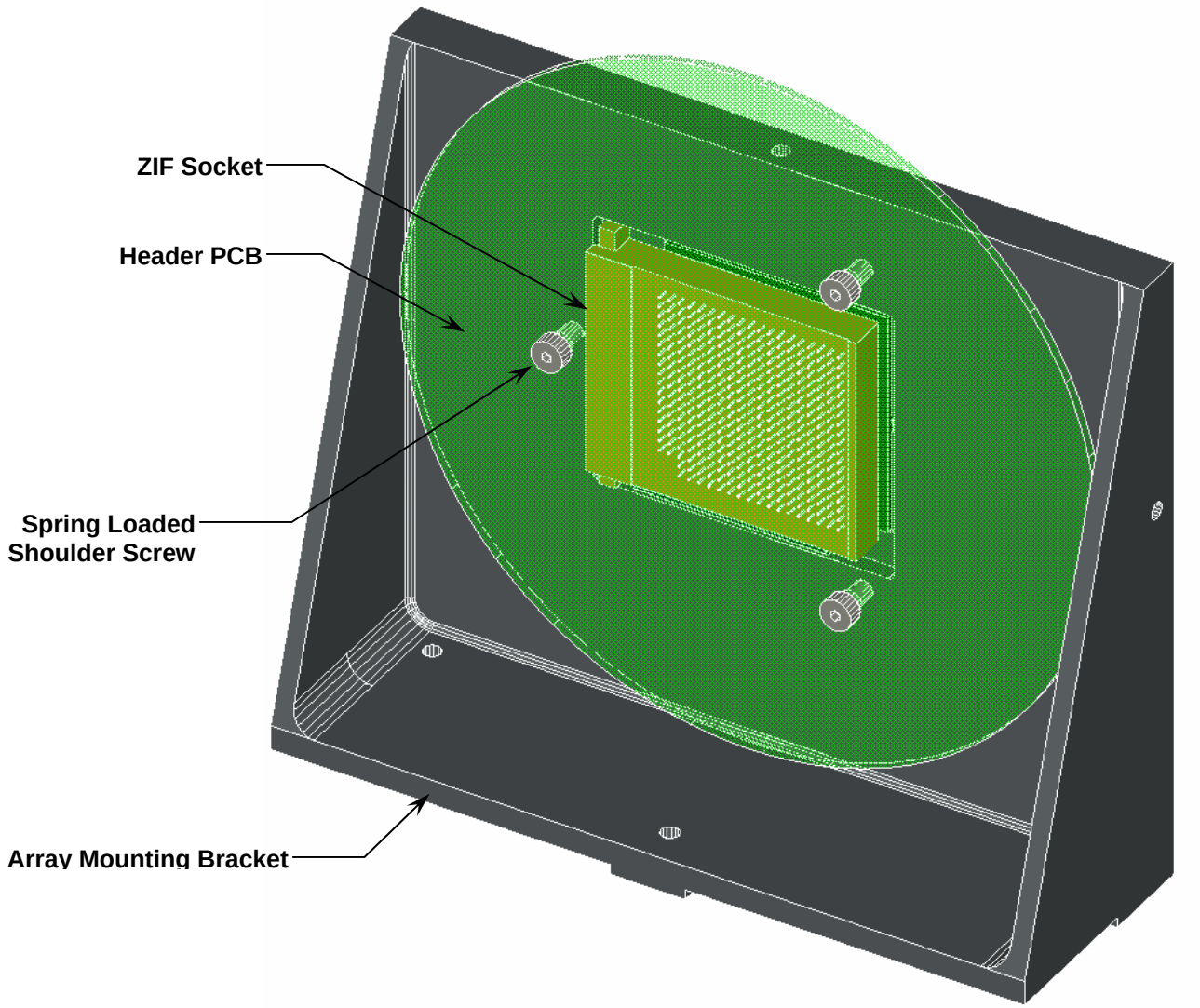

Figure 9 - Detector Array Mount

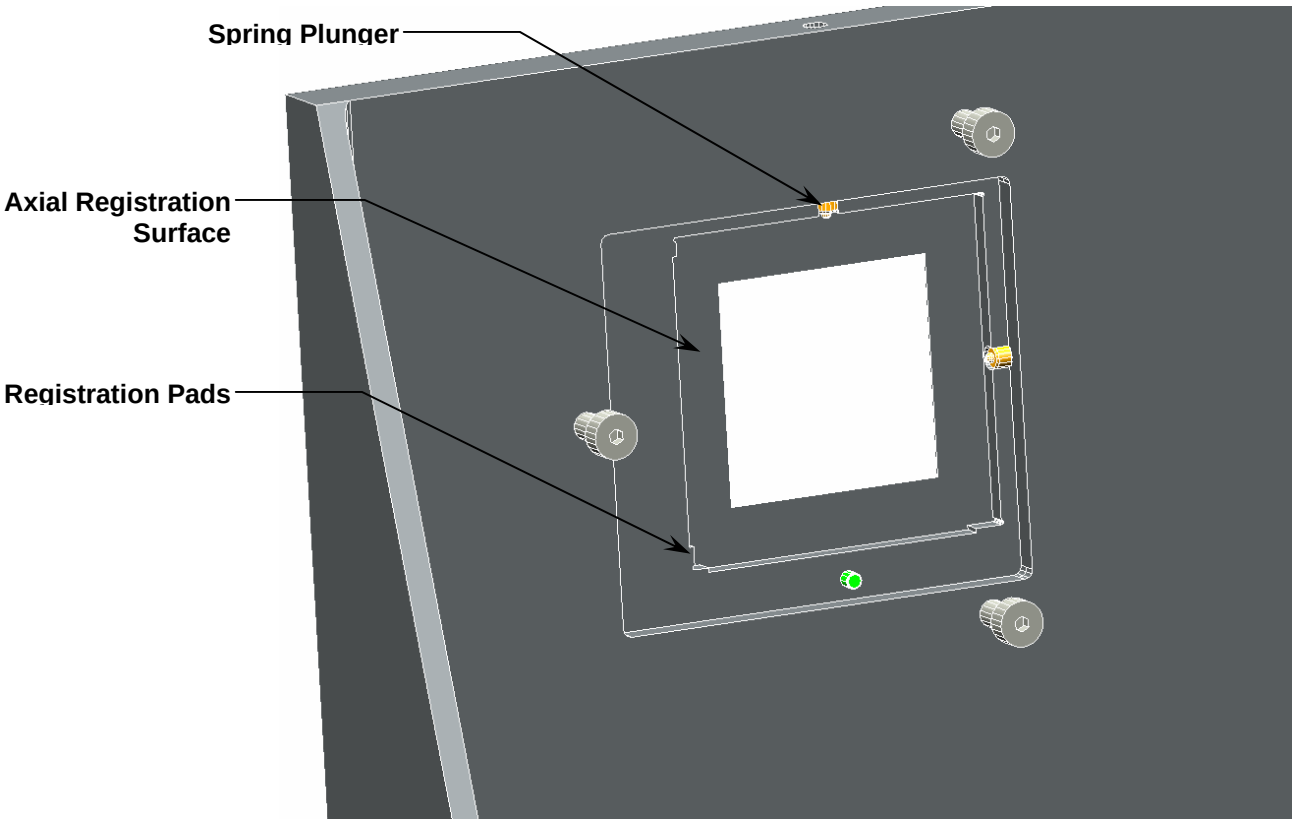

Figure 10 - Detector Carrier Registration Detail

The detector focus slide is a Univ. of Florida design adapted with a geared cam drive designed by SAO. The slide uses sapphire balls in machined raceways that are spring loaded together. The cam drive provides a 5-micron motion per motor step with a range of ± 2.5 mm. The cam is driven by a 200 steps/rev stepper motor that is common with all of the cold motors in the instrument. An LVDT is provided for position confirmation with an accuracy of 1 micron.

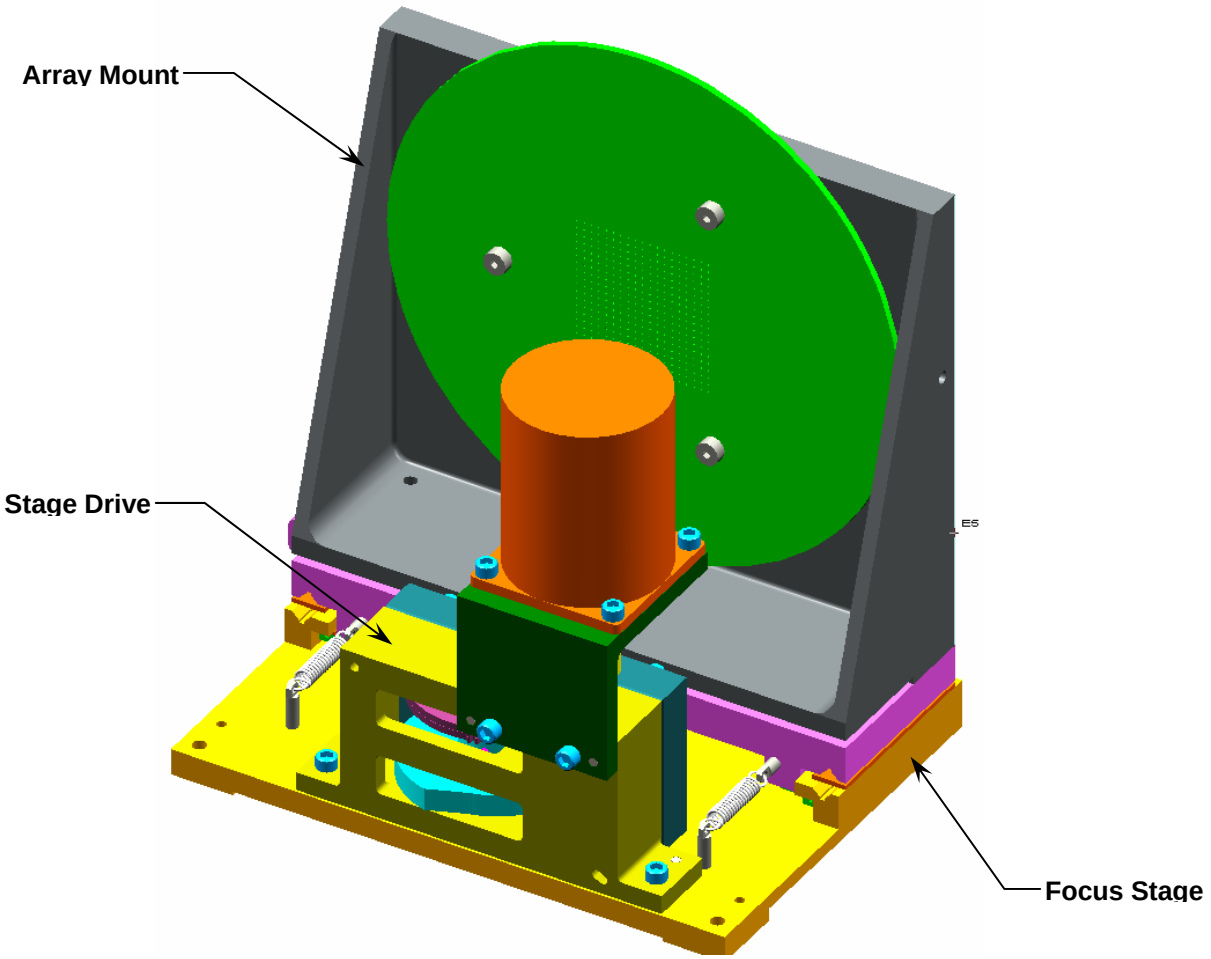

Figure 11 - Detector Focus Stage

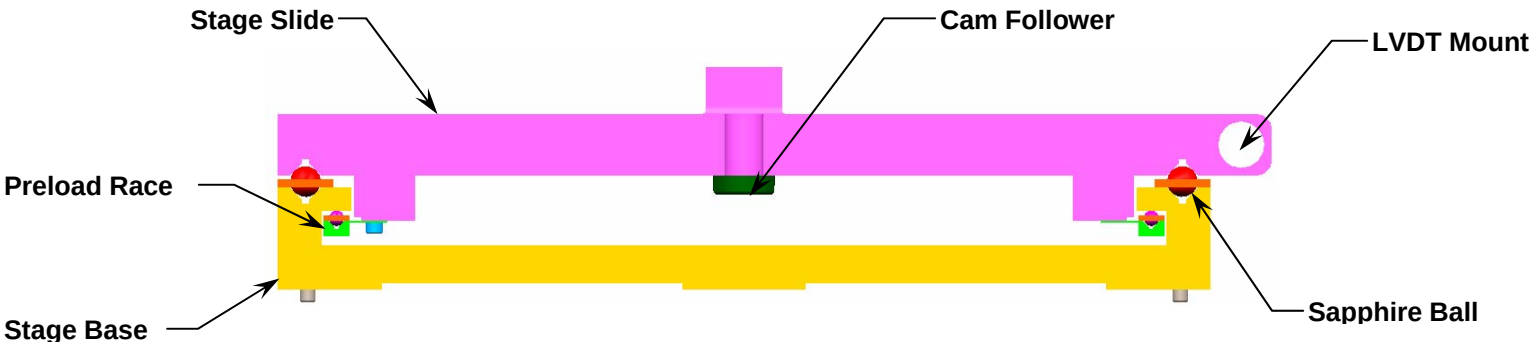

Figure 12 - Detector Focus Stage Front View

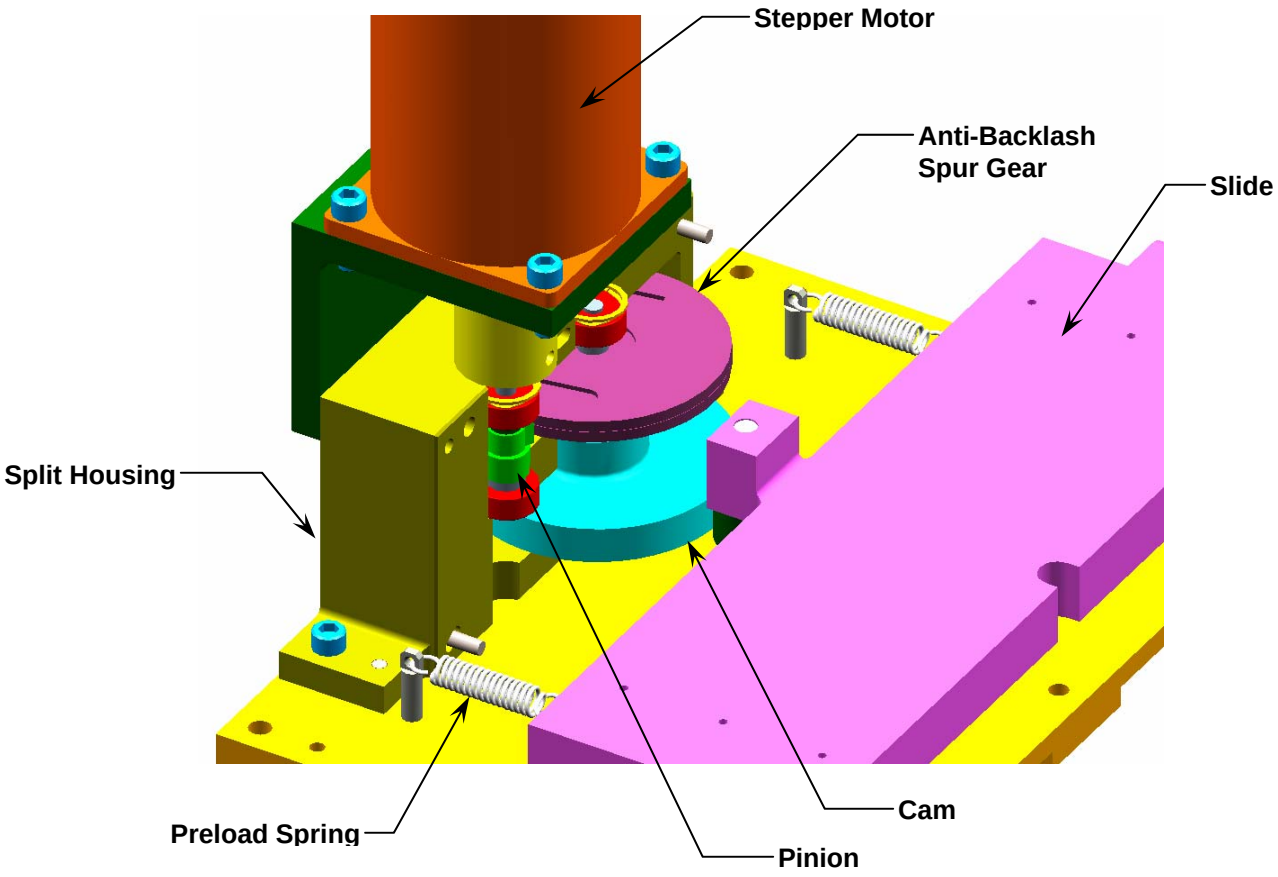

Figure 13 - Focus Stage Drive

116 Detector Pre-amplifier Assembly

The four preamplifier and voltage bias PCBs sit just outside the vacuum wall. They are soldered to the external pins of a standard 26-pin hermetic bulkhead connector. This minimizes the required cable length between the IR imager and pre-amplifiers. The pre-amplifiers are surrounded by a protective enclosure. The hermetic connector is mounted to a rectangular block with an o-ring seal. The rectangular block allows the cable on the inside of the vessel to pass through the hole in the mounting ring. The mounting ring can also be removed with all of the preamps attached. The rear cover provides access to the detector and cable connections in the rear of the instrument. The detector array mount can be removed through this rear port.

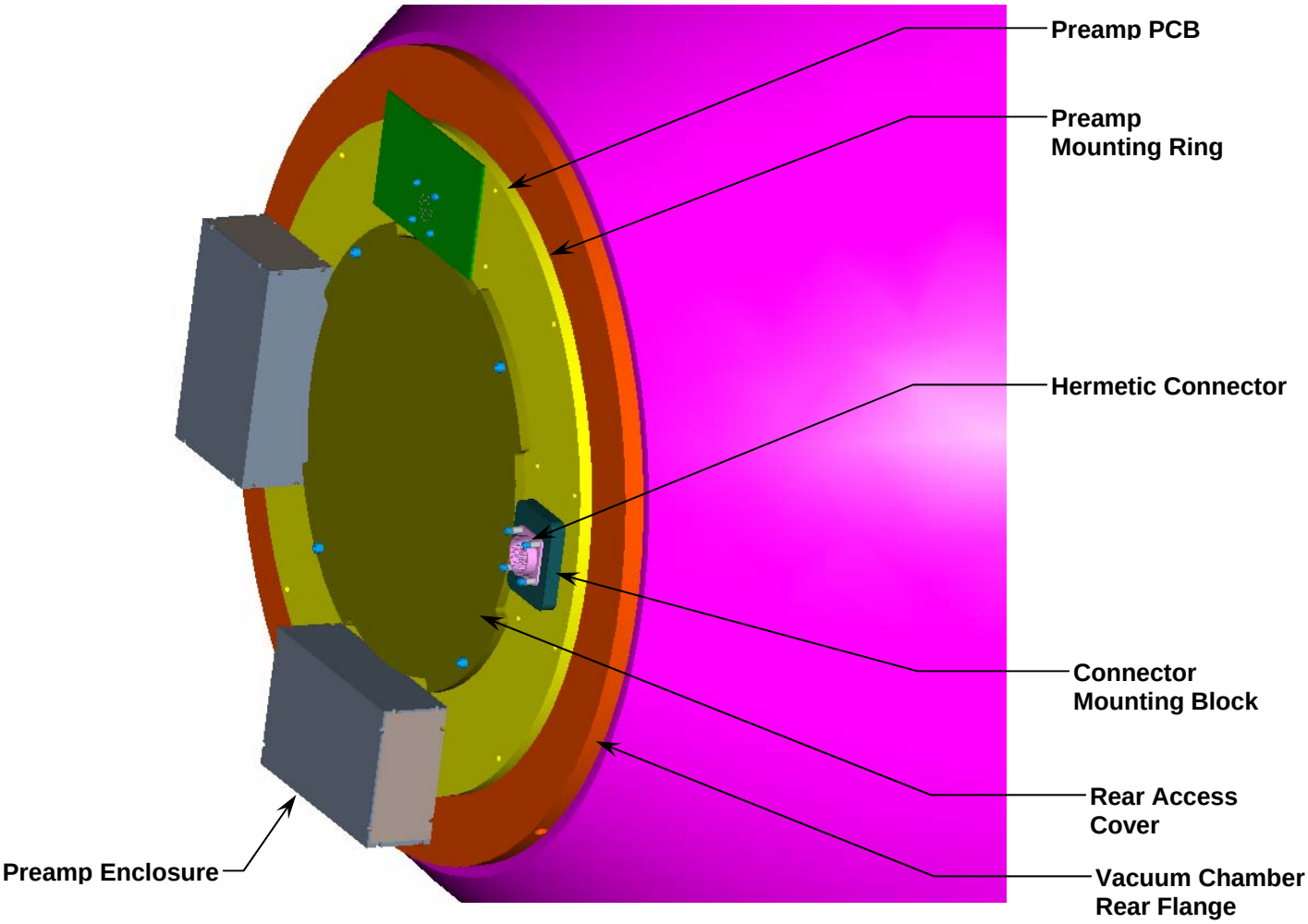

Figure 14 - Detector Preamp Mounting

117 Thermal Shield and Temperature Monitoring

The optical bench/dewar assembly is surrounded by one thin walled aluminum shield which has a thermal blanket applied to its outer surface. The shield is mounted to the optical bench's support ring with thermal isolators. Electrical connections pass though connectors mounted on the thermal shield flange. This makes it easy to remove the shield and provides a light-tight penetration of the shield. Eight Lakeshore RTD's will be placed in the camera section to provide temperature information.

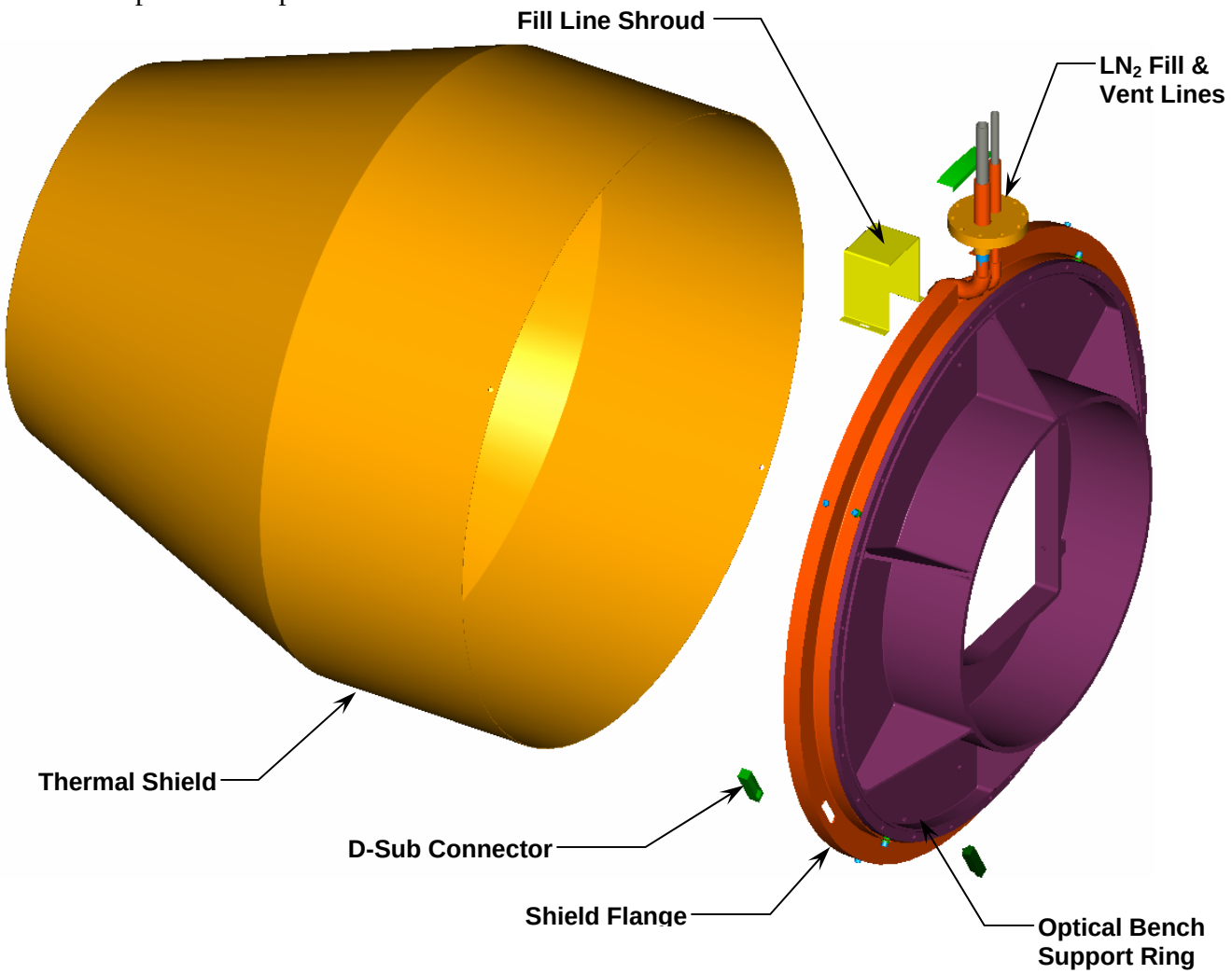

Figure 15 - Thermal Shield

120 Camera External Components

121 Zeolite Sorption Pump

A zeolite Sorption pump cartridge is mounted to the camera vacuum vessel to provide additional pumping capacity for the noble gases. It has a two isolation valves that allow it to be recharged in place without contaminating the internal vacuum.

122 Vacuum Gauge

The camera section has a Pfeiffer HPT-100 pressure gauge. The gauge has a range from one Atmosphere to 1 x 10-9 Torr. The gauge is baffled and mounted at a right angle to the vacuum housing to minimize thermal input.

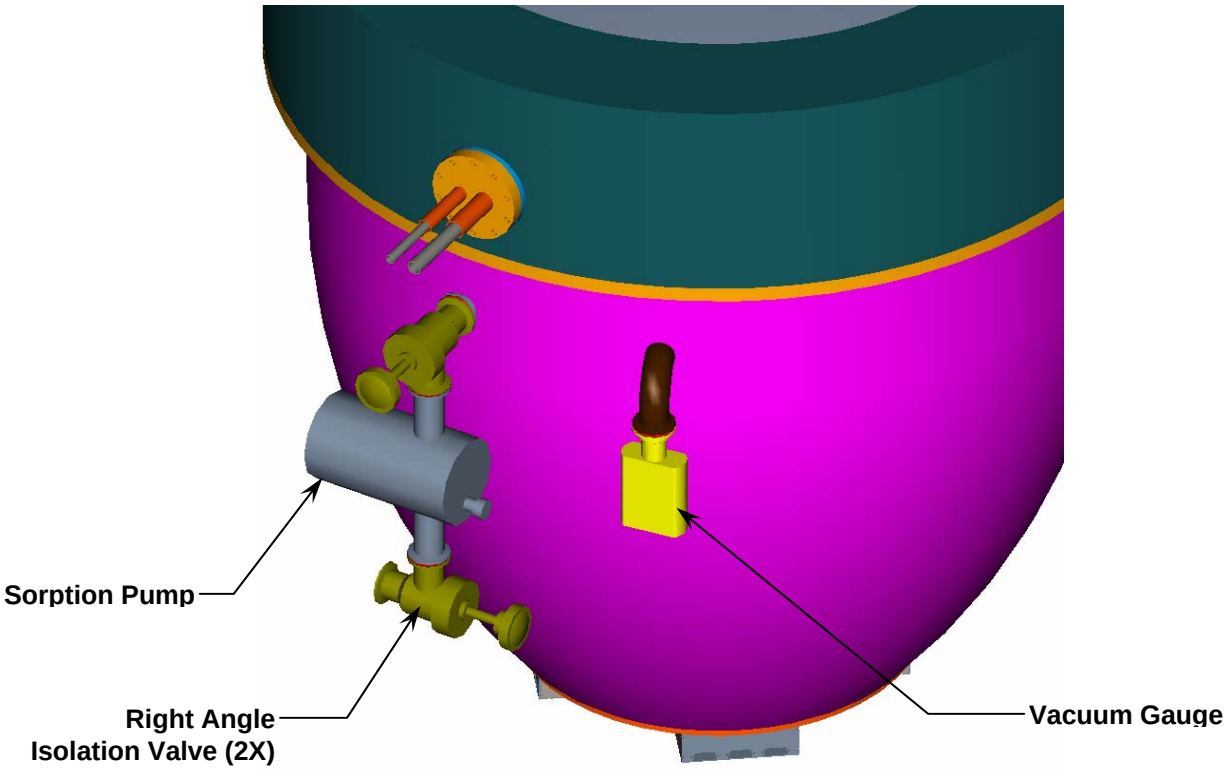

Figure 16 - External Vacuum Components

123 Vacuum Isolation Valve

A 40mm thick vacuum valve was designed to allow the 100 mm Slit to lens 3 required spacing. A VAT (Swiss vacuum manufacturer) valve insert was combined with an SAO designed motor driven-worm geared, ball screw. A set

of micro switches is used to sense the closed and open positions. The valve is currently scheduled for testing and results will be reported at the CDR.

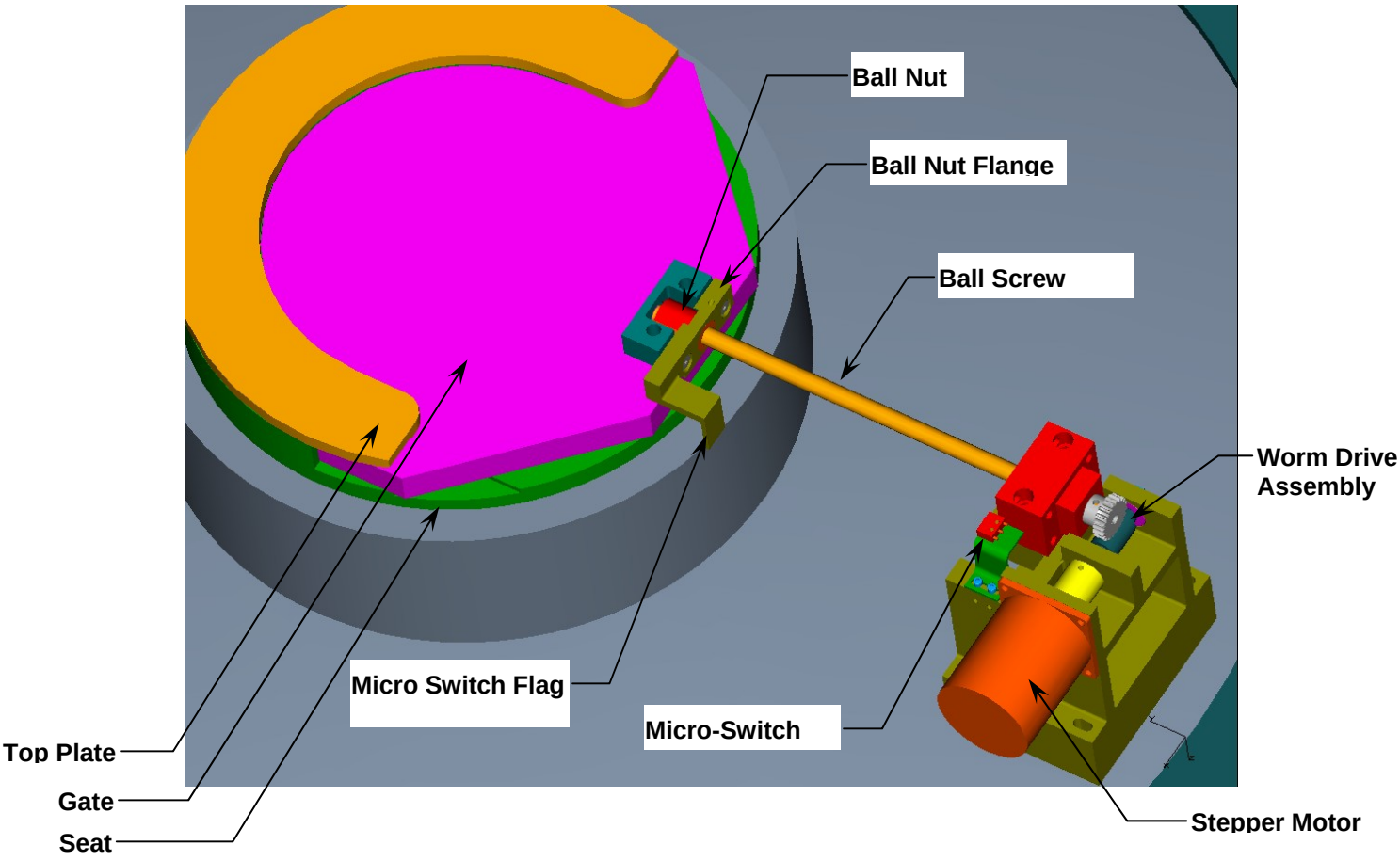

Figure 17 - Vacuum Isolation Valve

125 LN_2 Fill and Vent Feedthrus

The LN_2 fill and vent lines are made of ½ inch and ¾ inch stainless steel convoluted tubes that are welded to flanges on both ends. A v-groove is machined into the top of the optical bench and an indium ring is placed in the groove. The stainless flange is the bolted to the bench, crushing the indium ring, creating a vacuum seal. The fill and vent lines then continue on the inside of the dewar using standard aluminum tubing that is tack welded to the fins to hold them in place. The convoluted tubing is routed though a cut out in the thermal shield flange and underneath the thermal shield. A shroud is then mounted onto the side rail to prevent light leaks.

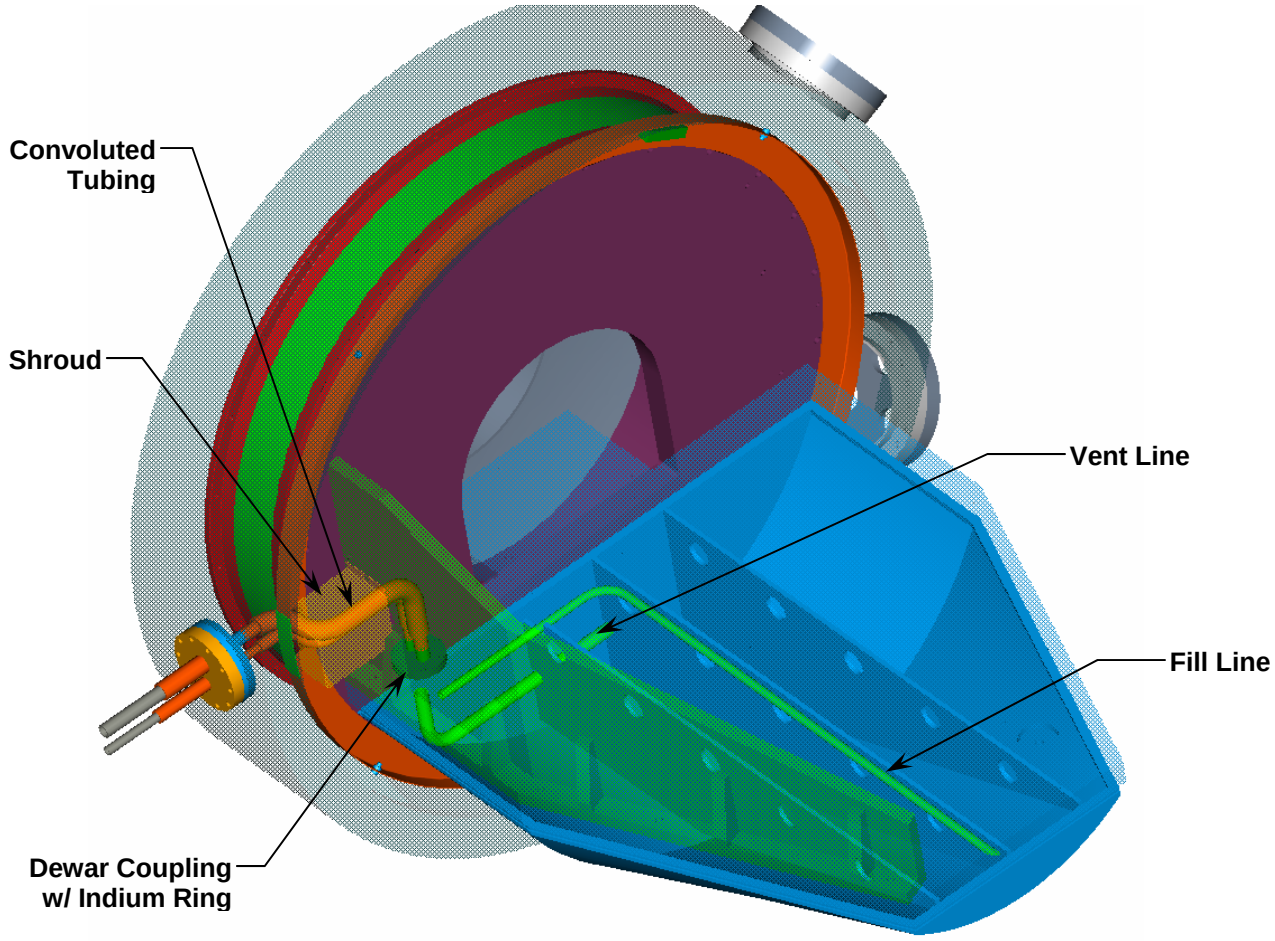

Figure 18 - LN_2 Fill and Vent Lines

126 Vacuum Housing

The vacuum housing is a tapered aluminum design with 0.220" thick walls and an aluminum flange that bolts to the instrument bulkhead. The tapered design is resistant to buckling and reduces the pressure head at the rear access port. Holes are tapped into the front and rear flanges are used to temporarily attach handles during installation and removal of the housing.

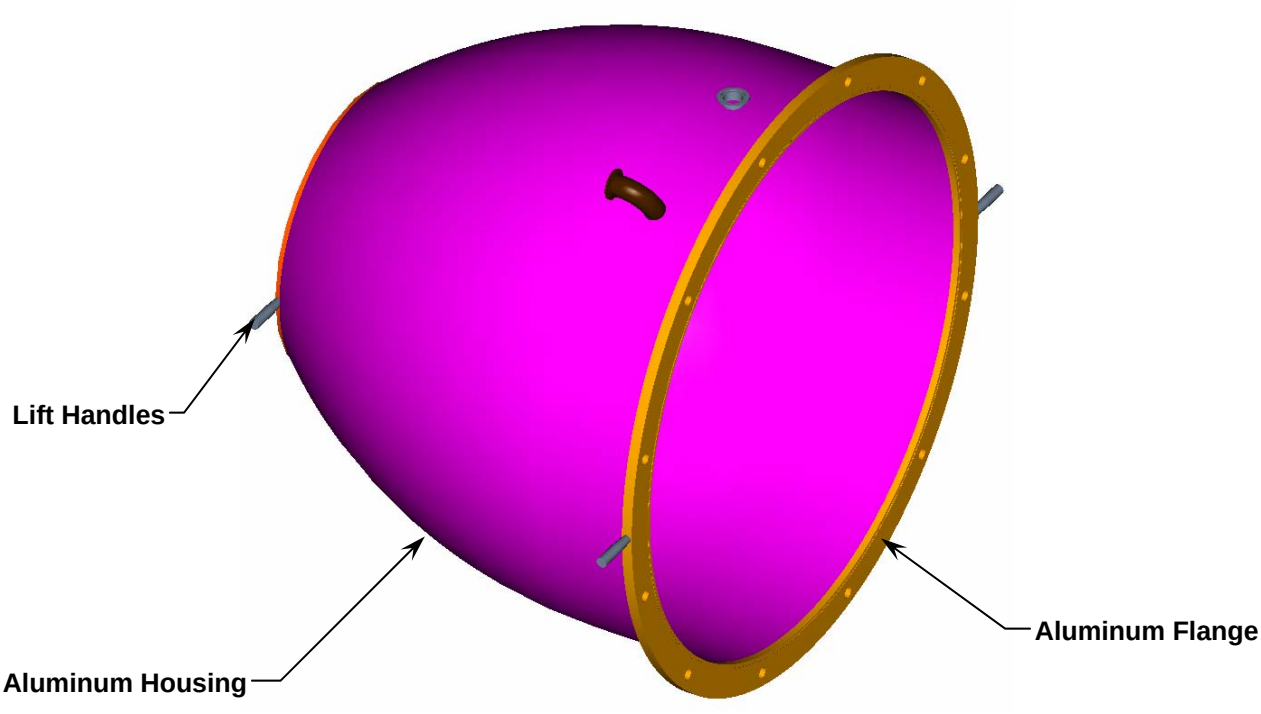

Figure 19 - Vacuum Housing

200 Camera Specifications

Issue	Requirement	Document	MMIRS Value
Multiple Grism Capability	Provide Grism Wheel w/ (5) 138mm Grisms and (1) open aperture	S-MMIRS-202 / Section 8.0 / p. 5	By Design
Multiple Filters Capability	Provide (2) Filter Wheels w/ (5) filters and (1) open aperture each	S-MMIRS-202 / Section 8.0 / p. 5	By Design
Additional Aperture Stops	Provide aperture stops on Filter Wheel to limit K and H+K bands fields of view	S-MMIRS-202 / Section 8.0 / p. 5	By Design
Lyot Stop	Provide a cold Lyot stop that optimizes the SNR	S-MMIRS-200 / Section 143 / p. 12	By Design
Grism Wheel Mechanism Repeatability	±50 microns in all axis	S-MMIRS-202 / Section 9.0 / p. 6	±5.1 microns X ±8.1 microns Y
Filter Wheel Mechanisms Repeatability	±50 microns in all axis	S-MMIRS-201 / Section 10.1 / p. 6	±5.1 microns X ±8.1 microns Y
Detector Focus Stage Resolution	≅5 microns	S-MMIRS-202 / Section 10.0 / p. 7	5 microns
Detector Focus Stage Travel	±2.5 mm	S-MMIRS-202 / Section 10.0 / p. 7	±2.5 mm
Access to Liquid Nitrogen Ports	LN2 ports and valves shall be accessible without instrument removal from CIR	S-MMIRS-200 / Section 332 / p. 19	By Design
Access to Electrical Connections	Connections shall be accessible without instrument removal from CIR	S-MMIRS-200 / Section 333 / p. 19	By Design
Safety - Mechanism back driving	No mechanism shall backdrive in the event of loss of power	S-MMIRS-200 / Section 371	By design

Grism Wheel Time to Function	Maximum of 30 seconds to any wheel position	S-MMIRS-200 / Section 372 / p.23	12.8 sec
Filter Wheels Time to Function	Maximum of 30 seconds to any wheel position	S-MMIRS-200 / Section 372 / p.23	12.8 sec
Grism Motor Drive Torque	Minimum Factor of Safety = 2.5	S-MMIRS-202 / Section 9.0 / p.6	FS = 4.0
Filter Wheel Motors' Drive Torques	Minimum Factor of Safety = 2.5	S-MMIRS-202 / Section 9.0 / p.6	FS > 4.0

MMIRS
Grism Wheel Motor Sizing Calculations

Justin Holwell

05/04/05

Introduction

The MMIRS grism wheel is driven by a stepper motor through a worm gear. The wheel is to be balanced so that the torque do to any imabalance is less than the torque due to friction. These calculations were used to size the stepper motor. An acceleration was assumed in order to solve for the maximum torque required to accelerate the load. The total move time of the wheel for a 180 degree rotation was then calculated.

Caculations for Worst Case

Load Parameters

$J_L := 6.367 \cdot lbf \cdot in \cdot sec^2$ Mass moment of inertia of load (from CAD model)

$T_d := 34.6 \cdot in \cdot lbf$ Torque to overcome detent spring force (from separate document for detent spring calculations)

$T_f := 14.083 \cdot in \cdot lbf$ Torque due to friction in bearings (from bearing friction calcs in separate document)

$T_L := T_f + T_d$ $T_L = 778.928\ ozf \cdot in$ Load Torque

Worm Gear Reduction

The grism wheel will have the worm gear teeth cut into it. A xxxx worm and worm gear were chosen. The gear calculations are included in a separate document.

$Teeth := 252$

$Starts := 2$

$N_r := \frac{Teeth}{Starts}$ $N_r = 126$ Gear ratio

$\eta_r := 0.63$ Efficiency of worm gear (see separate document for gear calculations)

$J_r := 9.821 \cdot 10^{-5} \cdot lbf \cdot in \cdot sec^2$ Mass moment of inertia of worm (from cad model)

Stepper Motor Specifications

$J_{motor} := 0.82 \cdot oz \cdot in^2$ Mass moment of inertia of motor

Torque Calculations

$J_{eq} := \frac{J_L}{N_r^2 \cdot \eta_r}$ Equivolent mass moment of inertia of Load reflected on the motor

$J_{eq} = 3.932\ oz \cdot in^2$

$J_{total} := J_{motor} + J_{eq}$ Total Mass moment of inertia of the system

$J_{total} = 4.752\ oz \cdot in^2$

$\alpha_{motor} := 179.64 \cdot \frac{rad}{sec^2}$ Maximum allowable angular acceleration of motor

$T_{max} := J_{total} \cdot \alpha_{motor} + T_L \cdot \left(\frac{1}{\eta_r \cdot N_r} \right)$ Maximum motor torque required to accelerate the load

$T_{max} = 12.024\ ozf \cdot in$

$T_{avail} := 33 \cdot newton \cdot cm$ Maximum motor torque available (Phytron VSS 52 @ 300 RPM @ 45 V)

$SF := \frac{T_{avail}}{T_{max}}$

$SF = 3.9$ Minimum expected torque safety factor. This is based a 2X factor of safety for the friction torque and detent spring force. If the assumed friction is less, then the motor torque factor of safety will increase.

Load Move Profile

$\omega_{motor.max} := 300 \cdot rpm$ Maximum allowable angular velocity of motor

$\omega_{load.max} := \frac{\omega_{motor.max}}{N_r}$ $\omega_{load.max} = 0.249 \frac{rad}{sec}$ Final (max) angular velocity of load during acceleration

$\alpha_{load.max} := \frac{\alpha_{motor}}{N_r}$ $\alpha_{load.max} = 1.426 \frac{rad}{sec^2}$ Angular acceleration of load

$t_a := \frac{\omega_{load.max}}{\alpha_{load.max}}$ $t_a = 0.175\ sec$ $t_d := t_a$ Load acceleration, constant velocity and deceleration times

$\theta_a := \frac{1}{2} \cdot \alpha_{load.max} \cdot t_a^2$ $\theta_a = 0.0218\ rad$ Angular displacement during acceleration

$\theta_{total} := \pi \cdot rad$ Total angular displacement

$\theta_c := \theta_{total} - 2 \cdot \theta_a$ $\theta_c = 3.098\ rad$ Angular displacement during constant velocity portion of move

$t_c := \frac{\theta_c}{\omega_{load.max}}$ $t_c = 12.425\ sec$ Time rotating at constant velocity

$t_{total} := t_a + t_c + t_d$ $t_{total} = 12.8\ sec$ Total move time

Inertia Matching

$J_{ratio} := \frac{J_{eq}}{J_{motor}}$ Ratio of driven inertia to the motor inertia

$J_{ratio} = 4.796$

$N_o := \sqrt{\frac{J_L}{\eta_r \cdot J_{motor}}}$

$N_o = 275.927$ Optimal gear ratio based on $J_{ratio} = 1$

MMIRS
Grism Wheel Friction Torque

Justin Holwell

05/0405

Introduction

The following calculations are used to determine the friction torque in the bearings for the Grism Wheel. The grism wheel is supported by three bearings, a normal ball bearing, an angular contact ball bearing and a thrust bearing (a custom sapphire ball bearing). The bearings will be coated with a dry lubricant like MoS_s, but because there is little data on rolling friction or bearing life for dry lubricants the friction torques are calculated using values recommended for standard lubrication. Because of this assumption, the friction torques are multiplied by a 2X safety factor to be conservative. The starting torques for each bearing are found and then summed to determine the total friction torque due to the bearings. The filter wheels are assumed to have have a equal to or lower starting torque since they are lighter and have a lower preload.

Calculations

Load Parameters

$F_r := 38 \cdot lbf$ Radial load on bearing

$F_a := 10 \cdot F_r$ Axial load on bearing due to preload of 10 g's

Deep Groove Ball Bearing Starting Torque

$r_{dg} := 12.5 \cdot mm$ Average ball contact radius

$\mu_{dg} := 0.0025$ Coefficient of rolling friction (Machine Design, pg. 482)

$M_{dg} := \mu_{dg} \cdot F_r \cdot r_{dg}$

$M_{dg} = 0.047\ in \cdot lbf$ Starting Torque

Angular Contact Ball Bearing Starting Torque

$r_{ac} := 12.5 \cdot mm$ Average ball contact radius

$\mu_{ac} := 0.006$ Coefficient of rolling friction (Machine Design, pg. 482)

$X := 0.35$

$Y := 0.57$

$P_{ac} := X \cdot F_r + Y \cdot F_a$ Equivalent bearing load

$M_{ac} := \mu_{ac} \cdot P_{ac} \cdot r_{ac}$

$M_{ac} = 0.679\ in \cdot lbf$ Starting Torque

Thrust Ball Bearing Starting Torque

$r_{th} := 2.8975 \cdot in$ Average ball contact radius

$\mu_{th} := 0.006$ Coefficient of rolling friction (assumed to be similar to angular contact ball bearing)

$M_{th} := \mu_{th} \cdot F_a \cdot r_{th}$

$M_{th} = 6.606\ in \cdot lbf$ Starting Torque

Total Starting Torque

$T_f := 2\left(M_{dg} + M_{ac} + M_{th}\right)$

$T_f = 14.664\ in \cdot lbf$ Starting torque due to friction (a 2X safety factor is used)

MMIRS
Grism Detent Spring Force Calculations

Justin Holwell

05/04/05

Introduction

The detent for the Grism Wheel is a spring loaded mechanism. The spring force must be large enough to overcome any friction in the wheel so that the wheel will rotate and the detent will bottom out. Once the detent is bottomed out the wheel is fully aligned. The calculations below solve for the spring force needed in the detent mechanism.

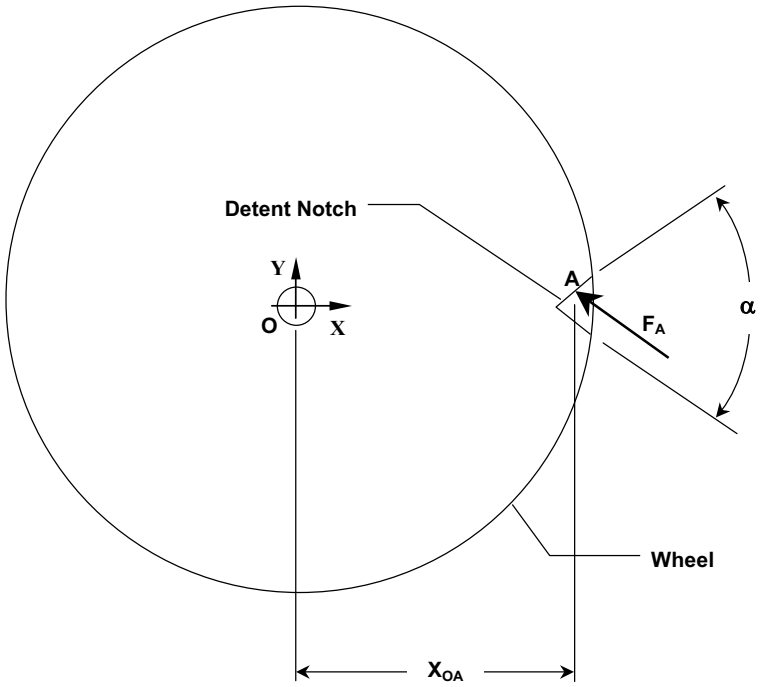

Calculations

Solve for spring force required

$T_f := 14.664 \cdot in \cdot lbf$ Friction torque in the wheel

$X_{OA} := 10.2 \cdot in$ Distance from wheel axis to detent feature

$\alpha := 90 \cdot deg$ The included angle of the detent feature

$$F_A := \frac{T_f}{X_{OA} \cdot \cos\left(\frac{\alpha}{2}\right)}$$

$F_A = 2.033\ lbf$ Force at contact point between detent notch and cam follower for equilibrium condition

$X_{AB} := 0.6875 \cdot in$

$Y_{AB} := 3.0 \cdot in$

$$F_s := F_A \cdot \frac{Y_{AB} \cdot \sin\left(\frac{\alpha}{2}\right) - X_{AB} \cdot \cos\left(\frac{\alpha}{2}\right)}{Y_{AB}}$$

$F_s = 1.108\ lbf$ Spring force required to match friction torque

$SafetyFactor := 2$

$F_{req} := SafetyFactor \cdot F_s$

$F_{req} = 2.216\ lbf$ Spring required for application

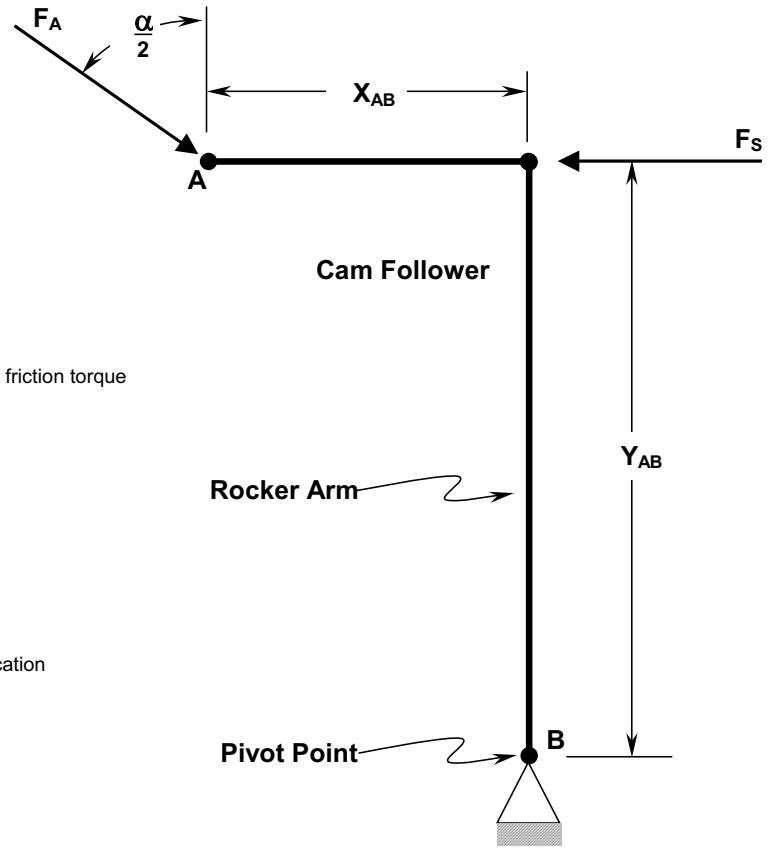

Spring Selection

$k := 3.5 \cdot \frac{lbf}{in}$ Spring rate for selected compression spring (Lee Spring LC-026E-10). The spring rate was chosen such that as the detent arm retracts the spring force increases no more that 20% above the force when the detent is in position.

$L_{free} := 1.125 \cdot in$ Free length of spring

$L_{solid} := 0.190 \cdot in$ Solid height of spring

$x_{in} := \frac{F_{req}}{k}$ Spring deflection when detent is in position

$x_{in} = 0.633\ in$

$x_{out} := x_{in} + 0.114 \cdot in$ Spring deflection when detent is retracted

$x_{out} = 0.747\ in$

$L_{in} := L_{free} - x_{in}$

$L_{in} = 0.492\ in$ Length of spring when detent is in position

$L_{out} := L_{free} - x_{out}$

$L_{out} = 0.378\ in$ Length of spring when detent is retracted

$L_{adjust} := L_{out} - L_{solid}$ Amount of adjustment available to increase force before spring reaches its solid height

$L_{adjust} = 0.188\ in$

$F_{out} := k \cdot x_{out}$ Spring force when detent is retracted

$F_{out} = 2.615\ lbf$

$F_{max} := k \cdot (L_{free} - L_{solid})$ Maximum force of spring

$F_{max} = 3.273\ lbf$

Spring Force vs Height Curve

$x := 0.190 \cdot in, 0.195 \cdot in .. 1.125 \cdot in$

$F(x) := k \cdot (L_{free} - x)$

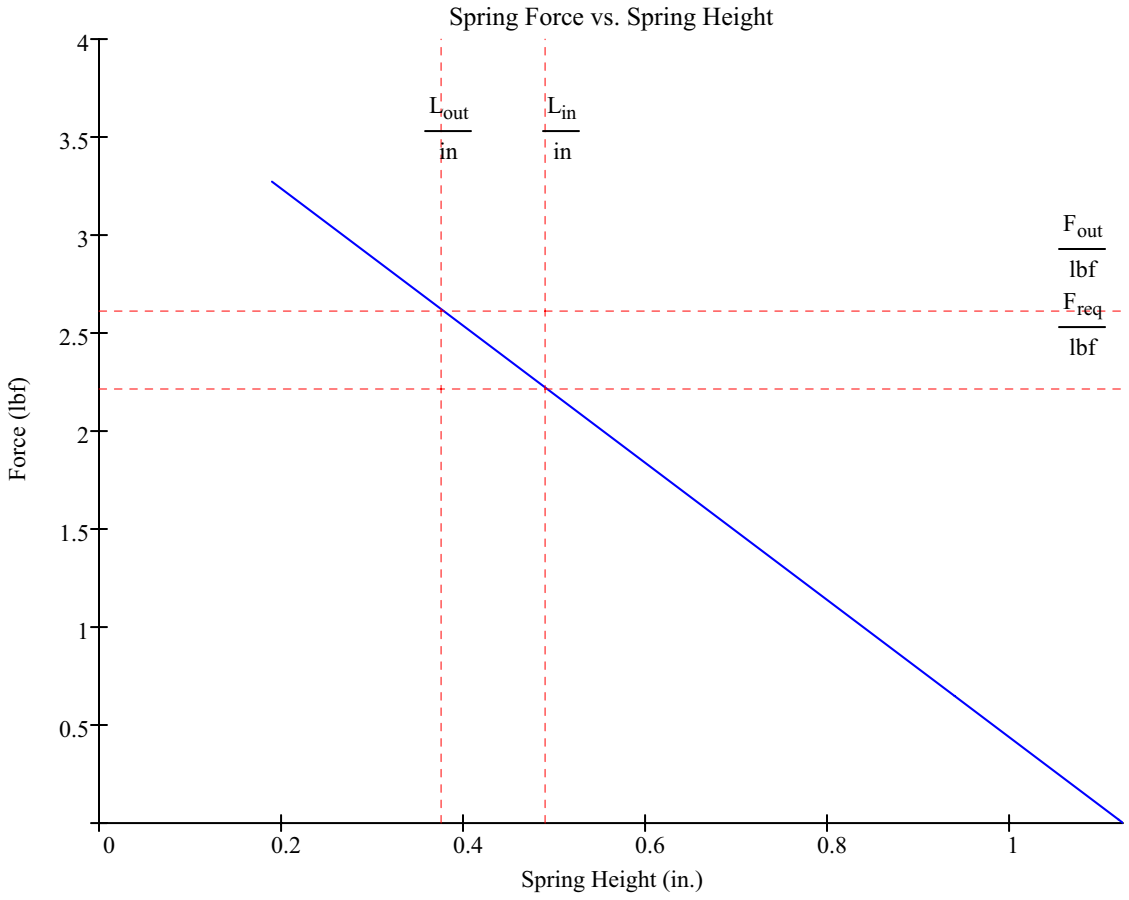

Torque on Wheel Due to Detent

$$F_{A.out} := F_{out} \cdot \frac{Y_{AB}}{Y_{AB} \cdot \sin\left(\frac{\alpha}{2}\right) - X_{AB} \cdot \cos\left(\frac{\alpha}{2}\right)}$$

Force at contact point between detent notch and cam follower when detent is retracted

$F_{A.out} = 4.798\ \text{lbf}$

$$T_d := F_{A.out} \cdot \left(X_{OA} \cdot \cos\left(\frac{\alpha}{2}\right) \right)$$

Maximum expected wheel torque required to overcome detent. Since a 2X safety factor was used for the wheel friction torque, the wheel torque, T_d, required to overcome the detent may be actually be less.

$T_d = 34.6\ \text{in} \cdot \text{lbf}$

MMIRS
Detent Repeatability Calculations

Justin Holwell

05/04/05

Introduction

Enter The grism and filter wheels are accurately positioned using a detent mechanism. The instrument requires that the wheels stop at each position repeatability within +/- 50 microns. The detent repeatability is a function the runout tolerance of the bearings used for the wheel, the detent arm pivot and the cam follower. The calculations below determine the repeatability of the detent mechanism.

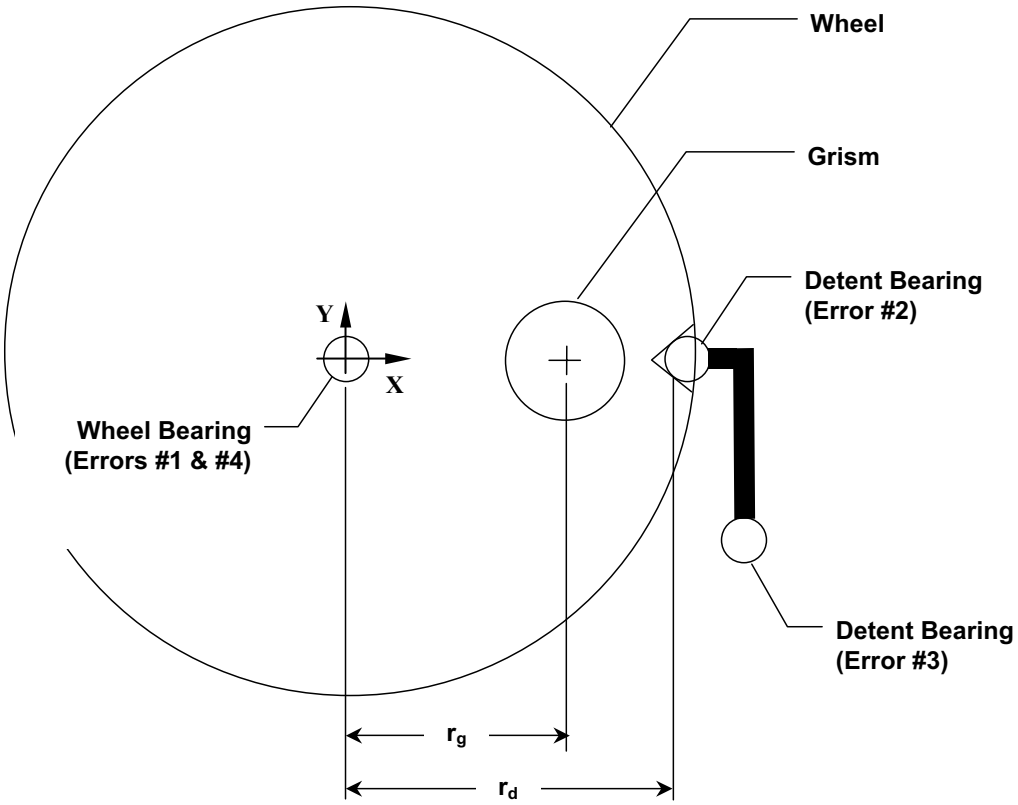

Calculations

Bearing Properties

$t_b := 0.0002 \cdot in$ Runout tolerance in bearings. It is assumed that all three bearings in system have similar runout tolerance.

Detent and Wheel Geometry

$r_g := 9.559 \cdot in$ Radius to grism from center of wheel

$r_d := 10.4 \cdot in$ Radius to detent notch in wheel from center of wheel

Error Calculations

$$e_{\theta 1} := \tan\left(\frac{t_b}{r_d}\right)$$

Rotational error in wheel due to runout tolerance in wheel bearing. This error is present when the runout in the bearing causes the center of the wheel to translate in the Y direction. This rotational error can be resolved into X and Y positional errors of the optic.

$$e_{\theta 1} = 3.967\ \text{arcsec}$$

$$e_{x1} := r_g - \left(r_g \cdot \cos\left(e_{\theta 1}\right)\right)$$

Positional error of optic in X direction.

$$e_{x1} = 1.768 \times 10^{-9}\ \text{in}$$

$$e_{y1} := r_g \cdot \sin\left(e_{\theta 1}\right)$$

Positional error of optic in Y direction.

$$e_{y1} = 1.838 \times 10^{-4}\ \text{in}$$

$$e_{x2} := e_{x1} \qquad e_{y2} := e_{y1}$$

$$e_{x3} := e_{x1} \qquad e_{y3} := e_{y1}$$

The rotational error of the wheel caused by the bearings in the detent are equal to the rotational error caused by the wheel bearings. Therefore, the positional errors for both bearings and the same as the wheel bearings.

$$e_{x4} := t_b$$

$$e_{x4} = 5.08\ \mu\text{m}$$

Positional error of optic due to runout tolerance in wheel bearing. This error is present when the runout causes the center of the wheel to translate in the X direction which also translates that optic in the X direction only.

Repeatability Calculations

$$E_x := \sqrt{e_{x1}^2 + e_{x2}^2 + e_{x3}^2 + e_{x4}^2}$$

RSS of the errors in the X direction

$$E_x = 5.08\ \mu\text{m}$$

Repeatability (+/-) of grism wheel in X direction

$$E_y := \sqrt{e_{y1}^2 + e_{y2}^2 + e_{y3}^2}$$

RSS of the errors in the Y direction

$$E_y = 8.087\ \mu\text{m}$$

Repeatability (+/-) of grism wheel in Y direction

$$E_\theta := \sqrt{3 \cdot \left(e_{\theta 1}^2\right)}$$

$$E_\theta = 6.87\ \text{arcsec}$$

Rotational repeatability of grism (this effect grism dispersion)

MMIRS
Grism Worm Gear Calculations

Justin Holwell

05/04/05

Introduction

A worm gear set was chosen to drive the grism and filter wheels. The diameteral pitch was chosen to allow adequate backlash for the detent mechanism to work properly. The calculations below are used to determine the dimensions and efficiency of the gear set.

The gear set was chosen to be a stainless steel worm and aluminum worm gear teeth cut into the grism wheel. The aluminum teeth will be hard anodized. Boston Gear was used as a reference for the worm dimensions and efficiency calculations.

Calculations

Worm and Worm Gear Parameters

$P := 12 \cdot in^{-1}$ Diametral Pitch

$l := 0.5236 \cdot in$ Lead

$\lambda := 9.4667 \cdot deg$ Lead Angle

$\phi := 14.5 \cdot deg$ Pressure Angle

$p := \frac{\pi}{P}$ $p = 0.262\ in$ Circular pitch

$a := \frac{1}{P}$ $a = 0.083\ in$ Addendum

$D_g := 21 \cdot in$ Pitch diameter of worm gear

$N_g := P \cdot D_g$ $N_g = 252.0000$ Number of teeth on worm gear

$D_t := D_g + 2 \cdot a$ $D_t = 21.167\ in$ Throat diameter of worm gear

$D_o := D_t + 0.6 \cdot a$ $D_o = 21.2167\ in$ Worm gear O.D.

$h_t := \frac{2.157}{P}$ $h_t = 0.17975\ in$ Whole depth of tooth

$D_w := 1 \cdot in$ Pitch diameter of worm

$d_o := D_w + 2 \cdot a$ Worm O.D

$d_o = 1.167\ in$

$d_r := d_o - 2 \cdot h_t$ Bottom diameter of worm

$$C := \frac{D_w + D_g}{2}$$

$C = 11.0000\ in$ Center distance between worm and worm gear

Efficiency Calculations

$\mu := 0.095$ Coefficient of friction

$$\eta := \frac{\tan(\lambda) \cdot (1 - \mu \cdot \tan(\lambda))}{\mu + \tan(\lambda)}$$

$\eta = 0.63$ Worm Set Efficiency

Expected Tooth Loads

$N_r := 126$ Gear Ratio

$T_w := 12.024 \cdot in \cdot ozf$ Torque on the worm (from Grism Motor Sizing Calculations)

$T_g := \eta \cdot N_r \cdot T_w$ Torque on the worm gear

$T_g = 59.366\ in \cdot lbf$

$$W_{tg} := 2 \cdot \frac{T_g}{D_g}$$ Tangential component of force on worm gear

$W_{tg} = 5.654\ lbf$

$$W_{tw} := \frac{2 \cdot T_w}{D_w}$$ Tangential component of force on worm

$W_{tw} = 1.503\ lbf$

$W_{aw} := W_{tg}$ Axial force on worm

$W_{aw} = 5.654\ \text{lbf}$

$W_{ag} := W_{tw}$ Axial force on worm gear

$W_{ag} = 1.503\ \text{lbf}$

$W_r := \frac{W_{tg} \cdot \tan(\phi)}{\cos(\lambda)}$ Radial force separating the two elements

$W_r = 1.482\ \text{lbf}$

Since the loads are very low and the worm gear (grism wheel) is hard anodized it is expected that wear of the aluminum worm gear will be minimal. Dry lubricants may also be investigated to further reduce amount of wear.

MMIRS
Isolation Valve Worm Gear Calculations

Justin Holwell

05/04/05

Introduction

A worm gear set was chosen to drive the ball screw for the isolation valve. The calculations below are used to determine the dimensions and efficiency of the gear set.

The gear set was chosen to be a stainless steel worm and aluminum worm gear. The aluminum teeth will be hard anodized to resist wear. Dry lubricants may be investigated to further reduce any wear on the aluminum worm gear. Boston Gear was used as a reference for the worm dimensions and efficiency calculations.

Calculations

Worm and Worm Gear Parameters

$P := 24 \cdot in^{-1}$		Diametral Pitch
$l := 0.1309 \cdot in$		Lead
$\lambda := 4.767 \cdot deg$		Lead Angle
$\phi := 14.5 \cdot deg$		Pressure Angle
$p := \frac{\pi}{P}$	$p = 0.131\ in$	Circular pitch
$a := \frac{1}{P}$	$a = 0.042\ in$	Addendum
$D_g := 0.833 \cdot in$		Pitch diameter of worm gear
$N_g := P \cdot D_g$	$N_g = 20$	Number of teeth on worm gear
$D_t := D_g + 2 \cdot a$	$D_t = 0.916\ in$	Throat diameter of worm gear
$D_o := D_t + 0.6 \cdot a$	$D_o = 0.941\ in$	Worm gear O.D.
$h_t := \frac{2.157}{P}$	$h_t = 0.09\ in$	Whole depth of tooth

$D_w := 0.5 \cdot in$ Pitch diameter of worm

$d_o := D_w + 2 \cdot a$ Worm O.D

$d_o = 0.583\ in$

$d_r := d_o - 2 \cdot h_t$ Bottom diameter of worm

$$C := \frac{D_w + D_g}{2}$$

$C = 0.6665\ in$ Center distance between worm and worm gear

Efficiency Calculations

$\mu := 0.05$ Coefficient of friction

$$\eta := \frac{\tan(\lambda) \cdot (1 - \mu \cdot \tan(\lambda))}{\mu + \tan(\lambda)}$$

$\eta = 0.62$ Worm Set Efficiency

Expected Tooth Loads

$T_w := 16.747 \cdot in \cdot ozf$ Torque on the worm (from Grism Motor Sizing Calculations)

$T_g := \eta \cdot N_g \cdot T_w$ Torque on the worm gear

$T_g = 13.027\ in \cdot lbf$

$$W_{tg} := 2 \cdot \frac{T_g}{D_g}$$ Tangential component of force on worm gear

$W_{tg} = 31.278\ lbf$

$$W_{tw} := \frac{2 \cdot T_w}{D_w}$$ Tangential component of force on worm

$W_{tw} = 4.187\ lbf$

$W_{aw} := W_{tg}$ Axial force on worm

$W_{aw} = 31.278\ \text{lbf}$

$W_{ag} := W_{tw}$ Axial force on worm gear

$W_{ag} = 4.187\ \text{lbf}$

$W_r := \frac{W_{tg} \cdot \tan(\phi)}{\cos(\lambda)}$ Radial force separating the two elements

$W_r = 8.117\ \text{lbf}$

MMIRS
Gate Valve Drive Train

Justin Holwell

05/04/05

Introduction

The isolation valve between the camera and MOS assemblies for MMIRS requires a custom design drive to open and close the gate. A worm gear driven ball screw was chosen for the linear motion. The drive must provide enough compression force to seal the valve. A worm gear was chosen so that the drivetrain would not backdrive when the valve is closed. Once the valve is closed,the power to the motor will be shut off and the worm will hold the gate in place. The calculations below were used to select the stepper motor size and worm gear ratio.

Calculations

Load Specs

$F_{min} := 451 \cdot lbf$ Minimum compression force to seal valve (from valve manufacturer VAT)

$F_{max} := 590 \cdot lbf$ Maximum compression force used to seal valve (from valve manufacturer VAT)

Worm Gear Specs

$N_w := 20$ Gear ratio

$\eta_w := 0.623$ Gear efficiency

Ball Screw Specs

$L := 0.125 \cdot in$ Ball screw lead (Nook Industries 0375-0125 SRT / SBN9578 ball screw and nut)

$\eta_s := 0.90$ Efficiency of screw

Required Motor Torque Calcs

$$T_s := \frac{F_{max} \cdot L}{2 \cdot \pi \cdot \eta_s}$$ Screw Backdriveing Torque (required to hold gate in place)

$T_s = 208.67\,ozf \cdot in$

$$T_{req} := \frac{T_s}{(\eta_w \cdot N_w)}$$ Required motor torque (to hold gate in place)

$T_{req} = 16.747\,ozf \cdot in$ $T_{req} = 11.826\,newton \cdot cm$

$T_{avail} := 65 \cdot newton \cdot cm$ Maximum motor torque available (Phytron VSS 52 @ 60V)

$$SF := \frac{T_{avail}}{T_{req}}$$

$SF = 5.5$ Safety Factor

Move Time

$d_{travel} := 8 \cdot in$ Travel distance of gate

$\omega_m := 300 \cdot rpm$ Angular velocity of motor

$$\omega_s := \frac{\omega_m}{N_w}$$

$speed := \omega_s \cdot L$

$$speed = 0.196\,\frac{in}{sec}$$ Linear speed of motor

$$Time := \frac{d_{travel}}{speed}$$

$Time = 40.7\,sec$ Time fully open or close valve

MMIRS
Ball Screw Stability for Isolation Valve

Justin Holwell
05/04/05

Introduction

The isolation valve uses a ball screw to open and close the gate. The ball screw provides an axial force on the gate to compress the o-ring and seal the gate opening. This analysis calculates the the elastic stability of the ball screw.

Assumptions

- The screw is modeled as a slender rod equal to its root diameter
- The ball screw is fixed at one end and pinned at the other
- The ball screw material is 17-4 PH stainless steel

Analysis

Ball Screw Properties

$P_{max} := 2624 \cdot newton$ Maximum compressive load applied to screw

$L := 8 \cdot in$ Length of screw between fixed bearings and ball nut

$d_r := 0.3 \cdot in$ Root diameter of ball screw

$E := 28600 \cdot ksi$ Modulus of elasticity of 17-4 PH stainless steel (http://www.matweb.com)

$I := \frac{1}{64} \cdot \pi \cdot d_r^4$ Moment of inertia for screw cross section

Critical load calculation

$L_e := 1 \cdot L$ Effective length of column for one fixed end, one pinned end (*Mechanics of Materials*, pg. 640)

$P_{cr} := \frac{\pi^2 \cdot E \cdot I}{L_e^2}$ Critical load at which column becomes unstable

$P_{cr} = 1.754 \times 10^3 \, lbf$

$SF := \frac{P_{cr}}{P_{max}}$ Factor of safety for load

$SF = 3.0$

Critical stress calculation

$A := \frac{1}{4} \cdot \pi \cdot d_r^2$ Area of column's cross-section

$\sigma_{cr} := \frac{P_{cr}}{A}$ Critical stress for column

$\sigma_{cr} = 24.8\,\text{ksi}$

$\sigma := \frac{P_{max}}{A}$ Normal Stress in column

$\sigma = 8.346\,\text{ksi}$

Conclusions

The buckling safety factor for the ball screw is more than adequate. A 3/8" ball screw will not buckle or yield under the load needed to seal the gate.

MMIRS
Detector Slide Resolution Calculations

Justin Holwell

01/07/05

Introduction

The detector focus slide is translated using a cam mechanism which is driven by a stepper motor. A resolution of 5 microns is required and the slide has to travel 5 mm. In order to get the resolution required an anti-backlash spur gear set was added to the drive train. The calculations that follow are used to determine the gear ratio and cam profile to provide the resolution required.

Calculations

$step := \frac{rev}{200}$ There are 200 steps per revolution for the stepper motor

$m_G := 5.5$ Gear ratio

$\theta_{cam} := 330 \cdot deg$ Degrees cam rotates from bottom of cam to top of its rise

$Rise\_distance := 5 \cdot mm$ Distance the cam profile rises over its full travel

$Rise\_steps := \theta_{cam} \cdot m_G$ Number of motor steps over the full travel

$Rise\_steps = 1008.3\ step$

$Resolution_{cam} := \frac{Rise\_distance}{Rise\_steps}$

$Resolution_{cam} = 4.96 \frac{\mu m}{step}$ Resolution of the cam profile in microns per motor step

MMIRS CAMERA SECTION OPTICS MOUNTING SYSTEM

George Nystrom
May 3, 2005

The Camera Section optics mounting system is comprised of two lens assemblies or Vee blocks that house six lenses each. One assembly houses the collimator optics and the other assembly houses the camera optics (see Figures 1 and 2).

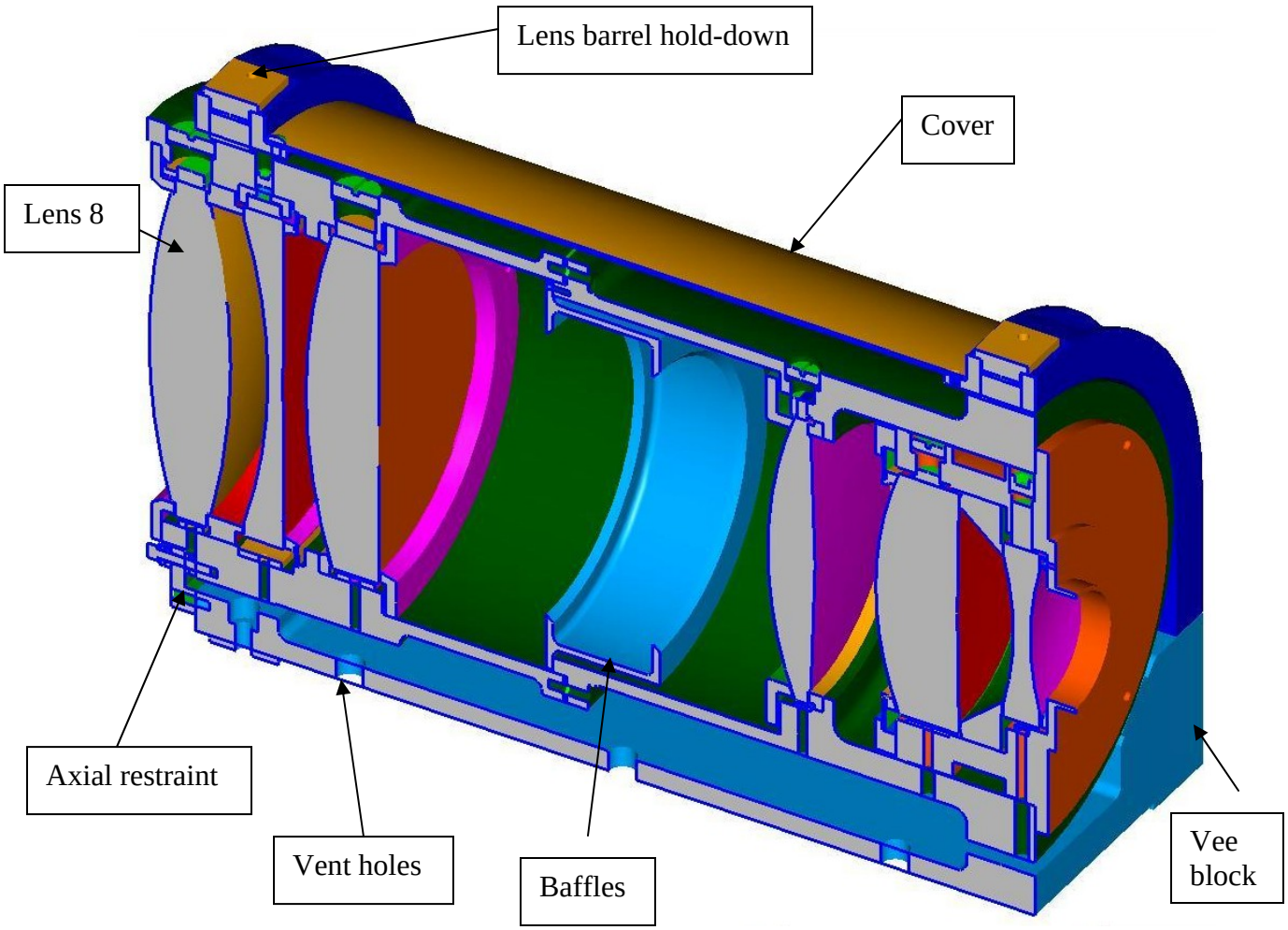

Figure 1: Lens assembly and Vee block for the camera optics.

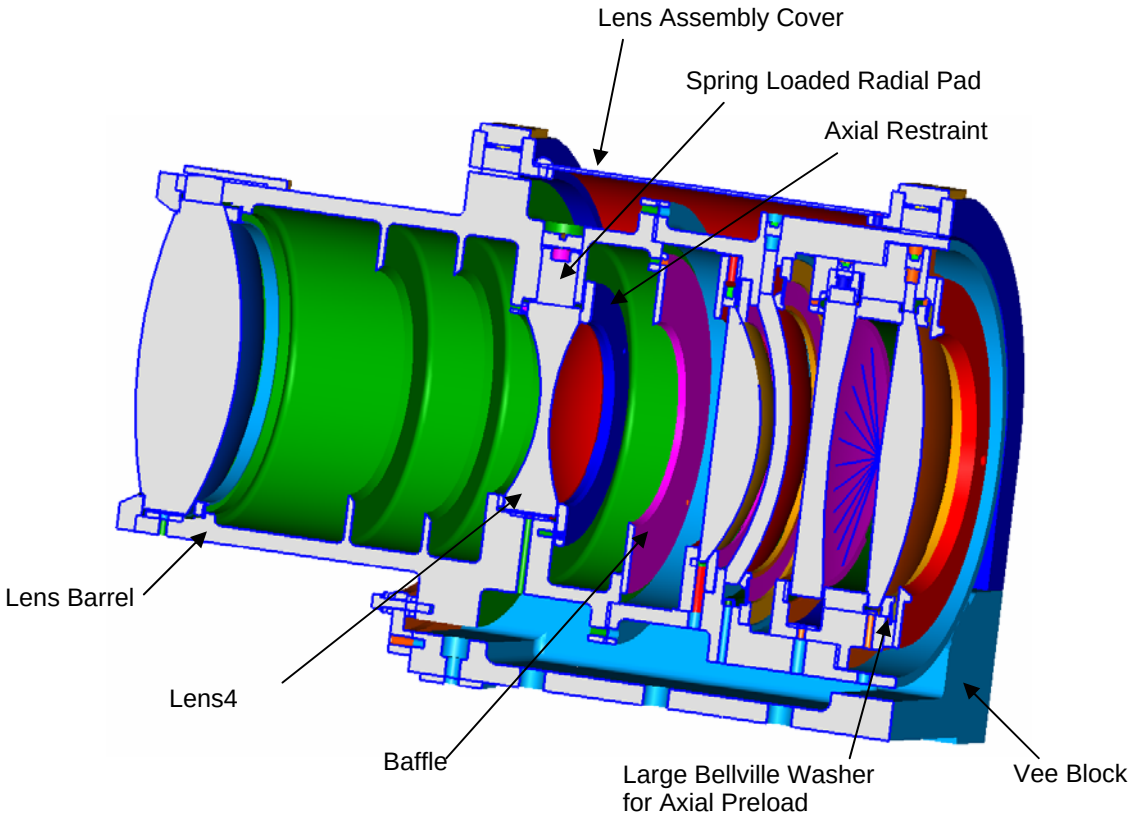

Figure 2 - Collimator Lens Assembly

The radial definition of each lens is accomplished with three Nylon pads equally spaced about the lens diameter. One of these pads is spring-loaded and the other two are fixed. These assemblies are designed to center all of the lenses within a given assembly at both ambient and cryogenic temperatures. This is accomplished by choosing a pad thickness for each lens that will exactly compensate for the lens diameter change between cryogenic and ambient temperatures (Bergner 11/08/04).

The axial definition of each lens is accomplished by a fixed, three-point restraint placed against a flat on the lens surface. This flat has been specified to be perpendicular to the lens generation axis to within 0.01mm. A spring-loaded, three-point axial restraint acts against the opposite surface of the lens by providing the force necessary to maintain the lens axial positioning. The spring force is provided by a large Bellville washer. The axial and radial three point mounts are aligned to eliminate parasitic forces. The mounts are designed for applied loads 10 (g) times the lens weight. The combined radial and axial forces are designed to not exceed 100-psi stressing within the lens. Each fixed axial mount will have a 3-mil Kapton foil against the lens and the spring-loaded mount will have a 10 mil Teflon ring. This will reduce the friction coefficient to 0.2 and 0.04, respectively. During temperature transitions slippage will occur between the lenses and mounts. The axial mount slippage results in radial force vectors, which are at most 2.04g. The lens radial temperature difference is accommodated by the spring-loaded radial

restraint. Since its force vector is 10g, the axial restraint slippage will not cause lens de-centering.

The lens barrels are fabricated from Aluminum, which are placed within an Aluminum Vee block mounting structure. A precision diameter placed at the end of each lens barrel provides registration with sufficient length to maintain the Hertzian stresses at acceptable levels. Two end support brackets apply a 10g spring load to the precision diameters to maintain each barrel's position within the Vee block. The +z end has a flat surface where the load is applied to eliminate barrel rotation and is fastened to the Vee block to maintain its axial position. Differential temperature effects during cool down and warm up are allowed to produce sliding within the blocks.

The Vee blocks have several tapped holes to allow thermal straps to be installed should additional thermal conduction be desired. This will be determined during initial testing. The lens barrels also have radial holes opposite the radial mounts to measure lens centration and also provide an evacuation path. The Vee block also has evacuation holes in its base to ensure that all volumes are adequately vented. A cover surrounds the lens barrel to provide both a light baffle and to facilitate thermal radiation exchange.

The Vee blocks mount to the optical bench through three mounting feet. The Vee blocks have four contact points with the lens barrels that are separated to maximize stability. The positioning capabilities of this mounting system are described in the structural and thermal sections.

Table 1 below lists the allowable lens position tolerances from Section II (Optical Specifications) and the compliance of the mount design with the specifications. Lens mounting and positioning calculations are available in the document: "MMIRS Collimator and Camera Lens Mount Calculations."

Table 1: Lens Compliance Table

LENS NUM	DECENTER (mm)		TILT (mrad)		AIRSPACE (mm)	
	SPEC	DESIGN	SPEC	DESIGN	SPEC	DESIGN
3	0.05	0.041	0.1	0.098	0.05	0.033 (TO SLIT)
4	0.05	0.025	0.1	0.11*	0.05	.043 (3 to 4)
5	0.05	0.031	0.1	0.12*	0.05	.033
6	0.05	0.041	0.1	0.09	0.05	.025
7	0.05	0.043	0.1	0.11*	0.05	.028
8	0.05	0.043	0.1	0.11*	0.05	.022
9	0.05	0.041	0.1	0.08	0.05	.046
10	0.05	0.022	0.1	0.09	0.05	.025
11	0.05	0.041	0.1	0.08	0.05	.028
12	0.05	0.041	0.1	0.1	0.05	.043
13	0.05	0.043	0.1	0.09	0.05	.03
14	0.05	0.043	0.1	0.10	0.05	.013

* These specifications exceeded the original specification (see Section II, however they are in compliance within the allowed contingency of the error budget.

MMIRS Camera Optics Mount Calculations

George Nystrom
May 3, 2005

100 MMIRS Lens Mount Design

Design parameters:

- Design stress is to be < 100 psi for both axial and radial loads.
- Design loading (static) is 10g
- Nylon thickness (radial), Henry Bergner memo 11/08/04
- The design is to have 3 pads of equal area & equally spaced. The axial and radial pads are aligned.

110 Mount Design Calculation for Lens 3

Lens weight = 4.46 pounds from Zemax file (D. Fabricant 10/20/04)

Radial force required: Fr = (10g's * lens weight) = 44.6 pounds

Axial force required: Fa = Fr

If the optics were displaced by a force greater than 10g, they will return to their original position. This is because the only restraining force is friction at the mounting surfaces. The worst case is in the radial direction where friction exists at both axial surfaces. A coefficient of friction for Mylar on glass was measured at ≤ 0.2 and for Teflon is 0.04. The worst case restraining force is 0.24 times 44.6 or 10.7 pounds, so therefore the restoring force is a factor of 4 greater than the restraining forces. In addition, the radial force vector arising from the axial restraint against the spherical surface has not been considered. This also helps insure that the optic will return to its original position.

Radial Stress: S = Fr/A
Stress axial: Fa/A where A is total area (in^2)

So therefore A =Fa/100 = 0.491 in-sq is required for a 100 psi stress. Solve for the total mounting area available based on the lens mounting diameters.

A_t = (pi/4) *(OD^2-ID^2)
A_t = 3.675 in^2

Where OD & ID are lens-mounting diameters (see excel spread sheet-Lens mounting dimensions or TK calculation file –Lens mount stress).

Solve for the minimum pad angular extent:

$P\alpha = (A/ A_t) * 360/3$

$P\alpha = 16.03$ degrees

The model shows that a 20-degree wide pad satisfies all lenses, except 5 & 12. However, thermal modeling shows a need for greater contact area. Therefore, all pads will have an angular extent of 40 degrees.

Axial chord length at pad center:

$C = 2R \sin a/2$ or $C = 2R \sin 20 = 01.905$ in

Therefore axial pads are (units as above):

OD= 5.78, ID = 5.36, A = 1.22, A/P = .408, Sa = 36.4 psi

The fixed radial hard points are the same size as the axial points (40 degrees) and the width takes advantage of the lens edge thickness and is set at 0.75 inches. The radial force is the same at all pads since the lens is in static equilibrium and therefore

$S = (44.6) / (1.905*.75) = 29.7$ psi at each fixed pad location.

The adjustable pad is a rod of diameter 0.75 inches, which has a matched radius to the lens diameter. Its contact area is a compound surface, which can be approximated by a circle giving the least contact area and therefore

$S = 44.6/ .7854*(.75^2) = 100.9$ psi.

The radial adjustable pad requires a special cantilever beam spring. Its solution uses standard equations with the input values and results given below. We needed to minimize the lens barrel diameter at lens 3 because it is placed immediately behind the valve plate. This allows is necessary to provide acceptable pumping conductance for a reasonable valve size.

The spring's design parameters are:

E = 10,600,000 psi, 6061-T6 al, b = .78, h = .125, L = 1.25

The spring then delivers a 45-pound force at a 0.019-inch deflection with a stress equal to 26162 psi. The force slope is .001 in/ 2.4 lbs. (TK file: radial spring lens 3)

120 Mount Design for Lenses 4-14

Lenses 4 through 14 follow the design approach shown for lens 3. Calculations for other areas of the lens mount designs, such as: Belleville springs, friction forces will available at the CDR review. The mechanical mounting stress is not the dominant lens stress. The dominant stress is caused by thermal gradients. We have detailed lens finite element models that are discussed in the thermal and structural sections, which address this area. Also, Belleville spring designs will be available at the CDR. The Bellevilles are designed to be insensitive to deflection, thereby making assembly to achieve the appropriate force level not a concern. The load curve for lens 6 is shown here as an illustration.

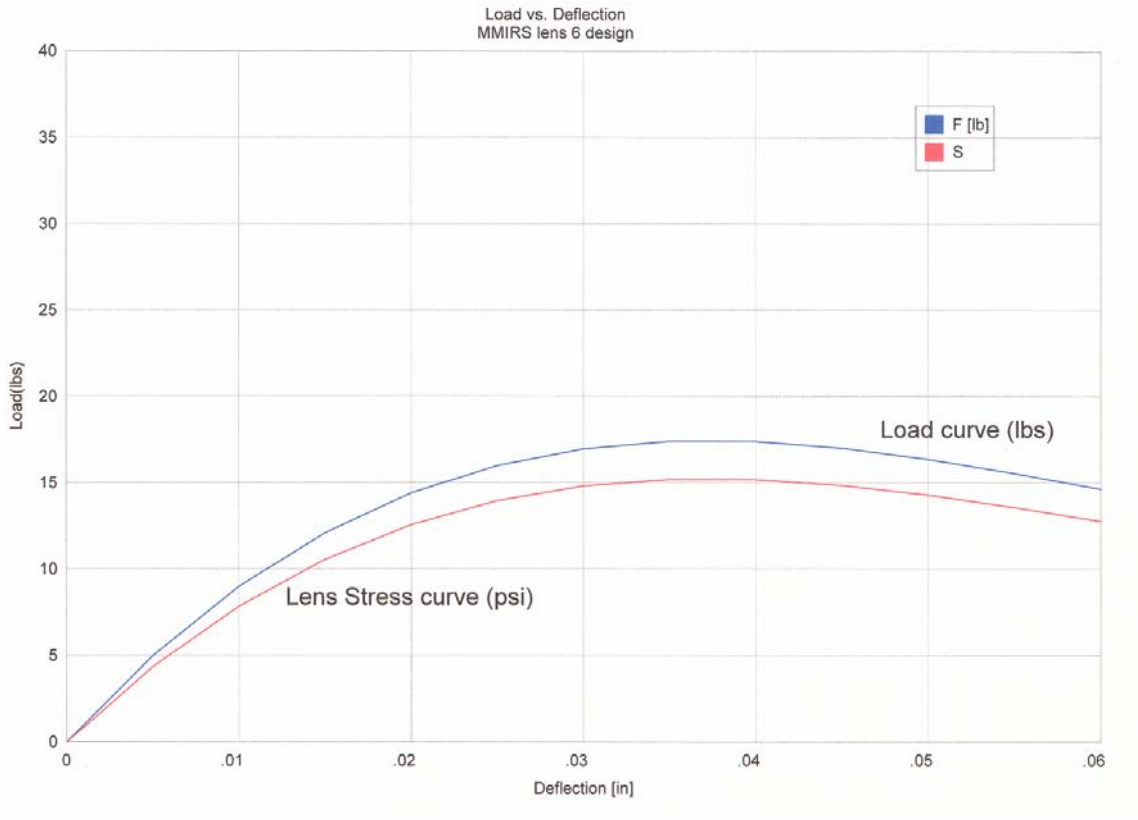

The desired load is 16 pounds and acceptable loads are from 0.025 to 053 inches of deflection. Radial spring loads are accomplished using various configurations of nylon interface pieces, which all have their loads applied using commercially available compression springs.

Table 1: Data for Lenses 4-9

ITEM	LENS 4	LENS 5	LENS 6	LENS 7	LENS 8	LENS 9	UNITS
Mat'l	CAF2	BAF2	ZNSE	FQTZ	CAF2	CAF2	
Wg	1.07	1.7	1.6	1.02	1.54	3.88	lbs
Fa	10.7	17	16	26.6	26.6	60	lbs
Fr	10.7	17	16	10.2	15.4	38.8	lbs
Sa	13.3	34	13.9	23.4	22.8	44.5	psi
Srf	10.6	128	42.5	10.7	40.2	35.3	psi
Sra	24.2	128	85	52	79.2	70	psi
A_t	2.41	2.99	3.43	3.4	3.5	4.0	in-sq
A_p	.267	.166	.382	.378	.389	.45	in-sq
A_r	1.0	.132	.382	.952	.383	1.09	in-sq
A_{ra}	.442	.132	.382	.196	.195	.555	in-sq

Table 2: Data for Lenses 10-14

ITEM	LENS 10	LENS 11	LENS 12	LENS 13	LENS 14	UNITS
MAT'L	S-FTM16	CAF2	BAF2	CAF2	S-FTM16	
Wg	1.62	3.69	2.31	2.47	.46	lbs
Fa	60	39.9	23.1	34.6	34.6	lbs
Fr	16.2	39.9	23.1	24.7	7.4	lbs
Sa	45.5	30	20.5	37	52	psi
Srf	12	27.3	69	21	6.7	psi
Sra	53.65	90.6	69	82	60.1	psi
A_t	3.95	3.69	3.36	2.80	2.00	in-sq
A_p	.439	.410	.186	.312	.22	in-sq
A_r	1.33	.1.34	.33	1.18	.68	in-sq
A_{ra}	.301	.41	.33	.301	.076	in-sq

The axial lens forces for lens 9,10,13 and 14 are higher because they are combined as a lens set.

200 Collimator Lenses (G5; Lenses 3-8)

Note: The lens cells are all designed so that a micrometer or CMM measurement can be made to determine the lens' radial positioning. This is accomplished through three radial holes sized for a close fit with a standard micrometer probe and our CMM probe. The holes are arranged in line with (opposite) the radial pads. The fits are computed using the example below for lens 3.

Lens: The lens diameter specification is 0.01 mm (.0004 inches). However, this analysis assumes the lens run out to be 0.001 (worst case), except for lens 4 and 5, which need to meet the specification. We will make the radial mounts once we have the exact dimension, so therefore:

Lens 3: 5.8634/5.8630 Radial mounts: 5.8630/5.8644
These dimensions yield a fit: 0/0.001 loose with the average = 0.0005 loose. Similar fits are used elsewhere.

Temperature effects are accounted for by calculating the displacement effects for all three positional requirements:

- De-centering uses the lens and mount properties in the formula (L*K*ΔT)*2.5%.
- Tilt uses expected thermal gradients in standard formulas for calculation.
- Airspace uses the same formula as de-centering except K is for Aluminum and L is the separation between components.

210 Decenter

Lens de-centering:	**Lens 3**	**Lens 4**
G2-G5 tilt effects & mating:	0.0005	0.0005
Lens mfg. Run out	0.001	0.0004

Lens/pads clearance	0.0005	0.0005
CTE	0.0004	0.0002
Concentricity pads-Mount OD	0.001	0.0005
RSS: inches (spec.)	0.0016 (0.0019)	0.0019 (.0019)

Lens de-centering:	**Lens 5**	**Lens 6**
G2-G5 tilt effects	0.0005	0.0005
Lens mfg. Run out	0.0004	0.001
Lens/pads clearance	0.0005	0.0005
CTE	0	0.0001
Lens cell clearance	0.0005	0.0005
Concentricity pads-cell OD	0.0008	0.0008
RSS: inches (spec.)	0.0012 (.00019)	0.0016 (.0019)

Lens de-centering:	**Lens 7**	**Lens 8**
G2-G5 tilt effects	0.0005	0.0005
Lens mfg. Run out	0.001	0.001
Lens/pads clearance	0.0005	0.0005
CTE	0.0003	0.0004
Concentricity pads to cell	0.0008	0.0008
Concentricity cell to mount	0.0008	0.0008
RSS: inches (spec.)	0.0017 (.0019)	0.0017 (.0019)

220 Tilt

Note: Lens tilts are computed by using the pads axial separation distances, i.e. pads midpoint radius and 120 degrees apart. Also, the tilt due to axial temperature differences at the pads is negligible.

Lens 3	**Tilt (arc-sec)**
Lens mfg surface error:	10.5
Axial restraint:	13.5
Lens barrel face:	9.2
3°K gradient across barrel:	6.2
1°K gradient between Vee supports:	0.6
RSS Total:	20.4 arc-seconds
Worst-case tilt is: (spec)	0.098 m-radians (0.1)

Lens 4	
Lens mfg surface error:	16.9
Axial restraint:	14.6
Lens barrel face:	5.6
3°K gradient across barrel:	2.1
1°K gradient between Vee supports:	0.6
RSS Total:	23.19
Worst-case tilt is: (spec)	0.11 m-radians (0.1)

Lens 5

Lens mfg surface error:	12.8
Axial restraint:	15.4
Lens barrel face:	15.9
3°K gradient across barrel:	2.1
1°K gradient between Vee supports:	0.6
RSS Total:	25.7
Worst-case tilt is: (spec)	0.12 m-radians (0.1)

Lens 6

Lens mfg surface error:	11.9
Axial restraint:	14.5
Lens barrel face:	11.3
3°K gradient across barrel:	2.1
1°K gradient between Vee supports:	0.6
RSS Total:	21.9
Worst-case tilt is: (spec)	0.09 m-radians (0.1)

Lens 7

Lens mfg surface error:	14.8
Axial restraint:	14.25
Lens barrel face:	11.7
3°K gradient across barrel:	2.1
1°K gradient between Vee supports:	0.6
RSS Total:	23.7
Worst-case tilt is: (spec)	0.11 m-radians (0.1)

Lens 8

Lens mfg surface error:	14.7
Axial restraint:	14.18
Lens barrel face:	11.7
3°K gradient across barrel:	2.1
1°K gradient between Vee supports:	0.6
RSS Total:	23.6
Worst-case tilt is: (spec)	.11 m-radians (0.1)

230 Spacing

For these calculations the measurement accuracy has been estimated to be 0.0005 inches. And the measurements are then RSS together. The RSS value is then added to the CTE error. The CTE error is 2.5 percent of (L*K*ΔT), where K is for aluminum and L is the lens spacing distance.

Lens 3: we estimate that it can be placed within 0.001 of the required dimension by Vee block placement. Added to this is the CTE error.

Airspace = .001 + .0003 = 0.0013 inches (0.033 mm)

Lens 3-4 spacing:
5 measurements required: RSS = .0011
CTE = .0006
Lens 3-4, Airspace: (spec) 0.0017 inches (0.0019)

Lens 4-5 spacing:
3 measurements required: RSS = .0008
CTE = .0003
Lens 4-5, Airspace: (spec) 0.0011 inches (0.0019)

Lens 5-6 spacing:
4 measurements required: RSS = .001
CTE = .000
Lens 5-6, Airspace: (spec) 0.001 inches (0.0019)

Lens 6-7 spacing:
4 measurements required: RSS = .001
CTE = .0001
Lens 6-7, Airspace: (spec) 0.0011 inches (0.0019)

Lens 7-8 spacing:
3 measurements required: RSS = .0008
CTE = .0001
Lens 7-8, Airspace: (spec) 0.0009 inches (0.0019)

300 Camera Lenses (G6; Lenses 9-14)

310 Decenter

Lens de-centering:	**Lens 9**	**Lens 10**
G3-G4 tilt effects & mating:	0.0005	0.0005
Lens mfg. Run out	0.001	0.0004
Lens/pads clearance	0.0005	0.0005
CTE	0.0004	0.0002
Concentricity pads-Mount OD	0.001	0.0002
RSS: inches (spec.)	0.0016 (0.0019)	0.0009 (.0009)

Lens de-centering:	**Lens 11**	**Lens 12**
G3-G4 tilt effects & mating:	0.0005	0.0005
Lens mfg. Run out	0.001	0.001
Lens/pads clearance	0.0005	0.0005
CTE	0.0004	0.0003
Concentricity pads-cell OD	0.001	0.001
RSS: inches (spec.)	0.0016 (.0019)	0.0016 (.0019)

Lens de-centering:	**Lens 13**	**Lens 14**
G3-G4 tilt effects & mating:	0.0005	0.0005
Lens mfg. Run out	0.001	0.001
Lens/pads clearance	0.0005	0.0005
CTE	0.0002	0.0001
Concentricity pads to cell	0.0008	0.0008
Concentricity cell to mount	0.0008	0.0008
RSS: inches (spec.)	0.0017 (.0019)	0.0017 (.0019)

320 Tilt

Lens 9	**Tilt (arc-sec)**
Lens mfg surface error:	9.6
Axial restraint:	10.1
Lens barrel face:	8.6
3°K gradient across barrel:	2.0
1°K gradient between Vee supports:	0.6
RSS Total:	16.53 arc-seconds
Worst-case tilt is: (spec)	0.08 m-radians (0.1)

Lens 10	
Lens mfg surface error:	9.8
Axial restraint:	11.7
Lens barrel face:	10.3
3°K gradient across barrel:	2.0
1°K gradient between Vee supports:	0.6
RSS Total:	18.57
Worst-case tilt is: (spec)	0.1 m-radians (0.1)

Lens 11	
Lens mfg surface error:	9.7
Axial restraint:	10.2
Lens barrel face:	9.4
3°K gradient across barrel:	2.0
1°K gradient between Vee supports:	0.6
RSS Total:	17.0
Worst-case tilt is: (spec)	0.08 m-radians (0.1)

Lens 12	
Lens mfg surface error:	11.5
Axial restraint:	13.7
Lens barrel face:	11.9
3°K gradient across barrel:	2.0
1°K gradient between Vee supports:	0.6
RSS Total:	21.6

Worst-case tilt is: (spec)	0.1 m-radians (0.1)

Lens 13

Lens mfg surface error:	13.5
Axial restraint:	9.6
Lens 13 & 14 stack up:	9.0
3°K gradient across barrel:	2.0
1°K gradient between Vee supports:	0.6
RSS Total:	18.96
Worst-case tilt is: (spec)	0.09 m-radians (0.1)

Lens 14

Lens mfg surface error:	18.6
Axial restraint:	6.8
Lens barrel face:	6.2
3°K gradient across barrel:	2.0
1°K gradient between Vee supports:	0.6
RSS Total:	20.9
Worst-case tilt is: (spec)	0.10 m-radians (0.1)

230 Element Spacing

The placement of the lenses will be accomplished by standard alignment and measurement techniques, including by moving the camera lens barrel within its Vee block.

Lens 8-9 spacing:

Placement to within:	RSS =	0.0010
		CTE = .0008
Lens 8-9, Airspace: (spec)		0.0018 inches (0.0019)

Lens 9-10 spacing:

4 measurements required:	RSS =	0.001
		CTE = .000
Lens 9-10, Airspace: (spec)		0.001 inches (0.0019)

Lens 10-11 spacing:

5 measurements required:	RSS =	0.0011
		CTE = .0001
Lens 10-11, Airspace: (spec)		0.0011 inches (0.0019)

Lens 11-12 spacing:

4 measurements required:	RSS =	0.0010
		CTE = .0007
Lens 11-12, Airspace: (spec)		0.0017 inches (0.0019)

Lens 12-13 spacing:
4 measurements required: RSS = 0.0010
CTE = .0002
Lens 12-13, Airspace: (spec) 0.0012 inches (0.0019)

Lens 13-14 spacing:
1 measurement required: RSS = 0.0005
CTE = .0000
Lens 13-14, Airspace: (spec) 0.0005 inches (0.0019)

Section V.

Guider/Wave Front Sensor

1. Guider/WFS Design
2. Description of the CCD electronics

MMIRS Guider and Wavefront Sensor

McLeod, McCracken, Martini 2005 May 02

100 Overview

Guiding and wavefront sensing (GWFS) on MMIRS will be performed using two identical units that are fed by a fixed pickoff mirror that surrounds the science beam. The field of the GWFS covers the region outside the 7'x7' science field out to a field radius of 7'. Each GWFS rides on a 2-axis translation stage and serves half of the available field. The camera can be focused and there is also a Guiding/Shack-Hartmann mode selector stage. One unit will operate in Guiding mode while the other will be used to derive wavefront information. Slow-speed guiding information will also be derived from the Shack-Hartmann data and used to control the instrument rotation angle. The existing GWFS used at Magellan are very similar in concept. Below we discuss the optical and mechanical layouts of the GWFS. The software is discussed in the Software section.

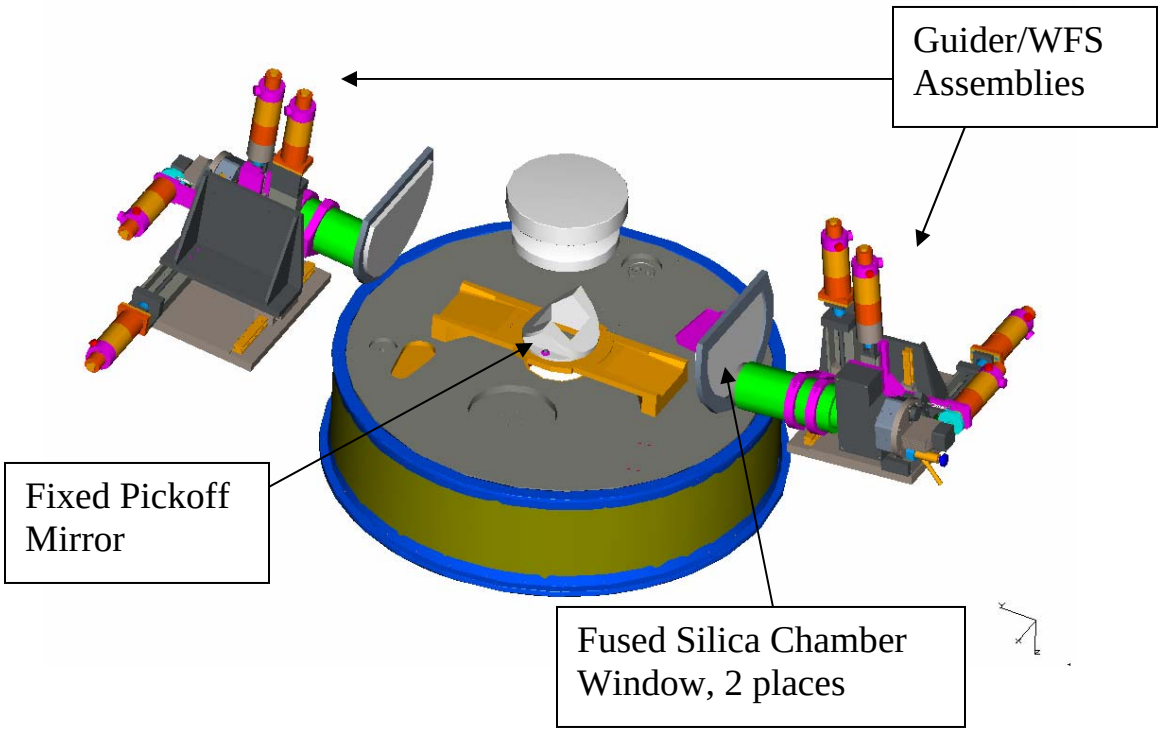

MOS Section with MMIRS Guider and Wave Front Sensor Assemblies

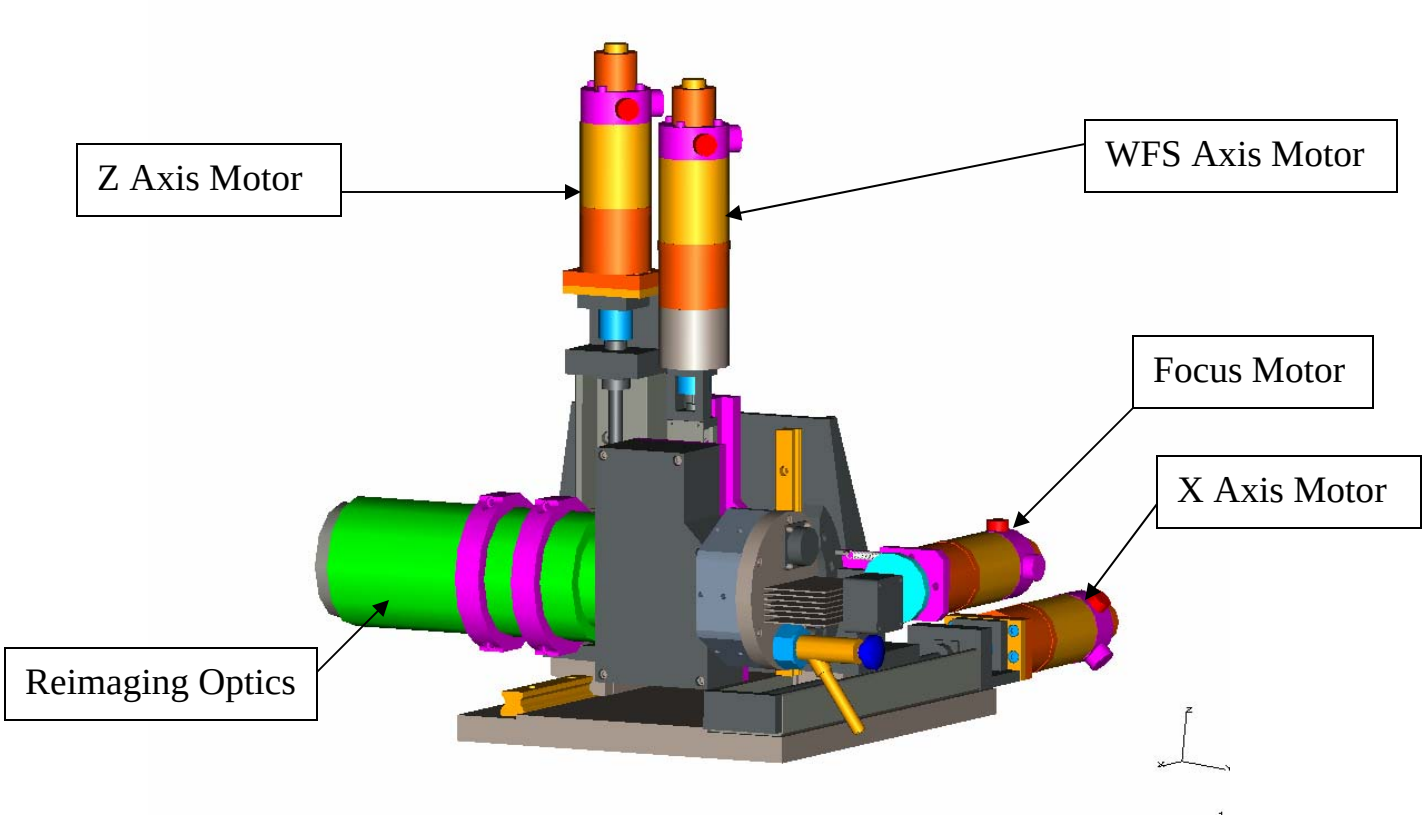

MMIRS Guider Wave Front Sensor Assembly

200 Optical Design

210 Guiding Mode

The optical layout is shown here. The optics are designed to work from 600nm to 900nm, rather than in the blue because MMIRS will be primarily a bright-time instrument. A 16mm thick fused silica flat serves as the vacuum pressure window and is large enough to cover the entire field of view. A symmetric custom doublet is used to collimate and reimage the focal plane onto the camera. A second 16mm piece of silica after the reimager makes the design symmetric.

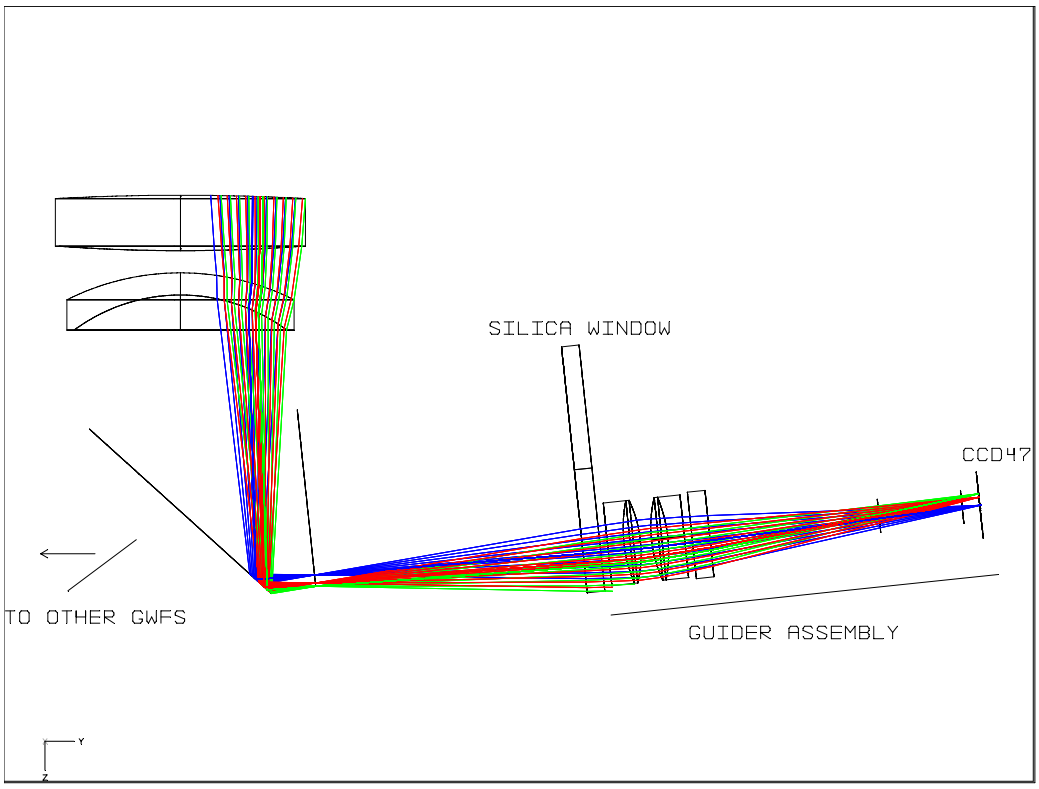

220 WFS Mode

To operate the GWFS in Shack-Hartmann mode, a stage containing two fold mirrors is moved into the beam. The first fold directs the light through a field stop. The 4" field stop is required to cut down the bright sky background, so that each spot image contains sky background only from its own subaperture. The beam is then folded on through a second collimator which forms a pupil image onto an Adaptive Optics Associates 600-40-S lenslet array. The final fold redirects the light back to the CCD camera. The distances are chosen so that the camera should not need to be refocused when switching between the two modes.

A 20 micron pinhole reference source illuminated by an LED used for calibrating the Shack-Hartman spot positions is located as shown. This location is in the reflected position of the center of the slit mask. To use the calibration source, the GWFS is moved in front of it using the X-Z stage. The calibration is performed to remove the effects of aberrations in the GWFS optics.

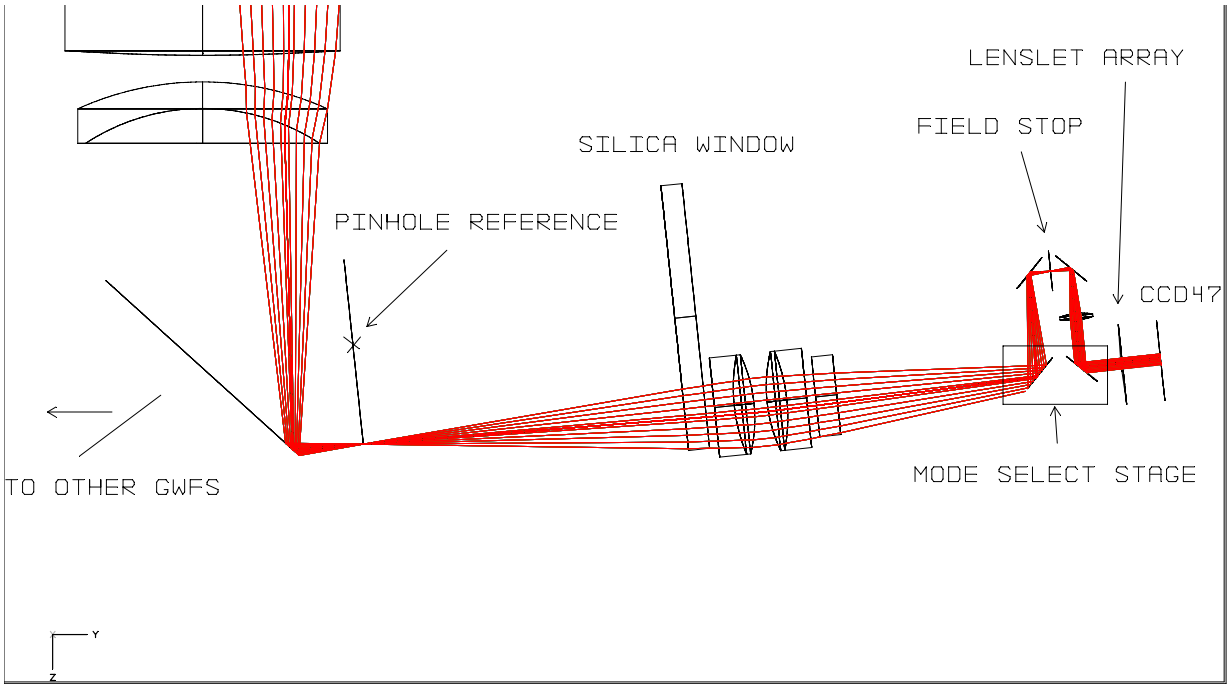

230 Optical Prescription

System/Prescription Data

File : C:\Documents and Settings\bmcleod\My Documents\ZemaxFiles\MMIRS\mmirs_guider_outside_wfs_apertures_48deg_new lenslet.ZMX
Title: MMIRS Camera
Date : TUE APR 26 2005

Surf	Type	Comment	Radius	Thickness	Glass
OBJ	STANDARD		Infinity	Infinity	
STO	STANDARD	PRIMARY	-16255.3	-6179.233	MIRROR
2	STANDARD	SECONDARY	-5150.89	6179.233	MIRROR
3	STANDARD		Infinity	1430.149	
4	STANDARD	LENS1	2126.526	50	CAF2
5	STANDARD		-1502.7	19.99995	
6	STANDARD	LENS2	229.6804	20	CAF2
7	STANDARD		162.3126	195.2	
8	COORDBRK		-	0	
9	STANDARD	PICKOFF	Infinity	0	MIRROR
10	COORDBRK		-	-114.8	
11	STANDARD		Infinity	-244	
12	STANDARD	WINDOW	Infinity	-16	SIL5C
13	STANDARD		Infinity	-6.826915	
14	COORDBRK		-	0	
15	STANDARD	REIMAGER	-10741.9	-15	SF5
16	STANDARD		-129.3031	-15.00169	BK7
17	STANDARD		112.3034	-10	
18	STANDARD		-112.3034	-15.00169	BK7
19	STANDARD		129.3031	-15	SF5
20	STANDARD		10741.9	-6.826915	
21	STANDARD		Infinity	-16	SIL5C
22	STANDARD		Infinity	-155.451	
23	COORDBRK		-	0	
24	STANDARD	FOLD	Infinity	0	MIRROR
25	COORDBRK		-	74.75	
26	COORDBRK		-	0	
27	STANDARD	FOLD	Infinity	0	MIRROR
28	COORDBRK		-	-16	
29	STANDARD	APERTURE	Infinity	-15.763	
30	COORDBRK		-	0	
31	STANDARD	FOLD	Infinity	0	MIRROR
32	COORDBRK		-	23.487	
33	STANDARD	EDMND 45212	82.92	3	SF5
34	STANDARD	(COLLIMATOR)	21.38	7.89	SK11
35	STANDARD		-28.75	40.373	
36	COORDBRK		-	0	
37	STANDARD	FOLD	Infinity	0	MIRROR
38	COORDBRK		-	-18.5	
39	USERSURF	LENSLET	-20.5	-1	BK7
40	PARAXIAL		-	0	
41	STANDARD		Infinity	-39.5	
IMA	STANDARD		Infinity		

240 Summary of Basic Properties

Guiding Mode

Pixel Size (binned x2)	26 microns = 0.16”
Field of View	80”
Image Quality	40micron RMS dia = 0.25”

WFS Mode

Collimator focal length	45mm
Collimator part numb	Edmund 45-212
Lenslet focal length	40mm
Lenslet pitch	0.6mm
Lenslet part number	Adaptive Optics Associates 600-40-S Substrate D
Number of illuminated spots	15 across diameter
Pixel size (binned x2)	0.18”/pixel
Spot separation	4.15” = 23 pixels
Field stop diameter	4” = 0.66 mm = 0.026in = #71 drill

300 Mechanical and Electrical Design

310 Translation Stages

The GWFS X and Z axes are mounted on THK KR33 rails and driven with an integrated ball-screw. Each axis also has a THK SHS rail and block operating as an outrigger for additional support. A Phytron ZSS 52 stepper motor with a 6.25:1 single stage planetary gearhead powers the stages. An integrated power-off brake will prevent the mechanism from backdriving. A Hymark magnetic linear encoder is used to sense position. The positioning tolerance requirement is ±200 microns. The encoder resolution is 5 microns and the step size is 4.8 microns, which is more than adequate to meet this specification. Controlling flexure of the guider relative to the slit mask is critical to keeping targets aligned with their slits during an observation. Flexure of the GWFS will be reported in Structural Analysis, Section VIII.

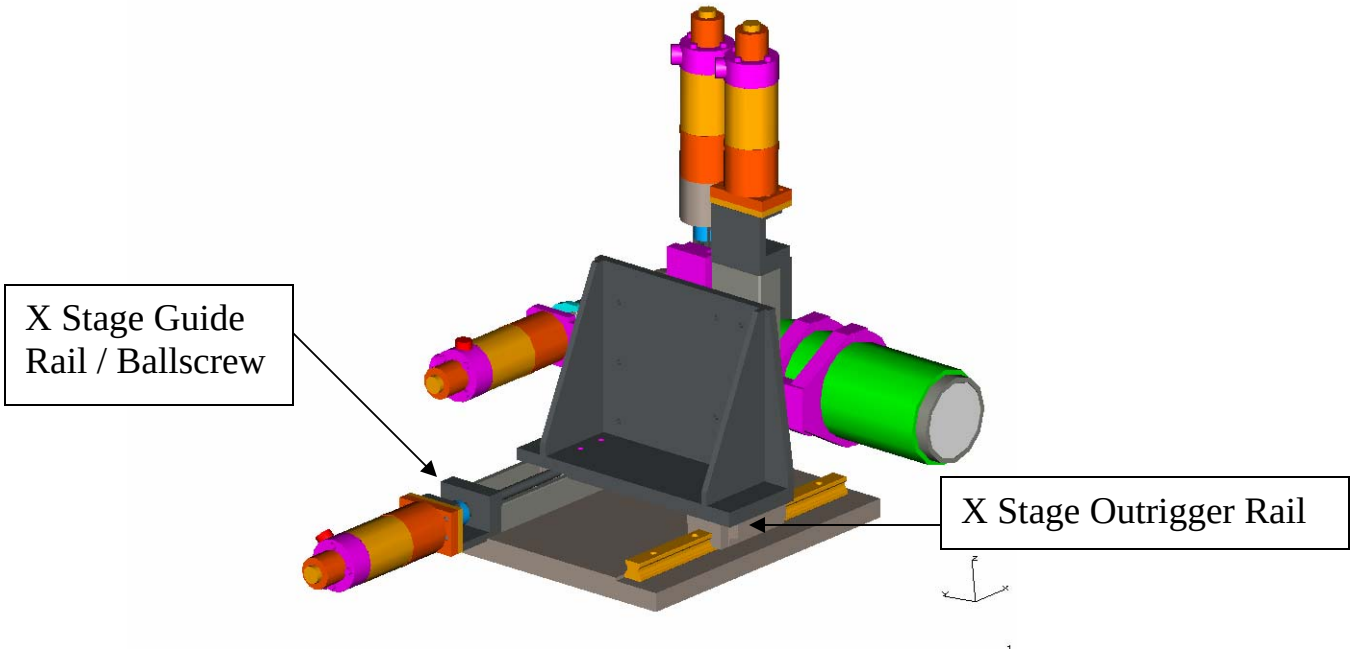

GWFS X Axis Stage

320 WFS Select Stage

The Wave Front Sensor select axis is mounted on THK KR30 rails and driven with an integrated ball-screw. A Phytron ZSS 52 stepper motor with a 6.25:1 single stage planetary gearhead powers the stage. An integrated power-off brake will prevent the mechanism from backdriving. A Hymark magnetic linear encoder is used to sense position. The positioning tolerance requirement is ±200 microns. The encoder resolution is 5 microns and the step size is 4.8 microns, which is more than adequate to meet this specification.

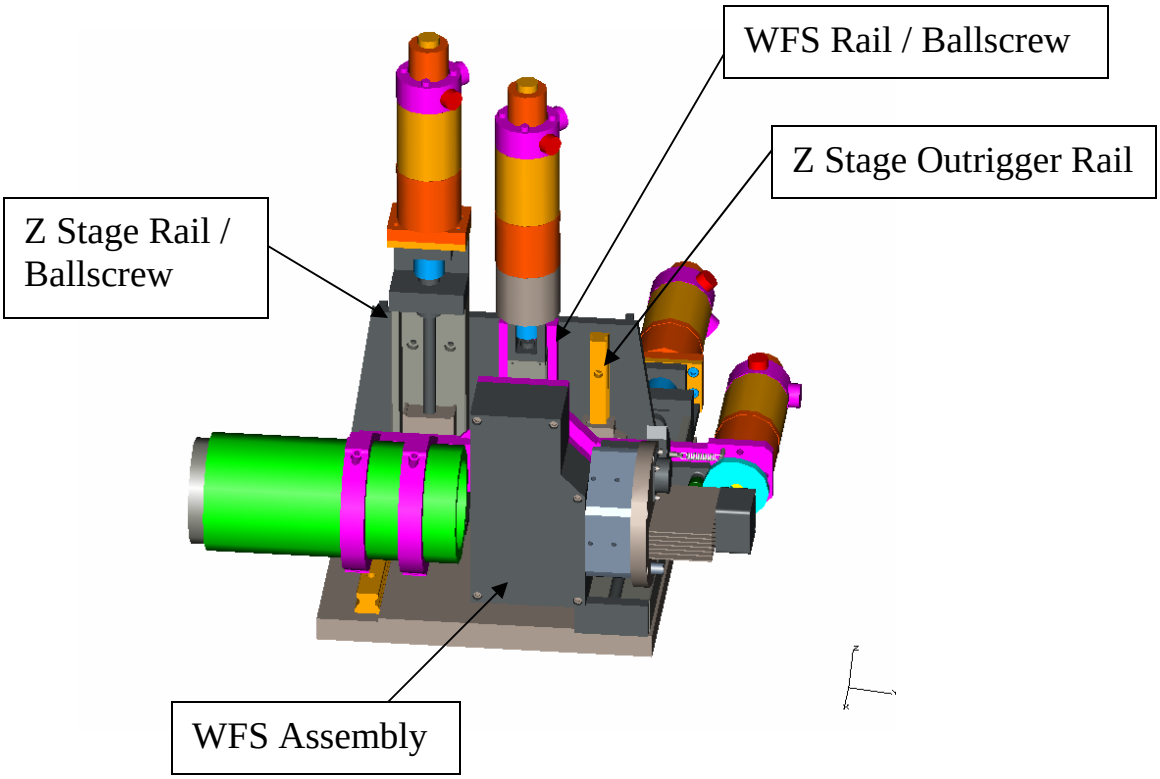

GWFS Z-Axis and Select-Axis.

330 Focus Stage.

The Guider Camera axis is mounted on THK RSR rails and driven directly with a cam mounted on the motor/gearhead output shaft. The moving (block) part of the stage attaches to the camera mount. A cam follower attached to the camera mount is spring-loaded against a cam with 2mm of lift. A Phytron ZSS 52 stepper motor with a 6.25:1 single stage planetary gearhead powers the stage. An integrated power-off brake will prevent the mechanism from moving after adjustment. A Hymark magnetic linear encoder is used to sense position. The positioning tolerance requirement is ±40 microns. The encoder resolution is 5 microns and the step size is 1.8 microns, which is more than adequate to meet this specification.

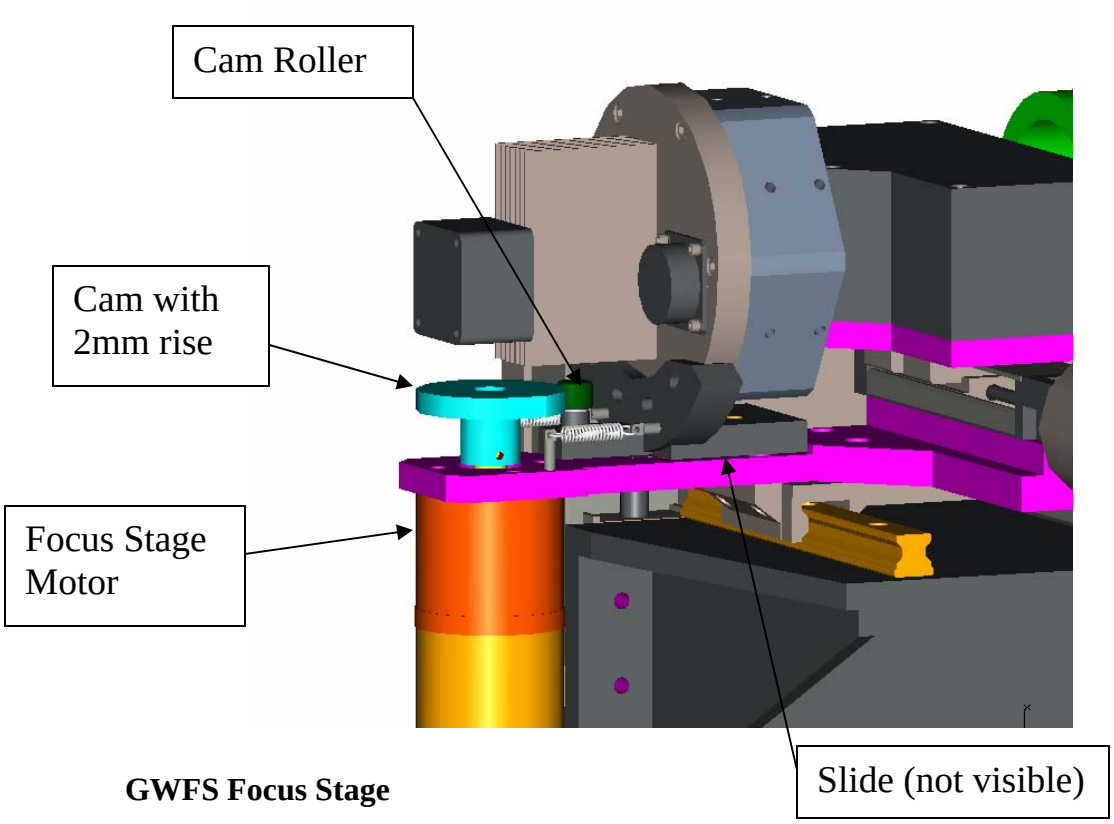

GWFS Focus Stage

MMIRS Guider Wavefront Sensor Assembly Summary					
Subassembly	**Travel Range Required**	**Travel Rate**	**Document**	**Requirements:**	**MMIRS Design Value**
	(mm)	**Full Travel Time**		**Positioning Accuracy (+/-)**	**Positioning Accuracy (+/-)**
		Motor Speed		**Encoder Resolution**	
				(um)	
Guider "X" Axis	+/- 70	18 mm/sec	S-MMIRS-200 / Section 315 / p. 18	200	7.8
		10 sec		10	
		1094 rpm			
Guider "Z" Axis	+/- 35	9 mm/sec	S-MMIRS-200 / Section 315 / p. 18	200	7.8
		10 sec		10	
		547 rpm			
Guider Camera Focus Axis	+/- 1	n/a	S-MMIRS-200 / Section 315 / p. 18	40	1.8
		10 sec		25	
		34.4 rpm			
Wave Front Sensor Axis	40	5 mm/sec	S-MMIRS-200 / Section 315 / p. 18	200	7.8
		10 sec		10	
		312.5 rpm			

400 CCD Camera

The CCD camera dewar is based on a Steward Observatory design, but modified to accept the larger CCD we are using and will be air-cooled instead of liquid cooled. The CCD is cooled with a Melcor three-stage thermoelectric cooler.

The CCD is clamped between two copper plates. The upper copper plate has a hole in it to expose the detector; the lower plate extends to the TEC. The cold side of the TEC will be soldered to the lower copper plate. The TEC's hot side will be clamped to the camera baseplate. The CCD and copper plate assembly will be mounted on Kel-F standoffs. Aluminum heatsink fins will be bonded into the guide camera baseplate and a small axial fan will draw air over the fins.

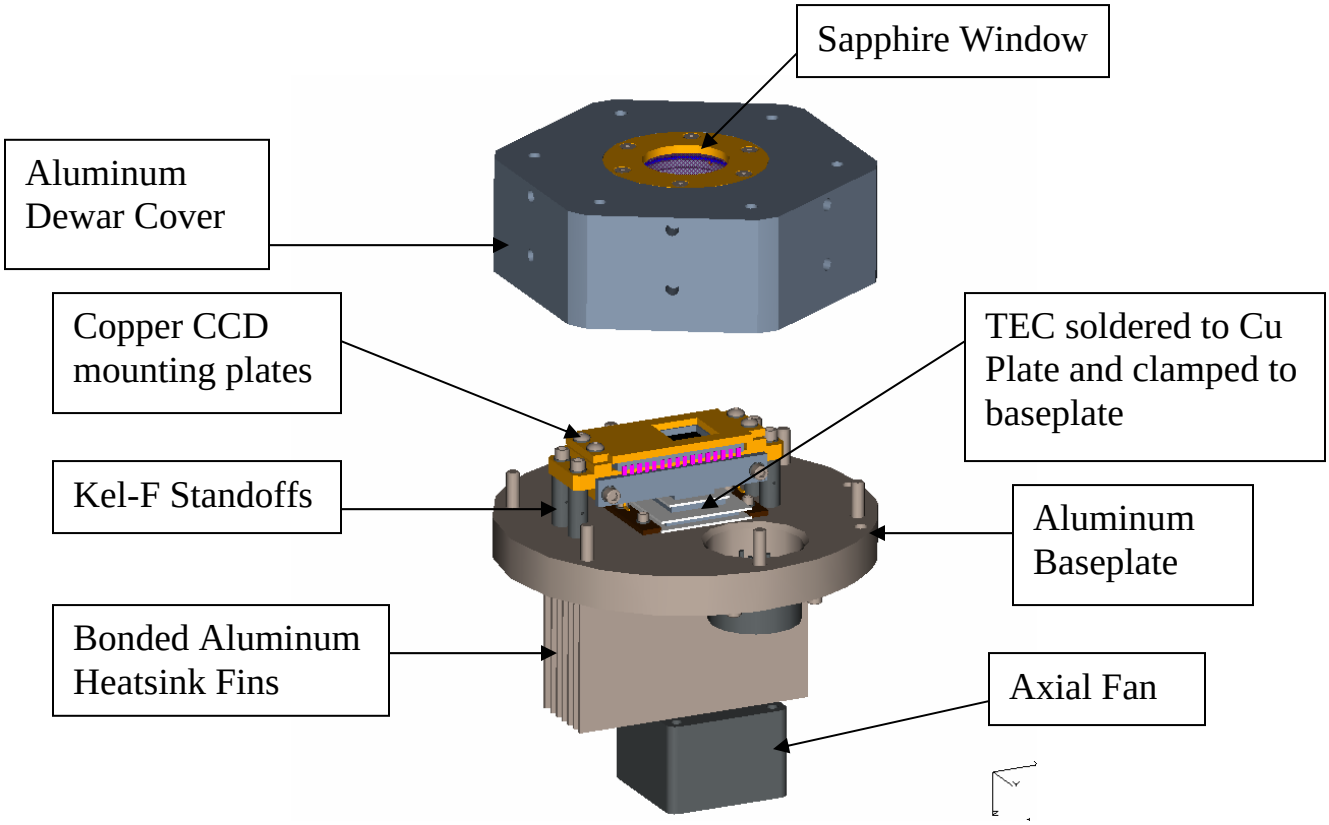

MMIRS Guider Camera

Assuming a 20C ambient and that the TEC's cold side must reach –30C, it is calculated that the TEC's hot side will dissipate 8.2 W to the ambient. A typical fan will dissipate an additional 3.4 W for a total of 11.6 W per guider at 20 C ambient. Note the TEC's contribution to this power dissipation is ambient temperature dependant. At a more typical ambient of 10 C the TEC's power dissipation is estimated at 4.3 W for a total of 7.7 W per guider.

500 Camera Electronics

The electronics are identical to those currently used at Magellan, with two differences. First, the camera head has been physically separated from the electronics box. A video buffer located in the camera head will provide a level of noise immunity. Second, a new optical fiber based interface is used to commicate with the computer, rather than a copper interface. This will provide much better lightning protection. A description of the guider electronics by Burley et al. follows this section. Even more detail can be found at http://www.ociw.edu/instrumentation/ccd/gcam.html.

600 Guide Star Density

The required field of view and sensitivity of the GWFSs are set by the surface density of suitable guide stars as a function of apparent magnitude.
Based on the expected sensitivity of the guide cameras and wavefront sensors, the goal is for a 15th magnitude or brighter guide star and a 14th magnitude or brighter star for the wavefront sensor. The required field of view is then set by the surface density of such stars.

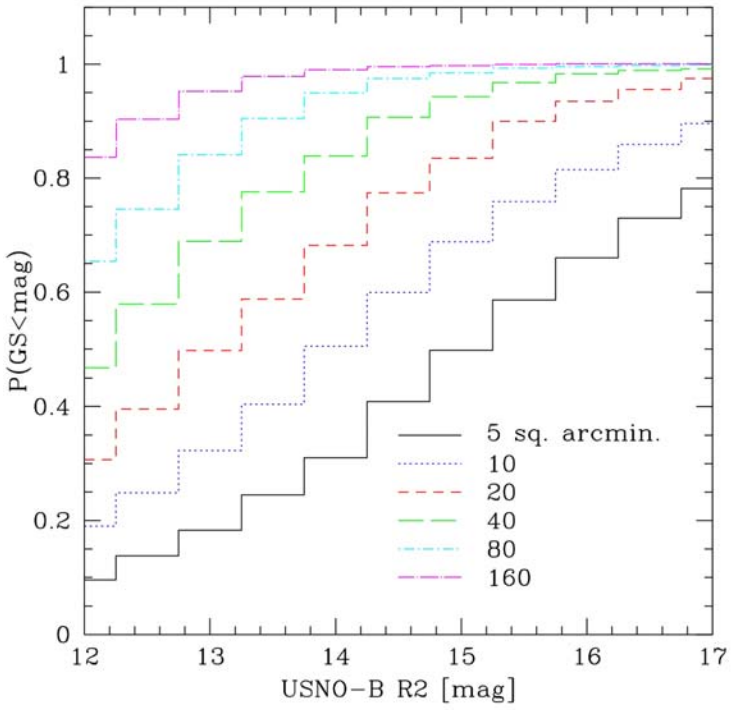

Figure 1: Probability of having a guide star within some surface area as a function of R magnitude. The field centers are randomly distributed across the entire sky. The second line from the top corresponds to one GWFS field.

The surface density of suitable guide stars was calculated with a series of realizations of various field sizes and apparent magnitude limits with the USNO-B catalog. In particular, a thousand randomly generated, uniformly distributed field centers were calculated and the presence or absence of USNO stars brighter than some apparent magnitude was recorded. These data were used to determine the probability that a given field size would contain a USNO star brighter than some apparent magnitude. Based on these calculations (see Figure above), the two GWFS fields of 80 sq. arc-minutes each are sufficient to identify appropriate stars. In particular, 14th magnitude and brighter stars will be available over 95% of the time.

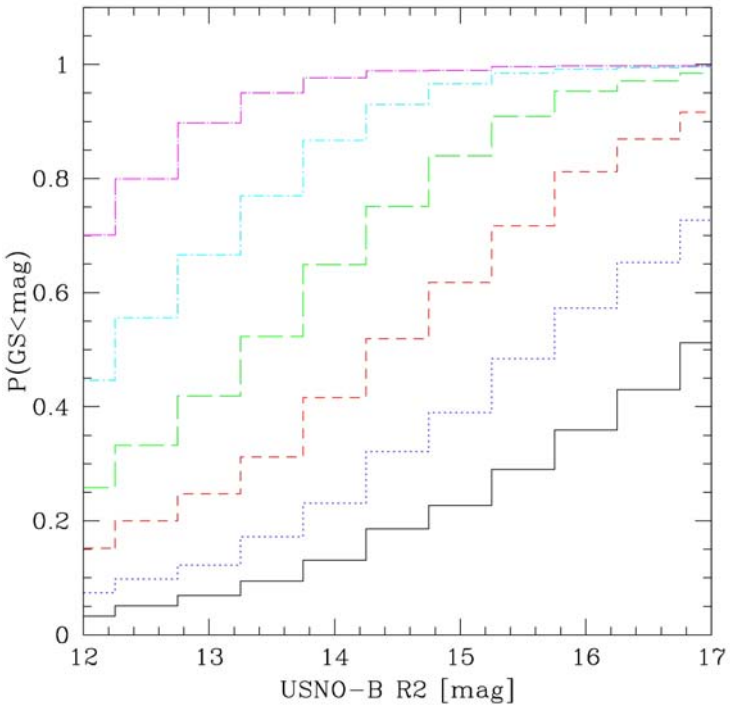

Figure 2: Probability of having a guide star within some surface area as a function of R magnitude for high Galactic latitude fields only (|b| > 70 degrees).

Many observations with MMIRS will likely target high Galactic latitude fields, which will have significantly lower stellar surface densities. To determine if the MMIRS GWFS fields are still sufficient, a new set of realizations were run for fields with Galactic latitude |b| > 70 degrees. This calculation (shown in Figure 2 above) still indicates that 14th magnitude stars will be available approximately 90% of the time. However, to insure that sufficiently bright stars are available for MOS observations, the MOS design software should include information on the availability of GWFS stars during mask design.

COMPACT CCD GUIDER CAMERA FOR MAGELLAN

Greg Burley, Ian Thompson and Charlie Hull
Observatories of the Carnegie Institution of Washington

Abstract: The Magellan guider camera uses a low-noise frame transfer CCD with a digital signal processor based controller. The electronics feature a compact, simple design, optimized for fast settling times and rapid readout rate. The camera operates (nominally) at –20 ºC with thermoelectric cooling. Multiple operating modes are supported, with software selectable binning, exposure times, and subrastering.

Key words: guider camera

The design objective for the Magellan guider camera was to build simple, low-power hardware with enough flexibility to operate in full-frame imaging mode, subrastered guiding mode, and Shack-Hartmann wavefront sensing mode.

The guider camera uses a Marconi CCD47-20 1024×1024×13 μm pixel, low-noise, back-illuminated, frame transfer CCD with a digital signal processor (DSP) based CCD controller. For reduced complexity, most of the digital logic functions are concentrated in the DSP and its internal peripherals, and a programmable logic chip (EPLD). A block diagram of the CCD camera is shown in Figure 1.

The CCD controller for the guider camera has a number of interesting properties. It features a programmable DSP56303 digital signal processor, which allows for software control of image size, subraster, binning, clock voltages, dual-slope signal processing, and exposure times. The circuit designs use simple op-amp and analog switch components for the clock driver and signal processing circuits[1]. The preamplifier[2] and signal processing circuits are optimized for fast settling times (less than 100 ns) to

maximize the pixel readout rate. The design has dual signal processing channels with 14-bit, 1.2 ìs conversion time analog-to-digital converters. Clock and bias voltages are set by digital-to-analog converters. The controller features temperature monitoring of the CCD, and digital control of TE cooler current. The on-board DC-DC converters (with heavily filtered outputs) generate +3.3V, ±5V, ±12V and +28V from 48V DC input.

In operation, the CCD system is controlled by commands and program code sent over the data link. The DSP is fast enough to directly generate the sequences used for the CCD parallel and serial transfers from on-chip memory[3], and write them to the sequence register. Each bit controls one of the CCD clock lines, with a clock driver to translate to CCD-level voltages. The DSP controls the dual-slope integrators and analog-to-digital conversion, extracts the signal pixel-by-pixel and multiplexes the digitized data onto an RS-485 serial link at 20 Mbps for up to 100 meters. Each of the ADCs, DACs, sequence register, and data link peripherals are memory mapped in the DSP to simplify the software design.

The basic sequence patterns programmed into the DSP memory (serial shift, parallel shift, read pixel, flush pixel) are combined to read out the array. With the appropriate sequences the CCD can be read out through one or both output amplifiers.

Table -1. Detector and readout specifications

Property	Value	Units
Image size	1024 × 1024	Pixels
Pixel size	13	µm
Read noise	5	e- (slow scan)
Readout rate (slow)	5.0	µs/pixel
Readout rate (fast)	2.5	µs/pixel
Dark current (-20 C)	2	e-/pixel/s
Frame rate (binned 4×4)	4	fps
Subraster rate (32×32 pixels)	40	fps

Table -2. Power estimate

Circuit block	Value	Units
Digital electronics	1.05	
Clock drivers	1.60	
Signal processing	2.50	
Preamplifiers	0.35	
TE cooler	6.50	
TOTAL	12.0	watts

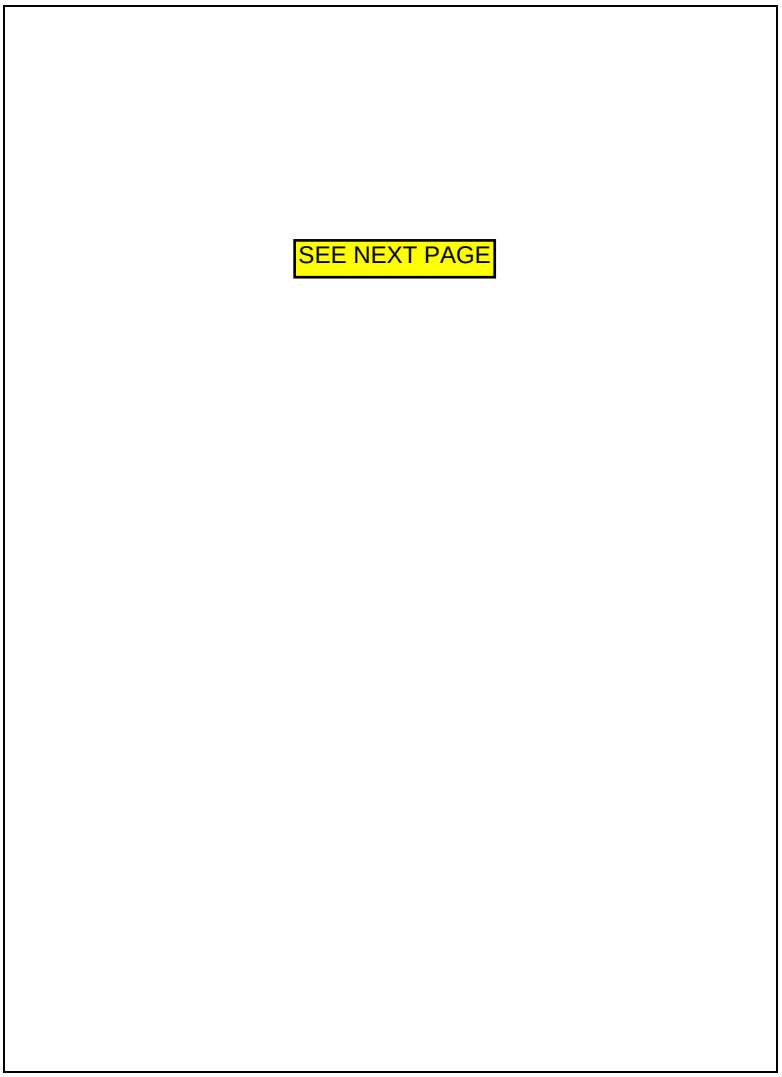

Figure 1. Magellan guider camera block diagram.

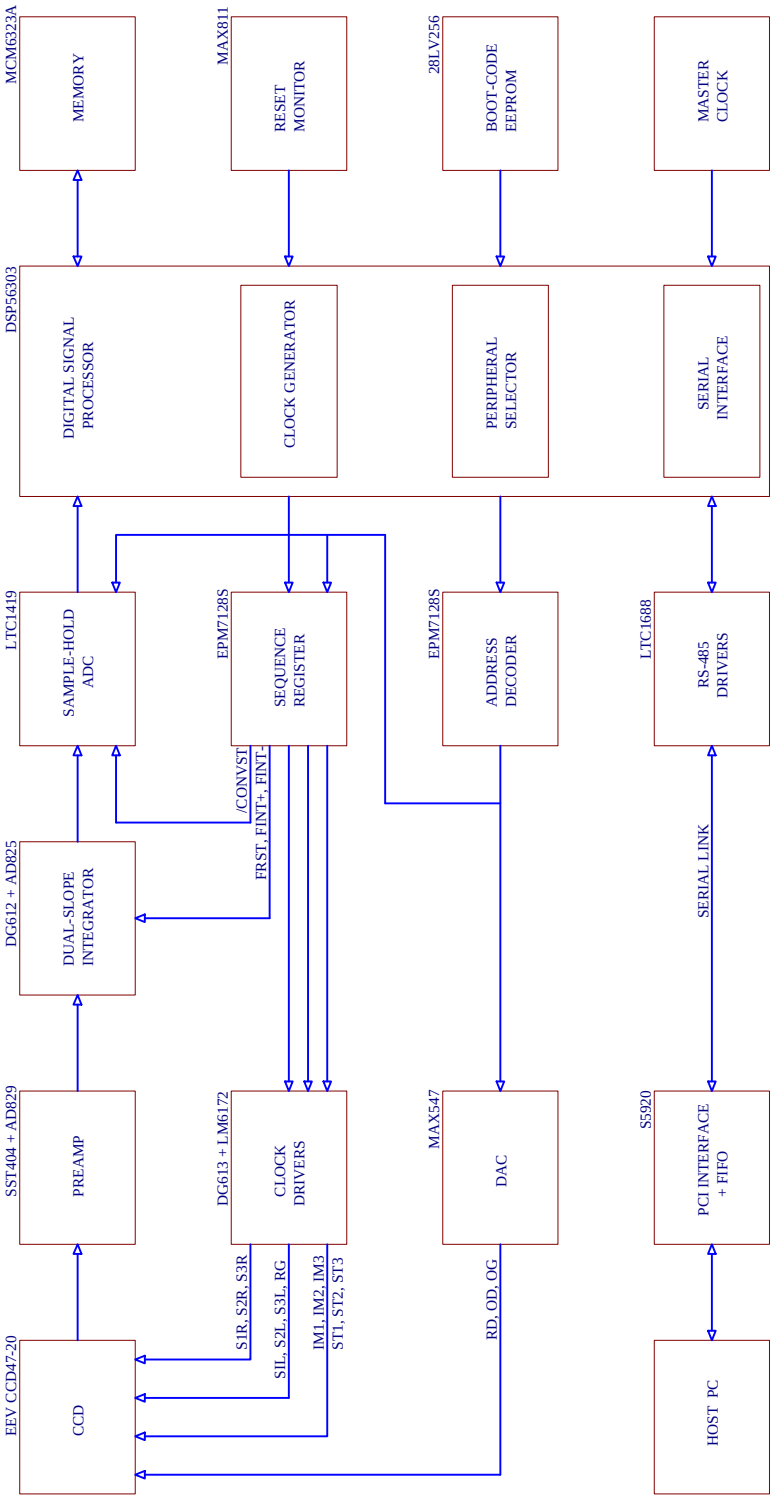
MCM6323A
MEMORY
MAX811
RESET MONITOR
28LV256
BOOT-CODE EEPROM
MASTER CLOCK
DSP56303
DIGITAL SIGNAL PROCESSOR
CLOCK GENERATOR
PERIPHERAL SELECTOR
SERIAL INTERFACE
LTC1419
SAMPLE-HOLD ADC
EPM7128S
SEQUENCE REGISTER
EPM7128S
ADDRESS DECODER
LTC1688
RS-485 DRIVERS
/CONVST
FRST, FINT+, FINT-
DG612 + AD825
DUAL-SLOPE INTEGRATOR
SERIAL LINK
SST404 + AD829
PREAMP
DG613 + LM6172
CLOCK DRIVERS
MAX547
DAC
S5920
PCI INTERFACE + FIFO
S1R, S2R, S3R
S1L, S2L, S3L, RG
IM1, IM2, IM3
ST1, ST2, ST3
RD, OD, OG
EEV CCD47-20
CCD
HOST PC

Physically, the guider camera consists of six circuit boards (DSP timing generator, signal processing, clock driver, power supply, backplane, and CCD header boards), and occupies a volume of less than 3.75 × 3.5 × 6.0 inches. An additional PCI interface board is used in the host computer.

The CCD is enclosed in a sealed, dry gas filled housing with an off-the-shelf two-stage thermoelectric (TE) cooler. The CCD temperature is monitored with an off-chip sensor (AD590) mounted inside the housing. An adjustable current source provides up to 3 amps to the TE cooler, which is rated for $\Delta T = 83$ ºC under ideal no-load conditions. In practice, a $\Delta T \approx 40$ ºC is achievable with a TE current of about 2 amps.

A liquid-cooled heat sink removed heat from the TE cooler hot side. Even at low flow rates (a few lites per minute), the entire CCD housing can be rapidly chilled to the fluid temperature (nominally 10 ºC at the telescope). The TE drive transistor is mounted on the heatsink as well, to prevent it overheating.

OCIW has open-sourced the design information for the guider camera, which is available at www.ociw.edu/~burley/ccd/guider.html. The on-line information contains a complete design description, including all schematics, pcb layouts, EPLD code, dsp source code, C subroutine library, and test results.

The guider cameras are in regular use on the two Magellan 6.5-m telescopes at Las Companas Observatory.

REFERENCES

1. J. Gunn et al, “Palomar Observatoy CCD camera,” PASP 99, 518-534 (1987).
2. J. Geary and S. Amato, “Camera electronics for the SAO Megacam,” SPIE 3355 Optical Astronomical Instrumentation (1998).
3. G. Burley et al, “A versatile CCD wavefront curvature sensor,” PASP 110, 330-338 (1998).

Section VI.

MMIRS Structural Analysis

Structural Analysis Overview

1. Optical Performance of the GWFS and Science Optics
2. Buckling Analysis of the MOS and Camera Sections
3. Lens 6 Analysis
4. Lens 1 Analysis
5. Radial Lens Mount Sizing for Nylon
6. Thermal Gradient Stress on Lenses 3-14
7. MMIRS Instrument Lift Cart Analysis

MMIRS Structural Analyses
Overview

The structural analysis performed since the PDR typically focused on either specific subsystems or global models. The subsystem analyses have been used to provide design direction to specific areas of the instrument, while the global models have been employed to provide direction to the large-scale design. These models are presented in this section and are briefly described below.

A high-fidelity, global structural model is in progress and will be presented at the CDR. This model will contain significantly more detail than the previous global models and will supercede those results that employed, or were bounded by, the earlier models.

The specific reports planned for CDR are:

Section VI.1 Optical Performance of the GWFS and Science Optics

Section VI.2 Buckling Analysis of the MOS and Camera Sections

Section VI.3 Lens 6 Analysis

The following reports are included in this data package:

Section VI.4 Lens 1 Analysis

This report summarizes an analysis of the updated lens mount design for L1.

Section VI.5 Radial Lens Mount Sizing for Nylon

This report summarizes an analysis of the updated lens mount design for L3-14.

Section VI.6 Thermal Gradient Stress on Lenses 3-14

This report summarizes the sensitivity of lenses L3-L14 to stress induced by thermal gradients.

Section VI.7 MMIRS Instrument Lift Cart Analysis

This report addresses the structural integrity of the instrument lift cart that is intended to support MMIRS (and other instruments) at Magellan.

Section VI.1

Optical Performance of the GWFS and Science Optics

This document will be available at the CDR.

Section VI.2

Buckling Analysis of the MOS and Camera Sections

This document will be available at the CDR.

Section VI.3

Lens 6 Analysis

This document will be available at the CDR.

SMITHSONIAN ASTROPHYSICAL OBSERVATORY **Central Engineering**

MEMORANDUM

MMIRS LENS 1 ANALYSIS

To: George Nystrom
From: Henry Bergner
Date: December 17, 2004
CC: John Boczenowski, Lester Cohen, Dan Fabricant, Bob Fata, Justin Holwell, Paul Martini, Ken McCracken, Brian McLeod, Tim Norton, Sang Park
File: c:\bergner\mmirs\lens01\lens01.wpd

Summary:

Stress in MMIRS lens 1 was determined considering the effects of pressure, temperature, lens seating, and friction. The highest stress in the lens was found to be 844 PSI that occurs at the center of the lens. This stress is due primarily to the radial thermal gradient.

Stress at the edge of the lens was found to be dependent upon friction and how the lens seats onto the housing. The maximum edge stress was determined to be 592 PSI.

The current material for lens 1 is calcium fluoride (CaF). This material is notorious for unpredictable failure modes at the stress levels reported here. Due to the "high" stresses from thermal effects and the fundamental uncertainties occurring when the lens seats, it is recommended that lens 1 should instead be constructed from fused silica.

Overview:

The purpose of this report is to determine what stress will be present in the MMIRS lens 1 when the instrument is operating. Lens 1 is unique in many respects and so the analysis must provide basic stress information to cover the unique requirements. First, lens 1 is the only lens in the system that seals outside pressure from the MOS vacuum vessel. Second, the outside pressure can be 14.7 PSI at sea level or 10.7 PSI on the mountain. The seal for the MOS vacuum vessel over this pressure range is accomplished with an o-ring seal. Third, the design baseline calls for the o-ring / housing seating loads to be as close to 85% / 15% as practical. Fourth, because the center of the lens sees more of the cold interior of the instrument than the lens edge, there is a steady state 10 degree C temperature gradient from the center to the lens OD. Fifth, the lens housing will have some flatness tolerance where the lens registrates axially on the housing. The contact areas of the lens on the housing greatly influence the lens stress distribution. Other issues, such as the effect of where the lens touches the housing radially and whether or not friction contributes to the stress in the optic, are other topics considered in this memo.

In the process of understanding the lens stress, three areas emerged as the most critical. The edge area near the OD on the bottom (vacuum) side where the pressure load is reacted produced critical stress. The bottom center of the optic and the internal center of the optic also produced areas of critical stress. Throughout this memo "stress" refers to the maximum principle stress. Maximum principle stress that exceeds the allowable value is a common failure mode for brittle materials.

Analysis Details:

Table 1 lists the most important load cases run on lens 1. The lens stress is fundamentally determined by the superposition of stress from o-ring loads (load case 1), seating loads on the steel housing (load cases 2-6), and thermal loads (load cases 7-9). Obtaining actual lens stress from Table 1 must first resolve the following questions: How is the load split between the o-ring and the housing? How exactly does the lens seat onto the housing? What role does friction play?

Table 1. Summary of FEM Load Cases Run on Lens 1

load case	description	stress, PSI		
		max bottom edge	bottom center	internal center
1	14.7 PSI on outside of lens, supported 360 degrees on o-ring	117	52	33
2	14.7 PSI on outside of lens, supported at two points on a diameter	7,150	220	165
3	14.7 PSI on outside of lens, supported by sine 2 theta without friction at minimum diameter contact area	495	228	23
4	14.7 PSI on outside of lens, supported by sine 2 theta with maximum friction at minimum diameter contact area	629	124	144
5	14.7 PSI on outside of lens, supported by sine 2 theta without friction at maximum diameter contact area	792	244	~0
6	14.7 PSI on outside of lens, supported by sine 2 theta with maximum friction at maximum diameter contact area	986	134	4
7	thermal gradient of +10 degrees C from lens center to OD without friction	~0	148	817
8	thermal gradient of +10 degrees C from lens center to OD, supported by sine 2 theta with maximum friction	5,220	735	987
9	thermal gradient of +10 degrees C from lens inner surface to outer surface	~0	~0	~0

The load split between the o-ring and the housing has two values: One at 14.7 PSI (sea level) and 10.7 PSI (on the mountain). Also, our maximum o-ring / housing load split is 85% / 15%. This load split must occur at 10.7 PSI. If the 85% / 15% occurred at 14.7 PSI, the housing would offload on the mountain to decrease housing seat load to something less than 15%. On the mountain total stress may be calculated from the following:

[total 10.7 PSI stress] = [o-ring unit stress]*0.85*10.7/14.7
+ [housing unit stress]*0.15*10.7/14.7
+ [thermal unit stress from o-ring]*0.85
+ [thermal unit stress from housing @10.7 PSI]*0.15

Equation 1.

For the total stress at 14.7 PSI, the o-ring / housing load split is calculated from knowing the o-ring load won't increase (since it's bottomed out already at 10.7 PSI). Its ratio at 14.7 PSI is:

0.85*10.7/14.7 or 62%

This leaves the remainder of 38% load coming from the housing stress. The sea level total stress may be calculated from the following:

[total 14.7 PSI stress] = [o-ring unit stress]*0.62
+ [housing unit stress]*0.38
+ [thermal unit stress from o-ring]*0.62
+ [thermal unit stress from housing @14.7 PSI]*0.38

Equation 2.

Next, we relate "o-ring unit stress", "housing unit stress", and "thermal unit stress" values from the above equations to specific load cases from Table 1. The simplest relationship is the o-ring unit stresses. The o-ring unit stresses are simply the values directly from load case 1 of Table 1.

Housing unit stresses are calculated from load cases 2-6. Load case 2 represents an extreme stress state with the lens supported at two points 180 degrees apart at the edge of the lens. The peak to valley deflection at the edge of the lens for this load case was 0.00075 inches. Since our flatness machining tolerance is between 0.0003 and 0.0005 inches, the lens housing does not allow this extreme load condition to actually exist. Load cases 3-6 deal with a more realistic scenario. By assuming some small tolerance exists in the lens, we will use the higher housing flatness tolerance of 0.0005 inches to generate boundary condition assumptions for load cases 3-6. Chart 1 shows the worst case machining tolerance for the lens housing: It assumes the 0.0005 inch tolerance follows a sine 2 theta variation around the support edge of the lens. This produces two contact areas about 180 degrees apart with the lens gapping off the housing between the contact areas. This edge behavior is similar for load cases 3-6. Figure 1 shows lens 1 deflection, also typical of load cases 3-6.

Load cases 3,4 to 5,6 show the effect of radial contact location on the stress. These load cases were run because the lens rests on a 0.200 inch wide flat of the housing. Under pressure load, line contact can take place at the inside or outside diameter of the flat, depending on the relative deflected angle of the lens vs the housing. Other modeling that included the housing has shown that the housing has a tendency to rotate "out from under" the lens. Because of this, we select load cases 5 and 6 for further consideration. Load cases 5,6 show the effect of friction on the lens stress. Since the effect of friction is relatively low, we further consider the "worst case" load case 6 to represent the "housing unit stress".

Chart 1. Housing Tolerance with FEM Contact / Gap Areas

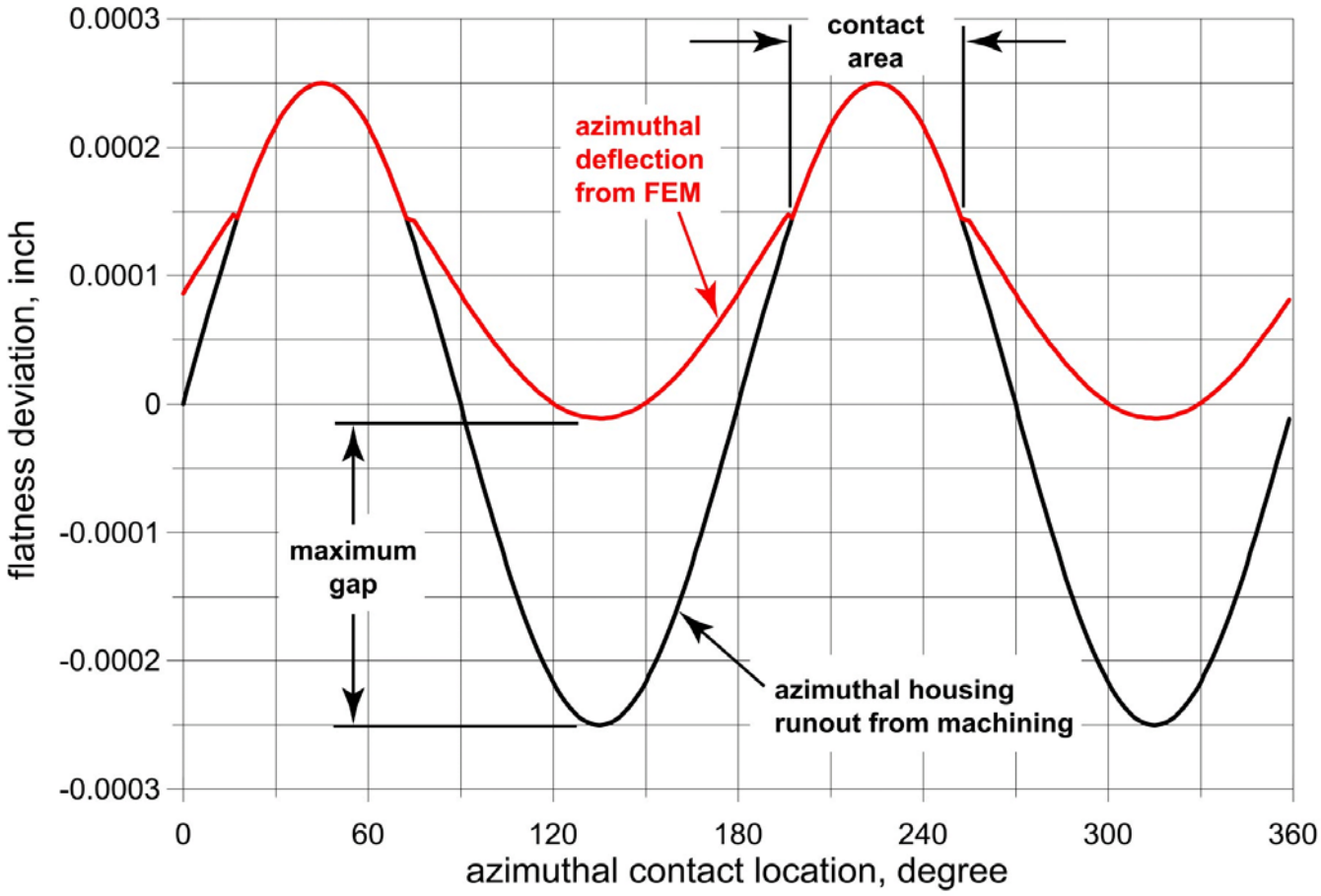

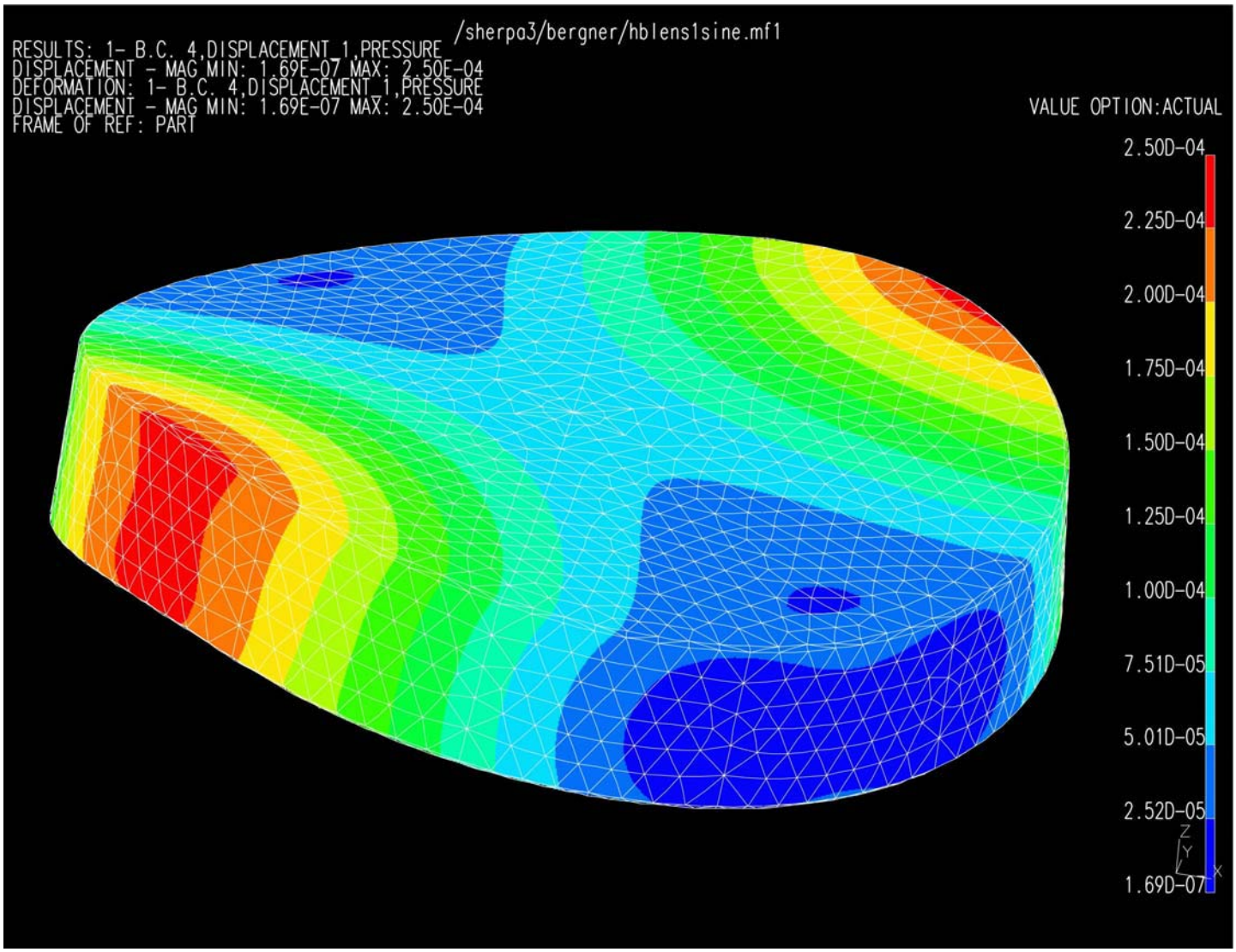

Figure 1. Typical MMIRS Lens 1
FEM Mesh and Deflected Shape with Pressure Load

Thermal unit stresses are derived from load cases 7-9. For "thermal unit stress from o-ring", we assume the o-ring contributes negligible friction and so we use load case 7 directly. Load case 8 assumes maximum friction by pinning the lens to a rigid steel housing along the contact area shown in Chart 1. Obviously friction plays a major role at the edge of the lens, being essentially stress free without friction (load case 7) then generating 5,220 PSI with maximum friction. To properly derive

stress at the edge of the lens, we need to determine if and how much the lens slips. This is determined by comparing the available friction to the actual load in the model. The stress may then be scaled by this ratio. The available friction load is given by:

$$S = P\pi r^2 \mu$$

where P is the pressure (10.7 or 14.7 PSI), r is the seal radius (4.37 inches), and is the coefficient of static friction (0.3). For 10.7 PSI, the available friction force is 193 pounds and for 14.7 PSI the available friction force is 265 pounds. For the load case 8 the friction load present at the boundary of lens 1 was 3,642 pounds. Two things become obvious: The lens will slip when it is exposed to the temperature gradient, and the stress will be greatly reduced at the edge from the load case 8 values. The resulting thermal unit stresses from housing were derived by the ratio of load case 7 (the slip) and 8 (the remaining available friction). Note that stress due the axial thermal gradients (load case 9) are heretofore neglected. Table 2 presents the derived unit load stresses.

Table 2. Derived Unit Stress Summary from Table 1

description	stress, PSI		
	max bottom edge	bottom center	internal center
o-ring unit stress	117	52	33
housing unit stress	986	134	4
thermal unit stress from o-ring	~0	148	817
thermal unit stress from housing @10.7 PSI	277	179	826
thermal unit stress from housing @14.7 PSI	380	190	829

Operational stress in lens 1 can now be determined by combining Equations 1 and 2 with the unit load cases listed in Table 2. The results of these calculations are listed in Table 3.

Table 3. Total Stress in Lens 1

description	stress, PSI		
	max bottom edge	bottom center	internal center
total stress @10.7 PSI	222	199	839
total stress @14.7 PSI	592	247	844

References:

1. SAO Master Series archive file, \\farpoint\hbergner\ideasbackup\hblens1sine.arc, dated December 17, 2004.

SMITHSONIAN ASTROPHYSICAL OBSERVATORY **Central Engineering**

MEMORANDUM

MMIRS RADIAL LENS MOUNT SIZING
UPDATED 11/08/2004 FOR NYLON

To: George Nystrom
From: Henry Bergner
Date: November 8, 2004
CC: John Boczenowski, Lester Cohen, Dan Fabricant, Bob Fata, Justin Holwell, Paul Martini, Ken McCracken, Brian McLeod, Tim Norton, Sang Park
File: c:\bergner\mmirs\celldiameter\celldiameter11082004.wpd

Scope:

Lenses 3-14 of the MMIRS optical design are to be radially supported on three nylon pads. Each pad is spaced at 120 degrees with two of the pads hard mounted and the third pad being spring loaded. This memo computes the required warm (room temperature) diameters for the nylon pads and the aluminum supports such that the lens-pad and pad-support diameters match exactly when cold (77 degrees K). The nylon pad thicknesses were sized to match the lens-pad assembly coefficient of thermal expansion (CTE) to the bezel/support CTE of aluminum. In theory, this provides lens centration at warm and cold operational temperatures.

The warm nylon pad thickness ranged from 0.100 to 0.601 inches. Although the nylon was sized to provide warm centration from a CTE standpoint, the warm diametral mismatch causes the thicker nylon pads to behave like leaf springs between the lens and the aluminum support. The thicker nylon pads may be slotted so they conform better to their mating parts at warm temperature.

Discussion:

The geometry and materials for the lenses were obtained from Reference 1, except that all cell / support material are aluminum. The lens geometries, material, and cell / support pad materials are listed in Table 1. CTE properties for the materials were obtained from LAE values, NIST values, publications in process, or vendor data sheets. The CTEs used in the analysis are listed in Table 2.

Table 1. Cold Lens Geometry and Cell / Support Pad Materials

lens number	lens properties			cell / support pad material
	cold diameter, mm	cold diameter, inch	material	
3	148.900	5.862	CAF2	Aluminum
4	100.000	3.937	CAF2	
5	122.770	4.833	BAF2	
6	139.700	5.500	ZNSE	
7	141.500	5.571	FQTZ	
8	142.300	5.602	CAF2	
9	163.100	6.421	CAF2	
10	159.600	6.283	S-FTM16	
11	161.700	6.366	CAF2	
12	137.000	5.394	BAF2	
13	116.500	4.587	CAF2	
14	84.300	3.319	S-FTM16	

Table 2. Material Thermal Properties

material	CTE value, per degree F	source / comment
BAF2	8.1792E-06	LAE value integrated from 293 to 77K
CAF2	7.7910E-06	LAE value integrated from 293 to 77K
FQTZ	1.5000E-07	Vendor data 0 to -50 C (32 to -58 F)
S-FTM16	4.2000E-06	To be published integrated from 24.85 to -196.15 C (76.73 to 321.1 F)
ZNSE	2.9790E-06	LAE value integrated from 293 to 77K
Aluminum	9.9820E-06	LAE value integrated from 293 to 77K
nylon	5.7022E-05	From NIST data 293 to 80K

The thickness of the nylon pad is sized such that the lens-pad assembly has the same CTE as the aluminum support and cell. For this condition to be met, the following equation applies:

$$\alpha_a \left(r_l + \Delta r_t \right) = r_l \alpha_l + \Delta r_t \alpha_t$$

where $_a$ is the CTE of aluminum, r_l is the lens radius, r_t is the thickness of the nylon pad, $_l$ is the lens CTE, and $_t$ is the nylon CTE. Solving for r_t produces the following:

$$\Delta r_t = r_l \left(\frac{\alpha_a - \alpha_r}{\alpha_t - \alpha_a} \right)$$

The spreadsheet of Reference 2 was used to calculate the cold r_t values listed in Table 2. Table 2 also lists the warm r_t values, lens OD, nylon ID and OD, and aluminum support ID.

During cold operation, the lens OD matches the nylon ID and the nylon OD matches the aluminum support ID exactly. However, when the assembly is warm, the fit up is a function of how well the warm lens OD matches the warm nylon ID and how well the warm nylon OD matches the warm support ID. Table 3 suggests that when warm, the nylon contacts the lens at its center (since the warm lens OD is always less than the warm nylon ID). It also suggests the nylon pad contacts the aluminum support at the edges (since the warm nylon OD is always greater than the warm support ID. This configuration causes the nylon to behave like a leaf spring between the lens and the support pad. This is not a problem on the thinner (~0.200 inches or less) nylon pieces because they will compress under the spring preloads. The thicker nylon pieces should be slotted axially to relieve the warm leaf spring effect of the nylon.

Table 3. Computed Geometry Requirements, Units Inch

lens number	cold nylon thickness	warm nylon thickness	warm lens OD	warm nylon ID	warm nylon OD	warm support pad ID
3	0.146	0.149	5.880	5.993	6.291	6.178
4	0.098	0.100	3.949	4.025	4.225	4.149
5	0.100	0.102	4.849	4.942	5.146	5.054
6	0.417	0.426	5.507	5.623	6.476	6.359
7	0.601	0.615	5.571	5.696	6.925	6.800
8	0.139	0.142	5.620	5.728	6.012	5.904
9	0.160	0.163	6.441	6.565	6.891	6.767
10	0.396	0.405	6.294	6.424	7.235	7.104
11	0.158	0.162	6.386	6.509	6.832	6.709
12	0.112	0.114	5.411	5.514	5.743	5.639
13	0.114	0.117	4.601	4.689	4.922	4.834
14	0.209	0.214	3.324	3.393	3.821	3.752

References:

1. SAO spread sheet, “MMIRS Preconstruction Optics Design”, dated November 5, 2004, by George Nystrom.

2. SAO spreadsheet, “celldiameter11082004.qpw”, dated November 8, 2004, by Henry Bergner.

SMITHSONIAN ASTROPHYSICAL OBSERVATORY **Central Engineering**

MEMORANDUM

THERMAL GRADIENT STRESS SURVEY FOR MMIRS LENSES 3-14, REVISION B

To: George Nystrom
From: Henry Bergner
Date: June 16, 2004
CC: Lester Cohen, Bruce Dias, Dan Fabricant, Bob Fata, Brian McLeod, Tim Norton, Sang Park
File: c:\bergner\mmirs\lenssurvey\lenssurveyrevb.wpd

Scope:

This survey was conducted to determine the sensitivity of the MMIRS lenses to thermal gradients. MMIRS lenses 3-14 were subject to unit temperature changes over their radial, axial, and diametral dimensions. For this survey, these were the only loads applied. In general, the radial temperature gradients produced the highest stress. The axial gradients produced about one tenth of the radial gradient stress. The diametral gradients produced about on tenth of the axial gradient stress. The CAF2 lenses produced the highest stress. Based on an allowable max / min principal stress of ±200 PSI, the smallest radial temperature change allowed was determined to be 1.39 degrees C on lens 4. These results must be applied to the thermal design of the MMIRS instrument.

Discussion:

The geometry and materials for the lenses were obtained from Reference 1. Elastic and thermal properties for the materials were obtained from vendor data sheets. The CTEs used in the analysis were chosen to obtain the highest stress for the cool down process: In all cases, this required using the room temperature CTE.

Each lens model was generated using a standard 4,000 element solid model that was modified to the particular diameters and curvatures of the optical prescription using the software of Reference 2. A typical finite element mesh is shown in Figure 1. The particular mesh shown is for lens 3.

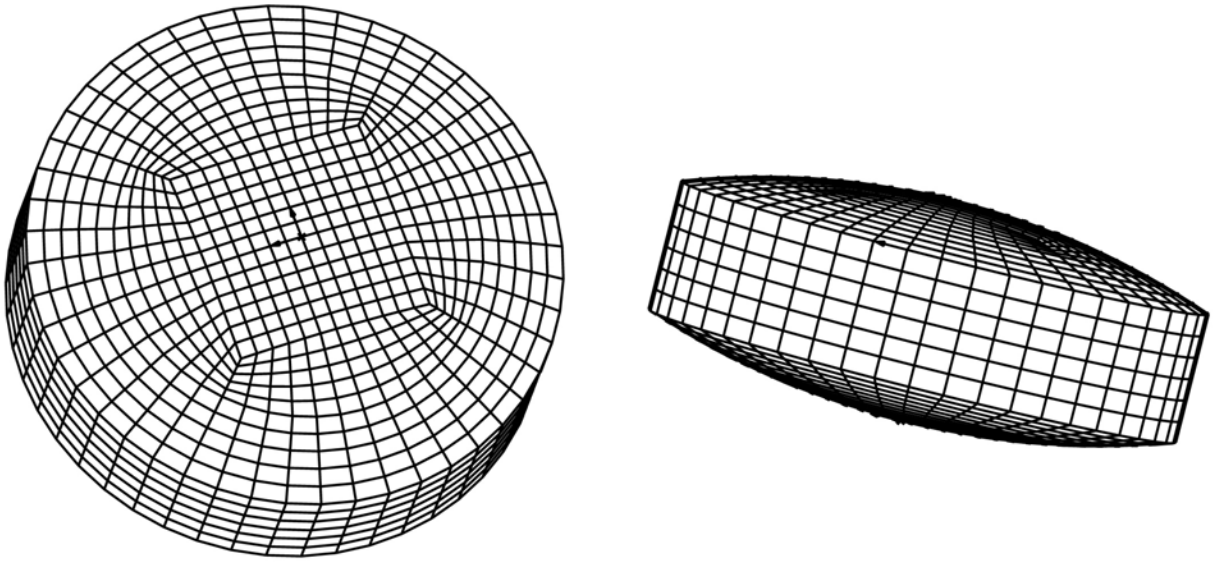

Figure 1. Typical Lens Finite Element Mesh

Radial, axial, and diametral thermal gradients were then applied to each lens. A typical stress distribution resulting from a 1.0 degree C radial temperature gradient is shown in Figure 2. The figure shows the maximum principal stress in PSI of the lens 4 half model. The resulting maximum and minimum principal stresses for each unit load case is listed in Appendix A for completeness. All models and results are in the I-DEAS archive file of Reference 3.

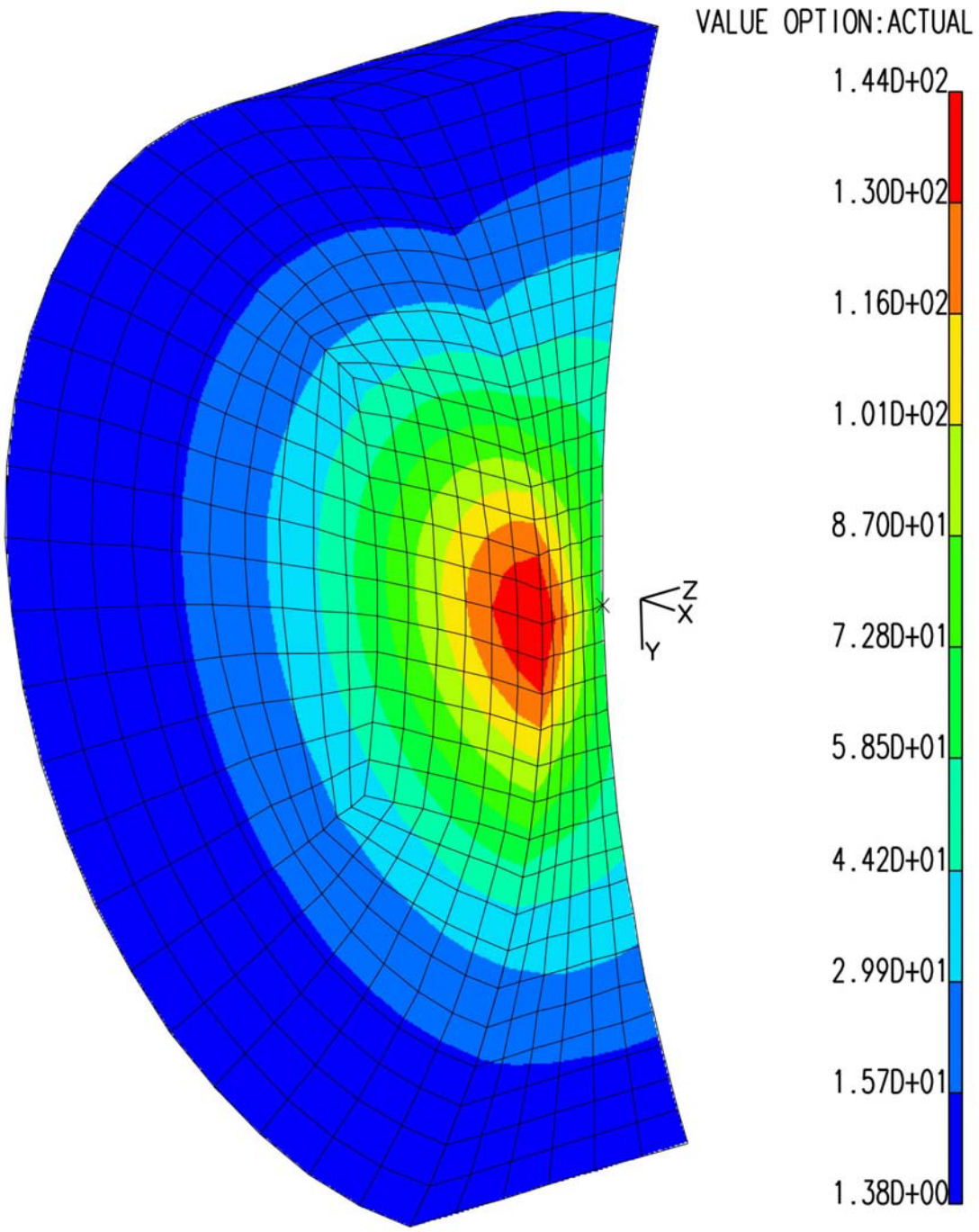

Figure 2. Typical First Principal Stress Distribution (units PSI) Due to a 1.0 Degree C Radial Temperature Gradient

Table 1 shows the maximum temperature gradient allowed over each lens using an allowable maximum or minimum principal stress of ±200 PSI. Table 1 clearly shows the smallest temperature gradients allowable are in the radial direction: Most lenses allow gradients of less than 4.0 degrees C with the smallest gradient of 1.39 degrees C occurring at lens 4. By inspection it is obvious that temperature gradients in the axial and diametral directions produce large allowable temperature gradients: Therefore it is unlikely that thermal gradients in these directions would cause any excessive stress in the lenses.

Table 1. Allowable Temperature Gradients (Degree C) for MMIRS Lenses

	allowable temperature		
lens number	radial gradient	axial gradient	dimetral gradient
3	2.18	46.30	222.22
4	1.39	48.31	555.56
5	3.97	42.74	370.37
6	4.83	222.22	1111.11
7	92.59	2777.78	22222.22
8	2.78	42.74	555.56
9	2.58	44.44	370.37
10	3.58	113.38	1234.57
11	2.47	44.44	358.42
12	3.83	48.31	483.09
13	2.22	46.30	252.53
14	5.05	156.49	1221.00

References:

1. SAO drawing, “MMIRS Optical Layout”, number MMIRS-100 revision 1, dated March 6, 2004.

2. SAO Visual C++ software, “LensMaker”, dated April 29, 2004, by Vladimir Kradinov.

3. SAO Master Series archive file, c:\bergner\mmirs\lenssurvey\analysis\hbmmirslens.arc, dated May 6, 2004.

Appendix A. Lens Principal Stress from a Unit Load 1.0 Degree C Temperature Gradient

lens number	radial stress, psi		axial stress, psi		diametral stress, psi	
	max	min	max	min	max	min
3	91.800	-72.000	4.320	-4.320	0.900	-0.900
4	144.000	-82.800	4.140	-3.600	0.360	-0.360
5	50.400	-46.800	4.680	-3.780	0.540	-0.540
6	41.400	-19.800	0.900	-0.540	0.180	-0.180
7	2.160	-1.800	0.072	-0.072	0.009	-0.009
8	70.200	-72.000	4.680	-4.320	0.360	-0.360
9	77.400	-72.000	4.320	-4.500	0.540	-0.540
10	55.800	-32.400	1.764	-1.710	0.162	-0.162
11	81.000	-72.000	4.320	-4.500	0.558	-0.558
12	52.200	-50.400	3.780	-4.140	0.414	-0.414
13	90.000	-75.600	4.140	-4.320	0.792	-0.792
14	39.600	-28.800	1.278	-1.278	0.164	-0.164

SMITHSONIAN ASTROPHYSICAL OBSERVATORY **Central Engineering**

MEMORANDUM

MAGELLAN LIFT CART WELDMENT ANALYSIS

To: Mark Ordway
From: Henry Bergner
Date: April 28, 2005
CC: John Boczenowski, Lester Cohen, Roger Eng, Dan Fabricant, Bob Fata, Justin Holwell, Brian McLeod, Ken McCracken, Paul Martini, Mark Mueller, Tim Norton, George Nystrom, Andy Szentgyorgyi
File: c:\bergner\liftcart\weldmentreport\liftcartweld.wpd

Scope:

The Magellan lift cart provides precise positioning and lift capabilities for the CIR Adapter, Wide Field Corrector, Magellan Top Box, and MMIRS. This report is the first in a series to provide analysis of the complete lift cart system. This report specifically addresses issues relating to the structural integrity of the lift cart weldment. These issues include stress in cart frame members, weld stress, bolt joint stress, and deflection analysis.

Load cases analyzed included Z gravity and lateral (X and Y) load cases for three configurations: lift cart on wheels, lift cart on jack screws, and lift cart hoist. All load conditions required a factor of safety of 5.0 and a load factor of 2.0. For these requirements, all structural margins of safety were found to be acceptable. The heaviest lift cart configuration analyzed was 9,990 pounds that included the MMIRS instrument, MMIRS stand, lift cart tray, and lift cart. The MMIRS instrument jacked to the maximum lift stroke produced many of the highest stress and load conditions.

Modeling Details:

The solid model for the lift cart is shown in Figure 1. The figure shows the complete cart including motor, shafts, and lift hardware. The tray is shown at the floor position while two struts are shown at the maximum lift stroke for illustration. Figure 1 does not include the instrument or the instrument stand.

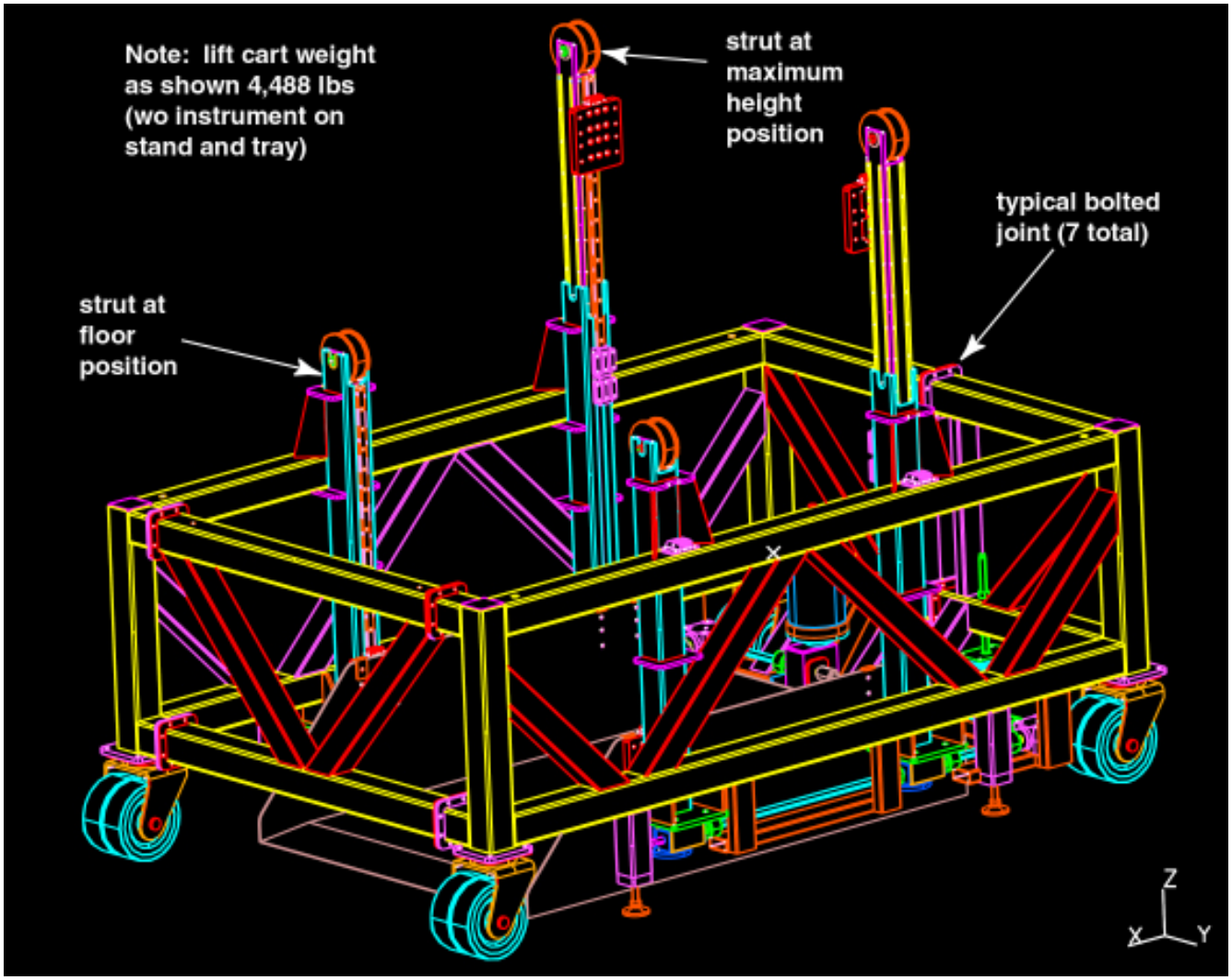

Figure 1. Magellan Lift Cart System

The lift cart FEA (retrievable as Reference 1) is shown in Figure 2. Figure 2 shows the critical stress configuration with the MMIRS instrument at the maximum lift stroke. This model geometry detailed the A500 Grade B steel members and the A36 steel plate supporting the motor. Features not clearly shown in the figure include details of the seven bolted joints and short, connecting beam elements that represent the weld joints. The MMIRS instrument, stand, and tray were represented as lumped masses. A very detailed model of the vertical split tubes is discussed later in this report.

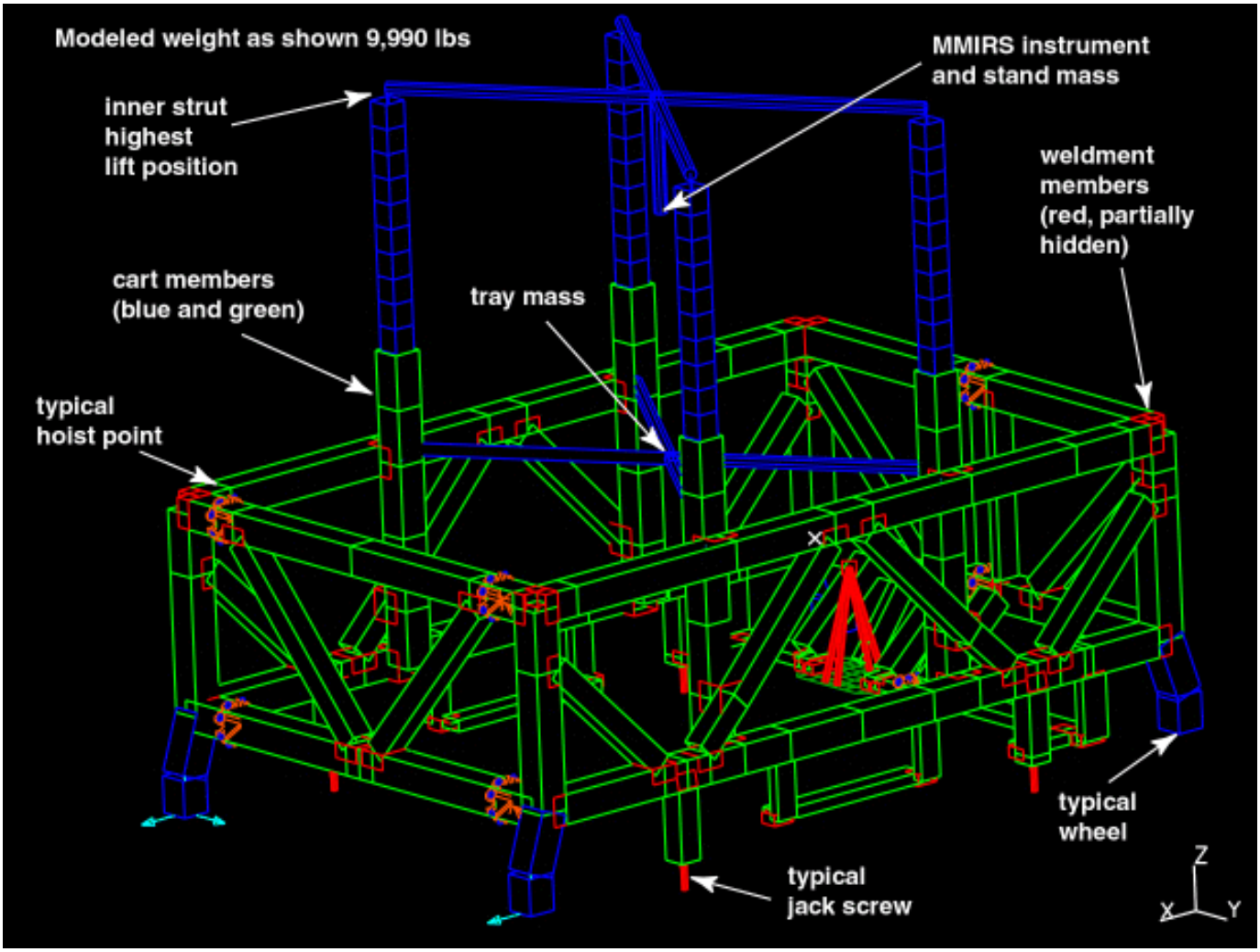

Figure 2. FEA for Magellan Lift Cart System

Table 1 lists the lift cart weights used in the analysis. The MMIRS instrument weight was considered the heaviest version possible for the instrument. The weights for the MMIRS stand and cart tray were estimated. The other weights listed in the table are actuals or very close to actual weights. Note all analysis used the full loaded weight of 9,990 lbs except for the hoist load case: Hoisting is not conducted with the 5,002 lb instrument weight or the 500 lb stand weight.

Table 1. Lift Cart Weights

Cart Item	Weight, pound
MMIRS instrument	5,002
MMIRS stand	500
cart tray	500
steel tubing and plates	2,308
lift hardware	320
gearboxs (2 total)	100
jacks (4 total)	220
motor and reducer gearbox	200
wheels (4 total)	840
total modeled weight, all load conditions except hoisting	9,990
total modeled weight, hoisting without instrument and stand	4,488

Load Cases Analyzed:

Table 2 shows the loads applied for each load configuration and direction. The table shows three configurations analyzed: On wheels, on jack screws, and hoisting. "Vertical -Z" loads have only Z load vectors present. All lateral load cases have a combined vertical load (LF 1.0) and a lateral load (LF 2.0). The FS applies the factor of safety to load 1 and load 2. Total vector load applied to the model is given by:

total load = FS * (load 1 * LF1 + load 2 * LF2).

Table 2. Load Cases Evaluated

load case	configuration	load description	FS	load 1	LF 1	load 2	LF 2
1	on wheels	vertical -Z	5.0	-1.0GZ	2.0	0	0
2		lateral +X	5.0	-1.0GZ	1.0	+0.1GX	2.0
3		lateral -X	5.0	-1.0GZ	1.0	-0.1GX	2.0
4		lateral +Y	5.0	-1.0GZ	1.0	+0.1GY	2.0
5		lateral -Y	5.0	-1.0GZ	1.0	-0.1GY	2.0
6	on jack screws	vertical -Z	5.0	-1.0GZ	2.0	0	0
7		lateral +X	5.0	-1.0GZ	1.0	+0.1GX	2.0
8		lateral -X	5.0	-1.0GZ	1.0	-0.1GX	2.0
9		lateral +Y	5.0	-1.0GZ	1.0	+0.1GY	2.0
10		lateral -Y	5.0	-1.0GZ	1.0	-0.1GY	2.0
11	hoisting	vertical -Z	5.0	-1.0GZ	2.0	0	0

A typical deflected shape and stress contour display is shown in Figure 3. The specific load case shown is load case 1. This load case is effectively 10 G's in the -Z direction. The maximum beam stress shown is 25.6 KSI.

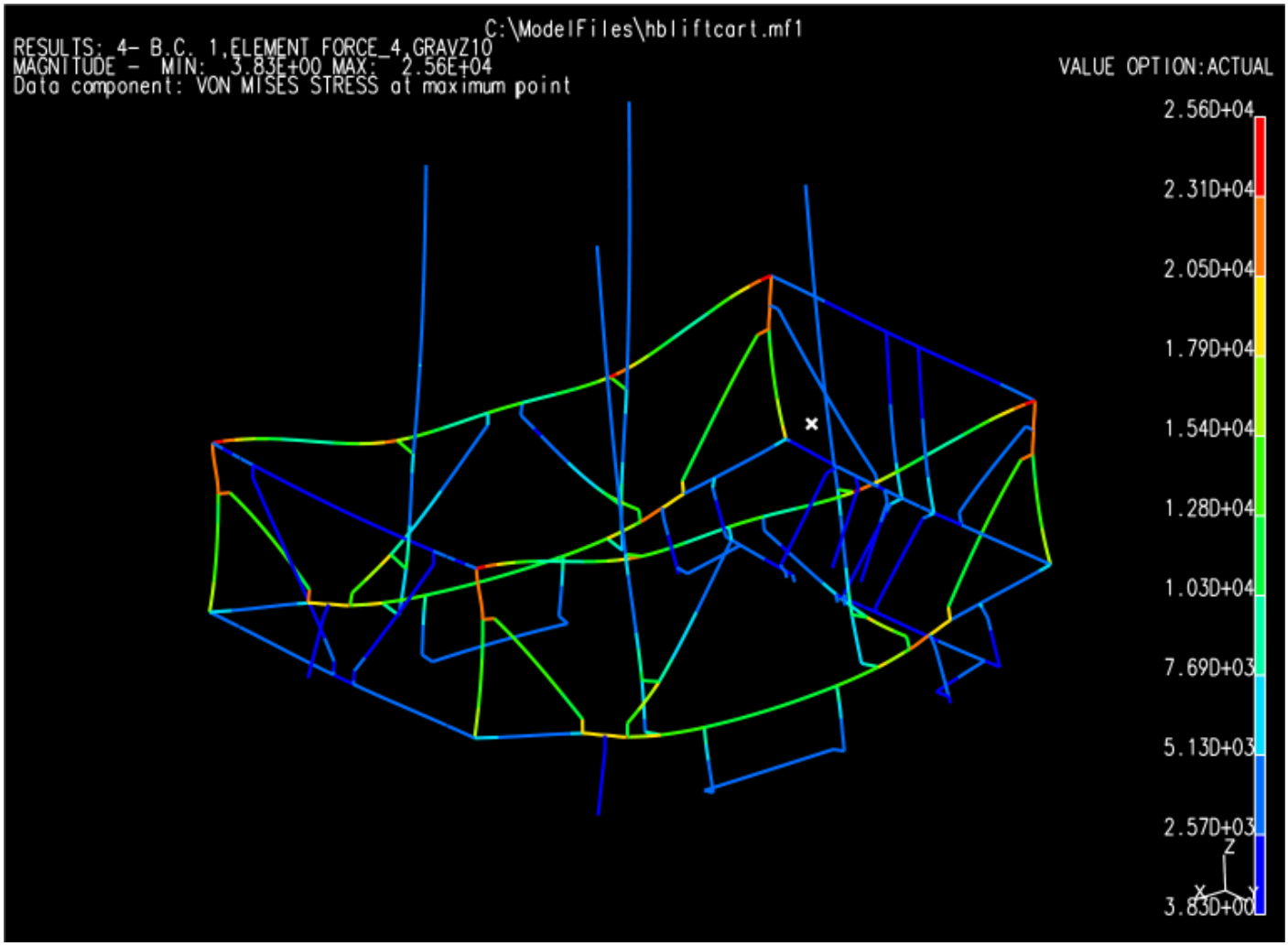

Figure 3. Typical Deflected Shape and Beam Stress for Load Case 1, -10GZ Total Load Vector

The maximum beam stress, bolt load, shell stress, and maximum model deflection for all load cases are summarized in Table 3. The beam stress listed is the maximum of beam and weld element stress: Typically, weld stress was about 10% higher than the maximum beam stress. The most critical stress was from load case 1 at 25.6 KSI. Maximum axial and shear bolt loads listed are the individual maximum bolt loads from 7 bolt patterns. Each bolt pattern typically consisted of 8 bolts. The most critical bolt load was from load case 4 at 3,290 pounds axial and 587 pounds shear. The only shell elements in the model were located under the motor. As listed, these stresses were quite low. The maximum deflection for all load cases was from load cases 9 and 10 at 0.93 inches. Note that these deflections "include" the built in factor of safety and load factors. Under normal operating conditions, the maximum deflection would be less than 0.1 inches.

Table 3. Analysis Stress, Load, and Deflection Results

load case	load description	beam stress, KSI	maximum axial bolt load, lb	maximum shear bolt load, lb	shell stress under motor, KSI	maximum deflection, inch
1	vertical -Z	25.6	867	400	3.3	0.18
2	lateral +X	16.6	370	114	2.6	0.32
3	lateral -X	15.4	549	315	1.1	0.39
4	lateral +Y	25.0	3,290	587	2.3	0.73
5	lateral -Y	24.7	3,080	623	1.8	0.72
6	vertical -Z	25.3	643	324	3.5	0.10
7	lateral +X	19.4	335	169	2.8	0.42
8	lateral -X	17.5	352	156	1.1	0.43
9	lateral +Y	20.0	2,710	608	2.7	0.93
10	lateral -Y	19.7	2,680	607	3.1	0.93
11	vertical -Z	15.4	701	151	3.4	NA

Margins of Safety:

The maximum allowable weld stress is equal to the base material (A500, Grade B YS 46 KSI): The allowable weld stress is therefore 46 KSI. The margin of safety for members and welds is therefore +0.80.

Table 4 lists the torque requirements and margins of safety for the critical bolt loads in Table 3. Bolt calculations were made using software of Reference 2. The calculations assume the bolt size of ½ - 13 UNC. The bolt type used is an alloy steel Unbrako with a breaking strength of 27,000 pounds. The torque is based on the Unbrako catalog specification that loads the bolt to about 70% of its rated strength. The thread engagement not computed because high strength nuts are using for all bolted joints. The joint preload and the coefficient of static friction of the joint (0.3) are then used to calculate the margin of safety. The margin of safety refers to joint slipping. Note that ultimate joint failure would exceed this by a significant, but difficult to compute, factor.

Table 4. Fastener Torque and Thread Engagement Requirements

external load, lb		torque, in-lb	joint preload, lb	margin of safety
axial	shear			
3,290	587	1,850	18,500	2.5

Detailed Tube Stress:

The 5 X 5 inch vertical square tubes support the inner 4 X 4 inch tubes. The jack screw / chain assembly allows for the maximum extension of the inner tube moving inside the outer tube. The inner tube is supported or shimmed inside the outer tube by 8 bearing surfaces, 2 on each face. In order for the outer tube to allow the rails on the inner tube to slide, the outer 5 X 5 tubes were required to be split on the internal face as shown in Figure 1. This geometry allows for a high stress to occur when the inner tube tries to "pry" out of the outer tube on the slotted side at full extension with the MMIRS instrument for load cases 4 and 5 (+/- Y lateral). This localized stress was quantified by detailing one of the four vertical inner / outer tube assemblies. Such detailing included not only the detailed tube geometry, but also modeling the 8 bearing surfaces with nonlinear gap elements. The analysis results for this load case is shown in Figure 4.

The maximum stress for this load case is 42.5 KSI. Based on the yield stress of 46 KSI for A500, Grade B, the margin of safety for this load case is +0.08. This margin of safety is acceptable. The model is retrievable at Reference 1.

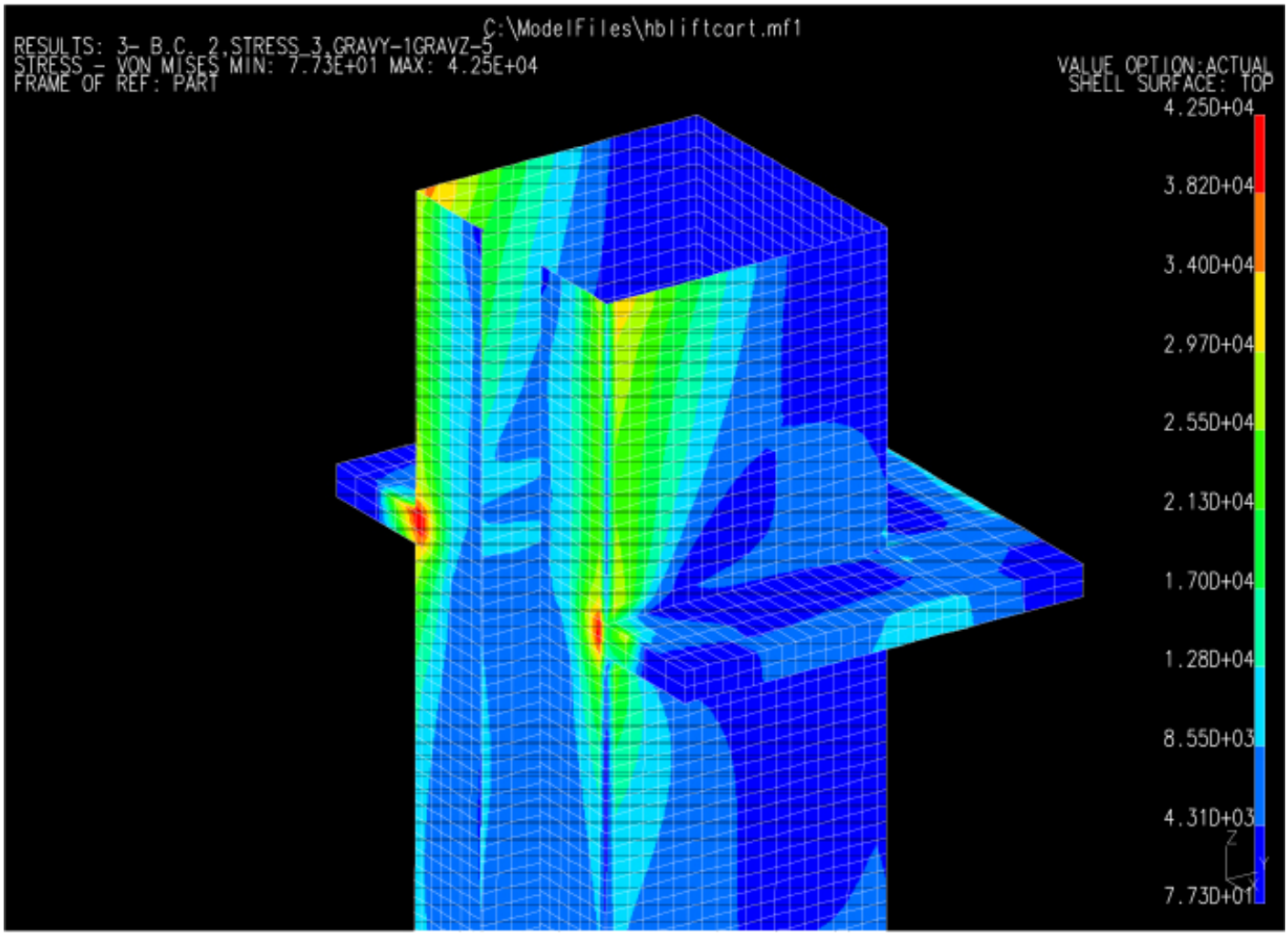

Figure 4. Detailed Pry Out Stress from +/- Y Loads

References:

1. Ideas Archive File, “hbliftcart.arc”, dated April 28, 2005, by Henry Bergner

2. Software “*boltcant*”, version 11/18/2003, by Henry Bergner.

Section VII.

MMIRS Thermal Analysis

1. MMIRS Design Compliance Matrix - Thermal
2. MOS Steady State Analysis
3. MOS Transient Analysis
4. MOS Thermal Finish Analysis Report
5. Camera Steady State and Transient Analysis
6. Camera Thermal Finish Analysis Report
7. Camera-Detector Steady State and Transient Analysis
8. Temperature and Stress Distribution in Optics

Item No.	Document	Document No.	Document Section	Requirement	Compliance Status	Completed by
					Requirement Satisfied	
					Requirement Needs work	
					Requirement not satisfied	
Therm.1	F&P	S-MMIRS-200	141 Thermal Shielding	The MMIRS shall contain sufficient thermal shielding to minimize heat loading on the cryogenic systems.	MOS: Dewar assembly is covered in thermal blankets. There is a floating passive thermal shield. Guider baffles are covered in thermal blanket/low ε surface finishes Camera: A system thermal shield is covered in thermal blankets	SP
Therm.2	F&P	S-MMIRS-200	173 Thermal Cycle Optics	Thermal cycles of the instrument shall not degrade or destroy the optics and coatings.	MOS: The temperature gradients within Lens 1 and 2 will not exceed the allowable stress level during the cooling and warming period Camera: the rate of cooling and heating will be maintained less than 0.2deg-C/min not to exceed the allowable lens stress	SP
Therm.3	F&P	S-MMIRS-200	222 Science Array Controller Thermal Interface	The array controller, power supplies and associated analog electronics shall be enclosed in a	All control electronic components are enclosed in the rack enclosure.	SP

MMIRS Design Requirement Compliance Matrix

THERMAL DESIGN

				MMIRS thermal rack enclosure.		
Therm.4	F&P	S-MMIRS-200	243 GWFS Array Thermal Interface	The CCD array will be contained within a separate dewar and will be cooled with a thermoelectric cooler.	GWFS will be cooled using a thermoelectric cooler but may be cooled using a heat sink assembly with a fan	SP
Therm.5	F&P	S-MMIRS-200	246 GWFS Array Controller Thermal Interface	The array controller shall be cooled by the instrument cooling system.	Inside electronic rack	SP
Therm.6	F&P	S-MMIRS-200	320 Thermal Performance	Thermal gradients in the MMIRS optical bench shall be minimized to prevent degradation of image quality.	All lenses are within 80+/-3K once a thermal stabilization is established.	SP
Therm.7	F&P	S-MMIRS-200	351 Cryostat	The total time to pump and thermally cycle MMIRS shall not exceed one week, including one day for cold tests and one day for engineering when the instrument is warm.	Approximately 36 hours are required to cool the camera section at a cooling rate of 0.2deg-C/min at the optical bench. Also, approximately 36 hours are required to warm the camera section at a cooling rate of 0.2deg-C/min at the optical bench. 3 days for cooling and warm-	SP

					up, 1 day for cold test, 1 day for warm-test, <1 day for pump-down, and <1 day for re-press yields less than one week cycle time	
Therm.8	F&P	S-MMIRS-200	352 MOS Section	The total time to thermally cycle the MOS section (with the gate valve closed) and exchange all slit masks shall not exceed nine hours.	The thermal cycle of the MOS section may be completed in approximately 4.8 hours, excluding the time to change MOS slit plates, (0.33hr to boil off excess LN_2, 2.5 hrs to warm-up, then 2.0 hrs to cool to the observation temperature).	SP
Therm.9	F&P	S-MMIRS-200	353 Hold Time	The steady-state hold time of the MOS and Camera Dewars shall each be 30 hours	MOS: Based on 31 watts absorbed = 32 hours of hold time at 22 liters of LN2 Camera: Based on 35.6 watts absorbed = 63.6 hours of hold-time at +25°C ambient with 50 liters of LN_2.	SP
Therm.10	F&P	S-MMIRS-200	354 Thermal Stability	The science detector assembly shall be thermally coupled to the LN2-cooled worksurface to provide maximum stability without requiring active control of the detector temperature	No active thermal control during the science observation period	

				during science operations.		
Therm.11	F&P	S-MMIRS-200	355 Science Array Thermal Interface	The array's fanout board shall be thermally strapped to the cryo-worksurface, and it shall additionally be controlled with a heater and temperature sensor mounted on the fanout board. The maximum rate of temperature change for the detector during warm up and cool down shall not exceed 0.2 K/min. The detector must be the warmest part of the instrument during warmup to protect it from contamination.	Completed by design	SP
Therm.12	F&P	S-MMIRS-200	356 Autofill	MMIRS shall be equipped with an autofill system when not mounted on the telescope.	TBD	SP

Therm.13	F&P	S-MMIRS-200	**700 Environment Requirements** 710 Altitude Environment 711 Transportation Altitudes 712	 MMIRS shall be capable of being transported, stored, and operated at either the MMT or Magellan Clay telescopes. MMIRS shall be capable of being transported at any altitude between -200 feet and 10,000 feet by any transportation mode. MMIRS shall be capable of being transported by commercial jet with pressurized cargo compartments at altitudes up to 50,000 feet. MMIRS shall be capable of being	The thermal analysis was performed using the 10K feet altitude condition to satisfy the design requirements.	SP

			Storage Altitudes 713 Operation Altitudes	stored in or out of its shipping container at any altitude between -200 feet and 10,000 feet. MMIRS shall be capable of being operated at any altitude between -200 and 10,000 feet.		
Therm.14	F&P	S-MMIRS-200	**700 Environment Requirements** **720 Temperature Environment** 721 Operational Environment 722 Survival Environment	 MMIRS operational environment shall be limited to -15 to +40 °C. MMIRS shall be capable of surviving a temperature of -51 to +71 °C without damage per MIL-STD-810E.	The thermal analysis was performed using the +25C ambient temperature condition to satisfy the design requirements.	

			723 Transportation Environment	MMIRS shall be capable of withstanding a temperature of -51 to +71 °C during transport without damage.		
Therm.15	Component Spec. (MOS)	S-MMIRS-201	400 Temperature Range	Temperature range: a. First element follows ambient temperature: 313 to 258 degrees Kelvin (40 to -15 Celsius). b. Second element is 313 to 248 degrees Kelvin (40 to -25 Celsius).	Lens 1: less than +21deg-C steady state temperature at +25C Ambient Lens 2: Less than +19 deg-C at steady state temperature at +25C Ambient	SP
Therm.16	Component Spec. (MOS)	S-MMIRS-201	500 Guider/Wave front Sensor	The pickoff mirrors for the GWFS shall be mounted on a structural support attached to the cold plate, which will provide a conductive thermal path for the mirrors.	Completed by design	KM
Therm.17	Component Spec. (MOS)	S-MMIRS-201	600 Dekker Wheel	operating temperature of ≈ 80	Dekker wheel is predicted at 82K (-191°C)	SP

				to 140 degrees Kelvin.		
Therm.18	Component Spec. (MOS)	S-MMIRS-201	700 MOS Wheel	The slit masks must be thermally coupled to the slit wheel with their cold operating temperature < 120 degrees Kelvin with a maximum change during the night observing time of 10 degrees Kelvin.	MOS wheel is predicted at 82K (-191°C)	SP
Therm.19	Component Spec. (Camera)	S-MMIRS-202	7.0.5 Optics	Maximum cooling rate: 1 degree K per Minute	Cooling rate is limited to less than 0.2deg-C/min not to exceed the thermal gradient requirements in the lens	SP
Therm.20	Component Spec. (Camera)	S-MMIRS-202	8.0 Filter and Grism wheels	All optics must be thermally coupled to their respective wheels with their cold operating temperature at 80 degrees Kelvin +/- 2K	All Grism/Filter wheel components are less than 83K once the thermal stabilization is established.	SP
Therm.21	Component Spec. (Camera)	S-MMIRS-202	11.0 Cryogenic System	The Camera section shall be designed to provide a minimum hold time of 40hours once cooled and	Camera: Based on 35.6 watts absorbed = 63.6 hours of hold-time at +25°C ambient with 50 liters of LN_2.	SP

				topped off		
Therm.22	Component Spec. (Camera)	S-MMIRS-202	810 Cryogenic System	The LN2 fill and vent lines shall be designed to minimize thermal conduction to the camera vacuum enclosure.	Completed by Design	JH
Therm.23	Component Spec. (Camera)	S-MMIRS-202	810 Cryogenic System	The rate of temperature change of the optical bench during warm up and cool down shall be set by the detector's heating and cooling rate of 0.2 degrees Kelvin per minute.	Heating and cooling rate are limited to less than 0.2deg-C/min not to exceed the thermal gradient requirements in the lens	SP
Therm.24	Component Spec. (Camera)	S-MMIRS-202	810 Cryogenic System	A system of radiation shields shall be designed to minimize heat loss between the cold component and the surrounding vacuum enclosure. Their effectiveness must satisfy the requirements for hold time stated.	The system thermal shield is covered in thermal blankets	

Therm.25	Component Spec. (Camera)	S-MMIRS-202	810 Cryogenic System	A system of temperature sensors shall be placed to map the camera section's thermal behavior	MMIRS Temperature Sensing and Heating Requirements	
Therm.26	Component Spec. (Camera)	S-MMIRS-202	900 Vacuum System	The vacuum vessel shall be constructed of aluminum with its internal surface polished to 4-6 micro inch roughness.	Al Alloy, thermal surface specified.	

Harvard-Smithsonian Center for Astrophysics
Smithsonian Astrophysical Observatory
Central Engineering

Document No. MMIRS-SP032305A Rev A

To: George Nystrom
From: Sang Park (Thermal Engineer)
Date: 25 March 2005

CC: Brian McLeod, Paul Martini, Henry Bergner, Ken McCracken, Justin Holwell, Mike Burke, Tim Norton, John Boczenowski, Bill Podgorski

References:

1. MMIRS-SP012505A Rev A; Subject: MOS Operational Thermal Cycle Profile, From: S. Park, To: G. Nystrom, 07 February 2005
2. MMIRS-SP030405A Preliminary; Subject: MOS Section Thermal Surface Finishes, From: S. Park, To: G. Nystrom, 04 March 2005

Subject: MOS Operational Steady State Temperature

1. SUMMARY/INTRODUCTION

A thermal analysis was performed to characterize the steady state temperature of the MOS section during Science Observation. The MOS thermal design requirements are:

- MOS wheel temperature shall be maintained below 120K (-153°C) and stabilized within 10°C during the science observation period.
- Hold time greater than 30hours.
- Lens 1 & 2 temperature gradient requirements: TBD
- Time to change MOS slit plates not to exceed 9 hours (See Reference 1 for further details)

This analysis has shown that the steady state temperature of MOS wheel is predicted at 82K (-191°C). Also, the 10°C stabilization was satisfied with the current design and its results are presented in Reference 1. The average steady state temperatures of the lens #1 and #2 are predicted at 294K (21°C) and 291K (18°C), respectively.

The MOS LN_2 Dewar is sufficient to provide at least 30 hours of hold-time, a design requirement, when it is half filled or an equivalent of 22 liters of liquid Nitrogen. This analysis had calculated that 31 watts of thermal load was absorbed from the environment via the natural convection on the chamber outer wall surfaces and through the conductive heat transfer at the bulkhead mounting points. Based on only the environment thermal load, the current design will provide 32 hours of hold-time at +25°C ambient with 22 liters of LN_2.

The pickoff mirror assembly, optical baffles and the Wave-Front Sensor/Guider are also the parts of the MOS. However, their thermal performances are a subject of a separate report.

2. MOS THERMAL DESIGN

Shown in the Figures 1 thru 3 are the thermal design features that are relevant to this analysis. The MOS assembly includes as a part of the thermal design the following features:

a) LN_2 Dewar
b) Thermal baffle, floating shield
c) Cold-shields above the MOS and Dekker wheels
d) G-10 thermal isolation ring
e) Sapphire ball-bearings
f) Thermal surface treatments to enhance thermal radiation heat transfer *(thermal radiation surface properties will be presented further in Section 3.2 Material Properties and Reference 2. MOS Section Thermal Surface Finishes).*

The following paragraphs describe the details of the thermal features.

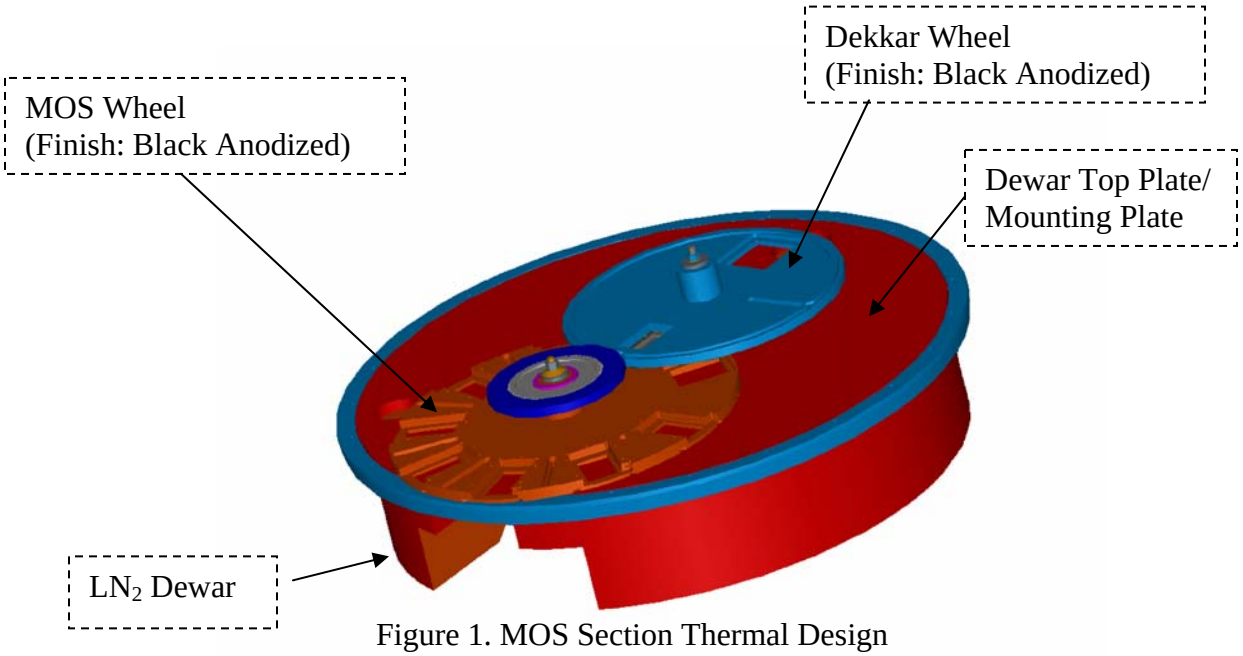

Figure 1. MOS Section Thermal Design
(G-10 Ring removed for clarity)

2.1. LN_2 Dewar

The MOS section LN_2 Dewar is constructed from Aluminum Alloy 6061-T6 with a 0.75" thick top plate also serving as a mounting platform for the MOS mechanisms and slit wheels. The walls of the MOS Dewar are 0.25" thick and there are also eight (8) internal baffles/stiffeners that are 0.25" thick. The top plate of the Dewar is finished with the black hard-anodized to enhance thermal radiation heat transfer. The external walls of the Dewar are assumed to be covered with 5-7 layer Multi-Layer Insulation (MLI) thermal blankets. The internal baffles, in addition to being a structural stiffener, will serve as a conductive path from LN_2 to the top plate during the science observation period.

2.2. G-10 Thermal Isolation

An isolation cylinder made from G-10 is used in the design to thermally isolate the Dewar and associated cold components from the warm environment. The G-10 isolation cylinder is assumed to be 0.128" thick and has bonded aluminum mounting rings at the each end which are secured to Dewar and vacuum chamber bulkhead.

2.3. Sapphire Ball Bearings

As a part of the mechanism designs, a set of sapphire balls are used under the MOS and Dekker wheels. These sapphire balls (3mm diameter) have high thermal conductivity at a low temperature (see Section 3.2 Material Properties) which enhance thermal conductance from to the wheels.

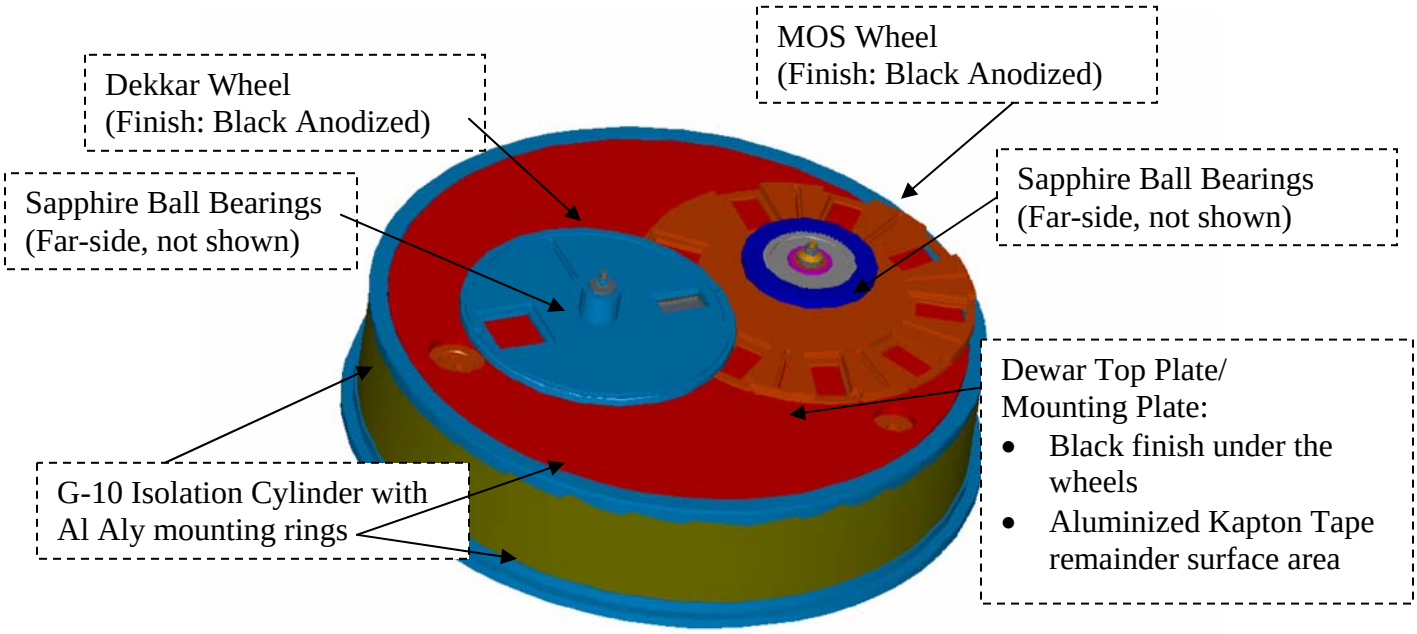

Figure 2. MOS Section Thermal Design

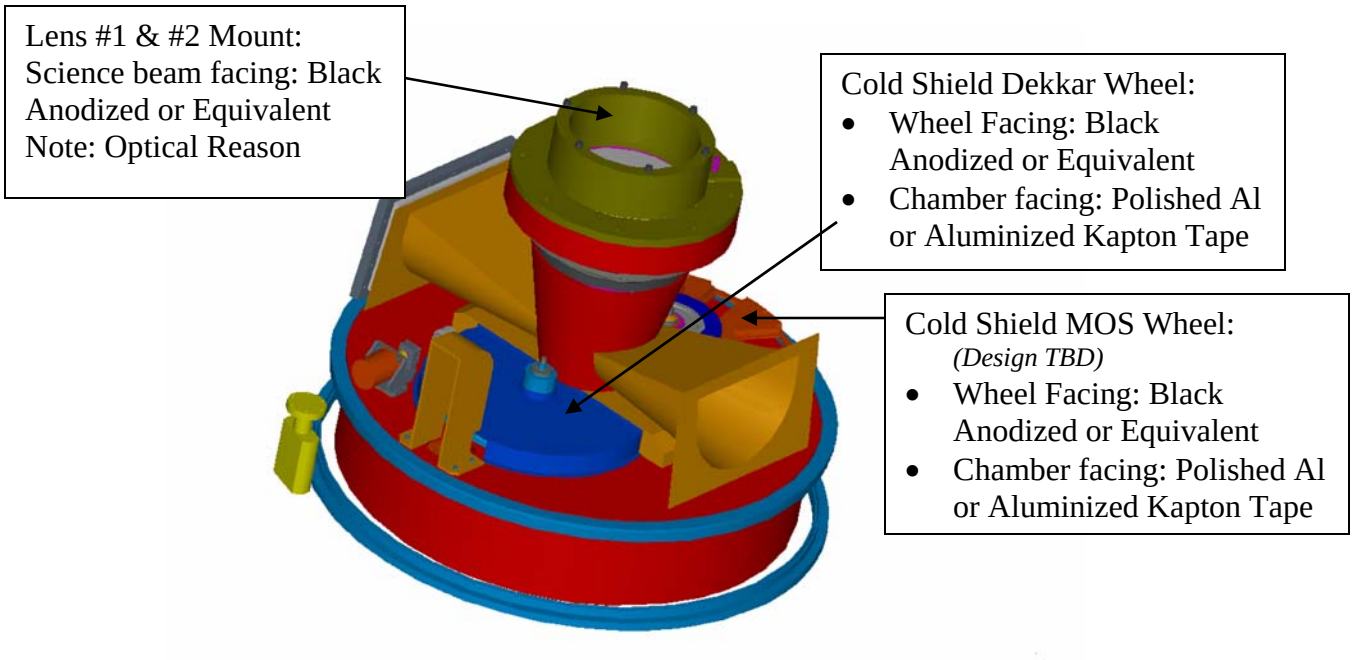

Figure 3. MOS Section Thermal Design

3. THERMAL MATH MODEL/THERMAL ANALYSIS

A detailed system level thermal math model was generated and is depicted in the Figures 4 thru 6 below. The thermal model is generated using Thermal Desktop® as a pre-and post processors. The thermal radiation heat transfer was calculated using RadCAD®. The temperatures were predicted using SINDA finite difference solver.

Included in the thermal model are the MOS vacuum Chamber, lens 1and 2 assembly, MOS Dewar/Wheel mounting plate assembly, MOS Wheel, Dekker Wheel, G-10 Isolation ring assembly, Thermal shields, and the instrument bulkhead.

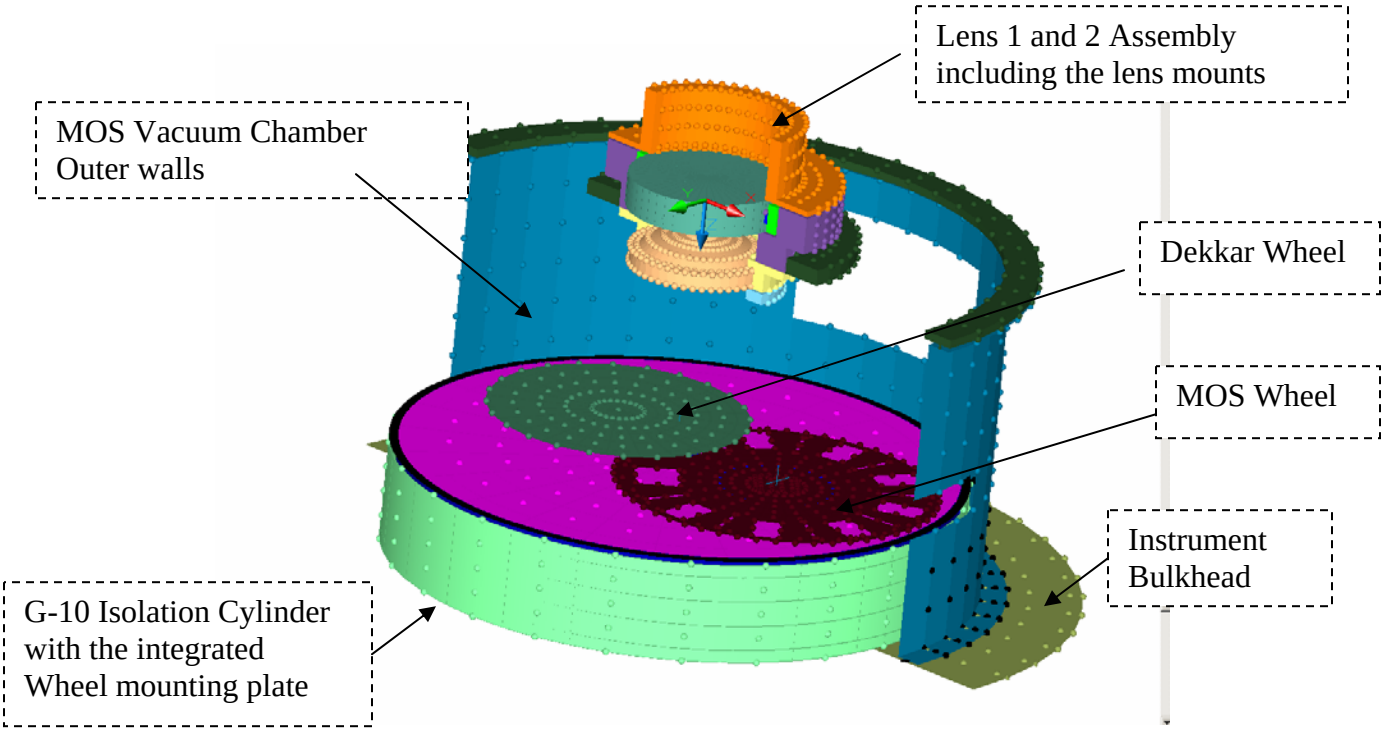

Figure 4. Detailed MOS Section Overall Thermal Math Model
(Parts of the model not shown for clarity)

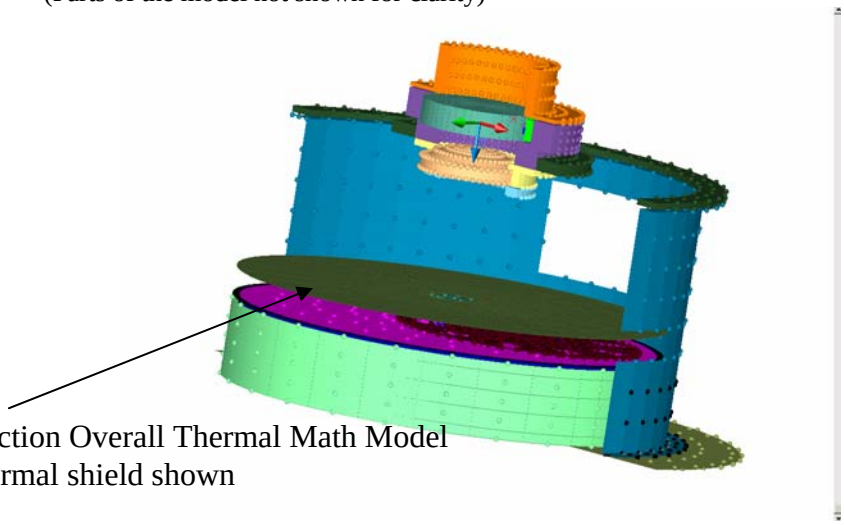

Figure 4a. Detailed MOS Section Overall Thermal Math Model
Floating thermal shield shown

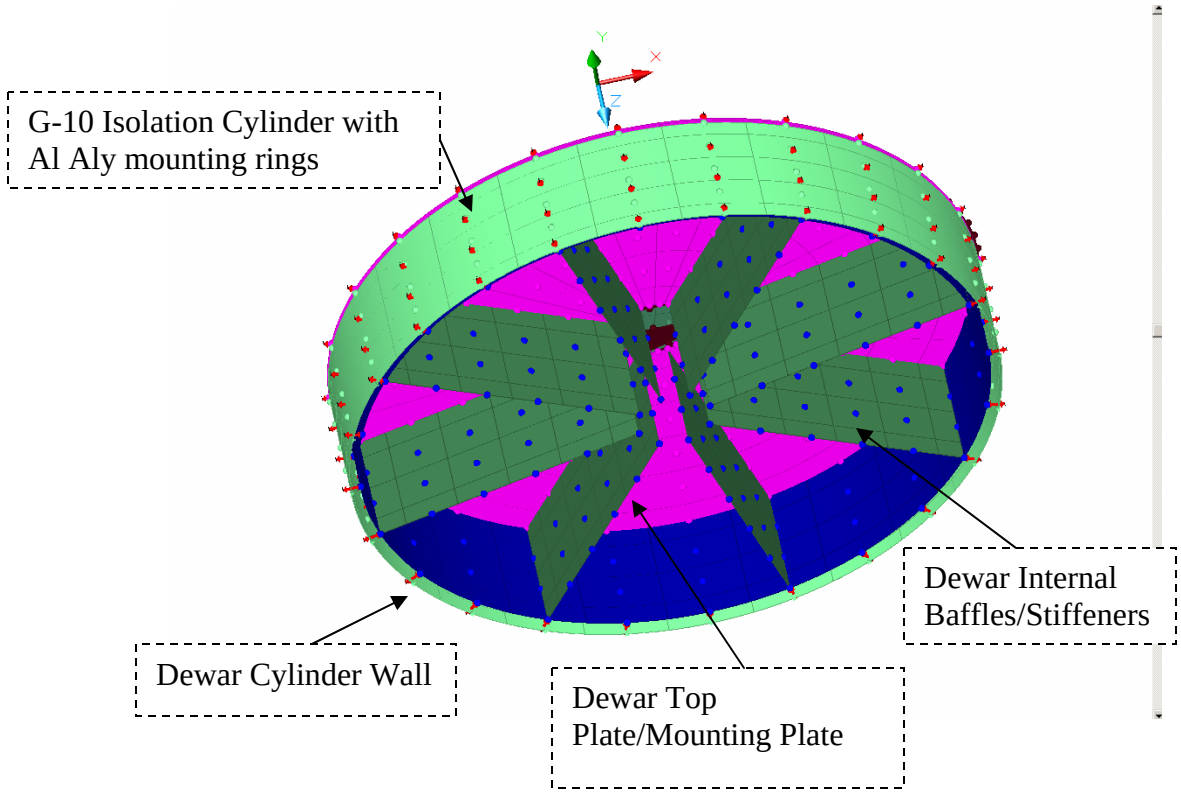

Figure 5. Thermal math model of the MOS Section: Bottom View

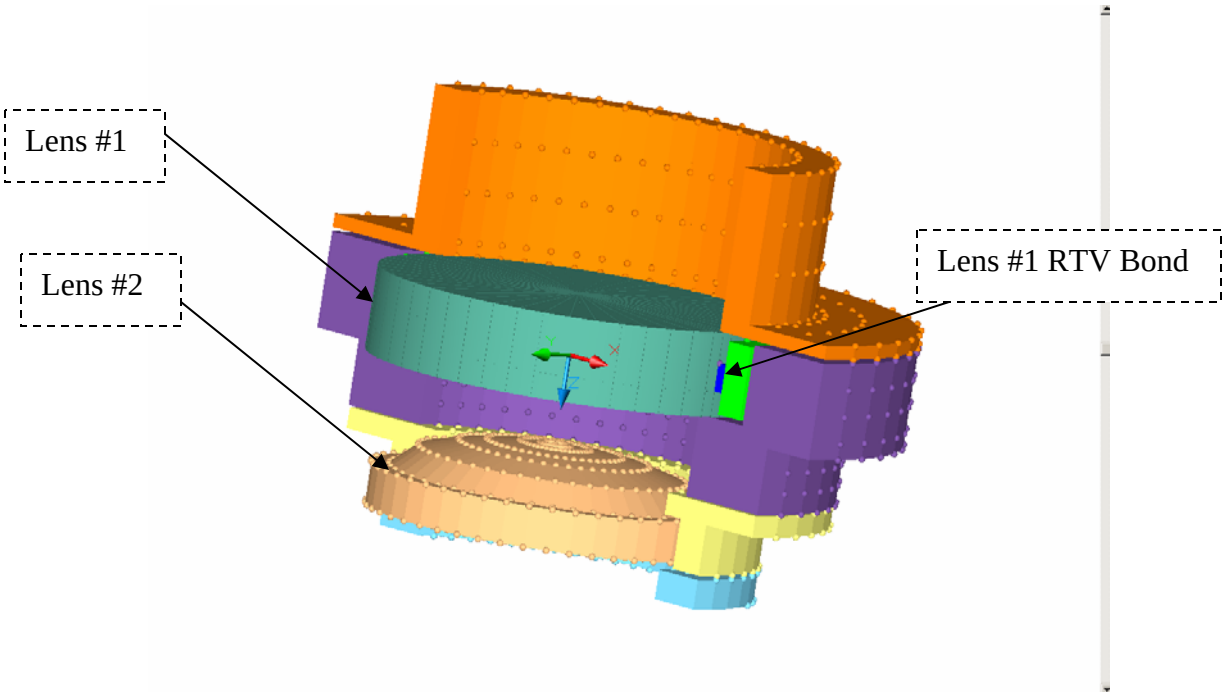

Figure 6. Thermal math model of the MOS Section: Corrector Lens 1& 2 Assembly
(Partial sectional view shown for clarity)

3.1. Analysis Assumptions

The following are the list of assumptions used during the steady state analysis.

- Boundary temperatures:
  - Bulkhead Mounting points = +25°C
  - Local Ambient Air Temperature: +25°C
  - Convective heat transfer Coefficient = 0.00366 w/in^2-°C (5.67 w/m^2-°C)
    - At 10k feet altitude
  - No thermal radiation heat transfer from the outer shell to the local ambient.
  - Bottom edge of the LN2 Dewar including the baffles: 77K (-196°C)
- No conductive path between the hub of the wheels and the center shaft bearings.

3.2. Material Properties

- Al Aly
  Density: 2700 Kg/m^3

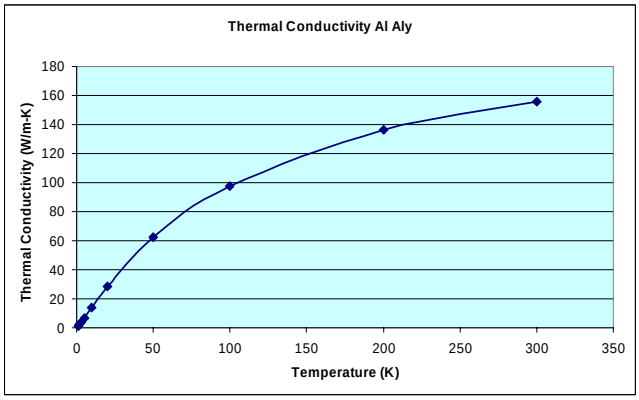

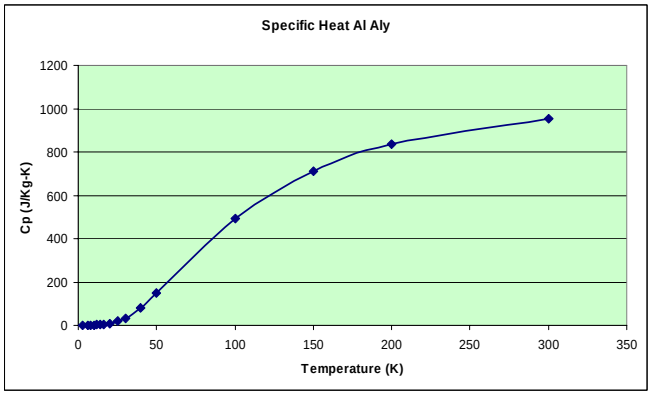

- G-10
  Density: 1790 Kg/m^3

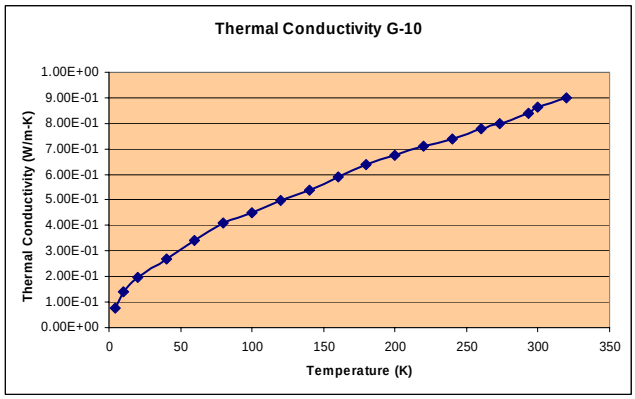

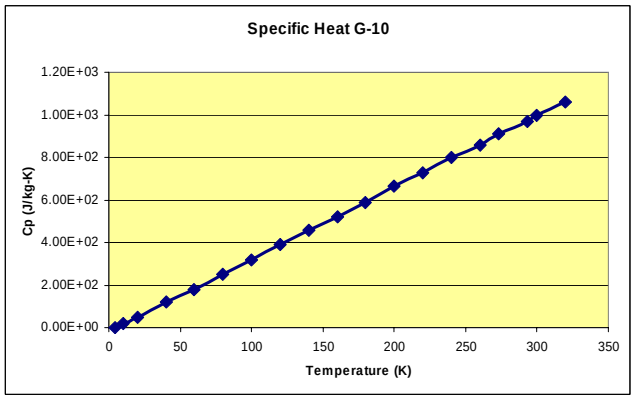

- Sapphire
  Density: 3970 Kg/m^3
  Specific Heat (Cp): 419 J/Kg-K

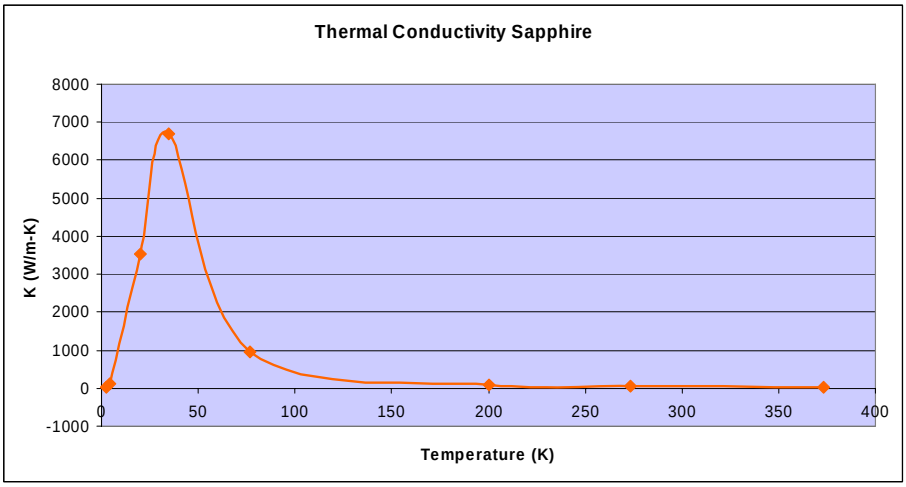

- CaF_2
  Density: 3180 Kg/m^3

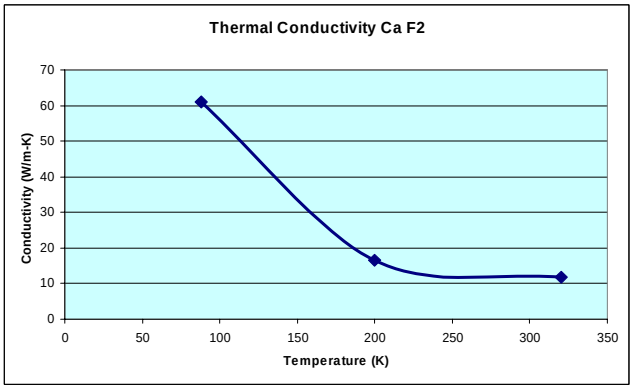

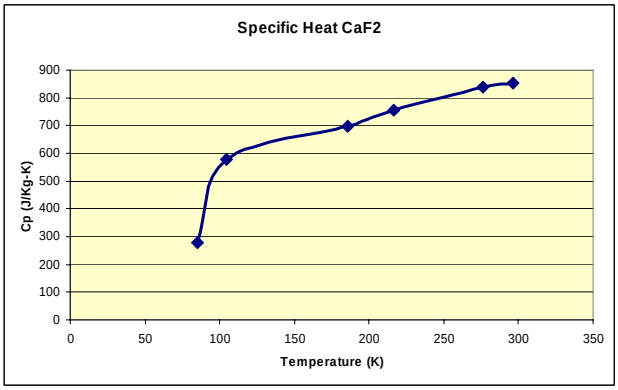

- Thermal Surface Properties

Further detailed descriptions of the thermal surface may be found in Reference 2, MOS Section Thermal Surface Finishes.

Description	Mat'l	Thickness		Thermal Surface Property	
				Outer	Inner
		inches		Emissivity	
MOS Mtg Plate Support	G-10	0.128		0.05	0.05
Dewar Top Plate	Al Aly 6061	0.625		0.9	n/a
Dewar Walls	Al Aly 6061	0.25		0.05	n/a
MOS Wheel	Al Aly 6061	0.625		0.9	0.9
Dekker Wheel	Al Aly 6061	0.5		0.9	0.9
MLI Blanket	Aluminized Mylar	0.00025/each layer		e* = 0.02-0.05	

4. ANALYSIS RESULTS

The results of the analysis are presented in the following Figures 7 thru 11.

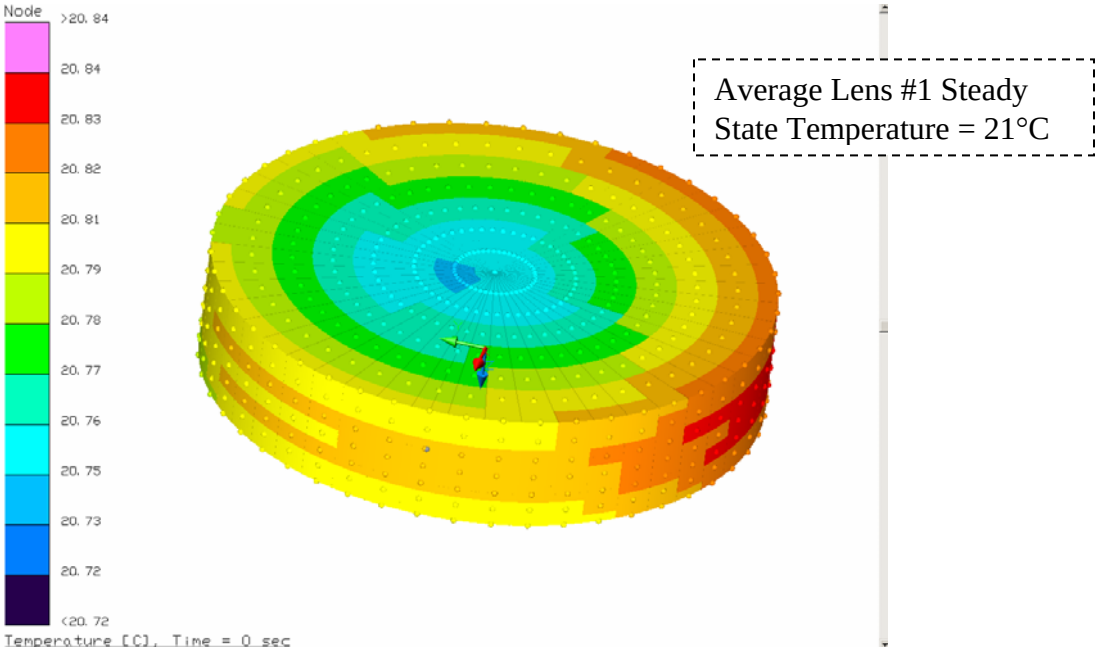

Figure 7. Steady State Temperature of Lens #1

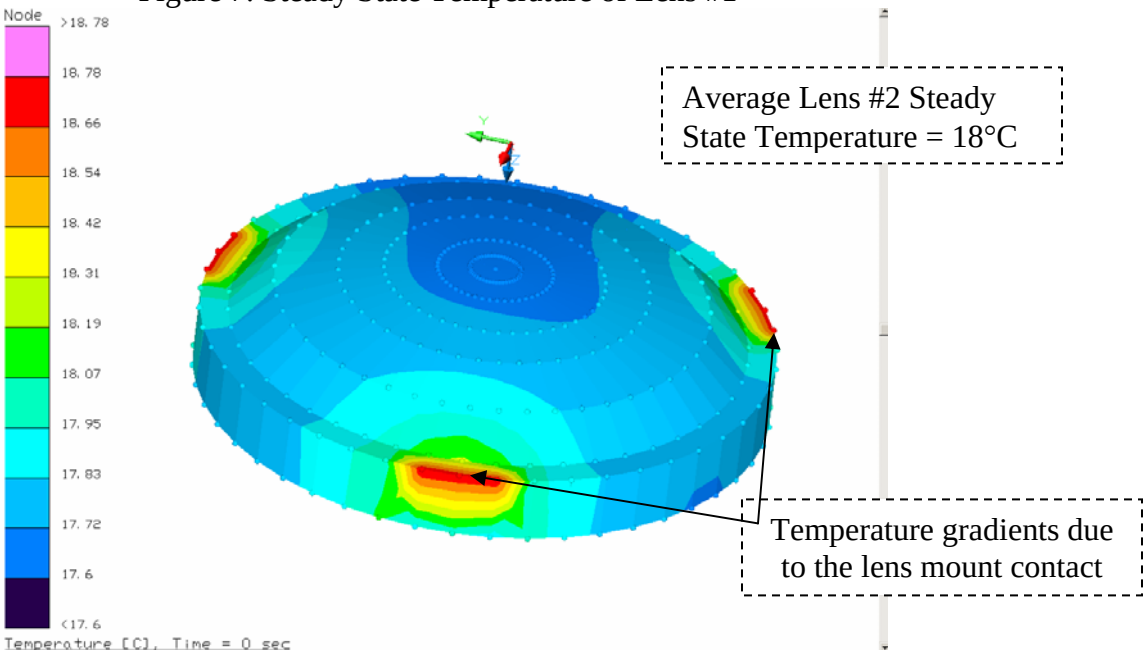

Figure 8. Steady State Temperature of Lens #2

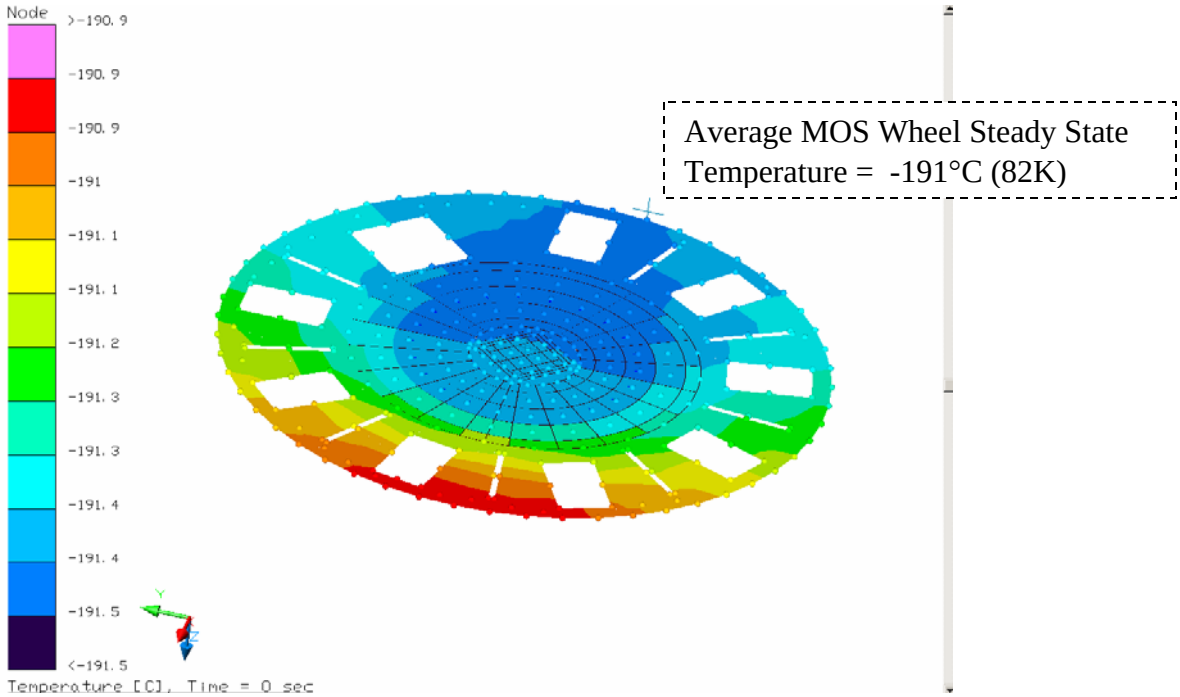

Figure 9 Steady State Temperature of MOS Wheel

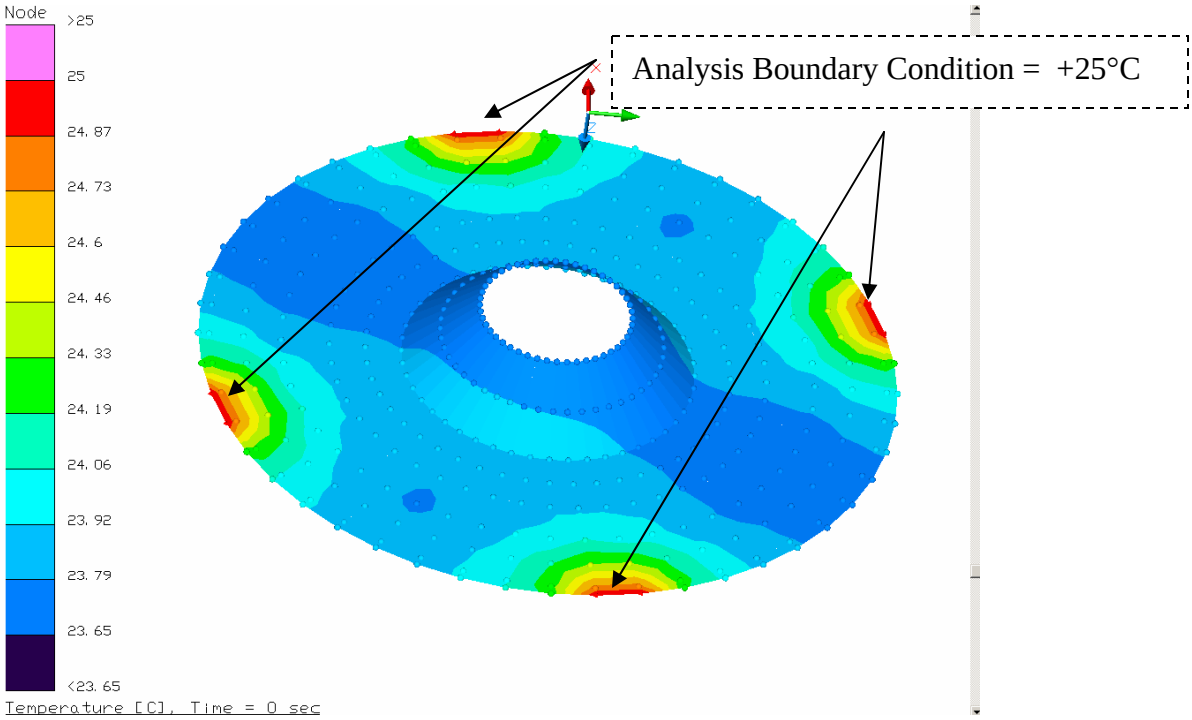

Figure 10. Steady State Temperature of Bulkhead

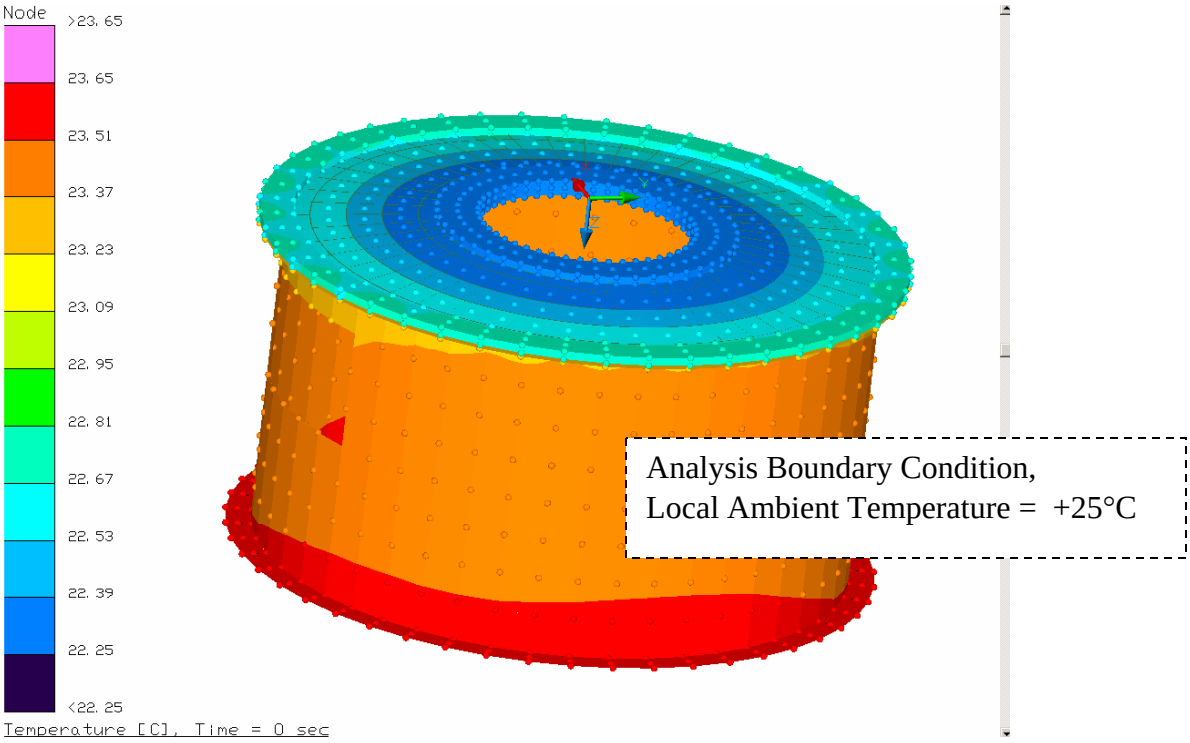

Figure 11. Steady State Temperature of MOS Vacuum Chamber

In addition to the steady state temperature, the thermal math model of the MOS section has predicted that 30.9 watts of thermal load was absorbed from the environment. Based on the energy balance from the model, a total of 12.3 watts were conducted in from the bulkhead mounting points and 18.6 watts were absorbed via convective heat transfer to the MOS vacuum chamber outer walls.

5. CONCLUSION

This analysis has shown that the steady state temperature of MOS wheel is predicted at 82K (-191°C), well below the requirement of 120K. As mentioned previously, the 10°C stabilization was satisfied with the current design and its results are presented in Reference 1. Also, this analysis has shown that the average steady state temperatures of the lens #1 and #2 are 294K (21°C) and 291K (18°C), respectively.

Based on the energy balance from the model, this analysis had calculated that 30.9 watts of thermal load was absorbed from the environment. Based on only the environment thermal load, the current design will provide 32 hours of hold-time at +25°C with 22 liters of LN_2. This analysis did not consider the internal thermal dissipations from the other mechanisms, such as drive motors. However, it is expected that the full Dewar, 51 liters (latest design, 3/14/05), will provide a total of 74 hours of hold-time. The MOS LN_2 Dewar is sufficient to provide the design requirement of 30 hours of hold-time.

Harvard-Smithsonian Center for Astrophysics
Smithsonian Astrophysical Observatory
Central Engineering

Document No. MMIRS-SP020305A Rev A

To: George Nystrom
From: Sang Park (Thermal Engineer)
Date: 07 February 2005

CC: Brian McLeod, Paul Martini, Henry Bergner, Ken McCracken, Justin Holwell, Mike Buke, Tim Norton, John Boczenowski, Bill Podgorski

Subject: MOS Operational Thermal Cycle Profile

1. SUMMARY/INTRODUCTION

A thermal analysis was performed to characterize the thermal transient behavior of the MMIRS MOS Section. This analysis showed that the current thermal design is sufficient to thermal cycle the MOS section within the allowable time limit of 9 hours.

During the operational phase of the instrument, a limit of 9 hours was imposed on the "turn-around" time or a "thermal cycle". A thermal cycle includes: a. Warm-up from the previous observation temperature using heaters including boiling off residual LN_2, b. Change of MOS Wheel slit plates, c. Return the MOS section to the observation temperature via cooling the instrument using LN_2.

Another requirement that was imposed on the MOS thermal design is that the MOS wheel temperature shall be maintained below 120K (-153°C) and stabilized within 10°C during the science observation period. The results of this analysis will show that the above requirements are satisfied with the current design.

2. MOS THERMAL DESIGN

The entire thermal design of the MOS section will be a subject of a later report. However, shown in the Figures 1 and 2 are the thermal design features that are relevant to this analysis. The MOS section includes as a part of the thermal design: a. LN_2 dewar, b. Warm-up heater, c. G-10 thermal isolation ring, d. Sapphire ball-bearings, e. thermal surface treatments to enhance thermal radiation heat transfer (thermal radiation surface properties will be presented further in Section 3.2 Material Properties). The following paragraphs describe the details of the thermal features.

2.1. LN_2 Dewar

The MOS section LN_2 Dewar is constructed from Aluminum Alloy 6061 (Al Aly 6061) with a 0.75” thick top plate also serving as a mounting platform for the parts of the MOS assembly. The walls of the MOS Dewar are 0.25” thick and there are also eight (8) internal baffles/stiffeners that are 0.25” thick. The top plate of the Dewar is finished with the black hard-anodized to enhance thermal radiation heat transfer. The external walls of the Dewar are assumed to be covered with 5-7 layer Multi-Layer Insulation (MLI) thermal blankets. The internal baffles, in addition to being a structural stiffener, will serve as a conductive path from LN_2 to the top plate during the science observation period.

2.2. Warm-Up Heater

The warm-up heaters are constructed from a thin low-outgassing Kapton insulator and they are intimately mounted on the walls of the Dewar. The heaters are sized to dissipate 1500 watts and will be controlled by a Croyocon Heater controller in conjunction with an external power supply sufficient enough to provide 1500 watts to the heaters. The heaters will have ON/OFF set points at +30/+35°C.

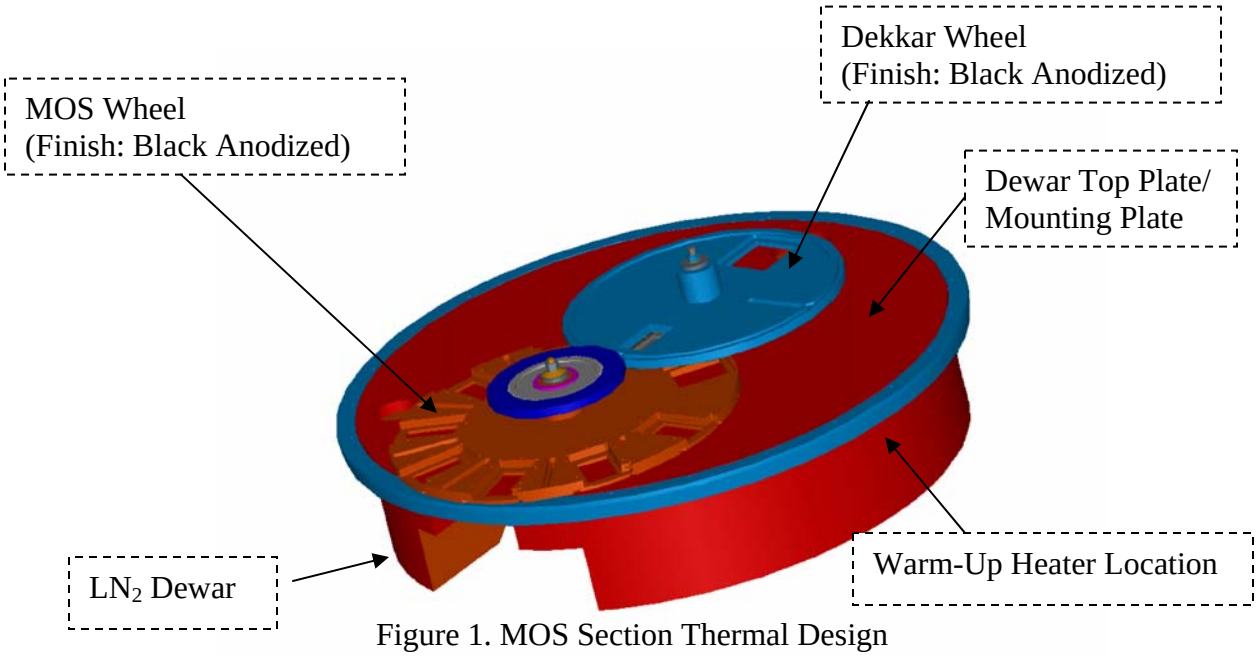

Figure 1. MOS Section Thermal Design
(G-10 Ring removed for clarity)

2.3. G-10 Thermal Isolation

An isolation cylinder made from G-10 was used in the design in order to thermally isolate the mounting plate of the MOS section (at a LN_2 temperature range) from the bulkhead (at a local ambient temperature range) of the instrument. The G-10 isolation cylinder is

assumed to be 0.128" thick and has Al Aly mounting rings secured to the both edges of the cylinder.

2.4. Sapphire Ball Bearings

As a part of the mechanism design, a set of ball bearings were used under the MOS and Dekkar wheels. These ball bearings (3mm diameter) are made from sapphire with the high thermal conductivity at a low temperature (see Section 3.2 Material Properties) to enhance thermal conductance from the mounting plates to the wheels.

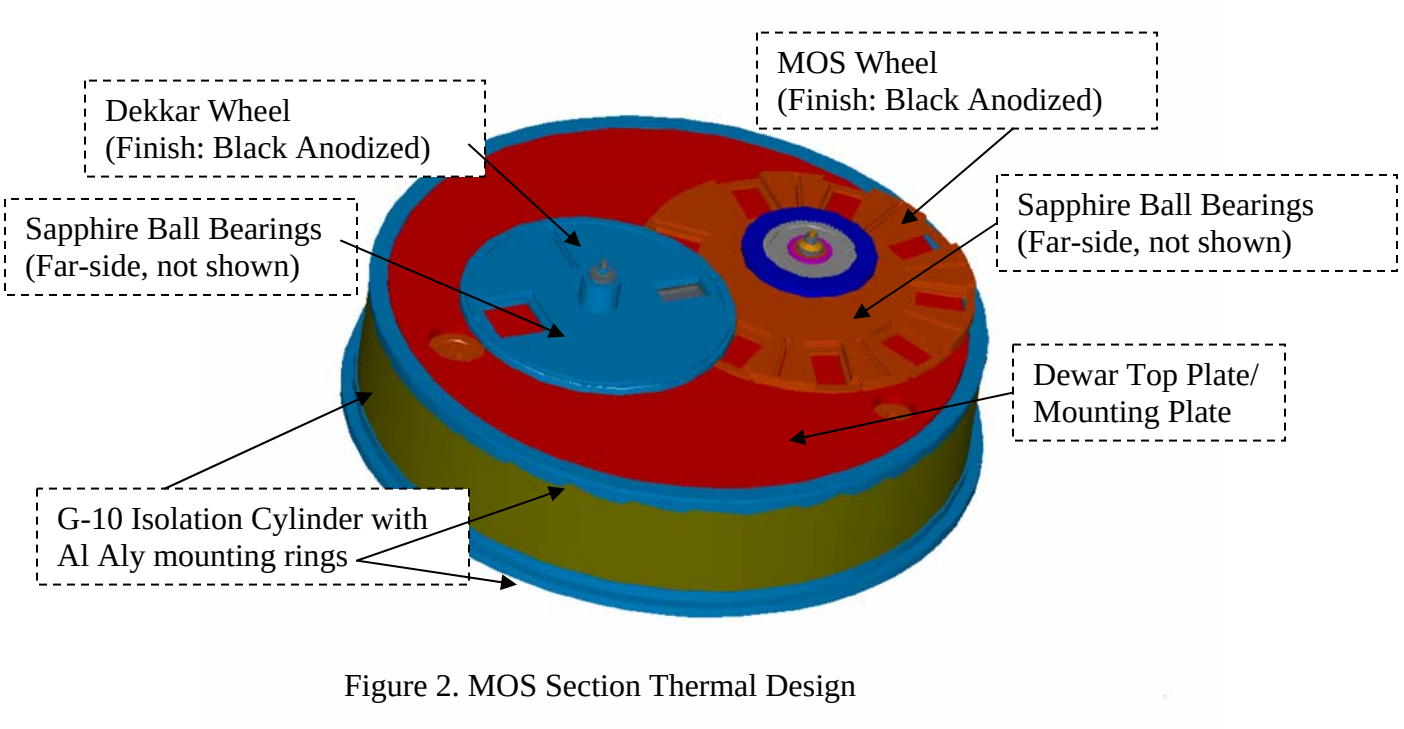

Figure 2. MOS Section Thermal Design

3. THERMAL MATH MODEL/THERMAL ANALYSIS

A reduced thermal math model was generated from the detailed overall thermal math model of the MOS section (See Figure 3). The detailed overall thermal math model of the MOS section will be a subject of a separate report. The reduced thermal model for the purpose of characterizing the MOS thermal cycle is depicted in the Figures 4 and 5 below. The reduced thermal model is generated using Thermal Desktop® as a pre-and post processors. The thermal radiation heat transfer was calculated using RadCAD®. The temperatures were predicted using SINDA finite difference solver.

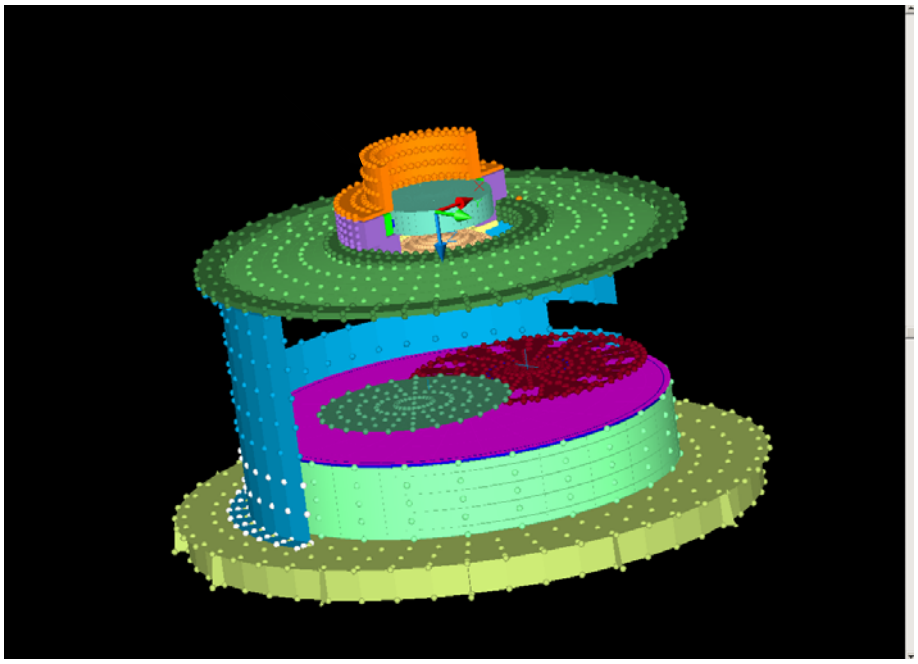

Figure 3. Detailed MOS Section Overall Thermal Math Model
(Parts of the model not shown for clarity)

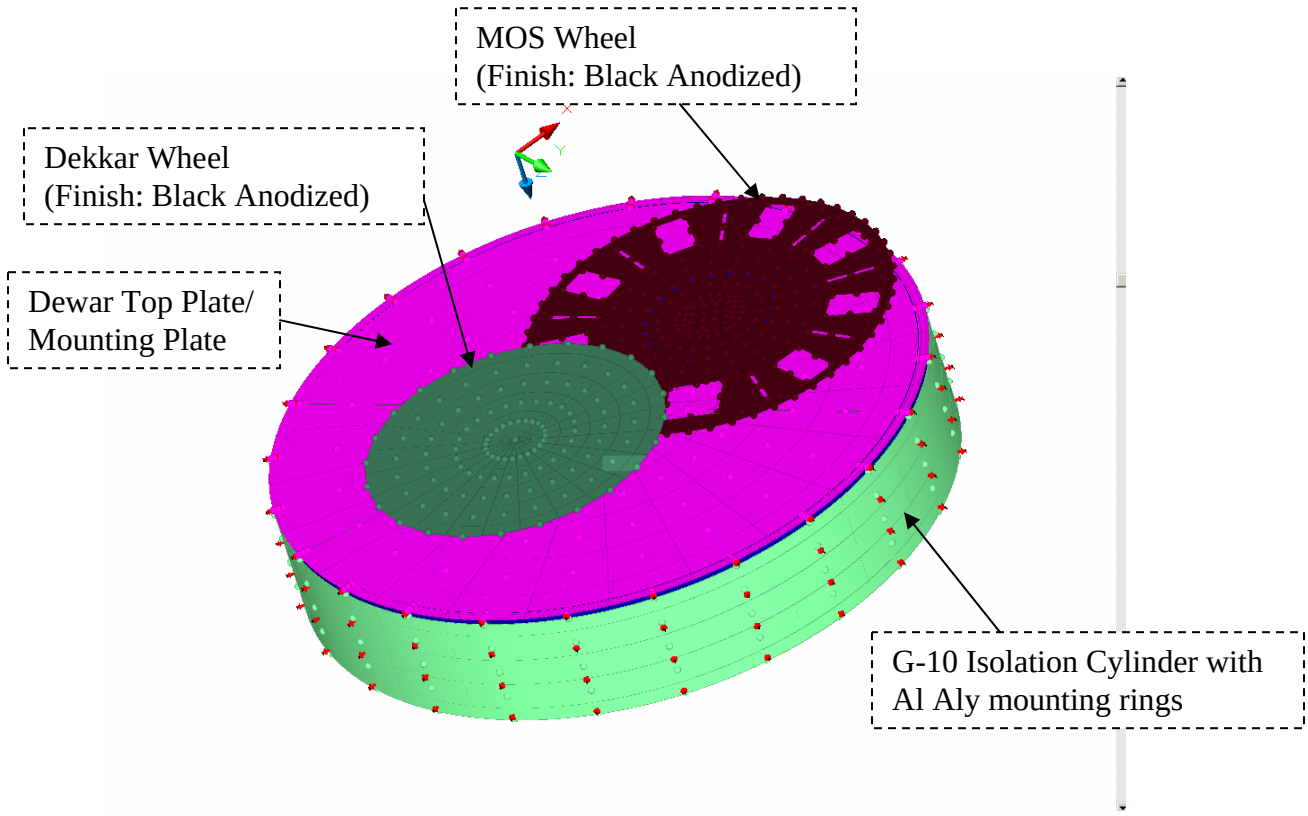

Figure 4. Reduced thermal math model of the MOS Section: Top View

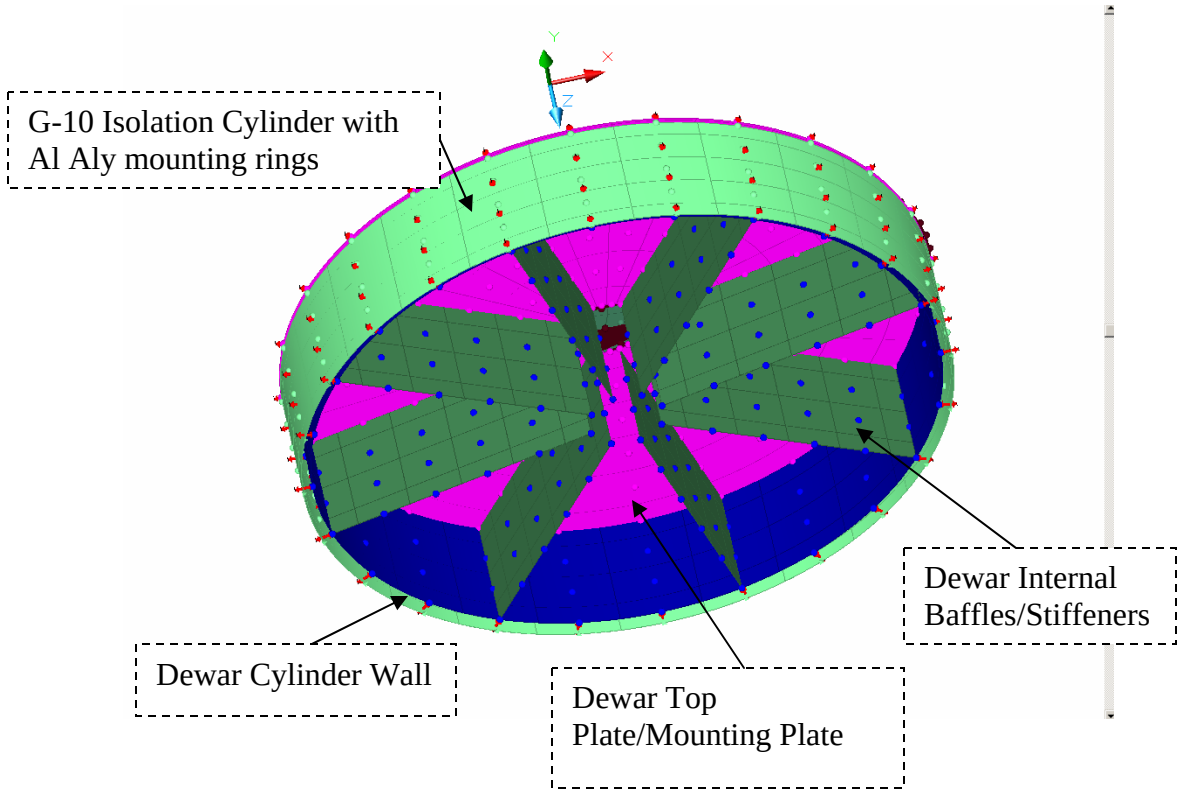

Figure 5. Reduced thermal math model of the MOS Section: Bottom View

3.1. Analysis Assumptions

2 cases were analyzed using the reduced thermal math model as follow:

Case 1. Warm-up Cycle
Case 2. Cooling Cycle

The following are the list of assumptions used during each case of the analysis.

Case 1. Warm-up Cycle Analysis Assumptions

- Initial temperature: 90K (-183°C)
- No LN_2 left in the Dewar
- Boundary temperatures:
  - Bulkhead side of the G-10 Cylinder = +25°C
  - Bottom edge of the LN2 Dewar including the baffles: 77K (-196°C)
- Warm-up heaters set points +30/+35°C
- Warm-up heater dissipation = 1500W evenly distributed around the cylinder portion of the Dewar
- 40w external heat load

No conductive path between the hub of the wheels and the center shaft bearings

Case 2. Cooling Cycle Analysis Assumptions

- Initial temperature: +25°C
- Boundary temperatures:
  - Bulkhead side of the G-10 Cylinder = +25°C

- Bottom edge of the LN_2 Dewar including the baffles: 77K (-196°C)

- Warm-up heaters OFF
- 40w external heat load
- No conductive path between the hub of the wheels and the center shaft bearings

3.2. Material Properties

- Al Aly
  Density: 2700 Kg/m^3

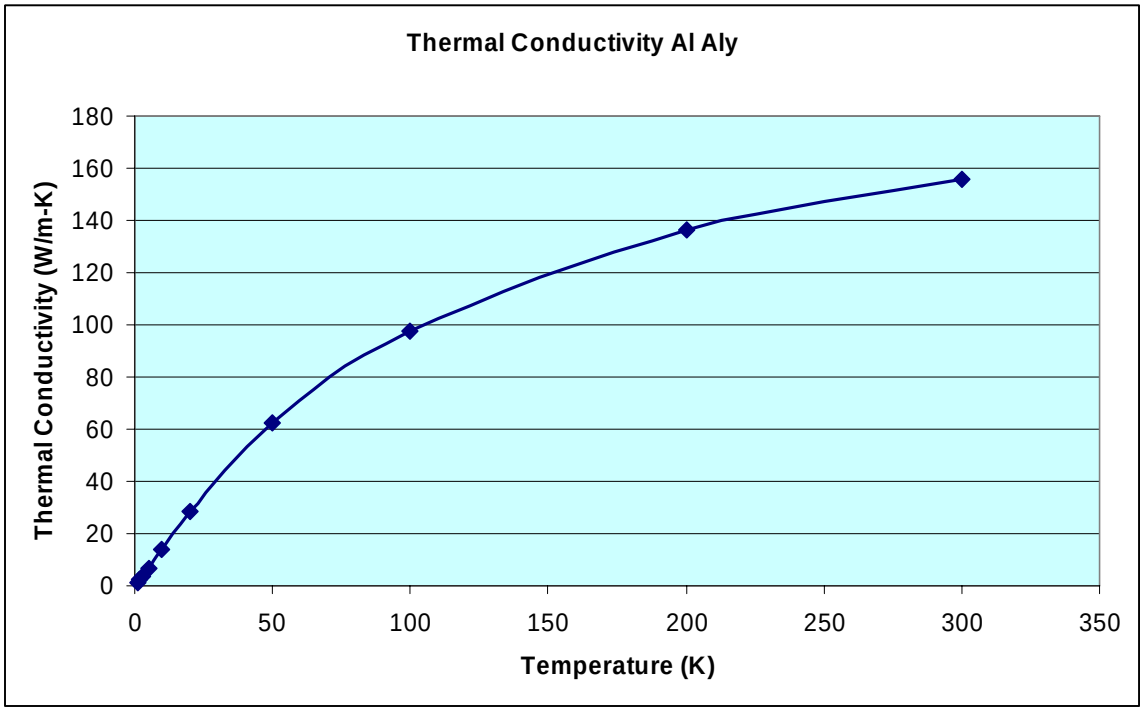

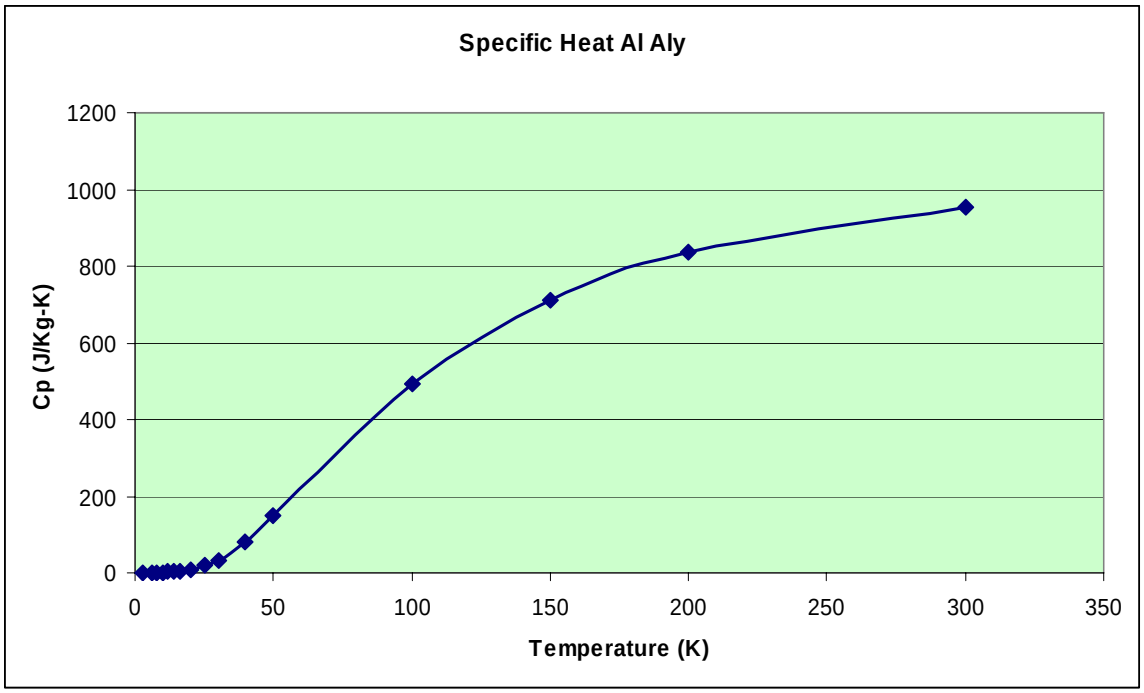

- G-10
  Density: 1790 Kg/m^3

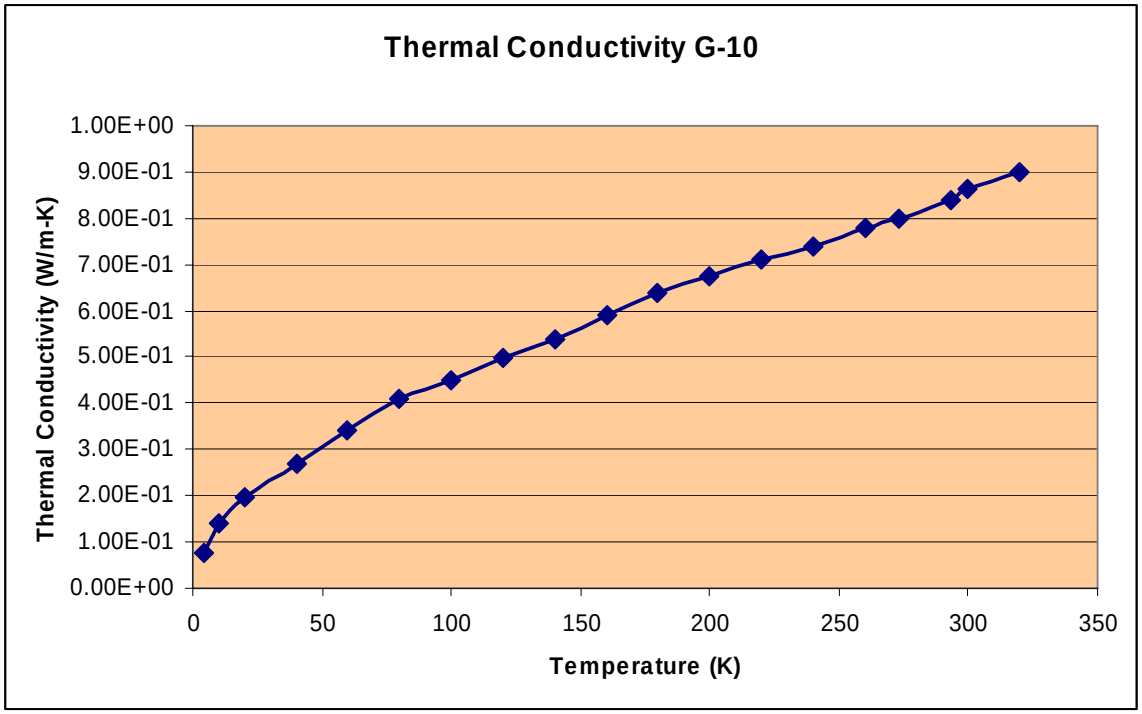

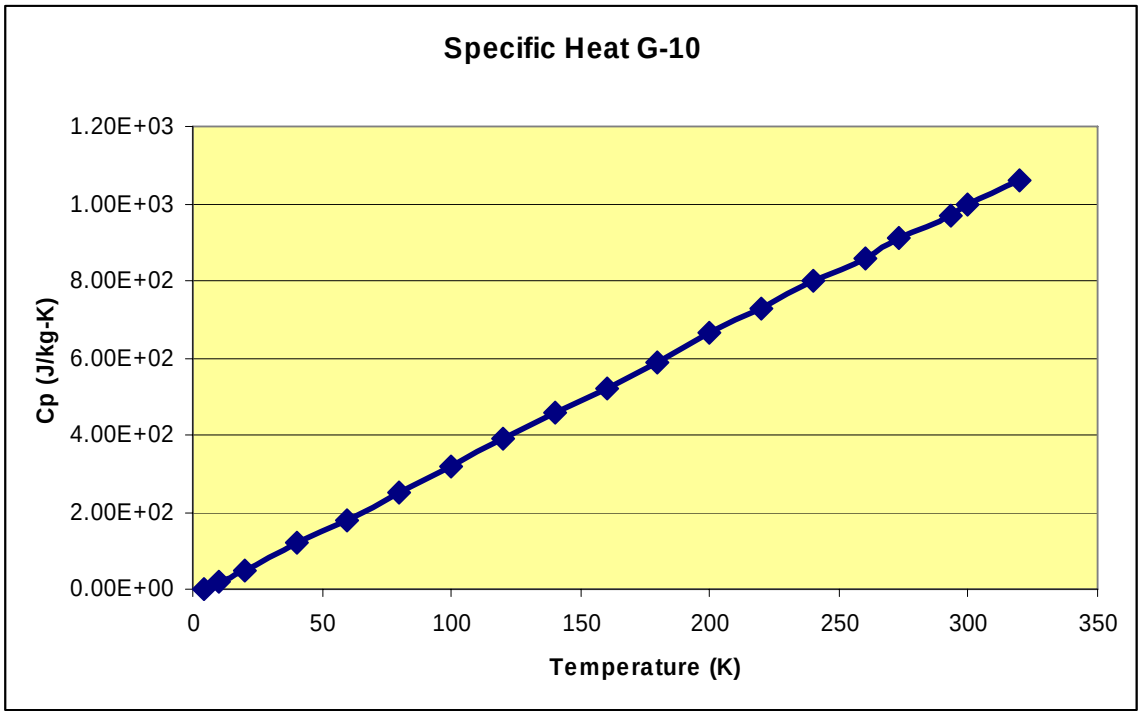

- Sapphire
  Density: 3970 Kg/m^3
  Specific Heat (Cp): 419 J/Kg-K

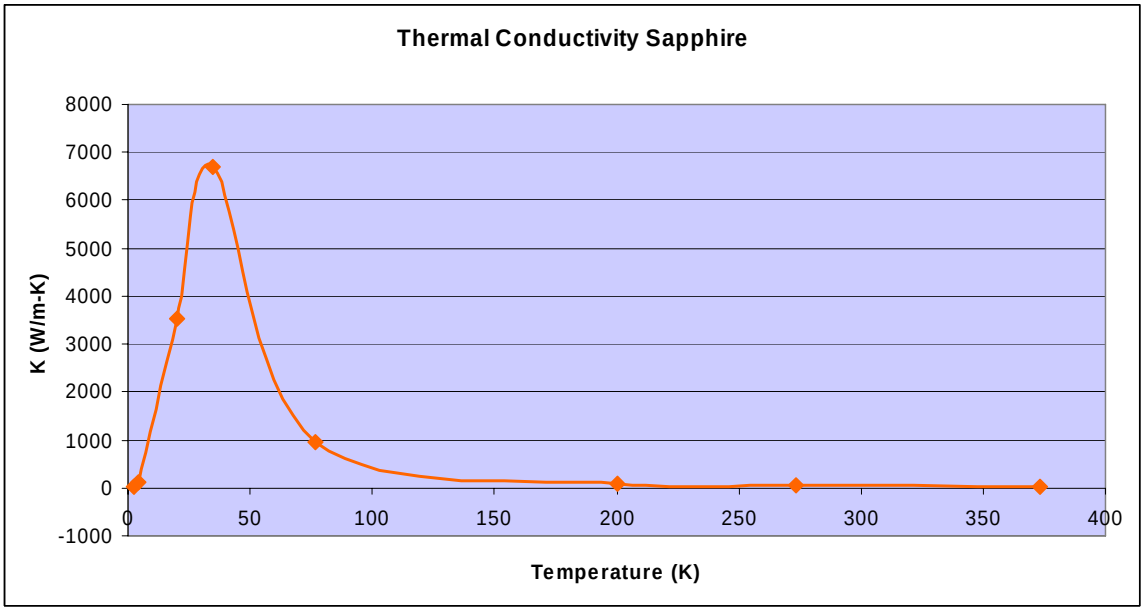

- Thermal Surface Properties

Description	Mat'l	Thickness		Thermal Surface Property	
				Outer	Inner
		inches		Emissivity	
MOS Mtg Plate Support	G-10	0.128		0.05	0.05
Dewar Top Plate	Al Aly 6061	0.625		0.9	n/a
Dewar Walls	Al Aly 6061	0.25		0.05	n/a
MOS Wheel	Al Aly 6061	0.625		0.9	0.9
Dekkar Wheel	Al Aly 6061	0.5		0.9	0.9
MLI Blanket	Aluminized Mylar	0.00025/each layer		e* = 0.02-0.05	

4. ANALYSIS RESULTS

The results of the analysis are presented in the following Paragraphs 4.1 thru 4.3.

4.1. Residual LN_2 Boil-off Analysis Result

Assumptions:
1. Dewar is ½ full (11 liters)
2. Heat of Vaporization of LN2 = 2.01E5 J/Kg (55.83 watt-hr/Kg)
3. Thermal Capacitance of LN2 at ½ full: 495.6 watt-hr
4. Warm-up heater dissipation: 1500w

Therefore, time to boil off excess LN_2= 0.33hrs (19.8min.)

4.2. Warm-up Cycle Analysis Result

The results of the analysis Case 1 (Warm-Up Cycle) is depicted in Graph 1 below:

Graph 1. MOS Section Warm-Up Cycle Profile

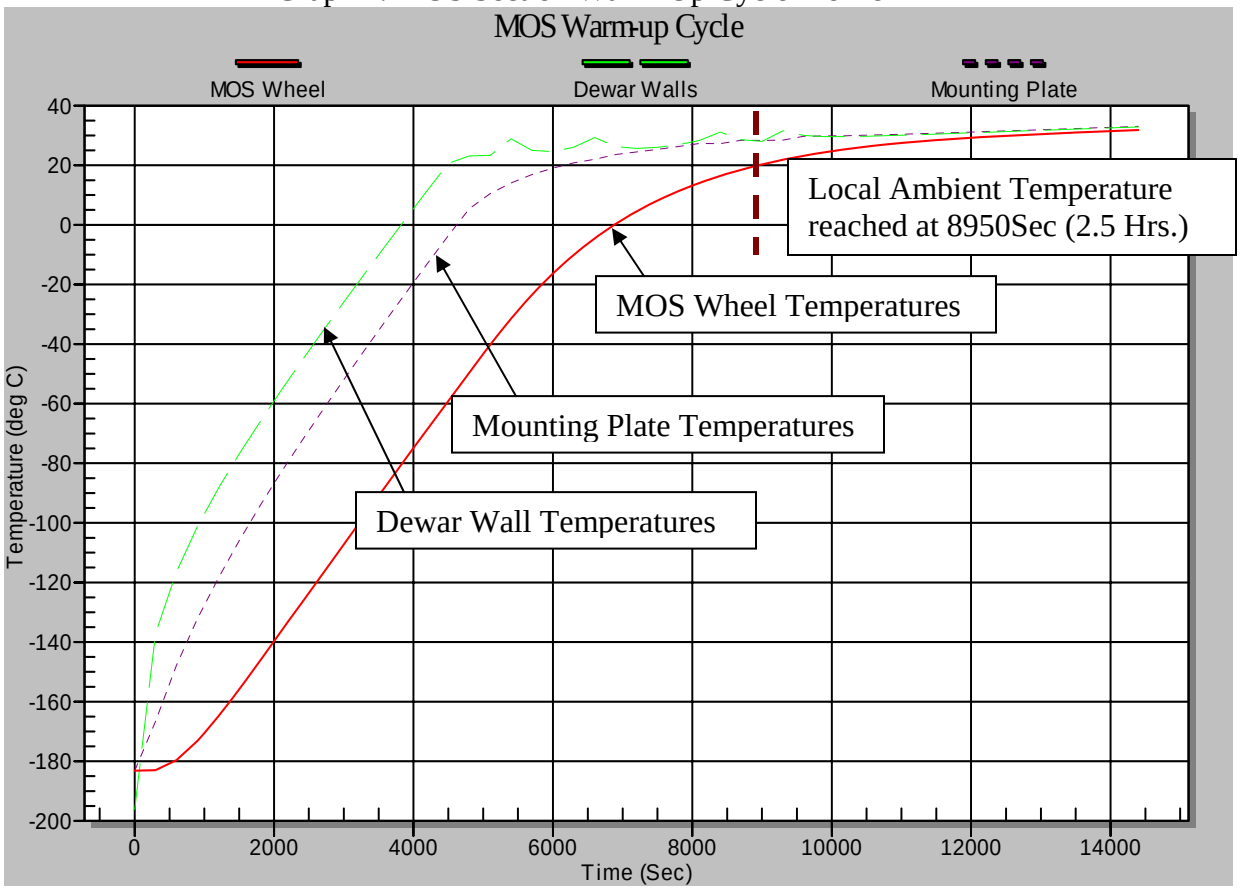

As depicted in Graph 1 above, the MOS wheel temperature reached above 20°C at 8950 Sec (2.5 Hrs.) after the initial warm-up.

4.3. Cooling Cycle Analysis Result

The results of the analysis Case 2 (Cooling Cycle) is depicted in Graph 2 below:

Graph 2. MOS Section Cooling Cycle Profile

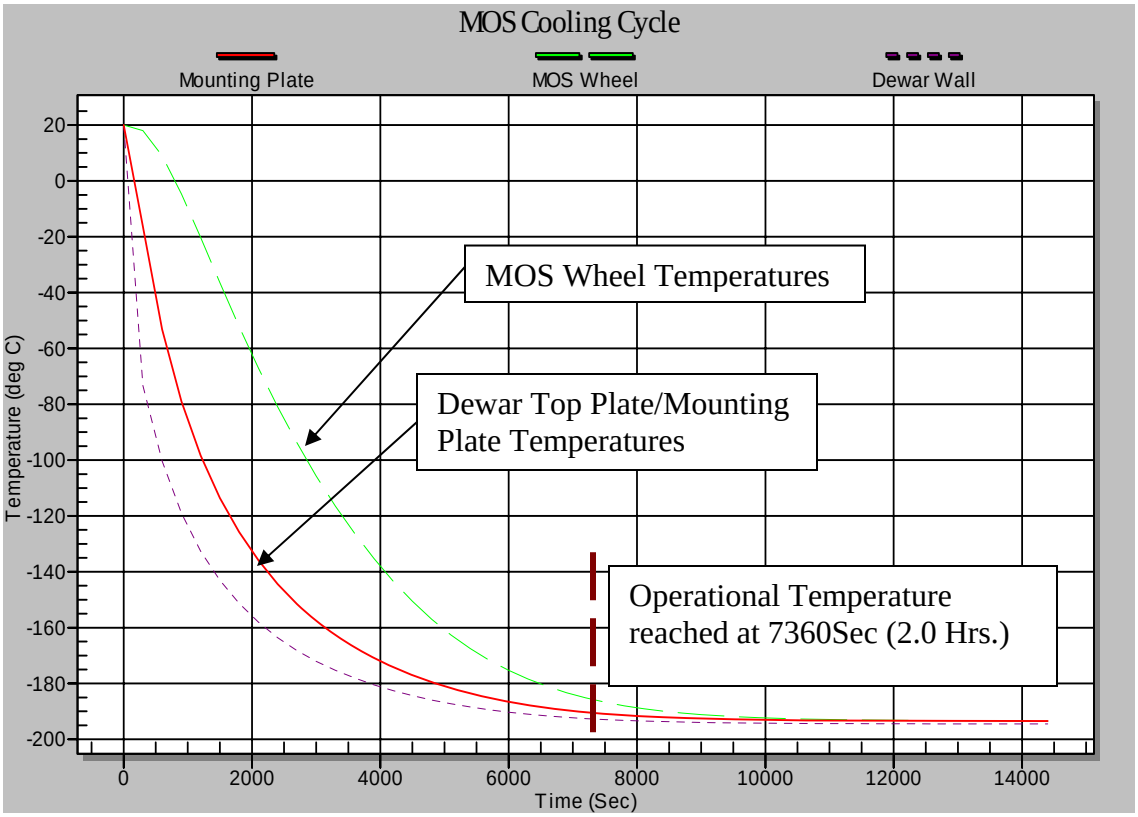

As depicted in Graph 2 above, the MOS wheel temperature reached below 120K and was stabilized within 10K from its steady state temperature at 7360 Sec (2 Hrs.) after the initial cool-down.

5. CONCLUSION

This analysis has shown that the thermal cycle of the MOS section may be completed in approximately 4.8 hours, excluding the time to change MOS slit plates, (0.33hr to boil off excess LN_2, 2.5 hrs to warm-up, then 2.0 hrs to cool to the observation temperature).

Harvard-Smithsonian Center for Astrophysics
Smithsonian Astrophysical Observatory
Central Engineering

Document No. MMIRS-SP030405A

To: George Nystrom
From: Sang Park (Thermal Engineer)
Date: 04 March 2005

CC: Brian McLeod, Paul Martini, Henry Bergner, Ken McCracken, Justin Holwell, Mike Buke, Tim Norton, John Boczenowski, Bill Podgorski

Subject: MOS Section Thermal Surface Finishes

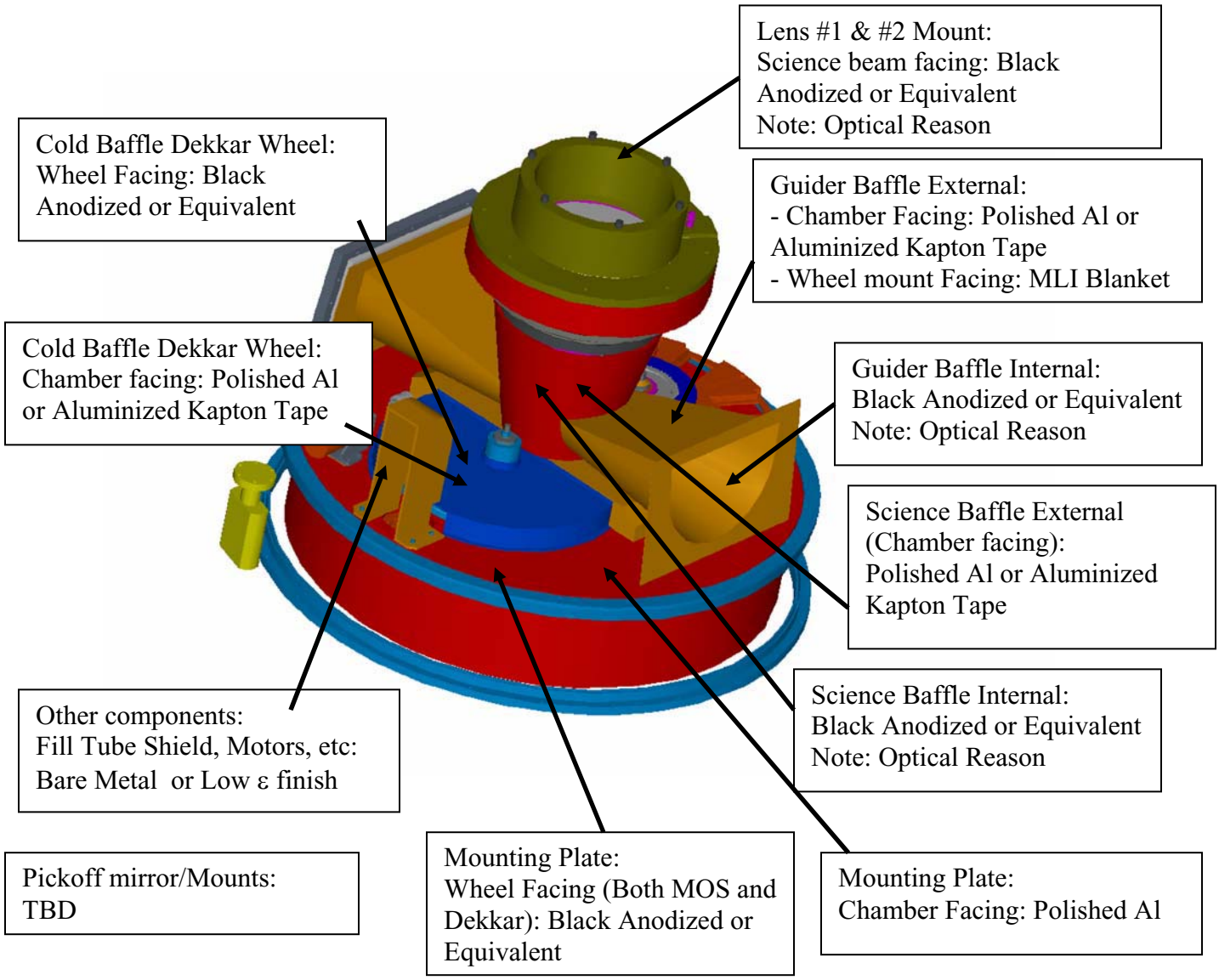

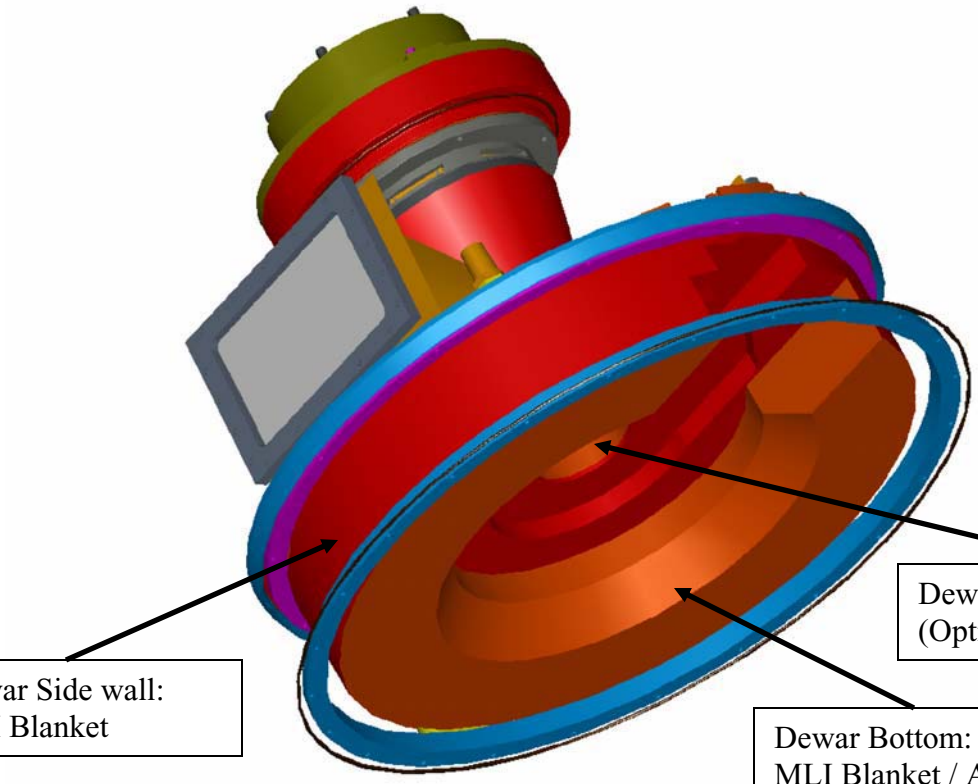

Dewar Side wall:
MLI Blanket

Dewar Aperture: Black
(Optical reason)

Dewar Bottom:
MLI Blanket / Aluminized

Bulkhead, Dewar facing:
Polished Aluminum

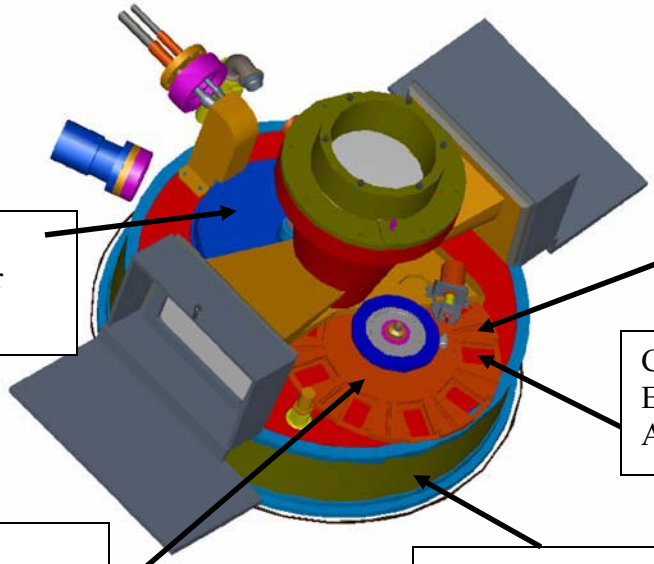

Dekkar Wheel:
Black Anodized or
equivalent

Cold Baffle MOS Wheel (TBD):
Wheel Facing/Internal: Black
Anodized or Equivalent

Cold Baffle MOS Wheel (TBD):
External: Polished Al or
Aluminized Kapton Tape

MOS Wheel:
Black Anodized or
equivalent

G-10 Chamber Facing:
MLI Blanket

Chamber Internal wall: Bare Aluminum except
G-10 facing potion: Polished Aluminum

Thermal Baffle (TBD): Polished Aluminum both
sides / Aluminized Kapton tape

Harvard-Smithsonian Center for Astrophysics
Smithsonian Astrophysical Observatory
Central Engineering

Document No. MMIRS-SP040405A Rev - (April 04 2005)
MMIRS-SP040405A Rev A (April 29 2005)
MMIRS-SP040405A Rev B (May 04 2005)

To: George Nystrom
From: Sang Park (Thermal Engineer)
Date: 04 May 2005

CC: Brian McLeod, Paul Martini, Henry Bergner, Ken McCracken, Justin Holwell, Mike Burke, Tim Norton, John Boczenowski, Bill Podgorski

References:

1. MMIRS-SP032805A Preliminary; Subject: MMIRS Camera Section Thermal Surface Finishes, From: S. Park, To: G. Nystrom, 28 March 2005
2. THERMAL GRADIENT STRESS SURVEY FOR MMIRS LENSES 3-14, REVISION B, File: c:\bergner\mmirs\lenssurvey\lenssurveyrevb.wpd, From: Henry Bergner, To: George Nystrom, Date: June 16, 2004
3. George's Memo, Lens Contact Pressure and Contact Surface Area
4. "Spacecraft Thermal Control Handbook" Vol. I, 2nd Edition, David Gilmore, The Aerospace Press/AIAA, 2002

Subject: MMIRS Camera thermal analyses

1. SUMMARY/INTRODUCTION

A thermal analysis was performed to characterize the steady state and transient temperatures of the MMIRS Camera section. The analysis is presented in 2 folds, Steady State temperature predictions and Transient temperature predictions.

Steady State Design Requirements:

- Lens temperature shall be maintained at 80K +/- 3K at steady state condition
- Hold time greater than 40hours.

Transient Design Requirement:

- Maintain below the lens temperature gradient requirements, as depicted in Table 1 during the cool-down and warm-up of the instrument.

This analysis has shown that all lenses are expected to be between 77K (-196°C) and 83K (-190°C) at a steady state condition assuming that the LN_2 boiling temperature is at 77K. Also, the Grism assembly is expected to reach an average steady state temperature of 81K (192°C). Also, the transient response of the prisms located within the Grism assembly will be discussed in this report.

The Camera LN_2 Dewar is sufficient to provide at least 40 hours of hold-time, a design requirement. This analysis has calculated that approximately 35.4 watts of thermal load

was absorbed from the environment via the natural convection on the chamber outer wall surfaces and through the conductive heat transfer at the bulkhead mounting points. Based on only the environment thermal load, the current design will provide 63.6 hours of hold-time at +25°C ambient with 50 liters of LN_2.

The results of the transient analysis has shown that the optical bench cooling rate (and warming rate) of 0.2°C/min (or less) is required to maintain the desirable temperature gradients within each lens.

Table 1. Allowable Temperature Gradients (Degree C) for MMIRS Lenses

	allowable temperature		
lens number	radial gradient	axial gradient	dimetral gradient
3	2.18	46.30	222.22
4	1.39	48.31	555.56
5	3.97	42.74	370.37
6	4.83	222.22	1111.11
7	92.59	2777.78	22222.22
8	2.78	42.74	555.56
9	2.58	44.44	370.37
10	3.58	113.38	1234.57
11	2.47	44.44	358.42
12	3.83	48.31	483.09
13	2.22	46.30	252.53
14	5.05	156.49	1221.00

Though the IR Detector is located in the Camera section of the instrument, the thermal performance of the detector will be a subject of a separate report.

2. CAMERA THERMAL DESIGN

Shown in the Figures 1 thru 4 are the thermal design features that are relevant to this analysis. The Camera assembly includes as a part of the thermal design the following features:

a) LN_2 Dewar with 1500watt warm-up heater
b) Thermal Shields
   - Overall Cold-Shield
   - Cold-Shields for Lens assemblies
c) G-10 thermal isolation ring
d) Sapphire ball-bearings
e) Multi-Layer Insulation (MLI) thermal blankets
f) Thermal surface treatments to enhance thermal radiation heat transfer *(thermal radiation surface properties will be presented further in Section 3.2 Material Properties and Reference 1. Camera Section Thermal Surface Finishes)*.

The following paragraphs describe the details of the thermal features.

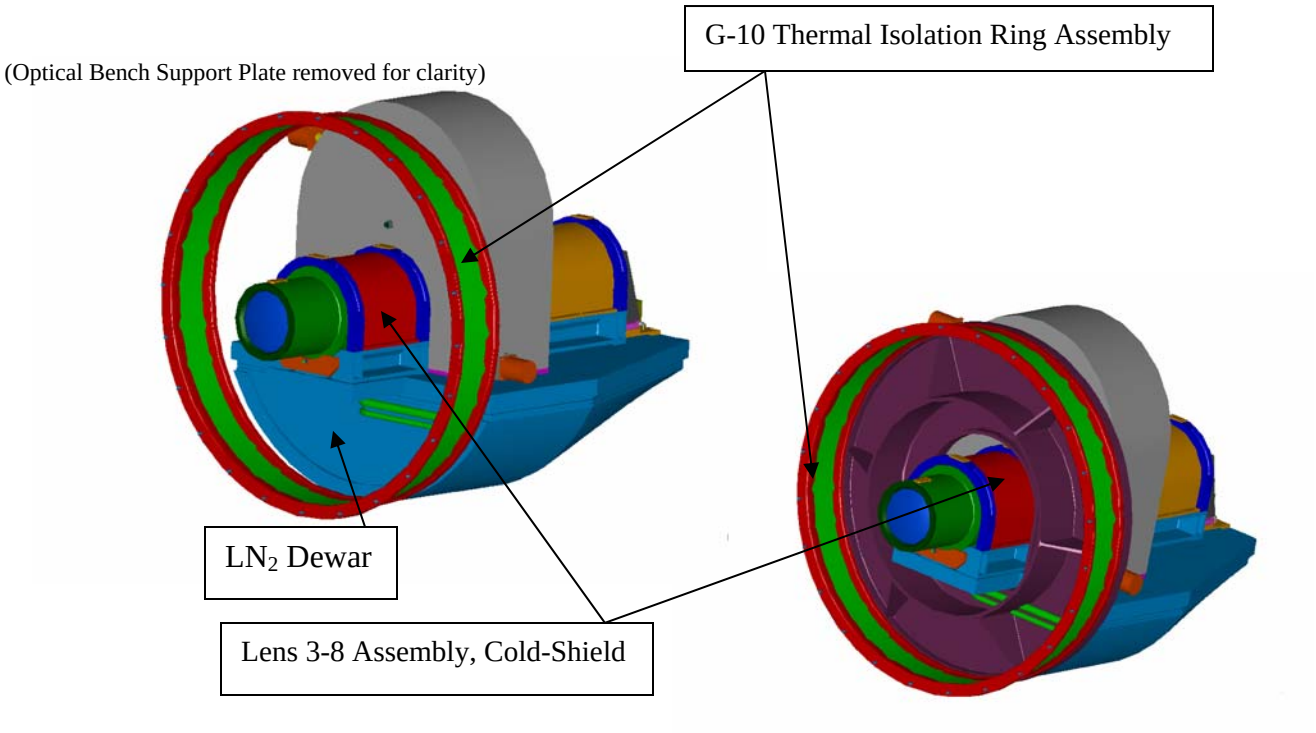

Figure 1. Camera Section Thermal Design

2.1. LN_2 Dewar

The Camera section LN_2 Dewar is constructed from Aluminum Alloy 6061-T6 with an equivalent 1.5” thick top plate also serving as an optical bench for the camera lens assemblies, Grism assembly, and the IR detector. The walls of the Camera Dewar are 0.25” thick and there are also three (3) internal baffles/stiffeners that are 0.25” thick. The internal baffles, in addition to being a structural stiffener, will serve as a conductive path from LN_2 to the top plate during the science observation period.

2.2. G-10 Thermal Isolation

An isolation cylinder made from G-10 is used in the design to thermally isolate the Dewar and associated cold components from the warm environment. The G-10 isolation

cylinder is assumed to be 0.128” thick and has bonded aluminum mounting rings at the each end which are secured to Dewar and optical bench support plate.

2.3. Sapphire Balls

As a part of the mechanism designs, a set of sapphire balls are used between Grism wheels. These sapphire balls (3mm diameter during this analysis) have high thermal conductivity at a low temperature (see Section 3.2 Material Properties) which enhance thermal conductance from to the wheels.

Figure 2. Camera Section Thermal Design
(Optical Bench Support Plate removed for clarity)

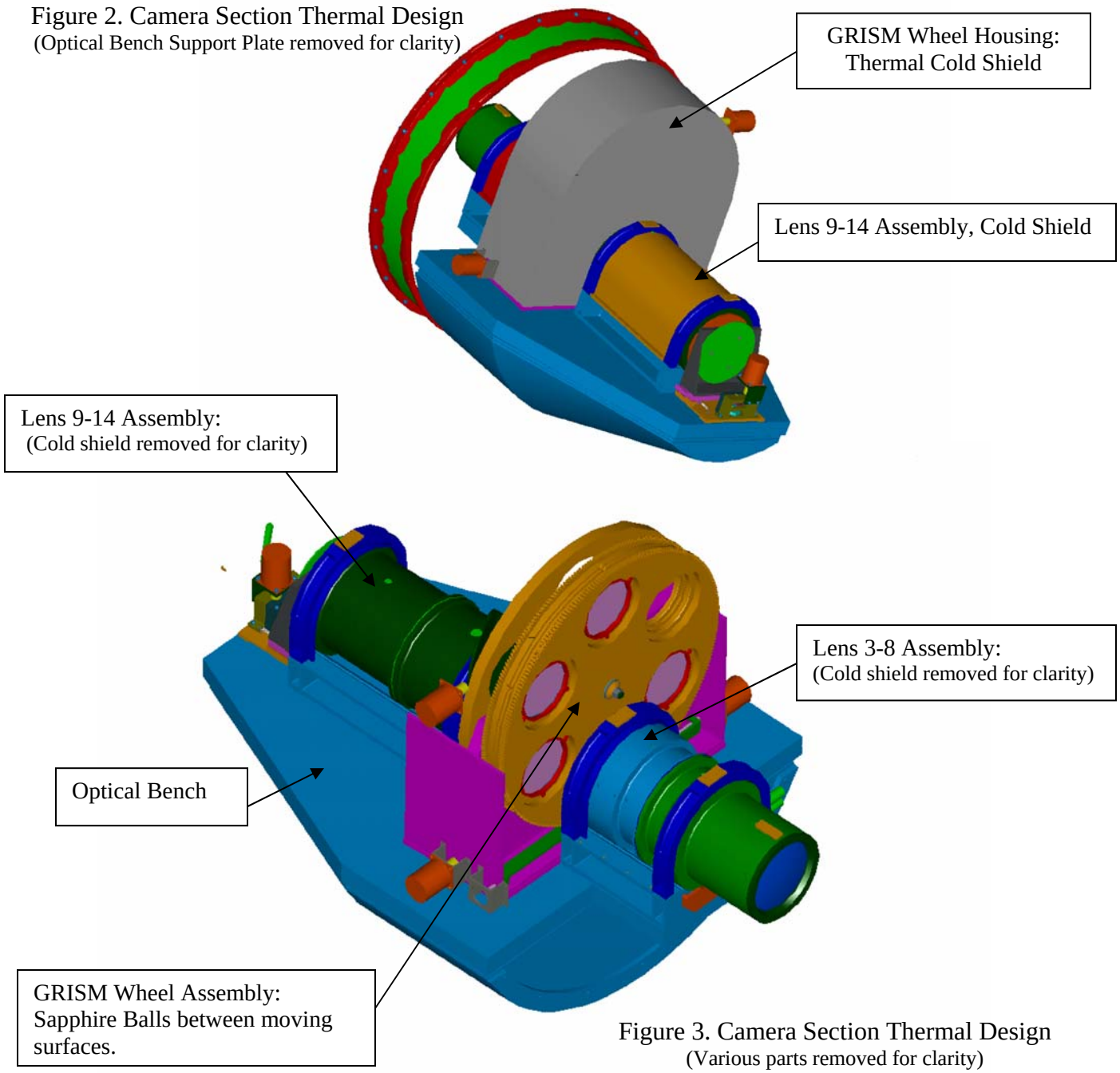

Figure 3. Camera Section Thermal Design
(Various parts removed for clarity)

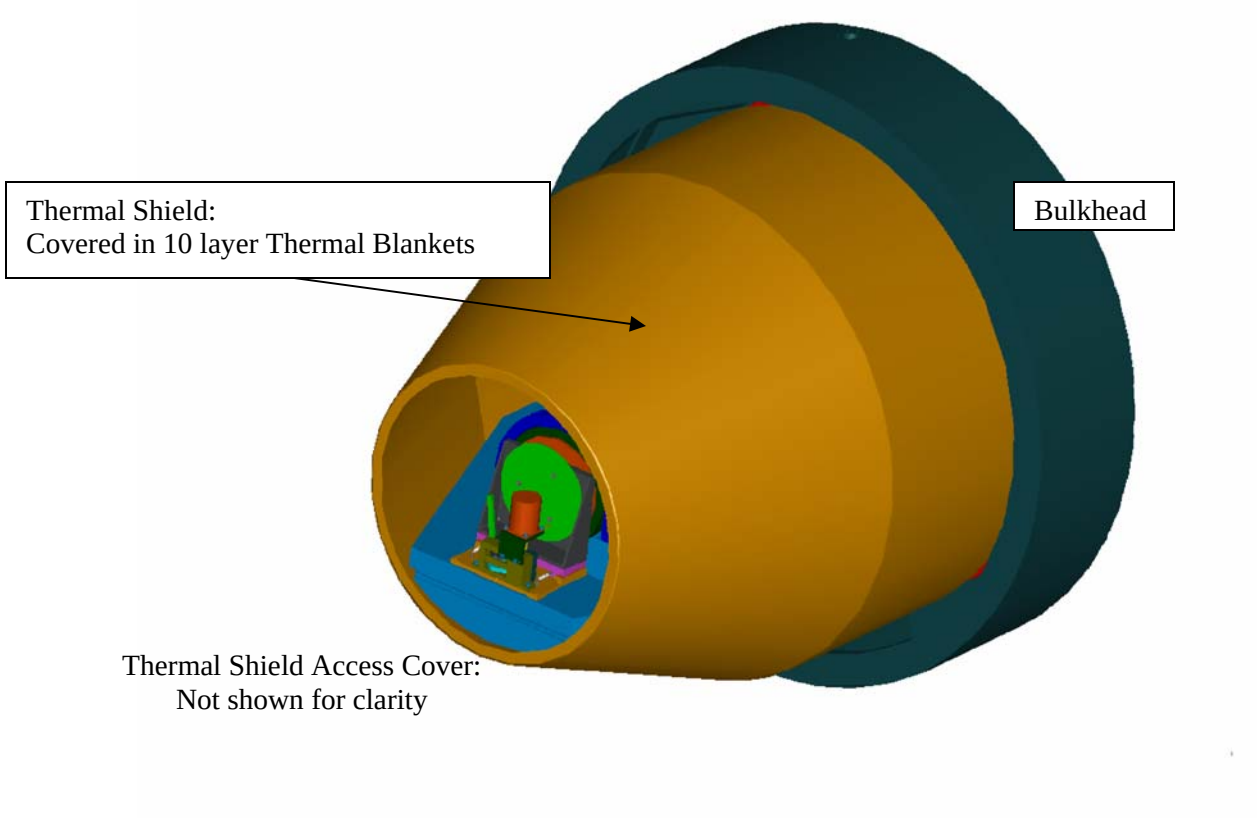

Figure 4. Camera Section Thermal Design
(Parts of the model not shown for clarity)

2.4. Thermal Shields

2.4.1. Overall Thermal Shield

The overall thermal shield as shown in Figure 4 is constructed from Aluminum Alloy, 0.040" thick and is finished with a thermal surface emissivity value of 0.1 or less on both surfaces. The external walls of the overall thermal shield are assumed to be covered with 10 layer Multi-Layer Insulation (MLI) thermal blankets to further insulate the camera section from the environmental effects. The MLI thermal blanket is made mostly of 0.0025" aluminized Mylar separated by Dacron mesh and effective emmisivity is assumed to be 0.03.

2.4.2. Lens Assembly Cold-Shield

The lens housing assemblies for lens 3-8 and 9-14 are shrouded in cold thermal shields as illustrated in Figures 1 & 2. They are constructed from Aluminum Alloy, 0.125" thick and are finished with a thermal surface emissivity value of 0.05 (Aluminized Kapton Tape, Aluminum side exposed) on the overall thermal shield facing side. The inner surface of the cold-shield is finished with black anodize, an equivalent emissivity value of 0.9.

2.4.3. Warm-up Heater

The warm-up heaters are constructed from a thin low-outgassing Kapton insulator and they are intimately mounted on the walls of the Dewar. The heaters are sized to dissipate 1500 watts and will be controlled by an Omega Heater controller in conjunction with an external power supply sufficient enough to provide 1500 watts to the heaters. The heaters will have ON/OFF set points at +25/+27°C and be able to control the warming rate to 0.2°C/min or less.

3. THERMAL MATH MODEL/THERMAL ANALYSIS

A detailed system level Camera thermal math model was generated and is depicted in the Figures 5 and 6 below. The thermal model was generated using Thermal Desktop® as a pre-and post processors. The thermal radiation heat transfer was calculated using RadCAD®. The temperatures were predicted using SINDA finite difference solver.

Included in the thermal model are the Camera vacuum Chamber, lens 3-8 assembly, lens 9-14 assembly, Grism wheel assembly, camera Dewar assembly, optical bench with a support plate and gussets, G-10 isolation ring assembly, thermal shields, and the instrument bulkhead.

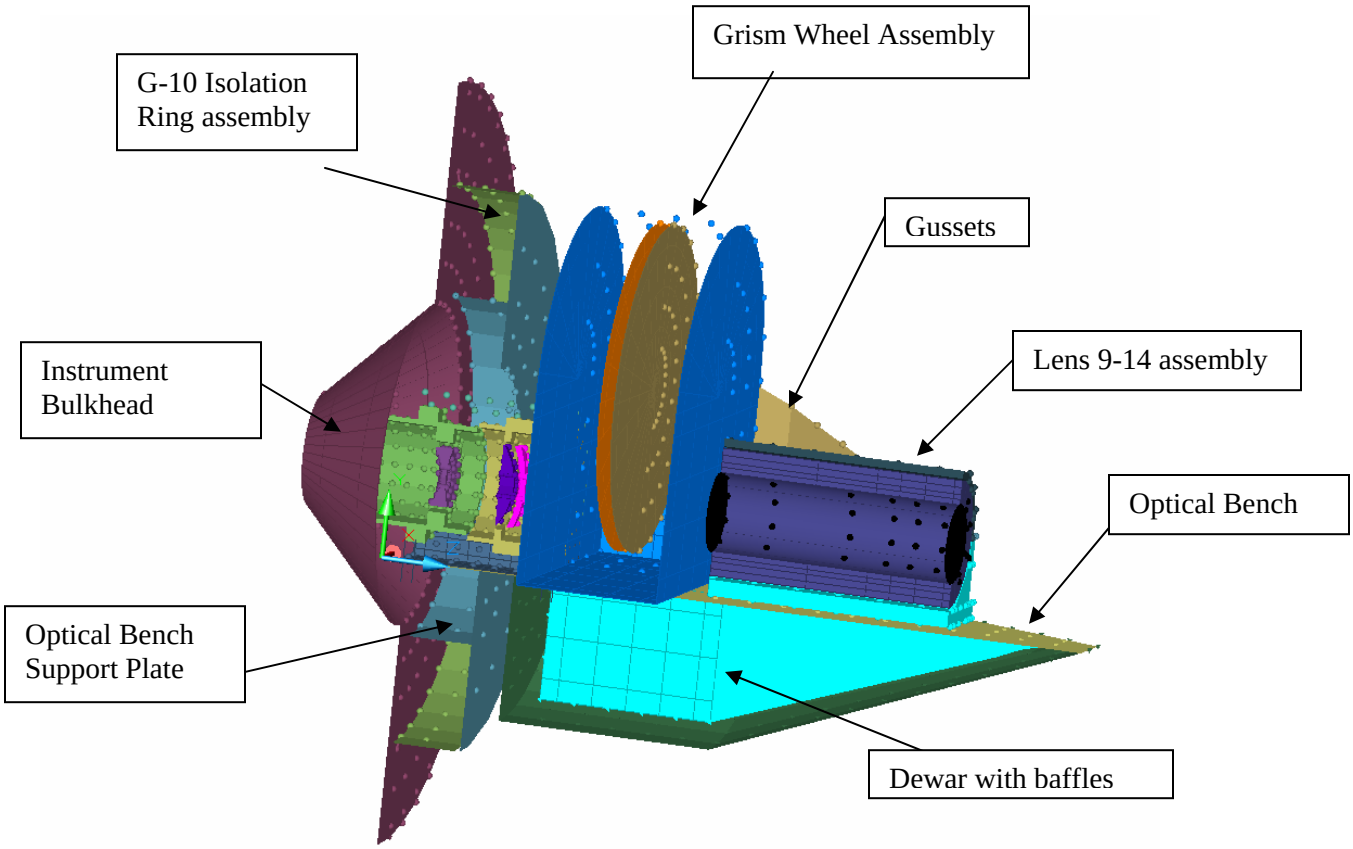

Figure 5. Detailed MMIRS Camera Overall Thermal Math Model, Cross-Sectional View
(Parts of the model not shown for clarity)

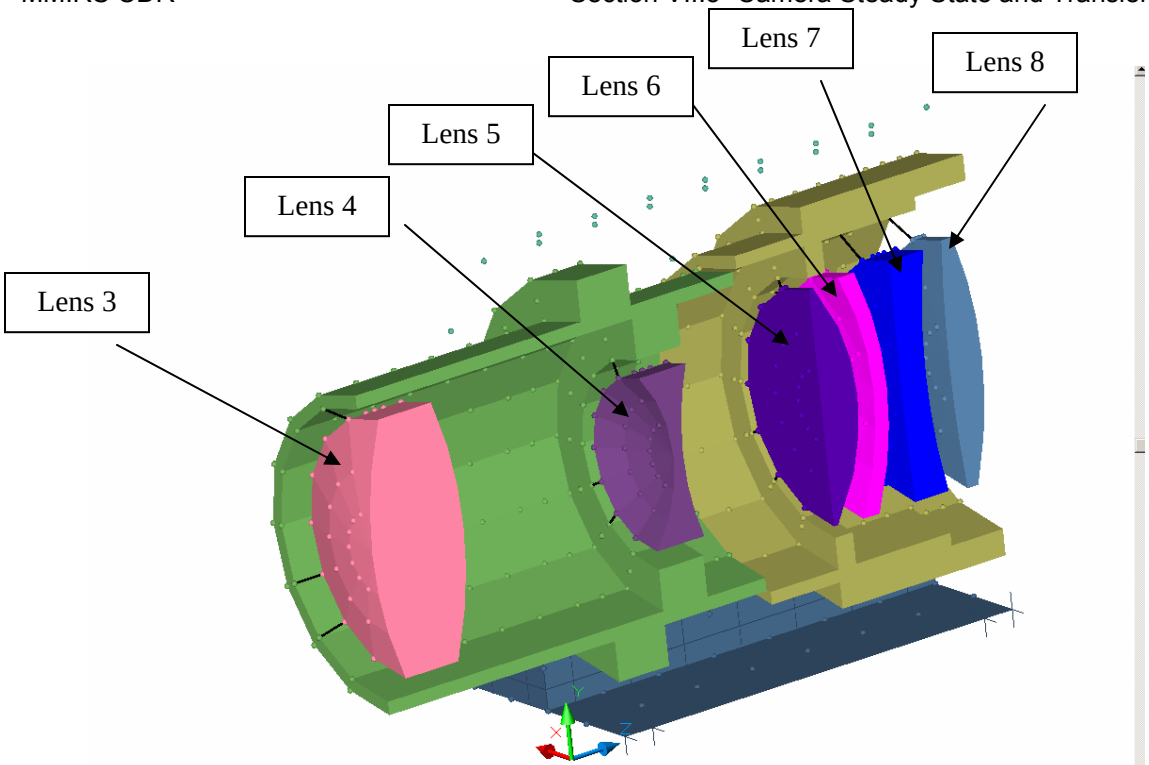

Figure 6. Detailed Camera Section, Lens 3-8 Thermal Math Model
(Parts of the model not shown for clarity)

3.1. GRISM Assembly (Prism 41-degree)
A separate thermal math model of the 41-degree Prism (Material: CaF_2), a part of the GRISM Assembly) was generated as depicted in Figure 7.

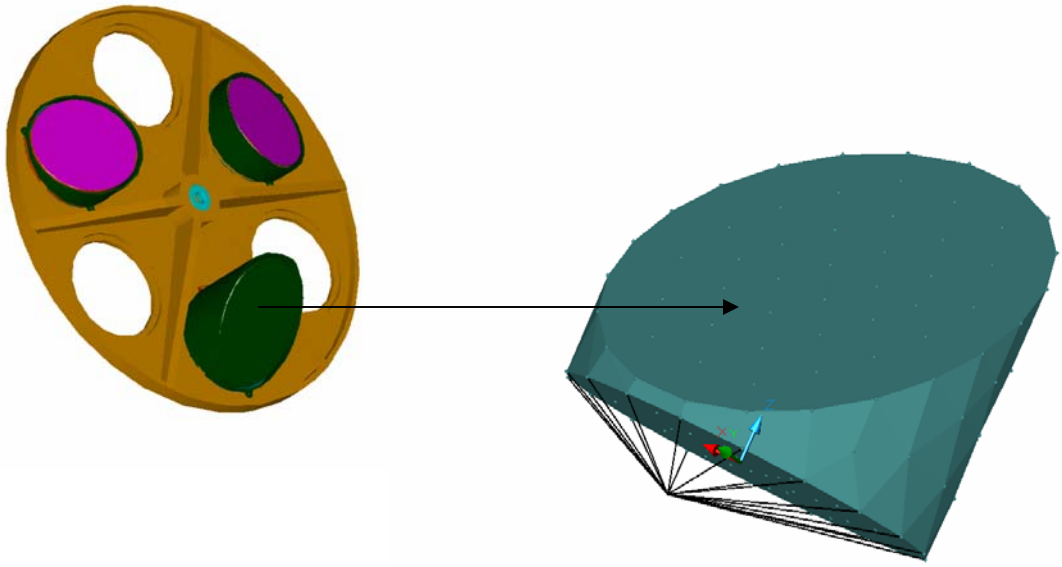

Figure 7. A separate detailed Thermal Math Model of the 41-Prism

3.2. Analysis Assumptions

3.2.1. The following are the list of assumptions used during the steady state analysis.

- Boundary temperatures:
  - Bulkhead Mounting points = +25°C
  - Local Ambient Air Temperature: +25°C
  - Convective heat transfer Coefficient = 0.00366 w/in^2-°C (5.67 w/m^2-°C)
    - At 10k feet altitude
  - No thermal radiation heat transfer from the outer shell to the local ambient.
  - Bottom edge of the LN2 Dewar including the baffles: 77K (-196°C)
- No conductive path between the hub of the Grism wheels and the center shaft bearings.

3.2.2. The following are the list of assumptions used during the transient analysis.

- Boundary temperatures:
  - Bulkhead Mounting points = +25°C
  - Local Ambient Air Temperature: +25°C
  - Convective heat transfer Coefficient = 0.00366 w/in^2-°C (5.67 w/m^2-°C)
    - At 10k feet altitude
  - No thermal radiation heat transfer from the outer shell to the local ambient.
  - LN2 Dewar including the baffles: 77K (-196°C)
- All initial temperatures are +25°C (298K)
- No conductive path between the hub of the Grism wheels and the center shaft bearings.

3.3. Material Properties

- Al Aly
  Density: 2700 Kg/m^3

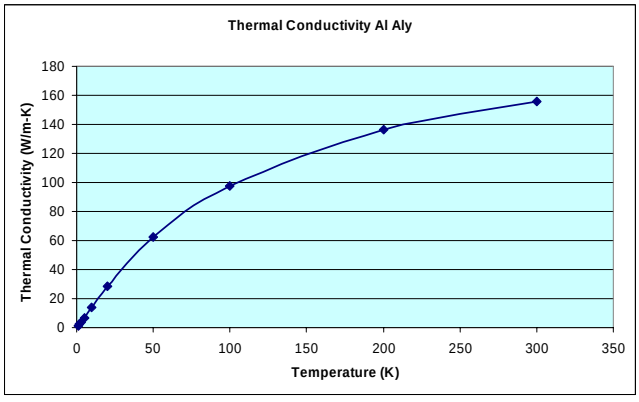

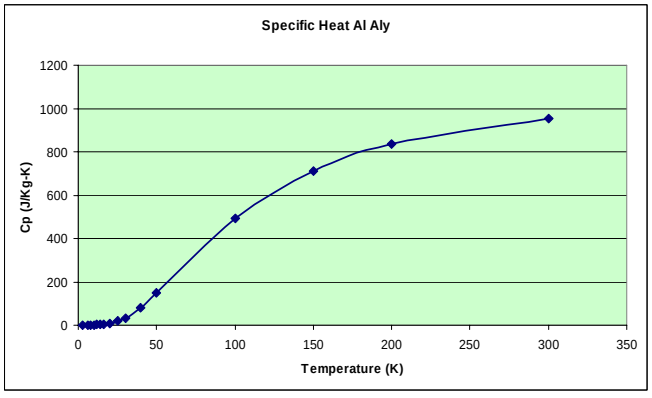

- G-10
  Density: 1790 Kg/m^3

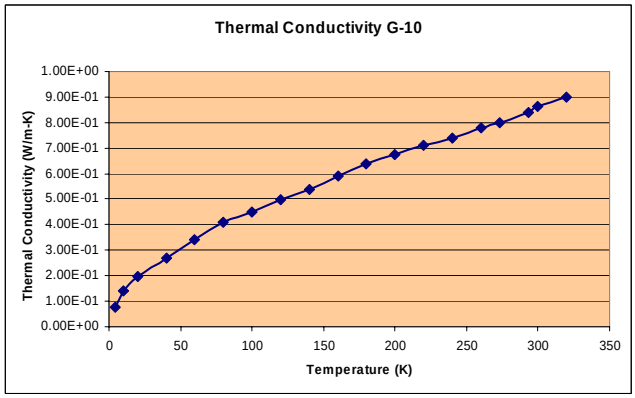

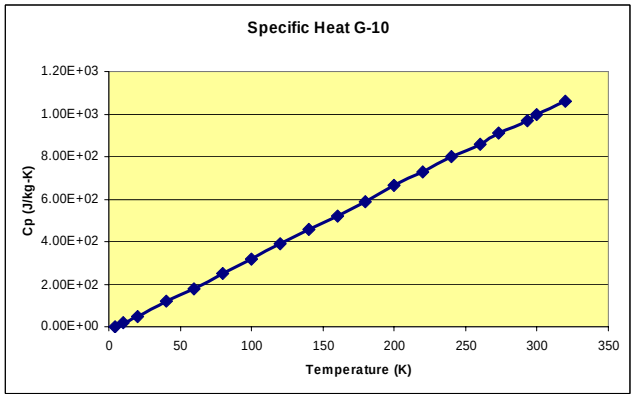

- Sapphire
  Density: 3970 Kg/m^3
  Specific Heat (Cp): 419 J/Kg-K

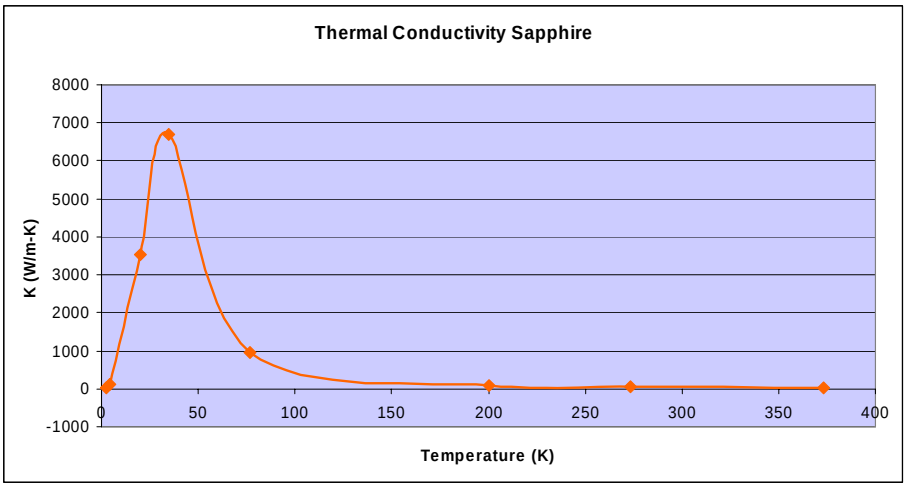

- CaF_2 (Lens 3, 4, 8, and Prisms)
  Density: 3180 Kg/m^3

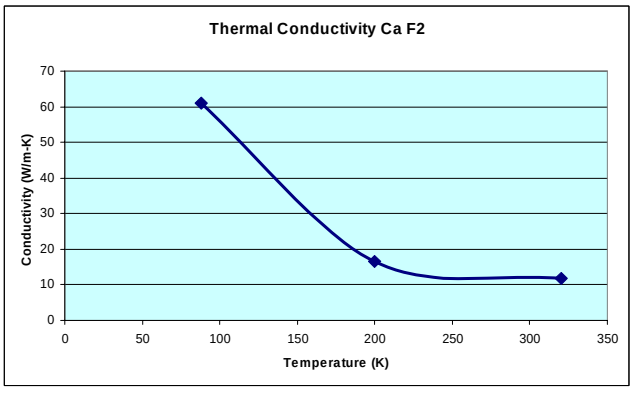

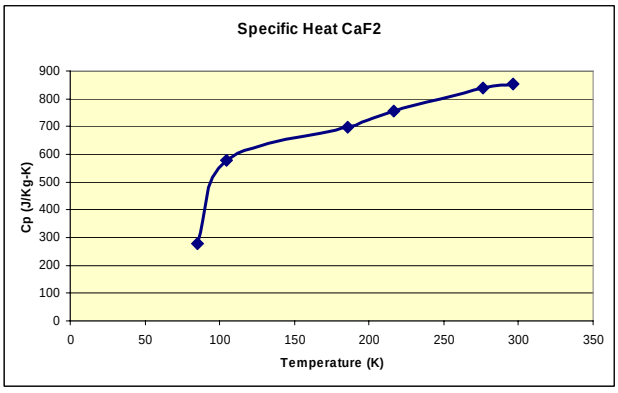

- Fused Quartz (Lens 7)
  Density: 2210 Kg/m^3

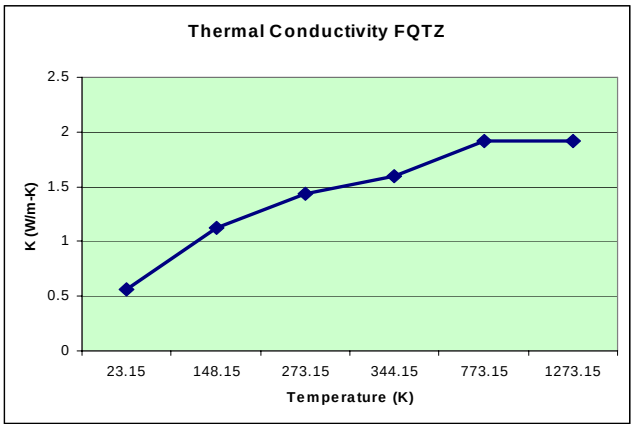

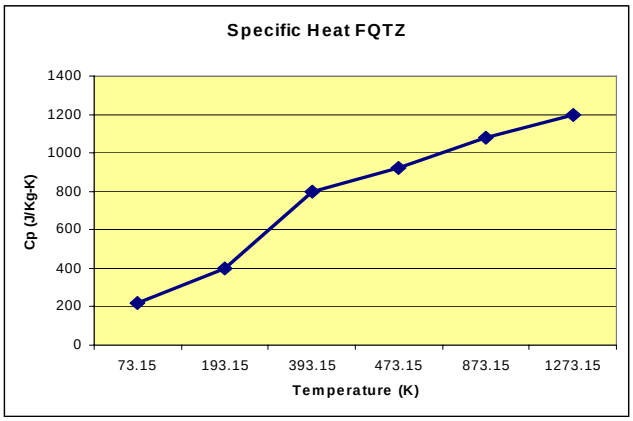

- BaF_2 (Lens 5)
  Density: 4890 Kg/m^3
  Thermal Conductivity: 11.72 w/m-K
  Specific Heat: 410 J/Kg-K

- ZnSe (Lens 6)
  Density: 5270.0 Kg/m^3
  Thermal Conductivity: 18 w/m-K
  Specific Heat: 339 J/Kg-K

- Contact Resistance
  - The following heat transfer coefficient value was obtained as per Reference 4* to calculate the contact conductance between the axial lens mounts and the lens: 1000 w/m^2-K

* Reference 4: "Spacecraft Thermal Control Handbook" Vol. I, 2nd Edition, David Gilmore, The Aerospace Press/AIAA, 2002, P259, Figure 8.11 Generalized heat-transfer coefficient vs. pressure for aluminum in vacuum.

- Bolted interfaces
  - The following thermal conductance values were obtained as per Reference 4** to calculate the heat transfer across the bolted interface based on different bolt sizes.
    - Screw 6-32: 0.42 w/K
    - Screw 8-32: 0.80 w/K
    - Screw 10-32: 1.32 w/K
    - Screw ¼-28: 3.51 w/K

** Reference 4: "Spacecraft Thermal Control Handbook" Vol. I, 2nd Edition, David Gilmore, The Aerospace Press/AIAA, 2002, P265, Table 8.4 Thermal Conductance Design Guideline from TRW

- Thermal Surface Properties

Further detailed descriptions of the thermal surface may be found in Reference 1, Camera Section Thermal Surface Finishes.

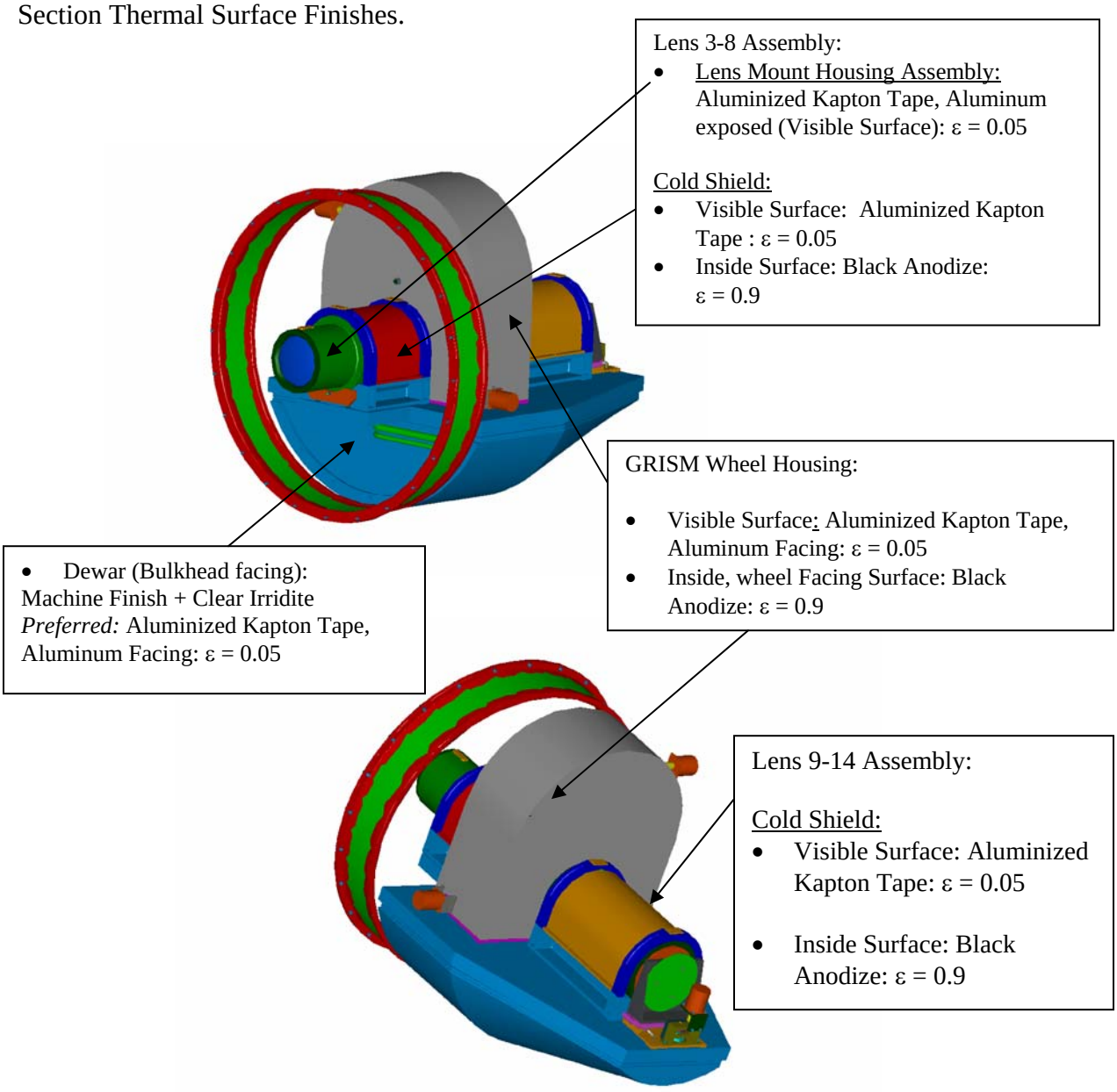

4. ANALYSIS RESULTS

The results of the analysis are presented in the following paragraphs. The results are presented in 2 parts, namely, steady state temperatures and transient temperature profiles.

4.1. Steady State Temperatures

Illustrated in the following figures 8 thru 10 are the steady state temperatures of the camera section.

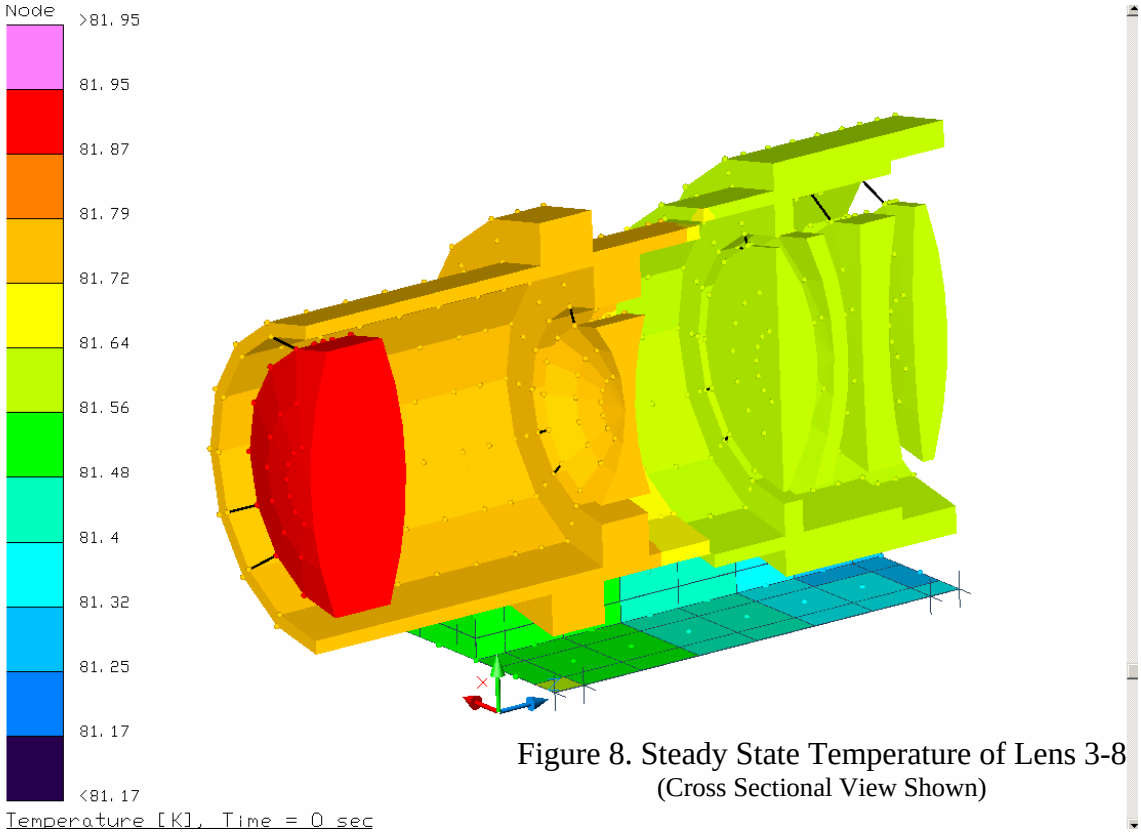

Figure 8. Steady State Temperature of Lens 3-8
(Cross Sectional View Shown)

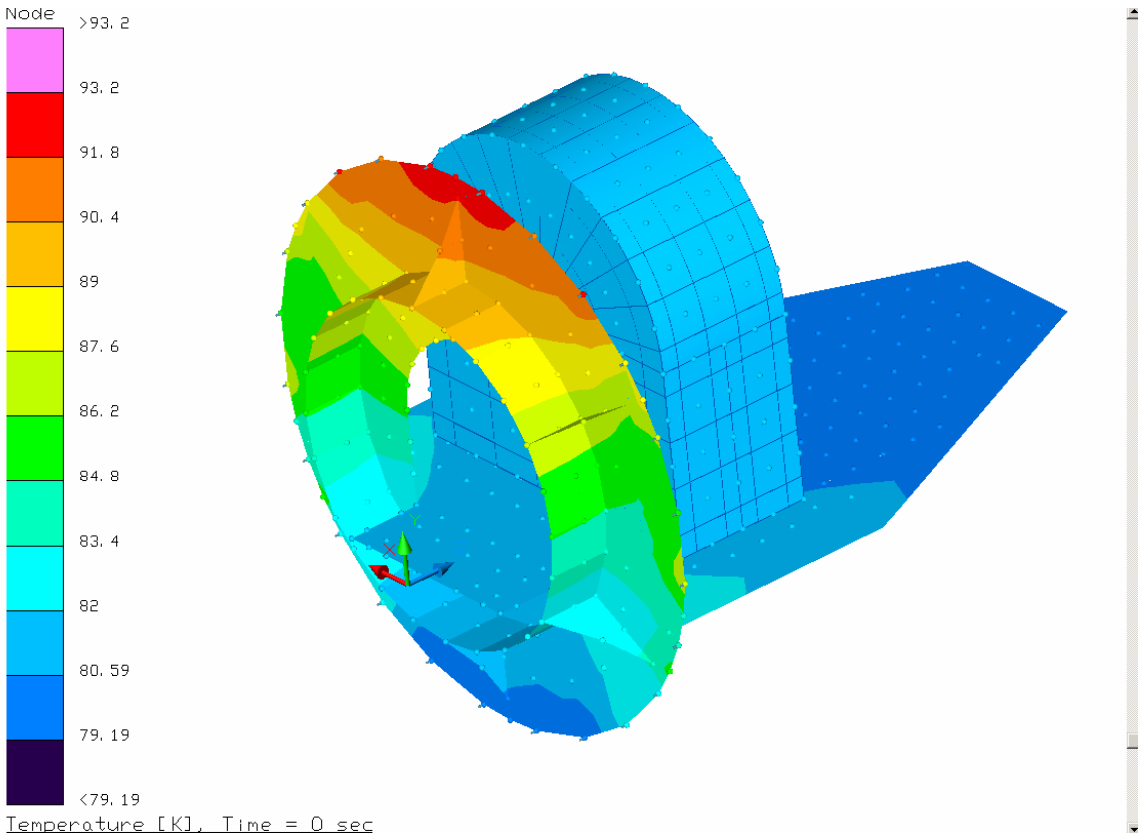

Figure 9. Steady State Temperature of the Major Structures of the Camera

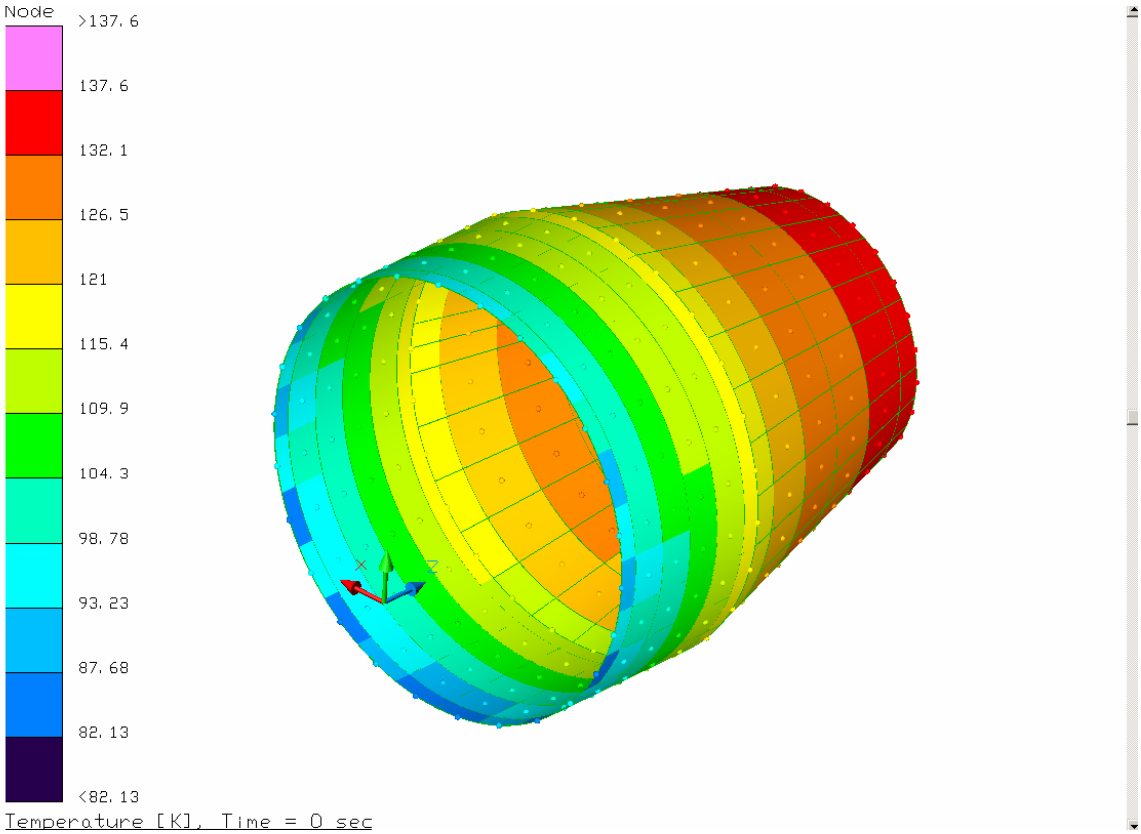

Figure 10. Steady State Temperatures of the Overall Cold-Shield

Using the boundary condition derived from the system level model, the detailed thermal math model of the 41-degree Prism predicted the following results as shown in Figure 10 and 10a.

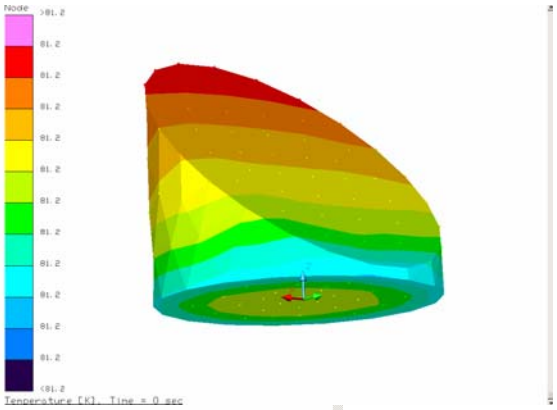

Figure 10a. Steady State Temperatures of 41-degree Prism (81.2K Calculated)

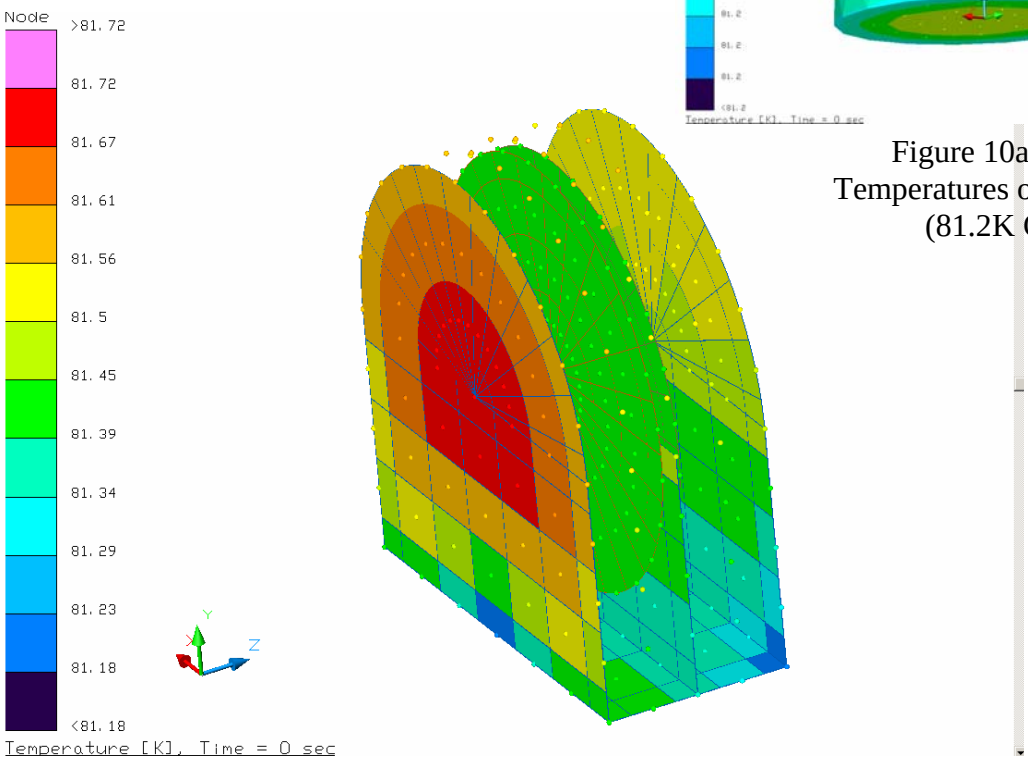

Figure 10. Steady State Temperatures of GRISM Assembly

In addition to the steady state temperature, the thermal math model of the Camera section has predicted that 35.4 watts of thermal load was absorbed from the environment. Based on the energy balance from the model, a total of 7.9 watts were conducted in from the bulkhead mounting points and 27.5 watts were absorbed via convective heat transfer to the Camera vacuum chamber outer walls.

4.2. Transient temperature Profiles

The transient results are presented in 2 parts:

- Case 1. During the cooling period of the Camera section.
- Case 2. During the warming period of the Camera section.

As stated previously, the requirement for the transient analysis is to maintain the lens temperature gradient below the requirements as depicted in Table 1 during the cool-down and warm-up of the instrument. As seen from the Table 1 the Lens 3 and 4 have the tightest temperature gradient requirements thus the presented results of this analysis are limited to those lens.

Also worth noting is that the transient temperature profile of the prisms in the Grism assembly is a subject of a separate report.

4.2.1. Case 1: The cooling profile of the Camera Lens.

The results of a parametric study as a part of the cooling period are presented herein. This parametric study was performed to compare the lens temperature gradients as a result of the optical bench cooling rate at 0.5°C/min (Case 1.1) and 0.2°C/min (Case 1.2).

4.2.1.1. Case 1.1: Camera Optical Bench Cooling rate at 0.5°C/min

Shown in Graph 1 and Figure 10 are the transient temperature response of the Lens 3 during a cooling down rate at 0.5°C/min. Shown in Graph 2 and Figure 11 are the transient temperature response of the Lens 4 during a cooling down rate at 0.5°C/min. However, it is evident that the cooling rate of 0.5°C/min will produce temperature gradients that are not acceptable when compared with the design requirements.

GRAPH 1: Lens #3, Camera Optical Bench Cooling rate at 0.5C/min
(Temperature K vs. Time Sec.)

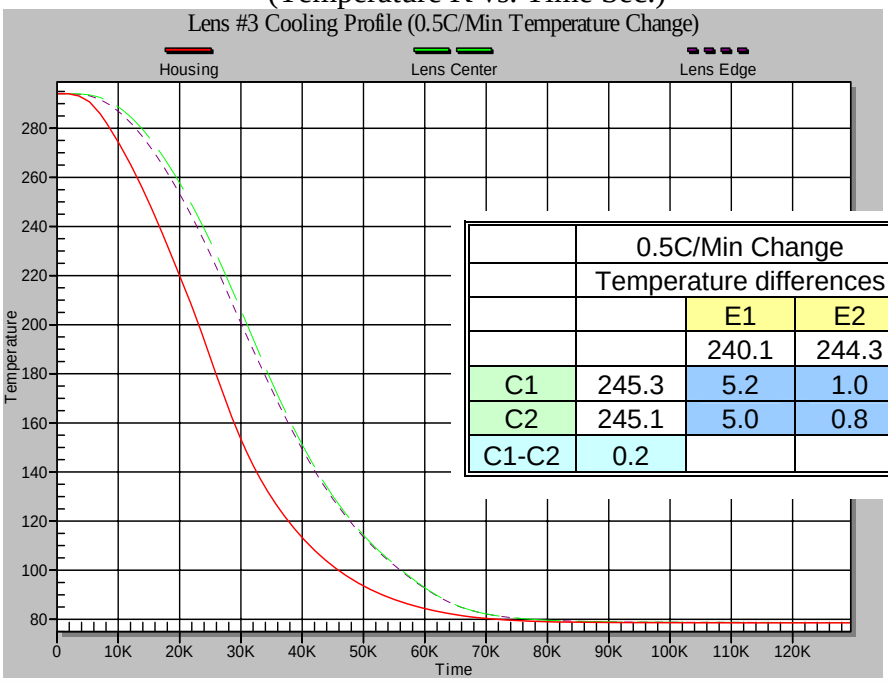

	0.5C/Min Change Temperature differences			
		E1	E2	E2-E1
		240.1	244.3	4.2
C1	245.3	5.2	1.0	
C2	245.1	5.0	0.8	
C1-C2	0.2			

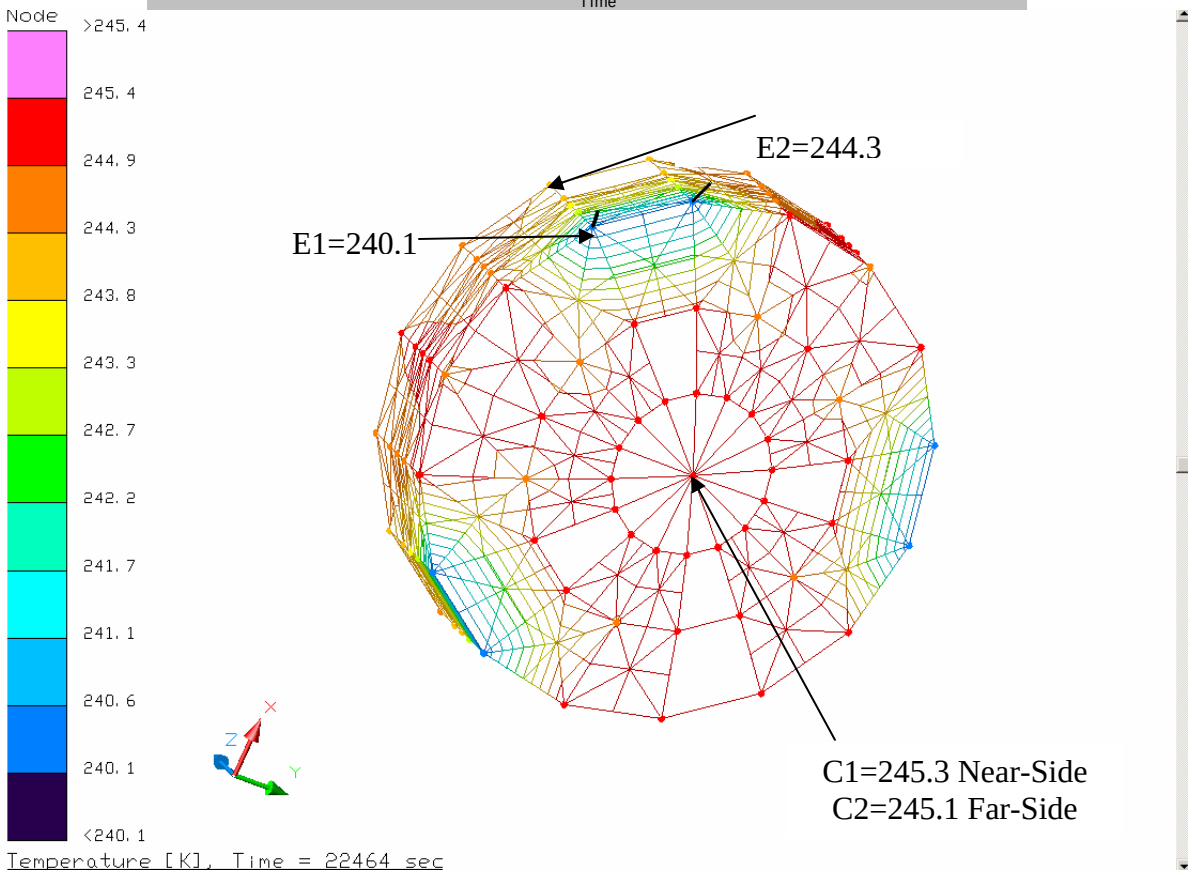

Figure 10. Lens 3 Temperature distributions during cool-down rate at 0.5C/min

GRAPH 2: Lens #4, Camera Optical Bench Cooling rate at 0.5C/min
(Temperature K vs. Time Sec.)

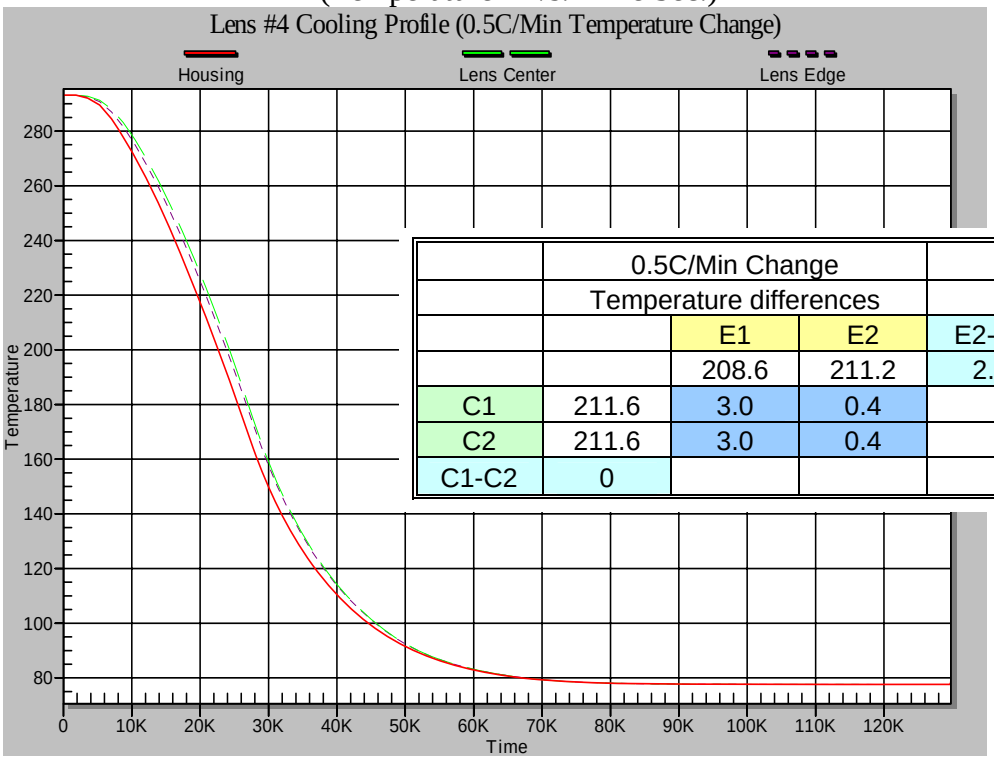

	0.5C/Min Change Temperature differences			
		E1	E2	E2-E1
		208.6	211.2	2.6
C1	211.6	3.0	0.4	
C2	211.6	3.0	0.4	
C1-C2	0			

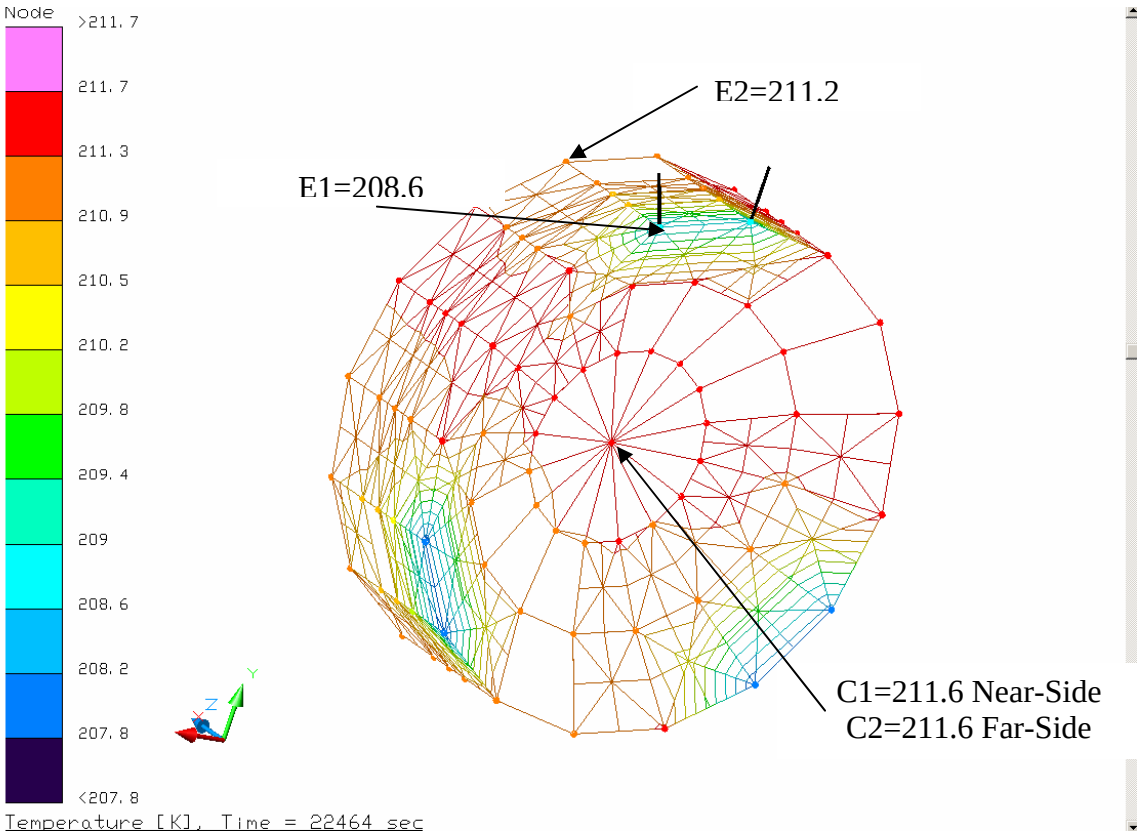

Figure 11. Lens 4 Temperature distributions during cool-down rate at 0.5C/min

4.2.1.2. Case 1.2: Camera Optical Bench Cooling rate at 0.2C/min

Shown in Graph 3 and Figure 12 are the transient temperature response of the Lens 3 during a cooling down rate at 0.2°C/min. Shown in Graph 4 and Figure 13 are the transient temperature response of the Lens 4 during a cooling down rate at 0.2°C/min.

GRAPH 3: Lens #3, Camera Optical Bench Cooling rate at 0.2C/min (Temperature K vs. Time Sec.)

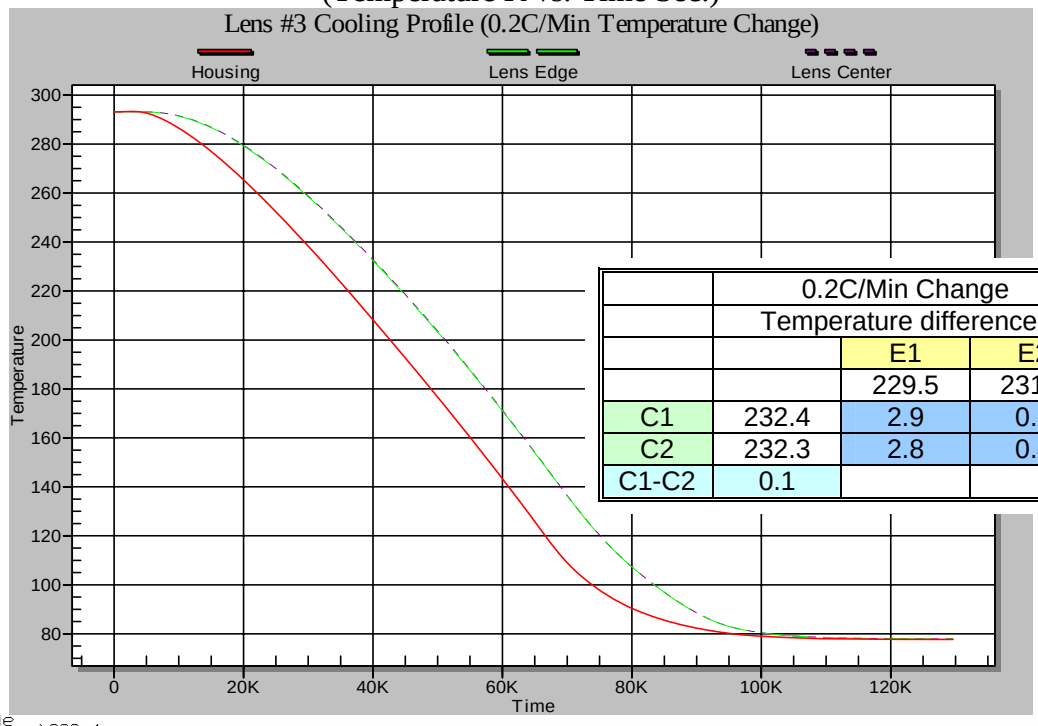

	0.2C/Min Change Temperature differences			
		E1	E2	E2-E1
		229.5	231.9	2.4
C1	232.4	2.9	0.5	
C2	232.3	2.8	0.4	
C1-C2	0.1			

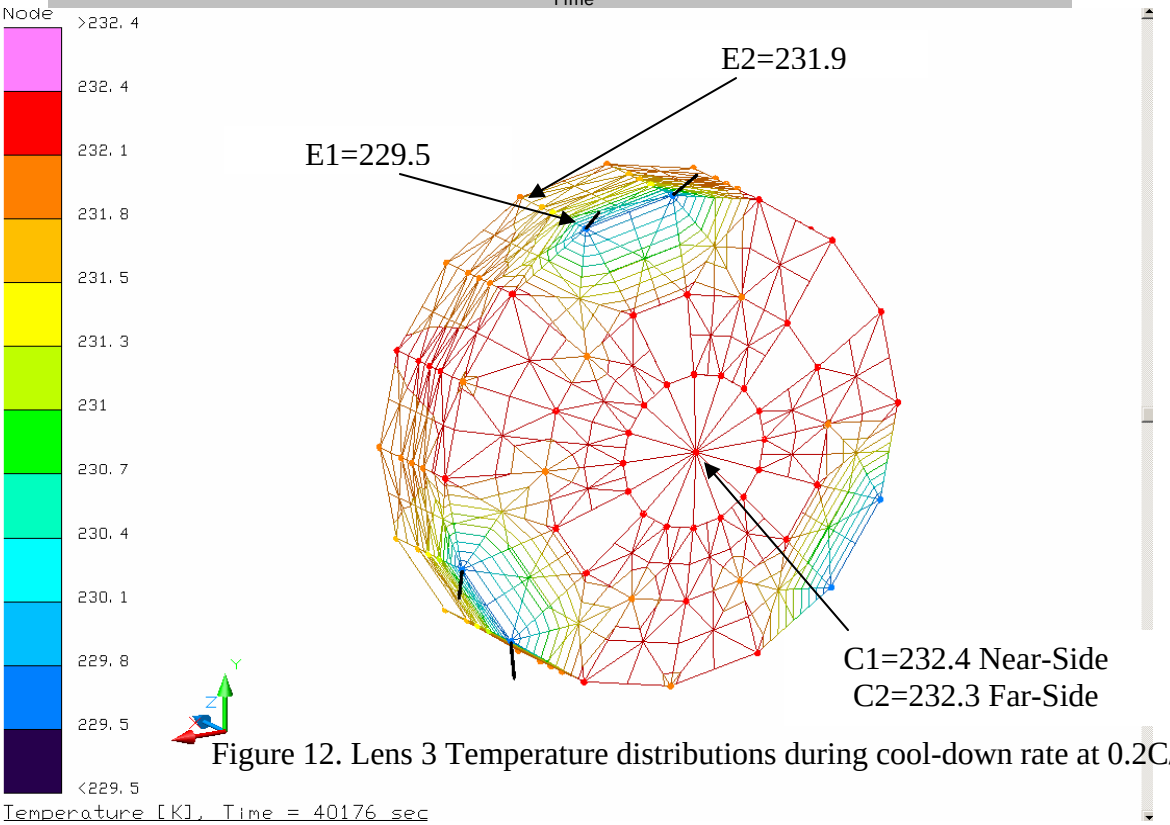

Figure 12. Lens 3 Temperature distributions during cool-down rate at 0.2C/min

GRAPH 4: Lens #4, Camera Optical Bench Cooling rate at 0.2C/min
(Temperature K vs. Time Sec.)

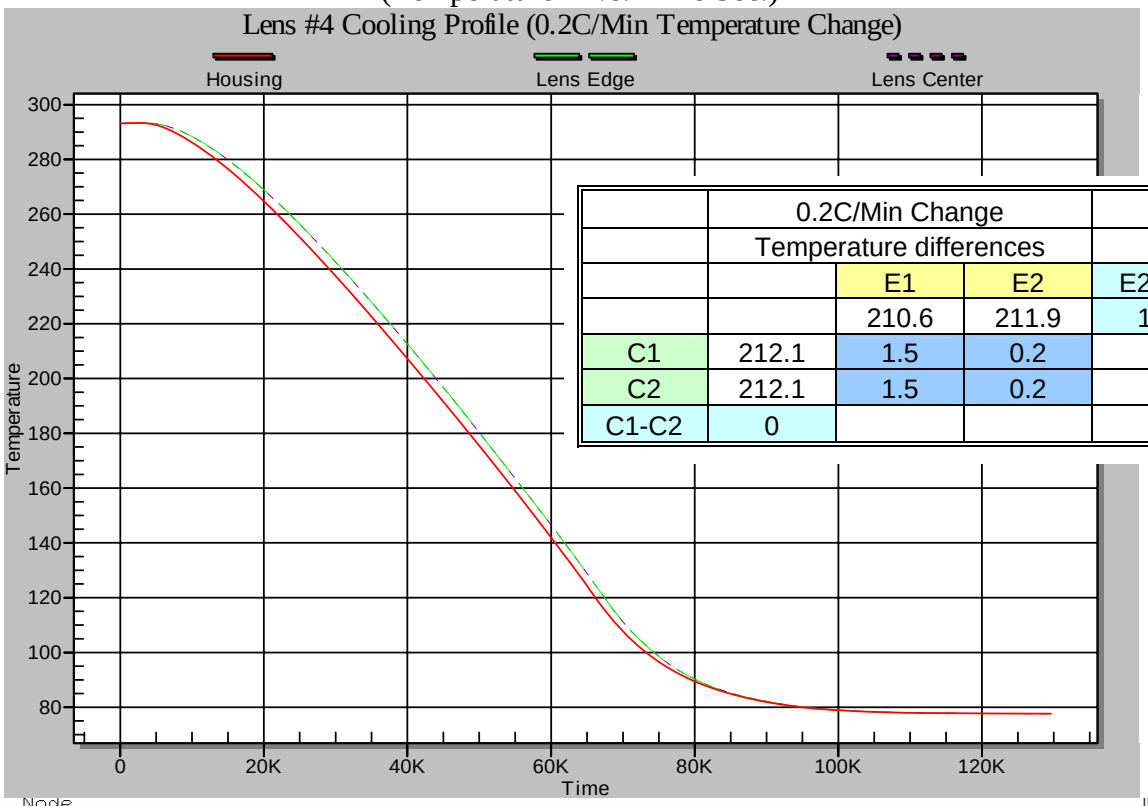

	0.2C/Min Change			
	Temperature differences			
		E1	E2	E2-E1
		210.6	211.9	1.3
C1	212.1	1.5	0.2	
C2	212.1	1.5	0.2	
C1-C2	0			

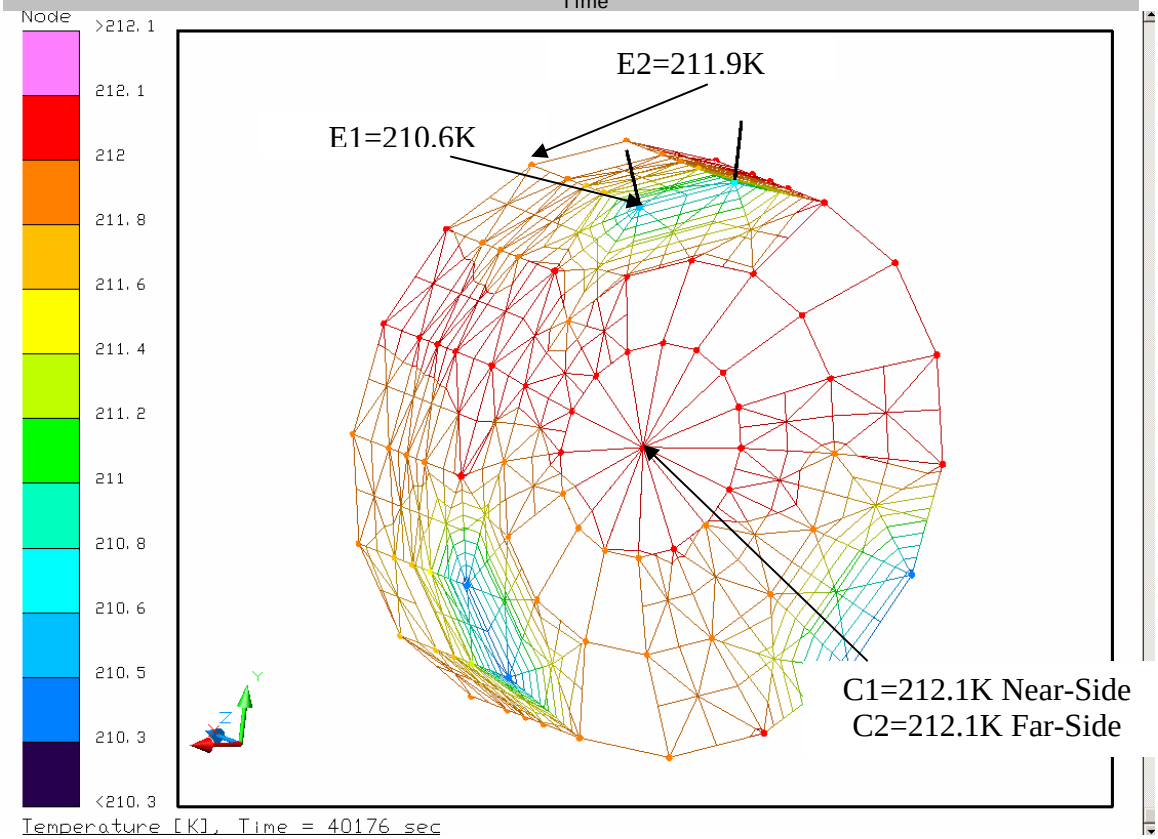

Figure 13. Lens 4 Temperature distributions during cool-down rate at 0.2C/min

4.2.2. Case 2: The warming profile of the Camera Lens

Shown in Graph 5 and Figure 14 are the transient temperature response of the Lens 3 during a warming rate at 0.2°C/min. Shown in Graph 6 and Figure 15 are the transient temperature response of the Lens 4 during a warming rate at 0.2°C/min.

GRAPH 5: Lens #3, Camera Optical Bench Warming rate at 0.2C/min (Temperature K vs. Time Sec.)

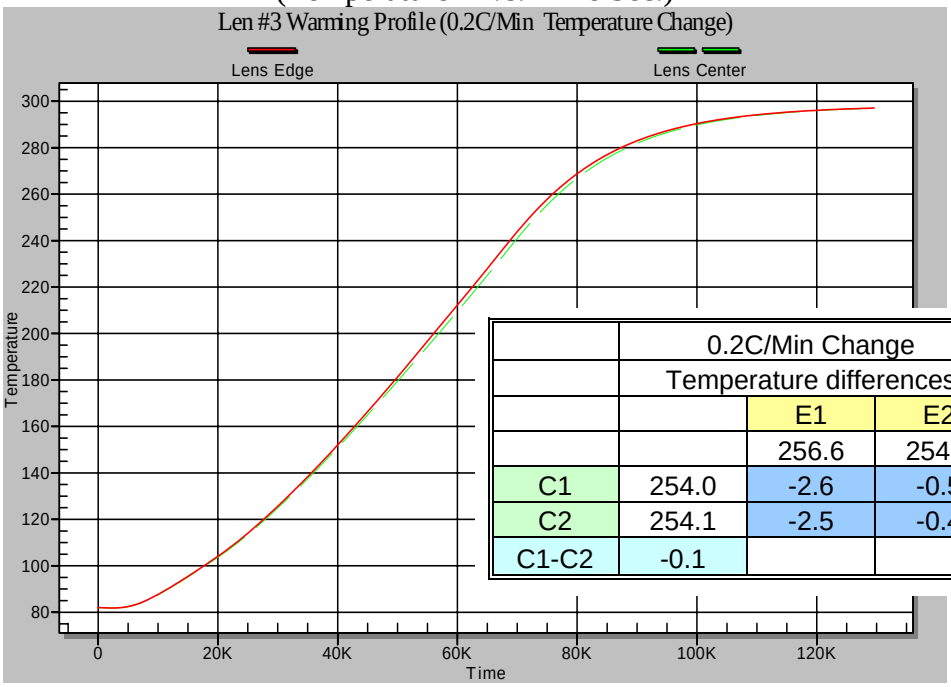

	0.2C/Min Change			
	Temperature differences			
		E1	E2	E2-E1
		256.6	254.5	-2.1
C1	254.0	-2.6	-0.5	
C2	254.1	-2.5	-0.4	
C1-C2	-0.1			

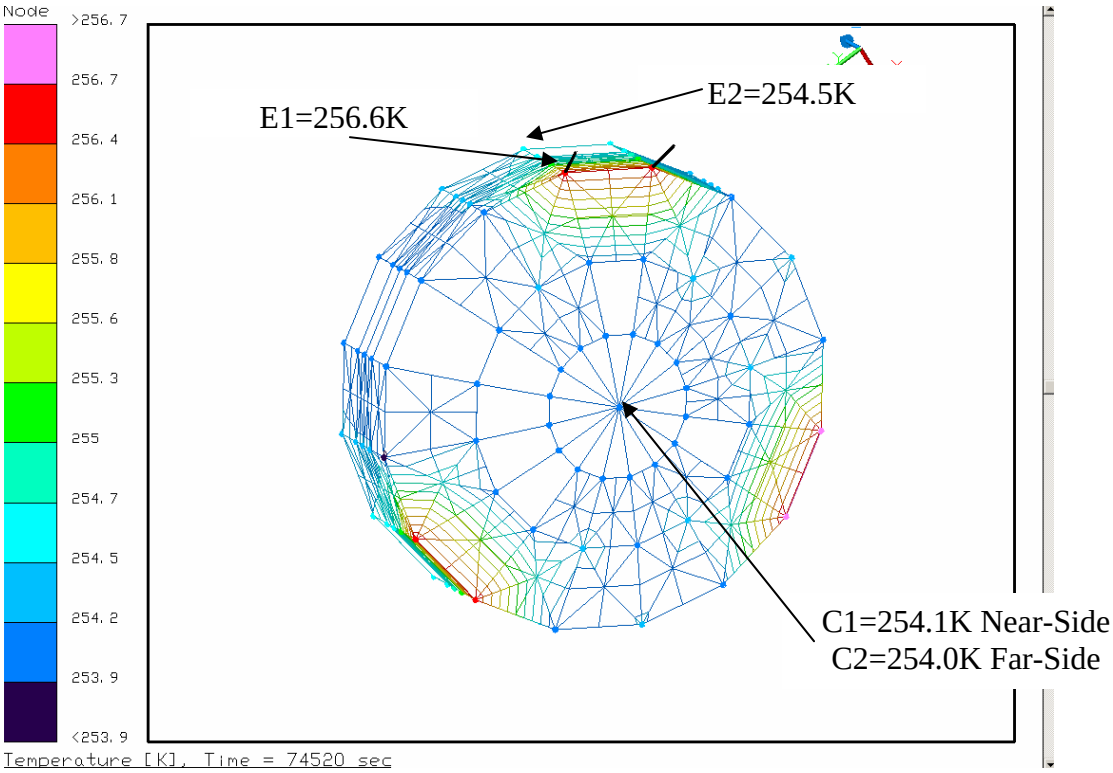

Figure 14. Lens 3 Temperature distributions during warm-up rate at 0.2C/min

GRAPH 6: Lens #4, Camera Optical Bench Warming rate at 0.2C/min
(Temperature K vs. Time Sec.)

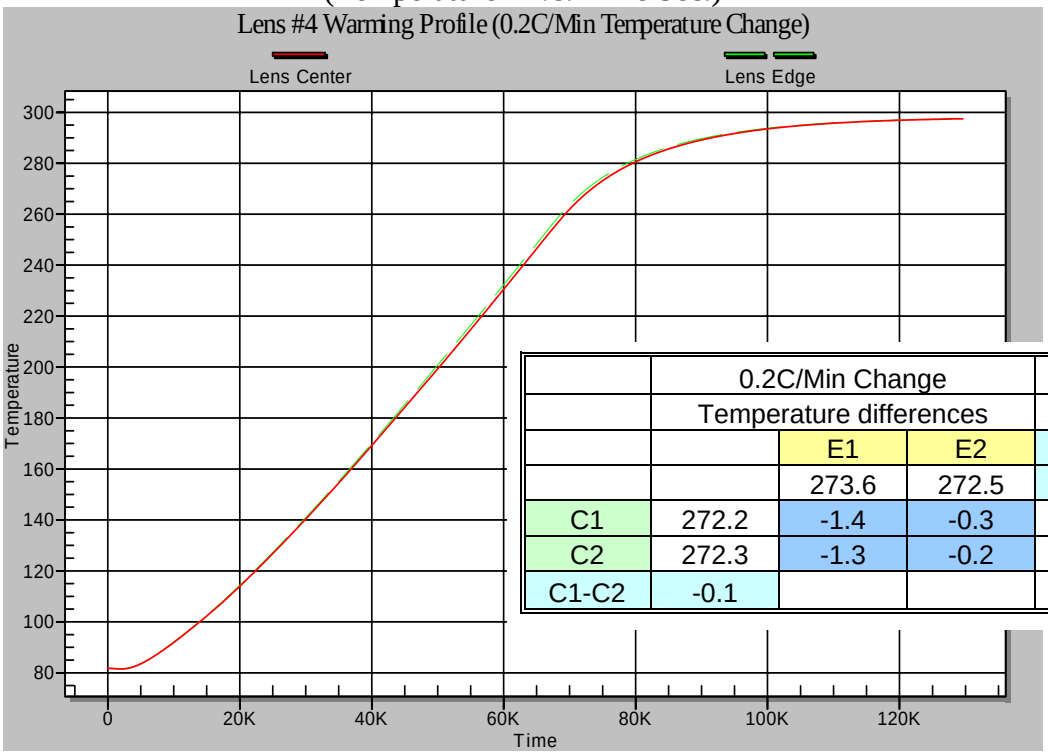

	0.2C/Min Change Temperature differences			
		E1	E2	E2-E1
		273.6	272.5	-1.1
C1	272.2	-1.4	-0.3	
C2	272.3	-1.3	-0.2	
C1-C2	-0.1			

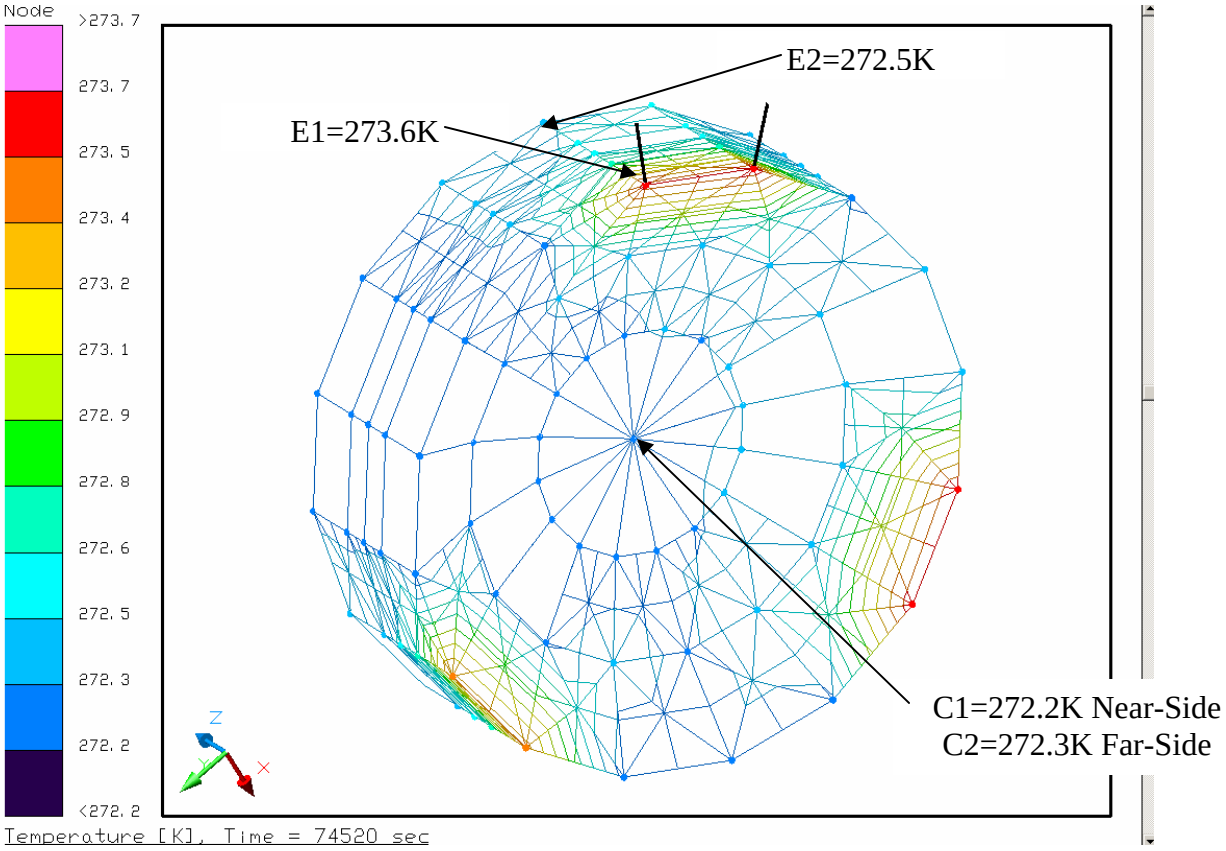

Figure 15. Lens 4 Temperature distributions during warm-up rate at 0.2C/min

4.2.3. Grism Transient analysis results

Shown in Graph 7 is the result of transient analysis of 41-degree prism during a cool-down rate of 0.2C/min.

GRAPH 7: Grism Assembly Transient Cooling Profile
(Temperature K vs. Time Sec.)

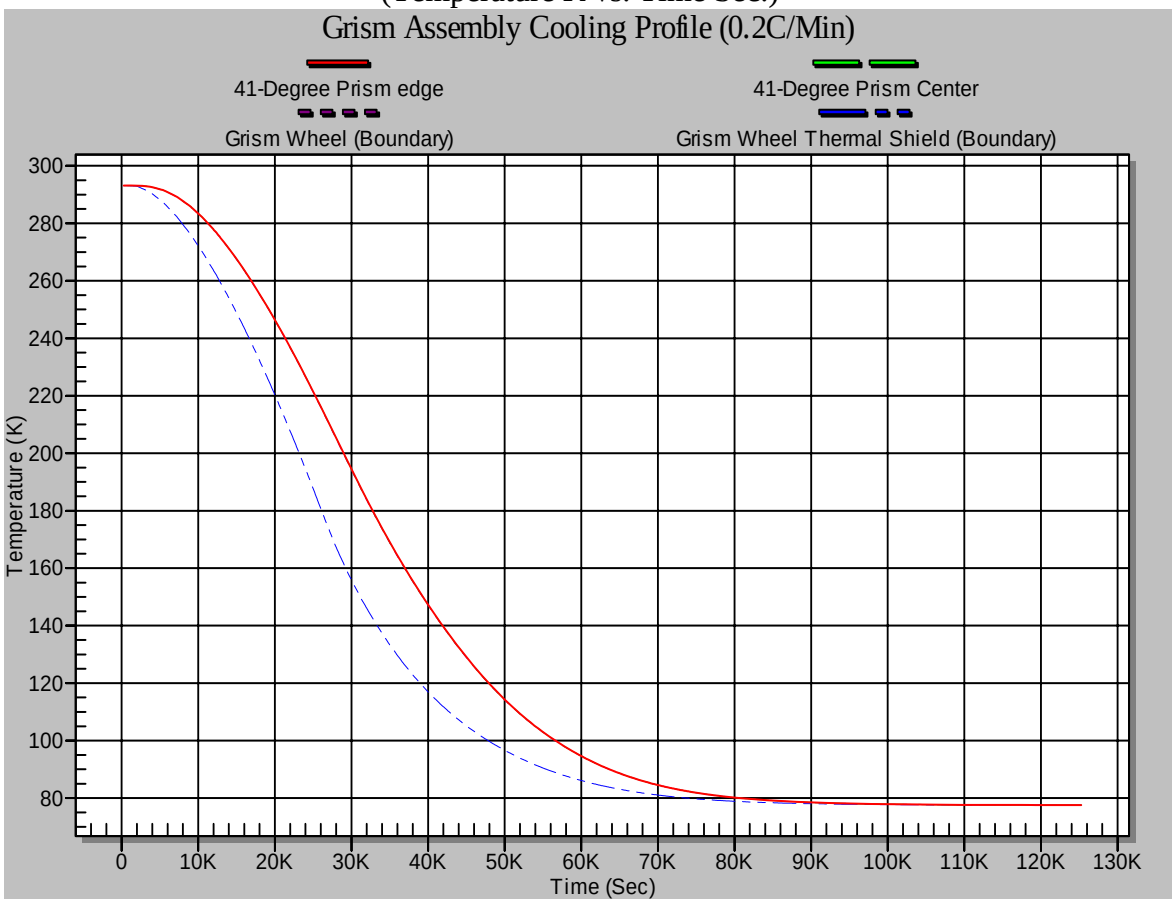

5. CONCLUSION / RECOMMENDATION

5.1. Steady State Analysis

This analysis has shown that all lens are expected to be between 77K (-196°C) and 83K (-190°C) at a steady state condition with the LN_2 boiling temperature is at 77K. This satisfies the steady state lens temperature requirement of 80.0 +/-3K. Also, the Grism assembly is expected to reach at an average steady state temperature of 81K (-192°C).

The Camera LN_2 Dewar is sufficient to provide at least 40 hours of hold-time, a design requirement. This analysis has calculated that approximately 35.4 watts of thermal load was absorbed from the environment via the natural convection on the chamber outer wall surfaces and through the conductive heat transfer at the bulkhead mounting points. Based

on only the environment thermal load, the current design will provide 63.6 hours of hold-time at +25°C ambient with 50 liters of LN_2.

5.2. Transient Analysis

This analysis has assumed that the optical bench temperature may be controlled at a specified rate and also that there's no temperature gradient within the optical bench. The results of the transient analysis has shown that the optical bench cooling rate must be less than 0.2°C/min in order to maintain the desirable temperature gradients within each lens as depicted in Table 1. The Lens 3 is required to be maintained less than 2.18°C radial gradient and this analysis has predicted the worst case gradient to be 2.9°C, slightly above the requirement. The Lens 4 is required to be maintained less than 1.39°C radial gradient and this analysis has predicted the worst case gradient to be 1.5°C, slightly above the requirement.

Also, during the warming period, the warming rate must be less than 0.2°C/min in order to maintain the desirable temperature gradients within each lens. The Lens 3 is required to be maintained less than 2.18°C radial gradient and this analysis has predicted the worst case gradient to be 2.6°C, slightly above the requirement. The Lens 4 is required to be maintained less than 1.39°C radial gradient and this analysis has predicted the worst case gradient to be 1.4°C.

Due to the sensitive nature of the lens materials, it is strongly recommended that a thermal test be performed before the final instrument is built to further understand the thermal transient behaviors of the instrument.

Harvard-Smithsonian Center for Astrophysics
Smithsonian Astrophysical Observatory
Central Engineering

Document No. MMIRS-SP032805A Rev -

To: George Nystrom
From: Sang Park (Thermal Engineer)
Date: 28 March 2005

CC: Justin Holwell, Brian McLeod, Paul Martini, Henry Bergner, Ken McCracken, Mike Buke, Tim Norton, John Boczenowski, Bill Podgorski

Subject: MMIRS Camera Section Thermal Surface Finishes

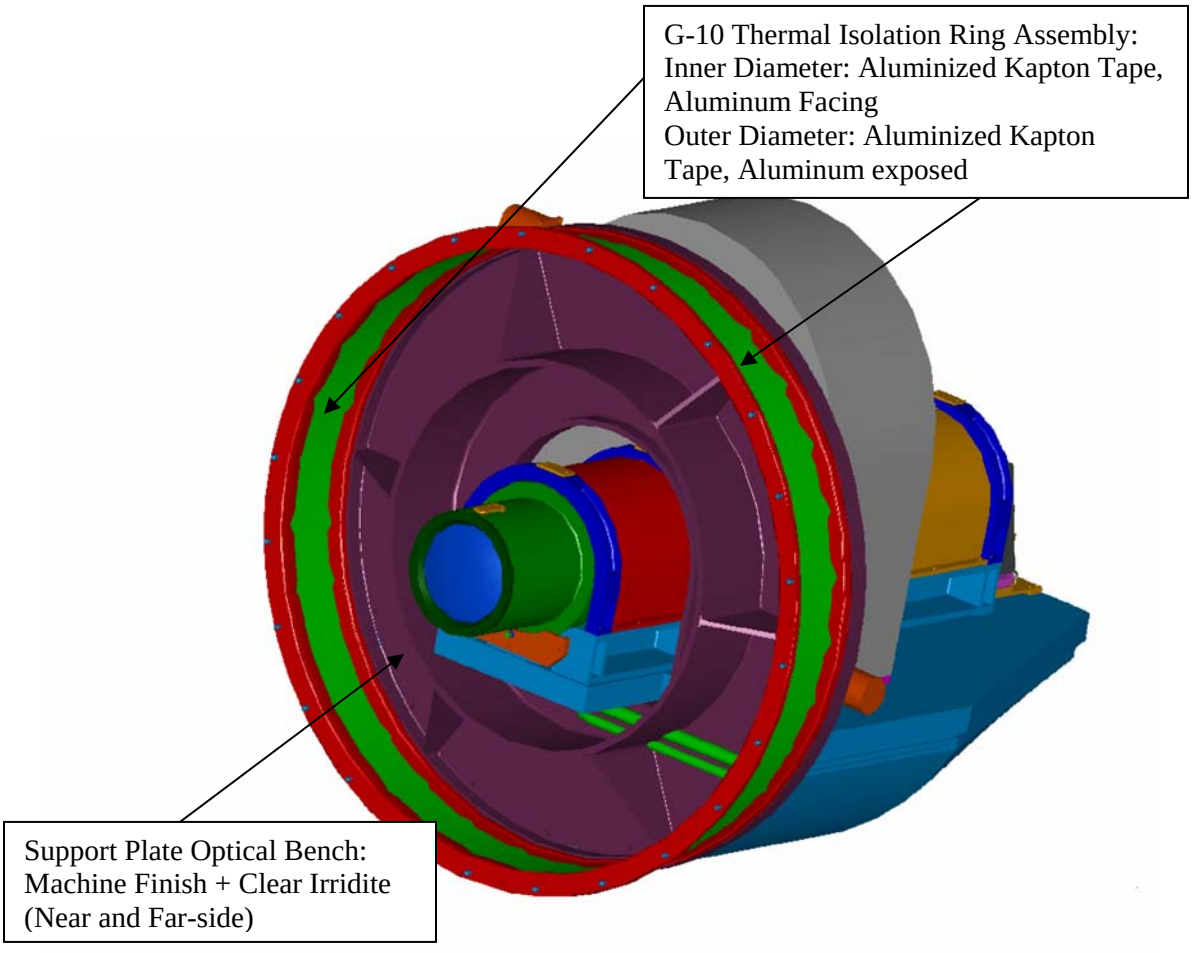

Lens 3-8 Assembly:
Lens Mount Housing Assembly:
Aluminized Kapton Tape,
Aluminum exposed (Visible Surface)

Cold Shield:
Visible Surface:
Aluminized Kapton Tape
Inside Surface: Black Anodize

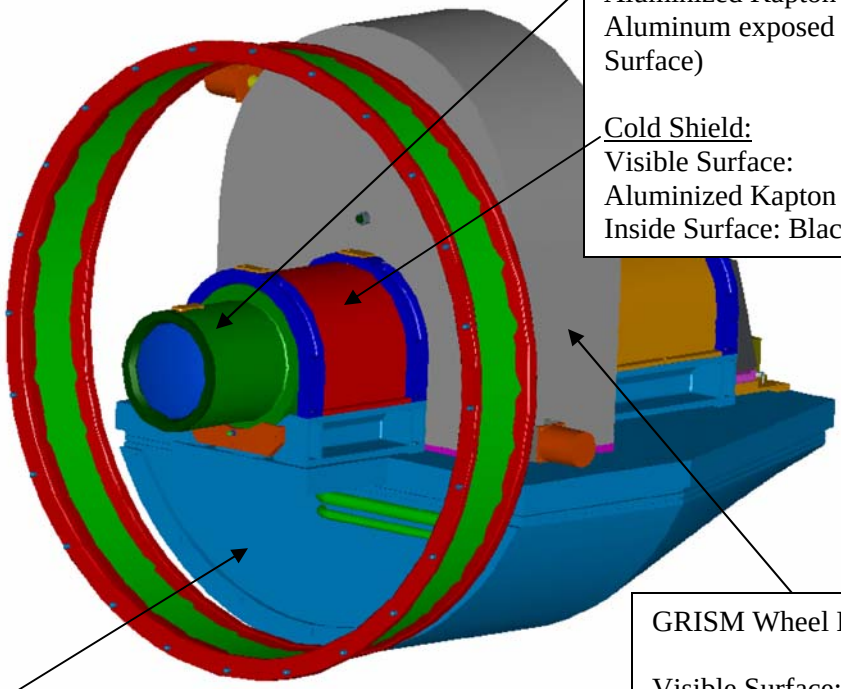

GRISM Wheel Housing:

Visible Surface: Aluminized Kapton Tape, Aluminum Facing

Inside, wheel Facing Surface:
Black Anodize

Dewar (Bulkhead facing):
Machine Finish + Clear Irridite
Preferred: Aluminized Kapton Tape, Aluminum Facing

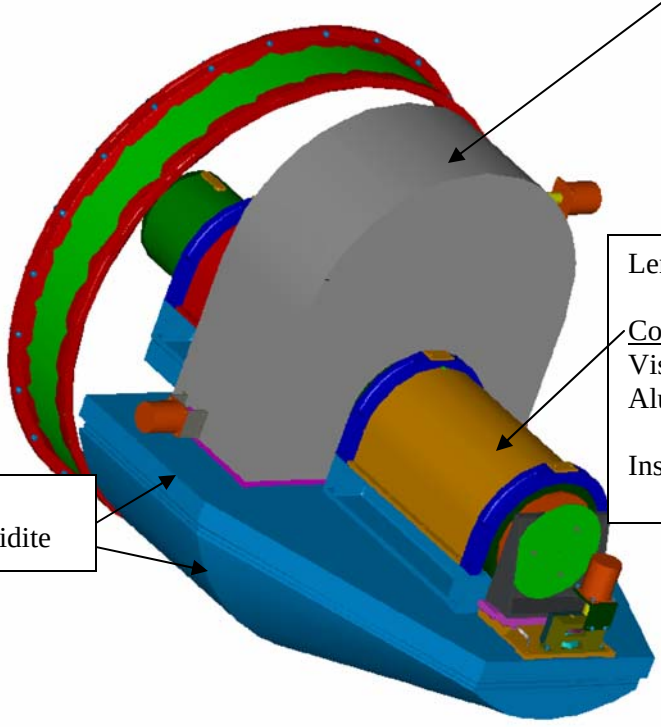

Lens 9-14 Assembly:

Cold Shield:
Visible Surface:
Aluminized Kapton Tape

Inside Surface: Black Anodize

Optical Bench / Dewar:
Machine Finish + Clear Irridite

Lens 9-14 Assembly:
Inside Surfaces: Black Anodize
(Cold shield removed for clarity)

Lens 3-8 Assembly:

Inside Surfaces: Black Anodize
(Cold shield removed for clarity)

Lens Mount Housing Assembly:
Aluminized Kapton Tape
(Visible Surface)

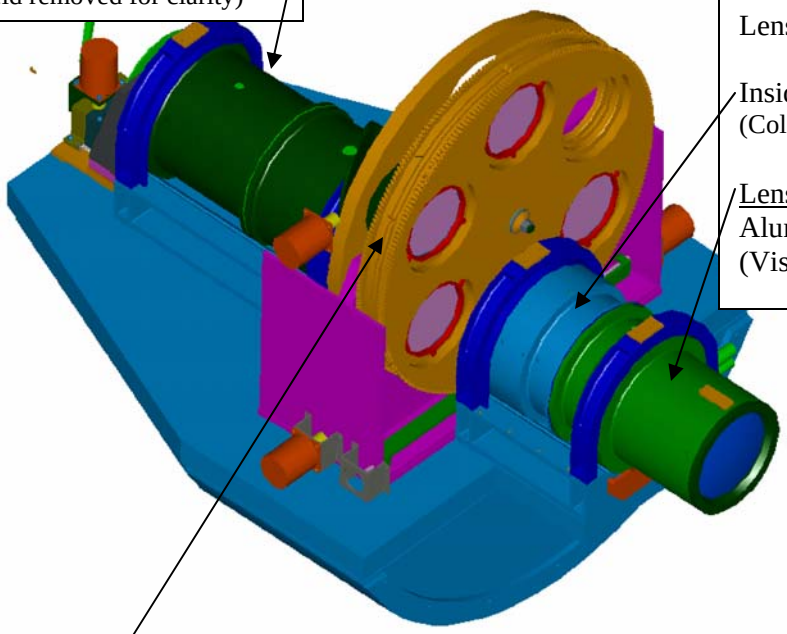

GRISM Wheel Assembly:

All Internal Surfaces: Black Anodize

Lens 9-14 Assembly:
Inside Surfaces: Black Anodize
(Cold shield removed for clarity)

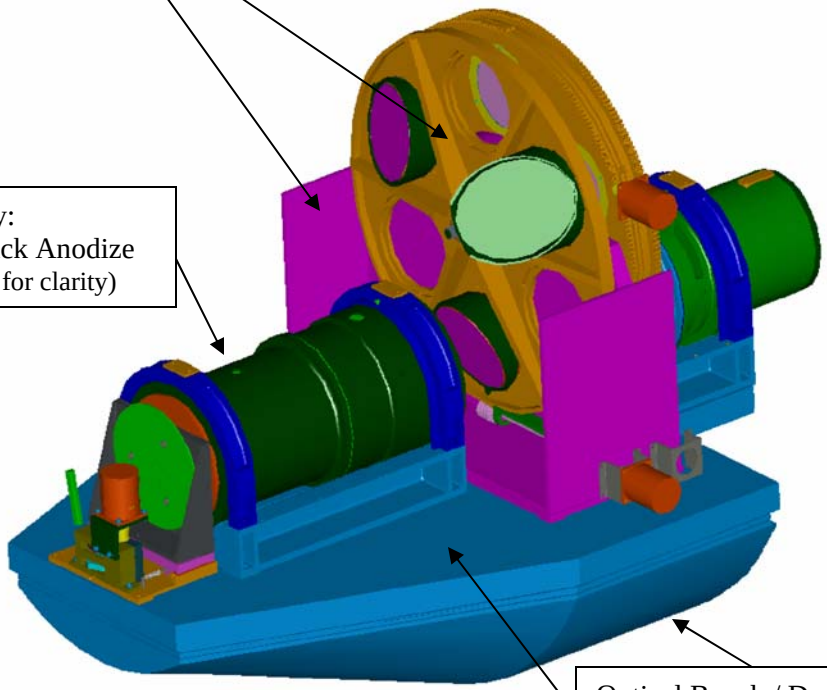

Optical Bench / Dewar:
Machine Finish + Clear Irridite

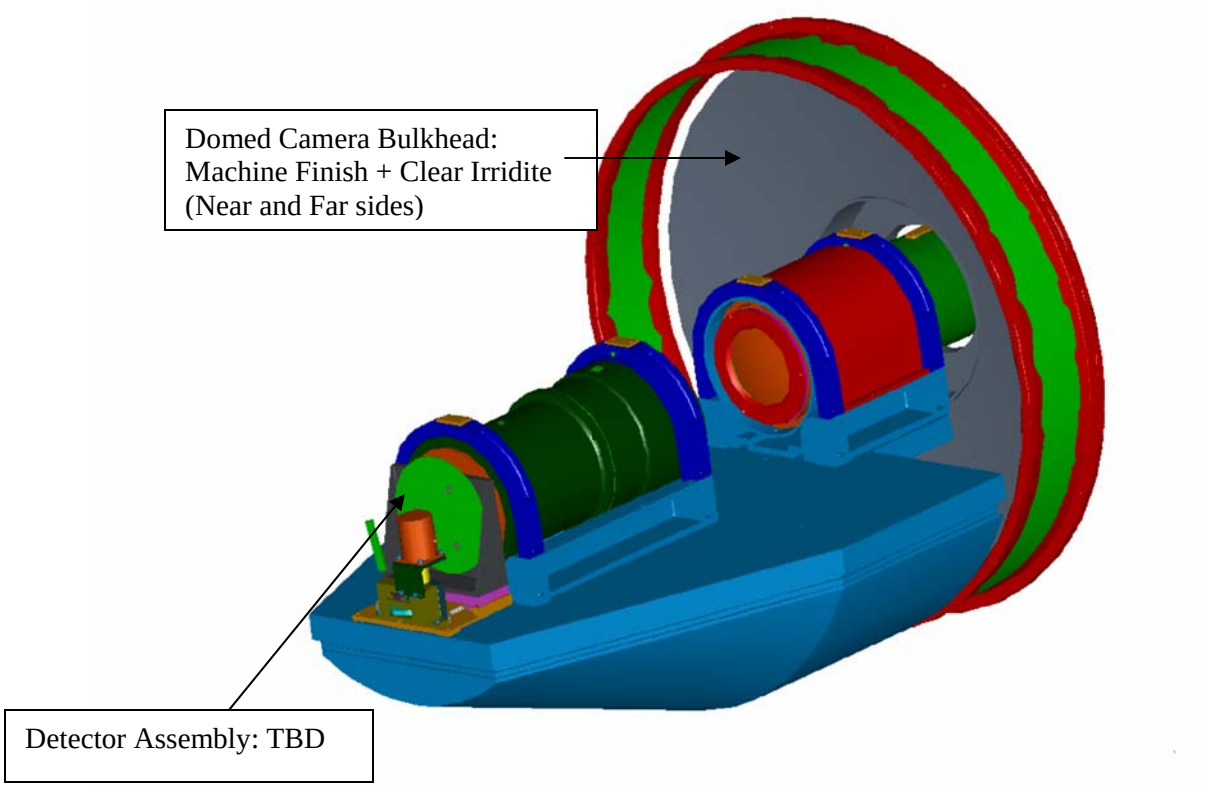
Domed Camera Bulkhead:
Machine Finish + Clear Irridite
(Near and Far sides)
Detector Assembly: TBD

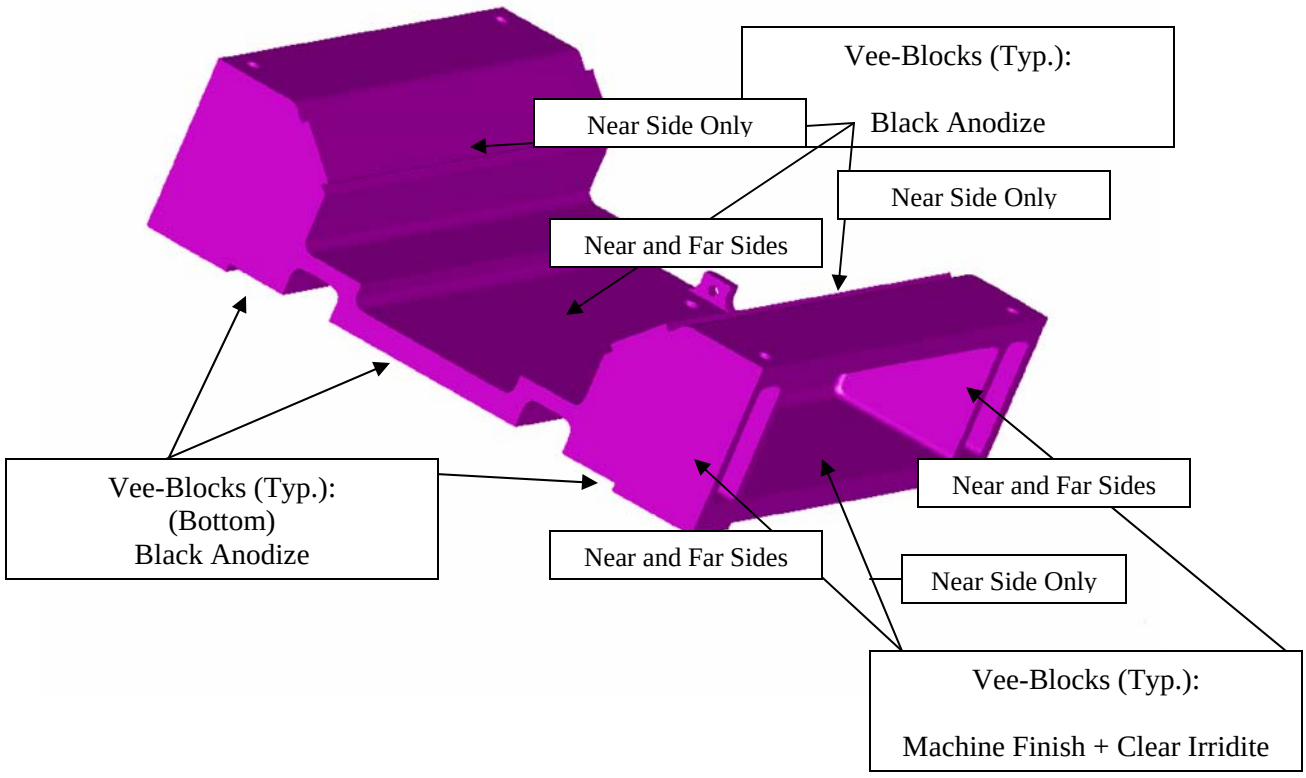
Vee-Blocks (Typ.):
Black Anodize
Near Side Only
Near Side Only
Near and Far Sides
Vee-Blocks (Typ.):
(Bottom)
Black Anodize
Near and Far Sides
Near and Far Sides
Near Side Only
Vee-Blocks (Typ.):
Machine Finish + Clear Irridite

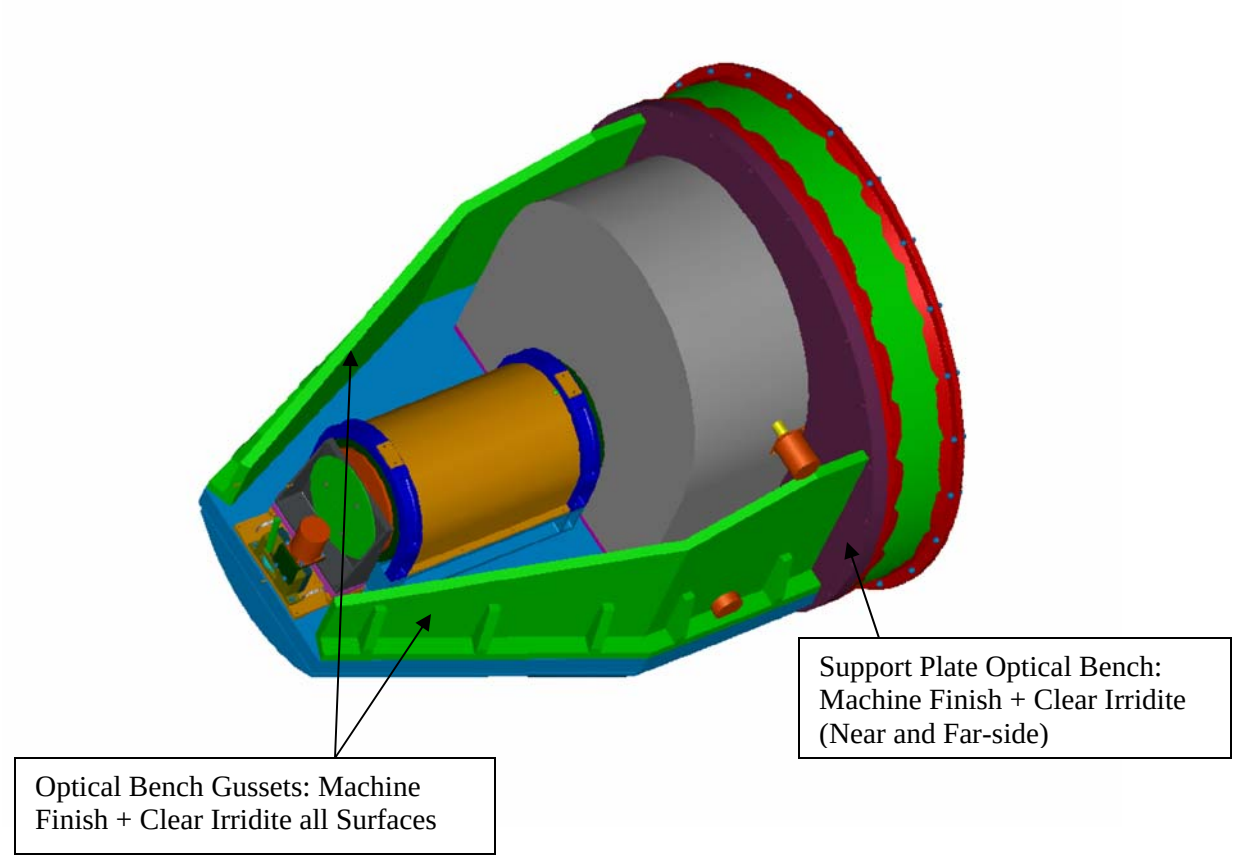
Support Plate Optical Bench: Machine Finish + Clear Irridite (Near and Far-side)
Optical Bench Gussets: Machine Finish + Clear Irridite all Surfaces

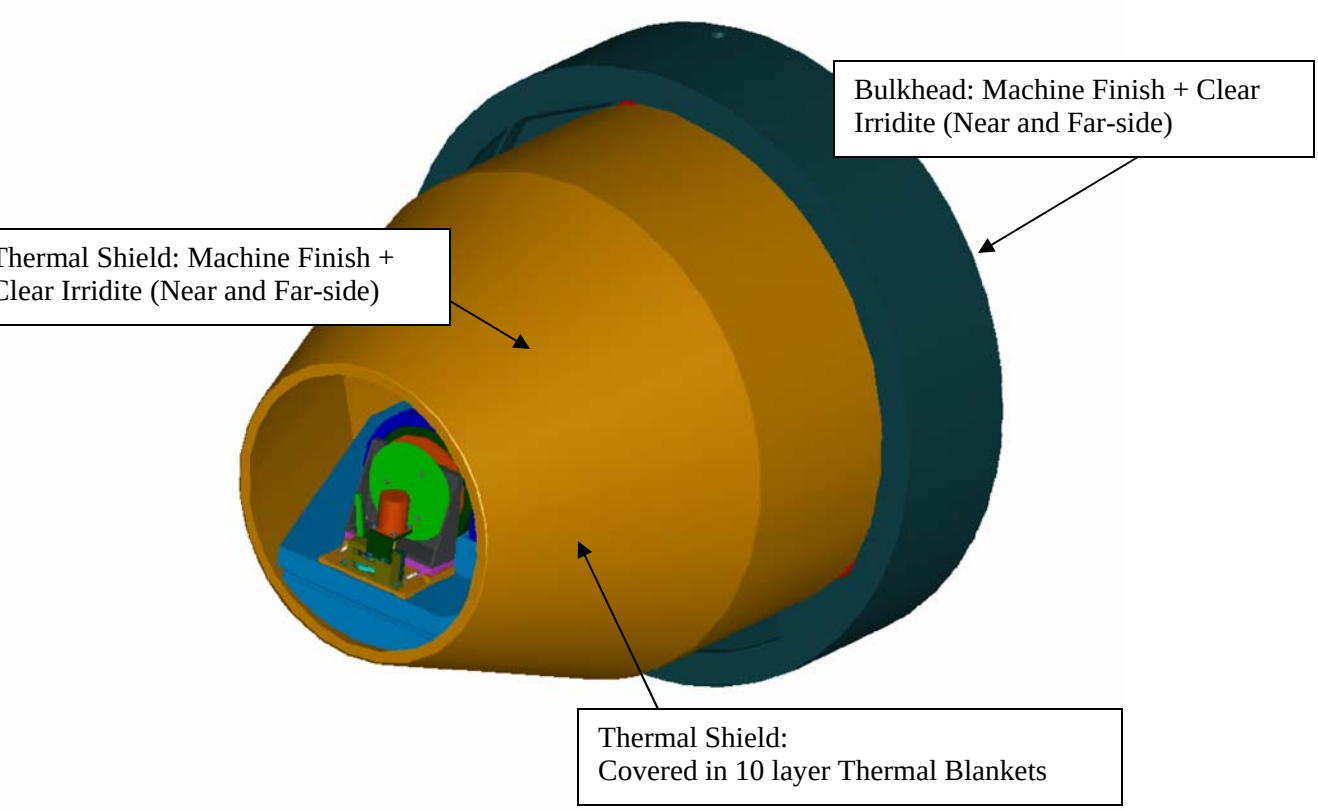
Bulkhead: Machine Finish + Clear Irridite (Near and Far-side)
Thermal Shield: Machine Finish + Clear Irridite (Near and Far-side)
Thermal Shield: Covered in 10 layer Thermal Blankets

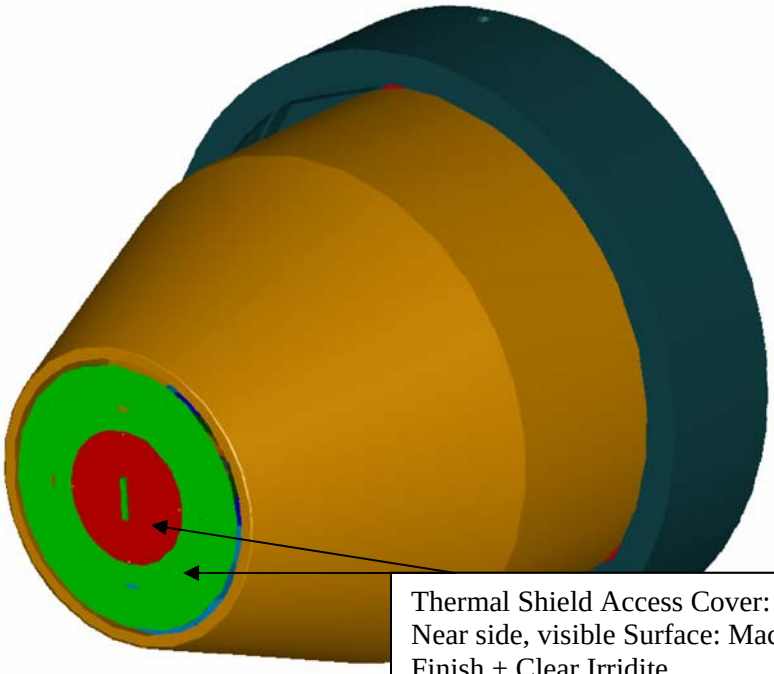

Thermal Shield Access Cover:
Near side, visible Surface: Machine Finish + Clear Irridite
Far side, visible Surface: Aluminized Kapton Tape, Aluminum exposed

Vacuum Chamber Outer Wall:
Machine Finish + Clear Irridite
(Near and Far-side)

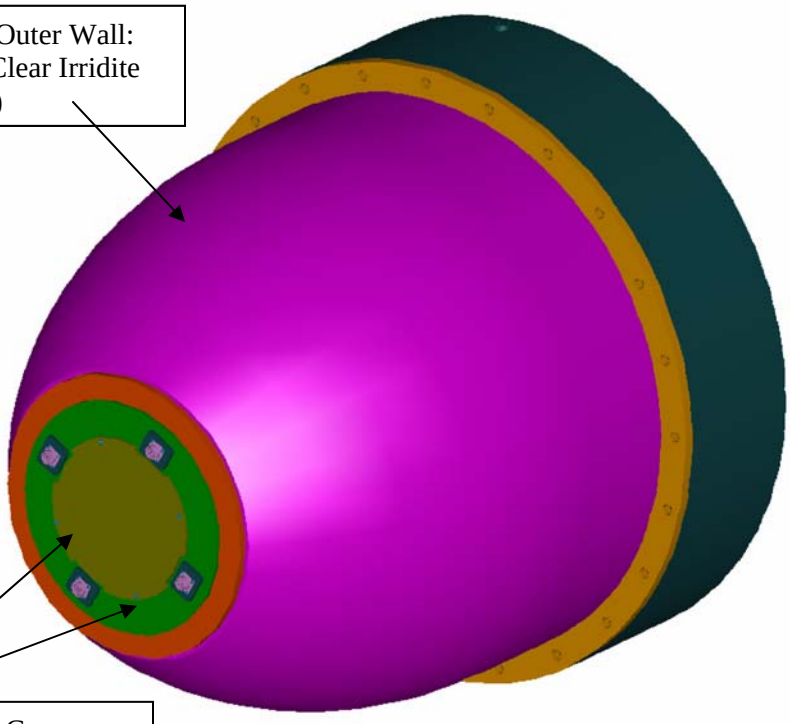

Vacuum Chamber Access Cover:
Near side, visible Surfaces:
Machine Finish + Clear Irridite

Section VII.7

Camera-Detector Steady State and Transient Analysis

This document will be available at the CDR.

Section VII.8

Temperature and Stress Distribution in Optics

This document will be available at the CDR.

Section VIII.

MMIRS Electrical Design

1. IR Array Electronics
2. Instrument Electronics
    - Overview
    - Block Diagrams
    - External Connections
    - Motion Control
    - Power Control Assignments
    - Temperature Control and Monitoring
    - Science Detector Thermal Control
    - Ethernet Connected Devices
    - Vacuum Pump Control
    - Emergency Stop (E-Stop)
    - Wheel Advance Control
    - Scanner
    - Grounding Plan
    - Interconnect Methodology
    - Overall Signal Flow Example
3. Instrument Electronics Rack Packaging
4. Electronics Rack Thermal Analysis

IR Array Electronics

System Overview and Grounding Scheme

Figure 1 shows a cartoon for the overall physical layout of the electronic system which hooks to and controls the Hawaii-2 NIR imager. The signals to and from the cold imager are conducted using 5-mil twisted-pair constantan wiring, terminating on four hermetic connectors soldered to four external preamplifier modules spaced around a heavy steel mount ring. This mount ring serves as system ground for the camera system, and will be electrically isolated from the rest of the structure and associated electrical grounds. The rest of the camera controller and associated power supplies will reference to this ground.

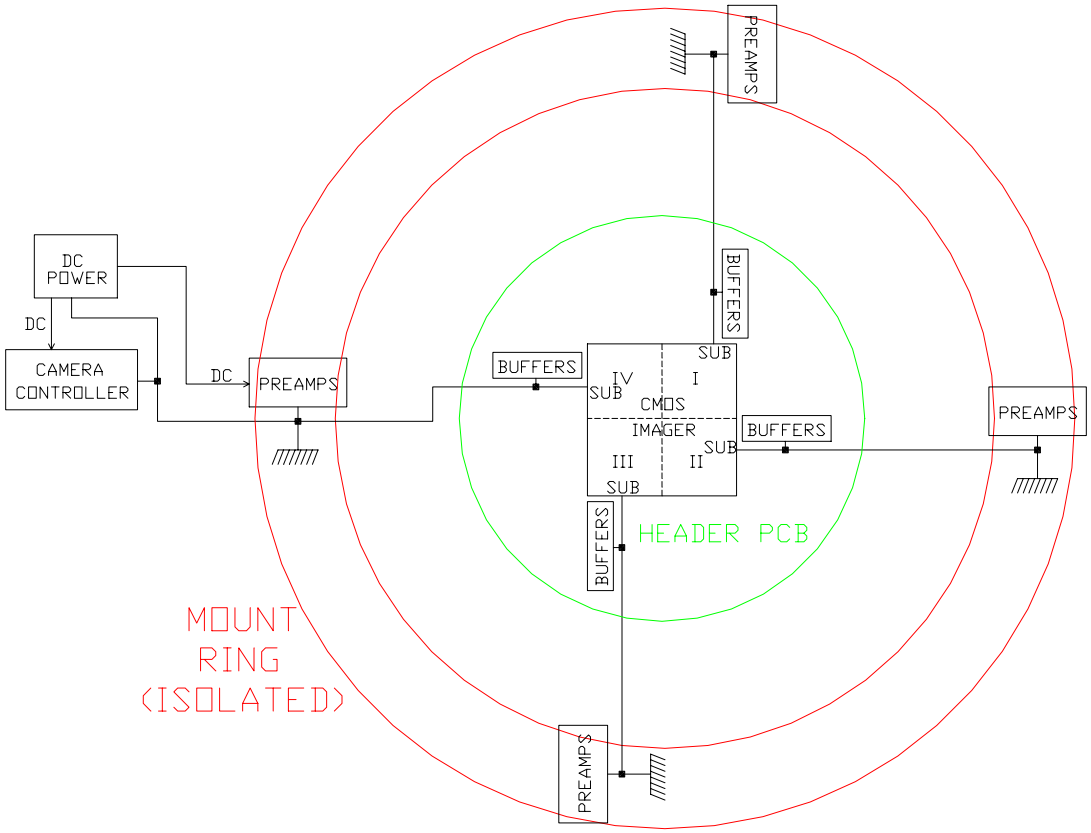

Fig. 1. Camera System overview and grounding scheme.

Imager Mount and Header Board

The Hawaii-2 imager plugs into a Yamaichi zero-insertion force (ZIF) socket, soldered to a 7-inch diameter cold header printed circuit board (PCB). This assembly serves the functions of routing signals to and from the imager, lateral and axial support for the spring-loading of the imager array against its precision locating structure, and as the main cooling mechanism for the imager and buffer amplifiers. A front view of the PCB artwork is shown in Figure 2.

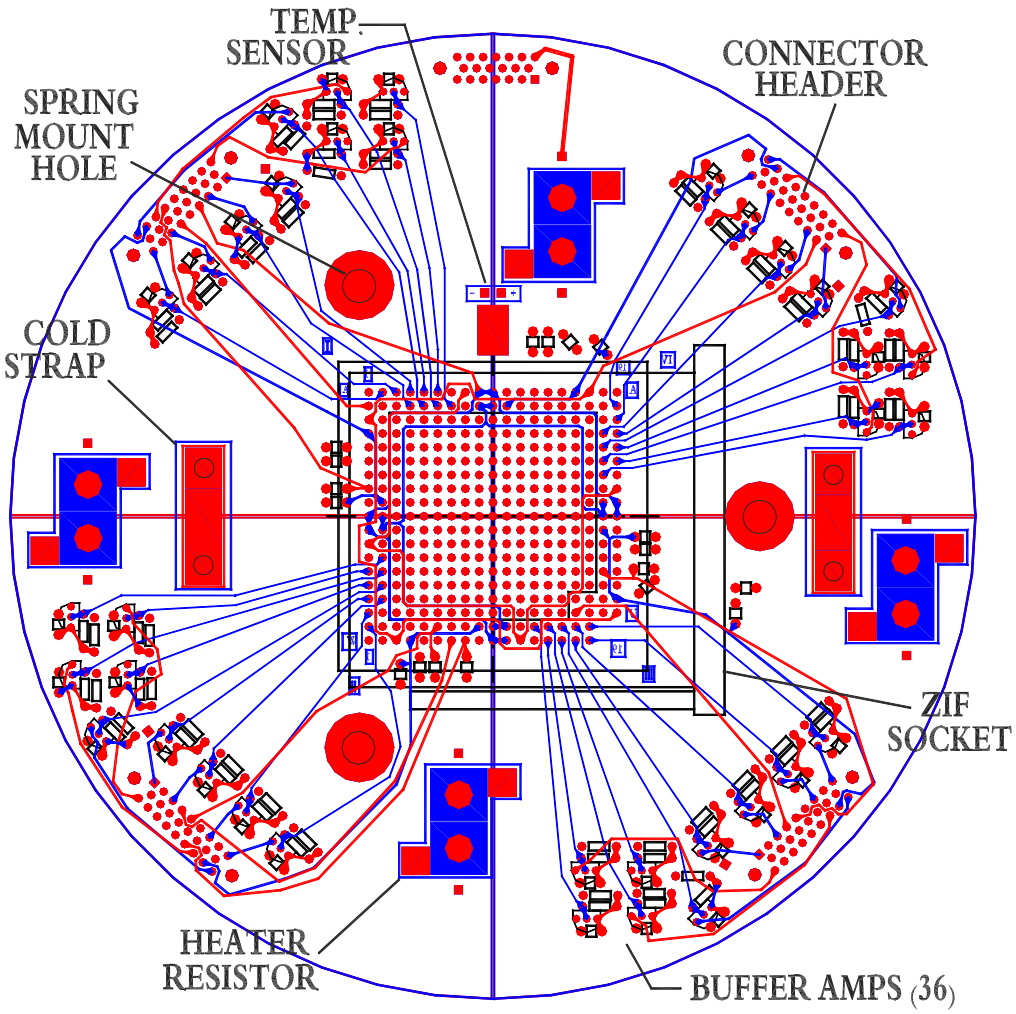

Fig. 2. Imager-side view of the Header PCB.

In the above view, only the front and back artwork are displayed to cut down on clutter. The actual board has eight layers, four plane and four routing. Two of the plane layers serve as cooling planes and conduct heat away from the inner 15 X 15 portion of the imager pin grid array to the two cold strap pads. In addition, there are planes for system ground and for VDDA (analog power for both imager and buffer amps). These latter two planes are isolated for each quadrant. A precision temperature sensor is clamped to the two cooling planes near the imager, and four 10W 10-ohm heater resistors are wired in series and thermally fasten to the cooling planes. The latter serve to both provide heating for safe warmup of the system for servicing and to provide temperature stabilization of the array while observing.

With the exception of the eight digital drive signals that run the imager multiplexer, all other bias and power voltages are generated by precision sources separately for each quadrant in order to minimize electronic crosstalk between quadrants, a scheme that we tested on the SAO Wide-field IR Camera (SWIRC) with good results. All signals to and from each quadrant are handled through a Positronic connector. Around each of these are

grouped the nine buffer amplifiers (8 video and 1 dummy pixel). A schematic drawing of this portion of the header PCB is shown below in Fig. 3.

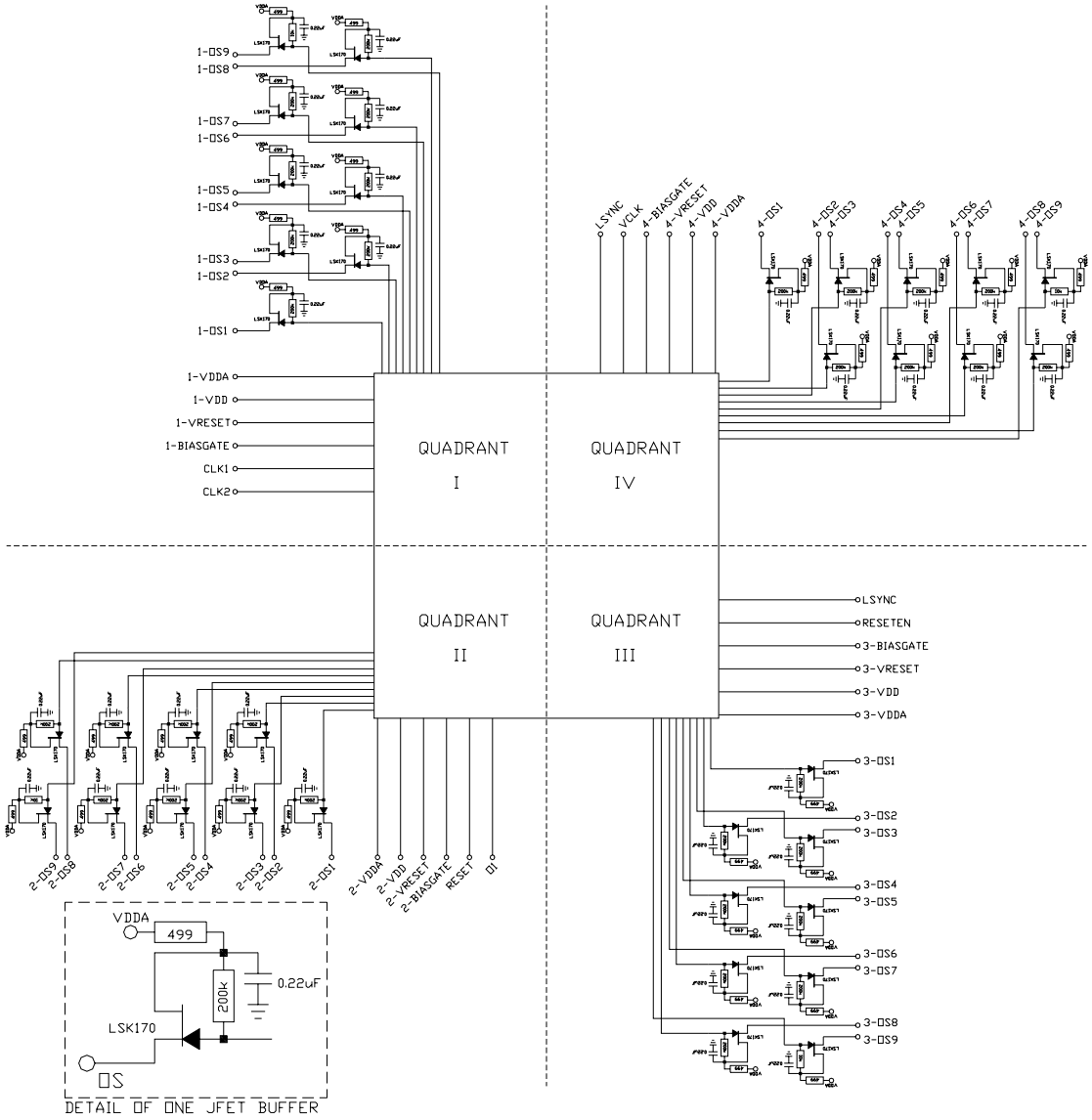

Fig. 3. Schematic of signals to and from the four quadrants of the Hawaii-2 imager. All critical ground and bias voltages are separate for each quadrant.

The ultra-lownoise JFET LSK170 is used in source-follower configuration, with the source loads being the inputs to the preamplifiers, outside the hermetic connectors. These JFETs have been tested at 77K and seem to function well there. Unlike SWIRC, which used cold CMOS opamps that dissipated about 380mW on the header board, the above configuration should produce negligible heating of the imager, both because the total dissipation is just 80mW and because more care is being used to connect to each output pin with a relatively long, very thin (6 mil) trace on the header PCB. We also expect that the heat extraction from the two cooling planes, hard clamped to the cold

support structure via flexible strapping, will be more efficient that what was used on SWIRC, which used a mechanical heat switch.

Preamplifier and Bias Voltage Boards

These four PCBs sit just outside the vacuum wall. They are soldered to the external pins of a standard 26-pin hermetic bulkhead connector. A view of the artwork for one of these 6-layer PCBs is shown in Figure 4.

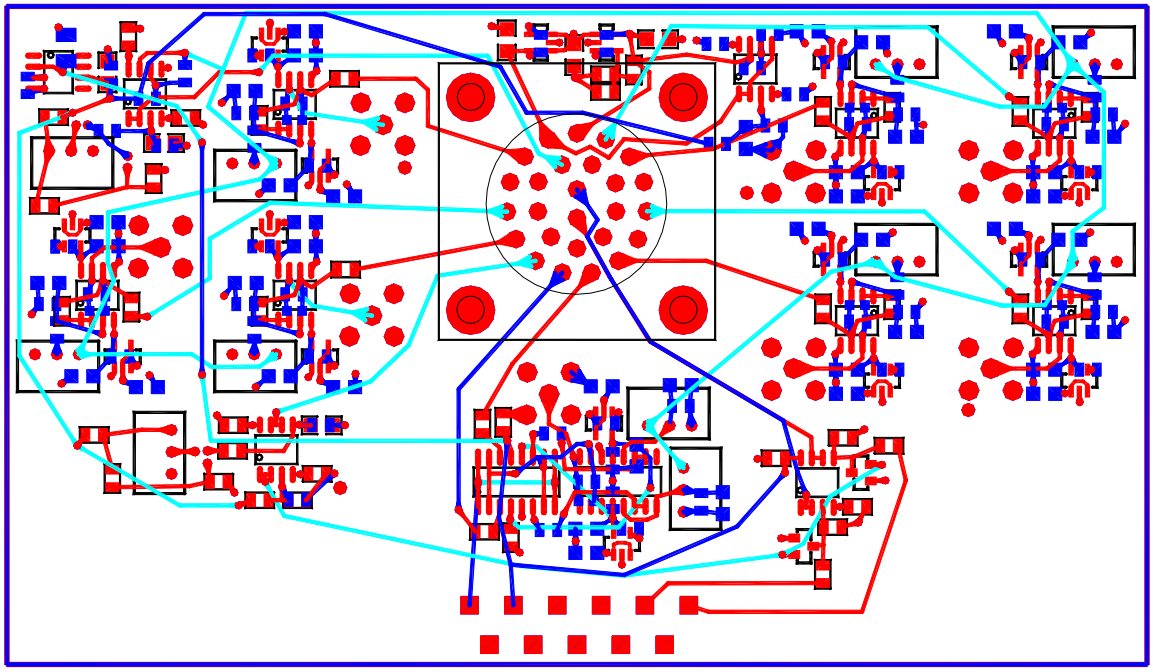

Fig. 4. Preamplifier and Bias PCB (6-layer, 3 routing and 3 planes).

Each of the nine preamplifiers per board serves to remove the rough DC offset coming from the DC-coupled cold buffer source followers and multiply the result by a gain factor of about five (settable by changing out feedback resistors). In addition, Channel 9 coming from the dummy reference pixel on the imager is multiplexed with Channel 1 video as the 129th pixel in each row, so that just eight video lines per quadrant are carried forward to the A/D boards in the camera controller, a scheme that has been successfully used on SWIRC.

In a significant change from SWIRC, we are going to generate precision, low-drift, low-noise bias and analog power voltages for each of the quadrants on this PCB. The four critical voltages are VDDA, VDD, VRESET, and BIASGATE, and they will all derive from a precision voltage reference rather than being generated on the driver board of the main camera controller. VDDA and VDD are fixed by imager specification to be +5.25V and +5.00V respectively, while VRESET and BIASGATE are variable. Once optimal values are established for the latter two, we intend to lock them down with fixed resistor dividers, as these values should not need routine adjustment in the field.

A schematic for this PCB is shown in Figure 5.

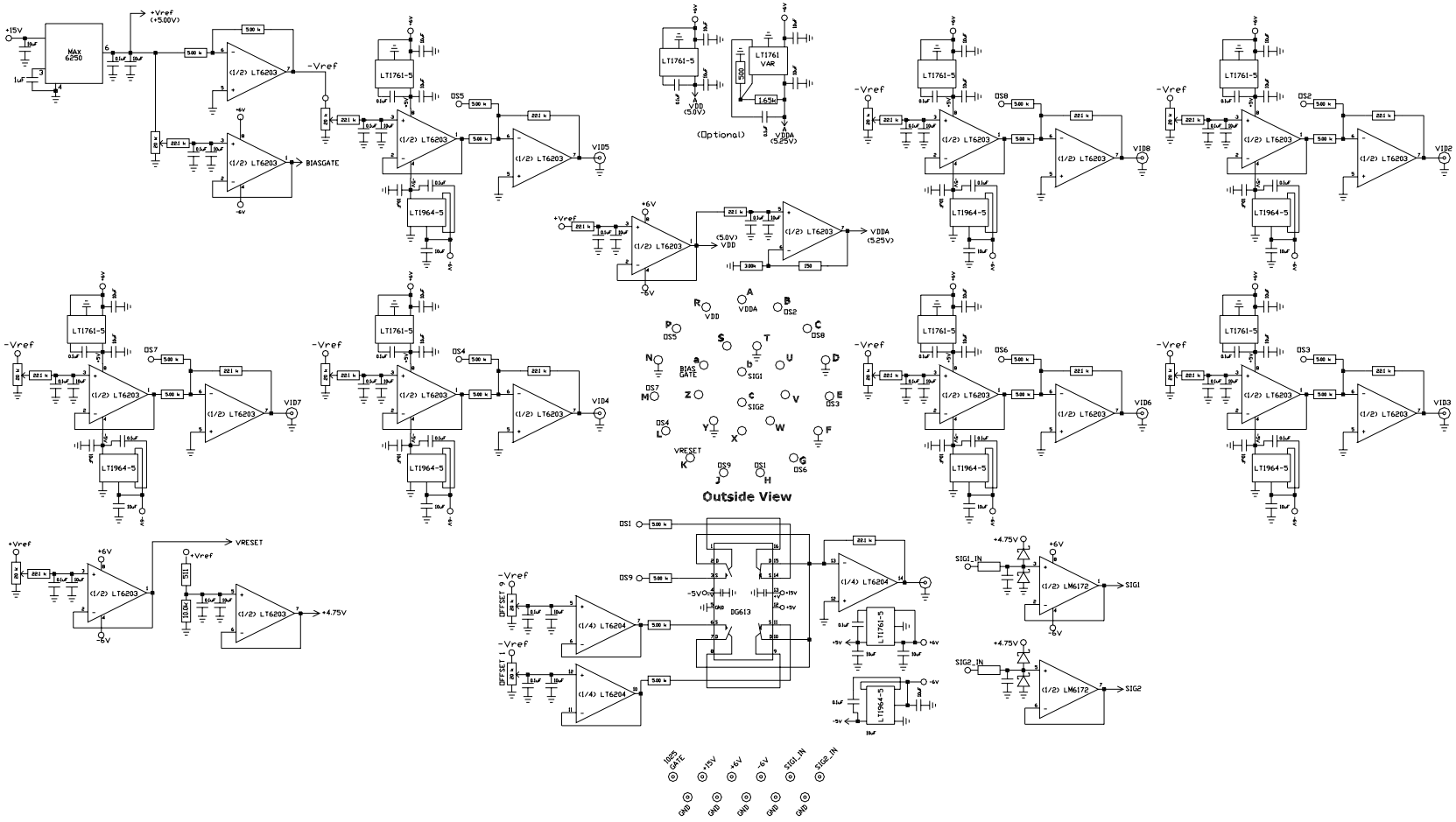

Fig. 5. Schematic of the Preamplifier and Bias PCB, soldered to each of the four hermetic connectors that serve each quadrant of the imager. Each preamplifier channel has its own local power regulation to maintain good signal separation, and the variable offsets for each channel derive from a precision voltage reference.

In addition to preamplification and bias voltage generation, filtered buffer amplifiers are provided for the digital drive signals that operate the imager multiplexer, two channels per board. These signals are common to all four quadrants of the imager, as our experience with SWIRC has shown that this scheme does not contribute any significant crosstalk between quadrants.

Camera Controller and Data Acquisition

The camera controller and data acquisition interface is a copy of what we are already using on the SWIRC camera on the MMT. This in turn is a direct derivative of the CCD controller that is has been used at all our telescopes for the past few years. The system was developed from the start to be simply extensible to very many readout channels, up to and including the 72-channel SAO Megacam, running all channels simultaneously at a pixel rate of 200kHz. Data acquisition and camera control is handled by a fiber-optically coupled commercial interface module from EDT, which mounts on the I/O board of the camera control unit.

All signals and power connections coming from and going to the camera controller will be carried on RG-174 coax cabling to each of the four Preamp/Bias modules. There is a 37-pin D-connector on the bottom of the backplane that supplies all required DC voltages and also the digital drive signals for the imager multiplexer. Each 4-channel video section also has a dedicated 25-pin D-connector on the backplane.

All software for camera control, data acquisition, and image analysis is now in place and has several years of development and heritage.

The MMIRS camera controller uses an identical board set to SWIRC, because we printed up enough PCBs to build two complete sets plus a few spare boards. A picture of the board set in shown in Figure 6. Only one of the eight 4-channel A/D boards is in the picture. The rest are nearing completion of part assembly in our lab.

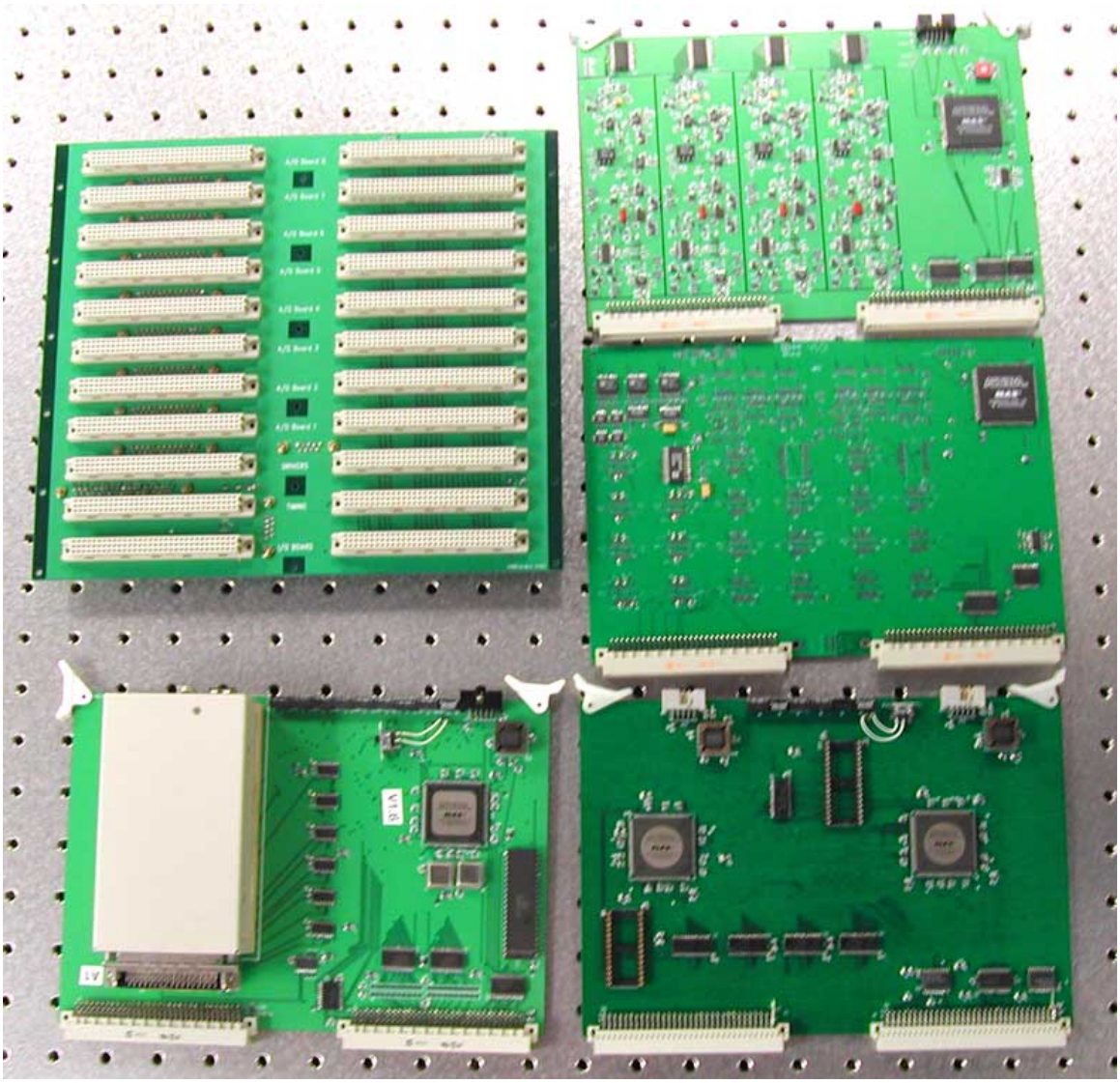

Fig. 6. Counterclockwise from the lower left is the I/O board with attached EDT fiber interface, the timing generation board for the system, the sparsely-populated driver board to supply the eight signals to the imager mux, one 4-channel A/D board, and finally the full 32-channel backplane to hold all the cards.

The critical task of taking the 32-channel video outputs from the preamplifier modules and converting to digital information is accomplished on the A/D boards. Each of the eight boards carries four synchronous analog processing channels. To ensure maximum channel separation, each channel has low-noise voltage regulation for the +/- 15V power planes, as well as both analog and digital +5V regulation for each A/D converter. A schematic diagram for one of the 32 A/D signal processing channels is shown in Figure 7.

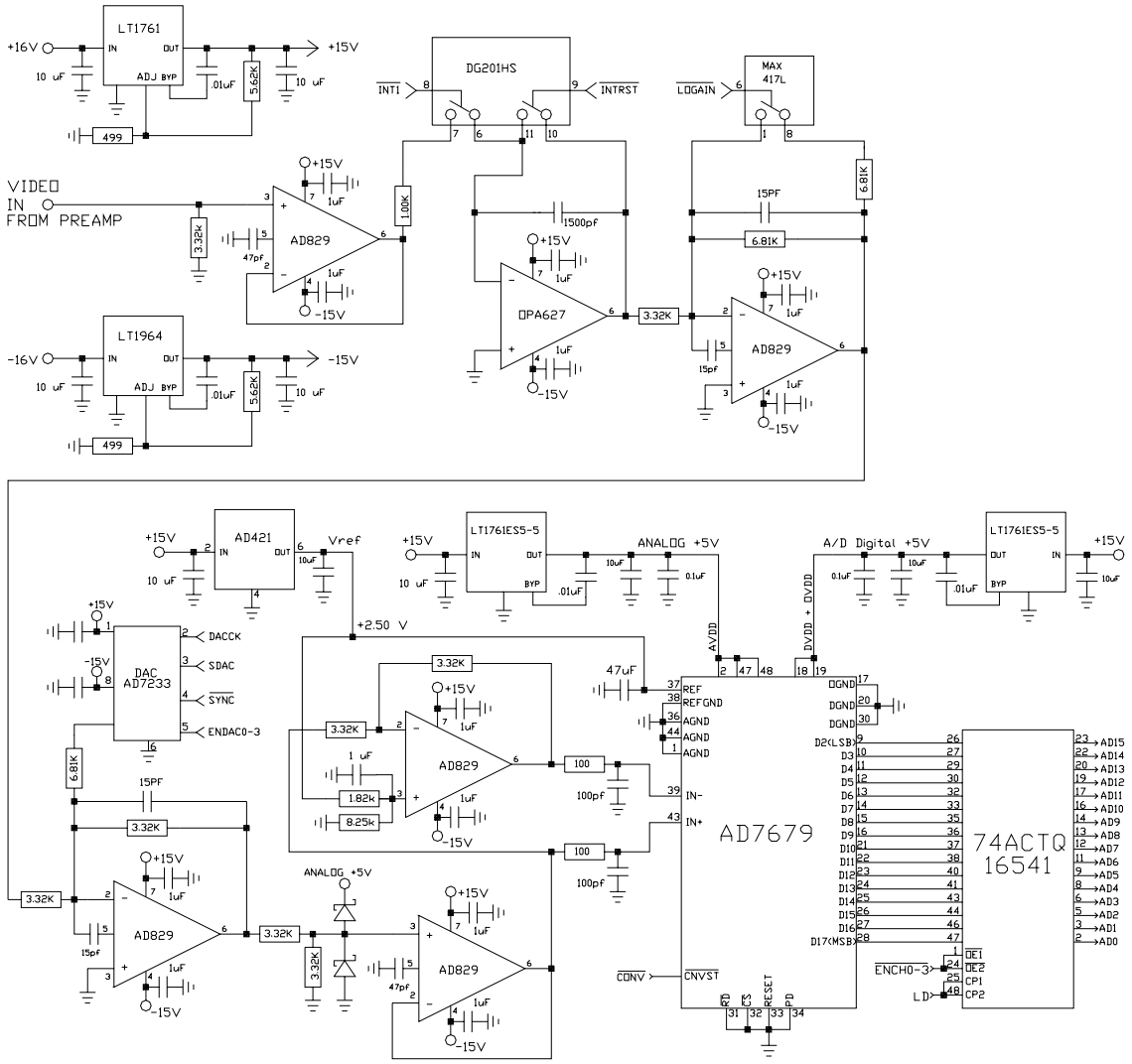

Fig. 7. Schematic of one channel of signal processing and A/D conversion. Low-noise components are used wherever possible. Fine control of DC offset is provided under computer control, and a gated integrator is used to optimally suppress high-frequency noise. The AD7679 converter is an 18-bit unit but only the top 16 bits are used, giving a net digitization noise of much less than 1 LSB. All 32 channels are processed and digitized simultaneously, with the 16-bit parallel data being strobed into the 16541 latches in the lower right. This data is then presented to the data bus (AD0-15) sequentially for each of the 32 channels for transmission through the EDT camera interface to the data acquisition computer, the transmission being accomplished in less than one pixel time, in time for the next pixel data to be latched.

SWIRC Performance and MMIRS Improvements

The realized performance so far with SWIRC is:
30e- read noise with one pair of reads
0.7sec frame rate (32-channels)
180000 e- full well
4.0 e-/adu gain
BIASGATE was 3.3-3.4V
VRESET was 0.5-1.0 V

It was noted above that drift and low-frequency noise in the latter two voltages are of some concern in getting the best read-noise performance from the Hawaii-2 imager. This is especially true of BIASGATE, as it feeds through to the output video with at least unity gain and perhaps higher. For this reason, these critical voltages will be derived from especially quiet, low-drift precision sources for MMIRS.

Also of great importance for achieving the best noise floor performance will be a more intensive effort to track low-frequency drift in the imager itself, as this is a dominant noise source. The reference pixel on the Hawaii-2 imager was provided for this purpose, and we intend to digitize it in our data train, but it is known that the implementation in Hawaii-2 was flawed and that most users of this device now ignore this information. What may prove to be more useful in tracking imager drifts are defective dark pixels in the image area. Extensive testing of methods for deriving electronic drifts from this information is planned.

MMIRS Electrical System

Mike Burke
Smithsonian Astrophysical Observatory
Central Engineering
1815 Massachusetts Ave
Cambridge, MA USA

1. Electrical System overview

The MMIRS electrical system is housed in two instrument mounted racks containing all control electronics for the system. One rack contains all motion control and provides the interface to facility power, network connectivity, and science fiber data links. The second rack contains all temperature, vacuum control, and the science detector electronics. Each rack houses a guider/ wave front sensor detector electronics interface. The science detector has pre-amplifiers off-rack near the detector to minimize noise, as do the guider wave-front sensor CCDs.

Rack 1 contains all motion control electronics, provides all external connections and the system ground reference. A Delta-Tau UMAC compact PCI motion control system is paired with Phytron stepper drives to provide control of all axes. The Delta-Tau system has been deployed on many SAO instruments and takes advantage of large code base and will also minimize the "learning curve" portion of the software and support efforts. The Phytron drives have built in diagnostics and setup, providing both flexibility in implementation and the diagnostic information needed to minimize risk. The drives are connected to the network and provide motor & amplifier temperature, bus voltage and run current. Rack 1 also provides for safety interlock combining inputs from Rack 2, an external MKS instruments differential pressure gauge and the motion control system. The connection to a serial barcode reader is also on Rack 1

Rack 2 houses temperature and vacuum control, and the science detector interface. Temperature control of the detector is provided by a Lakeshore 321 controller, and cryostat temperatures are monitored using two Lakeshore model 218s monitors. Chamber warm-up and cool down control is provided by three Omega Ethernet connected temperature controllers. Three Pfeiffer vacuum gauges are controlled by a Pfeiffer controller mounted in the rack. Vacuum pump control is provided by means of switched power to an externally mounted scroll pump and a rack mounted Varian turbo pump controller. Relay outputs from the Lakeshore, Pfeiffer and Varian controllers are routed to Rack 1 for interlock functions and read-out by the Delta-Tau system.

Features common to both racks are identical Guider/Wavefront sensor interfaces, and rack temperature monitoring. Each rack contains a power supply and interface electronics box that connects to the CCD pre-amp systems in the Guider cameras. Both racks also contain an Acromag 6 channel temperature monitor for rack temperature monitoring.

The following three pages show the overall electrical system diagram, followed by the rack diagrams.

REVISIONS				
ZONE	LTR	DESCRIPTION	DATE	APPROVED
			4-27-05	

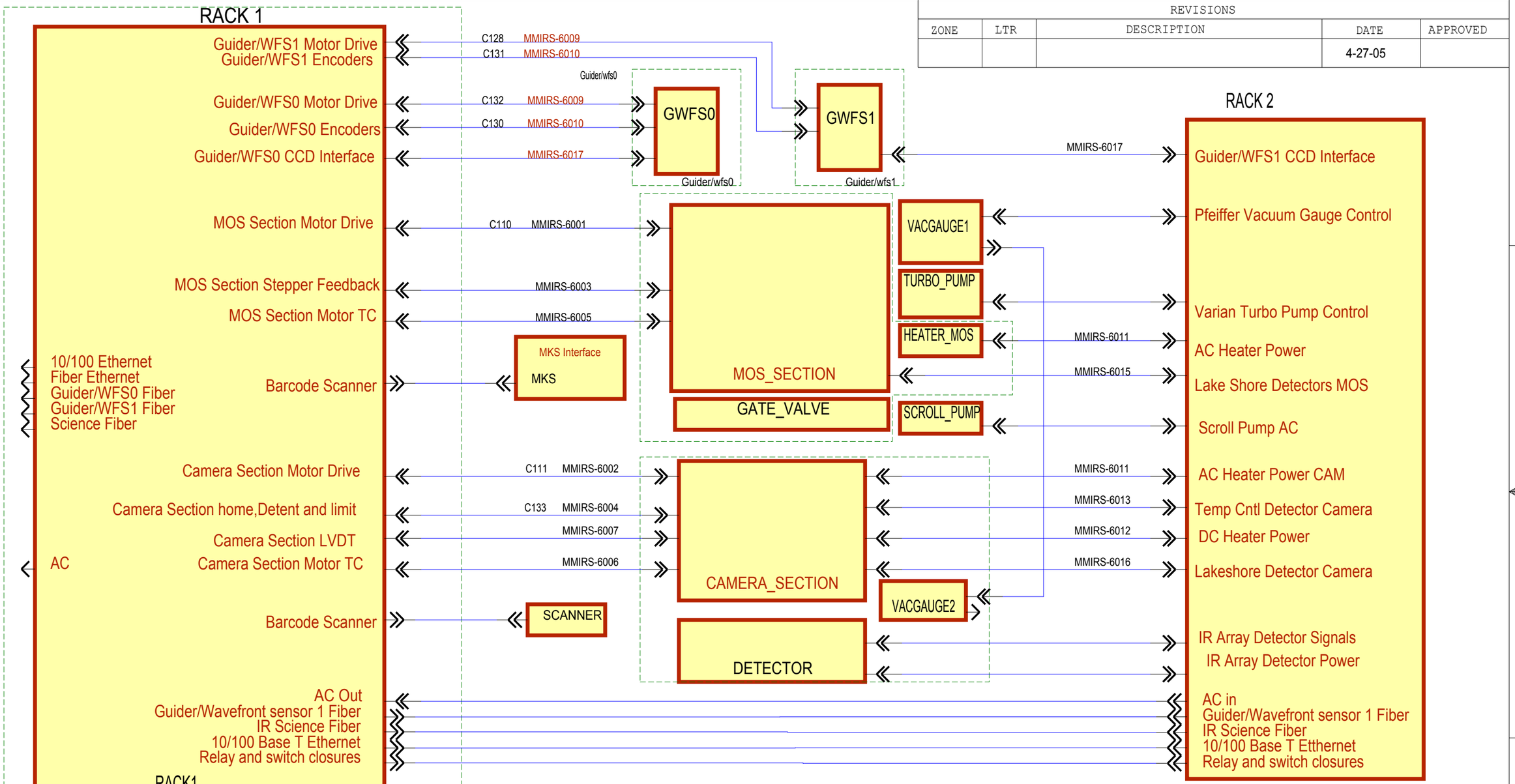

REMOVE BURRS AND BREAK SHARP EDGES	DR DATE	CHK DATE
UNLESS OTHERWISE SPECIFIED DIMENSIONS ARE IN INCHES	DSGN APPD DATE	
TOLERANCES ON FRACTIONS ± DECIMALS .XX ± .XXX ± ANGLES ±	DSGN APPD DATE	
MACH. FIN:	ENGR APPD DATE	
MAT'L: FIN:	PROJ APPD DATE	
NEXT ASSY	CONTRACT	

SMITHSONIAN ASTROPHYSICAL OBSERVATORY
CENTRAL ENGINEERING CAMBRIDGE,MA

MMIRS Electrical Top Level Diagram

SIZE	CODE IDENT NO.	DWG NO.	REV
B	50944		

SCALE | E3 CABLE Ver 6,2004,342 | SHEET 1 OF 16

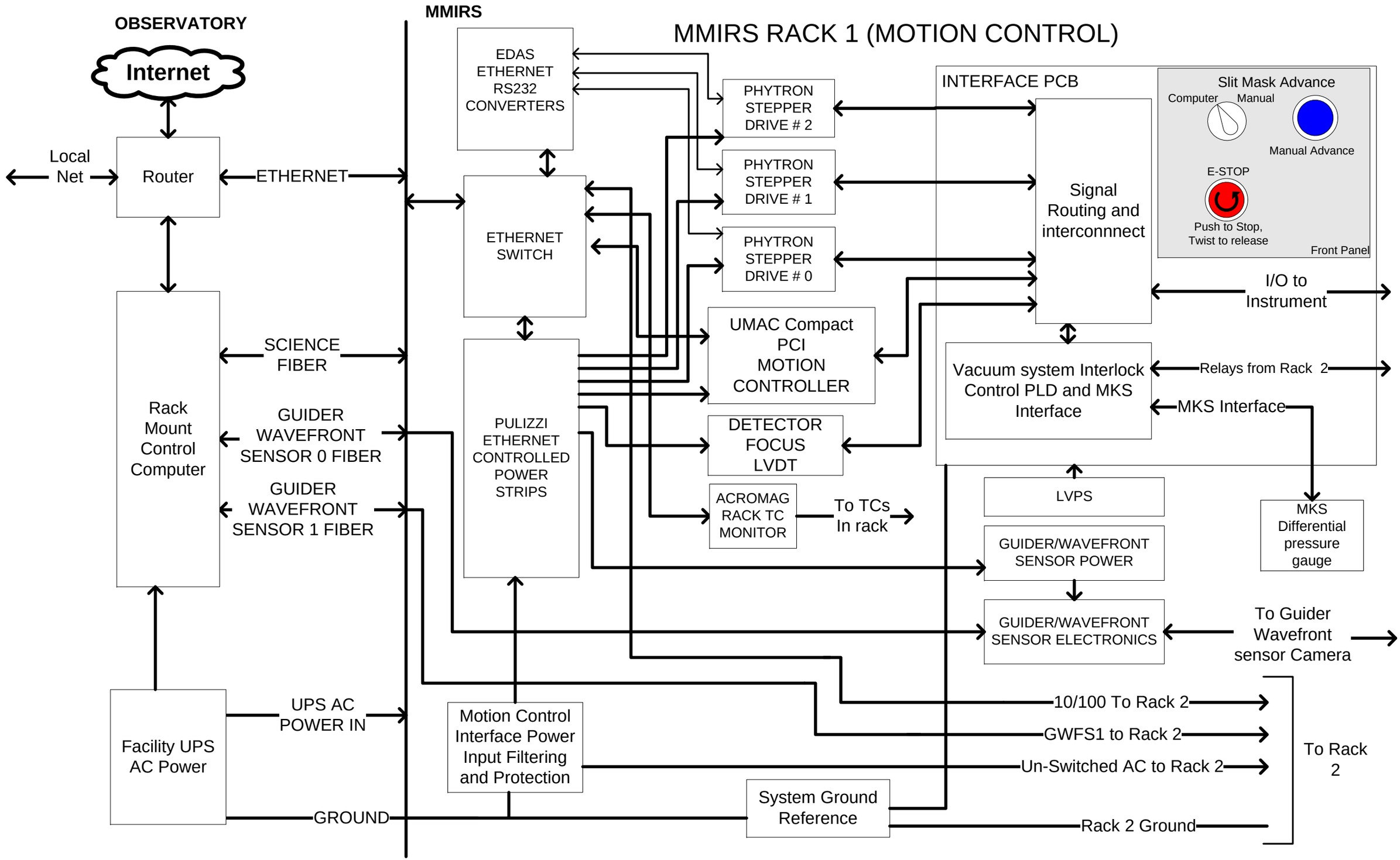
OBSERVATORY
MMIRS
MMIRS RACK 1 (MOTION CONTROL)
Internet
Local Net
Router
ETHERNET
EDAS ETHERNET RS232 CONVERTERS
ETHERNET SWITCH
PULIZZI ETHERNET CONTROLLED POWER STRIPS
PHYTRON STEPPER DRIVE # 2
PHYTRON STEPPER DRIVE # 1
PHYTRON STEPPER DRIVE # 0
UMAC Compact PCI MOTION CONTROLLER
DETECTOR FOCUS LVDT
ACROMAG RACK TC MONITOR
To TCs In rack
INTERFACE PCB
Signal Routing and interconnnect
Slit Mask Advance
Computer
Manual
Manual Advance
E-STOP
Push to Stop, Twist to release
Front Panel
I/O to Instrument
Vacuum system Interlock Control PLD and MKS Interface
Relays from Rack 2
MKS Interface
LVPS
MKS Differential pressure gauge
GUIDER/WAVEFRONT SENSOR POWER
GUIDER/WAVEFRONT SENSOR ELECTRONICS
To Guider Wavefront sensor Camera
Rack Mount Control Computer
SCIENCE FIBER
GUIDER WAVEFRONT SENSOR 0 FIBER
GUIDER WAVEFRONT SENSOR 1 FIBER
Facility UPS AC Power
UPS AC POWER IN
Motion Control Interface Power Input Filtering and Protection
GROUND
System Ground Reference
10/100 To Rack 2
GWFS1 to Rack 2
Un-Switched AC to Rack 2
Rack 2 Ground
To Rack 2

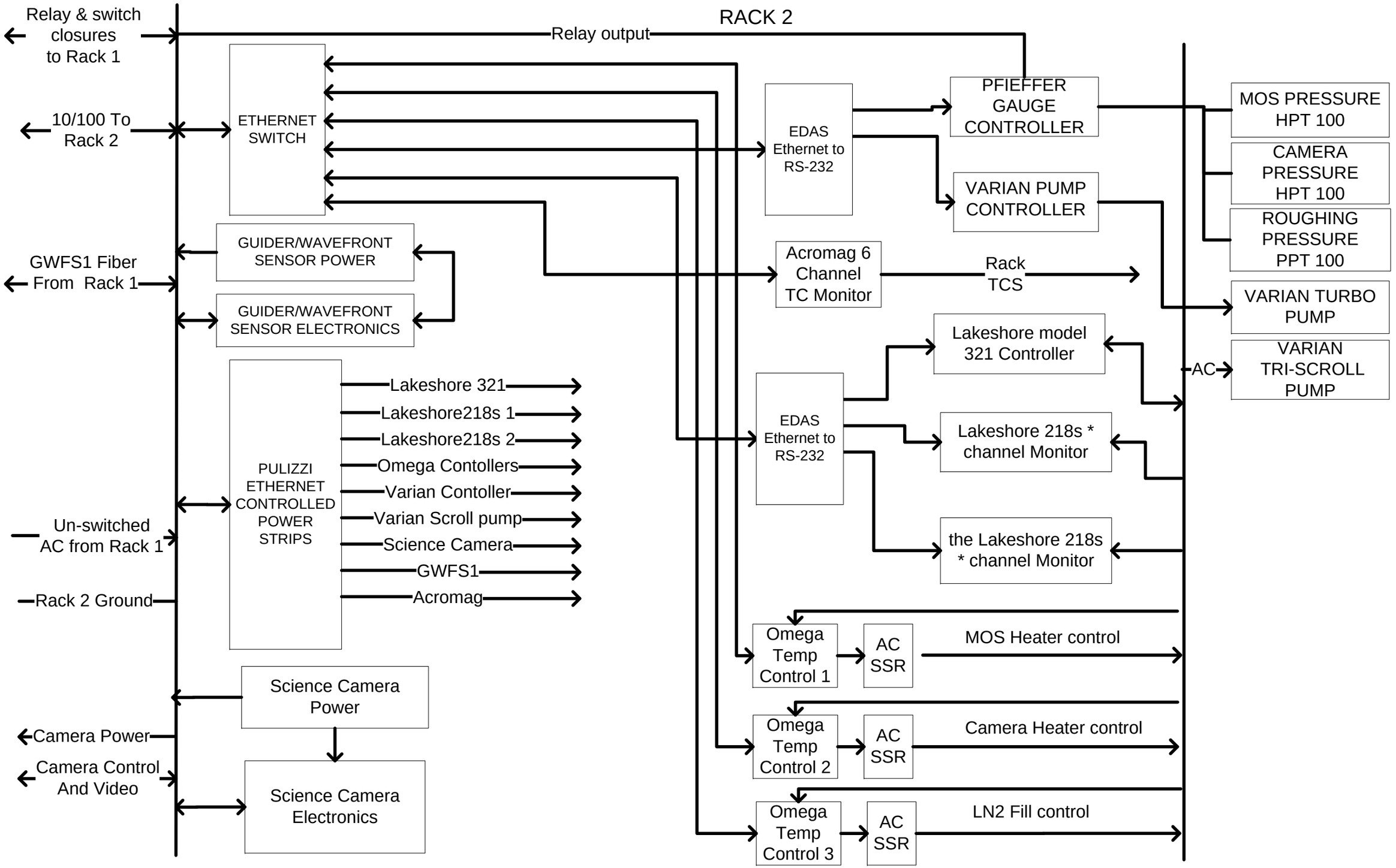
RACK 2
Relay & switch closures to Rack 1
Relay output
10/100 To Rack 2
ETHERNET SWITCH
EDAS Ethernet to RS-232
PFIEFFER GAUGE CONTROLLER
MOS PRESSURE HPT 100
CAMERA PRESSURE HPT 100
ROUGHING PRESSURE PPT 100
VARIAN PUMP CONTROLLER
VARIAN TURBO PUMP
GWFS1 Fiber From Rack 1
GUIDER/WAVEFRONT SENSOR POWER
GUIDER/WAVEFRONT SENSOR ELECTRONICS
Acromag 6 Channel TC Monitor
Rack TCS
Lakeshore model 321 Controller
AC
VARIAN TRI-SCROLL PUMP
PULIZZI ETHERNET CONTROLLED POWER STRIPS
Lakeshore 321
Lakeshore218s 1
Lakeshore218s 2
Omega Contollers
Varian Contoller
Varian Scroll pump
Science Camera
GWFS1
Acromag
EDAS Ethernet to RS-232
Lakeshore 218s * channel Monitor
the Lakeshore 218s * channel Monitor
Un-switched AC from Rack 1
Rack 2 Ground
Omega Temp Control 1
AC SSR
MOS Heater control
Science Camera Power
Omega Temp Control 2
AC SSR
Camera Heater control
Camera Power
Camera Control And Video
Science Camera Electronics
Omega Temp Control 3
AC SSR
LN2 Fill control

2. External connections

To simplify the cabling to the instrument a minimum number of external connections are used. The AC input of the instrument connects to the UPS power provided at the site. The instrument mounted racks are controlled by an off-instrument rack mounted computer system connected by fiber gigabit Ethernet. Three additional fibers provide connections to the IR array controller and the two guider CCD controllers

External connections	
Function	Connection
AC Line In-Single Phase 110VAC Line In	Keyed Three wire AC Outlet
Gigabit Fiber Ethernet-Primary network connection	SC
10/100 Ethernet- Alternate network connection	Standard RJ-45
Science Fiber	SC
Guider-wavefront sensor 0 fiber-MT-RJ Panel Jack	MT-RJ
Guider-wavefront sensor 1 fiber-MT-RJ Panel Jack	MT_RJ

3. Motion Control

The motion control system is a compact PCI (cPCI) version of the Delta-Tau UMAC system used by SAO in other instruments. All of the motion axes are driven by Phytron stepper motors and amplifiers. The Phytron drivers are mounted in three 4u 19 inch rack mount boxes. The seven "cold" axes use the same Phytron cryo-vac qualified motor, while the 8 Guider/Wavefront axes use a standard Phytron motor, four of which will be equipped with a brake. The Phytron driver provides for intelligent setup and control of motor run parameters and readout of motor temperature, bus voltage and current. The setup of the drives is provided by a serial interface on each Phytron box, which in turn connects to a serial to Ethernet converter. The Delta-TAU system provides real-time motor direction and control.

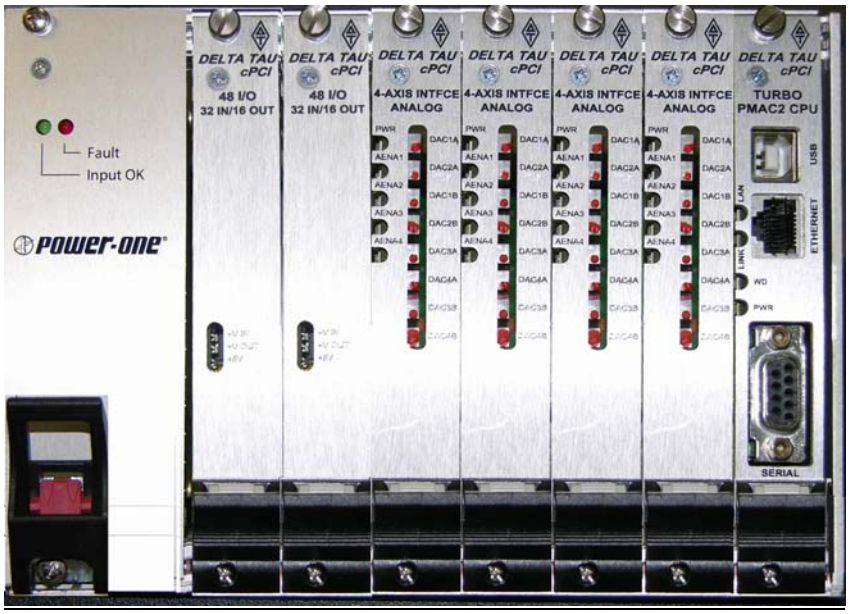

The system shown above is a 3U half-rack system comprised of system CPU, motion control and digital I/O. From left to right the modules shown are as follows, System Power, two ACC-11C Isolated 32-input / 16-output digital interface boards, four ACC24C2 4 axis analog servo and stepper interface boards, and a 240MHz control CPU with 10/100 Ethernet.

Phytron Motor control

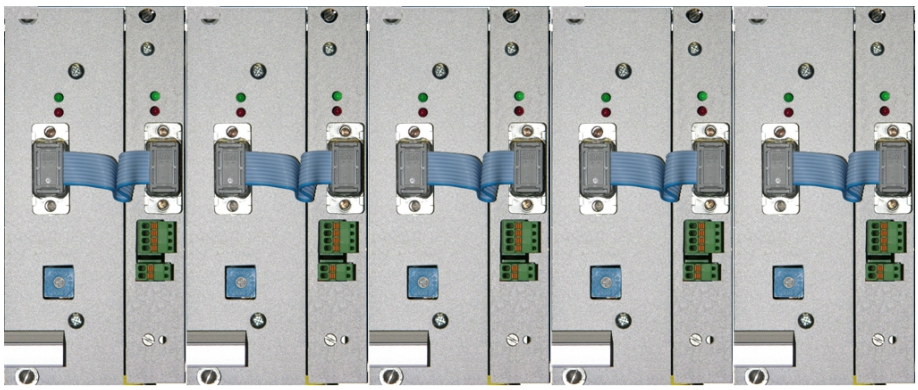

All motion axis are controlled by Phytron PAB93-70 programmable drives with motor temperature measurement option in a 6 slot 4u rack mounted 19 inch enclosure. MMIRS uses three of the drive boxes. Each box provides an RS-232 port for connection to the system for setup and parameter data logging. The drives run, boost and stop current and stepping modes are setup via this interface. The drives also provide measurements of bus voltage, Motor current, drive amplifier and motor temperature. The delta-Tau system drives the amplifiers pulse, direction and boost pins, and reads the amplifier fault status to implement closed loop control. All data logging and setup is performed by the off-instrument control computer through the RS-232 ports which in turn connect to the EDAS RS-232 to Ethernet converter

Delta-Tau Assignments

Delta-Tau axis assignments			
Number	Function	Phytron	Delta-Tau
Axis1	MOS Section - Dekker wheel	Phytron0-ch1	Axis card 0 ch 0
Axis2	MOS Section - Slit Mask	Phytron0-ch2	Axis card 0 ch 1
Axis3	Camera Section - Vacuum valve	Phytron0-ch3	Axis card 0 ch 2
Axis4	Camera Section - Filter wheel 1	Phytron0-ch4	Axis card 0 ch 3
Axis5	Camera Section - Filter wheel 2	Phytron0-ch5	Axis card 1 ch 0
Axis6	Spare	Phytron0-ch6	
Axis7	Camera Section - Grism wheel	Phytron1-ch1	Axis card 1 ch 1
Axis8	Camera Section - Detector Focus	Phytron1-ch2	Axis card 1 ch 2
Axis9	GWFS0 X	Phytron1-ch3	Axis card 1 ch 3
Axis10	GWFS0 Y	Phytron1-ch4	Axis card 2 ch 0
Axis11	Spare	Phytron1-ch5	
Axis12	GWFS0 Z	Phytron1-ch6	Axis card 2 ch 1
Axis13	GWFS0 Focus	Phytron2-ch1	Axis card 2 ch 2
Axis14	GWFS1 X	Phytron2-ch2	Axis card 2 ch 3
Axis15	GWFS1 Y	Phytron2-ch3	Axis card 3 ch 0
Axis16	GWFS1 Z	Phytron2-ch4	Axis card 3 ch 1
Axis17	GWFS1 Focus	Phytron2-ch5	Axis card 3 ch 2
Axis18	Spare	Phytron2-ch6	

Delta Tau connections		
For Axis 1-7 (Cryostat)		
Source	Delta-Tau Input	Description
Motor HOME Switch	HOME	zero when in home position
Motor DETENT Switch	USER	zero when in detent
Phytron FAULT Status	FAULT	One when drive in fault
LVDT (Camera focus only)	Analog input 1	Voltage proportional to position
For Axis 8-15 (Guider/WFS)		
Source	Delta-Tau Input	Description
Encoder A	ENCA	Encoder inputs
Encoder B	ENCB	Encoder inputs
Encoder C	ENCC	Encoder inputs
PLIM	PLIM	Postive travel limit, at limit when zero
MLIM	MLIM	Negative travel limit,at limit when zero

Delta-Tau Assignments

	Digital IO Assignments	
IN0	Estop Button state	zero=Normal, one =Stop
IN1	Computer/Manual button state	zero=Remote, one=Local
IN2	Advance wheel switch state	zero=not pushed, one= pushed
IN3	Temp alarm0	Zero=Alarm, one=Normal
IN4	Temp alarm1	Zero=Alarm, one=Normal
IN5	Temp alarm2	Zero=Alarm, one=Normal
IN6	Temp alarm3	Zero=Alarm, one=Normal
IN7	Vacuum valve relay status0	TBD
IN9	Vacuum valve relay status1	TBD
IN10	Vacuum valve relay status2	TBD
IN11	Vacuum valve relay status3	TBD

4. Pulizzi Power control assignments

All Rack AC Power is routed through Pulizzi IPC3402 Ethernet controlled AC switches.

Pulizzi AC control switch 0		**Pulizzi AC control switch 1**	
Location	RACK1	Location	RACK1
IP Address	TBD	IP Address	TBD
Output	**Function**	**Output**	**Function**
Outlet 1	Phytron Rack mount motor drive 0	Outlet 1	Acromag temperature monitor 0
Outlet 2	Phytron Rack mount motor drive 1	Outlet 2	Barcode scanner
Outlet 3	Phytron Rack mount motor drive 2	Outlet 3	E-STOP Power
Outlet 4	Compact UMAC Motion control System	Outlet 4	Spare
Outlet 5	EDAS	Outlet 5	Spare
Outlet 6	Guider/Wavefront camera electronics 0	Outlet 6	Spare
Outlet 7	Brake +24VDC power	Outlet 7	Spare
Outlet 8	Ectron LVDT signal conditioner	Outlet 8	Spare

Pulizzi AC control switch 2		**Pulizzi AC control switch 3**	
Location	RACK2	Location	RACK2
IP Address	TBD	IP Address	TBD
Output	**Function**	**Output**	**Function**
Outlet 1	Lakeshore Controller	Outlet 1	Ethernet switch
Outlet 2	Lakeshore Monitor 0	Outlet 2	Acromag Temperature monitor 1
Outlet 3	Lakeshore Monitor 1	Outlet 3	scroll pump
Outlet 4	Omega controllers (3).	Outlet 4	EDAS
Outlet 5	Pfeiffer gauge controller	Outlet 5	spare
Outlet 6	Guider/Wavefront camera electronics 1	Outlet 6	spare
Outlet 7	Varian vacuum valve control	Outlet 7	spare
Outlet 8	Science camera	Outlet 8	spare

5. Temperature control and monitoring

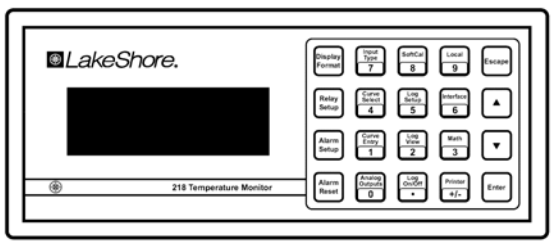

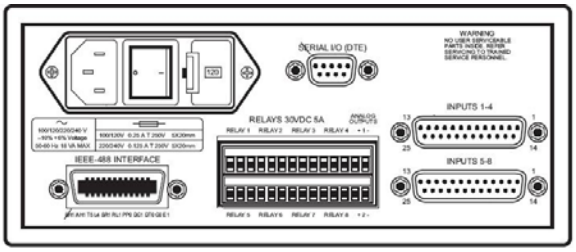

Lakeshore 218s monitor 0		
Input	Sensor	Description
channel 1	T1	Wheel enclosure: attached to the outer surface
channel 2	T2	Dewar: on side opposite bulkhead and facing wheels
channel 3	T3	Lens 3: attached to the lens mount, furthest from dewar
channel 4	T4	Vee block 1: attached to the inside of radiation shield at top, center
channel 5	T5	Detector mount: opposite the detector and near top
channel 6	T6	Detector mount: on detector header board
channel 7	T7	Dewar back: middle of side opposite bulkhead plate, near optical bench
channel 8	T8	Radiation shield: halfway along length and opposite the dewar

Engineering sensors will be allocated to the second lakeshore monitor. An external selection switch will support multiple inputs to the controller in the test and integration phase.

Lakeshore 218s monitor 1		
Input	Sensor	Description
	E1	Lens 2: Attached to the lens mount material or..
	E9	Lens 14: Attached to the lens mount or..
channel 1	E17	Grism wheel Rim of wheel for static test
	E2	Pickoff mirror: One of the two mirrors only or..
channel 2	E10	Vee block 2: Attached to the inside of the radiation shield at top, center
	E3	L2 baffle: Attached to the outside surface and facing the mask exchange port or..
channel 3	E11	Dewar front: Middle of side facing bulkhead plate, near optical bench
	E4	GWS baffle top: Outside surface facing top dome or..
channel 4	E12	Lens 9 dummy: Center of a dummy lens in the mount for lens 9
	E5	Slit mask wheel Rim of wheel for static test or..
channel 5	E13	Lens 10 dummy: Center of a dummy lens in the mount for lens 9
	E6	Lens 5: Attached to the lens mount or..
channel 6	E14	Detector dummy: Center of the ZIF socket
	E7	Lens 8: Attached to the lens mount or..
channel 7	E15	Electronics radiation shield Center of radiation shield behind detector
	E8	Lens 9: Attached to the lens mount or..
channel 8	E16	Wheel radiation shield Top of radiation shield over filter/grism wheels

Science Detector Thermal control

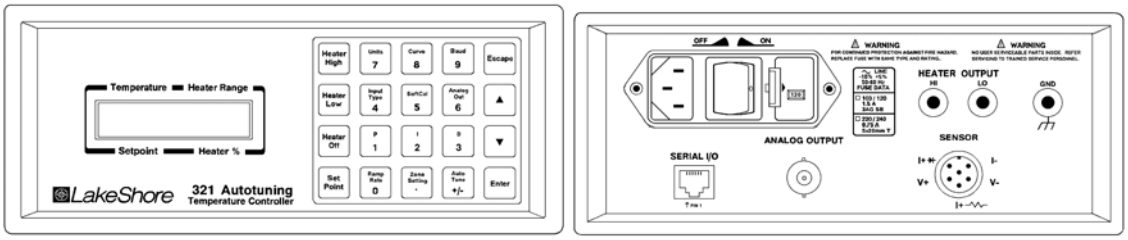

Lakeshore Model 321 Controller	
Input	Detector mount: on detector header board
Output	Science detector heater
Relay	To digital I/O

Omega Controllers

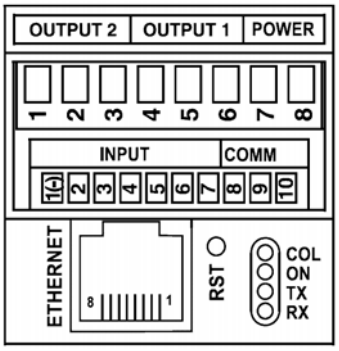

Three Omega model CNi16D54-EI PID controllers will be used for warm-up and cool-down of the instrument. Controller 0 will used for warm-up of the MOS section for slit mask changes. It will be programmed to warm up as quickly as possible. Controller 1 will be used to warm-up the camera section. It will be programmed to raise the temperature at a nominal rate 0.2C/minute. Controller 2 will be used to cool the camera section. The output will drive a solid state relay which drives a cryogenic solenoid valve that controls the flow of LN2. The rate of change will be maintained at a nominal 0.2 C/minute.

Omega Controller 0	
IP Address	TBD
Rack 2 Switch Port	0
Output	MOS Heater control
Input	K type TC in MOS Chamber

Omega Controller 1	
IP Address	TBD
Rack 2 Switch Port	1
Output- heater1	Camera Heater Control
Input TC or RTD	K type TC in Camera Chamber

Omega Controller 2	
IP Address	TBD
Rack 2 Switch Port	2
Output- heater2	LN2 Fill control
Input TC or RTD	K type TC

Acromag Thermocouple Rack housekeeping temperature monitors

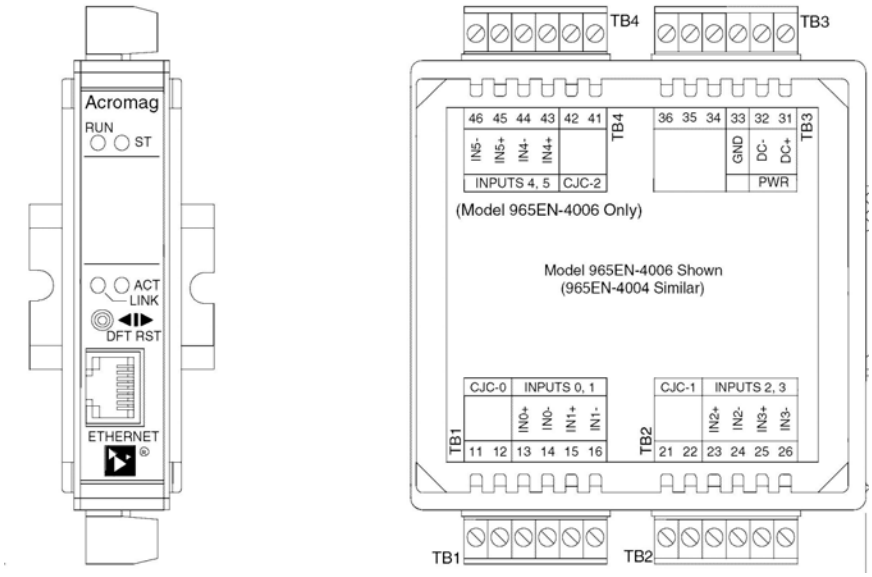

The Acromag units will be used to monitor rack temperatures. They will primarily be used during the initial testing of the rack cooling system, but during normal operation will provide a status to warn of an impending rack shutdown by the AC line in cutoff thermostat. For convenience each rack will have a standard mini K type thermocouple connector panel jack that will be read out at channel 6.

Acromag Monitor0 Rack 1	
IP Address	TBD
Rack 1 Switch Port	5
Channel1	heat exchanger inlet
Channel2	heat exchanger outlet
Channel3	rack ambient mid
Channel4	GWFS0 electronics
Channel5	Spare
Channel6	Panel jack

Acromag Monitor0 Rack 2	
IP Address	TBD
Rack 2 Switch Port	5
Channel1	heat exchanger inlet
Channel2	heat exchanger outlet
Channel3	rack ambient mid
Channel4	GWFS1 electronics
Channel5	Science detector electronics
Channel6	Panel jack

Phytron TCs

Phytron TCs are read back via EDAS0 RS-232 ports 0-2 in rack0. Refer to the Phytron serial protocol document and Phytron PAB manual for details. These detectors will be used primarily in the initial testing phase of the instrument. During normal operation, they will be monitored to check for motor overheating.

Phytron Drive TC Channels (all K type TC)	
phytron0_ch1	dekker motor temperature
phytron0_ch1	slit mask motor temperature
phytron0_ch2	gate valve motor temperature
phytron0_ch3	filter wheel 1 motor temperature
phytron0_ch4	filter wheel 2 motor temperature
phytron0_ch5	spare
phytron1_ch0	grism motor temperature
phytron1_ch1	detector focus motor temperature

6. Ethernet connected devices

All Ethernet connections are made via a Ruggedcom RSG2100 Industrial managed Ethernet switch. The switch is of a modular design to accommodate a variety of physical network interface layers.

Ethernet Assignments		
Subsystem	IP Address	Switch Connected to
cPCI system	TBD	Rack 1 Switch Port 0
EDAS0 Rack 1	TBD	Rack 1 Switch Port 1
EDAS1 Rack 1	TBD	Rack 1 Switch Port 2
Rack2 Ethernet switch	TBD	Rack 1 Switch Port 3
Pulizzi0 Rack 1	TBD	Rack 1 Switch Port 4
Pulizzi1 Rack 1	TBD	Rack 1 Switch Port 5
Acromag Monitor0 Rack 1	TBD	Rack 1 Switch Port 6
Spare	TBD	Rack 1 Switch Port 7
Spare	TBD	Rack 1 Switch Port 8
Spare	TBD	Rack 1 Switch Port 9
Spare	TBD	Rack 1 Switch Port 10
Spare	TBD	Rack 1 Switch Port 11
EDAS2 Rack 2	TBD	Rack 2 Switch Port 0
EDAS3 Rack 2	TBD	Rack 2 Switch Port 1
Pulizzi1 Rack 2	TBD	Rack 2 Switch Port 2
Pulizzi2 Rack 2	TBD	Rack 2 Switch Port 3
Acromag Monitor0 Rack 2	TBD	Rack 2 Switch Port 4
Omega0	TBD	Rack 2 Switch Port 5
Omega1	TBD	Rack 2 Switch Port 6
Omega2	TBD	Rack 2 Switch Port 7
Spare	TBD	Rack 2 Switch Port 8
Spare	TBD	Rack 2 Switch Port 9
Spare	TBD	Rack 2 Switch Port 10
Spare	TBD	Rack 2 Switch Port 11

7 Vacuum pump control

Varian Turbo-V301 pump controller

Varian vacuum control

MMIRS vacuum pumping is provided by a combination of a roughing pump and a turbo pump. The roughing pump is controlled by pushing a button of the Pulizzi power controller, and the turbo pump is controlled by a rack mounted Varian turbo-pump controller, which is also connected to a Pulizzi channel. The steps to achieve pumping are as follows..

1. Power up the Varian V600 Scroll pump by pressing the Pulizzi button that controls it. The Scroll pump will immediately run.
2. Power up the turbo pump controller by pressing the Pulizzi button that controls it.
3. Enable and run the Varian navigator 310 Turbo pump Turbo pump via the

The controller's RS-232 interface is connected to an EDAS RS-232 to Ethernet converter, to support remote operation.

8. Vacuum gauge Control

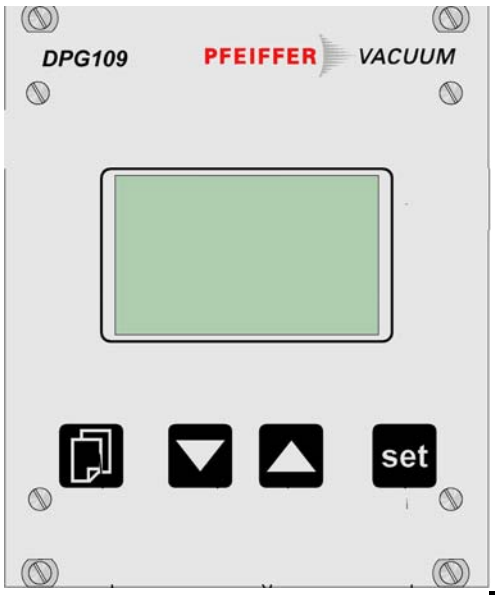

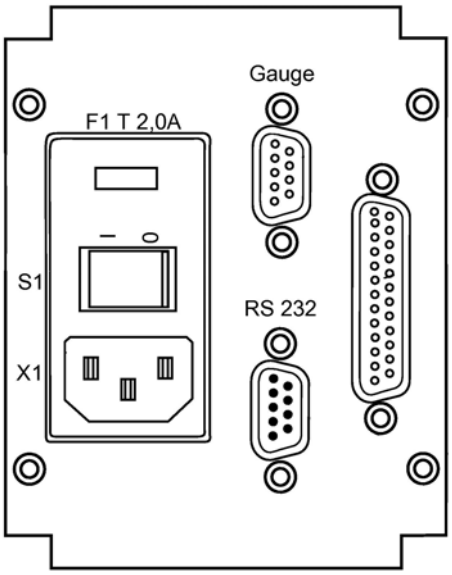

Pfeiffer Gauges

MMIRS utilizes three Pfeiffer vacuum gauges all controlled by a rack mounted controller. Rough pressure is measured by a PPT100 gauge, and each chamber is monitored by an HPT 100 sensor. The controller's RS-232 interface is connected to an EDAS RS-232 to Ethernet converter.

9. E-stop

The emergency stop function is selected by pressing a mushroom push button located on the front panel. Once the button is pressed it will lock in place, and must be turned to be un-latched. When in the latched state, all motion will stop, and all motion commands will be disabled. The switch closure directly disables the drives and also toggles a status bit that can be read by the Delta-Tau motion controller. Turning and unlatching the button re-enables motion.

10. Wheel advance control

Control of the wheel advance is provided by front panel switches and buttons and runs independent of the host system. The Slit Mask Advance is used to select between manual control and computer operation. Manual control mode is defined as having all axis movement disabled, except for on demand wheel advance. Computer control mode is the normal operating mode.

11. Scanner

The barcode scanner used in MMIRS is an OMRON V520-LGP6125 handheld CCD scanner with an RS-232 interface. The scanner connects to a panel mounted connector on Rack 1. The scanner is used to read barcodes when installing slit masks. When installing slit masks the system will query the scanner to store the mask ID associated with the MOS wheel position set by the user in “manual advance mode”.

12. Grounding Plan

Rack 1 provides the instrument its ground reference return and termination for safety grounds. The grounding plan assures that no current is flowing through enclosures and that common mode noise is minimized. In addition, the effects of EMI and electrostatic discharge are also minimized. The science detector maintains a separate ground reference to keep noise to a minimum. A high impedance path of 10 megohms from this isolated ground will be installed to protect against damage to the detector due to ESD. The MMIRS Cryostat and racks are not isolated from the telescope, but the science detector front end is.

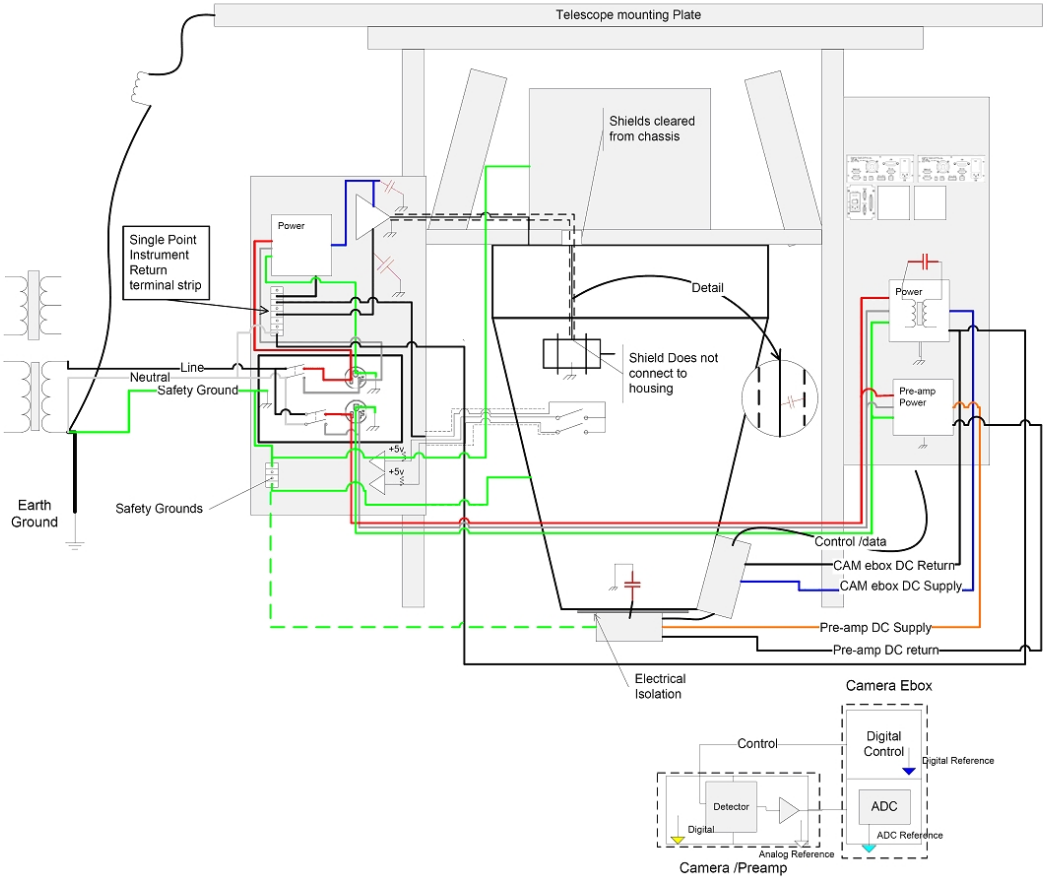

13. MMIRS Interlock Methodology

General:

The motion control signals for the MMIRS mechanisms should, in general, route to the interface printed wiring board (I/F PWB) and through a high pin count Complex Programmable Logic Device (CPLD) with appropriate opto-isolation and buffering logic. Signals applicable to interlocks (e.g. pressure ALARMS, temperature ALARMS, Emergency Stop etc.) would also route to the I/F PWB, through this logic. The purpose of the CPLD is primarily to implement any presently defined and future required interlock logic for the motion control mechanisms of the instrument. Use of a CPLD for this application allows for future additions to, or modifications of, the interlock scheme through the In-Circuit-Programming capability of modern devices. In addition to the interlock function, the CPLD allows for re-routing of signals and changes of signal polarity, should the need arise, without changing the printed wiring board. Routing all of the PMAC control and mechanism feedback signals through the I/F PWB also allows for a central location of all test points for troubleshooting. The JTAG programming/diagnostic port on the CPLD is also available for reading all signals passing in and out of the CPLD. This allows for a powerful secondary diagnostic tool independent of the PMAC or computer systems.

Implementation:

The interlock rules defined by “MMIRS Valve and Heater Interlock Conditions”, McLeod, Martini (Reference. 1) is presented in block diagram form in Figure 1. ALARM relay outputs of the Pfeiffer Gauge control and Lakeshore temperature control units are brought to the I/F PWB and are set for the conditions set out in Ref. 1. (Table 1 defines the relays used in Figure 1.)These signals are opto-isolated, and brought to an Altera CPLD (e.g. ACEX 1K family) along with the mechanism drive commands and feedback (Amp Enable, STEP, and DIRection from the PMAC ACC24C2A board. Mechanism LIMIT feedback signals and system Emergency Stop are similarly isolated and brought to the CPLD. Implementation of the interlock scheme defined in Ref. 1 is a matter of generating an Altera format source file, including pin definitions and Boolean equations, and compiling to the target device. The resulting object file can then be uploaded to the CPLD, in circuit, via the JTAG programming/diagnostic connector. The interlock conditions defined in Ref. 1 are simple Boolean logic equations involving camera and MOS temperature and pressure values. More complex interlocks, involving multiple axes are possible, and easily implemented, if required. Qualified Amp Enable signals are buffered and sent back to PMAC I/O as well as buffered versions of ALARM signals

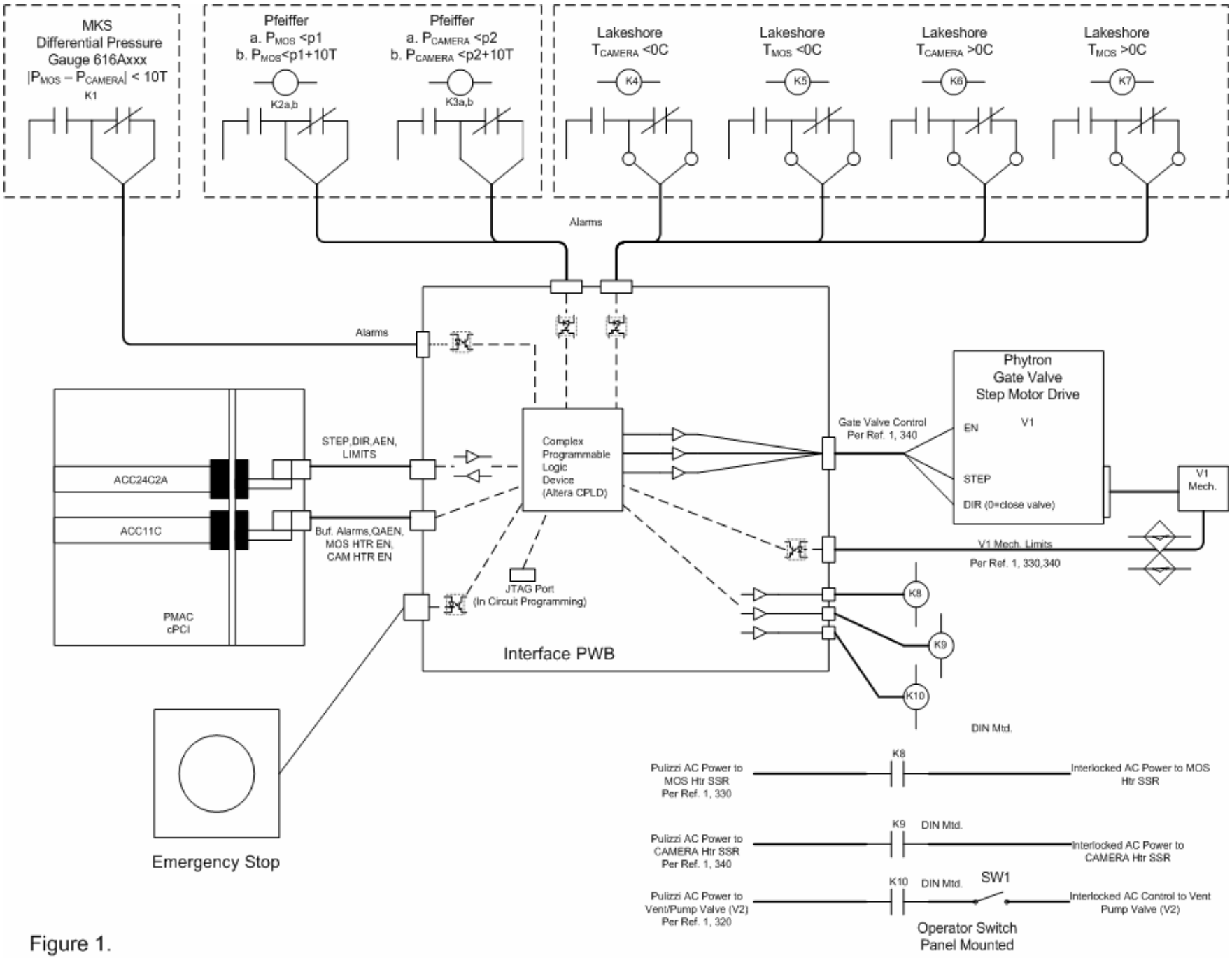

Figure 1.
MMIRS Interlock Scheme

Interlock Relay Summary and Description.

K1 – MKS Differential Pressure Sensor, N.O. Dry contacts. [1.]

Contacts closed when differential pressure between Camera and MOS sections is less than 10Torr.

K2 – Alarm relays internal to Pfeiffer DPG109 Gauge Control. N.O. contacts. [1, 2.]

a. Contacts closed when MOS pressure is less than p1.
b. Contacts closed when MOS pressure is less than p1+10Torr.

K3 – Alarm relays internal to Pfeiffer DPG109 Gauge Control. N.O. contacts. [1, 2.]

a. Contacts closed when CAMERA pressure is less than p1.
b. Contacts closed when CAMERA pressure is less than p1+10Torr.

K4 – Lakeshore relay associated with T_{CAMERA} ALARM. N.O. contacts. [1, 2.]

Contacts closed when $T_{CAMERA} < 0C$.

K5 – Lakeshore relay associated with T_{MOS} ALARM. N.O. contacts. [1, 2.]

Contacts close when $T_{MOS} < 0C$.

K6 – Lakeshore relay associated with T_{CAMERA} ALARM. N.O. contacts. [1, 2.]

Contacts close when $T_{CAMERA} > 0C$.

K7 – Lakeshore relay associated with T_{MOS} ALARM. N.O. contacts. [1, 2.]

Contacts close when $T_{MOS} > 0C$.

K8 – DIN rail mounted relay. N.O. contacts. [1, 3.]

Used to gate Pulizzi switched AC power to MOS heater solid state relay

Contacts close when Gate Valve, V1, is in LIMIT, closed.

K9 – DIN rail mounted relay. N.O. contacts. [1, 3.]

Used to gate Pulizzi switched AC power to CAMERA heater solid state relay

Contacts close when Gate Valve, V1, is in LIMIT, closed.

K10 – DIN rail mounted relay. N.O. contacts. [1, 3.]

Used to gate Pulizzi switched AC power to operator switch (SW1) for Backfill/Pumping Valve (V2) control.

Contacts close when Gate Valve, V1, is in LIMIT, opened AND $T_{MOS} > 0C$ AND $T_{CAM} > 0C$. OR

Contacts close when Gate Valve, V1, is in LIMIT, closed AND $T_{MOS} > 0C$

Notes:

1. Relay contacts chosen to provide safe condition in the event of Disconnect.
2. Pfeiffer relay outputs only configurable to switch when pressure is less than set point.
3. K8 and K9 could be replaced with a single, 2-pole relay to provide gated MOS/CAMERA heater AC.

14. Overall Signal flow example

The following pages show an example of the signal flow and cabling for the MOS section motion axes. The first diagram is an overall view of the connections and the functional elements used. The following pages are the cable drawings that provide the connections for the MOS section from the inside of Rack 1 through to the motors and switches in the MOS chamber. All MMIRS electrical design is done in this manner, with changes made at the top level (the first diagram) flowing to the interconnect drawings automatically.

REVISIONS				
ZONE	LTR	DESCRIPTION	DATE	APPROVED

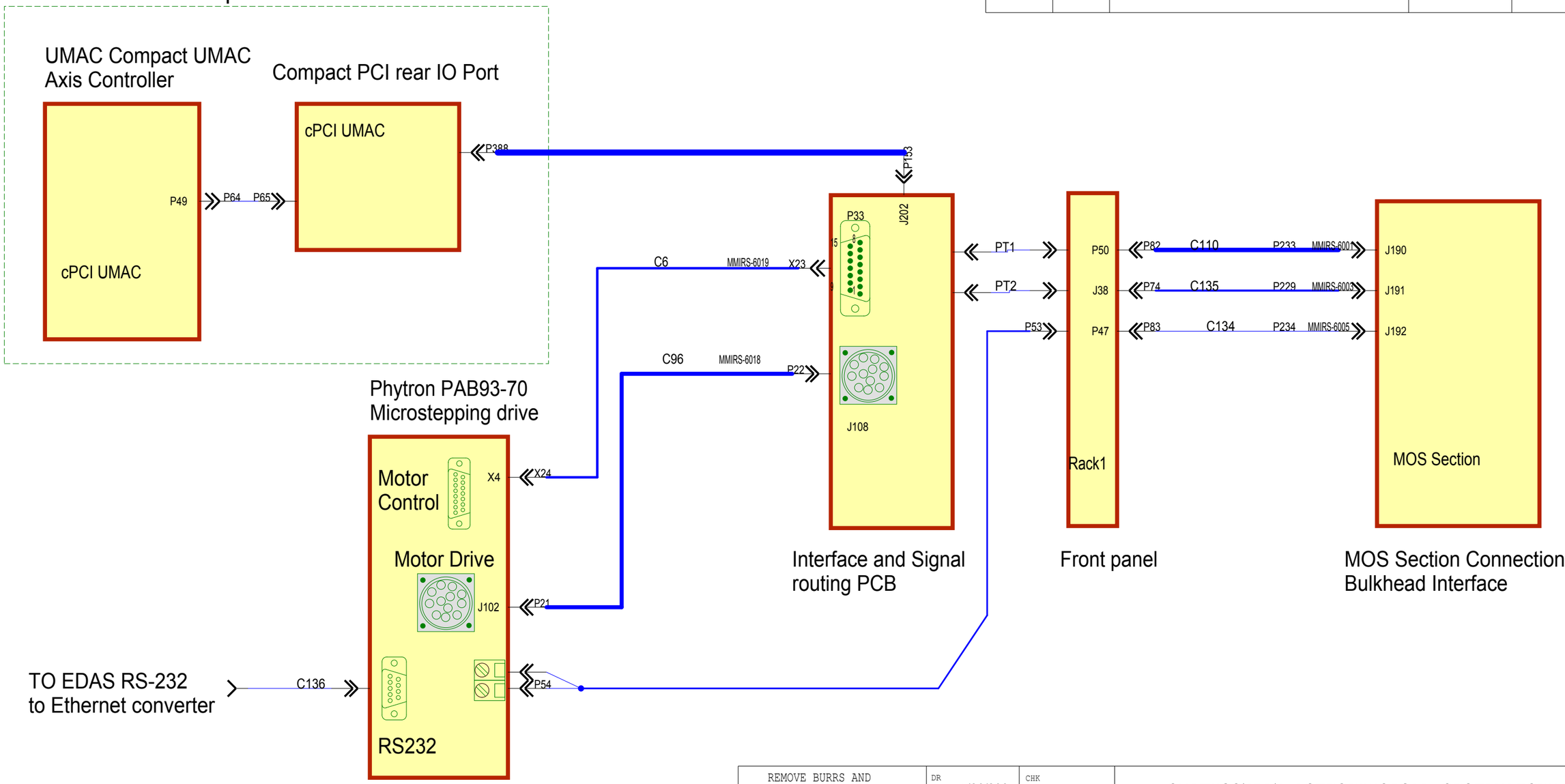

REMOVE BURRS AND BREAK SHARP EDGES	DR DATE 4/26/2005	CHK DATE
UNLESS OTHERWISE SPECIFIED DIMENSIONS ARE IN INCHES	DSGN APPD DATE	
TOLERANCES ON FRACTIONS ± DECIMALS .XX ± .XXX ± ANGLES ±	DSGN APPD DATE	
	ENGR APPD DATE	
MACH. FIN:	PROJ APPD DATE	
MAT'L: / FIN:	CONTRACT	
NEXT ASSY		

SMITHSONIAN ASTROPHYSICAL OBSERVATORY
CENTRAL ENGINEERING CAMBRIDGE,MA

MMIRS Electrical

Motion control System axis Interconnects

SIZE	CODE IDENT NO.	DWG NO.	REV
B	50944		

SCALE | E3 CABLE Ver 6,2004,342 | SHEET 6025 OF 25

REVISIONS				
ZONE	LTR	DESCRIPTION	DATE	APPROVED

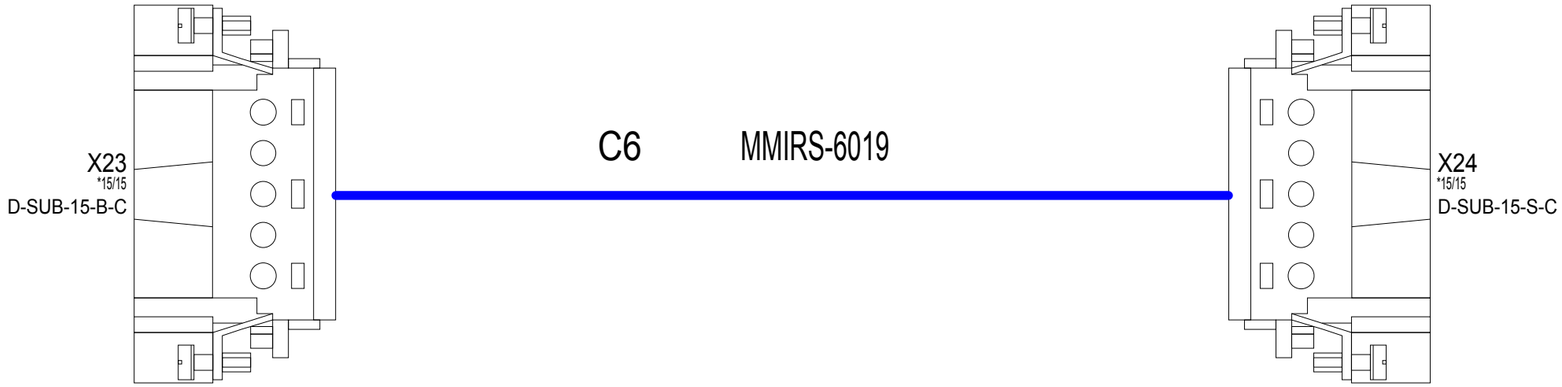

1	Axis_card0_ PUL1-/T1	X24:1	C6	1
2	Axis_card0_ PUL1+/W1	X24:2	C6	2
3	Axis_card0_ DIR1-/V1	X24:3	C6	3
4	Axis_card0_ DIR1+/U1	X24:4	C6	4
5	Axis_card0_ USER1	X24:5	C6	5
6	NC	X24:6	C6	6
7	NC	X24:7	C6	7
8	Axis_card0_ AGND	X24:8	C6	8
9	Axis_card0_ AGND	X24:9	C6	9
10	Axis_card0_ AENA1+	X24:10	C6	10
11	NC	X24:11	C6	11
12	Axis_card0_ HOME1	X24:12	C6	12
13	Axis_card0_ FAULT1	X24:13	C6	13
14	NC	X24:14	C6	14
15	Axis_card0_ FRET1	X24:15	C6	15

1	Axis_card0_ PUL1-/T1	X23:1	C6	1
2	Axis_card0_ PUL1+/W1	X23:2	C6	2
3	Axis_card0_ DIR1-/V1	X23:3	C6	3
4	Axis_card0_ DIR1+/U1	X23:4	C6	4
5	Axis_card0_ USER1	X23:5	C6	5
6	NC	X23:6	C6	6
7	NC	X23:7	C6	7
8	Axis_card0_ AGND	X23:8	C6	8
9	Axis_card0_ AGND	X23:9	C6	9
10	Axis_card0_ AENA1+	X23:10	C6	10
11	NC	X23:11	C6	11
12	Axis_card0_ HOME1	X23:12	C6	12
13	Axis_card0_ FAULT1	X23:13	C6	13
14	NC	X23:14	C6	14
15	Axis_card0_ FRET1	X23:15	C6	15

REMOVE BURRS AND BREAK SHARP EDGES

UNLESS OTHERWISE SPECIFIED DIMENSIONS ARE IN INCHES

TOLERANCES ON
FRACTIONS ± DECIMALS .XX ± .XXX ± ANGLES ±

MACH. FIN:

MAT'L: FIN:

NEXT ASSY

DR DATE 4/27/2005 CHK DATE

DSGN APPD DATE

DSGN APPD DATE

ENGR APPD DATE

PROJ APPD DATE

CONTRACT

SMITHSONIAN ASTROPHYSICAL OBSERVATORY
CENTRAL ENGINEERING CAMBRIDGE,MA

MMIRS Electrical
Phytron Motor control to Interconnect PCB

SIZE	CODE IDENT NO.	DWG NO.	REV
B	50944		

SCALE | E3 CABLE Ver 6,2004,342 | SHEET 6026 OF 25

REVISIONS				
ZONE	LTR	DESCRIPTION	DATE	APPROVED

1	NC	P22:1
2	Mtr_drv_A/_0	P22:2
3	Mtr_drv_A_0	P22:3
4	Mtr_drv_B_0	P22:4
5	Mtr_drv_B/_0	P22:5
6	NC	P22:6
7	Mtr_drv_fwdlim_0	P22:7
8	Mtr_drv_home_0	P22:8
9	Mtr_drv_revlim_0	P22:9
10	NC	P22:10
11	NC	P22:11
12	Mtr_drv_gnd_0	P22:12

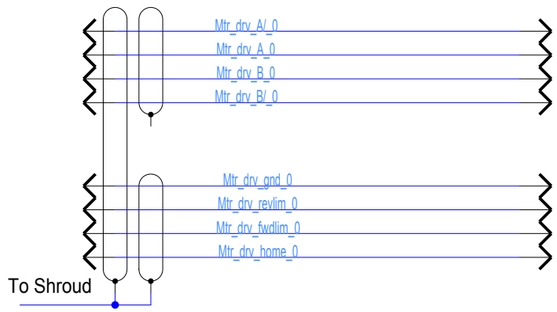

1	NC	P21:1
2	Mtr_drv_A/_0	P21:2
3	Mtr_drv_A_0	P21:3
4	Mtr_drv_B_0	P21:4
5	Mtr_drv_B/_0	P21:5
6	NC	P21:6
7	Mtr_drv_fwdlim_0	P21:7
8	Mtr_drv_home_0	P21:8
9	Mtr_drv_revlim_0	P21:9
10	NC	P21:10
11	NC	P21:11
12	Mtr_drv_gnd_0	P21:12

REMOVE BURRS AND BREAK SHARP EDGES	DR DATE 4/27/2005	CHK DATE
UNLESS OTHERWISE SPECIFIED DIMENSIONS ARE IN INCHES	DSGN APPD DATE	
TOLERANCES ON FRACTIONS ± DECIMALS .XX ± .XXX ± ANGLES ±	DSGN APPD DATE	
	ENGR APPD DATE	
MACH. FIN:	PROJ APPD DATE	
MAT'L: / FIN:	CONTRACT	
NEXT ASSY		

SMITHSONIAN ASTROPHYSICAL OBSERVATORY
CENTRAL ENGINEERING — CAMBRIDGE, MA

MMIRS Electrical

Phytron Motor Drive to Interconnect PCB

SIZE	CODE IDENT NO.	DWG NO.	REV
B	50944		

SCALE | E3 CABLE Ver 6,2004,342 | SHEET 6027 OF 25

REVISIONS				
ZONE	LTR	DESCRIPTION	DATE	APPROVED

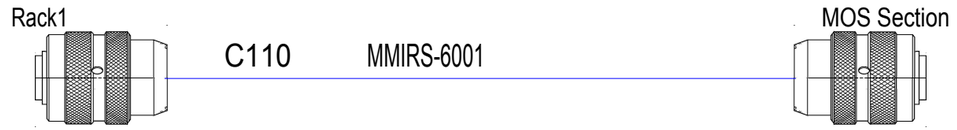

Rack1 P82

	Motor_drv1_A	MOS SectionP233:1
	Motor_drv1_A/	MOS SectionP233:2
	Motor_drv1_B	MOS SectionP233:3
	Motor_drv1_B/	MOS SectionP233:4
	drain1	MOS SectionP233:5
	Motor_drv2_A	MOS SectionP233:6
	Motor_drv2_A/	MOS SectionP233:7
	Motor_drv2_B	MOS SectionP233:8
	Motor_drv2_B/	MOS SectionP233:9
	drain2	MOS SectionP233:10

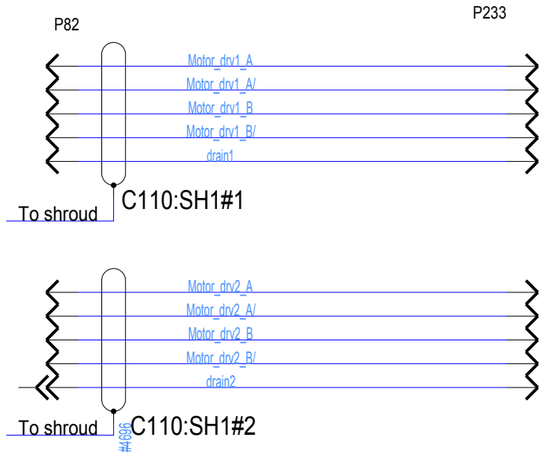

MOS Section P233

	Motor_drv1_A	Rack1P82:1
	Motor_drv1_A/	Rack1P82:2
	Motor_drv1_B	Rack1P82:3
	Motor_drv1_B/	Rack1P82:4
	drain1	Rack1P82:5
	Motor_drv2_A	Rack1P82:6
	Motor_drv2_A/	Rack1P82:7
	Motor_drv2_B	Rack1P82:8
	Motor_drv2_B/	Rack1P82:9
	drain2	Rack1P82:10

REMOVE BURRS AND BREAK SHARP EDGES	DR DATE 4/27/2005	CHK DATE
UNLESS OTHERWISE SPECIFIED DIMENSIONS ARE IN INCHES	DSGN APPD DATE	
TOLERANCES ON FRACTIONS ± DECIMALS .XX ± .XXX ± ANGLES ±	DSGN APPD DATE	
MACH. FIN:	ENGR APPD DATE	
MAT'L: FIN:	PROJ APPD DATE	
NEXT ASSY	CONTRACT	

SMITHSONIAN ASTROPHYSICAL OBSERVATORY
CENTRAL ENGINEERING CAMBRIDGE,MA

MMIRS Electrical

Phytron Motor Drive - Rack1 to MOS Chamber

SIZE	CODE IDENT NO.	DWG NO.	REV
B	50944		

SCALE | E3 CABLE Ver 6,2004,342 | SHEET 6028 OF 25

REVISIONS				
ZONE	LTR	DESCRIPTION	DATE	APPROVED

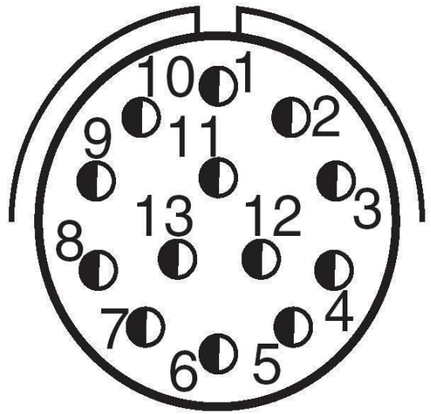

Rack1
P74

1	Axis_card0_ USER1	MOS SectionP229:1
2	Axis_card0_ HOME1	MOS SectionP229:2
3	Axis_card0_ AGND	MOS SectionP229:3
4	Axis_card0_ USER2	MOS SectionP229:4
5	Axis_card0_ HOME2	MOS SectionP229:5
6	Axis_card0_ AGND	MOS SectionP229:6

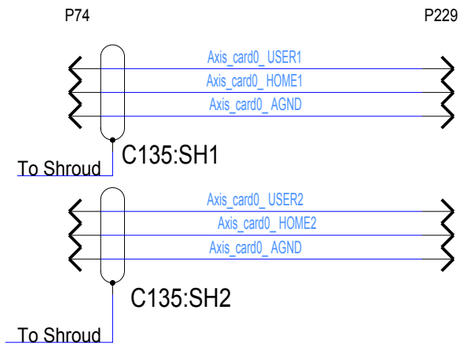

MOS Section
P229

1	Axis_card0_ USER1	Rack1P74:1
2	Axis_card0_ HOME1	Rack1P74:2
3	Axis_card0_ AGND	Rack1P74:3
4	Axis_card0_ USER2	Rack1P74:4
5	Axis_card0_ HOME2	Rack1P74:5
6	Axis_card0_ AGND	Rack1P74:6

REMOVE BURRS AND BREAK SHARP EDGES	DR DATE 4/27/2005	CHK DATE
UNLESS OTHERWISE SPECIFIED DIMENSIONS ARE IN INCHES	DSGN APPD DATE	
TOLERANCES ON FRACTIONS ± DECIMALS .XX ± .XXX ± ANGLES ±	DSGN APPD DATE	
	ENGR APPD DATE	
MACH. FIN:	PROJ APPD DATE	
MAT'L: / FIN:	CONTRACT	
NEXT ASSY		

SMITHSONIAN ASTROPHYSICAL OBSERVATORY
CENTRAL ENGINEERING CAMBRIDGE,MA

MMIRS Electrical

MOS home and detent switch cable-chamber to Rack1

SIZE	CODE IDENT NO.	DWG NO.	REV
B	50944		

SCALE | E3 CABLE Ver 6,2004,342 | SHEET 6029 OF 25

REVISIONS				
ZONE	LTR	DESCRIPTION	DATE	APPROVED

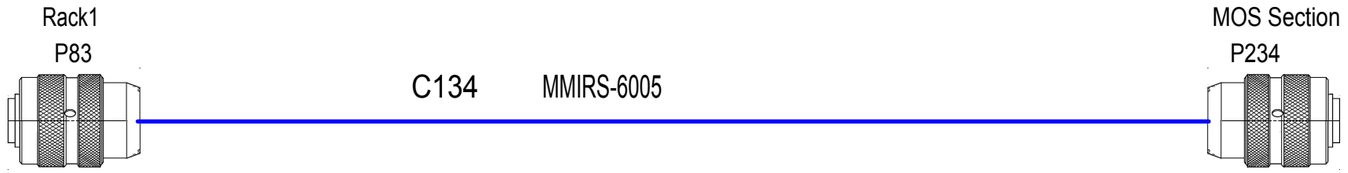

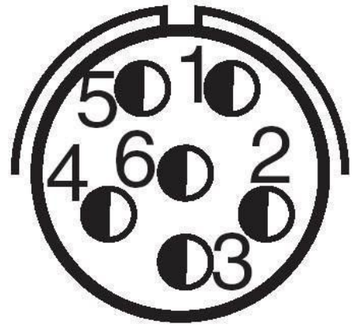

1	mtr_tc+_0	MOS SectionP234:1
2	mtr_tc-_0	MOS SectionP234:2
3	mtr_tc+_1	MOS SectionP234:3
4	mtr_tc-_1	MOS SectionP234:4
5		MOS SectionP234
6		MOS SectionP234

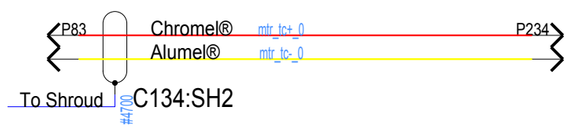

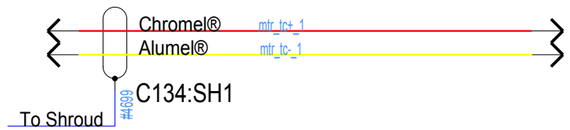

1	mtr_tc+_0	Rack1P83:1
2	mtr_tc-_0	Rack1P83:2
3	mtr_tc+_1	Rack1P83:3
4	mtr_tc-_1	Rack1P83:4
5		Rack1P83
6		Rack1P83

REMOVE BURRS AND BREAK SHARP EDGES	DR DATE 4/27/2005	CHK DATE
UNLESS OTHERWISE SPECIFIED DIMENSIONS ARE IN INCHES	DSGN APPD DATE	
TOLERANCES ON FRACTIONS ± DECIMALS .XX ± .XXX ± ANGLES ±	DSGN APPD DATE	
MACH. FIN:	ENGR APPD DATE	
MAT'L: FIN:	PROJ APPD DATE	
NEXT ASSY	CONTRACT	

SMITHSONIAN ASTROPHYSICAL OBSERVATORY
CENTRAL ENGINEERING CAMBRIDGE,MA

MMIRS Electrical

MOS Motor Thermocouple cable-chamber to Rack1

SIZE	CODE IDENT NO.	DWG NO.	REV
B	50944		

SCALE | E3 CABLE Ver 6,2004,342 | SHEET 6030 OF 25

REVISIONS				
ZONE	LTR	DESCRIPTION	DATE	APPROVED

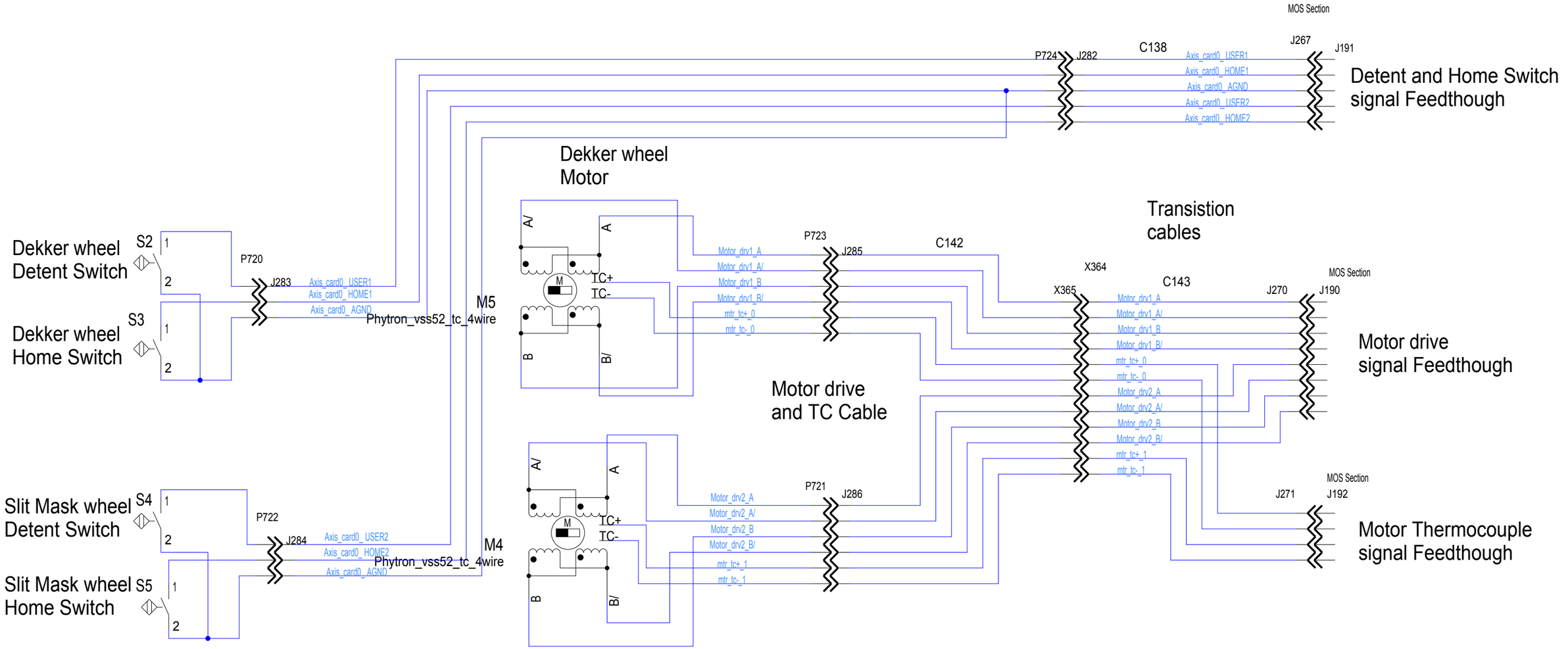

REMOVE BURRS AND BREAK SHARP EDGES	DR DATE 4/28/2005	CHK DATE
UNLESS OTHERWISE SPECIFIED DIMENSIONS ARE IN INCHES	DSGN APPD DATE	
TOLERANCES ON FRACTIONS DECIMALS ANGLES ± .XX ± .XXX ± ±	DSGN APPD DATE	
MACH. FIN:	ENGR APPD DATE	
MAT'L: FIN:	PROJ APPD DATE	
NEXT ASSY	CONTRACT	

SMITHSONIAN ASTROPHYSICAL OBSERVATORY
CENTRAL ENGINEERING CAMBRIDGE,MA

MMIRS Electrical
MOS Cryostat Motor and switch connections

SIZE	CODE IDENT NO.	DWG NO.	REV
B	50944		
SCALE	E3 CABLE Ver 6,2004,342	SHEET 6031 OF 25	

REVISIONS				
ZONE	LTR	DESCRIPTION	DATE	APPROVED

J283

1	Axis_card0_ USER1	P724:1	C139	1
2	Axis_card0_ HOME1	P724:2	C139	2
3	Axis_card0_ AGND	P724:3	C139	3

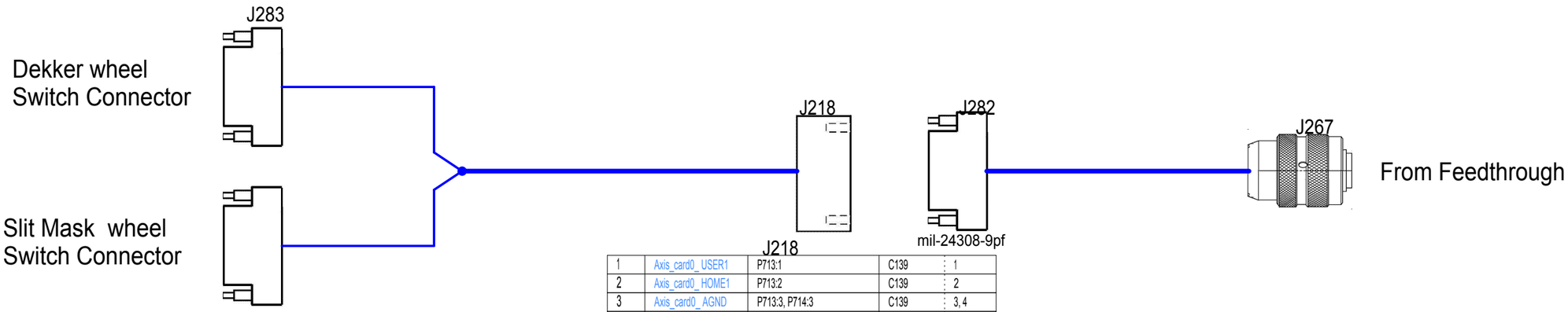

J284

1	Axis_card0_ USER2	P724:4	C139	5
2	Axis_card0_ HOME2	P724:5	C139	6
3	Axis_card0_ AGND	P724:3	C139	4

J218

1	Axis_card0_ USER1	P713:1	C139	1
2	Axis_card0_ HOME1	P713:2	C139	2
3	Axis_card0_ AGND	P713:3, P714:3	C139	3, 4
4	Axis_card0_ USER2	P714:1	C139	5
5	Axis_card0_ HOME2	P714:2	C139	6

REMOVE BURRS AND BREAK SHARP EDGES	DR DATE 4/29/2005	CHK DATE
UNLESS OTHERWISE SPECIFIED DIMENSIONS ARE IN INCHES	DSGN APPD DATE	
TOLERANCES ON FRACTIONS ± DECIMALS .XX ± .XXX ± ANGLES ±	DSGN APPD DATE	
	ENGR APPD DATE	
MACH. FIN:	PROJ APPD DATE	
MAT'L: / FIN:	CONTRACT	
NEXT ASSY		

SMITHSONIAN ASTROPHYSICAL OBSERVATORY
CENTRAL ENGINEERING CAMBRIDGE,MA

MMIRS Electrical

MOS Cryostat switch cables

SIZE	CODE IDENT NO.	DWG NO.	REV
B	50944		

SCALE | E3 CABLE Ver 6,2004,342 | SHEET 6032 OF 25

REVISIONS				
ZONE	LTR	DESCRIPTION	DATE	APPROVED

J286

1	Motor_drv2_A	X365:7	C142	7
2	Motor_drv2_A/	X365:8	C142	8
3	Motor_drv2_B	X365:9	C142	9
4	Motor_drv2_B/	X365:10	C142	10
5	mtr_tc+_1	X365:11	C142	11
6	mtr_tc-_1	X365:12	C142	12

X365

1	Motor_drv1_A	J285:1	C142	1
2	Motor_drv1_A/	J285:2	C142	2
3	Motor_drv1_B	J285:3	C142	3
4	Motor_drv1_B/	J285:4	C142	4
5	mtr_tc+_0	J285:5	C142	5
6	mtr_tc-_0	J285:6	C142	6
7	Motor_drv2_A	J286:1	C142	7
8	Motor_drv2_A/	J286:2	C142	8
9	Motor_drv2_B	J286:3	C142	9
10	Motor_drv2_B/	J286:4	C142	10
11	mtr_tc+_1	J286:5	C142	11
12	mtr_tc-_1	J286:6	C142	12

J270

1	Motor_drv1_A	X364:1	C143	1
2	Motor_drv1_A/	X364:2	C143	2
3	Motor_drv1_B	X364:3	C143	3
4	Motor_drv1_B/	X364:4	C143	4
5				
6	Motor_drv2_A	X364:7	C143	7
7	Motor_drv2_A/	X364:8	C143	8
8	Motor_drv2_B	X364:9	C143	9
9	Motor_drv2_B/	X364:10	C143	10

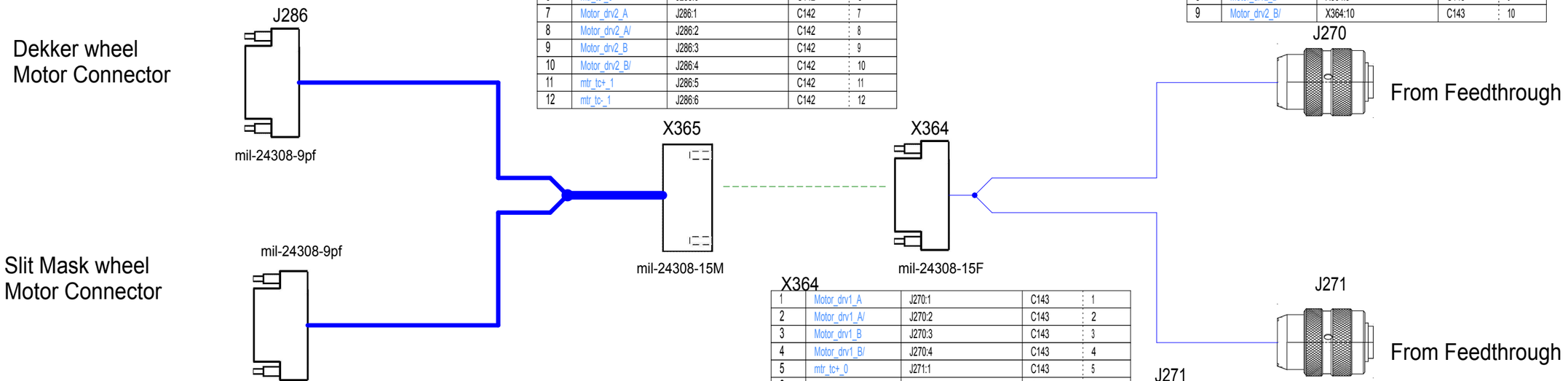

J285

1	Motor_drv1_A	X365:1	C142	1
2	Motor_drv1_A/	X365:2	C142	2
3	Motor_drv1_B	X365:3	C142	3
4	Motor_drv1_B/	X365:4	C142	4
5	mtr_tc+_0	X365:5	C142	5
6	mtr_tc-_0	X365:6	C142	6

X364

1	Motor_drv1_A	J270:1	C143	1
2	Motor_drv1_A/	J270:2	C143	2
3	Motor_drv1_B	J270:3	C143	3
4	Motor_drv1_B/	J270:4	C143	4
5	mtr_tc+_0	J271:1	C143	5
6	mtr_tc-_0	J271:2	C143	6
7	Motor_drv2_A	J270:6	C143	7
8	Motor_drv2_A/	J270:7	C143	8
9	Motor_drv2_B	J270:8	C143	9
10	Motor_drv2_B/	J270:9	C143	10
11	mtr_tc+_1	J271:3	C143	11
12	mtr_tc-_1	J271:4	C143	12
13				
14				
15				

J271

1	mtr_tc+_0	X364:5	C143	5
2	mtr_tc-_0	X364:6	C143	6
3	mtr_tc+_1	X364:11	C143	11
4	mtr_tc-_1	X364:12	C143	12
5				
6				

REMOVE BURRS AND BREAK SHARP EDGES	DR DATE 4/29/2005	CHK DATE
UNLESS OTHERWISE SPECIFIED DIMENSIONS ARE IN INCHES	DSGN APPD DATE	
TOLERANCES ON FRACTIONS ± DECIMALS .XX ± .XXX ± ANGLES ±	DSGN APPD DATE	
MACH. FIN:	ENGR APPD DATE	
MAT'L: / FIN:	PROJ APPD DATE	
NEXT ASSY	CONTRACT	

SMITHSONIAN ASTROPHYSICAL OBSERVATORY
CENTRAL ENGINEERING CAMBRIDGE,MA

MMIRS Electrical

MOS Cryostat Motor Drive and TC connections

SIZE	CODE IDENT NO.	DWG NO.	REV
B	50944		

SCALE | E3 CABLE Ver 6,2004,342 | SHEET 6033 OF 25

100 Electronic Enclosure Design

The are two electronics enclosures which house all of the control electronics for the system. For a complete list of the components in each rack see Electrical Section VIII. The enclosures are designed to allow for easy access to all of the components for setup and removal. The enclosures are also required to limit the heat dissipation into the atmosphere while keeping the electronics below their maxium operating temperature. The sections following discuss the mechanical and thermal design of the enclosures.

110 Enclosure Mechanical Design

The enclosure is based on an standard 19 inch rack mount design. The frame is assembled from a heavy-duty alumunim structural framing sytstem of modular extruded tubing manufactured by AMCO Engineering. The frame measures 24” wide x 51” tall x 25” deep.

There are two doors on the enclosure, one in the front and one in the rear. The rear door provides access to the cabling and any rear mounted compontents. The doors close and seal against a gasket using a multipoint latch.

The top, bottom and side panels are made of aluminum backed foamed polyurethane insulation sheets.

The back side of the enclosure contains panels for all of the electrical connections to the enclosure.

120 Enclosure Thermal Design

S-MMIRS-200, Section 650 states the enclosure shall contain an internal cooling system that limits its heat dissipation into the ambient environment. A maximum of 50 Watts heat dissipation for the entire instrument was given in the specification. Since each Guider/WFS was budgeted 10 Watts, the budget for each enclosure was determined to be 15 Watts. See the table below for the MMIRS heat dissipation budet.

Table 1 - MMIRS Heat Dissipation Budget

Component	Heat Dissipation Budget
Guider WFS	10 Watts (ea)
Electronics Enclosure	15 Watts (ea)
Total Heat Dissipation	50 Watts

To control the heat dissipation for the enclosures a liquid-to-air heat exchanger was selected. Since MMT and Magellan facility coolant supplies are different (methanol/water at MMT and ethylene glycol/water at Magellan) a separate, removable heat exchanger is needed for each site. The heat exchanger will be mounted such that it can be removed without removing or

disconnecting other components. Also, other components can be removed without removing or disconnecting the heat exchanger.

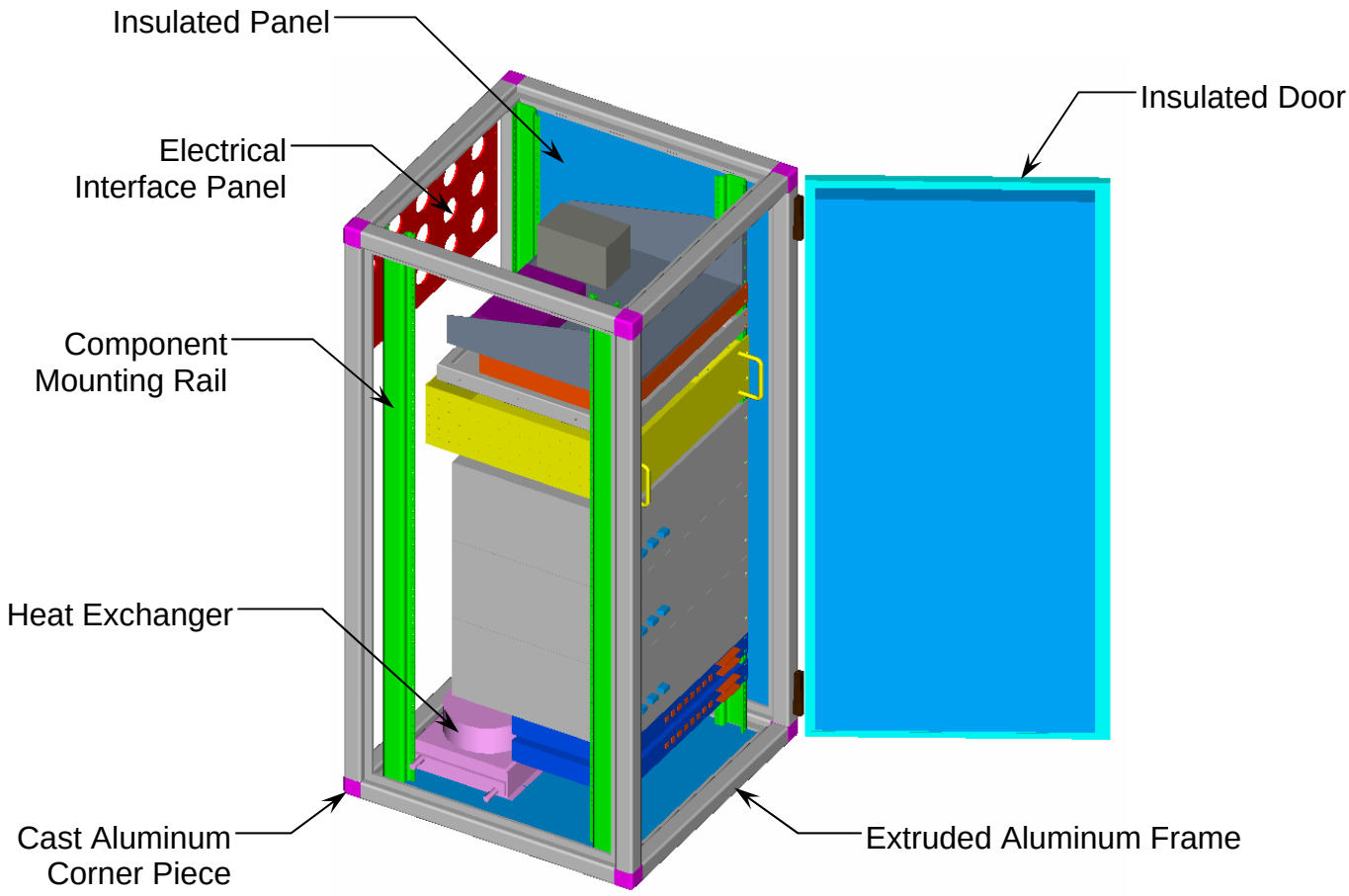

Figure 1 - Electronics Enclosure

121 Heat Exchanger Design

The goal is to cool cabinet air circulated in a closed loop using a liquid-to-air heat exchanger with incoming liquid @ 24.7C (76.5F). Maximum allowable temperature inside the cabinet was set at 35C which is 5C below the maximum operating temperature of the most sensitive component. A conservative estimate of the maximum heat load for an enclosure is 800 Watts. Below is an example of thermal model of the ethylene glycol/water-to-air heat exchanger:

Application Inputs
Heat load: 800 Watts
Max desired air temperature (entering the HX): 35C Max (95F)
Coolant: 10% EG / 90% water (Copper tubes OK)
Coolant flow: 2 GPM

Coolant temperature (entering the HX): 24.7C
800 watts / 35.0C (air entering HX) - 24.7C (water entering HX) = 77.7 Watts / deg C

Thermal Model
Heat Exchanger: (1) Thermatron Model 723 / Parallel circuit, with (2) Comair-Rotron Patriot Fans
Coolant flow: 2.0 GPM @ 3 PSIG
Coolant temperature (entering HX): 24.7C
Coolant temperature (exiting HX): 26.3C
Air flow: 360 ACFM @ 0.25" w.c. (pressure not corrected for density)
Air temperature (entering HX): 33.5C <35C = Good
Air temperature (exiting HX): 27.9C
Heat Load Dissipated: 800 Watts

The heat exchangers in both enclosures will be tied to the same facilities input line through a “tee”. The same is true for the return lines.

The heat exchangers for the glycol/water coolant will use coated copper tubing that is compatable with the coolant. The methanol/water heat exchangers will use stainless steel tubing because copper is not coorsively compatable with methanol.

In order to get proper air circulation inside the enclosure baffling my be required and adequate space has been alotted to add it if necessary.

122 Insulation Panels

The doors and panels on all sides will be insulated with a rigid, closed cell polyiscoyanurate foam. The foam will be sandwiched between two thin aluminum sheets to form the panel. When mounted the panels will compress a thin gasket to provide an adquate seal. The foam has a superior (Class 1) flammability building code classification as tested by Underwriters Laboratory and Factory Mutual.

130 Enclosure Mouting to Telescope

The two electronics enclosures are attached to the telescope mounting truss and ride along with the instrument. Four pads located on the underside of the telescope mounting truss provide anchor points for the electronics enclosures’ own truss. The electronics ensclosures’ truss consists of one inch aluminum tubes with a 0.120 inch wall thickness. Each end of the tube is threaded to accept a clevis. A clevis on one end of the tube is pinned to the anchor point on the telescope mounting truss. The clevis on the other end is pinned to a anchor bracket on the enclosure frame. Each tube and clevis assembly forms a turnbuckle that can be adjusted for length and then locked using jam nuts.

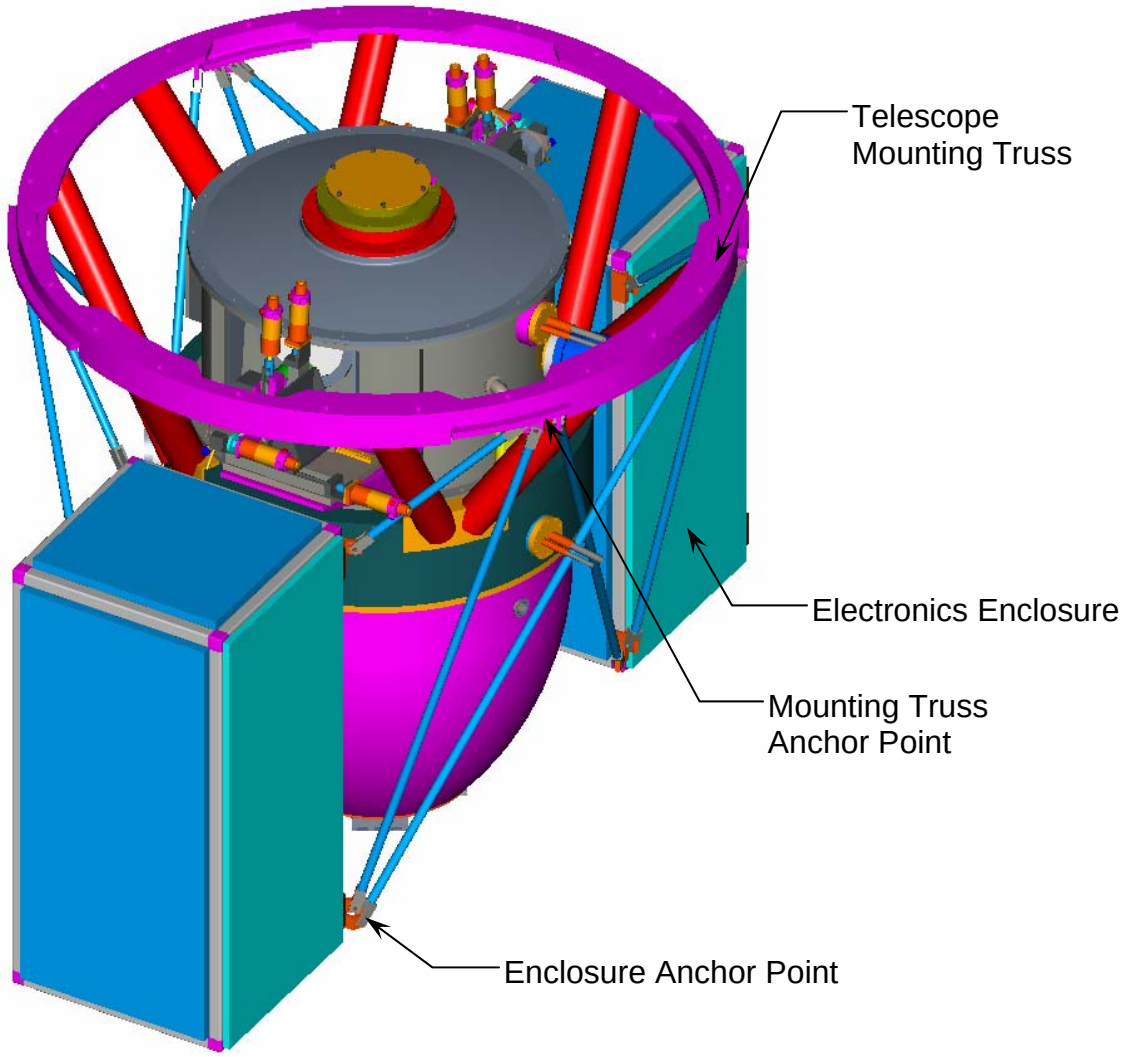

Figure 2 - Electronics Enclosures Mounted to Telescope

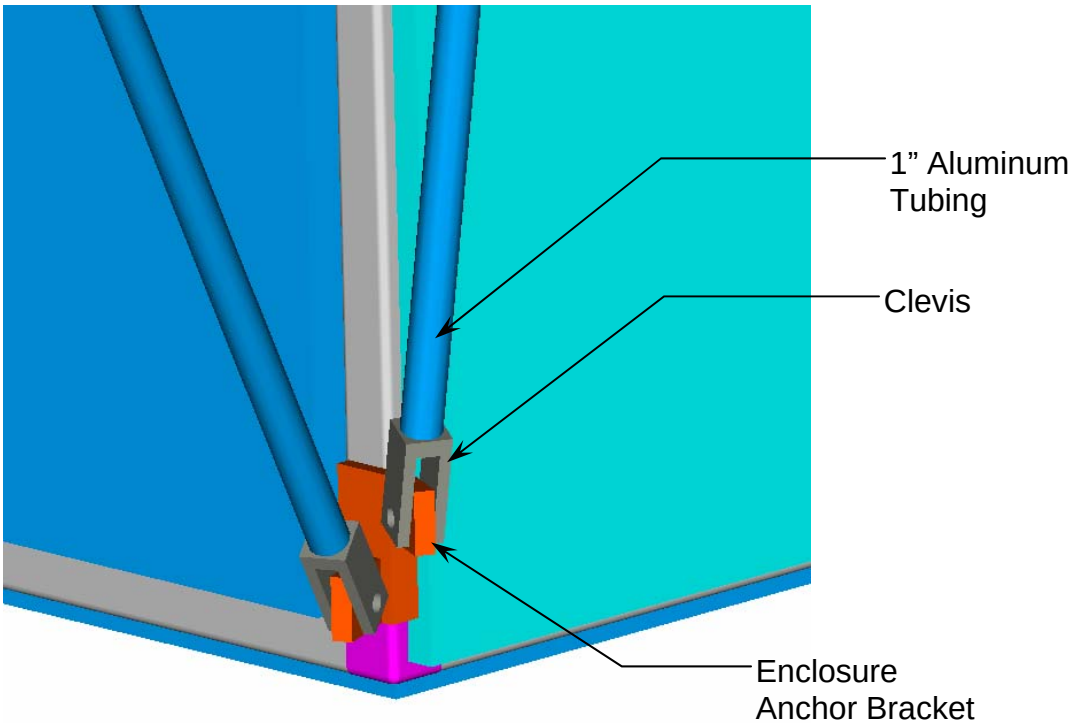

Figure 3 - Enclosure Anchor Point View

MMIRS
Electronics Rack Thermal Design Study

Justin Holwell

05/04/05

Introduction

The MMIRS Instrument requires two rack-mountable enclosures to house all of its electronics. It has been decided that the racks will be cooled using air-to-liquid heat exchangers. This design study documents the assumptions and calculations used in the thermal design for the enclosures.

There are two objectives for this design study:

Determine the size of the heat exchanger required to keep the maximum air temperature in the rack below the maximum temperature of the most temperature sensitive component in the rack.
Determine the insulation type and thickness that will ensure that the rate of heat transfer to the outside environment is less than the budgeted amount for the rack.

Requirements

- Maximum internal enclosure temperature is less than or equal to 35 deg C
- Heat dissipation is less than or equal to 30 watts total for both racks

Assumptions

- Steady state
- One-dimensional heat conduction (ignore corner effects)
- Conservative estimate of heat load = 800 Watts

Insulation Calculations

Rack Dimensions

$h := 1300 \cdot mm$ $w := 600 \cdot mm$ $d := 600 \cdot mm$ Height, width and depth respectively

$A_{surf} := 2 \cdot h \cdot w + 2 \cdot h \cdot d + 2 \cdot d \cdot w$ $A_{surf} = 41.333\ ft^2$ Surface area

$L_a := 1 \cdot mm$ Thickness of metal panels

Material Properties

$k_a := 64 \frac{watt}{m \cdot K}$ Thermal conductivity of stainless steel @ 300K

$k_b := 0.0206 \cdot \frac{watt}{m \cdot K}$ Thermal conductivity of insulation (polyurethane foam) @ 300K

Steady State Conditions

$T_{amb} := 299.85 \cdot K$ Maximum ambient air temperature

$T_i := 304.8 \cdot K$ Average Air Temperature in rack

$Q := 15 \cdot watt$ Allowable heat dissipation into the environment per rack

$\Delta T := T_i - T_{amb}$ $\Delta T = 4.95\ K$

Solve for Insulation Thickness

$$R_a := \frac{L_a}{k_a \cdot A_{surf}}$$

$R_a = 4.069 \times 10^{-6} \frac{K}{watt}$ Since the thermal resistance, Ra, of metal panel is extremely small it will be ignored

$$L_b := \frac{k_b \cdot A_{surf} \cdot \Delta T}{Q}$$

$L_b = 1.028\,in$ $L_b = 26.104\,mm$ Thickness of insulation panels

Heat Exchanger Sizing

MMIRS will travel to two different locations (Magellan and MMT) which have different liquid coolant provisions, two different heat exchangers are required.

Heat Exchanger Required Capacity

$Q_{load} := 800 \cdot watt$ Conservative estimate of heat load in one rack

$T_{air\_in} := 308.15 \cdot K$ Maximum temperature of air entering heat exchanger

$T_{coolant\_in} := 297.85 \cdot K$ Maximum temperature of coolant entering heat exchanger (~ 2 degrees below ambient)

$$HEX_{capacity} := \frac{Q_{load}}{T_{air\_in} - T_{coolant\_in}}$$

Capacity of heat exchanger required to dissipate the heat load.

$HEX_{capacity} = 77.7 \frac{watt}{K}$

Based on the heat exchanger capacity calculated above, the heat exchanger vendor Thermatron, sized heat exchangers for both applications using the following properties:

Air Properties (0.728 Bar / 35C)
1. Density = 0.0518 Lb/ft3
2. CPT = 0.2405 Btu/Lb.F
3. KT = 0.0155 Btu/(H.ft2.F/ft)
4. MUT = 0.0457 Lb/ft.H

10% EGW Properties (Avg 30C)
1. Density = 62.9 Lb/ft3
2. CPT = 0.946 Btu/Lb.F
3. KT = 0.333 Btu/(H.ft2.F/ft)
4. MUT = 2.56 Lb/ft.H

60% Methanol / 40% Water Mix (by volume) Properties (30C)
1. Density = 55.26 Lb/ft3
2. CPT = 0.7405 Btu/Lb.F
3. KT = 0.1747 Btu/(H.ft2.F/ft)
4. MUT = 2.543 Lb/ft.H

Thermotron's thermal model and calculated heat dissipated by the heat exchanger are listed below.

10% EGW Heat Exchanger Model
Heat Exchanger: (1) Model 723 / Parallel circuit, with (2) Comair-Rotron Patriot Fans
Coolant flow: 2.0 GPM @ 3 PSIG
Coolant temperature (entering HX): 24.7C
Coolant temperature (exiting HX): 26.3C
Air flow: 360 ACFM @ 0.25" w.c. (pressure not corrected for density)
Air temperature (entering HX): 33.5C <35C = Good
Air temperature (exiting HX): 27.9C
Heat Load: 800 Watts

60% Methanol / 40% Water Mix (by volume) Heat Exchanger Model
Heat Exchanger: (1) Model 733SBP2A02 / Parallel circuit, with (2) Comair-Rotron Patriot Fans
Coolant flow: 2.0 GPM @ 3 PSIG
Coolant temperature (entering HX): 24.7C
Coolant temperature (exiting HX): 27.1C
Air flow: 360 ACFM @ 0.25" w.c. (pressure not corrected for density)
Air temperature (entering HX): 34.5C <35C = Good
Air temperature (exiting HX): 28.8C
Heat Load: 800 Watts

Even though the heat load is a conservative estimate, the heat exchangers above provide no safety factor. The application will be reviewed to determine if the heat load can be reduced and/or if a larger heat exchanger should be selected. An attempt will be made to measure the load for various electronics modules to further refine the model. Other possibilities include increasing the coolant flow rates and/or usse two smaller heat exchangers per rack that will provide enough safety margin above the heat load.

Section IX.

MMIRS Software Design

1. Overview
2. Derived Requirements
3. Design Principles
4. Computer and Software Architecture

Software Components

5. Libraries and Utilities
6. Servers
7. Graphical User Interfaces, GUIs

8. System Management
9. Testing and Verification
10. Data Products
11. Schedule and Milestones

MMIRS/

CDR Software Section

- 1. **Overview**
- 2. **Derived Requirements**
- 3. **Design Principles**
- 4. Computer and Software Architecture
    - **Hardware and Network**
    - **MMIRS-Computer-Arch.pdf**
    - **Software Overview**
    - **Software Interconnect Diagram.pdf**
- Software Components
    5. **Libraries and Utilities**
    6. **Servers**
    7. **GUIs**
- 8. **System Management**
- 9. **Testing and Verification**
- 10. **Data Products**
    - **FITS Image Header Example.pdf**
    - **FITS MOS Header Example.pdf**
    - **Aperture Map Example.pdf**
    - **Data Reduction Software**
- 11. Schedule and Milestones
    - **Development Estimates**
    - **Release Schedule**

MMIRS/

Overview

SAO has been operating instruments at the 6.5m MMT for 5 years, starting with the Minicam imager at f/9 in 2000. In total we have now commissioned 5 instruments for operations at the MMT: 2 optical imagers (Minicam and Megacam), 2 fiber multi-object spectrographs (Hectospec and Hectochelle) and 1 infra-red imager (SWIRC), as well as a Shack-Hartmann wavefront sensor and the f/5 refractive corrector. As a result we have mature instrument control systems, a common observing environment, and a robust computer system to support multi-instrument observing.

The MMIRS instrument will use familiar instrument control systems to drive motors in the cryostat. The MMIRS science camera electronics are identical to SWIRC and the detector software is complete. The thermal-vacuum control systems are new, but largely decoupled from the instrument control and observing systems. The thermal-vacuum control systems require relatively simple computer support, as the bulk of the intelligence for controlling the systems resides in the hardware controllers, e.g. Omega and Lakeshore. The observing GUI will be largely identical to the Megacam and Hecto GUIs, with customizations as required to match up with the mechanisms in MMIRS.

The MMIRS instrument will also implement continuous wave-front sensing, which will be new to the MMT and will therefore require additional support from the facility. The MMIRS guiding system will be largely identical to the systems used with Megacam and Hectospec/chelle. Some additional software will be required to interface to the observatory wavefront sensing software and to interface to the guide camera X-Y stages.

We plan to operate MMIRS at the Magellan telescope as well, which will present a different environment and facility interface. However, we are currently in the process of preparing Megacam for operations at Magellan. This will require installation of our computer systems (identical to the MMT system) and writing a protocol translator to go between our instrument software and the observatory control system. We wrote a similar piece of code for the MMT several years ago. The completion of the Megacam installation at Magellan will require implementation of the majority of the telescope/facility interfaces required for MMIRS.

MMIRS/

Derived Requirements

Most MMIRS formal requirements are for the hardware. But there are many unwritten expectations and constraints based on our existing framework and the environments in which we'll be operating. From these contraints we derive these additional requirements.

- Observing interfaces for MMIRS should be as similar as possible to other SAO intrument interfaces.
- Operating interfaces (guiding, wave-front sensing) for MMIRS should be as similar as possible to other instruments at the same facility. The guider GUI will be new to the Magellan facility but will be in common with the Megacam guider.
- System must support multiple operational modes
    - Software must have test and/or simulator modes to enable easy use in non-observing settings, e.g. lab devopment, engineering, trouble-shooting and calibration modes.
    - Must have a test environement at SAO for development and debugging
- System must run on multiple computer systems at multiple facilities
    - Operate on private network
    - Operate behind a firewall
    - Devices will have private ethernet addresses that are constant so the instrument can be transported between SAO, MMT, and Magellan without reprogramming any IP addresses.
- Minimize Failure Conditions that Require Opening Camera Section of Cryostat
    - Failure of motor limits must be recoverable (must have hard stops)
- Dependability, Reliability, Recoverability
    - Previous software versions must be retrievable
        - System must be backed up
        - System must be under configuration control
        - System must be baselined
        - Software must be tested before installation

- Must have on-site spares to enable repair in < 24 hours
  - redundant computers
  - spare camera data controllers
  - spare phytrons
  - spare uMAC

- Integrity

  - Science Data must never be lost:

    3 copies made of each exposure

    - RAID5 system1:
      - 1 user accessible copy
      - 1 archived un-accessible copy
    - RAID5 system2:
      - 1 user accessible copy on data analysis computer

- Development Efficiency

  - Minimize Development Hours
    - Code ReUse
    - Table Driven Configurations
    - Table Driven Software

  - Support Parallel Devlopment
    Must support parallel lab development:
    - cryostat lab development
    - wfs/guide lab development

MMIRS/

Design Principles

- Client/Server Architecture using MSG protocol communication
    - Loosely Coupled Componets
    - Servers are controllable both from scripts as well as GUI buttons
    - All servers are accessible and runnable via telnet

- Protocol Translator Layers
  Isolate layers of code that contain the mappings necessary to operate in different environments
    - two different telescopes
        - telescope interface server
        - guideserver

- Maximize Code ReUse and Minimize Code Changes for Multiple Environments
    - Configuration Driven Services
        - Cal Lamps
        - Pulizzi Power Servers
        - EDAS converters
        - Lakeshore monitors and controllers
        - Omega heater controllers
        - Vacuum gauges
    - Table Driven Architecture (computer/server assignments)
    - Camera Parameters

- Incremental Development
  Implement a sparse operational framework as early as possible and continuously add functionality. Use existing code wherever possible. Make continuous incremental changes to gradually adapt and expand the system to full functionality. MMIRS system will integrate into the observing environments already in place at the MMT and Magellan, as well as the engineering environment at SAO.

- Multiple Interface Levels
    - Lab operations at SAO
    - Engineering operations at SAO and at telescopes
    - Calibration operations at SAO and the telescopes
    - Science observing operations at the telescopes

- Simulators
  We have simulators for many of the instrument and telescope components to allow end-to-end testing at SAO after delivery of the instruments.

- Standard File Formats/Header Keywords

  Our Science image FITS files use standard header keywords wherever possible. They conform to the keyword usage defined by NOAO and are common for all of our instruments.

  In addition to the science image frame, spectroscopic data requires an aperture map. This is stored as binary FITS table extension to the science image and also extracted into a plain ASCII Iraf-compatible list readable by IRAF APEXTRACT tasks.

MMIRS/

Hardware and Network

- Power

  The facility provides 120 V UPS quiet power which feeds our UPS device. All computer hardware is connected to the UPS. The UPS is specified to provide 30 minutes of backup, but is programmed to issue shutdown commands to the computers afer a 5 minute outage, ensuring a safe and orderly shutdown of all systems in the event of power loss. This also facilitates shutdown for impending thunderstorms. Simply shutting off power to the UPS will initiate automatic shutdown of the computers 5 minutes later, thus simplifying the shutdown procedure for the observatory staff.

- Computer Architecture

  The MMIRS computer system is built by networking identical linux server rack-mount systems. Our configuration requires a minimum of 3 units at the MMT and a minimum of 4 units at Magellan. The systems are otherwise identical and spare each other with the possible necessity of swapping special purpose PCI camera interface cards. The 3U units are mounted in our own computer rack with all the supporting equipment: UPS, ethernet switches, fans.

  Architecture Diagram

- Computer Hardware
  Each computer component in the MMIRS system will run the Fedora Core 2 linux operating system.

  - Dual Opteron 2.2 GHz. CPUs
  - 4 Gbytes memory
  - Dual Head Graphics Cards
  - 5 PCI Slots (for camera controllers) and other PCI computer devices
  - 6 x 250 Mbyte ATA data disks, RAID 3
  - 1 250 Mbyte ATA system disk
  - 2 Gigabit ethernet ports
  - 1 CDROM
  - 1 USB port

- Network Configuration

  The computers are all connected to our Gigabit ethernet switch. All the computers

have IP addresses in the private subnet range 192.168.1.1-256. One of the computers - Observer Workstation - also has an IP address in the public range and so is accessible from outside the telescope.

The 2 MMIRS instrument electronics racks will also be part of this private Gigabit ethernet and all ethernet devices in the racks will also be assigned IP addresses in the 192.168.1.1-256. This allows the hardware to move transparently between the 2 telescopes with no need to fiddle with IP addresses. Our network switches will connect to the facilities' Gigabit networks.

Computer Hardware Architecture

Observer computer

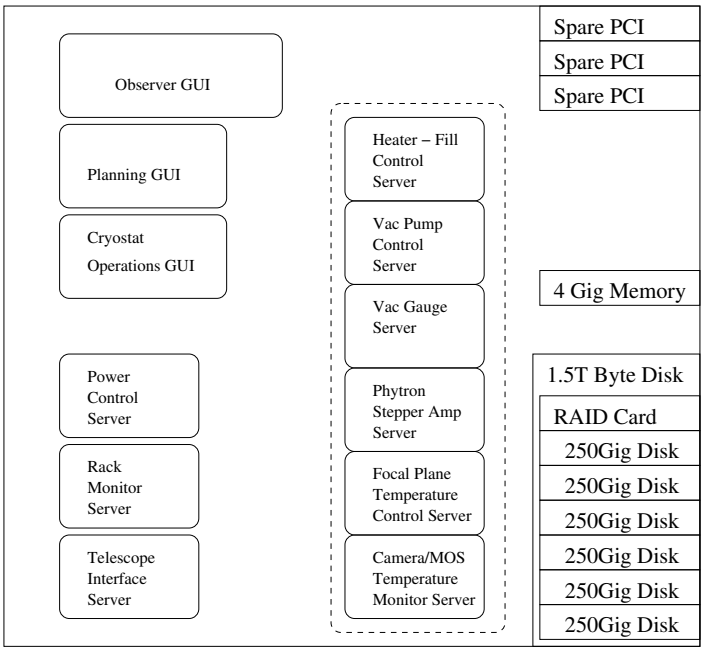

Science Data computer

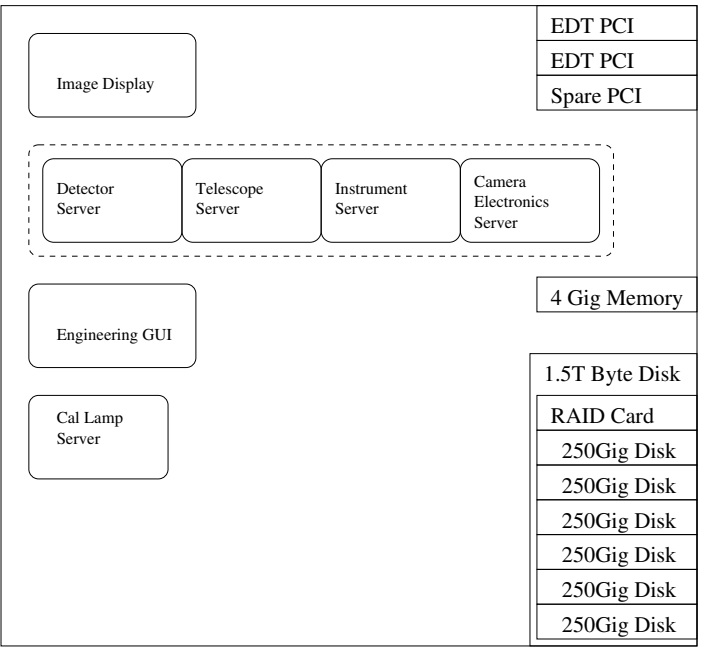

Guide computer

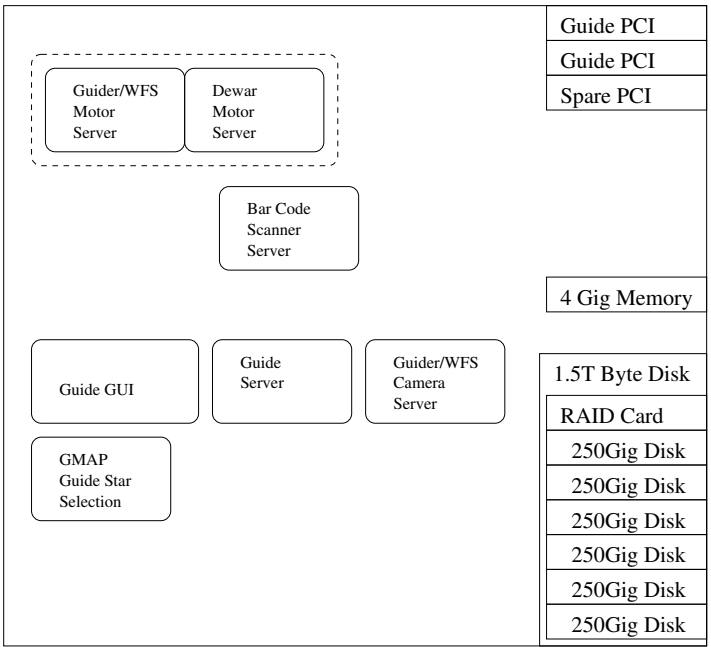

MMIRS/

Software Overview

Software Overview

The MMIRS software can be partitioned into 5 distinct subsystems each with its own environment and external interfaces. Only the Planning/MOS-slit design sub-system, WFS sub-system and the Telescope Interface Server have direct interaction with the observatory facilities.

- Engineering
  An engineering GUI is provided to allow testing and control of all MMIRS instrument hardware: thermal-vac and Motion Control. This system is completely self-contained within the SAO/MMIRS environment

- Cryostat monitoring & control
  The Cryostat system allows observers and observatory staff to control the heating and cooling of the MMIRS cryostat, and in particular to allow changing of MOS slitmasks. The interface must allow easy use by staff members while safe-guarding the instrument. This system is also completely self-contained within the SAO/MMIRS environment. This system interacts with the Thermal-Vac system which provides the interface to all of the cryostat thernal-vac devices.

- Planning
  The planning subsystem is primarily for use of MMIRS in the MOS mode. It allows the observer to plan an MOS observation and produce a slit-mask configuration file that is readable by the laser-cutting facility. This software must be accessible by users at their home institutions as well as at the observatories. The slit-mask configuration file must be usable at both the Magellan and MMT mask-cutting facility. This software will be taken from the existing system used by IMACS at Magellan, ensuring compatibility with the Magellan system. A translation layer will be added, if necessary for compatibiltiy with the MMT facility.

- Guiding & WaveFront Sensing
  The guiding and wavefront sensing subsystem must be compatible both with the SAO observing environment as well as the two telescope systems. This system has the most design and interface constraints. The Telescope Interface Server provides a critical protocol translation layer between the SAO instruments and the telescope control systems. It allows both the observing and guide correction interfaces to be uniform at both telescopes. The GuideServer provides the common interface to different Guide Camera systems. The MMIRS guide camera control protocol will be integrated into this

existing application. And we will adopt Magellan's GMAP guide star selection system for both observatories.

The Wave Front Sensing system will be provided by the Magellan facility. MMIRS must only supply a WFS definition file and the raw FITS images from the camera. The MMTO will need to add the capability to do continous wavefront sensing to support MMIRS.

- Observing
  The observing interface will be a variation of the SPICE/MICE GUIs currently in use for the existing SAO instruents. They have only 2 external interfaces. The telesope interface will be handled through the telescope interface server. The Guide interface will be implemented within the Guide Server. With these 2 systems in place, the observing system is completely de-coupled from the observatory system.

Software Interconnect Diagram

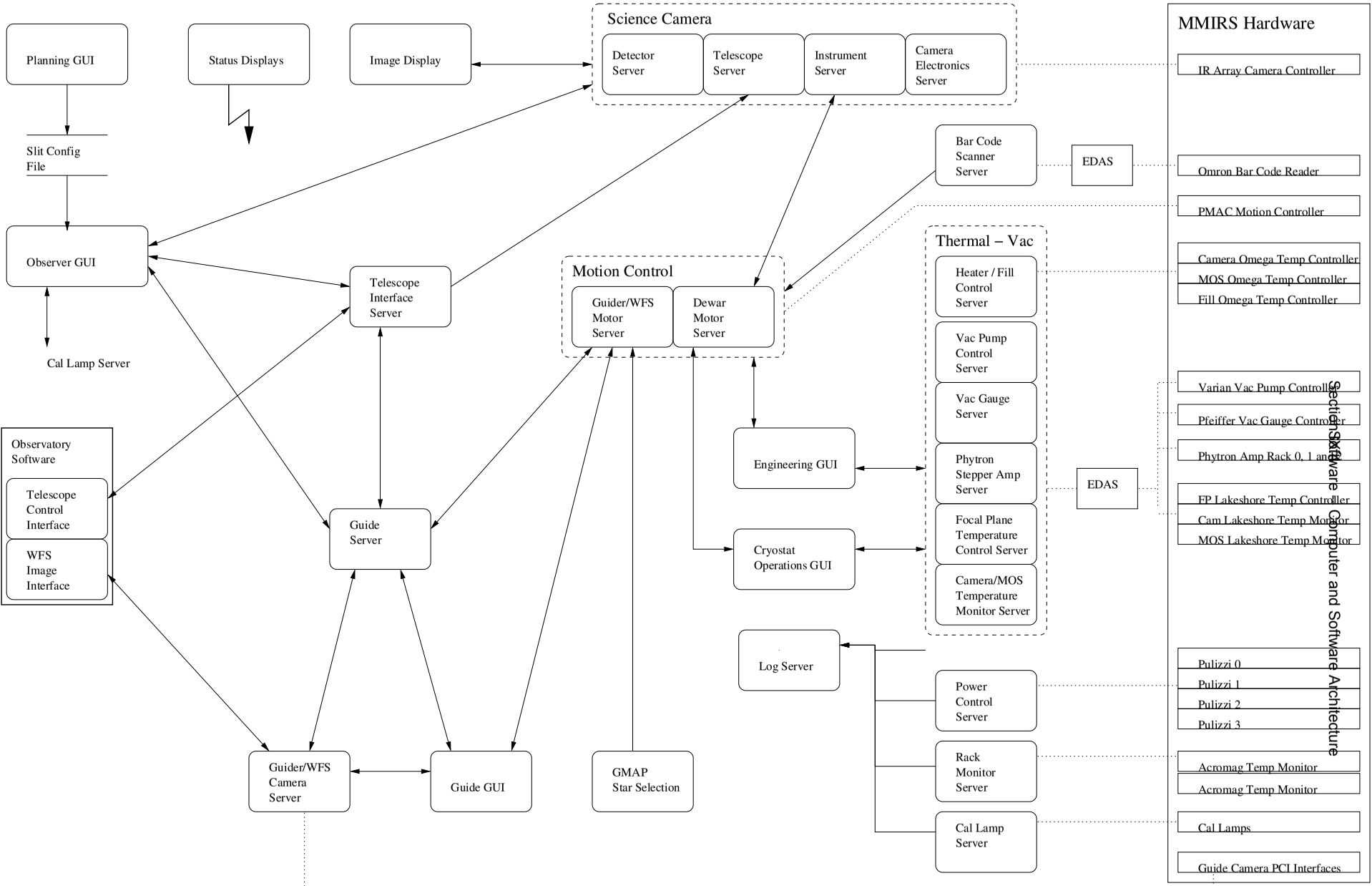

MMIRS/

Libraries and Utilities

The software is built using many common libraries and packages. These include SAO internal libraries developed for other instruments, external libraries from hardware vendors, external astronomy packages and utilities from the observatories where our instruments are deployed.

- SAO libraries and utilities
  - Inter-Process Communication: **msg protocol** The msg library (implemented in C and Tcl) is uses by all client and server applications to establish the communication of commands and status variables.
  - Database and Configuration Tables: Starbase tables are used for all the tabular data in the system. This includes all the internal software configuration tables as well as the observer object catalogs and aperture maps. The format is a simple ASCII tab-delimited table. The support tools allow sophisticated database manipulations including some astronomy specific functions.
  - FITS file read/write/keywords The fitsy library (implemented in C and Tcl) provides a light-weight interface to read and write FITS files.
  - IRAF-style parameter interface SAO written tools use our param interface library which emulates the IRAF parameter interface familiar to most astronomers
  - Observers Database A database of each exposure is automatically generated by postprocessor code that builds a starbase table from selected header keywords from each exposure image. (This is the same database that's joined with observer comments to generate the observers logfile).
  - Archiving The archiving at the MMT is implemented with a script that queues files for transfer to SAO via the print queue mechanism. This is called as a postprocessor to each exposure.
  - Power control The powserv Tcl library is used to control all the Pulizzi devices and supports the multiple models/communication protocols.
  - Temperature Monitoring The lakeshore Tcl library developed for SWIRC controls the communication with the Lakeshore devices. It will be expanded to add control commands to the existing monitoring coommands.

- cmac communications A Tcl library package developed to standardize PMAC motion control implementations.

- Hardware Interface Libraries
  - Serial-to-ethernet communication The EDAS library delivered from Intelligent Design and wrapped for Tcl is used to communicate with all the serial-port devices

  - Detector Electronics communication The EDT library delivered from EEV and with a few local enhancements is used for all communication with the science camera electronics.

- External Libraries and Utilities
  - Astronomical computations **slalib** is used to perform all the astronimical computations
  - Image Display DS9 is used for all our image display
  - IRAF The NOAO/IRAF system is installed to support basic image analysis, such as focus, seeing measurements.

- Observatory Compatibility Packages

  - SlitMask Generation
  - GMAP guide star selection software
  - Magellan telescope C interface library (Skip Schaller)

MMIRS/

msg protocol

SAO has developed a simple ASCII-over-tcp protocol to allow clients and servers to be written without significant effort on getting things to talk to each other.

This protocol is used for nearly all Inter Process Communication by the F5 instruments at the MMT.

The MMTI message passing protocol is an ASCII protocol based on TCP sockets. The protocol is described here.

- Newline terminated variable length ASCII message packet.
- Packet Format.

```
    [#] command args \n
```

  - Optional Packet Number.
  - Command and Args.
  - Terminator - A Newline character terminates the message.

- Message length. - The length of a message is not implicitly limited by the protocol. Currently the C implementation Messaging library limits messages to 512 characters.

- Commands - No commands are specifically defined in the protocol. The MMTI Messaging library defines the following:

```
        set      set a value
        get      get a value


        ack      positive acknowledge and return value.
        blk      positive acknowledge and data block.
        nak      negative acknowledge and return error.


        sub      subscribe to a value
        uns      unsubscribe to a value
```

```
lst      list available server commands
```

This command set supports the publish/subscribe design pattern used in all servers. Servers then publish additional commands to support their specific functions.

- Inter Packet Data

  Commands may define inter packet data. The sender and receiver of this data must each agree to write/read exactally the same number of bytes or define a logical EOF character.

  There is no provision for protocol resyncronization if commands get confused sending or receiving interpacket data.

  During the development of the F5 instruments for the MMT standard methods for sending interpacket data over msg sockets have been developed. FITS files are routinly sent as counted binary blocks using the fitsy library to read the correct number of bytes as indicated in the FITS headers. ASCII tables are read and written with the starbase routines that support the use of the form feed character as a logical end of file mark.

- Server access authentication - the msg library supports host based authentication via an enumerated list of allowed hosts.

MMIRS/

Servers

All servers are implemented either in C or TcL using the **msg protocol** socket communication library. This ensures that all servers can be operated either from scripts or from GUIs.

- **Telescope interface server**
- **Science Camera**
  - **Detector**
  - **Instrument**
  - **Telescope**
  - **camera electronics commands**

- Guiding/Wave Front Sensing
  - **Guide server**
  - **WFS - Guider camera server**

- **Motion Control Server**
  - **PMAC Control Server**
  - **MOS wheel push buttons**

- **Bar Code scanner server**

- Thermal Vacuum
  - **Vac gauge server**
  - **Vac pump control server**
  - **Heater - Auto Fill control server**
  - **Camera - Mos section temperature monitor**
  - **Focal Plane Temperature Control**
  - **Phytron Stepper Amp server**

- Hardware Control
  - **Cal lamp server**
  - **Power Control Server**
  - **Rack monitor server**

- **Log Server**

MMIRS/Servers/

Telescope interface server

Overview

The telescope interface server provides a standard messaging protocol interface for our software to access telescope information and control telescope functions. It also provides a translation layer where the telescope model and coordinate systems expected by our system can be implemented on top of the model provided directly by the facility. The most important example of this concept is the use of **instrument offset (instaz,instel)** coordinate system used to define the dithering of all of our instruments, but not available at Magellan.

Derived From

This interface has already been written for the MMT telescope. An analogous server will be written in Tcl to interface to the Magellan telescope control system using Skip Schaller's C library interface. (This will be be required for Megacam at Magellan also).

The server in operation at the MMT is a fairly simple 1 to 1 command and value translator. At the Magellan telescope the control model is significantly simpler and less sophisticated. The telescope interface server for Magellan will have to emulate several features that are available at the MMT:

- Target RA, Dec independent of current pointing position
- Instrument Offsets
- Clearable Instrument Offset registers
- Clearable Guide Offset registers

Interface (Msg Protocol)

- Telescope Commands
  - **azeloff** azoffset eloffset
    Set the Az El offset from the base pointing direction
  - **azelrel** azoffset eloffset
    Add to the Az El offset from the base pointing direction.
  - **instoff** azoffset eloffset
    Set the instrument offset from the base pointing direction.
  - **instrel** azoffset eloffset
    Add to the instrument offset from the base pointing direction.
  - **radecoff** raoffset decoffset
    Set the Ra Dec offset from the base pointing direction.

- **radecrel** raoffset decoffset
  Add to the Ra Dec offset from the base pointing direction.
- **azelerr** azerror elerror roterror
  Add to the Az, El and Rotation error from the pointing direction. This is the command used to add guide corrections to the pointing direction.
- **slew** ra dec posangle
  Request a slew to a new position. To be confirmed by telescope operator.

- Status Variables (Published Variables)
  - Telescope pointing
    - Target position
      - **ra** including RA/Dec offsets and Inst offsets
      - **dec** including RA/Dec offsets and Inst offsets
      - **pa** position angle
      - **epoch**
      - **ha**
      - **airmass**
      - **rot** Current rotator angle
      - **cat_id** Object name from catalog
      - **cat_ra** RA from catalog
      - **cat_dec** Dec from catalog
      - **cat_epoch** Epoch from catalog

  - Telescope Offsets
    - **raoff**
    - **decoff**
    - **eloff**
    - **azoff**
    - **instazoff**
    - **insteloff**

  - Time and Date
    - **dateobs**
    - **mjd**
    - **ut**
    - **lst**

  - Tracking Status
    - **strack** Is the telescope tracking?
    - **drives** Are the drives on?
    - **inpos** Is the telescope in position?

- Secondary Mirror Control

- Relative Offset Motions
  - **transxerr**
  - **transyerr**
  - **focuserr**
  - **tiltxerr**
  - **tiltyerr**
  - **thetazerr**

- Current Position Status variables
  - **transx**
  - **transy**
  - **focus**
  - **tiltx**
  - **tilty**
  - **thetaz**

MMIRS/Servers/

Science Camera

Overview

This server (written in C) provides all the functions necessary to configure a science camera and its supporting hardware (e.g. filter wheel, shutter), perform an exposure, read out the data and write a standard FITS data file with complete header keywords recording the telescope, instrument and detector readout information.

Derived From

The science camera server program consists of 4 servers bundled into a single executable. The 3 main servers: detector, instrument and telescope are taken directly from NOAO's ICE servers and can be run directly from an IRAF/ICE client interface. The only modification to the traditional ICE architecture is the writing of the final science data FITS file. This is written by the detector server rather than by the client.

We've added a "msg" protocol communication interface to the baseline ICE architecture to support Tcl/Tk clients that provide both status and control functions that allows the system to conform to our software architecture. Normal MMIRS observing will use the msg interface.

Current Status

The science camera software is largely complete. A new instrument server module will need to be configured for MMIRS to control the cryostat stages. The interface will be very similar to the existing SWIRC interface and Hecto interfaces. A new telescope interface will be added for the Magellan telescope to support both Megacam and MMIRS.

MMIRS/Servers/

Detector

Overview

This module is part of the ICE camera server and provides all of the interaction with the science camera. It configures the camera electronics, programs the camera readout parameters and receives DMA science data from the camera. The data stream is de-scrambled and written to a single FITS image file. The sequencing of the exposure steps is controlled by the client (either IRAF/ICE or Tcl/Tk msg client).

Derived From

The existing ICE detector server has 2 cameras defined: detsao for all the CCD detectors and detir for the infra-red detectors. This module is complete and operational.

Interface

- Commands
  - detir_open
  - detir_close
  - detir_rparam
  - detir_wparam
  - detir_rinfo
  - detir_areaddata
  - detir_awaitdata
  - detir_maxbytes
  - detir_action <action code>
    - Actions
      - AD_INIT (1)
      - AD_FLUSH (2)
      - AD_PREPARE (3)
      - AD_READ (4)
      - AD_READ (5)
      - AD_START_EXPO (6)
      - AD_PAUSE_EXPO (7)
      - AD_CONT_EXPO (8)
      - AD_STOP_EXPO (9)

- AD_IDLE (10)
- AD_WAIT_EXPO (11)
- AD_CHANGE_EXPO (12)
- AD_FCLOSE (100)

- Parameters (Published Variables)
  - dettype; / **entry in cap file** /
  - detfiletype; / **detector output pixel type** /
  - preflash; / **preflash** /
  - gain; / **gain** /
  - dwell; / **sample integration time** /
  - rdnoise; / **read noise** /
  - delay0; / **no-op delay after each pixel** /
  - delay1; / **no-op delay after each row** /
  - detpixtype; / **detector pixel type** /
  - exptime; / **exposure time (milliseconds)** /
  - caltime; / **cal exp time (milliseconds)** /
  - nscanrows; / **number of scan rows** /
  - imagetype; / **type of frame** /
  - colbin; / **binning factor** /
  - coltotal; / **total visible** /
  - colfirst; / **start of data readout** /
  - collast; / **end of data readout** /
  - colusct; / **underscan total** /
  - coluscw; / **underscan width (binned)** /
  - coluscm; / **underscan margin** /
  - colosct; / **overscan total** /
  - coloscw; / **overscan width (binned)** /
  - coloscm; / **overscan margin** /
  - rowbin; / **binning factor** /
  - rowtotal; / **total visible** /
  - rowfirst; / **start of data readout** /
  - rowlast; / **end of data readout** /
  - rowusct; / **underscan total** /
  - rowuscw; / **underscan width (binned)** /
  - rowuscm; / **underscan margin** /
  - rowosct; / **overscan total** /
  - rowoscw; / **overscan width (binned)** /
  - rowoscm; / **overscan margin** /
  - biasloc; / **preferred biassec location** /
  - datasecx1; / **datasec start column** /
  - datasecx2; / **datasec end column** /
  - datasecy1; / **datasec start row** /

- datasecy2; / **datasec end row** /
- biassecx1; / **biassec start column** /
- biassecx2; / **biassec end column** /
- biassecy1; / **biassec start row** /
- biassecy2; / **biassec end row** /
- trimsecx1; / **trimsec start column** /
- trimsecx2; / **trimsec end column** /
- trimsecy1;
- trimsecy2; / **trimsec end row** /
- ccdsecx1; / **ccdsec start column** /
- ccdsecx2; / **ccdsec end column** /
- ccdsecy1; / **ccdsec start row** /
- ccdsecy2; / **ccdsec end row** /
- origsecx1; / **origsec start column** /
- origsecx2; / **origsec end column** /
- origsecy1; / **origsec start row** /
- origsecy2; / **origsec end row** /
- naxis1; / **naxis1** /
- naxis2; / **naxis2** /
- namps; / **number of pre-amps** /
- timeleft; / **timeleft** /
- camtemp; / **camera temperature** /
- dewtemp; / **dewar temperature** /
- rvshift; / **reverse vertical shift** /
- ashift; / **reverse ampreadout** /
- maxbyte; / **max dma xfer size** /
- maxbuff; / **max buf xfer size** /
- maxnrow; / **max buf xfer size (rows)** /
- chunksize; / **actual dmabuf xfer size** /
- rowsize; / **actual row size (bytes)** /
- nfexpo; / **number of focus exposures** /
- nrvshift; / **number of rows to shift** /
- elaptime; / **elapsed exposure time** /
- acttime; / **actual exposure time** /
- xpreskip; / **X preskip** /
- xunderscan; / **X underscan** /
- xskip; / **X skip** /
- xdata; / **X data** /
- xpostskip; / **X postskip** /
- xoverscan; / **X overscan** /
- ypreskip; / **Y preskip** /
- yunderscan; / **Y underscan** /
- yskip; / **Y skip** /

- ydata; / **Y data** /
- ypostskip; / **Y postskip** /
- yoverscan; / **Y overscan** /
- headcode; / **detector head code i.d.** /
- longtime; / **long exposure time** /
- newtime; / **new exposure time** /
- scandir;
- outtype;
- seqno; / **current seqno** /
- detname / **detector name** /
- imagename / **type of frame** /
- objecttitle / **object name** /
- deterror / **detector error string** /
- micromc / **object ucode - MMTI signal** /
- microcs / **compile string** /
- microtk / **ucode token - MMTI idle signal** /
- microma / **ucode macro - MMTI no idle signal** /
- microsc / **source ucode - MMTI serial freeze** /
- microls / **ucode list - MMTI serial unfreeze** /

- header / **header parameter block** /
- filename / **name of image file** /
- configname / **name of config file** /
- shutconfig / **name of shutconfig** /
- ccdconfig / **name of ccd program file** /
- rotangle / **telescope rotation angle** /
- configroot / **name of guide config root** /
- ccdsigfile / **name of ccd signale file** /
- ccdpromprog / **name of prom file** /
- ccdgain / **ccd gain setting** /
- camgain / **camera gain setting** /
- rinfo / **header card** /

MMIRS/Servers/

Instrument

Overview

This module is part of the ICE camera server and acts primarily as a protocol translation layer between the client and the MMIRS cryostat to provide a uniform instrument interface. It translates the instrument configuration into commands to the uMAC motion server. It controls these stages in the cryostat:

- filter (instrfilter)
- decker (decker)
- grism (disperser)
- aperture (image,long-slit, slitmask-id)
- focus (instrfocus)

It also records the cyrostat status and the complamp status in FITS cards for storage in the data file header.

Derived From

The existing ICE instrument server has 4 instruments defined: mini/megacam, hectospec, hectochelle and swirc. A new MMIRS module will be added that will borrow heavily from the existing modules.

Interface

- Commands
    - instrmmir_open
    - instrmmir_close
    - instrmmir_rparam
    - instrmmir_wparam
    - instrmmir_rinfo
    - instrmmir_action <action code>
        - AI_INIT (1)
        - AI_FOCUS (3)
- Parameters (Published Variables)

- instrtype **entry in cap file**
- instrname **instrument name**
- instrerror **instrument error string**
- instrfilters **filter id**
- aperture **aperture**
- disperser **disperser**
- decker **decker**
- tiltpos **grating tilt position**
- instrfocus **instrument focus**
- dispaxis **dispersion axis**
- fts **filter database**
- instrfocus **instrument focus**
- complamp **comparison lamp**
- rinfo **header card**

- Unused - allowed by ICE

    - callamp **internal comparison lamp**
    - probepos **probe pos file**
    - instrcoll **instrument collimator focus**
    - tvfilt **tv filter**
    - scanoffset **offset from center (1/10 mic)**
    - scanstep **scan step (1/10 microns)**
    - posangle **position angle**

MMIRS/Servers/

Telescope

Overview

This module is part of the ICE camera server and provides a translation layer between the client and the different telescopes. It is used only for status (not commanding). It syncronises the telescope status variables and formats the FITS cards of telescope information for the science data file header

Derived From

The module for interface to the MMT telescope is complete. The module for interface with the Magellan computer will be essentially identical and will be completed for Megacam.

Interface

- Commands
    - telmag_open
    - telmag_close
    - telmag_rparam
    - telmag_wparam
    - telmag_rinfo
    - telmag_action <action code>

      o AT_INIT (1)

- Parameters (Published Variables)
    - telname **telescope name** /
    - tazoff **tel azimuth offset (arcsec)** /
    - teloff **tel elevation offset (arcsec)**/
    - azoff **inst azimuth offset (arcsec)** /
    - eloff **inst elevation offset (arcsec)**/
    - telerror **telescope error string** /
    - dateobs **date of obs.** /
    - ut **universal time** /
    - st **sidereal time** /
    - jd **Julian date** /
    - ra **right ascension** /
    - dec **declination** /

- epoch **epoch of ra & dec** /
- ha **hour angle** /
- zd **zenith distance** /
- airmass **airmass** /
- telfocus **telescope focus** /
- telfdelta **telescope focus delta** /
- telfilters **telescope filters** /
- teltemp **tel. temperature** /
- windspeed **wind speed** /
- winddirection **wind direction** /
- humidity **humidity** /
- seeing **seeing** /
- rotangle **rotation angle** /
- pressure **barometer** /
- longitude **longitude** /
- latitude **latitude** /
- altitude **altitude** /
- pa **parallactic angle** /
- catid **catalog id** /
- catra **catalog ra** /
- catdec **catalog dec** /
- catrapm **catalog ra proper motion** /
- catdecpm **catalog dec proper motion** /
- catepoch **catalog epoch** /
- catcoord **catalog coord** /
- rinfo **header card** /

MMIRS/Servers/

camera electronics commands

- Overview
  This server is implemented ONLY through the msg protocol and it handles commanding of the camera electronics which is unique to SAO controllers.

- Derived From
  This implementation is taken from the SAO CCD cameras and is used as is.

- Interface

  - Commands

    - **ccdsigtab** <starbase signal table>
      Download the signal table on the socket
    - **ccdsigbin** <file name of signal program binary>
      Download the binary signal file specified
    - **ccddownload**
      Download the binary file
    - **ccddownfile** <ccdprogram filename>
      Download the binary file specified
    - **ccdcmd** <4byte hexcode>
      Download the hex code specified
    - **ccdidle** <on,off>
      Activate/De-Activate the idle program
    - **ccdsfreeze** <on.off>
      Activate/De-Activate the serial freeze program

MMIRS/Servers/

Guide server

Overview

The Guide server is a C program using the **msg protocol** library. It retrieves FITS images from the guide camera server, computes guide corrections and sends them to the telescope.

The current guide server moves its guide boxes by changing the subimage configuration in the guide camera. For MMIRS the guide server will move the guide cameras by sending a motion command to the Guider/WFS Motor Control server.

A configuration file describing the MMIRS guide cameras will have to be developed.

Derived From

This program is already in use at the MMT. It has been used with the Minicam camera at F5 and F9, and is currently used with Megacam, Hectospec and Hectochelle at F5. The program is extensivly configurable for various camera sizes, positions, rotation angles and pixel scales.

Commands

- start - start the guider.
- stop - stop the guider.
- tick - make one pass through the guide loop.
- guidelog - set the guide log output file name.

- tweakboxes - center a set of guide boxes on their guide stars.
- transfer - move one set of guide boxes to the same az/el relative positions around their guide star images as are measured in another set of guide boxes.

- ditherinst - move the guide boxes and telescope in instrument coordinates.
- ditherazel - move the guide boxes and telescope in azel coordinates.

Variables

The guide server has a few variables that control its operation.

- state - state of the guide loop : running (1) or stopped (0)

- send - should guide errors be sent to the telescope
- ngoodboxes - the number of guide boxes with accepable SNR
- error - last error message for GUI

- ActiveBoxList - a list of guide box numbers to use in computing guide errors
- TransferBoxList - a list of guide boxes that were used to transfer guideing from one set of cameras to another.
- FullBin - full image binning
- BoxBin - guide box image binning
- BoxSize - guide box size in arcseconds
- ImageSize - guide image size in arcseconds
- Exposure - guide image exposure in seconds
- BackgroundWidth - width of area in pixels around the guide box to compute the background
- TelescopeDiameter - the diameter of the primary in meters.
- PrimaryFRatio -
- CassFRatio
- FocusUnits - units of the focus positioning.

- rot - last value of rotator recieved from the telescope

The guide server has many variables that control its configuration.

- GuiGeometry - prefered screen size and position for GUI
- FullImageList - a list full size star finder images.

- NumberOfCameras - the number of physical cameras in the system
- CameraN_Name
- CameraN_XSize
- CameraN_YSize
- CameraN_XPixelSize
- CameraN_YPixelSize
- CameraN_Binning
- CameraN_Radius
- CameraN_Rotation
- CameraN_CamAngle
- CameraN_Parity
- CameraN_Defocus
- CameraN_Bitpix

- NumberOfImages - the logical number of input images
- ImageN_Name

- ImageN_Camera
- ImageN_Exposure - exposure time for this image
- ImageN_Defocus
- ImageN_FullImage - Image number that this sub image is extracted from

These variables configure the source, placement and use of the image on the GUI

- ImageN_Grid - x, y position of the image in the GUI
- ImageN_GridWidth - size of the image
- ImageN_GridHeight
- ImageN_GridRotate - should the image to rotated such that +el is up?
- ImageN_GridRotation - static rotation offset for the image
- ImageN_GridZoom - initial zoom for the image
- ImageN_ImageSizePix
- ImageN_ShmKeys - shared memory key of FITS data
- ImageN_ShmSize - size of FITS data in memory
- ImageN_Config - updated when the image size is reconfigured
- ImageN_Update - updated when new data is available in shared memory

- NumberOfBoxes - the total number of guide boxes
- BoxN_Image - extract the box from image N
- BoxN_X - x pixel center of box
- BoxN_Y - y pixel center of box
- BoxN_SigmaXYThresh - maximum xy centroid error to allow guiding from a box
- BoxN_SigmaFWHMThresh - maximum FWHM error to allow focus adjustment from a box

These values are computed and made available for display on the GUI

- BoxN_FWHM
- BoxN_CenX
- BoxN_CenY
- BoxN_CenAz
- BoxN_CenEl
- BoxN_Counts
- BoxN_Background
- BoxN_Noise
- BoxN_SigmaXY - estimated error in centroid
- BoxN_SigmaFWHM - estimated error in FWHM
- BoxN_BoxSizePix
- BoxN_Locked - box locked and used in guiding state

- NumberOfErrors - the number of errors to try to correct.

  This may have a value of 2, 3 or 4, using 4 will try to mantain telescope focus in addition to az, el and rotation.

- Error_Name
- ErrorN_Gain - proportional gain for this error
- ErrorN_Offset - fixed offset on error
- ErrorN_Step - maximum value of output error
- ErrorN_Sample - number of error samples to average before sending a correction.
- ErrorN_LookB - number of seconds of "lookback" to maintain on errors already sent.

MMIRS/Servers/

WFS - Guider camera server

The WFS/Guide camera server will be based on software obtained from Greg Burley.

The software provided by Burley is in the form of a callback library which is intended to be used with a GUI toolkit. We will use most of the library functions as callbacks from our server commands and stub out the calls in the camera functions which initiate updates of the user interface. Camera servers for the Hectospec and Megacam guiders that use this command set already exist.

WFS / Guide camera protocol commands:

- **imageconfig** n x y size bin

  Configure the guide camera image *n* imaging area to begin at pixel *x*, *y* and be a square pixel box of *size* pixels with on chip binning *bin*

- **set guide** onoff

  The camera is guideing and any shutter control server should take action to uncover the guide camera.

- **set FILENAME** filename

  A filename to save the guide images in. The default is guide0.fits and does not change between images.

- **expose** type exptime

  Take a guide exposure. Type may be "full" or "box". A full image is the full guide camera size and box is a subimage as specified in the imageconfig command.

- **get** ImageN

  Return a fits data block with FITS image data from Image*N*

MMIRS/Servers/

Motion Control Server

Overview

The motion control server is an instance of the **PMAC Control Server**, configured to manage motors within the MMIRS Cryostat and Guide/WFS system. Its control layout is dictated by configuration files, such as those detailed on the **PMAC Control Server** page. Its client and server sides are generated by the same program, and feature MMIRS-specific commands.

The motion control server is defined to control axes responsible for:

- Positioning the IR array in focus.
- Rotating the grism wheel.
- Rotating both filter wheels.
- Sliding the gate valve open and closed.
- Rotating the MOS and Dekker wheels.
- Positioning both guide cameras in x, y, focus, and WFS select stage.

Configuration of this server and data reporting are further detailed on the **PMAC Control Server** page. Briefly, the server references three files: one for the overall system layout, a second for generic motor settings, and a third for specific motor settings. Most useful running and configuration data generated by the PMAC is available through user interfaces to engineers and observers.

Derived From

- PMAC control systems
  All of the SAO instruments have used PMAC control servers, starting with the Megacam topbox shutters and filter wheel. A more sophisticated example is the fiber positioner system for Hectospec/chelle. The MMT F5 Wave Front Sensor motor axes were a second-generation devolopment, implemented with the new framework allowing table definable axis definitions and parameters. The MMIRS PMAC development will also be built on this new framework.

- Instrument control systems
  The high level instrument commands are modeled directly from the instrument commands for Megacam topbox and Hecto spectrograph benches. These commands tie directly to the ICE instrument server.

Commands

Motors within the Cryostat and outside of the Cryostat can be considered operationally separate for reasons of their differing responsibilities and independent function. Here their commands will be broken into distinct categories, with further separation between high-level and low-level control.

- Cryostat
  - High-Level
    - filter <name>
      Discerns via uploaded starbase table where to move each filter wheel in order to expose the requested filter, by name.
    - dekker <name>
      Moves the dekker wheel to the designated slot, identified by name and lookup table.
    - mos <id>
      Functionally identical to filter wheel movement, where ID can be a barcode, name, or other designation.
    - grism <name>
      Moves the grism wheel to a designated slot, identified by name and lookup table.
    - focus <mm>
      Moves the IR Array focus stage by a given amount, in millimeters.
    - valve <open/close>
      Opens or closes the gate-valve. A series of checks are performed, documented elsewhere.

    - filtdb <starbase table>
      Uploads new filter wheel definitions via starbase table.
    - mosdb <starbase table>
      Uploads new MOS wheel definitions via starbase table.
  - Low-Level

    Each coordinate system has fine positioning control, these commands are:

    - array <counts>
    - grism <counts>
    - filter <T counts> <B counts>
    - valve <counts>

        - mosdek <M counts> <D counts>

      It is worth pointing out that the given counts is offset by a defined motor scale. Typically a straightforward scale is assigned, where for example the 'array' focus would be in millimeters, and the top 'filter' rotation would be in degrees.

- Guide/WFS
    - High-Level
        - collimator <in|out> <in|out>
          Moves the collimator in or out of the light path, for WFS 1 and 2.
    - Low-Level
        - wfs1 <X counts> <Y counts> <F counts> <C counts>
        - wfs2 <X counts> <Y counts> <F counts> <C counts>

      Here counts will likely be defined in millimeters, however it is yet to be determined.

There exist a plethora of other commands, not necessary to the operation or interaction of the motion control server. A few are worth noting:

- command <text>
  Sends given text to the PMAC, and returns its response.
- abortCS <csName>
  Issues an abort request to the given coordinate system.
- killCS <csName>
  Abruptly stops all motion on the given coordinate system.
- killServer
  Closes communication with the PMAC and allows the server to exit.
- postGather <gatherList>
  Sets the next gather to register the passed gather variables.
- getGather
  Returns gather configuration and data from PMAC system memory.
- unmap <varName>
  Determines and returns the PMAC-name of a passed variable.
- listprog <progName>
  Returns the entire program listing for a given program name.
- listplc <plcName>
  Returns the entire PLC listing for a given PLC name.

Variables

Although it is hardly informative, attached to this page is a file of the currently 1615 published variables that are available for the MMIRS setup. In practice only a fraction of these are used.

Reference

- The **PMAC Control Server** page contains further detail.
- Interfaces detailed on /MMIRS/Engineering GUI**?** and /MMIRS/Observing GUI**?** pages.
- A list of published variables is attached to this page.

MMIRS/Servers/

PMAC Control Server

The PMAC Control Server is software to allow setup-specific motor control through a powerful generic interface.

Configuration

Configuation is determined by a few basic setup files in human-readable format. The server interprets an overall setup file, interprets a motor-generic setup file, then looks for motor-specific setup files. Both the motor-generic and motor-specific setup files contain control information determined to be optimal for the motors in question. To stress the point, settings found among most motors would be set for all motors by an entry in the motor-generic file, then overridden for atypical motors in their motor-specific files.

With regards to the overall setup file, the config command takes coordinate system and motor specification arguments. For example, mmirs.tcl:

```
# Define and create programs foreach motor.
preprocess::config mmirs
        array  {F  1                    }
        grism  {G  2                    }
        filter {T  5    B  6            }
        valve  {V  3                    }
        mosdek {M 15    D  4            }
        wfs1   {X  7    Y  8    F  9    S 10}
        wfs2   {X 11    Y 12    F 13    S 14}
```

Here, a control name of mmirs creates clients and servers, mmirsClient and mmirsServer, respectively. They address motors 1 through 15, with 5 and 6 assigned to coordinate system 'filter'. The complete name of motor 6 becomes 'filterB', a convention that avoids conflicts.

The following is an example of a default setup file, mmirs/default.setup:

```
defn defaultSetup {a} {



        &[\${a}Coord]
        #[\${a}Motor]->+[\${a}Scale][\${a}AxisLetter]+0



        p0 = [var \${a}MHomeLimTrig 2]
```

```
        p0 = [var \${a}PHomeLimTrig 2]
        p0 = [var \${a}HomeAgainst  0]
        p0 = [var \${a}HomeFlagTrig 1]


        [\${a}Feedback    ] = DLR#10C000
        [\${a}AxisEnable  ] =       1
        [\${a}Homed       ] =       0
        [\${a}HasLimits   ] =       1


        [\${a}HomeSpeed   ] =     160
        [\${a}HomeOff     ] =       0
        ...
}
```

And, an example of a motor-specific setup file, mmirs/filterB.setup:

```
var filterBScale             200.0
var filterBGUIScale       614400.0


defn loadSettings_filterB { } {


        [filterBiFlagMode   ] = DLR#20001


        [filterBiFolError   ] =  85000
        [filterBiFolWarning ] =  70000
        [filterBiPSoftLimit ] =      0
        [filterBiMSoftLimit ] =      0
        [filterBiErrDecel   ] =      1.2
        [filterBiMaxVel     ] =  10000
        [filterBHasLimits   ] =      0
        ...
}
```

It is worth pointing out that in the above examples, filterB.setup overrides the default.setup variable HasLimits. By default, motors will be regarded as having limits, but when filterB. setup is loaded it redefines this variable.

Reporting

The PMAC motor control system creates a large amount of useful data for each coordinate system and motors defined therein. This information is relayed back through interfaces to be available to engineers and observers. At the engineering level one can set any number of configuration parameters motor by motor. For safechecking purposes these values are not automatically ported back into setup files, so if new optimal settings are determined they are to be entered by hand.

Software is currently in development to graph acute motor behavior over the course of movement commands. Values available for inspection include Commanded, Target and Actual Positions, Bias, Encoder and DAC Voltage. It is hoped that this reporting will assist in fine tuning of individual motors.

Interfacing

The server interacts with the PMAC using a mixed ascii/binary tcp-based protocol developed and documented by DeltaTau. The server-side connection is managed by a C library which allows for simpler packet management and data parsing than would be possible in tcl.

There exist both engineering-level and observing-level graphical user interfaces for interaction with the PMAC control server. The server uses an ascii-based protocol implemented by a tcl library named msg. The operational abilities of msg are not addressed here in detail, suffice it to note that the library trivializes data synchronization between the server and clients. It is not intended that a server will operate with more than one client at a time, though the software does support this functionality.

The user interfaces are out of the scope of this page, but are addressed further on the Engineering GUI**?** and Observing GUI**?** pages. Further interfaces are to be referenced from the GUIs**?** page.

Command-Line Arguments

The PMAC control server accepts a few command-line arguments to direct its operation. Some arguments, like '-setup' are required while others are solely for debugging purposes. An argument list with brief explanations of their function can always be obtained via the '-help' argument, or no arguments at all. The complete list follows:

- -help
  Display a list of acceptable arguments with brief descriptions.
- -setup <name>
  Load the setup defined by the provided name. The setup data is loaded as a tcl file

from a standard directory, eg: setups/<name>.tcl. Further data is loaded from a subdirectory of the same name, eg: setups/<name>/<motorName>.tcl.

- -stdout
  Pipes everything to stdout that it would send to the PMAC, though indented. This proves invaluable to debugging as it allows direct examination of the PMAC programming.
- -pmac
  Sends commands to the PMAC. If this option is not given, no data is written to the PMAC, and the system is assumed to be in an operable manner.
- -clients
  Dynamically creates the client and server communications code. Client and server code is specific to setups and is named accordingly.
- -server
  Starts the server, which listens for clients and ties communication/control through to the PMAC.
- -sim <server|pmac|none></server>
  Simulation level at which to run the server. Either there can be no simulation (the default), PMAC simulation where outputs are disabled but the PMAC appears to move motors, or server simulation where the PMAC is never interfaced. This argument makes no difference unless the -server argument is also given.

Reference

- Low-level PMAC control and systems design derived from:
  - MMT f/5 Wave Front Sensor
  - Hecto Fiber Positioner
  - Magellan/Megacam Topbox
- High-level server software derived from the Magellan/Megacam Topbox.
- Applications to MMIRS include **Motion Control Server** instantiation.
- Interfaces detailed on /MMIRS/Engineering GUI**?** and /MMIRS/Observing GUI**?** pages.

MMIRS/Servers/

MOS wheel push buttons

Overview

A PMAC PLC program will implement the push button MOS wheel operation. A PLC program is a constantly running pmac program. Nominally there is at least 1 PLC running monitoring safety status. Additional user-defined PLCs can be added. In this case the PLC will monitor the state of the manual buttons, and invoke the necessary PMAC programs to move the filter wheel.

Derived From

This is almost identical to the push button operation for the Megacam filter wheels

Components

There will be 2 PLC programs:

- The **local** switch will disable all computer driven motion control
- The **advance** push button will move the MOS wheel 1 slot position with each button press.

MMIRS/Servers/

Bar Code scanner server

The bar code scanners server interfaces to the Omron bar code scanner via an RS-232 serial port connected to EDAS Ethernet-to-serial interface and makes the current bar code available to the science camera server.

A similiar bar code scanner server already exists for the MMT MegaCam instrument. This server will be written as part of the Megacam/Magellan effort.

Msg Protocol Interface:

- Published Variables
  - sdata - current scanned bar code.

MMIRS/Servers/

Vac gauge server

Overview

The Vacuum Gauge Server is a simple tcl program using the **msg protocol** library. It connects to the Pfeiffer vacuum gauge through an EDAS ethernet to RS-232 serial converter. It obtains the current vacuum reading from the gauge and publishes as a **msg protocol** variable.

Derived From

The server will use the **Power Control Server** control framework and the EDAS communications library as a basis for its implementation.

Commands

NONE

Variables

- mos_vacuum - the current pressure in the mos section in Torr
- cam_vacuum - the current pressure in the camera section in Torr

Reference

The Pfeiffer gauge protocol is documented here **Pfeiffer vacuum protcol rs232 485 PM488BN_C.pdf**

MMIRS/Servers/

Vac pump control server

Overview

The Vacuum Pump Control Server is a simple tcl program using the msg protocol library. It connects to the Varian vacuum pump through an EDAS ethernet to RS-232 serial converter. The server will allow the

Derived From

The server will use the **Power Control Server** control framework and the EDAS communications library as a basis for its implementation.

Commands

- state on|off

Variables

- state - on/off state of the vacuum pump.
- speed
- current
- power
- temp

Reference

varian turbo-70 controller turbo-catalog.pdf

MMIRS/Servers/

Heater - Auto Fill control server

Overview

The Heater and Auto Fill Control Server is a simple tcl program using the **msg protocol** library. It connects to the Omega PID temperature controllers via ethernet. The server allows the PID loop to be started and its set point and parameters to be controlled.

Derived From

The server will use the **Power Control Server** control framework as a basis for its implementation.

Commands

- autofillpid on|off
- mosheat_pid on|off
- camheat_pid on|off

Variables

- autofillpid - when the state is set to on the PID loop is closed and active control begins.
- mosheat_pid
- camheat_pid

- autofillset - target control value for the PID loop in degrees K
- mosheat_set
- camheat_set

- autofullramp - ramp rate of target control value in degrees K/min
- mosheat_ramp
- camheat_ramp

- autofillP - PID control proportional gain setting
- autofillI - PID control integral gain setting
- autofillD - PID derivitive gain setting

- camheat_P

- camheat_I
- camheat_D

- mosheat_P
- mosheat_I
- mosheat_D

Reference

Omega-iSeries-Communications.pdf

MMIRS/Servers/

Camera - Mos section temperature monitor

Overview

The Camera - Mos section temperature monitor server is a simple tcl program using the msg protocol library. It connects to the Lakeshore temperature monitor via an EDAS ethernet to RS-232 converter. It obtains the current temperature from the monitor and publishes it as a msg protocol**?** variable.

Derived From

The server will use the **Power Control Server** control framework and the EDAS communications library as a basis for its implementation. In addition the comunications library for the Lakeshore 218 has been developed for the SWIRC camera at the MMT.

Commands

NONE

Variables

- cam_temperature
- mos_temperature

Reference

Lakeshore **218_Manual.pdf** page 75

MMIRS/Servers/

Focal Plane Temperature Control

Overview

The Focal Plane Temperature Control server is a simple tcl program using the msg protocol library. It connects to the Lakeshore PID temperature controller via an EDAS ethernet to RS-232 converter. The server allows the PID loop to be started and its set point and parameters to be controlled.

Derived From

The server will use the **Power Control Server** control framework and the EDAS communications library as a basis for its implementation.

Commands

- fp_pid on|off

Variables

- fp_pid - when the state is set to on the PID loop is closed and active control begins.

- fp_set - target control value for the PID loop in Kelvin
- fp_ramp - ramp rate for target control value in Kelvin /min
- fp_P - PID control proportional gain setting
- fp_I - PID control integral gain setting
- fp_D - PID derivitive gain setting

Reference

Lakeshore **321_Manual.pdf** page 60.

MMIRS/Servers/

Phytron Stepper Amp server

Overview

The Phytron Stepper Amp server is a simple tcl program using the msg protocol library. It connects Phytron stepper amplifier an EDAS ethernet to RS-232 serial converter.

The server allows the amp settings for each motor to be setup. The motor temperature for each motor within the dewar can be read back.

Derived From

The server will use the **Power Control Server** control framework and the [EDAS communications library] as a basis for its implementation.

Commands

Variables

- motor temps

Reference

Phytron motor drive with diagnostics and rs485 control PAB93-70.pdf

Phytron Temperature measurement module TEO gb.pdf

MMIRS/Servers/

Cal lamp server

The cal lamps server interfaces to the calibration lamp Electronics to allow calibration exposures with various lamps to be made.

The code to control this function will be integrated into the powserver software and will require writing a small tcl module to control the hardware hardware.

The hardware for the calibration lamps is not yet defined. Choosing pulizzi power control of Webdac boxes will allow reuse of the existing cal lamp system used with Hectospec.

MMIRS/Servers/

Power Control Server

Overview

The Power Control Server connects to Pulizzi Engineering 120v rack mounted power intelligent power controllers. These controllers allow remote switching of eight 120v outlets each. They are connected directly to the ethernet and each is assigned an IP address.

A configuration file allows the individual outlets in a controller to be assigned a name and then the status and control of that outlet is available by name from the server.

Multiple controllers may be controled from a single server and multiple servers may be run at the same time with different configurations.

An example config file section:

```
# Bench pulizzi - pulz9
#
array set pulizzi9 {
        edas edas2 port 1 lock none


        attn    @@@@
        reply   ONLINE!
        prot    @@@@


        J1      spec_steppers
        J2      spec_camera
        J3      spec_bench
        J4      hsshutter
        J5      chelle_steppers
        J6      chelle_camera
        J7      chelle_bench
        J8      chelle_grating
}
```

Derived From

The Power Control Server program is currently used with the F5 instruments at the MMT.

Commands

- The low level outlet names J1 through J8 can be used to command control of the outlets. For example to turn J1 off the server regognizes the command:

```
J1 off
```

- Each named outlet from the configuration file is registered as a command and can be commanded similarly to the low level outlet names.

Variables

- The low level outlet names J1 through J8 are published as variables and can be used to set or get the value of an outlet. For example to turn J1 off the server recognizes the command:

```
set J1 off
```

To get the value of J3 the server recognizes the command:

```
get J1
```

and replies with the state of J3.

Reference

The power control software provides a framework for publishing a set of named controlable values that has been used with several other devices in addition to the Pulizzi Engineering intelligent power controllers. A new device can be integrated into the framework by providing a set of routines and the names of the low level values to be controled.

Routines:

- _open - Open the device, provide any necessary initialzation
- _close - Close the device
- _stat - Poll the current values of the controlled values
- _set - Set the value of a controlled value

The F5 instruments at the MMT also use this framework to control WebDAC 100 I/O boxes,

LabJack U12 I/O boxes and a Blitz shutter controller. Two higher level drivers called plugset and valuset allow groups of names to be controlled from a single named control value. When the high level plugset name is set all of the values in the group are set to the same value. This is typically used to switch groups of pulizzi outlets on and off together or to set the control voltages of several outputs at the same time. The plugset type is restricted to on/off control while the valueset type allows the value to be floating point. This distinction is used when automatically generating a user interface for controlling power control server servers.

MMIRS/Servers/

Rack monitor server

Overview

The Rack monitor server is a simple tcl program using the **msg protocol** library. It connects to the Acromag Ethernet 4-6 channel TC monitor in each rack. It obtains the rack temperature reading from the monitor and publishes as a msg protocol variable.

Derived From

The server will use the **Power Control Server** control framework and the [EDAS communications library] as a basis for its implementation.

Commands

NONE

Variables

- rack1_temperature
- rack2_temperature

Reference

Acromag ethernet TC monitor 965EN_751a.pdf

Acromag Ethernet 4-6 channel TC monitor 965EN.pdf

MMIRS/Servers/

Log Server

Overview

The Log server tcl program using the **msg protocol** library. It connects to each of the other servers in the control system and subscribes to selected variables that the other servers publish. It writes the values of these selected variables to several log files at specified intervals.

The Log server is a client of all the other servers in the system and is a server only as a convenience. It is included in the servers list because it runs as a daemon without a GUI.

Derived From

The **msg protocol** library and various specialized lab loggers currently in use.

Commands

NONE

Variables

- The log server published all of the variables that is subscribes to providing a one stop shopping source of system wide info.

Reference

MMIRS/

GUIs

- **Planning GUI**

- **Observing GUI**
- Image Display - DS9

- **Guide GUI**
- **GMAP star selection**

- **Cryostat Operations**

- **Engineering GUI**

- Status Displays
  - **Instrument Configuration GUI**
  - Cryostat VAC/TEMP charts
  - **Exposure Status Display**
  - **Telescope Status Display**
    - **code sample.pdf**

MMIRS/GUIs/

Planning GUI

Overview

The planning GUI is used to layout slit masks and create the CNC input for the slit mask cutting machine.

The slit mask program used for IMACS will be adapted for use with MMIRS

Observing GUI

Overview

This is a TclTk GUI interface that provides an interface to both engineering and science observing. It provides status lights, pull-down selection lists and buttons to control observing. Its most important function is sequencing all the steps necessary for observation sequence. It also provides reminders if subsystems are not in nominal configuration.

Derived From

The observing GUI will be based on the "spice" GUI used with Hectospec/chelle and the "mice" GUI used with Megacam and SWIRC.

Fundamental observing sequence and exposure sequence already exist for both imaging and spectroscopic mode. Support for multiple observing modes must be added and as well as an interface to do specialized tasks such as mask alignment.

Components

MICE display

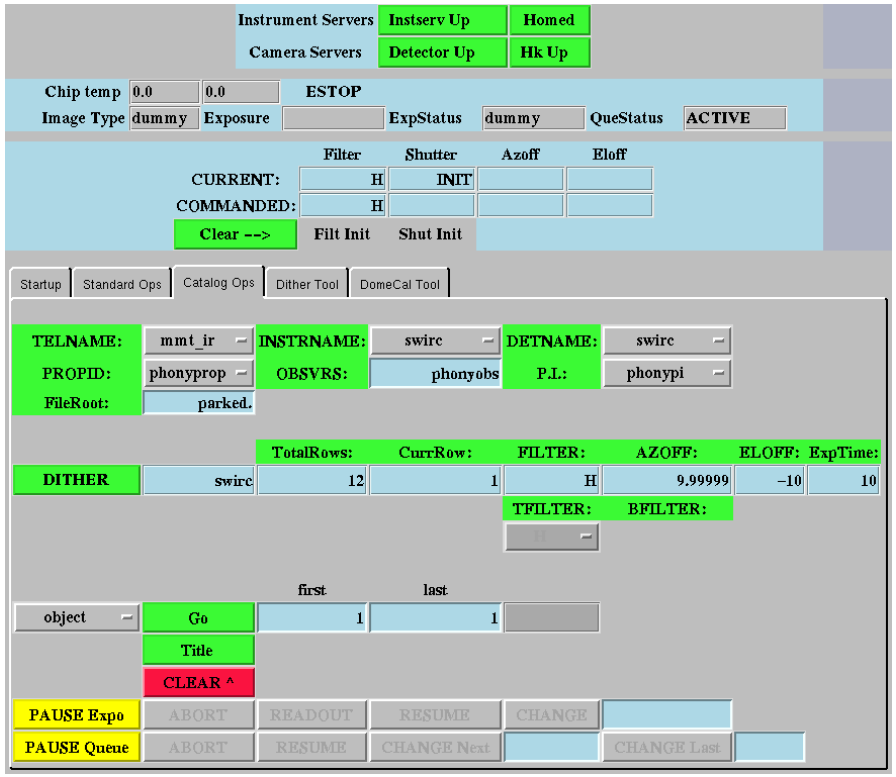

- Status Display
  - Red/Green state for power to each device
  - Red/Green state for status of all software device servers
- Pages
  - StartUp Page
    This page provides a column of buttons to allow the observer to sequentially go through to power up the electronics and start the associated server applications
    - Cryostat
    - Thermal Vac
    - Guide/WFS
    - Callamps
  - Standard Operations
    - Housekeeping Display
      - Focal Plane temperature
      - Callamp status
      - MOS temp/pressure
      - Camera temp/pressure
    - Exposure Display
      - Count within the exposure loop
      - Exposure type, e.g. skyflat, object, etc.
      - State of current exposure, e.g. exposing, readout, etc.
    - Configuration
      Name of current configuration file (MOS only)
    - Instrument Display
      Shows Actual and Commanded values for each of the axes:
      - Filter
      - Grism
      - Decker
      - MOS
      - Focus
      - Gate Valve
    - Configuration

Entry boxes for manual offsets, filter, grism, focus MOS

- Operation
  Line for each type of exposure including parameters

  - Auto Operations
    Similar to standard operations, but accepts a catalog name that describes a sequence of exposures that it will automatically sequence. The catalog nominally allows specification of filter, exposure time and telescope dither offsets.

- Dither Tool
  This tool facilitates the creation and formatting of the observing catalog. This example shows a sample dither pattern.

- ObsLog
  A utility for allowing the observer to add comments to the automatic observing log generated by the system. The resulting PostScript log file is shown.

MMT OBSERVATORY SWIRC LOG

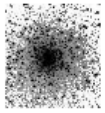

Page 49

UT Date 04/21/2005 *Observers* Brown, Hora, Wyatt *Focus* ____

File	*Title*	*Exp*	*Filt*	*UT*	*RA*	*Dec*	*Air*	*Instel*	*Instaz*	*Comments*
DEEPDARK.0966	deepdark	60	J	12:00	+17:41:00.4	+68:55:45	1.27	300	280	
DEEPDARK.0967	deepdark	60	J	12:01	+17:40:04.6	+68:55:45	1.27	0	280	
DEEPDARK.0968	deepdark	60	J	12:02	+17:39:08.8	+68:55:45	1.27	-300	280	
P138-C.0969	p138-c	3	J	12:05	+17:13:44.5	+54:33:21	1.12	0	0	check focus
P138-C.0970	p138-c	3	J	12:06	+17:13:44.5	+54:33:21	1.12	0	0	3x3
P138-C.0971	p138-c	3	J	12:07	+17:13:37.6	+54:33:21	1.13	-60	0	
P138-C.0972	p138-c	3	J	12:07	+17:13:37.6	+54:32:21	1.13	-60	60	
P138-C.0973	p138-c	3	J	12:07	+17:13:44.5	+54:32:21	1.13	0	60	
P138-C.0974	p138-c	3	J	12:07	+17:13:51.4	+54:32:21	1.13	60	60	
P138-C.0975	p138-c	3	J	12:08	+17:13:51.4	+54:33:21	1.13	60	0	
P138-C.0976	p138-c	3	J	12:08	+17:13:51.4	+54:34:21	1.13	60	-60	
P138-C.0977	p138-c	3	J	12:08	+17:13:44.5	+54:34:21	1.13	0	-60	
P138-C.0978	p138-c	3	J	12:08	+17:13:37.6	+54:34:21	1.13	-60	-60	
P138-C.0979	p138-c	3	H	12:09	+17:13:44.5	+54:33:21	1.13	0	0	H band, wrong focus
P138-C.0980	p138-c	3	H	12:09	+17:13:37.6	+54:33:21	1.13	-60	0	
P138-C.0981	p138-c	3	H	12:10	+17:13:44.5	+54:33:21	1.13	0	0	3x3 focus wrong again
P138-C.0982	p138-c	3	H	12:10	+17:13:37.6	+54:33:21	1.13	-60	0	
P138-C.0983	p138-c	3	H	12:10	+17:13:37.6	+54:32:21	1.13	-60	60	
P138-C.0984	p138-c	3	H	12:11	+17:13:44.5	+54:32:21	1.13	0	60	
P138-C.0985	p138-c	3	H	12:11	+17:13:51.4	+54:32:21	1.13	60	60	

File Table

	filts	exptime	azoff	eloff
1	H	10	9.99999	-10
2	H	10	-10	-9.99999
3	H	10	10	-5.61665e-06
4	H	10	0	0
5	H	10	-10	5.61665e-06
6	H	10	10	9.99999
7	J	20	9.99999	-10
8	J	20	-10	-9.99999
9	J	20	10	-5.61665e-06
10	J	20	0	0
11	J	20	-10	5.61665e-06
12	J	20	10	9.99999

MMIRS/GUIs/

Guide GUI

Overview

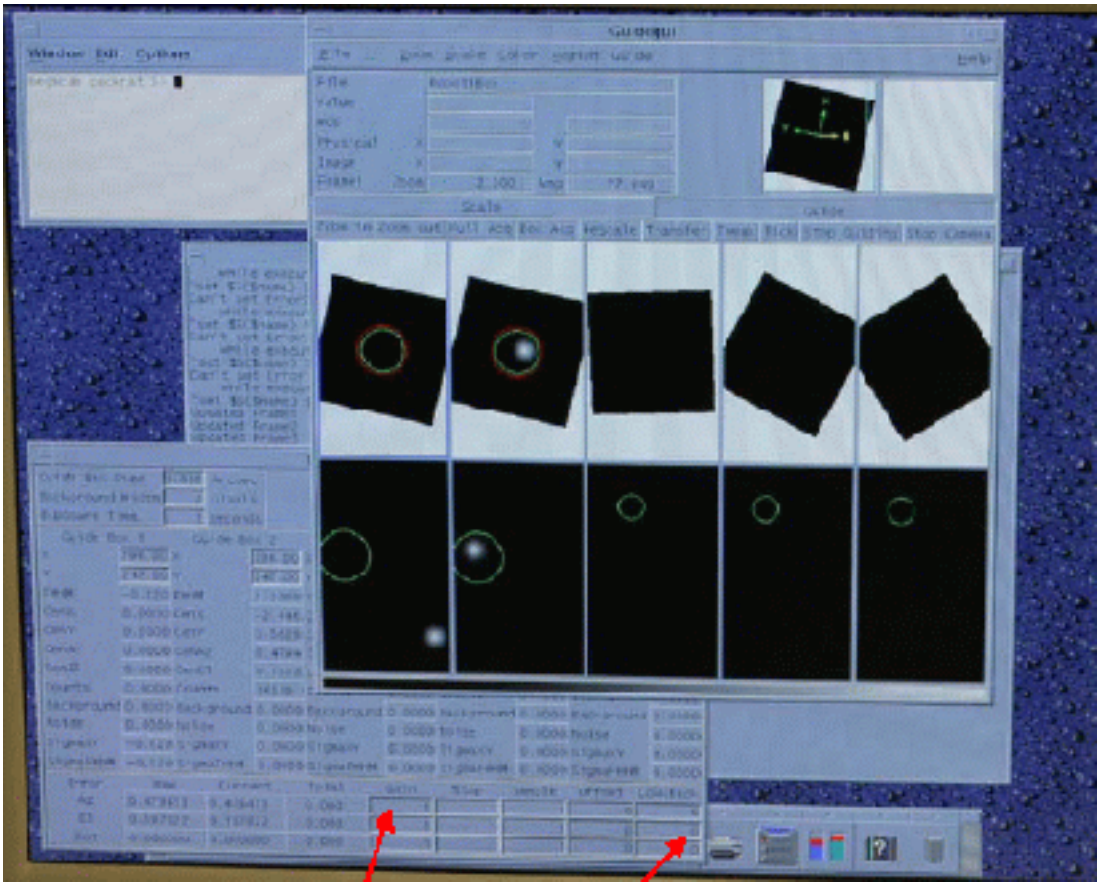

The Guide GUI is a tcl scripted enhancement to the SAO ds9 image display progam which itself is written in tcl/tk. The GUI connects to a currently running guide server and reads in the guide camera and image descriptions. It builds the GUI from these descriptions.

The GUI allows the real time image of the guide stars to be viewed in a ds9 frame and the guider corrections to be started and stopped. In addition the parameters controlling the guide servo loop are available. Time series plots of the total and sent corrections can be displayed to observe guider performance and debug guiding issues.

Derived From

The guide GUI is currently in use for Megacam, Hectospec and Hectochelle at the MMT.

MMIRS/GUIs/

GMAP star selection

Overview

Utility to select stars for the guide and wavefront sensing camera

Derived From

This is Magellan's GMAP star selection utility. We will use it for our guide star and wave-front sensing star selection.

We must provide:

- a script that positions the cameras
- a geometry file that defines the camera field of view:
  14' box with 7' inscribed circle excised.

MMIRS/GUIs/

Cryostat Operations

Overview

The Cryostat Operations GUI is a procedural type interface that leads the user through a task by presenting a list of steps and checking the status of the system to assure the order and safety of each step. This GUI will be used when performing the following tasks:

- Warm up
- Cool down
- Mask change

Derived From

Similar interfaces have been created for the Hectospec positioner fiber and guide star set up precedures. The Hectospec GUI is shown here.

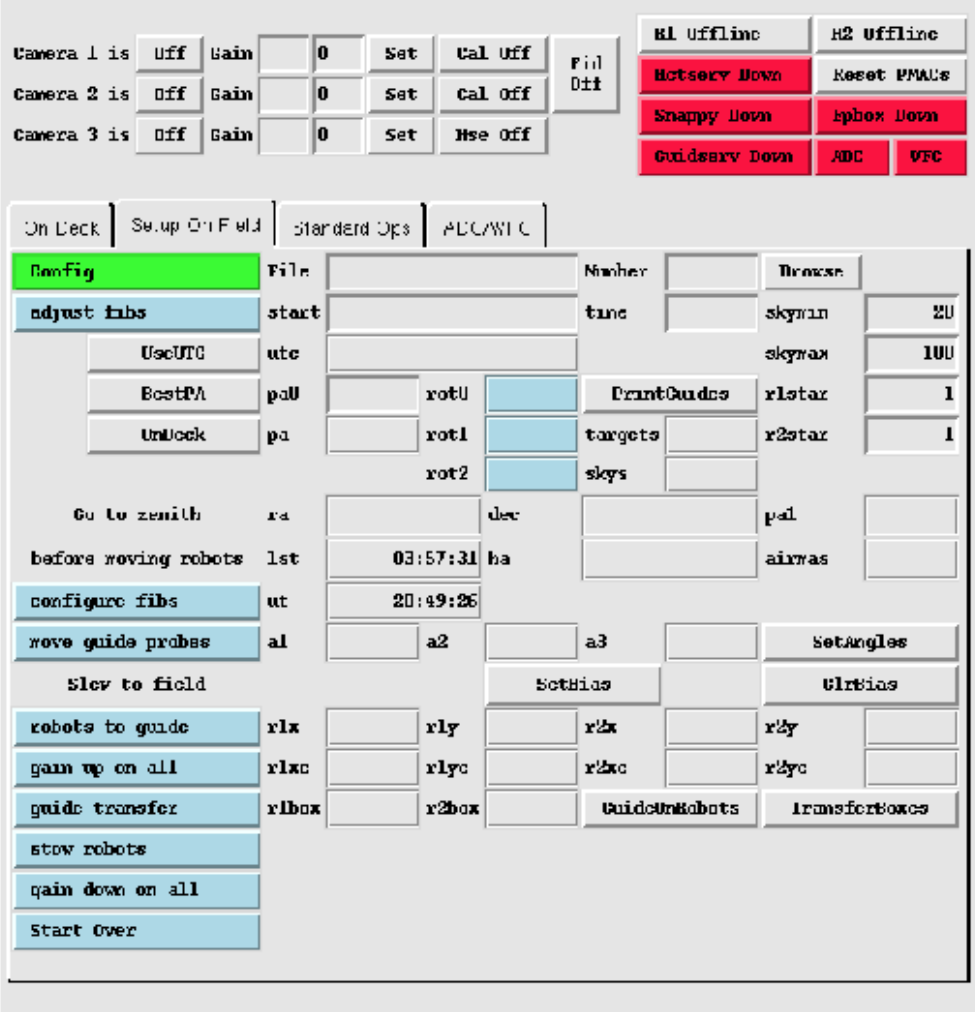

MMIRS/GUIs/

Engineering GUI

The Engineering GUI allows fine control over and evaluation of the system.The motor control interface gives engineers a means for fine tuning all motors defined.

Motor Control Inteface

On startup the user is shown a list of coordinate systems and motors therein; see attached **pmacGUI.gif**. For each coordinate system, the user has buttons to command:

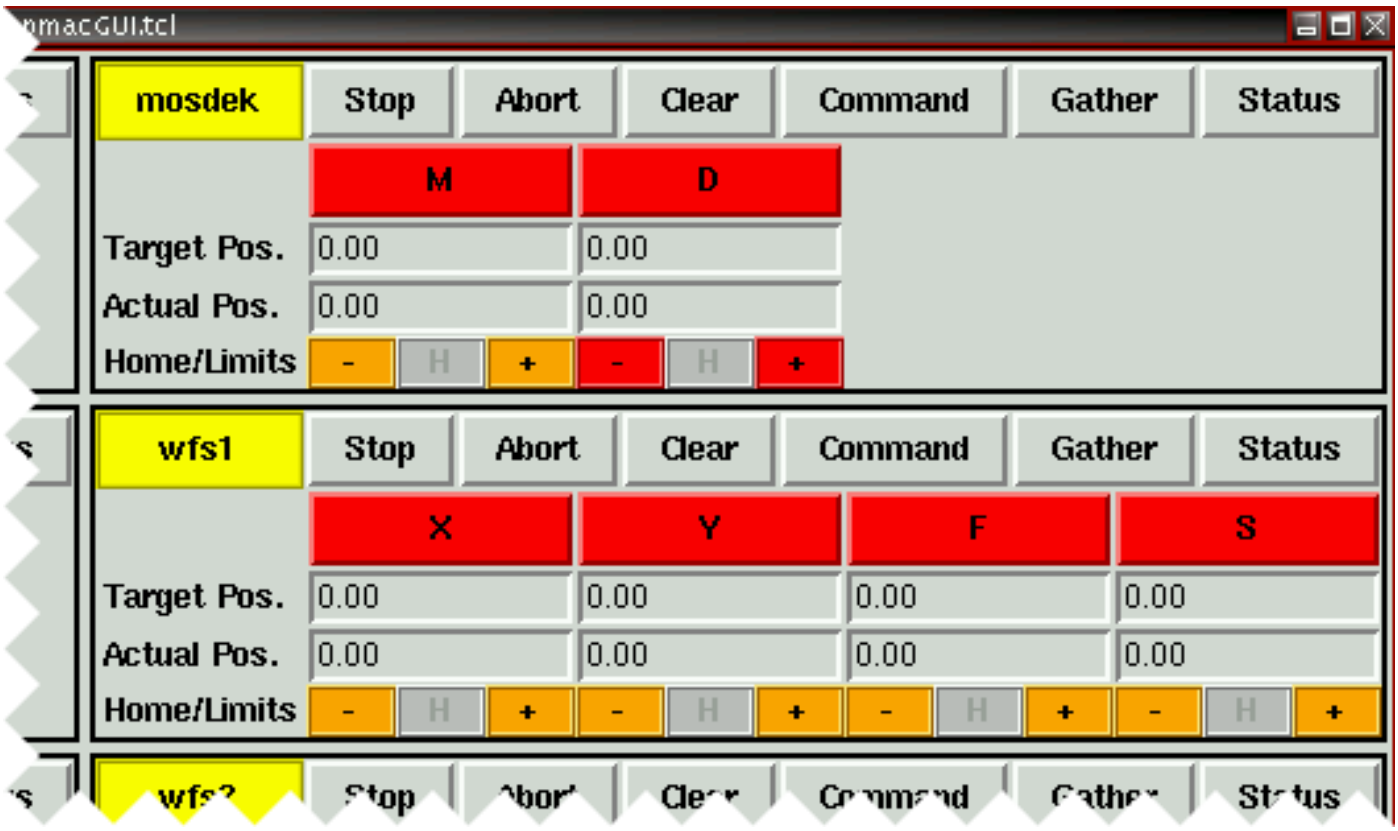

- Stop
  Halts and disables (offline) all motors.
- Abort
  Halts all motion programs and enables (online) all motors.
- Clear
  not yet completed
- Command
  Opens interface to command positions, below.
- Gather
  Opens interface to define gather data, below.
- Status
  Opens interface to display status bits, below.

For each motor a name-button is displayed in corresponding color status, where red indicates

the motor is offline, and green online. The user can click on its name-button to open the general readout interface, below. The general readout interface allows for futher readout interfaces, categorizing data access by relevance. For example, the button at the bottom of the general readout interface opens the debug readout interface. Both interfaces are discussed later. For each motor one is also shown Target and Actual positions, home status, and limit switch status. The home status label illuminates green when the motor has been homed. Each of the limit switch status labels show red for hardware- and software-limit triggered, orange for hardware-limit triggered, yellow for software-limit triggered, and green for neither limit triggered.

Command Interface

The command interface features a series of entries and buttons useful for sending movement instructions to individual motors and coordinate systems. The per-axis buttons are:

- Home
  Sends a home command, calling the home program for the individual motor.
- Stop
  Sends a requested stop motion command, decelerating the motor to a halt.
- Move
  The move button next to the blue entry sends a move request corresponding to the position entered in the blue entry box. If the position is '-' the motor stays in its current position.
- Move
  The move button next to the green entry box behaves similarly.

There also exist two buttons that request coordinate system wide events. These buttons are:

- Move all to 1st Position
  Requests a synchronized movement of all axes to their first (blue) positions. As noted above, any motors with a requested move of '-' stay in their current positions.
- Move all to 2nd Position
  Requests a synchronized movement of all axes to their second (green) positions.

Gather Interface

The gather interface allows for a selection of PMAC data to be recorded during subsequent

motor movements. For each motor one can check the data of interest, up to a total of 48 requests. This data is relayed to the PMAC where it is held until the next move command.

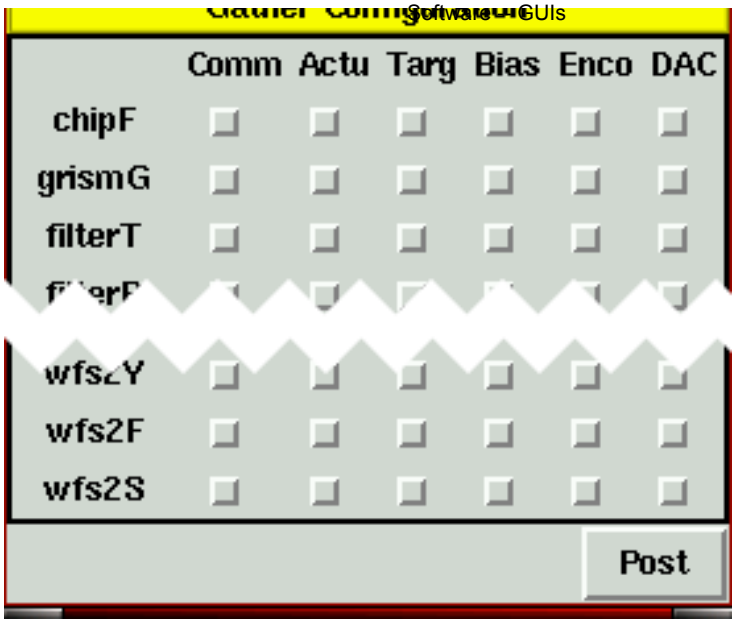

There exists only one button for this interface:

- Post
  Sends the current data selection to the **/MMIRS/Servers/PMAC Control Server**.

When a move is requested, the PMAC shuffles the gather selections into active memory and issues a gather command. Data can then be read out of the gather buffer and displayed graphically for easy interpretation. Readout and display software is currently in development. Access to a display interface will likely necessitate another button on this gather interface, however such design is yet to be determined.

Status Interface

The status interface is a non-interactive display of coordinate system wide status bits. For each motor, the PMAC stores a 48-bit word of status information, of which a selective amount is displayed. This interface pools this information for each motor registered to the requested coordinate system, and represents each bit as an on (red) or off (grey) circle.

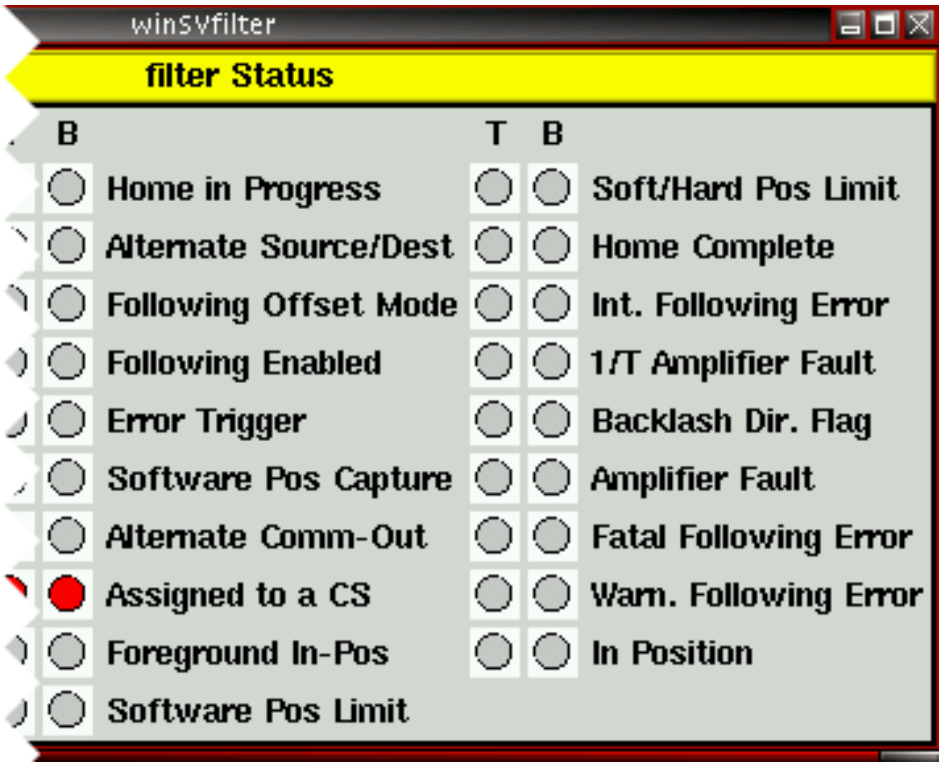

There is opportunity in the software to toggle display bits on and off, and those shown have been determined fundamental to engineering.

Reference

- The Engineering GUI connects to the **/MMIRS/Servers/PMAC Control Server**.
- Observers are intended to use the **Observing GUI**.

MMIRS/GUIs/

Instrument Configuration GUI

This display shows, at a glance, the current configuration of the Megacam shutter and filter wheels. A similar display will be created for MMIRS.

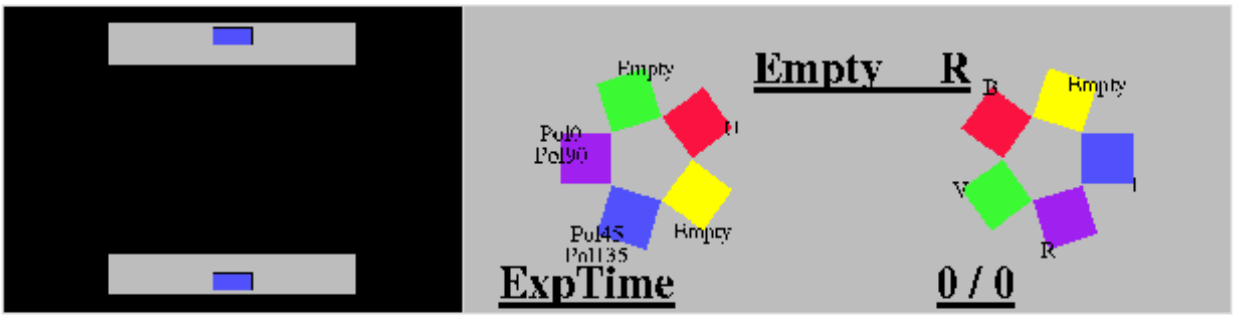

MMIRS/GUIs/

Exposure Status Display

This display shows the status of the current exposure and will need only minor updating for MMIRS.

Camera	SPEC
Shoe	YES
Config	ngc1234
Time left	5000
Total time	15000
File name	ngc1234.0074
Directory	SPEC/2003.0716
Filters	NONE
Image type	object
Exposure Status	exposing
Guiding	YES
Guide	YES
Boxes	2
Correcting	YES
GValid	YES
Grating	270 gpm
Wavelength	Wb
Focus	-0.235

MMIRS/GUIs/

Telescope Status Display

This display shows the current status of the telescope pointing, including the various types of offsets.

Object Name	
Catalog RA	-01:00:00.00
Catalog Dec	-100:00:00.00
Epoch	2000.00
Pos Ang	-360.02
Az Offset	0.00
El Offset	0.00
InstAzOff	0.00
InstElOff	0.00
RA Offset	0.00
Dec Offset	0.00
RA total	-01:00:00.00
Dec total	-100:00:00.00
Par Ang	-360.0000
Hour Ang	-00:00:00.008
Airmass	1.00
Azimuth	179.9822
Elevation	89.9575
Rot Ang	0.0224
Focus	0
Date	2005-04-29
MJD	53489.75441
UT	18:06:20
LST	01:13:58.253

mountdisplay Thu Jan 20 14:50:31 2005 1

```
#!/usr/bin/env wish

#lappend auto_path $env(MMTITCL)
load $env(MMTILIB)/libtclsignal.so

set sub_list {
    TELESCOPE   ra      ra       {}
    TELESCOPE   dec     dec      {}
    TELESCOPE   pa      pa       setposang
    TELESCOPE   ha      ha       {}
    TELESCOPE   airmass airmass  {reformat %.2f}

    TELESCOPE   az      az       {reformat %.4f}
    TELESCOPE   el      el       {reformat %.4f}
    TELESCOPE   rot     rot      {reformat %.4f}

    TELESCOPE   cat_id  cat_id   {}
    TELESCOPE   cat_ra  cat_ra   to_hms
    TELESCOPE   cat_dec cat_dec  to_hms
    TELESCOPE   epoch   epoch    {reformat %.2f}

    TELESCOPE   dateobs dateobs     {}
    TELESCOPE   ut      ut          {}
    TELESCOPE   lst     lst         {}
    TELESCOPE   mjd     mjd         {}

    TELESCOPE   instazoff instazoff {reformat %.2f}
    TELESCOPE   insteloff insteloff {reformat %.2f}
    TELESCOPE   azoff     azoff     {reformat %.2f}
    TELESCOPE   eloff     eloff     {reformat %.2f}
    TELESCOPE   raoff     raoff     {reformat %.2f}
    TELESCOPE   decoff    decoff    {reformat %.2f}

    TELESCOPE   focus     focus     {reformat %.0f}
}

set gui_list {
    "Object Name"  cat_id   lightblue black
    "Catalog RA"   _cat_ra  lightblue black
    "Catalog Dec"  _cat_dec lightblue black
     Epoch         _epoch    lightblue black
    "Pos Ang"      posang   lightblue black

    "Az Offset"    _azoff      orange black
    "El Offset"    _eloff      orange black
    "InstAzOff"    _instazoff  orange black
    "InstElOff"    _insteloff  orange black
    "RA Offset"    _raoff      orange black
    "Dec Offset"   _decoff     orange black

    "RA total"     ra       lightblue black
    "Dec total"    dec      lightblue black
    "Par Ang"      _pa       lightblue black
    "Hour Ang"     ha      lightblue black
    "Airmass"      _airmass  lightblue black

     Azimuth       _az       lightgreen black
     Elevation     _el       lightgreen black
    "Rot Ang"      _rot      lightgreen black
    "Focus"        _focus    lightgreen black

    "Date"         dateobs  yellow       black
    "MJD"          mjd      yellow       black
    "UT"           ut       yellow       black
    "LST"          lst      yellow       black

}

set bg_color yellow
set fg_color black
set font  "*-times-bold-r-normal--*-240-*-*-*-*-*-*"

lappend auto_path $env(MMTITCL)

proc setposang { name index op } {
    global posang rot pa _pa
    catch { set posang [format %.2f [expr $pa - $rot]] }
    set _pa [format %.4f $pa]
}

proc reformat { format name index op } {
    upvar #0 $name var
    global _$name
    set _$name [format $format $var]
}

proc to_hms { name index op } {
    upvar #0 $name var
    global _$name
    set _$name [hms $var]
}

proc dualtemp { name index op } {
    upvar #0 $name var
    global _$name
        # Convert Celsius to Fahrenheit and display both.
        set AT_F [ format "%02.2f" [expr (($var * 9./5.) + 32.)] ]
    set _$name "$var C/$AT_F F"
}

proc hms { decimal }  {

    global parameters

    if {$decimal < 0} {
        set signchar "-"
        set decimal [expr $decimal * -1]
    } else {
        set signchar " "
    }

    set decimal [expr int($decimal * 360000 + 0.5)/360000.]
    set degrees [expr int($decimal)]
    set frac_degrees [expr {$decimal - $degrees}]
    set decimal_minutes  [expr $frac_degrees * 60]
    set arc_min [expr int($decimal_minutes) ]

    set frac_degrees_sec [expr $decimal_minutes - $arc_min]
    set arc_sec [expr $frac_degrees_sec * 60]

    # Check if we are on a Linux system.  If os, use the degree symbol.
    # Else, use the caret to indicate degrees.
    return [format "${signchar}%02d:%02d:%05.2f"  [expr $degrees] [expr int($arc_min)]
 $arc_sec]
}

# Connect to the servers
foreach { server name var code } $sub_list {
```

mountdisplay Thu Jan 20 14:50:31 2005 2

```
    if {![info exists $server]} {
        msg_client $server
        msg_keepalive $server 5000 5000
    }
    msg_subscribe $server $var $var $code

}

# Build the GUI
wm title . "MMTO Status"
set w {}
foreach { label var bg fg } $gui_list {
    grid \
            [ label $w.l_${server}_$var -text $label -relief groove        \
                                -width 14 -font $font                       \
                                -bg $bg -fg $fg                            ] \
            [ entry $w.e_${server}_$var -textvariable $var                  \
                                -state disabled -relief sunken              \
                                -width 14 -font $font                       \
                                -bg $bg -foreground $fg        \
                                -justify center                            ]
}
```

MMIRS/

System Management

To simplify the management of the computer systems at remote observatories we use the following tools and procedures:

- CVS -- Concurrent Versions System
  All source code is maintained in a backed-up repository in Cambridge using CVS. Source code can be edited on any of our computers at any site and then checked back into the repository. Prior versions of the code can be recovered from the repository if necessary.

- Cron Jobs
  - Daily cron jobs clean old logs and old data files
  - Daily cron jobs terminate and restart all server logs

- Acct Management
  Before the start of each new observer, the observing account is restored from a pristine archival copy. This insures that any modifications to the environment made by previous observers will not hamper the next observer.

- Bootstrapper
  The bootstrapper is a shell script we have developed to simplify the installation of all our software onto a new computer system. It sets up user accounts, installs packages such as Tcl/Tk and Iraf, and checks out all the SAO developed code out of the CVS repository.

- System Backup
  Critical directories on each of the remote computers are backed up to Cambridge automatically. This eliminates the need to write backup tapes at the remote sites.

- Instrument Data Archiving
  Automatic scripts copy the previous night's data to Cambridge each day where they are archived on disk and to tape. In practice this means that it is not necessary for each observer to transport their own data home on physical media. It is made available to them over the network from the archive after their run. The bandwidth from the MMT is adequate that even Megacam data can be transferred to Cambridge automatically. From Magellan, however, it will be necessary to physically transport the data, most likely using USB hard drives.

- Shadow system
  We maintain at SAO a computer system identical to the MMT system and the future

Magellan system. This gives us the capability to test all software in Cambridge before installing in at the observatories.

MMIRS/

Testing and Verification

Overview

Each component in the system must be verified that it meets the specifications. This applies most directly to the hardware control components.

Each component must also be tested for robustness to verify that it can perform thousands of repetitions without errors. Automated tests will be defined and scripts will be written to control them and to log results.

In addition, the software must support the defined system tests.

- Component Verification

  For each hardware server, the software must be tested and verified against the performance specifications. The software will be base-lined at completion of each component.

  - The Project Engineer must provide the test specification and support equipment.
  - The software team must provide the software, operating instructions and logging of the test.
  - The Project Scientist must sign off on the performance of each of the components.

- System Verification

  The system will be operated using the science and observing GUI interfaces. The Project Scientist must define the test and sign off on the performance. The software will be base-lined at test completion.

- Pre-Ship Test

  The project scientist will define the pre-ship test. Upon successful completion of the pre-ship test the software will be base-lined in CVS.

- Post-Ship Test

  The pre-ship baselined software will be installed at the remote site. The post-ship test

will be performed. Discrepancies will be recorded and troubleshooting will isolate the components.

- Installation Test

  The post-ship test software will be re-exercised after installation on the telescope.

MMIRS/

Data Products

In this section we present examples of the following data products:

- A FITS header for an exposure taken in imaging mode
- A FITS header for an exposure taken in MOS mode
- A sample of an aperture map that gets appended as a FITS table to the spectral image.
- We end with a brief survey of Data reduction packages.

imagehdr.lst Mon May 02 14:05:55 2005 1

```
RDCS2.0698.fits[2048,2048][real]: rdcs2
No bad pixels, min=0., max=0. (old)
Line storage mode, physdim [2048,2048], length of user area 3524 s.u.
Created Tue 00:00:00 01-Jan-1980, Last modified Tue 00:00:00 01-Jan-1980
Pixel file "RDCS2.0698.fits" [ok]
PCOUNT  =                    0 /NO RANDOM PARAMETERS
GCOUNT  =                    1 /ONE GROUP
BZERO   =                24495
BSCALE  =                    1 /REAL = TAPE * BSCALE + BZERO
DATA-MAX=                52833
DATA-MIN=                -3843
FILENAME= 'MMIRS/2007.0421/RDCS2.0698'
NAMPS   =                   32
READALT =                    T /INITIAL READ VIA LINE RESET MODE
DETSIZE = '[1:2048,1:2048]   '
CCDSEC  = '[1:2048,1:2048]   '
AMPSEC  = '[1:2048,1:2048]   '
DATASEC = '[1:2048,1:2048]   '
DETSEC  = '[1:2048,1:2048]   '
ORIGSEC = '[1:2048,1:2048]   '
TIMFIRST= '2007-04-21 06:18:40' /UT TIME AT START OF FIRST READOUT
TIMLAST = '2007-04-21 06:19:40' /UT TIME AT END OF LAST READOUT
CCDSIGNM= '/data/mmti/src/ccdacq/lib/runlib/ir32asc.bin' /IR SIGNAL FILE
SERIALID= 'Hawaii2-34        '
GAIN    =                    4 /GAIN, ELECTRONS PER ADU
RDNOISE =                   31 /NOISE, ELECTRONS
FOWLNUM =                    1 /NO. FRAMES IN BEGINNING AND IN ENDING SAMPLES
CCDTMOUT=                    0 /EDT CONTROLLER TIMEOUTS
SECPIX1 =                 0.15 /X PIXEL SCALE, ARC-SEC
SECPIX2 =                 0.15 /Y PIXEL SCALE, ARC-SEC
OBJECT  = 'rdcs2             ' / object name
OBSERVAT= 'Magellan          ' / observatory
OBSERVER= 'Brown, Hora, Wyatt' / observers
PROPID  = 'SAO-3             ' / observing proposal ID
PI      = 'W. Brown          ' / principal investigator
DARKTIME=               60.000 / total elapsed time, seconds
IMAGETYP= 'object            ' / object, flat, bias, etc.
EXPTIME =               60.000 / actual integration time, seconds
DATE-OBS= '2007-04-21T06:18:33' / UT date (yyyy-mm-ddThh:mm:ss) of observation s
TELESCOP= 'Clay_F5           ' / telescope name
CORRCTOR= 'NONE              ' / telescope corrector
UT      = '06:18:33          ' / universal time (start of exposure)
ST      = '12:52:42.459      ' / sidereal time
MJD     = 53481.262889999998151 / modified julian date
RA      = '+13:50:45.96      ' / right ascension (hh:mm:ss)
DEC     = '+60:07:03.00      ' / declination (dd:mm:ss)
EQUINOX =            2000.0000 / equinox of RA and Dec
AIRMASS =                1.155 / airmass
ROTANGLE= '25.34660536       ' / telescope rotator angle (degrees)
TELFOCUS= '10336.410         ' / telescope focus
SITENAME= 'LCO'
SITEALT =                 2282         / meters
SITELAT = '-29:0.2'                    / d:m
SITELONG= '70:42.1'                    / d:m
DETECTOR= 'ir_hawaii2        ' / detector name
CCDSUM  = '1 1               ' / on chip summation
INSTRUME= 'mmirs             ' / instrument name
FILTER  = 'J                 ' / instrument filters
TFILTID = '2                 ' / filter id
TFILTNIC= 'J                 ' / filter nickname
TFILTSER= '0002              ' / filter serial#
BFILTID = '0                 ' / filter id
BFILTNIC= 'Emp               ' / filter nickname
BFILTSER= '0000              ' / filter serial#
------------------------------------------------------------
 Cryo Image  Configuration
------------------------------------------------------------
DECKER  = 'OPEN              ' / dekker position
MOS     = 'IMAGE             ' / mos-wheel position
GRISM   = 'NONE              ' / grism wheel position
INSFOCUS= '2345.6            ' / instrument focus
------------------------------------------------------------
 Image specific keywords
------------------------------------------------------------
OBSMODE = 'IMAGING           ' / instrument mode
RADECSYS= 'FK5               ' / Coordinate System
CTYPE1  = 'RA---TAN          ' / Axis 1
CTYPE2  = 'DEC--TAN          ' / Axis 2
CRVAL1  =            207.69150 / Target RA position
CRVAL2  =             60.11750 / Target Dec position
------------------------------------------------------------
 End Image specific keywords
------------------------------------------------------------
POSANGLE=           -180.03700 / telescope position angle
HA      = '-00:58:11.620     ' / hour angle
INSTAZ  = '-34.00000000      ' / instrument azimuth offset(arcsec)
INSTEL  = '-11.00000000      ' / instrument elevation offset(arcsec)
PARANGLE= '-154.6907600      ' / telescope parallactic angle(degrees)
TELAZ   = '0.00000000        ' / telescope azimuth offset(arcsec)
TELEL   = '0.00000000        ' / telescope elevation offset(arcsec)
CAT-ID  = 'RDCS2             ' / telescope catalog obj name
CAT-RA  = '13:50:49          ' / telescope catalog ra
CAT-DEC = '60:07:07          ' / telescope catalog dec
CAT-RAPM= '                  ' / telescope catalog ra proper motion
CAT-DCPM= '                  ' / telescope catalog decproper motion
CAT-EPOC= '2000.00000000     ' / telescope catalog epoch
RECID   = 'clay_f5.20070421.061716' / archive ID for observation
CRPIX1  =                1024.5
CRPIX2  =                1024.5
CD1_1   =  -4.166666548373E-05
CD1_2   =  -9.900641886603E-09
CD2_1   =  -9.900641886603E-09
CD2_2   =   4.166666548373E-05
LTV1    =                    0
LTV2    =                    0
LTM1_1  =                    1
LTM2_2  =                    1
```

moshdr.lst Mon May 02 14:10:29 2005 1

```
RDCS2.0598.fits[2048,2048][real]: rdcs2
No bad pixels, min=0., max=0. (old)
Line storage mode, physdim [2048,2048], length of user area 3524 s.u.
Created Tue 00:00:00 01-Jan-1980, Last modified Tue 00:00:00 01-Jan-1980
Pixel file "RDCS2.0598.fits" [ok]
PCOUNT  =                    0 /NO RANDOM PARAMETERS
GCOUNT  =                    1 /ONE GROUP
BZERO   =                24495
BSCALE  =                    1 /REAL = TAPE * BSCALE + BZERO
DATA-MAX=                52833
DATA-MIN=                -3843
FILENAME= 'MMIRS/2007.0421/RDCS2.0598'
NAMPS   =                   32
READALT =                    T /INITIAL READ VIA LINE RESET MODE
DETSIZE = '[1:2048,1:2048]   '
CCDSEC  = '[1:2048,1:2048]   '
AMPSEC  = '[1:2048,1:2048]   '
DATASEC = '[1:2048,1:2048]   '
DETSEC  = '[1:2048,1:2048]   '
ORIGSEC = '[1:2048,1:2048]   '
TIMFIRST= '2007-04-21 06:18:40' /UT TIME AT START OF FIRST READOUT
TIMLAST = '2007-04-21 06:19:40' /UT TIME AT END OF LAST READOUT
CCDSIGNM= '/data/mmti/src/ccdacq/lib/runlib/ir32asc.bin' /IR SIGNAL FILE
SERIALID= 'Hawaii2-34        '
GAIN    =                    4 /GAIN, ELECTRONS PER ADU
RDNOISE =                   31 /NOISE, ELECTRONS
FOWLNUM =                    1 /NO. FRAMES IN BEGINNING AND IN ENDING SAMPLES
CCDTMOUT=                    0 /EDT CONTROLLER TIMEOUTS
SECPIX1 =                 0.15 /X PIXEL SCALE, ARC-SEC
SECPIX2 =                 0.15 /Y PIXEL SCALE, ARC-SEC
OBJECT  = 'rdcs2             ' / object name
OBSERVAT= 'Magellan          ' / observatory
OBSERVER= 'Brown, Hora, Wyatt' / observers
PROPID  = 'SAO-3             ' / observing proposal ID
PI      = 'W. Brown          ' / principal investigator
DARKTIME=               60.000 / total elapsed time, seconds
IMAGETYP= 'object            ' / object, flat, bias, etc.
EXPTIME =               60.000 / actual integration time, seconds
DATE-OBS= '2007-04-21T06:18:33' / UT date (yyyy-mm-ddThh:mm:ss) of observation s
TELESCOP= 'Clay_F5           ' / telescope name
CORRCTOR= 'NONE              ' / telescope corrector
UT      = '06:18:33          ' / universal time (start of exposure)
ST      = '12:52:42.459      ' / sidereal time
MJD     = 53481.262889999998151 / modified julian date
RA      = '+13:50:45.96      ' / right ascension (hh:mm:ss)
DEC     = '+60:07:03.00      ' / declination (dd:mm:ss)
EQUINOX =             2000.0000 / equinox of RA and Dec
AIRMASS =                1.155 / airmass
ROTANGLE= '25.34660536       ' / telescope rotator angle (degrees)
TELFOCUS= '10336.410         ' / telescope focus
SITENAME= 'LCO'
SITEALT =                 2282        / meters
SITELAT = '-29:0.2'                   / d:m
SITELONG= '70:42.1'                   / d:m
DETECTOR= 'ir_hawaii2        ' / detector name
CCDSUM  = '1 1               ' / on chip summation
INSTRUME= 'mmirs             ' / instrument name
FILTER  = 'J                 ' / instrument filters
TFILTID = '2                 ' / filter id
TFILTNIC= 'J                 ' / filter nickname
TFILTSER= '0002              ' / filter serial#
BFILTID = '0                 ' / filter id
BFILTNIC= 'Emp               ' / filter nickname
BFILTSER= '0000              ' / filter serial#
------------------------------------------------------------
 MOS configuration  keywords
------------------------------------------------------------
OBSMODE = 'MOS               ' / instrument mode
DECKER  = 'slit              ' / dekker position
MOS     = 'brown2            ' / mos-wheel id
GRISM   = 'NONE              ' / grism id
INSFOCUS= '2345.6            ' / instrument focus
APERTURE= 'rdcs2_11          ' / aperture
----- NO WCS keywords -------------------------------------
POSANGLE=           -180.03700 / telescope position angle
HA      = '-00:58:11.620     ' / hour angle
INSTAZ  = '-34.00000000      ' / instrument azimuth offset(arcsec)
INSTEL  = '-11.00000000      ' / instrument elevation offset(arcsec)
PARANGLE= '-154.6907600      ' / telescope parallactic angle(degrees)
TELAZ   = '0.00000000        ' / telescope azimuth offset(arcsec)
TELEL   = '0.00000000        ' / telescope elevation offset(arcsec)
CAT-ID  = 'RDCS2             ' / telescope catalog obj name
CAT-RA  = '13:50:49          ' / telescope catalog ra
CAT-DEC = '60:07:07          ' / telescope catalog dec
CAT-RAPM= '                  ' / telescope catalog ra proper motion
CAT-DCPM= '                  ' / telescope catalog decproper motion
CAT-EPOC= '2000.00000000     ' / telescope catalog epoch
RECID   = 'clay_f5.20070421.061716' / archive ID for observation
LTV1    =                    0
LTV2    =                    0
LTM1_1  =                    1
LTM2_2  =                    1
```

apertable2.txt Wed May 04 23:20:20 2005 1

```
# Sample Hectospec aperture file.  This file is appended to the data as a FITS table extension
# A similar file will be generated for MMIRS slit definitions
#
```

aperture	beam	object	ra	dec	target	fiber	platex	platey
1	1	target	14:34:10.797	34:31:50.509	8965	41	210.546000	172.343000
2	1	target	14:34:05.400	34:47:23.550	10336	70	69.836000	244.473000
3	1	target	14:33:30.810	34:35:03.951	9238	42	137.914000	117.206000
4	1	target	14:33:57.157	34:46:37.806	10268	69	67.361000	225.406000
5	0	sky	0:00:00.000	0:00:00.000	-1	43	151.387000	133.066000
6	1	target	14:33:16.460	34:44:06.510	10041	68	44.703000	139.110000
7	1	target	14:32:28.274	34:38:52.288	9575	44	37.299000	26.784000
8	1	target	14:33:35.565	34:44:31.504	10087	67	61.885000	175.379000
9	1	target	14:34:26.006	34:33:31.940	9103	45	213.085000	209.021000
10	1	target	14:33:19.017	34:43:31.024	9991	66	52.523000	140.547000
11	1	target	14:32:29.678	34:18:56.865	8063	291	210.374000	-76.054000
12	1	target	14:32:24.299	34:36:46.563	9405	20	50.802000	8.810000
13	1	target	14:32:20.790	34:28:57.419	8766	292	113.890000	-38.529000
14	0	sky	0:00:00.000	0:00:00.000	-1	19	247.089000	57.954000
15	1	target	14:32:37.541	34:15:44.563	7815	293	247.381000	-79.380000
16	1	target	14:33:17.431	34:25:52.574	8576	18	202.617000	45.355000
17	1	target	14:32:33.833	34:20:17.972	8171	294	203.077000	-61.477000
18	1	target	14:32:51.785	34:30:42.133	8883	17	132.682000	25.259000

MMIRS/

Data Reduction Software

Data Pipeline:

Three potential software packages for multislit spectroscopic data reduction have been identified:

- the COSMOS package written by Gus Oemler at Carnegie for IMACS: **http://www.ociw.edu/~oemler/COSMOS.html**
- the Gemini software for GMOS **http://www.gemini.edu/sciops/instruments/gmos/gmosIndex.html**
- a data reduction pipeline under development by Armondo Gil de Paz for EMIR **http://www.ucm.es/info/emir/**

MMIRS/

Development Estimates

Most of the MMIRS software modules are derived from similar modules for other instruments. We assign a complexity value by considering the amount of code reuse, the number of interfaces and the interconnectedness of the module. Modules that are de-coupled from the overall observing environment are inherently less complex that those that are part of the telescope and facility interaction.

Also many of the GUIS and some servers are already implemented for existing instruments. The major effort in these cases involves integrating the new components in the existing code and then regression testing all of the instruments to re-certify the code.

e.g.

- Guide Server
- Observing GUI
- Guide GUI

New infrastructure will be developed for some of the components that will ultimately similify development and coding but does incur some infrastructure development costs.

The complexity codes range from:

- 0 - code complete
- 1 - least complex
- 3 - most complex

```
Hardware Control


   complexity  module                                          estimate
   ----------  ------                                          --------


       1        barcode scanner server                             2 wks
               (megacam topbox has a barcode scanner)


       2       pmac motion control server
               dewar motors (steppers/no encoders)                8 wks
               wfs/guide motors                                   4 wks
               push button - PLC                                  1 wk


       2       Engineering GUI                                    1 wk


       1       science camera server                              2 wks
```

```
                5 science cameras already deployed using the same
                server software
                    detector - done
                    instrument - 1 page
                    telescope - done
                    HK - mostly done


        1       Thermal Vac Control
                Multiple hardware and protocols


                HK monitoring (IR array)                                1 wk
                    SWIRC has HK monitoring code
                focal plane heater                                      1 wk
                    all ccd cameras have a heater - this one is easer
                cryo heaters                                            1 wk
                vacuum gauge                                            1 wk
                vacuum pump                                             1 wk
                Power Control Server


        2       Rack Monitor                                            2 wk
                (clunky binary format protocol)


        1       calibration lamp                                        ?


        2       wfs/guide camera server                                 2 wk
                similar to Carnegie Magellan camera


        2       Log Server                                              2 wk
                (infrastructure development)


External connections


    complexity  module                                          estimate
    ----------  ------
--------


        0      magellan telescope protocol translator                   0 wk
                done for megacam
```

```
        2       wfs                                                     1 wk
                an interface to megallan wfs server
                unknown MMT interface


        3       Planning GUI                                            4 wks
                MDF generator


        3       GMAP Guide Star interface                               4 wks


        2       guide server                                            4 wks
                mmt instruments all use current guide server
                needs upgrade for new camera type


Operations


    complexity  module                                          estimate
    ----------  ------                                          --------


        2       cryostat operation                                      4 wk
                startup
                heatup
                cooldown
                pump


        2       observing gui                                           6 wks
            observing sequence and exposure sequence already exist
            for both imaging and spectroscopic instruments
            Need to add support for multiple modes and MOS operation
            with mask alignment, etc.


                imaging
                mos
                longslit


        1       obslogger/commenter                                     1 wks
                done for megacam, hectospec and hectochelle
                needs exposure collapser for swirc/mmirs


        2       guidegui                                                4 wks
```

Add dual WFS/Guide support
Upgrade for new DS9 interface

Status Displays

complexity	module	estimate
2	dewar status similar to megacam topper display - more components	3 wk
2	guide motor status similar to megacam topper display - more components	3 wk

Software For Assembly and Test

complexity	module	estimate
0	subassembly build up and ad hoc testing	
	During any week where there is sub assembly testing some level of software support will be required.	
1	full up machanical system testing	
1	performance testing	

MMIRS/

Release Schedule

Release 1	Test Dewar Support	7/05
Science Camera Server 1 Detector Server only Thermal Vac Server 1 Cam/Mos Heater (Omega) AutoFill Control (Omega) Cam/Mos Temp Monitor (Lakeshore) FP Temp Control (Lakeshore)		
Release 2	Motor Components Wfs/Guide Components	10/05
Engineering GUI Motion Control Server 1 MOS Motors WFS/Guide Motors WFS/Guider Camera Server Thermal Vac Server 2 Phytron Stepper Amp Vac Gauge (Pfeiffer)		
Release 3	Cryostat Motor Control Electronics Rack support	1/06
Motion Control Server 2 High Level Functions Rack Monitor Barcode Scanner Power Control Server		
Release 4	Integration	4/06
Integrated Science Camera Server with instrument control and telescope status		
Observers GUI		

with spectral and imaging modes		
Cryostat Operations GUI including Interlock connections		
Guide Server and GuideGUI		
Release 5	Telescope	7/06
Planning GUI		
GSTARS		
Release 6	2nd Telescope	12/06

Section X.

Miscellaneous

1. Observatory Interface
    a. MMIRS Observatory Interface
    b. MMT Telescope Bearing Moment
    c. Magellan Telescope Bearing Moment
2. Vacuum System
3. Temperature Sensing
4. Gate Valve Interlock

MMIRS Observatory Interface

George Nystrom
May 4, 2005

100 Space Requirements

The MMT is the limiting envelope for the MMIRS instrument. Figures 1 and 2 describe the MMT instrument volume and rotator envelope and how well MMIRS fits within it. MMIRS will have 33.6 inches clearance with the elevation axis support weldments and 4.1 inches clearance with the instrument lift's floor channels. A possible encroachment on the MMT envelope as defined in MMTO-TM #00-1 is shown in Figure 1. We have contacted MMTO personnel to investigate if the defined envelope could be changed to accept MMIRS and are awaiting their investigation. The electronics boxes will need to be modified should the presently defined envelope need to be maintained. Figure 2, describes the allowable swing arc and MMIRS compliance with it. MMIRS fits well within this envelope. The Magellan envelope is vastly larger in all dimensions and therefore no interference is expected.

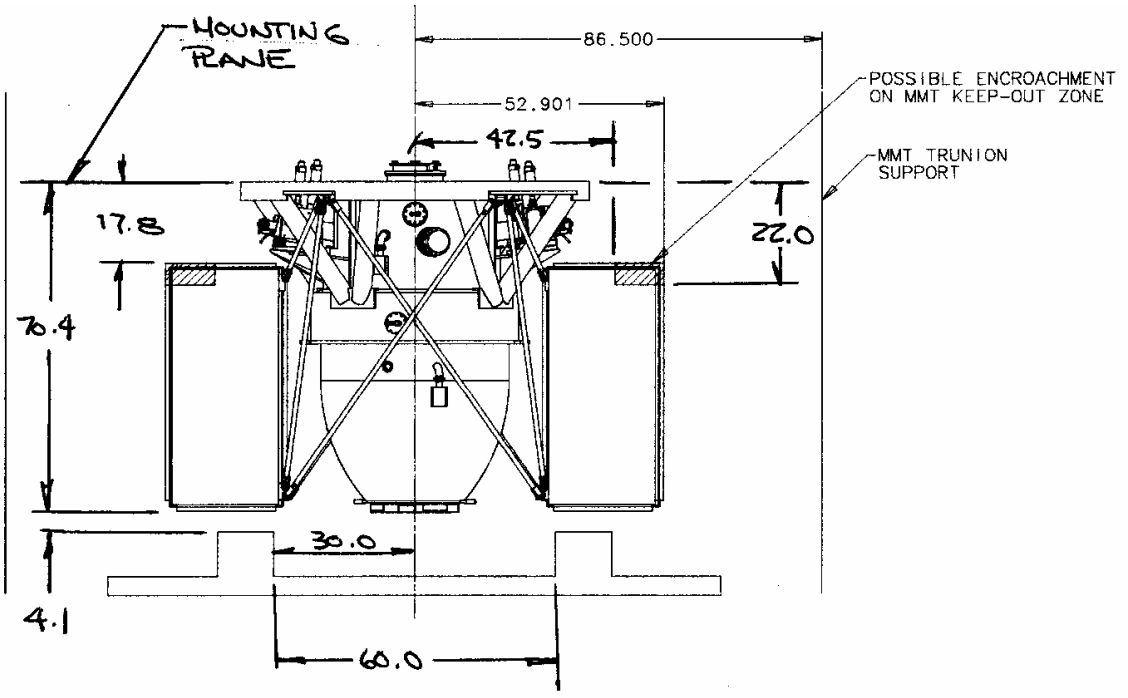

Figure 1: MMIRS space envelope at the MMT.

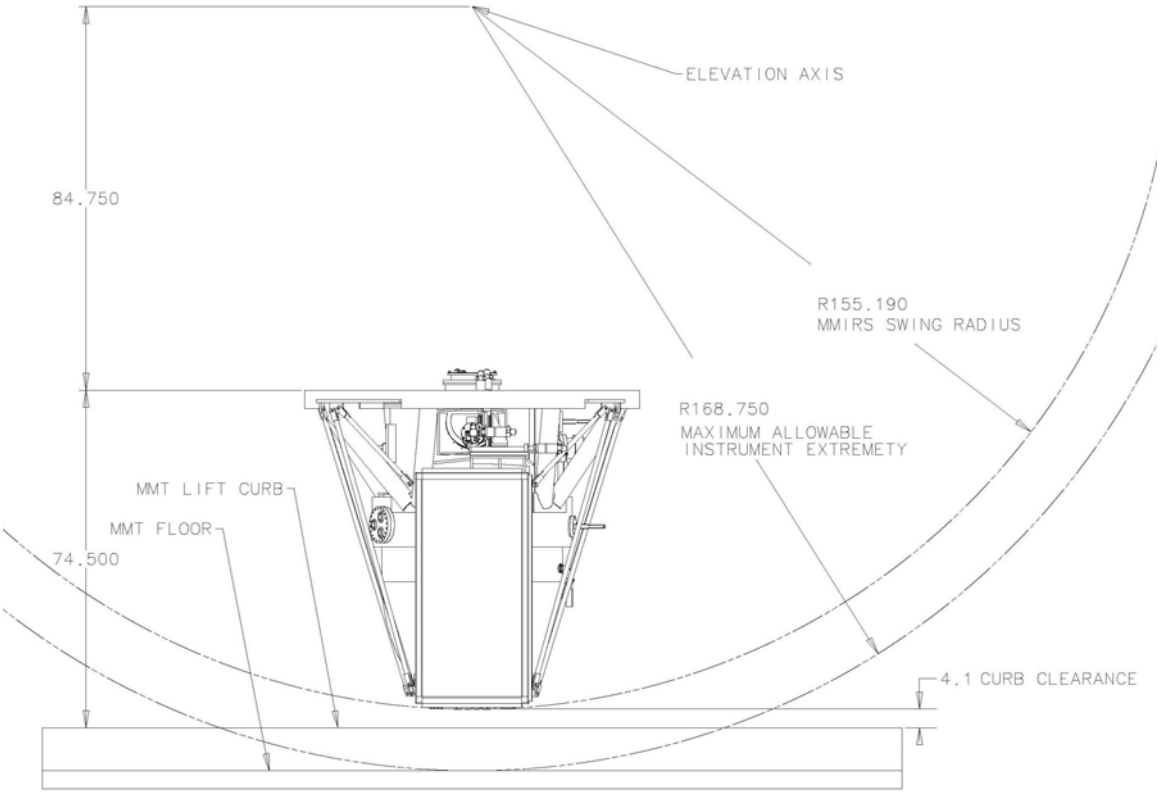

Figure 2: MMIRS clearance at the MMT.

110 Requirements from the F&P

The following sections address particular space and accessibility requirements from the F&P.

111 Electronic enclosures

Section 331 of the F&P specifies that the electronics enclosures be included in the space envelope evaluation. This has been done and is shown in Figures 1 & 2 above.

112 Access to Liquid Nitrogen ports

Section 332 of the F&P specifies that the LN2 ports shall be readily accessible. This is the case at both telescopes; however a small platform will be required to reach the MOS fill port at Magellan due to the instrument's height above the floor.

112 Electrical connections

Section 333 of the F&P specifies that all electrical connections to external equipment be accessible and that they may be disconnected without removal of the instrument from the CIR. This requirement is met by this design.

200 Mass and Center of Gravity Requirements

210 MMT

The MMIRS-MMT Center of Gravity (CG) location with respect to the instrument mounting surface and the telescope's central axis is listed below. These calculations are with respect to the telescope's axis definitions and all dimensions are in inches:

X-X = -0.127 Y-Y = 0.63 Z-Z = 28.728

Therefore the interface specifications (TM#00-1) and compliances are:

	Requirement	MMIRS
Cantilever Moment Specification (in-lbs):	150,000	93,180
Rotational imbalance Specification (in-lbs):	12,000	2,040
Mass Specification (lbs):	4,400	3243.7

The calculations for the CG and resultant moments are shown in attachment: "MMT Bearing Moment Calculations"

220 Magellan

The MMIRS-Magellan CG location with respect to the instrument rotator surface and the telescope's central axis is:

X-X = -0.092 Y-Y = .457 Z-Z = 26.632

The interface specifications (03SE004) and compliances are:

	Requirement	MMIRS
Cantilever Moment Specification (in-lbs):	150,000	119,076
Rotational imbalance Specification (in-lbs):	12,000	2,040
Mass Specification (lbs):	5,000	4,471

These calculations included the SAO supplied CIR with the origin at the telescope-bearing mounting surface.

The calculations for the CG and resultant moments are shown in attachment: "Magellan Telescope Bearing Moment Calculations"

300 Telescope mounting truss

The telescope mounting truss is a welded tubular truss made from A-36 steel in order to match the properties of the t MMT and Magellan CIR. It has a circular base ring for CIR attachment with a raised outer diameter to provide axial and radial stiffness. The truss mounts to the bulkhead between the MMIRS MOS and Camera Sections. The CIR mounting surface and the Cryostat's mounting surfaces will be final machined parallel to each other to within 0.003 inches. This is so that the Lyot stop can be properly positioned

during assembly and will not require further adjustment required at the telescope. The truss has eight 4-inch diameter by ½-inch wall thickness steel tubes welded to the base ring at the midpoints between the ring's CIR mounting holes. Similarly, at the Cryostat's interface, the tubes are welded to the ring segments. These segments are bolted to the bulkhead. Gussets are used at each tube end to stiffen the bolted interfaces. Gussets are also used between tubes to limit tube bending. The truss tubes are arranged to provide easy access to the MOS mask exchange panel and clearance around the Guider/WFS systems.

The base ring also provides four (4) raised platforms. These platforms are used to mount the two electronic racks and provide a mounting interface to the Magellan and MMT installation carts. These platforms are concentric with the base ring and have a U-shaped cross-section. The platforms have mounting holes for the electronics racks' mounting trusses and to secure the MMIRS to the installation carts. Some CIR mounting holes are covered by these platforms; however large holes are provided to allow the bolts to be installed.

The truss design calculations are covered in the structural section.

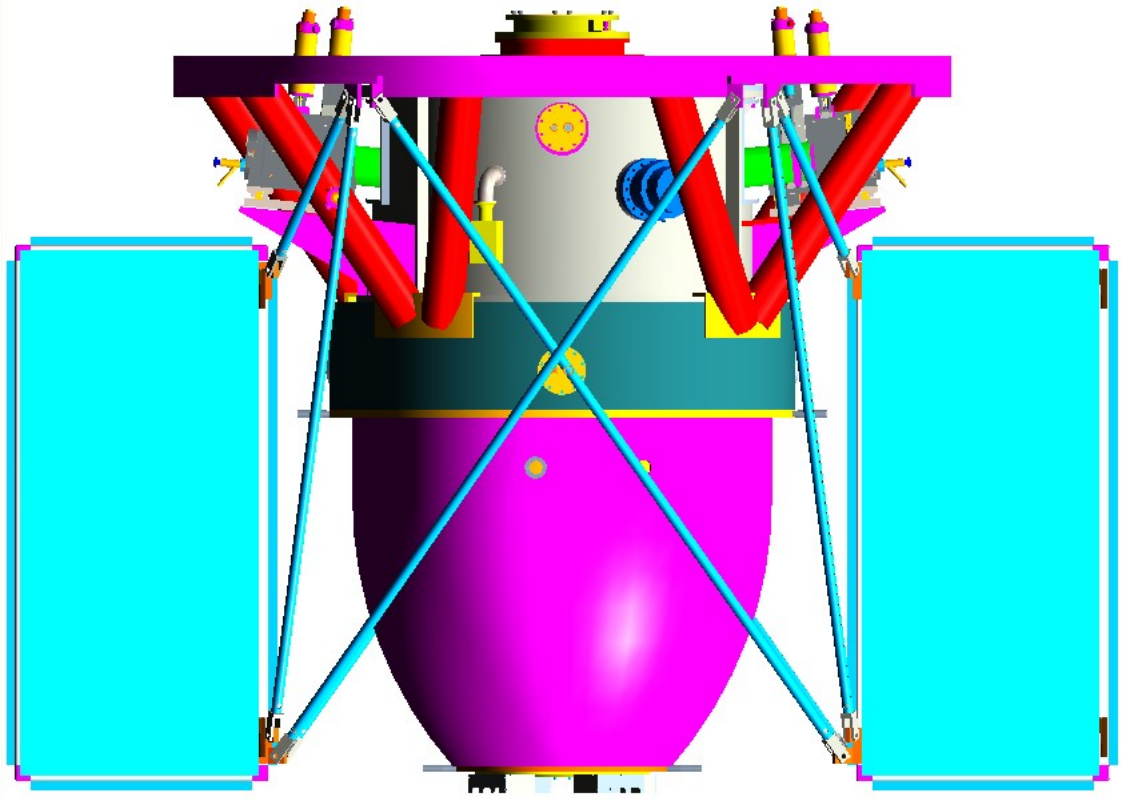

Figure 3: Intrument mounting truss.

MMIRS
MMT Telescope Bearing Moment Calculations

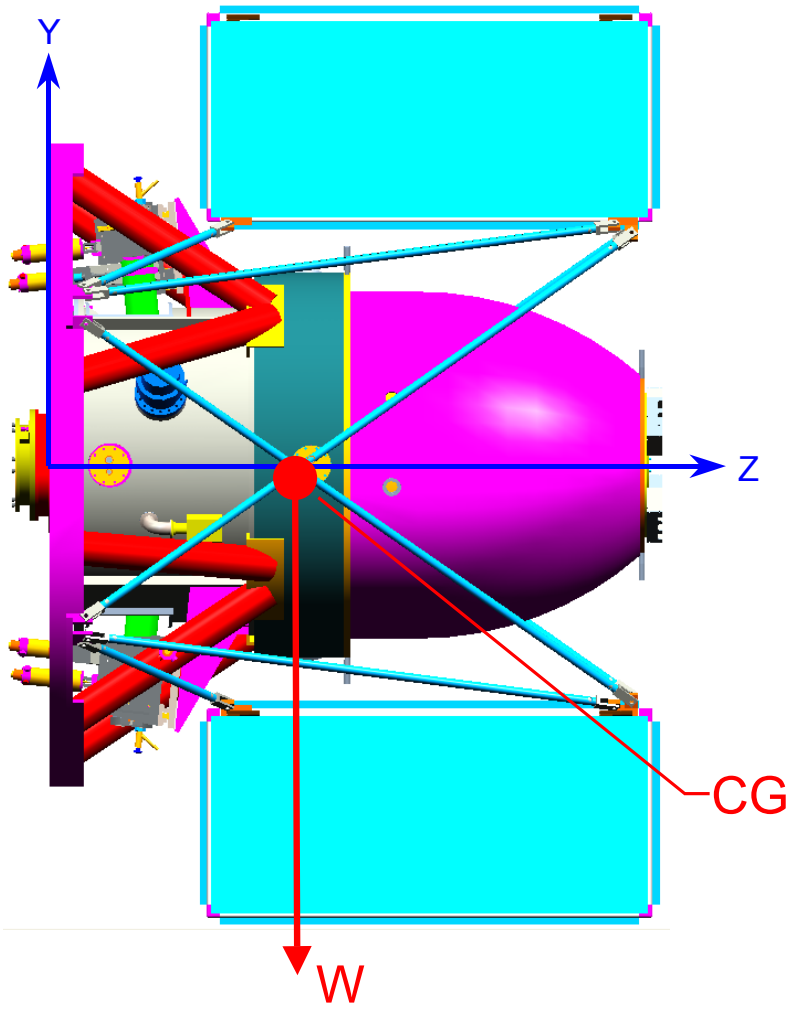

List the center of gravity for all components and their respective weights

$$CG_{L1} := \begin{pmatrix} 0 \\ -5.17 \\ 19 \end{pmatrix} \text{ in} \qquad W_{L1} := 90.4 \cdot \text{lbf}$$

Center of Gravity and Weight of MOS LN_2

$$CG_{L2} := \begin{pmatrix} 0 \\ -11.625 \\ 42.804 \end{pmatrix} \text{ in} \qquad W_{L2} := 141.6 \cdot \text{lbf}$$

Center of Gravity and Weight of Camera LN_2

$$CG_{Assy} := \begin{pmatrix} -0.18 \\ -0.49 \\ 21.9 \end{pmatrix} in \qquad W_{Assy} := 2289.7 \cdot lbf$$

Center of Gravity for Instrument Assembly

$$CG_{Rack1} := \begin{pmatrix} 0 \\ 40 \\ 48.84 \end{pmatrix} in \qquad W_{Rack1} := 427 \cdot lbf$$

Center of Gravity for Electronics Rack #1

$$CG_{Rack2} := \begin{pmatrix} 0 \\ -40 \\ 48.84 \end{pmatrix} in \qquad W_{Rack2} := 295 \cdot lbf$$

Center of Gravity for Electronics Rack #2

Vectorize weights and CG for each axis

$$W := \begin{pmatrix} W_{Assy} \\ W_{Rack1} \\ W_{Rack2} \\ W_{L1} \\ W_{L2} \end{pmatrix}$$

$$X := \begin{pmatrix} CG_{Assy_1} \\ CG_{Rack1_1} \\ CG_{Rack1_1} \\ CG_{L1_1} \\ CG_{L2_1} \end{pmatrix}$$

$$Y := \begin{pmatrix} CG_{Assy_2} \\ CG_{Rack1_2} \\ CG_{Rack2_2} \\ CG_{L1_2} \\ CG_{L2_2} \end{pmatrix}$$

$$Z := \begin{pmatrix} CG_{Assy_3} \\ CG_{Rack1_3} \\ CG_{Rack2_3} \\ CG_{L1_3} \\ CG_{L2_3} \end{pmatrix}$$

Find composite CG and weight for all components

$i := 1 .. 5$

$$CG_{total} := \begin{bmatrix} \frac{\sum_i (X_i \cdot W_i)}{\left(\sum_i W_i\right)} \\ \frac{\sum_i (Y_i \cdot W_i)}{\left(\sum_i W_i\right)} \\ \frac{\sum_i (Z_i \cdot W_i)}{\left(\sum_i W_i\right)} \end{bmatrix}$$

$$CG_{total} = \begin{pmatrix} -0.127 \\ 0.63 \\ 28.728 \end{pmatrix} \text{ in}$$

Composite CG for assembly liquid nitrogen and electronics racks

$$W_{total} := \sum W$$

$W_{total} = 3243.7\,\text{lbf}$ Total weight supported by telescope bearing

Solve for the moment about the point at (0,0,0)

$$\text{Weight} := \begin{pmatrix} -W_{total} \\ 0 \\ 0 \end{pmatrix}$$

Gravity applied in the -X direction is worst case. (Note: Picture above shows gravity in the -Y direction just for illustrative purposes)

$$M := CG_{total} \times \text{Weight}$$

$$M = \begin{pmatrix} 0 \\ -7765 \\ 170 \end{pmatrix} \text{ft}\cdot\text{lbf}$$

Moment Vector due to the weight

$$M_y := M_2$$

$$M_z := M_3$$

$M_y = -7765\,\text{ft}\cdot\text{lbf}$ Magnitude of the moment about the Y-Axis

$M_z = 170\,\text{ft}\cdot\text{lbf}$ Magnitude of the imbalance moment about the Z-Axis

MMIRS
Magellan Telescope Bearing Moment Calculations

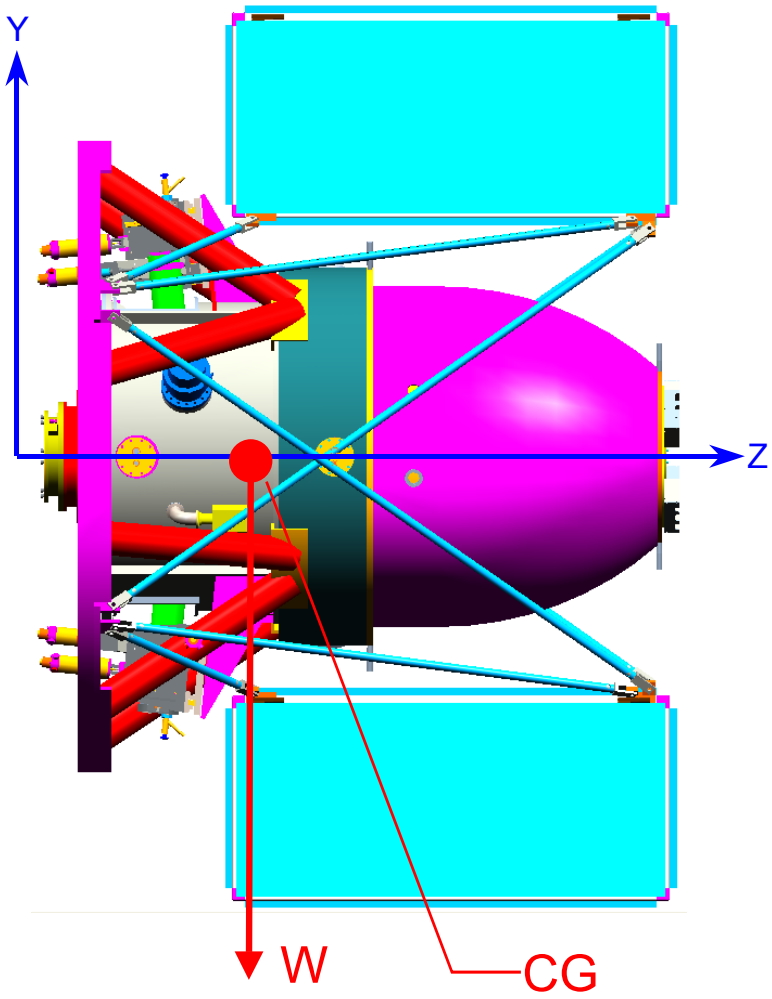

List the center of gravity for all components and their respective weights

$$CG_{L1} := \begin{pmatrix} 0 \\ -5.17 \\ 26.781 \end{pmatrix} \text{in} \qquad W_{L1} := 90.4 \cdot \text{lbf}$$

Center of Gravity and Weight of MOS LN_2

$$CG_{L2} := \begin{pmatrix} 0 \\ -11.625 \\ 50.585 \end{pmatrix} \text{in} \qquad W_{L2} := 141.6 \cdot \text{lbf}$$

Center of Gravity and Weight of Camera LN_2

$$CG_{Assy} := \begin{pmatrix} -0.18 \\ -0.49 \\ 29.68 \end{pmatrix} in \qquad W_{Assy} := 2289.7 \cdot lbf$$

Center of Gravity and Weigth for Instrument Assembly

$$CG_{Rack1} := \begin{pmatrix} 0 \\ 40 \\ 51.48 \end{pmatrix} in \qquad W_{Rack1} := 427 \cdot lbf$$

Center of Gravity and Weight for Electronics Rack #1

$$CG_{Rack2} := \begin{pmatrix} 0 \\ -40 \\ 51.48 \end{pmatrix} in \qquad W_{Rack2} := 295 \cdot lbf$$

Center of Gravity and Weight for Electronics Rack #2

$$CG_{CIR} := \begin{pmatrix} 0 \\ 0 \\ 3.558 \end{pmatrix} in \qquad W_{CIR} := 1227.5 \cdot lbf$$

Center of Gravity and Weight for Telescope CIR Adapter

Vectorize weights and CG for each axis

$$W := \begin{pmatrix} W_{Assy} \\ W_{Rack1} \\ W_{Rack2} \\ W_{L1} \\ W_{L2} \\ W_{CIR} \end{pmatrix} \qquad X := \begin{pmatrix} CG_{Assy_1} \\ CG_{Rack1_1} \\ CG_{Rack1_1} \\ CG_{L1_1} \\ CG_{L2_1} \\ CG_{CIR_1} \end{pmatrix}$$

$$Y := \begin{pmatrix} CG_{Assy_2} \\ CG_{Rack1_2} \\ CG_{Rack2_2} \\ CG_{L1_2} \\ CG_{L2_2} \\ CG_{CIR_2} \end{pmatrix} \qquad Z := \begin{pmatrix} CG_{Assy_3} \\ CG_{Rack1_3} \\ CG_{Rack2_3} \\ CG_{L1_3} \\ CG_{L2_3} \\ CG_{CIR_3} \end{pmatrix}$$

Find composite CG and weight for all components

$i := 1 .. 6$

$$CG_{total} := \begin{bmatrix} \frac{\sum_i \left(X_i \cdot W_i\right)}{\left(\sum_i W_i\right)} \\ \frac{\sum_i \left(Y_i \cdot W_i\right)}{\left(\sum_i W_i\right)} \\ \frac{\sum_i \left(Z_i \cdot W_i\right)}{\left(\sum_i W_i\right)} \end{bmatrix}$$

$$CG_{total} = \begin{pmatrix} -0.092 \\ 0.457 \\ 26.632 \end{pmatrix} \text{ in}$$

Composite CG for assembly liquid nitrogen and electronics racks

$$W_{total} := \sum W$$

$W_{total} = 4471.2 \text{ lbf}$

Total weight supported by telescope bearing

Solve for the moment about the point at (0,0,0)

$$\text{Weight} := \begin{pmatrix} -W_{total} \\ 0 \\ 0 \end{pmatrix}$$

Gravity applied in the -X direction is worst case. (Note: Picture above shows gravity in the -Y direction just for illustrative purposes)

$$M := CG_{total} \times \text{Weight}$$

$$M = \begin{pmatrix} 0 \\ -9923 \\ 170 \end{pmatrix} \text{ft·lbf}$$

Moment Vector due to the weight

$$M_y := M_2$$

$$M_z := M_3$$

$$M_y = -9923\,\text{ft·lbf}$$

Magnitude of the moment about the Y-Axis

$$M_z = 170\,\text{ft·lbf}$$

Magnitude of the imbalance moment about the Z-Axis

MMIRS Vacuum System

G. Nystrom, 03 May 2005

100 System Description

The MMIRS vacuum system components and arrangement are shown in Figure 1. It is composed of a Varian Turbo pump, model V301 with a Varian Tri-Scroll 600 roughing pump. Vacuum pressure recording is accomplished using a Pfeiffer vacuum gauge controller, Model DPG 109. It controls and provides pressure measurement from two Pfeiffer model HPT-100 and a PPT-100 sensors. The HPT-100 is used to measure the MOS and Camera chambers from one Atmosphere down to 1 x 10^{-9} Torr. The PPT-100 sensor is used to measure chamber pressure during initial evacuation and the Turbo pumps fore-line pressure when operating. The PPT-100 has a range from one Atmosphere down to 1 x 10^{-4} Torr.

The turbo pump is permanently attached to the MOS section. The exhaust port of the turbo pump connects through V2 to the roughing pump and the backfill system.

Evacuation of the camera section is performed by opening the isolation gate valve (V1). During initial testing, when the two sections may not be mated, the camera section can be pumped through valve V6.

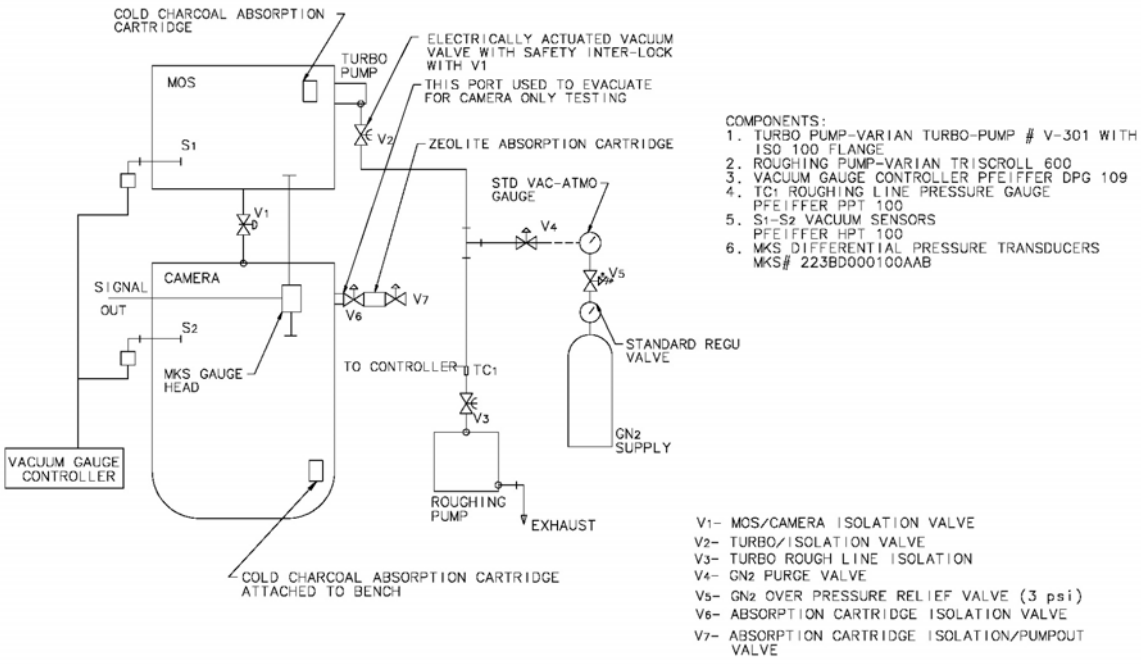

Figure 1 – The MMIRS vacuum system, from SAO drawing C-MMIRS 102

110 Isolation Gate Valve

A custom gate valve assembly has been fabricated by VAT, a respected manufacturer of vacuum equipment. The valve is operated by an SAO designed drive system. This valve, designated V1, requires a safety interlock protocol, which is outlined in a memo titled "MMIRS Gatevalve Interlock". The implementation of the interlock is described in the Electonics section.

120 Backfill System

A manually controlled backfill system is planned. It is shown on drawing C-MMIRS-102. The backfill system connects to the MOS chamber via V2 an electrically operated solenoid valve. To prevent backfilling of the MOS or Camera sections when they are cold, V2 is connected to the Interlock System.

The backfill system uses a standard Dry Nitrogen bottle outfitted with a regulator/valve. Also an over-pressure valve in placed between the bottle and MOS chamber to prevent its over-pressurization, which could lead to possible damage to internal components. A valve also is placed in front of the roughing pump to prevent flow in that direction. A pressure gauge is also in the backfill line to allow determination as to when the MOS chamber is at atmospheric pressure.

200 Pump Out Times

The MOS and Camera chambers have evacuation volumes of 192 and 617 liters respectively. The expected evacuation pump down curves are attached as Figures 2 and 3. These curves are for a clean instrument after initial out-gassing. The properties used in the evaluation are: O-ring leakage, surface volumes and materials, connector leak rates and valve (V1& V2) conductances.

The MOS only evacuation time to 1×10^{-4} Torr is less than 30 minutes, which is within specification as described in section 373 and shown in figure 2 below. The MOS+Camera evacuation time to 1×10^{-4} Torr is specified as < 4 hours, Figure 3 below shows that this specification is achieved.

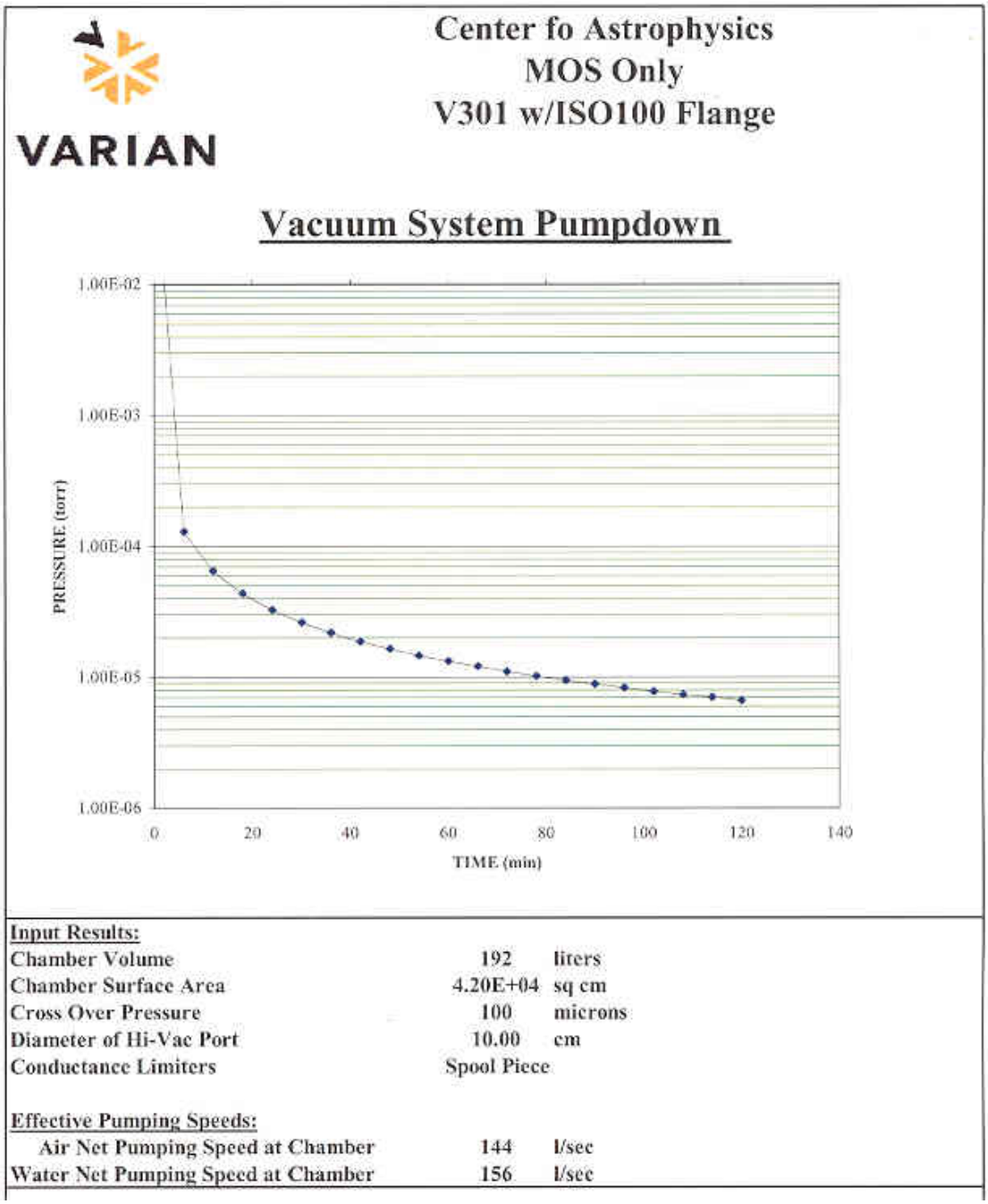

Input Results:		
Chamber Volume	192	liters
Chamber Surface Area	4.20E+04	sq cm
Cross Over Pressure	100	microns
Diameter of Hi-Vac Port	10.00	cm
Conductance Limiters	Spool Piece	
Effective Pumping Speeds:		
Air Net Pumping Speed at Chamber	144	l/sec
Water Net Pumping Speed at Chamber	156	l/sec

Figure 2 -- MOS Pumpdown Curve

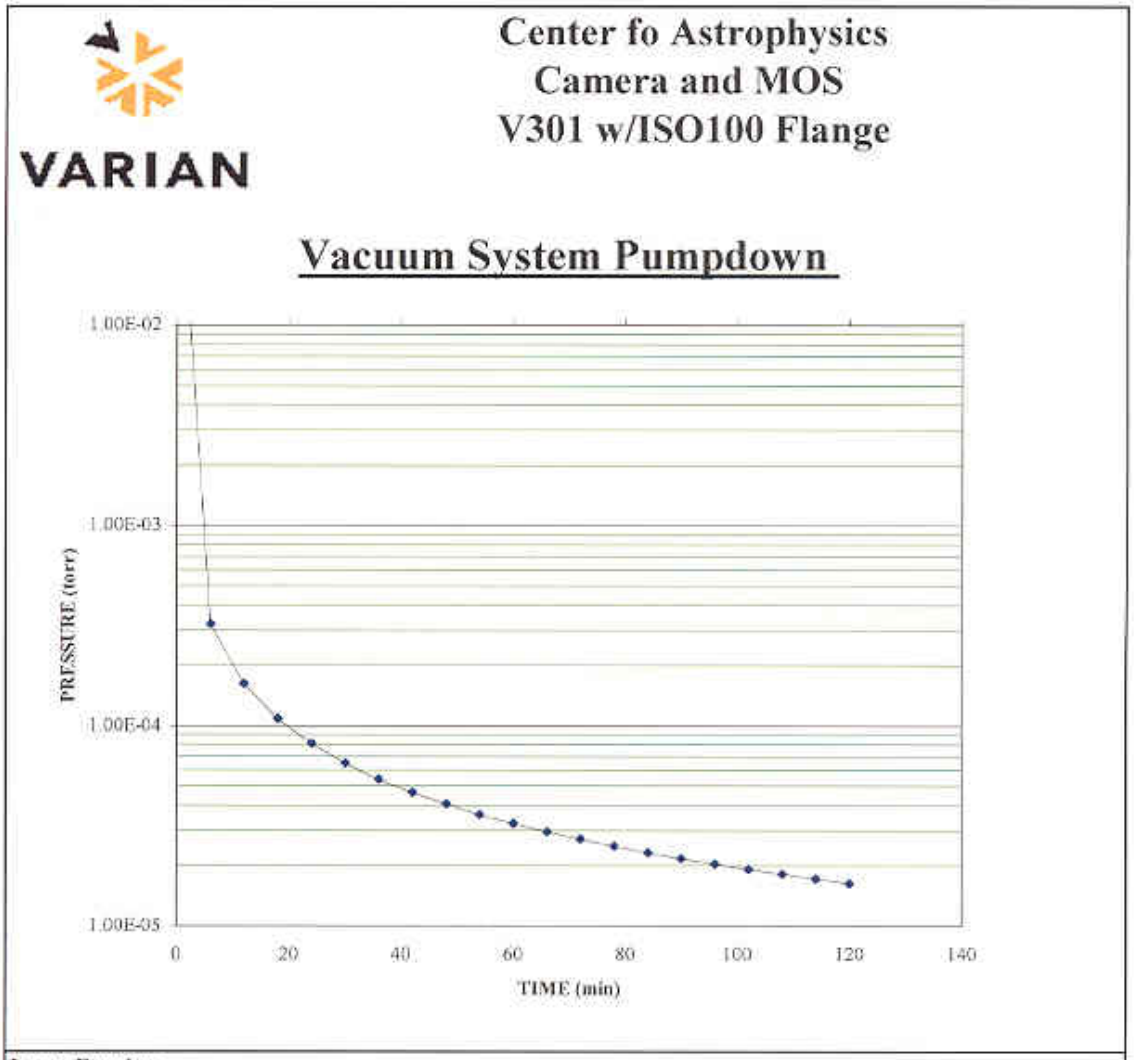

Input Results:		
Chamber Volume	809	liters
Chamber Surface Area	1.05E+05	sq cm
Cross Over Pressure	100	microns
Diameter of Hi-Vac Port	10.00	cm
Conductance Limiters	Spool Piece	
Effective Pumping Speeds:		
Air Net Pumping Speed at Chamber	144	l/sec
Water Net Pumping Speed at Chamber	156	l/sec

Figure 3. MOS+Camera Pumpdown Curve

300 Gettering

Vacuum maintenance during cold operation is required because O-ring seals are intrinsically leaky due to diffusion of nitrogen through rubber. MMIRS will have charcoal adsorption cartridges placed in each chamber and intimately attached to a cold surface. The charcoal will be contained using sintered metal filters. The Ohio State Astronomy MATHCAD document (Atwood-O'Brien) was used to calculate the effectiveness of the Charcoal pump. The camera section has a predicted pressure rise to $1.7*10^{-5}$ Torr after 180 days of cold operation using the Charcoal pump. A simple flow meter measuring LN2 boil-off can be used to evaluate the change in vacuum isolation.

The Camera section also has a warm Zeolite canister to pump water during initial pumpout phases, The Zeolite canister can be recharged via bake-out while in place using its isolation valves (V6 and V7).

MMIRS Temperature Sensing and Heating Requirements

Paul Martini
April 29, 2005

100 Overview

The MMIRS instrument will require a number of temperature sensors and heaters in order to monitor and maintain the optical elements and detector at their required temperatures, insure rapid cycling of the MOS Section, for diagnostics purposes during instrument assembly, and to monitor the long-term health of the instrument. This document describes the expected number and location of the temperature sensors and provides some guidelines on the temperature controllers.

The estimated temperature sensor requirements are:

- MOS Section: 2
- Camera Section: 6
- Electronics Racks: 5
- Engineering: 17

The total heater requirements are:

- High Power: 2
- Low Power: 1

200 Temperature Sensing Requirements

The temperature sensing requirements have been divided into four categories: MOS Section, Camera Section, Electronics Racks, and Engineering. The first three sections correspond to the recommended sensors for regular operation. The fourth corresponds to the expected additional temperature sensors that will be required during initial instrument assembly and checkout, but will not be monitored during regular operation. Nevertheless, all of these sensors should be permanently installed and cabled so that they may be connected to the temperature monitors in the electronics racks if necessary, and without opening the instrument. This will likely require a simple breakout box or jumper box installed in one of the electronics racks.

Note that temperature sensors in the electronics racks shall likely use a different temperature monitor than those inside the MOS and Camera Sections (see Section 230 below). A LakeShore Temperature Monitor is recommended for the temperature sensors inside the MOS and Camera Sections.

210 MOS Section

The following areas should have a temperature sensor:

- T1: Wheel enclosure: attached to the outer surface
- T2: Dewar: on side opposite bulkhead and facing wheels

The subtotal for the MOS Section is two temperature sensors. The locations of these sensors are indicated in Figure 1.

220 Camera Section

The following areas should have a temperature sensor:

- T3: Lens 3: attached to the lens mount, furthest from dewar
- T4: Vee block 1: attached to the inside of the radiation shield at top, center
- T5: Detector mount: opposite the detector and near top
- T6: Detector mount: on detector fan-out board
- T7: Dewar back: middle of side opposite bulkhead plate, near optical bench
- T8: Radiation shield: halfway along length and opposite the dewar

The subtotal for the Camera Section is 8 temperature sensors. The locations of these sensors are indicated in Figure 1. Temperature sensors T5 or T7 shall be connected in a feedback loop with the fill valve and heater to control the rate of change of temperature.

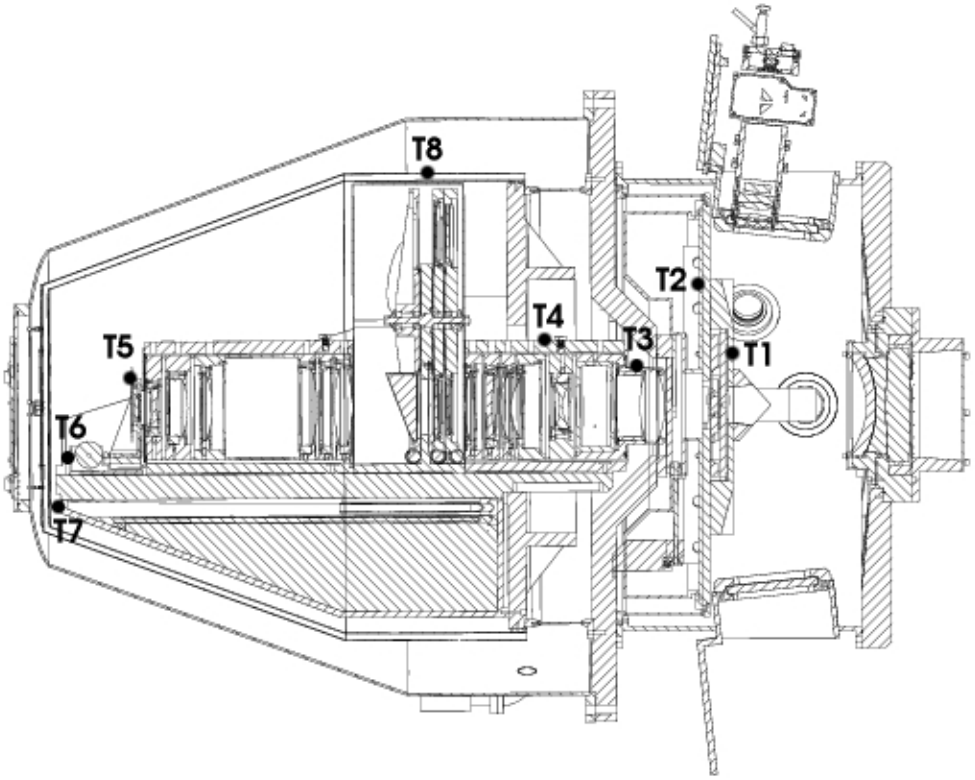

Figure 1: Locations of the temperature sensors for regular operation.

230 Electronics Racks

Temperature sensors will be necessary in each rack and up to one particularly heat-sensitive electronics component per rack may also be monitored individually. These sensors do not need to be part of the temperature monitors for the sensors inside the instrument. One option for these sensors is what we used in the PANIC instrument: the Omega CNi16D controller with embedded Ethernet. These units are small and cheap.

The subtotal for the electronics racks is expected to be five temperature sensors.

240 Engineering Sensors

We expect to require the following, additional sensors during the integration and testing phase.

MOS section:

- E1: Lens 2: Attached to the lens mount material
- E2: Pickoff mirror: One of the two mirrors only
- E3: L2 baffle: Attached to the outside surface and facing the mask exchange port
- E4: GWS baffle top: Outside surface facing top dome
- E5: Slit mask wheel: Rim of wheel (for static test!)

Camera section:

- E6: Lens 5: Attached to the lens mount
- E7: Lens 8: Attached to the lens mount
- E8: Lens 9: Attached to the lens mount
- E9: Lens 14: Attached to the lens mount
- E10: Vee block 2: Attached to the inside of the radiation shield at top, center
- E11: Dewar front: Middle of side facing bulkhead plate, near optical bench
- E12: Lens 9 dummy: Center of a dummy lens in the mount for lens 9
- E13: Lens 10 dummy: Center of a dummy lens in the mount for lens 9
- E14: Detector dummy: Center of the ZIF socket
- E15: Electronics radiation shield: Center of radiation shield behind detector
- E16: Wheel radiation shield: Top of radiation shield over filter/grism wheels
- E17: Grism wheel: Rim of wheel (for static test!)

Additional temperature sensors may exist in the cryogenic motors. The present layout anticipates that they will not be used.

The subtotal for engineering sensors is expected to be 17 temperature sensors. The locations of these sensors are indicated in Figure 2. Note that the MOS section baffles are not shown, and therefore E3 and E4 have been placed at their approximate spatial location.

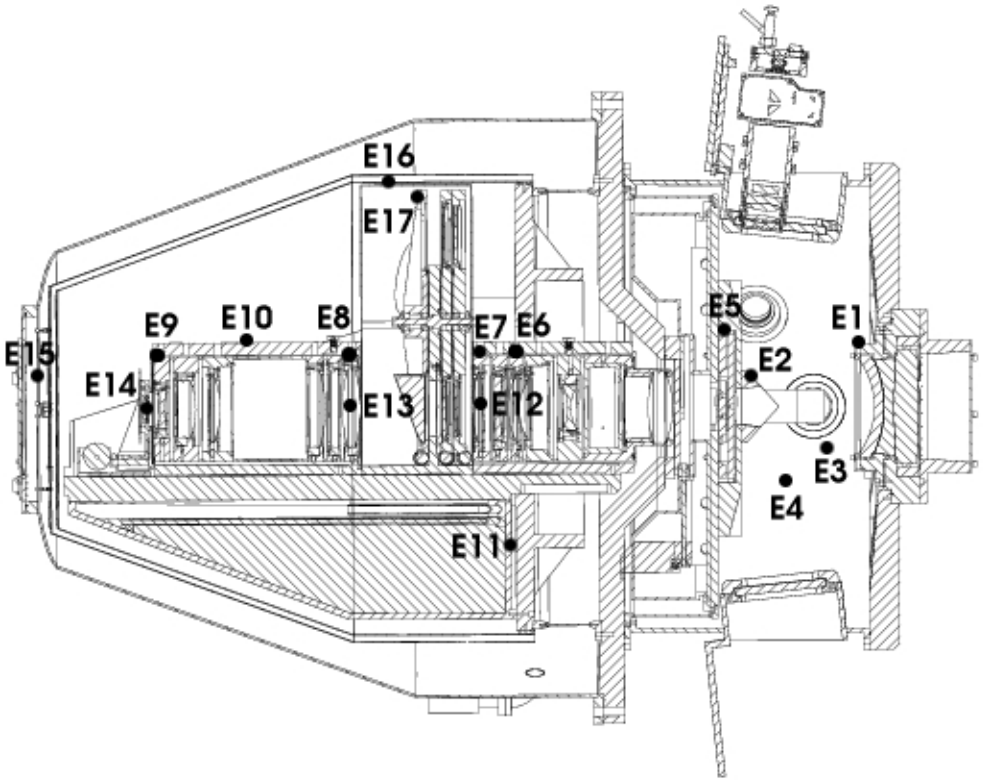

Figure 2: Locations of the temperature sensors for engineering checkout.

300 Heating Requirements

MMIRS will require two high power heaters for thermally cycling the MOS and Camera dewars and one low power heater for potential use in controlling the detector cooldown rate and insuring its temperature stability.

310 High Power Heaters

Heating elements will be required for thermal cycling of the two dewars. The MOS Dewar heater must be of sufficiently high power so that the time to cycle the MOS Dewar meets the specification in the F&PR. Both Ohio State and Florida use kapton sheet heaters from MINCO. They use the Omega C8502 temperature controller. The locations for these heaters should be:

- MOS Dewar: Attached to cylindrical wall
- Camera Dewar: Attached to rounded side facing outer radiation shield

320 Low Power Heaters

The following heating elements will be required:

- Detector mount: located on the heater board

This heater and controller must maintain high temperature stability at the detector.

MMIRS Valve and Heater Interlock Conditions

Draft, Paul Martini December 27, 2004
Released, Brian McLeod April 4, 2005

100 Overview

MMIRS contains two electrically controlled valves. A gate valve (V1) is located between the MOS and Camera sections of the MMIRS instrument and provides a vacuum seal when the MOS section is opened for slit mask exchange. This gate valve is a critical component as the *instrument would be seriously damaged* if the gate valve opens when the MOS section is at atmospheric pressure and the Camera section is under vacuum and at cryogenic temperatures. A second valve (V2) is located outside the turbo pump in the MOS section, and allows the instrument to be backfilled with dry nitrogen. This valve must also be opened when pumping the dewar, as it is located between the turbo and the roughing pump. This document specifies the conditions under which these two valves can be opened.

200 Standard Procedures

The following standard procedures need to be permitted by the interlock system, while preventing the cold Camera dewar from being exposed to atmospheric pressure or outgassing from a warm MOS dewar.

210 Slit Mask Exchange

The slit mask exchange process begins with both dewars cold and under vacuum. First the gate valve is closed, then the MOS heater is turned on. Once the MOS section reaches ambient temperature, the backfill valve is opened and the MOS section is vented with dry nitrogen. At this point the backfill valve (V2) can be closed while the masks are exchanged. Once the masks are exchanged, V2 must be reopened and the MOS chamber pumped out. When the MOS chamber reaches 10^{-5} Torr, V2 is closed, the pump is turned off, and it will be filled with LN2. Once the MOS temperature goes below 200K the gate valve may be reopened. The slit mask exchange procedure is described in more detail in the document “MMIRS Slit Mask Exchange Procedure.”

220 Camera Section Maintenance

To perform maintenance on the Camera Section requires warming both the MOS and Camera sections. If the MOS section is at atmospheric pressure, it must be pumped down to equalize the pressure in the two sections. The gate valve is opened then V2 is opened and both sections are vented with dry nitrogen through V2.

After maintenance, the gate valve is opened if necessary. V2 is opened and pumping begins. When both sections reach 10^{-5} Torr, the gate valve is closed and each section is filled. Once both sections are cold, the gate valve may be reopened. The warmup procedure is described in more detail in the document "MMIRS Warmup Cooldown Procedure."

300 Required Logic

310 Gate Valve (V1)

The required logical conditions to open the gate valve (V1) are:

- $|P_{MOS} - P_{Cam}| < 10$ Torr.

AND

- ($T_{MOS} > 0C$ AND $T_{Cam} > 0C$) OR ($T_{MOS} < 0C$ AND $T_{Cam} < 0C$)

These conditions will only avoid catastrophic failure, in particular damage to the optical elements and the detector. To insure the long-term performance of the instrument, however, there are additional recommendations specified in section 360 below.

No restrictions need to be placed on closing the gate valve.

320 Backfill/pumping Valve (V2)

The required logic to open the vent/pump valve (V2) is

- (V1 Open) AND ($T_{MOS} >= T_{amb}$) AND ($T_{Cam} >= T_{amb}$)

OR

- (V1 Closed) AND ($T_{MOS} >= T_{amb}$)

330 MOS Heater

The MOS heater may only be turned on when V1 is Closed.

340 Camera Heater

The Camera heater may only be turned on when V1 is Closed.

350 Required components

The MOS and Camera sections each require one pressure sensor and one temperature sensor. An air temperature sensor is required and must be located outside the electronics enclosure. The MOS temperature sensor shall be placed in a location which is the last to warm up during the heating process. This is expected to be on the cold baffle. The Camera section sensor shall also be placed in a location which is the last to warm up. This is expected to be near Lens 3. These locations will be confirmed during initial tests.

360 Sensor Failures

The interlock system must be failsafe. In the event of a sensor failure, V1 and V2 must not be enabled. However, it may be necessary to override the interlock to allow replacement of the failed sensor.

370 Additional recommendations:

A dry air purge should always be used to vent the dewar. This minimizes the risk of condensation in the unexpected event that the interior temperature is less than the ambient dew point. It also minimizes the adsorption of water onto aluminum surfaces. After the dry air purge, the instrument should be allowed to sit X minutes to allow a final temperature equilibration. This time period will be determined during initial testing.

In the case of slit mask exchange, the slit and dekker wheels should be placed in the dark position before opening the gate valve. This insures that Lens 3 will be exposed to a relatively cold surface once the gate valve is opened, rather than the significantly higher heat load of the entrance window. This is not a lockout condition, but should be part of the slit mask exchange procedure.

Section XI.

Operations and Maintenance

1. Observing Overview
2. Slit Mask Exchange Procedure
3. Warm Up and Cool Down Procedure
4. Maintenance and Serviceability
5. Shipping and Installation Plans
6. Assembly and Test Plan

MMIRS Observing Overview

Paul Martini
April 4, 2005

100 Overview

The MMIRS instrument has three observational modes: wide-field (7'x7') imaging, longslit spectroscopy (7' slit length) and multislit spectroscopy over most (4'x7' useable, 2'x7' full spectral range) of the imaging field of view. This document describes representative observing sequences for each of these modes, including target acquisition, setup of the guider and wavefront sensor, representative observation sequences, calibration data, required mechanisms for each mode, and estimates of how frequently the mechanisms will be moved.

200 Imaging

MMIRS can obtain broadband *YJHK* images with a 7'x7' field of view. This is the simplest observing mode and requires the fewest mechanisms and mechanism changes. The science goal of the observing scenario discussed here is to detect extremely faint objects in a field with low surface density.

210 Instrument Configuration

The only mechanism that may change during imaging observations is the filter wheel. The remaining mechanisms will be set to the following positions and not changed:

- Slit Wheel: Imaging Aperture
- Dekker Wheel: Imaging Aperture
- Grism Wheel: Imaging Aperture

220 Slew Telescope to Target

The telescope will be slewed to the target coordinates and then a short exposure will be obtained to verify that the telescope is pointed at the correct field.

In the case of a field with few or no bright objects, a pair of dithered, short exposures may be differenced to detect sources fainter than the sky background. In this instance, a short exposure will be obtained, the telescope offset on order 10'', another short exposure with the same integration time will be obtained, and then one exposure will be subtracted from the other. This process is used to remove the bright sky background, which varies substantially from pixel-to-pixel (relative to typical faint targets) due to pixel-scale sensitivity variations in the detector.

230 Setup GWFS

Separate stars for direct guiding and the wavefront sensor now need to be acquired. From the known position of the telescope and existing catalogs of suitable guide stars the coordinates of all candidate stars within the field of view of the guiders are known. One

star will then be selected for each guide camera and the X-Y stages will be moved to place these stars in the centers of their respective detectors.

Once the star for direct guiding is approximately centered on its detector, the guider software will be activated and used to maintain the star at the same position on the guide camera by sending offset commands to the telescope.

The wavefront sensor star will also be centered on its detector using the X-Y stages. In particular, it must be located at the correct position for the WFS aperture. Once the star is correctly positioned, the mirrors and Shack-Hartmann array will be moved into the beam and the WFS software activated.

240 Observations

To mitigate the effect of bright sky emission, bad pixels, and the intrapixel sensitivity of the detector array, imaging observation consist of many short to moderate length exposures (no more than several minutes) separated by small telescope offsets (dithers) of on order 10’’, depending on the image quality on a given night and the characteristic size of the objects under study.

241 Exposure Time

The time between dithers will be on order several minutes, although the detector array may be read several times between dithers, depending on the sky and object flux. For example, if the total time between dithers is chosen to be three minutes (this number can depend on the sky conditions and filter), this time will be divided into several shorter exposures such that the total counts accumulated from the sky (or the brightest science targets) do not exceed the range in which the detector is linear. This sets the time *T* of an individual exposure. *N* exposures will be obtained so that the product *TxN* equals the desired time between dithers.

Each time the telescope is offset or dithered, the guider and WFS X-Y stages have to be moved to exactly compensate for the telescope motion. Note that to maximize observing efficiency, the X-Y stages need to be quite exact so that no new guide star acquisition is necessary. This constraint is not particularly tight, however. The specification for the precision of the X-Y stages is driven instead by dithers in spectroscopic mode, as described below in section 350.

242 Dithers and Macros

Long exposures of very faint objects can require up to several hundred telescope dithers. The dither process will therefore be automated so that the observer can request a set number of dithers, all with the same offset size (although in different directions) and same exposure sequence at each step.

243 Change Filter, Repeat

Additional observations in other filters could then be obtained by changing the filter, calculating the time *T* of an individual exposure (because the sky brightness is different in each filter) and beginning a new dither sequence.

250 Calibration

The calibration data required for imaging are flat field exposures, standard star observations, and potentially dark exposures.

251 Flat Fields

Flat field exposures are used to remove the pixel-to-pixel sensitivity variations of the detector array. Flats are best obtained by observing the twilight sky as will likely provide the most uniform illumination of the detector. To obtain twilight flats, the instrument is configured as above for imaging and the desired filter is selected. At twilight, the telescope will then be slewed to a relatively blank field and a series of exposures will be obtained. The exposure times will be chosen to provide a relatively large number of counts, yet not exceed the linearity range of the detector. The best exposure time will change with time as the sky background darkens/brightens. The telescope will be dithered between these observations to eliminate faint stars when these data are combined. Note that the GWFS will not be used when flat fields are obtained.

252 Standard Stars

Standard stars will be observed in the same manner as the observations described in section 240, although the exposure times will be substantially less and the GWFS will not be necessary.

253 Darks

Dark frames are sometimes acquired to estimate and subtract, if necessary, any background due to the instrument itself. The detector dark current is likely to be completely negligible, although may contain some structure. Darks may not be necessary for MMIRS, although they are easily obtained if desired. To obtain darks, the instrument is configured with the Dekker wheel in the dark position. Exposures of the desired length can then be obtained.

260 Estimates of Mechanism Use

After the instrument is configured for imaging and the GWFS stars have been selected, the only mechanisms that will move are the filter wheel (if there are filter changes) and the guider X-Y stages. The filter wheel will likely move most often when the same field is being observed in multiple filters, such as for standard star observations, although a dither sequence will still require at least several minutes. More typically, the filter wheel will move on order once per hour. The GWFS X-Y stages will move most frequently during short, guided observations and this may correspond to as frequently as every 30 seconds (although in this case it may not be possible to close the loop with the wavefront sensor).

More typically, the telescope with be moved on order every few minutes. Finally, the slide to select the wavefront sensor will be used at the beginning and end of the observations of each field. Estimates for mechanism use in imaging mode are summarized in Table 1 below.

Table 1: Estimated Mechanism Use in Imaging Mode

Mechanism	Most Frequent [min]	Typical [min]
Filter Wheel	1	60
X-Y Guider	0.5	2
WFS Select	10	60

300 Long Slit Spectroscopy

MMIRS can obtain spectroscopy with a 7' long slit. A range of slit widths are provided and all can be used with either the *J*, *H*, or *K* moderate-resolution grisms, and either of the *J+H* or *H+K* low-resolution grisms. The science goal of the observing scenario discussed here is to obtain a spectrum of a small (relative to the slit length), faint object.

310 Instrument Configuration

All of the mechanisms in MMIRS will be moved when the spectroscopic mode is used. The initial configuration, however, will be the same as above for imaging mode. Imaging mode will be used to confirm, as described above in section 220, that the telescope is pointing at the correct target. Once the target is ready for spectroscopic observations, the Slit wheel, Dekker wheel, grism wheel, and perhaps the filter wheel will need to move to switch from imaging to spectroscopic mode.

320 Slew Telescope to Target

The telescope will be slewed and the target verified exactly as described above in section 220 for imaging observations. A small offset should be used to crudely position the target near the center of the detector. The instrument may be rotated if a specific slit angle is desired for the science observations.

330 Setup GWFS

The setup is identical to that described in Section 230 above.

340 Position Target on Slit

Once the GWFS has been set up, sufficiently accurate and precision telescope motions should be possible to place the target on the slit in one or at most two iterations. The exact position of the slit image relative to the detector should already be known, so the relative position of the target and the slit center (in pixels) can be used to offset the target directly to the slit. Once the target is located at a pixel position corresponding the slit center the slit wheel and Dekker wheel will be moved to place the desired slit and the Dekker long slit aperture in the science beam. Now another exposure will be obtained to verify that the target is in fact centered on the slit. If the target is faint, two exposures may be necessary in a manner similar to that outlined above in section 220. However, in this case the offset should be parallel to the long axis of the slit. If the target does not appear to be perfectly centered on the slit, small additional offsets may be necessary. Once the target is centered on the slit, the grism wheel and perhaps the filter wheel will be moved to finish preparations for spectroscopic mode. The filter wheel will only need

to be changed if either the *J+H* or *H+K* grism will be used, as likely one of the broadband (*JHK*) filters will be used to position the target on the slit.

350 Observations

Once the instrument has been configured for the desired spectroscopic mode, the observations can begin. Often this will entail observations of the target at multiple positions along the slit. Bad pixels, fringing, and accurate sky subtraction are the main motivations for dithering the target along the slit.

310 Exposure Times

Typically the observations will be of relatively faint targets and therefore require up to hours of total exposure time. The length of individual exposures will depend on the sky subtraction algorithm and the brightness of the OH airglow lines. Assuming that a 2-D model of the sky can be computed for each observation, the main limitation on the length of an exposure will be when the OH airglow lines approach the nonlinear regime of the detector, at least at wavelengths were accurate sky subtraction is desired. If this occurs, modeling and subtracting the sky lines will be more difficult. This may occur in approximately ten minutes for the brightest lines and in practice will depend on the slit width.

320 Dithering along the Slit

As for imaging, the size of the dither step should be several times the characteristic size of the object and the X-Y stages of the GWFS will need to move to exactly compensate for the telescope offset. Note that because of the narrow width of the slits, the precision of the telescope and GWFS offsets are critical.

360 Calibration

The calibration data required for spectroscopy are a reasonably featureless hot star to correct for (variable) telluric absorption, a flux standard (which may be identical to the hot star), flat fields, wavelength calibrations, and images of the slits on the detector. Flat fields and wavelength calibration frames may be desired at the exact same telescope orientation as the observations.

361 Correction for Telluric Absorption

The atmosphere in the near-infrared region is riddled with absorption bands, primarily due to water. These bands are largely unresolved at the resolution(s) of MMIRS and they also vary in strength with time and position on the sky. To obtain the best telluric correction, a hot star should be observed once every half hour and as close to the object position as possible (within approximately 10 degrees and 0.1 in airmass). Note that in practice this is quite difficult to achieve, especially once the overhead associated with setting up spectroscopic observations is taken into account. Once selected, the observations of these standards are identical to the observations described above, although the exposure times are typically much shorter. Unlike in imaging mode, these calibration frames will likely require use at least the guider. The wavefront sensor is not likely to be needed.

362 Flux Standard

Flux standards are used to place spectroscopic observations on a relative or absolute flux scale. These observations are identical to those described above for the telluric correction, and in some cases one of the telluric correction stars may also serve as a flux standard. Unlike the telluric correction, only one flux standard is likely to be observed in a given night.

363 Flat Fields

As for imaging, spectroscopic flat field exposures are used to remove the pixel-to-pixel sensitivity variations of the detector array. However, unlike in imaging, the flat fields have several sources of pixel-to-pixel variation that arise on a range of scales on the detector. The main two are fringing in the detector itself (discussed in a separate document) and variations in the slit width. Properly correcting for fringing requires observations of a uniform illumination source with the same instrument orientation (to minimize differences in flexure) as the science observations. These observations will be obtained by placing the diffuser in the Dekker wheel and illuminating it with a quartz lamp. These observations should only require several minutes. The GWFS will not be used while the flatfields are obtained. There will also be a variation in the transmission of the slit itself due to variation in the slit width due to mechanical imperfections. This variation in transmission can be removed with the same flat field obtained for the fringing correction. Finally, there is a large-scale variation in the grism transmission itself (blaze function), although this can be removed with the flux standard observation.

364 Wavelength Calibrations

For all sufficiently long spectroscopic exposures (likely on order a minute or longer), the OH airglow lines themselves can be used for wavelength calibration. Short exposures, such as the telluric correction and flux calibration, will need to use observations of calibration lamps to calculate the dispersion solution. These lamp exposures will be obtained with the GWFS inactive and with the instrument at the same orientation as the observations to minimize the effect of flexure.

365 Slit Images

Observations during daylight of all of the spectroscopic slits that will be used during the night will be valuable to exactly predetermine where a given slit’s image falls on the detector.

370 Estimates of Mechanism Use

Spectroscopic mode heavily uses most of the mechanisms in MMIRS. A typical, conservative estimate of mechanism use is for a 30 minute observation of a faint target split into 3 dithered, ten minute exposures. This observation would start with the instrument in imaging mode, movement of the GWFS stages to acquire stars, and then the slit wheel, Dekker wheel, grism wheel, and filter wheels would be moved to change into spectroscopic mode. There are then on two telescope/GWFS offsets with ten minute separations. This observation would then be followed by a flatfield exposure (Dekker wheel motion, GWFS off). Observation of a telluric correction star provides an estimate

of heavy mechanisms usage. As above, the setup requires motion of all of the mechanisms, although the dithers are only on order ten seconds apart. While the guider will need to be active during these observations, the wavefront sensors will not. The estimates for mechanism use in spectroscopic mode are summarized in Table 2.

Table 2: Estimated Mechanism Use in Longslit Mode

Mechanism	Most Frequent [min]	Typical [min]
Slit Wheel	1	30
Dekker Wheel	1	30
Filter Wheel	1	30
Grism Wheel	1	30
X-Y Guider	0.2	10
WFS Select	5	30

400 Multislit Spectroscopy

The multislit mode of MMIRS allows slit placement over a 4'x7' field, although complete wavelength coverage can only be obtained for the central 2'x7'. This option is similar to the longslit mode described in section 300, except that the alignment process is more critical and thus may require additional iterations with the telescope/GWFS X-Y stages. The science goal of the observation discussed here is to obtain spectroscopy of many faint objects.

410 Instrument Configuration

The initial configuration for multislit spectroscopy is identical to the configuration described in section 310 for longslit spectroscopy.

420 Slew Telescope to Target

The telescope will be slewed and the target verified exactly as described above in section 220 for imaging observations. A small offset should be used to crudely position the target near the center of the detector. In addition, the instrument will need to be rotated to the position angle of the multislit mask.

430 Setup GWFS

This setup is identical to that described in Section 230 above.

440 Mask Alignment

Mask alignment is similar to the alignment of a single object on the longslit, although because rotation is critical as well this step will likely require one or two additional iterations.

441 Initial Offset and Rotation

The first iteration for mask alignment will require an image of the field and an image of the slit mask, where the later was presumably obtained during the day or in twilight. The slit mask will typically contain three to five alignment stars and software will be used to

measure the centers of the alignment boxes in the slitmask image and the centers of the stars in an image of the field. These data will be used to calculate the position offset and rotation necessary to place the alignment stars at the centers of the boxes and thereby the objects in their slits. The GWFS X-Y stages will then move to compensate for the telescope motions. Depending on the precision of the offsets and rotations, a second iteration may be necessary to insure that the alignment stars are coincident with all of the boxes. Once this has been confirmed, the slit mask and Dekker wheels will be moved into position.

442 Final Mask Alignment

Now that the slit mask is in the optical path, a second observation of the field will be obtained to determine that the alignment stars fall in their boxes and perform an additional iteration with the telescope. This will be necessary for a number of reasons: the mask image was obtained when the MOS temperature was still equilibrating, the slit mask wheel repeatability is not perfect, and because the initial alignment offsets and rotations were not of the necessary precision. The image just obtained through the slit mask will now be used to determine the centers of the alignment boxes and the positions of the stars in these boxes will be used to calculate new offsets and rotations. This step should only require one iteration before spectroscopic observations can begin.

450 Observations

The grism (and perhaps filter) wheel will now be moved into place to begin spectroscopic observations. The considerations for exposure time and dithering are similar to those discussed above in section 350 for longslit mode. Dithering along the slits in a multislit mask may provide to be quite challenging, and also would reduce the number of individual slits in the mask, so it may be that a 2-D sky model will be generated instead. If the observations are not dithered, then the GWFS X-Y stages do not need to be moved and instead multiple exposures at the exact same telescope position will be obtained.

460 Calibrations

The calibrations required for multislit spectroscopy are identical to those described above for longslit spectroscopy in section 360. Note that telluric and flux standard observations can be obtained through one of the slits in the multislit mask to minimize the number of modes that require calibration data.

470 Estimates of Mechanism Use

The estimates of mechanism use for longslit spectroscopy in Table 2 are also reasonable estimates for multislit spectroscopy.

MMIRS Slit Mask Exchange Procedure

Paul Martini
April 25, 2005

Overview

The MMIRS instrument has slit masks cooled to cryogenic temperatures in a separate dewar (hereafter the MOS section) that is smaller than the main dewar (hereafter the Camera section). The MOS section is smaller and separate so that slit masks may be exchanged during daylight and with time to spare to obtain calibration data. The goal is for the slit mask exchange procedure to last no longer than eight hours. The mask exchange procedure involves warming up the MOS section, exposing it to atmospheric pressure, exchanging the slit masks, pumping it out, and cooling the slit masks back to cryogenic temperatures. This document describes the slit mask exchange procedure in detail. The current time estimate is eight hours.

Procedure

The entire exchange procedure is currently estimated to require eight hours, which does not include time for calibration exposures. If possible, the procedure should be shortened further to allow more time for calibration exposures and to give the observatory staff more leeway on exactly when they exchange slit masks. This procedure may either be performed exclusively by the observatory staff, or begun by the observer (or telescope operator) and completed by the daytime staff. It is expected that MMIRS will be mounted on the telescope for this procedure.

1 Close Gate Valve [0 minutes]

The gate valve will be closed through the instrument's user interface. This operation may be performed by the observer, the telescope operator, or another member of the observatory staff. Once the gate valve is closed it shall be impossible to open the gate valve again unless the interlock conditions are met. These conditions are described in the document "MMIRS Valve and Heater Interlock Conditions." The Dekkar wheel shall be placed in the dark position.

2 Activate MOS heaters [120 minutes]

The MOS heaters shall be activated by a button on the instrument's user interface. This activation should require additional confirmation (see also the interlock conditions). The MOS heaters shall warm up the MOS section until they are at the ambient temperature. The MOS heaters shall turn off automatically when this temperature is reached. This shall be accomplished through the use of an autotuning temperature controller, which shall have a temperature sensor attached to the MOS LN2 vessel

Note: Activation of the MOS heaters will likely be the last part of this procedure performed by either the observer or the telescope operator. In principle the MOS heaters may be activated as soon as the gate valve is closed

3 Introduce dry air to MOS [30 minutes]

It is important that no condensation occur within the MOS section, which would happen if the MOS is exposed to humid air when some of the interior is still colder than the dew point. Lens 2 is particularly crucial in this respect. Introduction of dry air will facilitate rapid equilibration of the interior temperatures through conductive heating. This step requires the availability of a dry air supply at both telescopes. The dry air feed shall be connected to the vacuum pumping port of the MOS section.

4 Disable Remote MOS Mechanism Control [0 minutes]

Remote control of the Slit and Dekker wheels shall be disabled by flipping a toggle switch next to the MOS access panel. Flipping this switch shall also activate a neighboring “wheel advance” button to facilitate slit mask exchange (see #6 below) and reset the software table of mask IDs and slit positions.

5 Open MOS access panel [10 minutes]

The MOS access panel shall be opened by removing the bolts around the MOS access panel. A bolt driver of the proper size shall be attached by a cable to the instrument electronics racks (so it is not lost) and have a small holster for storage in the electronics racks (similar to the bar code reader mentioned in #7).

6 Exchange Slit Masks [20 minutes]

The wheel advance button shall be used to advance the slit mask wheel until the first slit mask is centered in the MOS access panel. Each slit mask is mounted in a mask holder, which shall be unclamped and clamped with fasteners integrated into the wheel and plate assembly. After a slit mask has been exchanged, this process shall be repeated until all of the new masks are placed in the instrument.

Note 1: This step assumes that the new set of slit masks have already been mounted into their holders. This may be done either by the observer or the observatory staff and assumes the existence of at least two complete sets of mask holders. If no new mask needs to be loaded into a given position, an empty holder shall be loaded to maintain the balance of the wheel.

Note 2: During assembly and testing, we will determine if a blank mask must be loaded into the holder in order to maintain the balance of the wheel.

Note 3: The dry air purge could remain on under humid conditions to insure a positive pressure of dry air inside the MOS section during the slit mask exchange process.

7 Record Mask IDs [10 minutes]

The barcode reader and associated software shall be used to read and record the ID of each slit mask in the wheel. The wheel advance button shall be used to advance the wheel to each of the slit mask positions. To insure that all of the slit masks in the wheel are known (and correct) all of the slit mask positions should be scanned at this step, regardless of whether or not all of the slit masks were exchanged. This information

should then be automatically updated on the instrument control software so that the current mask configuration may be easily checked (again) against the observer's request when the mechanisms are exercised (see #10).

Note: For empty slit mask holders, a special bar code will be required so that these positions may be specifically flagged as empty. This bar code may be printed on the outside of the instrument, or some other convenient place.

8 Close MOS access panel [10 minutes]

The MOS access cover shall be bolted back into place. Care shall be taken to insure that the O-ring is properly seated.

9 Enable Remote MOS Mechanism Control [0 minutes]

The switch next to the MOS access panel shall be toggled to return remote control of the MOS mechanisms to the instrument control GUI and disable the wheel advance button.

10 Exercise MOS Mechanisms [10 minutes]

The Slit and Dekker wheels shall be briefly exercised to insure that both wheels are functioning properly and to double check that the proper masks are loaded into the wheel. The Dekkar wheel shall be placed into the dark position.

11 Pump Out MOS Dewar [30 minutes]

The vacuum pumps for the MOS section shall be activated until the target pressure is achieved.

12 Cool MOS Dewar [240 minutes]

LN2 shall be used to fill the MOS LN2 vessel and cool the MOS section to its operating temperature.

13 Open Gate Valve [0 minutes]

The gate valve shall be opened by pressing a button on the instrument control interface, provided the interlock conditions have been met. At this point the instrument should be ready for the observer to take calibration data.

Calibration Frames

Once the gate valve has been opened the observer will likely obtain images of each mask for alignment purposes as well as arc and flat exposures for quick-look calibration during the night.

MMIRS Warm Up and Cool Down Procedure

Paul Martini
April 25, 2005

Overview

This document describes the steps required to warm up and cool down the MMIRS instrument. The MMIRS instrument is divided into two sections. The first is a smaller section (hereafter the MOS section), which contains the corrector optics and the Slitmask and Dekker wheels. The second, larger section (hereafter the Camera section) contains the camera and collimator optics, the grism and filter wheels, and the detector. These two sections can be hermetically separated with a gate valve. The MOS section will be warmed up and cooled down on a regular basis, a procedure which will require on order eight hours total. The Camera section will require substantially longer as both the optics and the detector are very sensitive to thermal shocks and therefore should not be exposed to a gradient of greater than 0.1K/minute. As the operating temperature is 77K (220K below ambient), the fastest warm up and cool down time is therefore approximately 37 hours. In practice the warm up and cool down may require up to twice as long.

This document only describes the warm up and the cool down procedure for the entire instrument. The warm up and cool down procedure for the MOS section alone is described in the document “MMIRS Slit Mask Exchange Procedure”. As MMIRS will require over a day to warm up or cool down, it is assumed that MMIRS will be mounted on its handling cart, and not the telescope, during the warm up and cool down procedures.

Warm Up Procedure

The assumed starting point for the warm up procedure is that MMIRS has just been removed from the telescope after a night of observing and moved to a work area. Prior to removal from the telescope, MMIRS may be oriented to dump the remaining LN2 in the MOS and Camera sections.

1 Close Gate Valve

The gate valve between the MOS and Camera sections shall be closed. This may be done prior to removal from the telescope.

2 Activate Heaters

The MOS and Camera section heaters shall be activated to warm up the instrument. The Camera section heater shall be connected to the designated temperature sensor (described in the document MMIRS Temperature Sensing and Heating Requirements) in an active control loop to insure that the warm up rate for the Camera section will not exceed the maximum rate prescribed above. There are no specific restrictions on the warm up rate for the MOS section. Once the temperature sensors in each section are equal to the ambient temperature value, the heaters shall shut off automatically.

3 Open Gate Valve

Once both the Camera and MOS sections reach the ambient temperature the gate valve between them shall be opened.

4 Dry Air Fill

MMIRS should be filled with dry air (assumed to also be at the ambient temperature) via the vacuum port. A pressure gauge shall be used to insure the instrument is backfilled to ambient pressure. This fill will insure that all surfaces inside the instrument are sufficiently warm so that no condensation occurs when the instrument is exposed to ambient conditions.

5 Open to Ambient Conditions

After MMIRS has had time to come into equilibrium with the dry air fill, which should require on order 30 minutes, the instrument may be exposed to ambient conditions.

Cool Down Procedure

The cool down procedure is expected to start immediately after the instrument has been sealed. At the start of the cool down procedure it is assumed that the gate valve is open. The final cover to be installed on the MOS section is the MOS access panel. The final steps for sealing the Camera section will be installation of the main radiation shield and the outer vacuum case.

The instrument is assumed to be oriented horizontally on its cart with the V-block above the optical bench. The electronics racks are unlikely to be mounted on the instrument itself, but will be properly cabled and powered on so that the temperatures and pressures may be monitored during the cool down procedure.

1 Vacuum Pump

The instrument will be pumped via the port on the MOS section. The camera section will therefore be evacuated via the MOS section. MMIRS shall typically be pumped to a pressure of 10^{-5} Torr.

2 Close Gate Valve

The gate valve shall be closed so that the potentially much more rapid cool down of the MOS section does not affect the Camera section, particularly lens 3.

3 Camera Section LN2 Fill

The Camera Section will be cooled no faster than the maximum rate specified above. This is the maximum rate as measured by a temperature sensor on the top surface of the optical bench (see the document MMIRS Temperature and Sensing Requirements), the surface to which the VEE blocks and detector are mounted. The rate of LN2 supply will be controlled by a Cryogenic Valve connected via a feedback loop to the temperature sensor. This feedback loop will open and close automatically to control the LN2 rate per

minute and be designed to insure that the cool down rate does not exceed the maximum rate.

4 Notes on Potential Software

Two large LN2 supply dewars will be required to complete the Camera section cool down. When the tanks are swapped, the feedback control loop will likely need to be reset. The details of this procedure will be determined during initial cool down tests and may require specific software.

During the cool down two specific conditions will arise that may require automatically shutting down the Cryogenic Valve. These are the above condition when the external tank is empty and the case when the instrument is completely full, yet not at the set temperature. A stop condition for the autofill will be explored during integration and testing.

5 MOS Section LN2 Fill

LN2 shall be added to the MOS section. No restrictions are placed on the MOS section cool down rate.

MMIRS MAINTENANCE AND SERVICEABILITY

Paul Martini
May 2, 2005

100 Introduction

This document presents an outline of the maintenance and servicing plan for the MMIRS instrument and in particular is intended to address the specifications laid out in sections 820 – 850 of the MMIRS Functional and Performance Requirements (F&P) document (S-MMIRS-200). If there are any discrepancies between this document and the F&P, the F&P shall prevail.

200 Maintenance

MMIRS has been designed for a minimum of regular maintenance by the observatory staffs, both through a careful integration and test plan prior to commissioning and the use of instrument monitors to diagnose potential problems early. Demand on the time of the observatory staff will also be lessened by an autofill system, which shall be used to provide LN2 when MMIRS is not mounted on the telescope, and by a computer-controlled warm up and cool down system, as this procedure requires approximately 36 hours.

The mode of MMIRS that will require the most observatory staff support is the MOS mode, which shall require cutting slit masks, warming up the MOS Section, exchanging slit masks, and cooling down the MOS Section. This procedure is described in detail in “MMIRS Slit Mask Exchange Procedure.” The next subsections outline the expected maintenance that will be requested of observatory staff, as well as an outline of the plan to provide suitable training and documentation.

210 Routine Maintenance

MMIRS will require several, regular maintenance tasks and servicing by local observatory staff. These actions will include:

Daily filling of the MOS and Camera Sections with LN2 [when on telescope]
Monitoring the Autofill System [when off telescope]
Cutting MOS Masks
Slit Mask Exchange
Installation on and Removal from the Telescope

220 Training

An introduction shall be provided to the observatory staff during the commissioning runs at each observatory. In any event, some assistance by the observatory staff will be essential for the assembly and disassembly of MMIRS at each facility and this will provide an excellent opportunity to explain the instrument at the system level.

Training will be provided for all of the tasks outlined in the Routine Maintenance section above. Training, documentation, and spares will also be provided to handle expected failure scenarios. These are described further in the section on “Failure Scenarios” below.

230 Instrument Team Participation

MMIRS will require the presence of one or more members of the instrument team during the first few visits to each observatory, both for assembly and disassembly as well as troubleshooting and streamlining operations. The instrument team's presence is expected to be particularly necessary during assembly, initial installation on the telescope, and disassembly prior to shipping. After several iterations of assembly and disassembly, the need for the presence of members of the instrument team will be reevaluated.

240 Specialized Maintenance

Other maintenance tasks for MMIRS may include filter and grism changes, as well as repair or replacement of the temperature sensors inside the Dewar. These operations will require the presence of the instrument team, but as they are not time critical they can be performed before or after the instrument is shipped between observatories.

300 Reliability

MMIRS has been designed for reliability, including by selection of mechanical components from known and recommended vendors (including cryo-rated components were appropriate). Reliability is particularly important for components inside the Dewar as these components will require at least one week for repair (see the section on Major Failures below). The most critical components inside the Dewar are the Phytron motors, as they are not static and are required for regular operations. However, these motors are quite robust. They are rated for over four million revolutions, which is over an order of magnitude more than expected for the specified ten-year lifetime. Another critical area is the integrity of the vacuum vessels, particularly the areas around the LN2 fill ports. This will require monitoring of the pressure inside the Dewar and care that the O-rings in the vicinity of the fill ports are not frozen and damaged through contact with LN2.

400 Lifetime

The F&P specifies that MMIRS shall be designed for a lifetime of ten years without a major overhaul and the current design is expected to meet this requirement. The components inside the Dewar that are most likely to require maintenance during a major overhaul are the motors and micro-switches, although during a major overhaul the mechanisms would be lubricated again. The MMIRS components outside of the Dewar can be readily swapped during dark time or when MMIRS is being (dis)assembled for shipment between the two observatories. Replacement of these components is therefore not considered to constitute a major overhaul.

500 Failure Scenarios

The amount of effort and time lost to repair a failure will depend on whether or not the instrument must be warmed up in order for the failure to be repaired. Failures that do not require opening the instrument will be termed minor failures, while those that do will be termed major failures.

510 Minor Failures

Minor failures are failures of components outside of the Dewar that can easily be replaced and therefore should cause the loss of no more than one night of observing time. Several of the most likely sources of failure are:

Power Supply
Electronics Board
Cable
Computer
GWFS Stage

These types of failures could be addressed by the local staff, perhaps after phone consultation with the appropriate member of the instrument team. Spares for these components will be provided, as well as suitable documentation and training for the most common scenarios.

520 Major Failures

Major failures are defined to be failures that occur inside the instrument, and consequently will require thermally cycling the instrument and the travel of members of the instrument team to the observatory. Repair of a major failure will require approximately one week. An example is the failure the Grism Wheel motor in the next subsection.

521 Filter Wheel Motor Failure

A motor failure is most likely to occur during the night, since that is when the motors experience the most use. Once a motor failure has been diagnosed, the PI shall be called for consultation and a confirmation that opening the instrument is the only remedy for the problem. This may require consultation with several other members of the instrument team and therefore a final decision to warm up the instrument may wait until the following morning. Once the decision has been made to open the instrument, MMIRS should be removed from the telescope and the warm up procedure begun. As the warm up procedure requires at least 36 hours, members of the instrument team should be able to travel to either observatory before the warm up is complete. The warm up procedure is described in “MMIRS Warm Up and Cool Down Procedure.” Once the instrument is warm and backfilled with dry air, the instrument may be opened for repair. This will involve disconnecting the detector electronics, removing the vacuum housing of the Camera Section, and then removing the radiation shield. All of the motors will then be accessible and can be readily exchanged. After tests of the new motor, the instrument can be pumped out and cooled down again.

530 Catastrophic Failures

Catastrophic failures are defined to be failures which put the instrument out of service for at least six months. The two major sources of catastrophic failure are failure of the infrared array detector and failure of one or more optical elements. Both of these catastrophic failure scenarios will require long lead-time replacements.

Section XI.5

Shipping and Installation Plans

This document will be available at the CDR.

MMIRS Assembly and Test Plan

Paul Martini, Brian McLeod
April 25, 2005

Overview

This document outlines the assembly and test plan for the MMIRS instrument. The details of these tests are or will be described in other documents. The purpose of this document is to present the overall plan for the assembly and testing of various components and to note the requirements of each step. This plan has been divided into three sections: minor component tests, major component tests, and system integration. Within these broad sections, the individual tests are in approximately chronological order, although subsets of the minor and major component tests can be carried out in parallel. Many of the minor component tests are already underway and are meant to establish the operation and performance of key (though small in size) components, as well as to establish software control of these components. The major component tests are centered on the initial assembly of three physically large, yet somewhat separable components: the MOS section, the Camera section, and the Electronics Racks. The system integration tests involve the final assembly and verification of the entire instrument.

Minor Component Tests

These are tests of individual components that will be performed prior to their integration into the MMIRS structure, particularly into the MOS and Camera sections.

Motor

This will verify that the software can control a motor. The required components are a motor and the corresponding electronics and software. This test has been completed.

Cold Motor

This will verify the performance of the motors under vacuum and cryogenic conditions. The required components are John Geary's small dewar, a motor, and software.

Gate Valve Mechanism

This will verify software and hardware control of the gate valve. The required components are the gate valve, motor, and associated software and electronics.

Cryogenic Valve

This will verify proper operation of the cryogenic solenoid valve and how well the cool down rate of the test dewar can be controlled by the Omega Temperature Controller. The required components are the detector test dewar, the cryogenic valve, and the Omega Temperature Controller.

Detector Mount Thermal Behavior

This will verify and measure the thermal behavior of the detector mount during cool down. The required components are the detector mount, the LakeShore Temperature Monitor, associated thermal sensors, and the detector test dewar. Only a Hawaii-2 chip carrier will be installed for this test.

Detector Mount Slide

This will verify the operation of the detector slide and the LVDT. The test will be performed with the detector mount and slide in the detector test dewar at 77K. The required components are the detector mount (and slide), LVDT, and the test dewar.

Detector Electronics

This will verify the detector readout electronics. The required components are the detector mount, detector electronics, the test dewar, and an engineering-grade array. Once performance is verified with the engineering-grade array, the science array will be installed and characterized.

Guide Camera Electronics

This will verify the guide camera readout electronics. The required components are a guide camera and the associated readout electronics and software.

Guide Camera Mechanisms

This will verify the operation of the guide camera X-Y-Z stages and the WF-select slide. Required components are a complete guider camera and associated mechanisms, control electronics, and software.

Major Components

These tests are intended to verify the performance of the larger components before the instrument is assembled into its final form, particularly before the electronics racks are fully populated and cabled, and before the MOS and Camera sections are mated. The MOS and Camera section tests can in principle be performed in parallel.

Corrector Lens Alignment

This will verify that lenses 1 and 2 have been correctly installed. The positions of the lenses will be measured with the measuring machine.

MOS Section Vacuum Integrity

This will verify that the MOS section is properly sealed. A flat plate will be required to seal the bottom of the MOS section (in place of the bulkhead provided by the top of the Camera section). The vacuum system will be required for this test.

MOS Section Thermal Cycle

The MOS section shall be thermally cycled to verify the gross thermal behavior and the operation of the thermal sensors and heaters. The LakeShore temperature monitor and associated thermal sensors (and wiring) are required for this test.

Slit and Dekker Wheel Mechanisms

This will test control of the slit and dekker wheels and the detent repeatability. The slit and dekker wheels will need to be balanced and installed in the MOS section prior to this test. An alignment telescope will be used for the repeatability test. Note that this is a warm test.

Slit Wheel Alignment

This will verify that the slit wheel is in the focal plane. This test will require pressurizing the LN2 vessel of the MOS section to mimic the pressure differential of regular operations. The slit wheel will be populated with empty slit mask holders. The co-planarity of the slit mask and the MOS mounting surface will be measured with lasers and mirrors.

Camera Section Vacuum Integrity

This will verify that the Camera Section is properly sealed. The gate valve must be installed for this test. No components will be installed on the optical bench.

Camera Section Thermal Cycle

The Camera section shall be thermally cycled to verify gross thermal behavior and the operation of the thermal sensors, heaters.

Optical Bench Flexure

This will test flexure of the optical bench supported by the G10 ring. The weight and moment of the final components will be mimicked with a counterweight attached to the bench and the Camera section shall be rotated to a range of orientations. The angle between the bulkhead and the surface of the optical bench at each orientation shall be measured with a laser mounted on the bench and a mirror on the bulkhead. This test should be performed before any mechanisms are installed on the optical bench.

VEE Block and Optics Barrel Alignment

The VEE blocks shall be attached to the optical bench using reference surfaces machined into the optical bench.

Grism and Filter Wheel Mechanisms

This will be a warm test of the filter and grism wheels and the associated software. The filter and grism wheels will need to be balanced and installed in the Camera section prior to this test. The motors, cables, and control software will also be required.

Detector Slide

This will be a warm test of the motion and control of the detector slide on the optical bench with the final electronics and cables.

Camera Section Thermal Characterization

The Camera section shall be thermally cycled with the cryogenic valve to verify that the cool down and warm up procedure can produce a rate of 0.1 K/minute. Thermal sensors

on the camera barrel (including dummy lenses), collimator barrel, and the center of the detector socket shall be used to characterize the thermal behavior of the Camera section.

Electronics Racks Power Dissipation and Safety Conditions

This will test the insulation and thermal control of the two electronics racks. In particular, the temperature monitors, heat exchanger, and safety shutdown conditions will be tested. The racks should be fully populated (or at least with the components which dissipate 90% of the anticipated power). Both of the heat exchanger units should be tested.

Guider/WFS Alignment

This will determine the alignment and operation of the Guider/WFS mounted on the MOS Section and that the CCD cameras and the slit mask plane share the same focal surface. *The details of this test are under development.*

Slit Mask Exchange

This will verify the entire slit mask exchange procedure (with the exception of opening and closing the gate valve). This test includes a cold test of the Slit and Dekker wheel motions.

Optics Positioning

The lenses shall be integrated into the collimator and camera barrels and their positions verified with the CMM.

System Integration

These tests will verify the final integration of the entire system and will be performed once the MOS and Camera sections have been integrated and the electronics racks fully populated with their components. At this stage the instrument shall be placed on its cart.

Valve and Interlock

This test will involve pumping out the entire, mated instrument and verifying the gate valve seal and the interlock conditions for the gate and vacuum valves.

Penultimate Thermal Cycle

This test will involve a complete thermal cycle of the entire instrument, except without the detector and optics barrels installed. Temperature sensors shall be used to measure the cool down and warm up rates of the optics barrels and the detector mount. The alignment of the slit mask wheel, VEE blocks, and detector mount shall be verified. All of the mechanisms shall be exercised.

Ultimate Thermal Cycle

This test will involve pumping out the entire, mated instrument with the optics and detector installed. This test will verify the optical alignment.

Section XII.

Management

1. MMIRS Project Schedule
2. MMIRS Integration & Test Flow Chart
3. Status of PDR Action Items
4. Known/Open Issues

MMIRS Project Schedule

ID	Task Name
1	**Major Milestones**
2	Critical Design Review (CDR)
3	Pre-Ship Review
4	Ship to MMT
5	First Light
6	**Detector**
7	Engineering Prototype Test Complete at MMT
8	**Detector Electronics**
9	Design boards rev 1 (32 channel) - SWIRC
10	Manufacture boards rev 1 - SWIRC
11	Test multiplexer rev 1 - SWIRC
12	Test Engineering Array - SWIRC
13	Test 32 Channel SWIRC at MMT
14	Final Board Design
15	Manufacture final boards & cables
16	Cryo Test Chip Carrier
17	Cryo Test Multiplexer
18	**Detector - Rack Electronics**
23	**Focus/Detector Slide**
24	Receive and Review Detector Mount Design from U of F
25	Focus Slide Detail Design
26	Internal Cabling/Interconnect Design
27	Procure Focus/Detector Slide Components
28	Procure/Fabricate Cables
29	Assemble Focus Slide - Warm - Without Array
30	Test Focus Slide - Warm - Without Array
31	Test Slide - Cryo/Vac - Without Array
32	**Detector Preamp Packaging**
33	Design Preamp Packaging & PCB
34	Procure Components
35	Fabricate PCB
36	Assemble & Test Components
37	**Detector - Science Array & Slide Integration**
38	Assemble Slide, Detector Elecronics & Engineering Array
39	Cryo Test Assembly - with Engineering Array
40	Assemble Slide, Detector Electronics & Science Array
41	Test with Science Array - Warm
42	Cryo Test with Science Array
43	Detector Performance Evaluation
44	**Optics**
45	**Lenses**
46	Complete Preliminary Lens Design
47	Generate Specs
48	Generate Warm Optic Calculations/Specifications
49	Generate Drawings
50	Prepare RFQ
51	RFQ Submitted to Vendors
52	Vendor Selection
53	Phase I Optic Procurement (S-FTM16 Blanks)
54	Receive S-FTM16 Melt Data
55	Review Vendor Test Plate Data
56	Update Optics Design
57	Issue Contract
58	Optic Procurement - Post Test Plate
59	Optic Acceptance Test/Inspection
60	**Grisms**
61	Complete Design

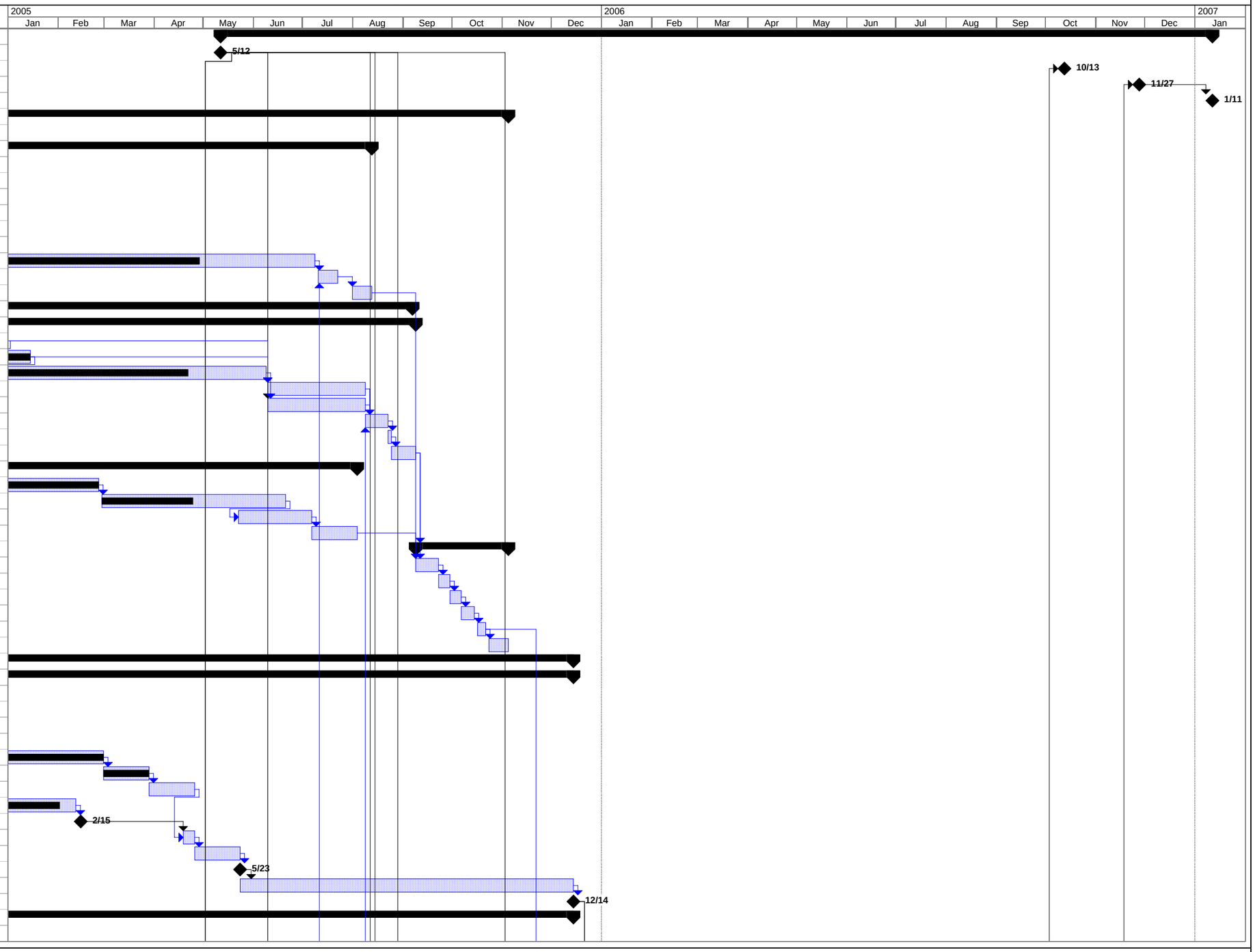

MMIRS Project
CDR Data Package Copy

Task Progress Summary External Tasks Deadline
Split Milestone Project Summary External Milestone

MMIRS Project Schedule

ID	Task Name
62	Generate Specs
63	Generate Drawings
64	Prepare RFQ
65	RFQ Submitted to Vendors
66	Vendor Selection
67	Procure Grism
68	Grism Acceptance Test/Inspection
69	**Filters**
70	Generate Spec Agreements with Consortium
71	Consortium RFQ
72	Procure Filters
73	Filter Acceptance Test/Inspection
74	**Software**
75	**Motor Control Software**
76	Investigate UMAC S/W Requirements
77	Develop Test Support S/W for Motor Control
78	Motor Control & Drive SW Ready for Test Support
79	Write UMAC toolkit
80	**Release Milestones**
81	Rel 1 - SCI Cam Serv 1, Therm Vac Serv 1
82	Rel 2 - Eng GUI, Mot Cntrl Serv 1, WFS/G Serv, Therm Vac Serv 2
83	Rel 3 - Mot Cntrl Serv 2, Rack Mon, Barcode, Pwr Cntrl
84	Rel 4 - Integ SCI Cam Serv, Obs GUI, Cryo Ops GUI, GuideServ GUI
85	Rel 5 - Planning GUI, GSTARS
86	**Electronics**
87	Design Complete
88	System Block Diagram and Interconnect Complete
89	**Electronics Rack/Packaging**
90	Receive U of F Rack Design
91	Design MMIRS Electronics Rack/Package & Internal Cabling
92	Fabrication Drawings
93	Procure Components
94	Fab & Assemble Components
95	Fab & Assemble Internal Cables
96	Assemble/Test of Rack Components and Cabling
97	**Interconnect Cabling**
98	Detail Design of Interconnect Cabling
99	Procure Components
100	Fab & Assemble Interconnect Cabling
101	Bakeout of Cables for Vacuum Use
102	**Ground Support Equipment (GSE) and Prototyping**
103	**Test Dewar - GSE**
104	Design
105	Procure/Fabricate
106	Assemble & Test (Qualify) the Test Dewar
107	**Motor Test and Evaluation**
108	Design Motor/Control Prototype Setup
109	Procure Components (including test motor)
110	Assemble & Test Motor/Control Prototype - warm
111	Cryo Test Motor
112	Purchase All Motors
113	Qualification Tests of All Motors
114	**Gate Valve Test Assembly**
115	Design Pump Station Assembly
116	Procure Components
117	Assemble & Prep for Gate Valve Testing (see below for Gate Valve Test)
118	**Thermal & Structural Analysis**

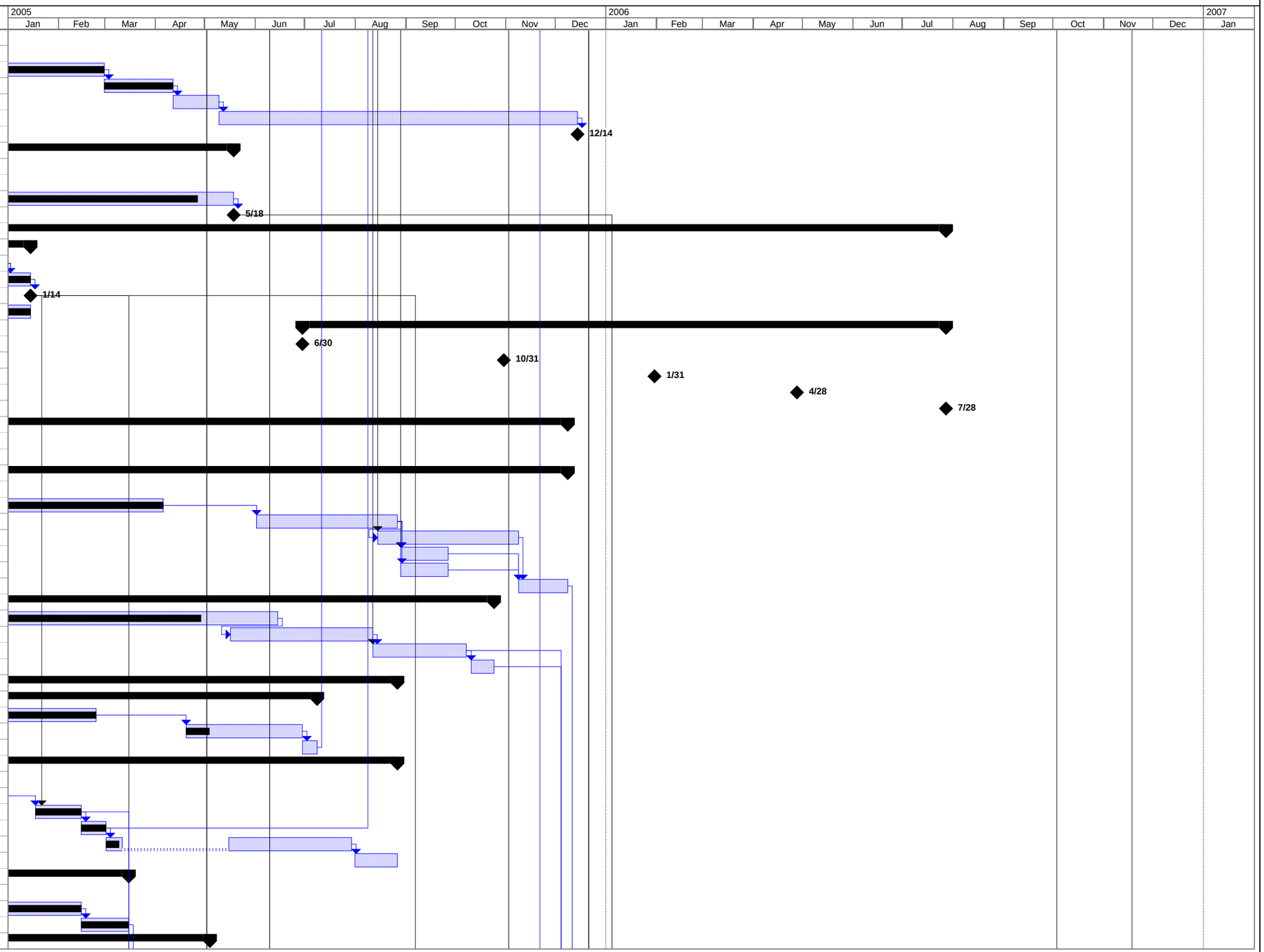

MMIRS Project
CDR Data Package Copy

Task Progress Summary External Tasks Deadline
Split Milestone Project Summary External Milestone

MMIRS Project Schedule

ID	Task Name
119	**Thermal Analysis**
128	**Structural Analysis**
146	**Cryostat - MOS SECTION**
147	Refine Concept Design (updates from PDR review, etc.)
148	MOS Detail Design - Critical Components
149	Detail Design Complete
150	Procure Parts
151	**MOS Vacuum Chamber**
152	Fabricate Chamber
153	Procure Vacuum Components (Top Plate, Seals, Windows, etc.)
154	Assemble ISO/Ring & Wheel Mtg Plate
155	Assemble Ring & Mtg Plate to Chamber
156	Assemble Components to Chamber Assembly
157	**Dewar Assembly**
158	Procure Dewar
159	Leak Test LN2 Dewar
160	Attach Fill Lines
161	**MOS Chamber & Dewar Assembly & Test**
162	Integrate Dewar Assembly with Vacuum Chamber Assembly
163	Install Vac Gauge & Thermal Sensors
164	Vacuum Leak Check & Thermal Cycle
165	Disassemble & Clean
166	**Dekker & MOS Wheel Mounting Plate Assembly**
167	**Dekker Wheel Sub-Assembly**
168	Mount Dekker Wheel Components to Wheel Mtg Plate
169	Test Dekker Drive System
170	**MOS Wheel Sub-Assembly**
171	Mount MOS Wheel Components to Wheel Mtg Plate
172	Test MOS Wheel Drive System
173	Dis-assemble & Clean Dekker & MOS Wheel Components
174	**Corrector Lens Assembly**
175	Fit Check Corrector Lens Mount to Chamber
176	Bond Lens 1 to Cell
177	Build-up Lens 1 into L1 Sub-Assembly
178	Build-up Lens 2 Sub-Assembly
179	Integrate L1 Sub-Assembly and L2 Sub-Assembly
180	Optical Test of Corrector Lens Assembly
181	**WFS & Guider Assembly #1**
182	**WFS & Guider Subassembly (without Lab Camera)**
183	Procure Components
184	Assemble on Test Stand (with Lab Camera & Dummy Mass)
185	Align Optics with Test Source
186	Perform Motion Test
187	Perform Image Motion Testing
188	**WFS Instrument Camera Sub-Assembly**
189	Procure Components
190	Assemble & Test
191	**WFS & Guider Assembly (with Instrument Camera)**
192	Integrate WFS Camera Sub-Assembly
193	Perform System Test
194	WFS #1 Ready for Installation & Test in Cryostat
195	**WFS & Guider Assembly #2**
196	**WFS & Guider Subassembly (without Lab Camera)**
197	Procure Components
198	Assemble on Test Stand (with Lab Camera & Dummy Mass)
199	Align Optics with Test Source
200	Perform Motion Test

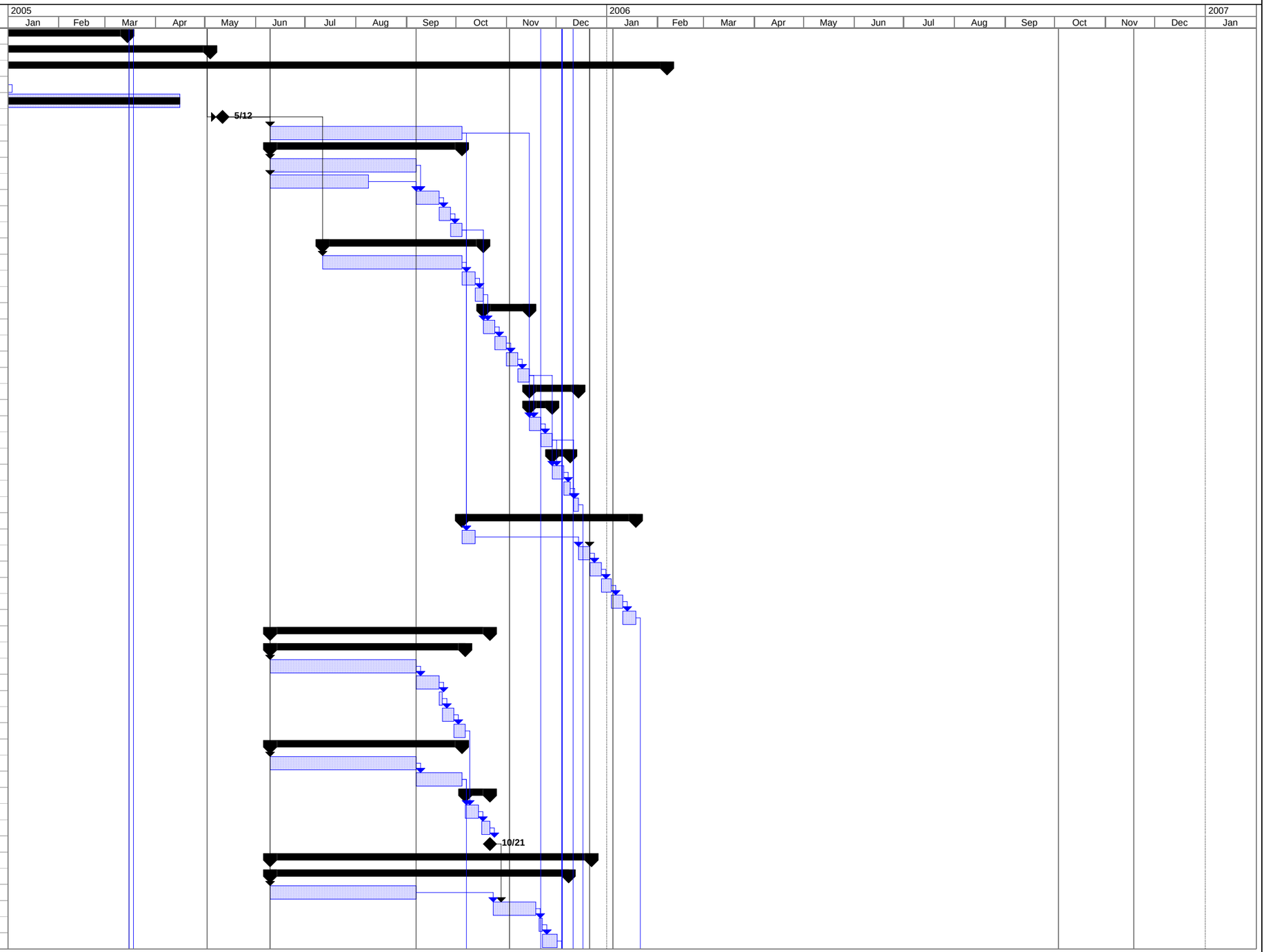

MMIRS Project
CDR Data Package Copy

Task Progress Summary External Tasks Deadline
Split Milestone Project Summary External Milestone

MMIRS Project Schedule

ID	Task Name
201	Perform Image Motion Testing
202	**WFS Instrument Camera Sub-Assembly**
203	Procure Components
204	Assemble & Test
205	**WFS & Guider Assembly (with Instrument Camera)**
206	Integrate WFS Camera Sub-Assembly
207	Perform System Test
208	WFS #2 Ready for Installation & Test in Cryostat
209	**MOS Section Thermal-Vac Test (without Guider/WFS)**
210	Prepare MOS Chamber & Dewar Assembly for Thermal-Vac Test
211	Perform Thermal-Vac Test
212	Clean & Install Corrector Lens Assembly
213	Perform Thermal-Vac Test
214	Prepare for Integration and Test with Camera Section
215	**Cryostat - Camera Section**
216	Refine Concept Design (updates from PDR review, etc.)
217	Camera Detail Design - Critical/Long Lead Components
218	Detail Design Complete
219	**Vacuum Chamber Subassembly**
220	Procurement of Vacuum Chamber
221	Procurement of Components
222	Assemble & Vacuum Leak Test
223	**Optical Bench Subassembly**
224	Procurement of Optical Bench (with its Dewar) and LN2 Lines
225	Detail Inspection & Clean for Vacuum
226	**Gate Valve Subassembly**
227	Receive Quote from VAT (vendor)
228	Procure Gate Valve Components
229	Test with Motor Drive on Test Plate
230	Assemble & Test Vacuum Integrity on Pump Station Test Setup
231	**Grism Subassembly**
232	Procure Components (including mass simulators)
233	Assemble with Grism & Filter Mass Simulator
234	Test Drive System & Detents - warm
235	Dissassmble Components for Clean Prep
236	Clean Prep all Components for Vacuum Use
237	Re-Assemble (with Grism & Filter mass simulators)
238	**Optical Components Subassembies**
239	Procure Vee Block #1 Components
240	Procure Vee Block #2 Components
241	Assemble Test Mirrrors into Cells
242	Assemble to Mounts with Test Mirrors
243	Assemble Deliverable Lenses into Cells
244	**Camera Section Assembly & Test**
245	Assemble LN2 Lines to Optical Bench
246	Vacuum Leak Test & Thermal Cycle
247	Integrate Thermal Isolator and Bulkhead
248	Integrate Vacuum Valve
249	Integrate Focus Slide Subassembly
250	Integrate Grism/Filter Subassembly (optic mass simulators)
251	Integrate Optic Components Subassemblies (with Test Optics)
252	Integrate Vacuum Chamber and Thermal Shrouds
253	Vacuum Leak Test and Thermal Cycle
254	Dissassemble to Remove Test Optics and Mass Simulators
255	Install and Align Optics (see Optical Comp. Subassemblies)
256	Install Test CCD
257	Vacuum Leak Test and Thermal Cycle

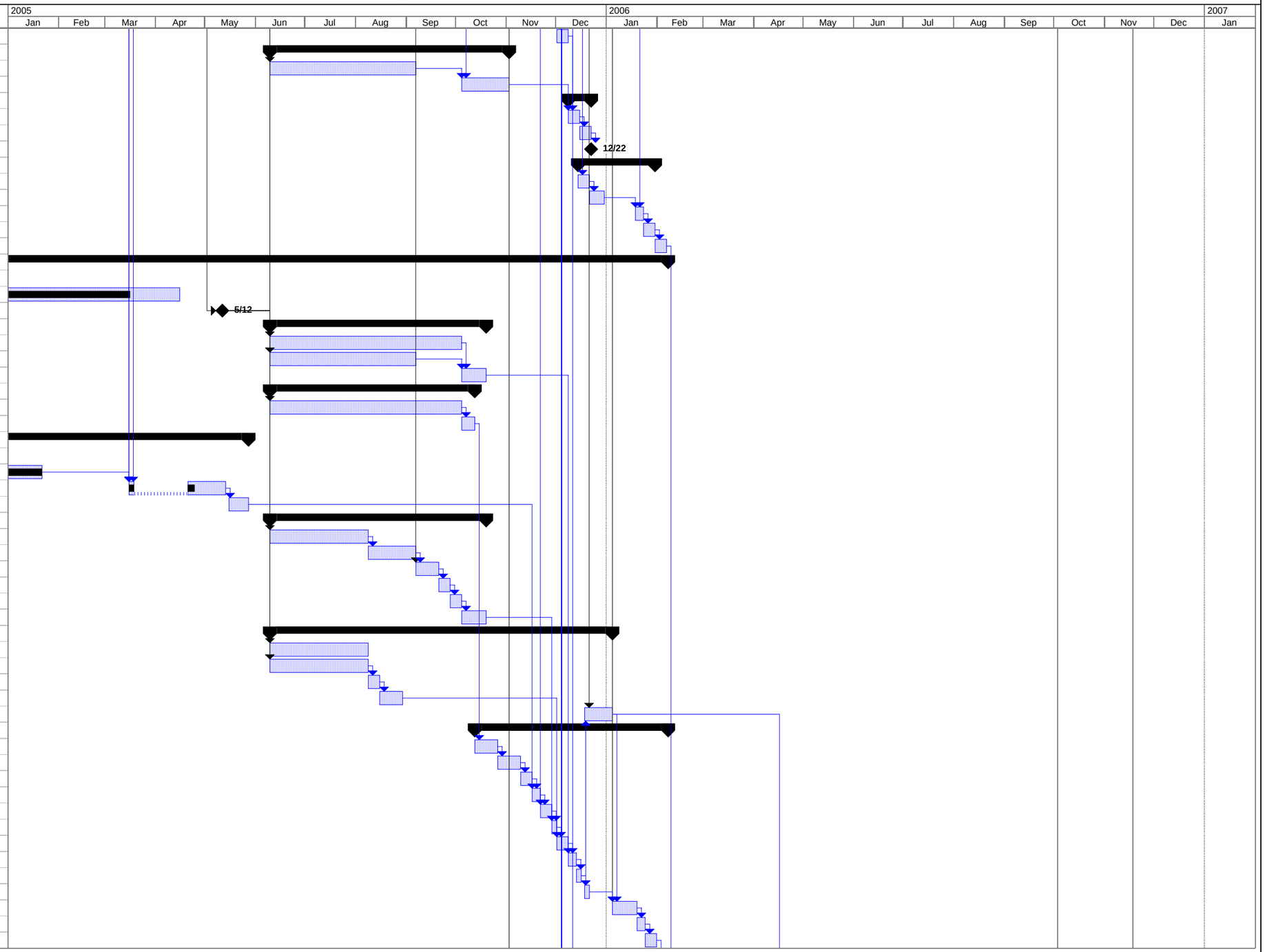

MMIRS Project
CDR Data Package Copy

Task Progress Summary External Tasks Deadline
Split Milestone Project Summary External Milestone

MMIRS Project Schedule

ID	Task Name
258	Prepare for Integration and Test with MOS Section
259	**Cryostat Assembly**
260	Camera Section Ready (without CCD)
261	MOS Section Ready (without WFS)
262	Electronics Rack & Interconnect Cables Ready
263	Integrate Camera and MOS Sections, Connect Cables to Rack
264	Perform Electrical Functional Tests
265	Evaluate Optical Alignment
266	Verify MOS & Camera Assembly
267	Install Turbo Pump on MOS Section
268	Perform Vacuum Leak Test
269	Perform Thermal Vacuum Test
270	Compare Thermal Vac Test Data to Model
271	Open and Install CCD Array
272	Install Optical Mounts (see Optical Component Subassemblies)
273	Evacuate Vacuum Chamber
274	Perform End-to-End Testing (without WFS)
275	Cryostat Testing Complete, Ready for Testing at SAO Telescope Simulator
276	**Telescope Mount**
277	Procure & Inspect
278	Inspect and Tests Fit to Telescope Simulator
279	**All Systems Testing at SAO Telescope Simulator**
280	Prepare Telescope Simulator
281	Evacuate and Cool Cryostat
282	Assemble Cryostat to Telescope Mount
283	Install WFS's (2)
284	Assemble Electronics Racks to Telescope Mount
285	Install Cabling for Racks
286	MMIRS Ready for Installation on Telescope Simulator
287	Mount MMIRS to Telescope Simulator
288	MMIRS Functional Test - Initial
289	Test Analysis
290	Vent MOS Chamber & Change Slits
291	MMIRS Functional Test - Final (if required)
292	Test Analysis
293	MMIRS Functional Test Complete
294	**Prepare & Ship to MMT**
295	Disassemble & Prepare for Shipment
296	**Shipping Containters**
300	Ship to MMT

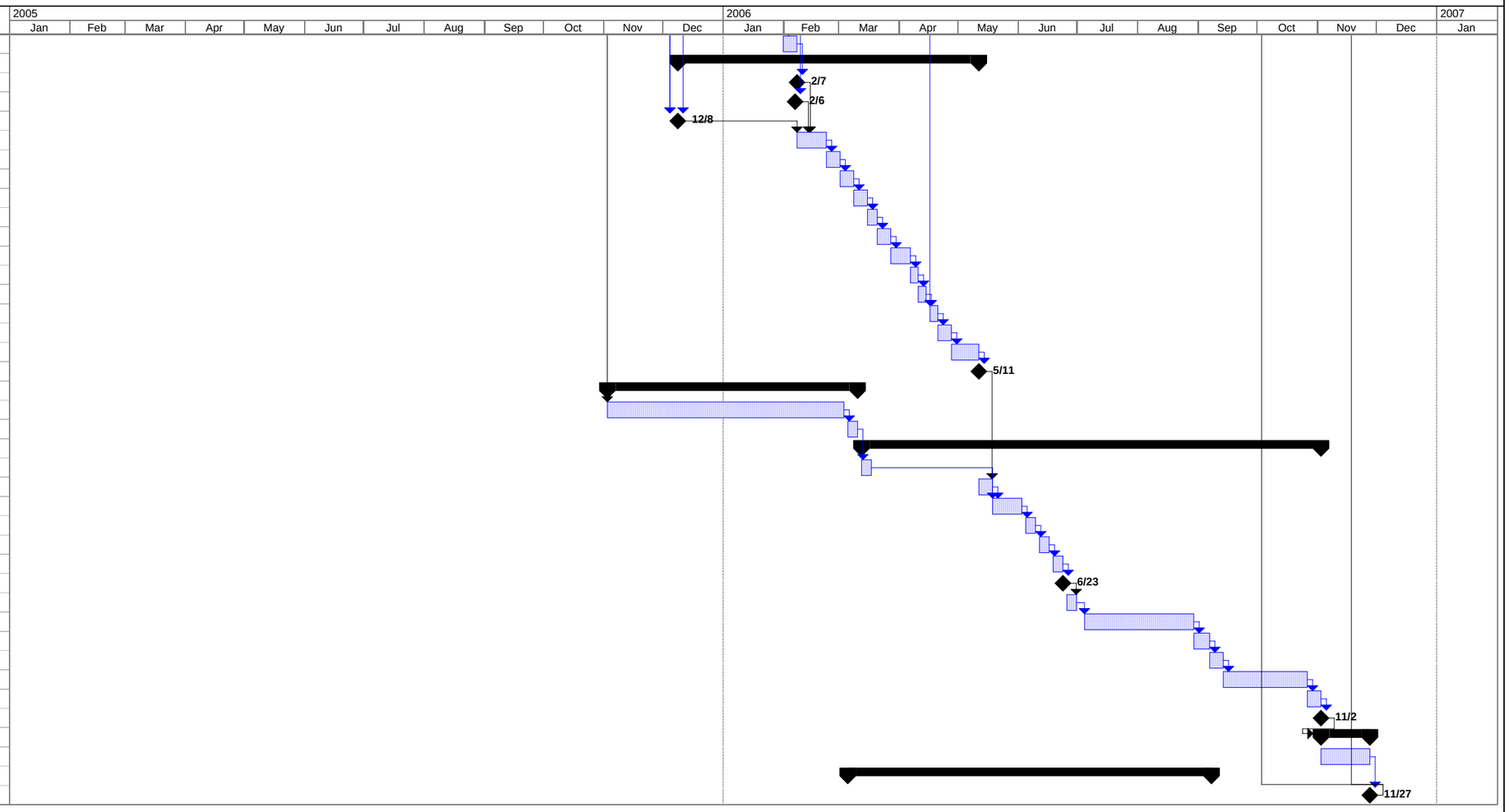

MMIRS Project
CDR Data Package Copy

Task | Progress | Summary | External Tasks | Deadline
Split | Milestone | Project Summary | External Milestone

REVISIONS				
ZONE	LTR	DESCRIPTION	DATE	APPROVED
		9/9/04		

MMIRS MAJOR COMPONENTS

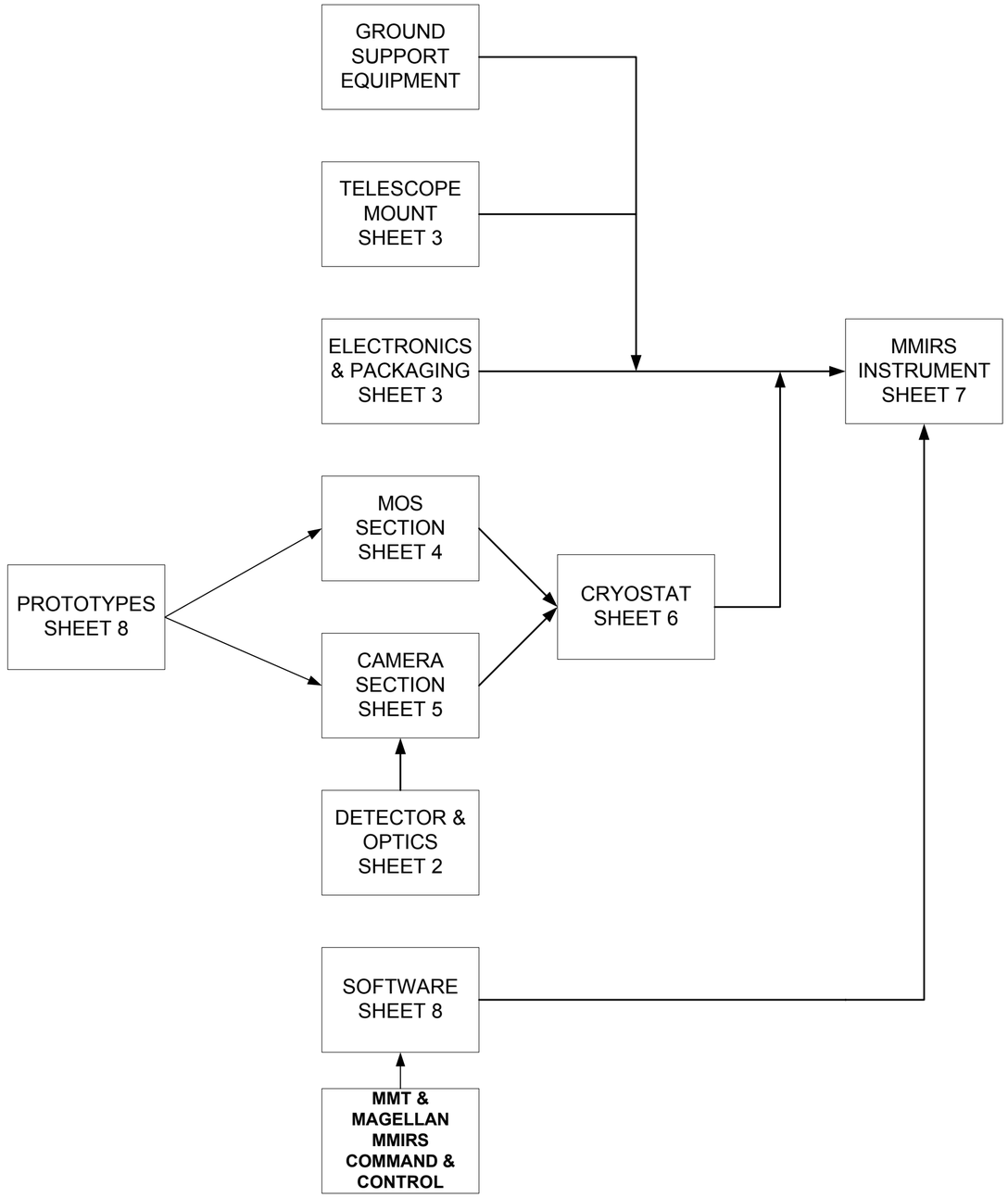

MMIRS PROGRAM FLOW SYSTEM

REMOVE BURRS AND BREAK SHARP EDGES	DRN DATE	CHK DATE
UNLESS OTHERWISE SPECIFIED: DIMENSIONS ARE IN MILLIMETERS	DSGN APPD DATE	
TOLERANCES ON DECIMALS ± .X ± .XX ANGLES ± .3 ± .13 FRACTIONS ± .25°	DSGN APPD DATE	
MACH. FIN. 1.6	ENGR APPD DATE	
MATL: FIN:	ENGR APPD DATE	
NEXT ASSY	CONTRACT	

SMITHSONIAN ASTROPHYSICAL OBSERVATORY
CENTRAL ENGINEERING — CAMBRIDGE, MA

MMIRS FLOW CHART

SIZE	CODE IDENT NO.	DWG NO.	REV
C	50944	MMIRS-301	1

SCALE	NONE	Visio Pro V2000	SHEET 1 OF 8

REVISIONS				
ZONE	LTR	DESCRIPTION	DATE	APPROVED
		9/9/04		

FOCUS SLIDE
DETECTOR MOUNT
PC BOARD
INTERNAL CABLING

SEE SHEET 8 → CRYO/VAC TESTED FOCUS SLIDE

REPEAT THIS LOOP UNTIL PERFORMANCE IS MET

DETECTOR → DESIGN FOCUS/DET SLIDE → DETECTOR PREAMP PACKAGING → DETECTOR RACK PACKAGING → ARRAY/SLIDE ASS'Y & CRYO/TEST → DETECTOR PERFORMANCE EVALUATION → MOD'S IF REQUIRED → EXCHANGE FLT ARRAY WITH ENG. UNIT → CONTINUE PAGE 5

TEST FIRST WITH ENG ARRAY THEN FLIGHT

DETECTOR SWIRC PROTOTYPE

BOARD DESIGNS
OPERATIONAL SOFTWARE
ELECTRONICS DESIGNS

COMPLETE ELECTRONICS DESIGN → PURCHASE ELECTRONICS & PCB'S → BUILD AND TEST PCB'S

PREPARE LENS & COATING SPEC.'S

FTSM16
TEST PLATE FIT

PREL. OPTICS DESIGN COMPLETE → PREPARE LENS DRAWINGS → PREPARE QUOTATION → SOLICIT VENDOR QUOTES → SELECT VENDOR → RECEIVE MELT DATA → UPDATE OPTICAL DESIGN & DRAWINGS → RECEIVE AND INSPECT OPTICS → OPTICS TO CRYOSTAT OR COATING VENDOR

LENS DESIGNS
GHOST ANAL
BAFFLES

WARM OPTICS CAL'S

COATING QUOTATION WILL BE EITHER PART OF OPTICS PROCUREMENT OR INDEPENDENT VENDOR

PREPARE LENS COATING QUOTATION → SOLICIT VENDOR QUOTES → SELECT VENDOR → RECEIVE AND INSPECT OPTICS → OPTICS TO CRYOSTAT ASS'Y

PREPARE GRISM SPEC.'S

GRISM DESIGNS COMPLETE → PREPARE GRISM DRAWINGS → PREPARE QUOTATION → SOLICIT VENDOR QUOTES → SELECT VENDOR → ORDER GRISM OR GRISMS → RECEIVE AND INSPECT GRISMS → GRISMS TO CRYOSTAT ASS'Y

FILTERS → JOIN CONSORTIUM → ORDER FILTERS → RECEIVE FILTERS → INSPECT FOR LIGHT LEAKS & REPAIR → FILTERS TO CRYOSTAT ASS'Y

FILTERS → SPECIFY SPECIAL FILTERS → ORDER FILTERS → RECEIVE FILTERS → INSPECT FOR LIGHT LEAKS & REPAIR → FILTERS TO CRYOSTAT ASS'Y

MMIRS PROGRAM FLOW DETECTOR AND OPTICS

SMITHSONIAN ASTROPHYSICAL OBSERVATORY
CENTRAL ENGINEERING — CAMBRIDGE, MA

MMIRS FLOW CHART

SIZE	CODE IDENT NO.	DWG NO.	REV
C	50944	MMIRS-301	1

SCALE NONE | Visio Pro V2000 | SHEET 2 OF 8

REVISIONS				
ZONE	LTR	DESCRIPTION	DATE	APPROVED
		9/9/04		

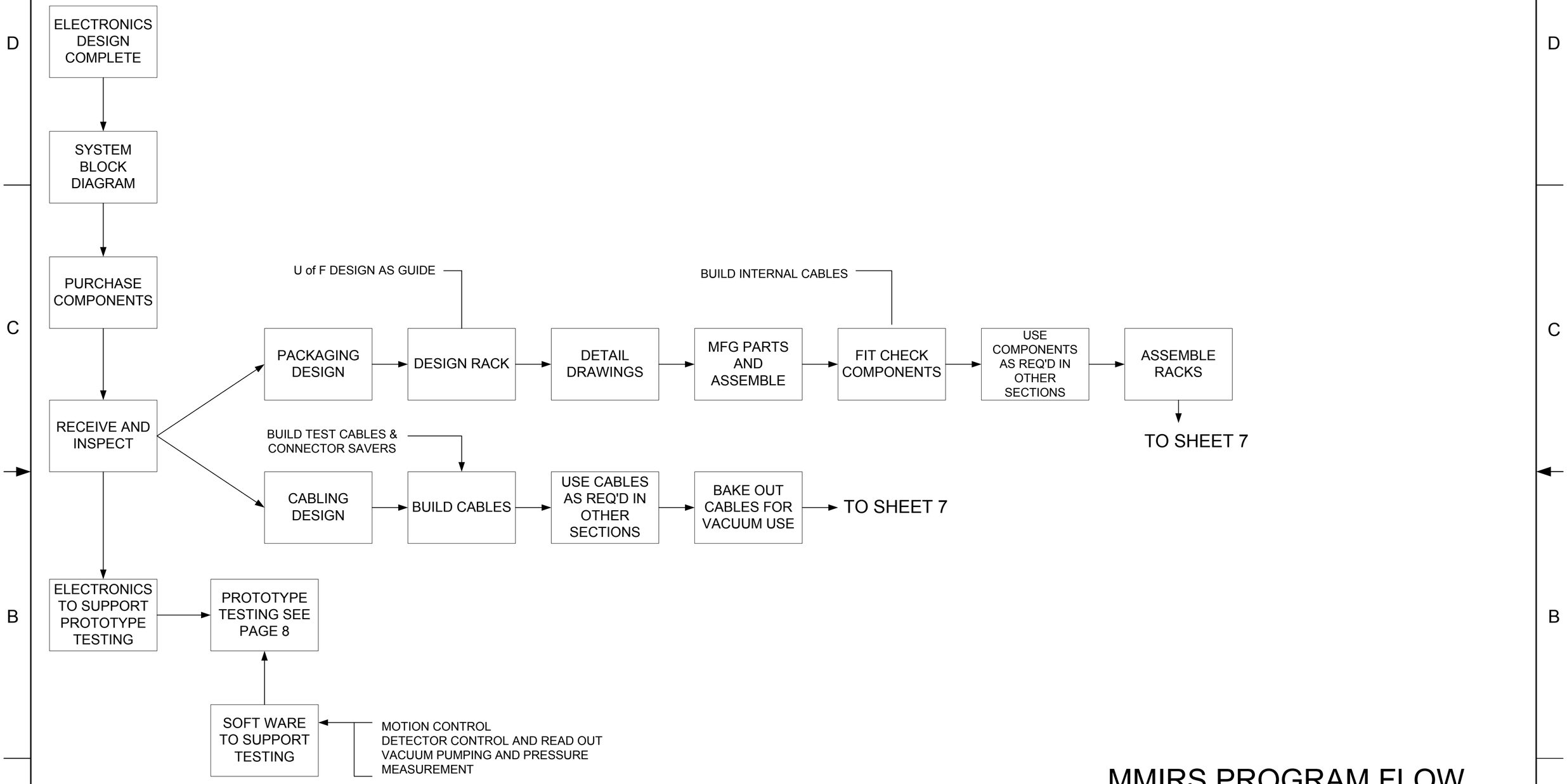

MMIRS PROGRAM FLOW ELECTRONICS AND SOFTWARE

SMITHSONIAN ASTROPHYSICAL OBSERVATORY
CENTRAL ENGINEERING — CAMBRIDGE, MA

MMIRS FLOW CHART

SIZE	CODE IDENT NO.	DWG NO.	REV
C	50944	MMIRS-301	1

SCALE	NONE	Visio Pro V2000	SHEET 3 OF 8

REVISIONS				
ZONE	LTR	DESCRIPTION	DATE	APPROVED
		9/9/04		

PURCHASE, RECIEVE & INSPECT PARTS

PREPARE DETAIL DRAWINGS

MOS SECTION

BOT TEST PLATE
TOP PLATE & SEAL LENS APERTURE WINDOWS

FABRICATE MOS VACUUM CHAMBER

PURCHASE WITH CAMERA CHAMBER

PURCHASE VACUUM COMPONENT

ASSEMBLE ISO/RING & MTG PLATE

2

ASSEMBLE PLATE TO CHAMBER

ASSEMBLE REMAINING ITEMS

ASSEMBLE DEWAR & FILL LINES

INSTALL VAC GAUGE & TEST THERMAL SENSORS

VACUUM LEAK CHECK & THERMAL CYCLE

DIS-ASSEMBLE & CLEAN

MOUNTING PLATE ASSEMBLY

LEAK TEST LN2 DEWAR

ATTACH FILL LINES

INSTALL TURBO PUMP

MAKE UP TEMPORARY ROUGHING & VENT SYSTEM

DEKKER WHEEL

WARM ASS'Y TO MTG PLATE

TEST DRIVE SYSTEM

MOS WHEEL ASSEMBLY

WARM ASS'Y TO MTG PLATE

TEST DRIVE SYSTEM

SOFTWARE
POSITIONING
STABLITIY

DIS-ASS'Y & CLEAN FOR VACUUM

RE-ASS'Y TO PREV. VAC TEST CONF.

VACUUM LEAK CHECK & THERMAL CYCLE

COLD TEST MECHANISMS

CLEAN AND INSTALL LENS ASS'Y

VACUUM LEAK CHECK & THERMAL CYCLE

COMPLETE MOS SECTION PER PROCEDURE

1

TO SHEET 7

DESIGN & MAKE FIXTURE

FIT CHECK MOUNT TO CHAMBER

CORRECTOR LENS ASSEMBLY

FIT CHECK LENS TO MOUNTS

BOND LENS 1 TO CELL

ASSEMBLE LENS 1 INTO CELL

ASSEMBLE LENS 2 INTO CELL

ASSEMBLE LENS 1 & 2 TOGETHER

WFS & GUIDER ASSEMBLY

WFS/GUIDER AS TEST ON PAGE 8

INSTALL CAMERA

TEST CAMERA & SOFTWARE OPERATION

SYSTEM TEST

TEST FIT TO MOS CHAMBER

TO SHEET 7

REPEAT FOR SYSTEM 2

NOTES:
1. ASSEMBLE PER PROCEDURE MMIRS-P-TBD?
2. PRE-ASSEMBLY AND TESTING TO USE PROCEDURE STATED IN NOTE 1 FOR DEBUGING OF PROCEDURE.

MMIRS PROGRAM FLOW MOS SECTION

SMITHSONIAN ASTROPHYSICAL OBSERVATORY
CENTRAL ENGINEERING — CAMBRIDGE, MA

MMIRS FLOW CHART

SIZE	CODE IDENT NO.	DWG NO.	REV
C	50944	MMIRS-301	1

SCALE	NONE	Visio Pro V2000	SHEET 4 OF 8

REVISIONS				
ZONE	LTR	DESCRIPTION	DATE	APPROVED
		9/9/04		

SEE NOTES 1 & 2

PURCHASE, RECEIVE & INSPECT PARTS

PREPARE DETAIL DRAWINGS

CAMERA SECTION

LAB PUMPING SYSTEM

PURCHASE VACUUM VESSEL

INSPECT & VAC LEAK TEST

BUY VACUUM SYSTEM COMPONENTS

USE LAB PUMP

VALVE BULKHEAD
MOS CHAMBER

TESTED FOCUS SLIDE PAGE 2

HOLD IN TEST STAND

INSTRUMENT FOR TEST

REPEAT AS REQ'D

OPTICAL BENCH

DETAIL INSP. & CLEAN FOR VACUUM

RE-ASSEMBLE AND ATTACH LN2 LINES

ASSEMBLE ISOLATOR & BULKHEAD

INSTALL FOCUS SLIDE AND DETECTOR

ASSEMBLE VAC. VALVE

ASSEMBLE CAMERA SECTION

VACUUM LEAK CHECK & THERMAL CYCLE

CAMERA SECTION TESTING

GRISM WHEEL
FILTER WHEEL
DRIVES

BUY VAC VALVE AND ALL PARTS

TESTED VALVE ASS'Y FROM PAGE 8

OPEN VACUUM VESSEL

REMOVE MOUNTS AND TEST MIRRORS

GRISM ASSEMBLY

ASSEMBLE PER PROCEDURE

WARM TEST DRIVES + DETENTS

DIS-ASS'Y CLEAN FOR VACUUM

REASSEMBLE

INSTALL & ALIGN LENS CELLS INTO MOUNTS

USE DUMMY MASS FOR GRISMS & FILTERS

ENG ARRAY INSTALLED (REF)

ASSEMBLE TEST MIRRORS INTO CELLS

ASSEMBLE INTO MOUNTS

ASSEMBLE MOUNTS ONTO BENCH AND ALIGN

EVACUATE & TEST

CLEAN ALL PARTS FOR VACUUM

FIT CHECK MOUNTS TO OPTICAL BENCH

PREPARE FOR MOS ASS'Y

VEE BLOCK 1

MEASURE LENS DIA. & MACHINE CELLS

FIT CHECK LENS TO CELLS

ASSEMBLE LENS INTO CELLS

READY FOR CRYOSTAT ASSEMBLY
SEE SHEET 6

VEE BLOCK 2

NOTES:
1. ASSEMBLE PER PROCEDURE MMIRS-P-TBD
2. PRE-ASSEMBLY AND TESTING TO USE PROCEDURE STATED IN NOTE 1 FOR DEBUGGING OF PROCEDURE.

MMIRS PROGRAM FLOW
CAMERA SECTION

SMITHSONIAN ASTROPHYSICAL OBSERVATORY
CENTRAL ENGINEERING — CAMBRIDGE, MA

MMIRS FLOW CHART

SIZE	CODE IDENT NO.	DWG NO.	REV
C	50944	MMIRS-301	1
SCALE NONE	Visio Pro V2000	SHEET 5 OF 8	

REVISIONS				
ZONE	LTR	DESCRIPTION	DATE	APPROVED
		9/9/04		

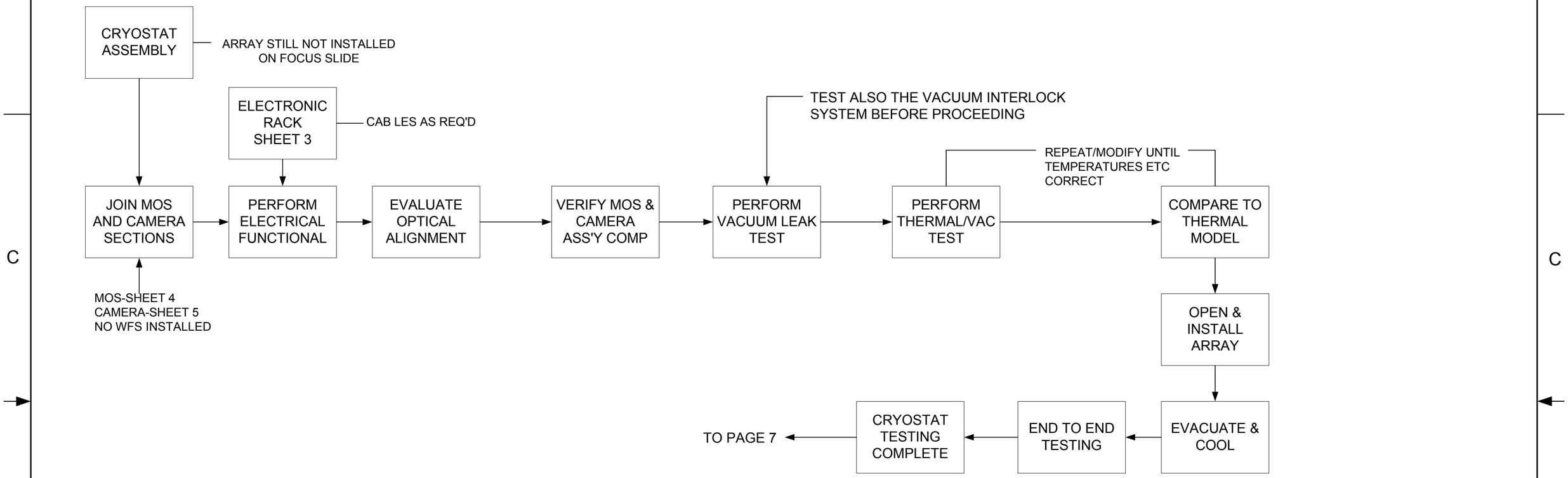

NOTES:
1. ASSEMBLE PER PROCEDURE MMIRS-P-TBD
2. USE PROCEDURE STATED IN NOTE 1 FOR PRE-ASSEMBLY TASKS TO DEBUG PROCEDURE FOR FINAL ASSEMBLY

MMIRS PROGRAM FLOW CHART CRYOSTAT

SMITHSONIAN ASTROPHYSICAL OBSERVATORY
CENTRAL ENGINEERING — CAMBRIDGE, MA

MMIRS FLOW CHART

SIZE	CODE IDENT NO.	DWG NO.	REV
C	50944	MMIRS-301	1

SCALE	NONE	Visio Pro V2000	SHEET 6 OF 8

REVISIONS				
ZONE	LTR	DESCRIPTION	DATE	APPROVED
		9/9/04		

TESTED CRYOSTAT FROM PAGE 6

MAINTAIN CRYOSTAT CAMERA VACUUM & TEMPERATURE FOR ENTIRE TESTING PERIOD UNLESS PROBLEMS REQUIRE TEARDOWN

INSTALL WFS (2) AFTER MOUNT ASSEMBLED

HANDLING FIXTURE REQUIRED

MOVE ALL MMIRS COMPONENTS TO THE MMT TELESCOPE ROTATOR SIMULATOR AREA

CRYOSTAT

EVACUATE &COOL DOWN CRYOSTAT

FLIGHT ARRAY INSTALLED

ASSEMBLE TO TELESCOPE MOUNT

1

START OF TEST FLOW AT TELESCOPE

ASSEMBLE ELECTRONICS RACKS TO FRAME

CONNECT ALL CABLES CRYOSTAT TO RACKS

MOUNT MMIRS TO MMT SIMULATOR

TELESCOPE MOUNT

RECEIVE AND INSPECT

TEST FIT TO MMT SIMULATOR

BE AWARE OF DIFFERENCES WITH ROTATOR

TELESCOPE COMPUTER SYSTEM

PERFORM FUNCTIONAL TEST

LOAD FINAL SOFTWARE

LOG DATA & EVALUATE RESULTS

ELECTRONICS RACKS

PLACE ELECTRONICS IN RACKS

MAKE CABLE CONN'S AND TESTS

REPEAT THIS LOOP UNTIL REQUIREMENTS SATISFIED

USE & DEBUG PROCEDURE RECORD TIME REQ'D

VENT MOS CHAMBER & CHANGE SLITS

PERFORM VENTING AND REPAIRS-IF REQUIRED

END TESTING

BRING CRYOSTAT TO ROOM TEMP & PRES.

DIS-ASSEMBLE TO SHIPMENT CONFIG.

PREPARE FOR SHIPMENT

SHIP TO TELESCOPE

RECEIVE & INSPECT

EVACUATE &COOL DOWN CRYOSTAT

PICKUP &REPEAT FLOW STARTING AT 1

MGSE

DESIGN AND FABRICATE FIXTURES

CRYOSTAT HOLDER
CRYOSTAT SLING
MOS HOLDER
MOS SLING
ALIGNMENT FIXTURES
TELESCOPE INSTALLATION

EGSE

DESIGN AND FABRICATE EQUIPMENT

CONTROL COMPUTER
TELESCOPE CABLES
MOTOR TEST BOX
TEST CABLES

MGSE & EGSE USED AS REQ'D IN FLOW

WRITE SHIPPING PROCEDURE

FIT CHECKS PRESSURE TESTS

SHIPPING CONTAINERS

DESIGN SHIPPING CONTAINERS

PURCHASE OR FAB CONTAINERS

RECEIVE & INSPECT

TEST

AVAILABLE FOR SHIPPING

SMITHSONIAN ASTROPHYSICAL OBSERVATORY
CENTRAL ENGINEERING CAMBRIDGE, MA

MMIRS FLOW CHART

SIZE	CODE IDENT NO.	DWG NO.	REV
C	50944	MMIRS-301	1

SCALE	NONE	Visio Pro V2000	SHEET 7 OF 8

REVISIONS				
ZONE	LTR	DESCRIPTION	DATE	APPROVED
		9/9/04		

PURCHASE 1 MOTOR WITH OPTION TO BUY 12 AFTER QUALIFICATION

TEST AND DEBUG MOTOR ELEC. & SOFTWARE

MOTOR OPERATION, COLD PARAMETERS, TORQUE VS SPEED

MOTOR QUALIFICATION → PURCHASE MOTOR → WARM TEST MOTOR ELEC. & SOFTWARE → CYRO/VAC TEST MOTORS → PURCHASE MOTORS OR SELECT & QUALIFY NEW MOTOR TYPE → MOTORS AVAILABLE FOR USE

DESIGN AND BUILD CYRO/ VAC TEST CHAMBER → QUALIFY CHAMBER → CYRO/VAC TEST MOTORS

SMOOTHNESS OF MOTION ,LVDT & ELEC. PARAMETERS

MOTOR & LVDT OPERATION, COLD PARAMETERS

MEASURE COOLING RATE AND FINAL ARRAY TEMP.

USE QUALIFIED MOTOR

DETECTOR FOCUS SLIDE → DETAIL MFG PARTS & FAB → PURCHASE SLIDE COMPONENTS → RECEIVE, INSPECT AND ASSEMBLE SLIDE → WARM TEST DRIVE & SOFTWARE → CYRO/VAC TEST SLIDE → INSTALL TEST ARRAY & CYRO/ VAC TEST

DESIGN & BUILD TEST PLATE

VACUUM VALVE → PURCHASE VALVE → DETAIL MFG PARTS & FAB → RECEIVE, INSPECT AND ASSEMBLE VALVE → WARM TEST DRIVE & SOFTWARE → WARM TEST VALVE SEALING

DETECTOR → BUILD PCB'S, OTHER ELEC. & CABLES → PERFORM PRELIMINARY BENCH TESTS → ASSEMBLE ON TESTED FOCUS SLIDE → CYRO/VAC TEST USING ENG. ARRAY → CYRO/VAC TEST USING FLIGHT ARRAY → REMOVE FLIGHT ARRAY → FOCUS SLIDE TO CAMERA ASSEMBLY

INSTALL LAB CAMERA WITH DUMMY MASS FOR TESTING

TEST ALL MOTION DEVICES & SOFTWARE

ROTATE WFS THRU OPERATIONAL RANGE AND MEASURE IMAGE MOTION

WFS → ASSEMBLE 1 UNIT ON TEST STAND → ALIGN OPTICS WITH TEST SOURCE → MOTION TESTING → IMAGE MOTION TESTING → ANALYZE RESULTS AND MAKE CHANGES IF REQUIRED

SOFTWARE → MOTION CONTROL → WFS SERVOS, CRYOSTAT SERVOS (MOS, DEKKER, GATE VALVE, FILTER WHEELS, GRISM WHEEL, FOCUS SLIDE) → OTHER REQ'D SOFTWARE → CRYOSTAT HOUSEKEEPING, DETECTOR CONTROL & READOUT, THERMAL SYSTEM, VACUUM SYSTEM & INTERLOCK

SOFTWARE → SCIENCE & FACILITY SOFTWARE → DETECTOR DATA MGMT, OBSERVATIONAL ROUTINES, FACILITY INTERFACE, MMIRS-TELESCOPE CONTROL

MMIRS PROGRAM FLOW PROTOTYPES

REMOVE BURRS AND BREAK SHARP EDGES

UNLESS OTHERWISE SPECIFIED: DIMENSIONS ARE IN MILLIMETERS

TOLERANCES ON
DECIMALS ± .X ± .XX
ANGLES ± .3 ± .13
FRACTIONS ± .25°

MACH. FIN. 1.6

MATL: FIN:

NEXT ASSY

DRN DATE | CHK DATE

DSGN APPD DATE

DSGN APPD DATE

ENGR APPD DATE

ENGR APPD DATE

CONTRACT

SMITHSONIAN ASTROPHYSICAL OBSERVATORY
CENTRAL ENGINEERING CAMBRIDGE, MA

MMIRS FLOW CHART

SIZE	CODE IDENT NO.	DWG NO.	REV
C	50944	MMIRS-301	1

SCALE NONE | Visio Pro V2000 | SHEET 8 OF 8

Comments and Responses from MMIRS PDR 06 July 2004

MT=Mark Trueblood
DF=Dan Fabricant
RF=Bob Fata
JJ=Jeff Julian
MO=Mark Ordway
TB=Todd Boroson
JH=Joe Hora
EH=Ed Hertz
AS=Andrew Szentgyorgyi
GN=George Nystrom
BM=Brian McLeod
TN=Tim Norton

Number	Comment	SAO Response/Action	Actionee	Status
001	MT: Concerned we are not following proper order: Requirements --> Design.	SAO to publish F&P. Plan to send out by 30 July, 2004. The document will be released with TBR/TBD's where no spec has been resolved.	BM	Closed
002	JJ: Flamingos2 filters from OCLI and Barr have pinholes. They had to blacken them using microscope.	SAO will specify appropriately and perform acceptance inspection.	BM	Closed
003	MT: Asked how we will align cold pupil.	Alignment by design, fabrication and assembly. Confirmation at telescope integration.	BM	Closed
004	EH: Questioned necessity of having G2, G3, and G4 in Zemax tolerancing.	An explicit flexure calculation will be done which combines the IDEAS model with ZEMAX analytical tool – to be presented at CDR	BM	Closed
005	JH: Asked what is scale change when we refocus from J->H-> K.	Worst case is between J and H where the image position at the corner of the field shifts by 15 microns.	BM	Closed
006	JJ: Discussion of CaF2 allowable stress. UF uses 1500PSI. We've been using 200 as a nominal limit, but the front window shows 400. DGF thought 400 would be ok if it were single crystal CaF2.	Adopted 400 psi.		Closed
007	RF: Asked about rotational constraint of lenses in cryo mounts.	BM @ PDR: I don't think this is a big issue as the tolerances on rotation will be 10's of degrees even if we try to optimize wedges on lenses.	BM	Closed
008	RF: Asked if lenses deflections from 3pt mount is acceptable.	BM@PDR: This needs to be analyzed.	GN	Closed

		Analysis to be presented at CDR.		
009	RF: Concerned about tolerance stackup of tilts in lens barrels. Discussed whether you would want to face off a whole stack of components. Alternatively can we optimize by rotating the spacers?	BM@PDR: Goal is to rely on machining tolerances. SAO will design with groups of lenses.	GN	Closed
010	JJ: In Flam they had threaded lens barrel assembly to minimize stackup errors and simplify warm/cold switchover. Also recommended treating groups of lenses to prevent stack up of tolerances.	SAO will design with groups of lenses.	GN	Closed
011	DF: Are we concerned about Janos ability to not exceed 2% loss value used in throughput assumptions?	Coating spec calls for R<0.5% avg. At least one vendor claims this is achievable. Janos claims to do R<1.5%	PM/BM	Closed
012	JJ: Are we going to test plate the optics?	BM/DF @ PDR: Yes		Closed
013	JJ: Given the tight tolerances, is there adequate budget in the thermal and structural areas?	See MMIRS-S-203	PM	Closed
014	JJ: Will we perform tests to quantify lens mount pad shrinkage?	GN @ PDR: Yes		Closed
015	JJ: Will there be some sort of cushioning material used on the lens mount axial restraints?	GN @ PDR: Kapton tape		Closed
016	MT: Asked about interlock on Electronics rack doors. We have no formal requirement, but is this needed for safety?	No interlocks are planned.	T.Gauron	Closed
017	MO: Suggested coordinating cabling with Megacam Magellan Topbox so we have interchangeability.	Designs are reviewed and used where applicable.	T. Gauron	Closed
018	MT: Warned of problems with Phytron motors on GNIRS and NIRI. Need to do incoming cryo tests/inspection.	SAO to perform.	GN	Closed
019	MT: Asked about LVDT stability, but then retracted when he got units sorted out: 2.5mm * 0.001 = 2.5um. This is less then spec so OK.	No action needed.		Closed
020	DF: Do we even need the LVDT?	SAO to include for positional information.	BM	Closed
021	JJ: UF puts temp sensors in racks to cut power if temp exceeded, eg if cooling is turned off.	SAO to include.	MB/TG	Closed
022	JJ: Watch out for noise pickup from focus and temp sensors on detector electronics.	SAO is advised. Detector electronics are going in own housing/cabinet and will be tested for noise.	MB	Closed
023	JJ: UF found it useful to increase motor current temporarily via software during Integration and Test. Apparently not possible with stepper drivers we are using?	Not available. SAO to use hardware change in current limiting resistor.	MB	Closed
024	DF: Asked about access to MOS wheels for changeout. JJ suggests making opening much larger.	SAO to incorporate a larger opening.	GN	Closed

025	DF: Suggests removing flat from bottom of Lens 1 and put curve on mating piece. We need to check on impact on required tolerance.	Design discussion held and use of flat approved.	GN	Closed
026	MT: Questions 80+/-3 on MOS specs. Need to review.	Established T<120K, within 10K of final temp for operation.	BM	Closed
027	TB: Asked if 1 pix repeatability on MOS wheel is good enough. Impact on flats?	MOS Repeatability will be 10 microns. In addition we plan to have continuum and HeNeAr lamps outside the MOS window. System flexure is relevant and will be presented at CDR.	BM	Closed
028	DF: Suggests making mockup of mask insertion mechanism	Enlarged opening & using proven U of F design.	GN	Closed
029	DF: Concerned about torque of stepper motors. Do we have enough margin?	Design calculations and torque margin to be presented in CDR data package.	GN	Closed
030	JJ: UF bearing races are V-grooves on one side, flat on other. Moly-disulfide powder burnished in.	SAO changed to incorporate this design.	GN	Closed
031	DF: Need to verify 3000 rpm on steppers.	SAO subsequent design change results in 1500 RPM. Calculations to be presented in CDR data package.	GN	Closed
032	JJ: Questions need for gearbox on motor. Tradeoff w/ higher pitch worm? Use flexible coupling on drive.	Design calculations to be presented in CDR data package.	GN	Closed
033	JH: Are motor specs adequate for warm operation.	Specs are de-rated for cryo environment.	GN	Closed
034	JH: What is time lag between imaging and cutting of slit masks. Would be desirable to do imaging and spectroscopy in same observing run.	Magellan requires several week lead time for mask manuf. Will use outside shop in Arizona, so same-run img/spect not possible.	BM	Closed
035	DF: Need FEA of thermal standoff ring. Doesn't it introduce bending forces? (I'm sure this is planned if not already done.)	Design and analysis done and to be presented at CDR.	GN	Closed
036	JJ: Filter washers. Suggests using indium instead of teflon because off higher thermal conductivity.	SAO agrees to use either indium or silver foil.	GN	Closed
037	JJ: Make opening in outer filter wheel or grism wheel large enough so that access to inner filter wheel is easy.	Design incorporated and will be presented at CDR.	GN	Closed
038	DF: Think about servicing issues now.	SAO to include procedures in CDR data package, ie “Slit Mask Exchange”, “Warm up and Cool Down” procedures.	GN	Closed
039	MT: Filter wheel access. Can we make it easier to change filters?	See #037	GN	Closed
040	GN: Concerned about accuracy of home switches. How repeatable are	SAO to analyze and report at CDR.	GN	Closed

	they. Do they guarantee that we will actually get centered in detent? MT suggested talking to Doug Simons about NIRI experience with Hall sensors.			
041	AS: Concerned if we increase backlash, will that cause problems with stepper motor performance?	See #040	GN	Closed
042	TN: How accurately do we need to set limit switches on valve. How do we know if we are really closed?	SAO is building prototype for test.	GN	Closed
043	JG: Suggests test purge of MOS chamber with small amount of GN2 to verify gate valve integrity before completely backfilling.	See "MMIRS Warm Up and Cool Down Procedure" part of CDR data package.	GN	Closed
044	DF: Put handles on outer shell of instrument if they are heavy.	Lift features are added where necessary.	GN	Closed
045	MT: Suggests writing Operational Concepts Document to include Observing Procedures and Installation Procedures (loading dock to telescope)	Draft Installation Plan to be presented at CDR.	BM	Closed
046	EH: Check CG moment of instrument.	See CDR Data Package.	GN	Closed
047	DF: Can we minimize detector connection by using bellows assy inside dewar? JJ says they use hermetic D-connectors on radiation shields.	Considered but not implemented. Design to be presented at CDR.	GN	Closed
048	RF: Questions Henry's Lens mount model (Slide #12) -- are the constraints correct?	Boundary constraints in the model were correct to the extent the lens was modeled in a linear way. Lens mount design has changed and re-analyzed.	HB	Closed
049	JJ: Are we being too conservative by specifying flexure limits from zenith to horizon rather than for duration of observation?	Flexure limits have been changed to be for 2 hour observation	BM/PM	Closed
050	JJ: Is GrafTech really necessary? Does it adversely affect optical alignment?	GrafTech eliminated from design.	GN/SP	Closed
051	DF: Can we weld v-block to bench to increase thermal efficiency? Much discussion of thermal design. This needs much closer scrutiny.	V-blocks not welded. Revised thermal analysis indicates adequate thermal contact with a bolted interface. Transient analysis showed that the optical bench will require less than 0.2C/min cooling / heating rates. Contact conductance between the optical bench and the V-block is sufficient	GN/SP	Closed
052	JJ: Questions steady state thermal load of 100W and would like to discuss assumptions/calculations in more detail with Sang Park.	Thermal model of MOS section has been reviewed and revised. Current model indicates about 35 Watts.	GN/SP	Closed

053	BM: Sang mentioned continuous LN2 flow during cooldown. Not what I had envisioned.	Camera Dewar will be cooled actively at a rate of 0.2C/Min using controlled LN2 fill.	GN/SP	Closed
054	JJ: Has empirical rate of cooling of LN2 cooled dewars. He would like to review cool down calculations/assumptions with Sang Park.	See #053. Camera Dewar will be cooled actively at a rate of 0.2C/Min.	GN/SP	Closed
055	BM: Need to understand cooling rate of slit plates. How important is stability below max acceptable operating temp. IE. if 120K is acceptable can we continue to cool to 80K while observing?	See #026	BM	Closed
056	JJ: Suggests using LN2 boiloff to cool radiation shield.	SAO agrees to include in design.	GN	Closed
057	TB: Need more detail on Fabrication, Integration and Test phases. Break down by subassy and staffing requirements. Wants it for Sept report for payment.	SAO generated I&T Flow chart and detailed schedule submitted with the MMIRS First Annual Report on 27 September 2005.	TN-GN-BM	Closed

MMIRS OPEN ISSUES

Date: 05/05/2005

The following is a list of open issues as posted on the internal MMIRS website:

1. Specifically where is MOS LN2 vessel heater servo sensor location?
2. Where is ambient air sensor for interlock?
3. Mike B and Tom G to define whether or not there is a specialized SAO cable required for power/ethernet at each facility
4. Lens 2 Mount Design - Ken to update mount design details
5. Need to add provision for shimming detector tilt (perhaps an open discussion at the CDR)
6. Discussion of Calibration Lamps
7. Compute temp gradient in Guider window on mos chamber and on CCD camera.
8. Covers for guiders -- to address after CDR.
9. Penetrations for guider motors in light shield above MOS.
10. GWFS pinhole reference.
11. What is the procedure if the pressure starts to rise during observations, indicating there is a vacuum leak somewhere?
12. Think about implications of 71C shipping extreme.
13. Think more about requirements for gate valve interlock.